Technical Report Documentation Page

1. Report No. TX -97/0-1704-8	2. Government Accession No.	3. Recipient's Catalog No.
4. Title and Subtitle Evaluation of Roadway Lighting Systems Designed by Small Target Visibility (STV) Methods		5. Report Date December 2000 6. Performing Organization Code TECH
7. Author(s) Sanjaya Senadheera, Olkan Culvalci, Bobby Green, Douglas D. Gransberg, and Karl Burkett		8. Performing Organization Report No. 1704-8
9. Performing Organization Name and Address Texas Tech University Departments of Engineering Technology, Mechanical Engineering, and Civil Engineering Box 43107 Lubbock, Texas 79409-3107		10. Work Unit No. (TRAIS) 11. Contract or Grant No. Project 0-1704
12. Sponsoring Agency Name and Address Texas Department of Transportation Research and Technology P. O. Box 5080 Austin, TX 78763-5080		13. Type of Report and Period Cover Final Report 14. Sponsoring Agency Code

15. Supplementary Notes
Study conducted in cooperation with the Texas Department of Transportation.
Research Project Title: "Evaluation of Roadway Lighting Systems Designed by STV Methods"

16. Abstract
The project's objective is to evaluate the design of roadway lighting systems by the Small Target Visibility (STV) method and determine if it is indeed practical, worthwhile design methodology and should be adopted by the Department. This evaluation will compare STV to current design methods and asses the potential liability associated with making the change. The project consists of seven tasks. The first is to conduct a comprehensive, international literature review to identify roadway lighting issues and their relationship to accident reduction potential. The review will also include a search for risk management and tort liability issues that relate to the subject. Tasks 2, 3, and 4 involve the development of experiments to establish a benchmark of empirical data from which to evaluate STV and compare it with current design methods. Task 5 is the synthesis of the first four tasks into a formal plan of experiments and the conduct of those experiments directed by the Project Director. Task 6 consists of further experimental work as well as detailed analysis of the impact of STV on the Department's lighting design program, and a recommendation of STV standards language and design and construction tolerances. Task 7 is a comprehensive final report.

17. Key Words Small Target Visibility, Roadway Lighting, Luminaire	18. Distribution Statement No restrictions. This document is available to the public through the National Technical Information Service, Springfield, Virginia 22161

19. Security Classif. (of this report) Unclassified	20. Security Classif. (of this page) Unclassified	21. No. of Pages 315	22. Price

Form DOT F 1700.7 (8-72)

EVALUATION OF ROADWAY LIGHTING SYSTEMS DESIGNED BY Small Target Visibility (STV) METHODS

by

Sanjaya Senadheera, Ph.D.
Olkan Culvalci, Ph.D.
Bobby L. Green, P.E.
Douglas D. Gransberg, P.E.
and Karl Burkett

Report Number: TX-97/0-1704-8
Project Number 0-1704

Research Sponsor:
Texas Department of Transportation

Texas Tech University
Departments of Engineering Technology
Mechanical Engineering
and Civil Engineering

Box 41023
Lubbock, Texas 79409-3107

Implementation Statement

At this point in time, experimental work has not been completed to validate the inferences made in this report. If the experimental work does indeed support the conclusions, a recommendation will be made that the Texas Department of Transportation choose not to implement Small Target Visibility (STV) design methodology even if it is adopted as a National standard for roadway lighting design.

Dissemination of this information will best be accomplished through the Traffic Operations Division. A letter clearly stating the policy for roadway lighting design should be published and disseminated to all districts.

Author's Disclaimer

The contents of this report reflect the views of the authors who are responsible for the facts and the accuracy of the data presented herein. The contents do not necessarily reflect the official view or policies of the U.S. Department of Transportation, Federal Highway Administration, or the Texas Department of Transportation. This report does not constitute a standard, specification, or regulation.

Patent Disclaimer

There was no invention or discovery conceived or first actually reduced to practice in the course of or under this contract, including any art, method, process, machine, manufacture, design or composition of matter, or any new useful improvement thereof, or any variety of plant, which is or may be patentable under the patent laws of the United States of America or any foreign country.

Engineering Disclaimer

Not intended for construction, bidding, or permit purposes. The engineer in charge of the research study was Phillip T. Nash, P.E., Texas 66985.

Trade Names and Manufacturers' Names

The United States Government and the State of Texas do not endorse products or manufacturers. Trade or manufacturers' names appear herein solely because they are considered essential to the object of this report.

Prepared in cooperation with the Texas Department of Transportation and the U.S. Department of Transportation, Federal Highway Administration.

SI* (MODERN METRIC) CONVERSION FACTORS

APPROXIMATE CONVERSIONS TO SI UNITS

Symbol	When You Know	Multiply By	To Find	Symbol
LENGTH				
in	inches	25.4	millimeters	mm
ft	feet	0.305	meters	m
yd	yards	0.914	meters	m
mi	miles	1.61	kilometers	km
AREA				
in^2	square inches	645.2	square millimeters	mm^2
ft^2	square feet	0.093	square meters	m^2
yd^2	square yards	0.836	square meters	m^2
ac	acres	0.405	hectares	ha
mi^2	square miles	2.59	square kilometers	km^2
VOLUME				
fl oz	fluid ounces	29.57	milliliters	mL
gal	gallons	3.785	liters	L
ft^3	cubic feet	0.028	cubic meters	m^3
yd^3	cubic yards	0.765	cubic meters	m^3
NOTE: Volumes greater than 1000 l shall be shown in m^3.				
MASS				
oz	ounces	28.35	grams	g
lb	pounds	0.454	kilograms	kg
T	short tons (2000 lb)	0.907	megagrams (or "metric ton")	Mg (or "t")
TEMPERATURE (exact)				
°F	Fahrenheit temperature	5(F-32)/9 or (F-32)/1.8	Celcius temperature	°C
ILLUMINATION				
fc	foot-candles	10.76	lux	lx
fl	foot-Lamberts	3.426	candela/m^2	cd/m^2
FORCE and PRESSURE or STRESS				
lbf	poundforce	4.45	newtons	N
lbf/in^2	poundforce per square inch	6.89	kilopascals	kPa

APPROXIMATE CONVERSIONS FROM SI UNITS

Symbol	When You Know	Multiply By	To Find	Symbol
LENGTH				
mm	millimeters	0.039	inches	in
m	meters	3.28	feet	ft
m	meters	1.09	yards	yd
km	kilometers	0.621	miles	mi
AREA				
mm^2	square millimeters	0.0016	square inches	in^2
m^2	square meters	10.764	square feet	ft^2
m^2	square meters	1.195	square yards.	yd^2
ha	hectares	2.47	acres	ac
km^2	square kilometers	0.386	square miles	mi^2
VOLUME				
mL	milliliters	0.034	fluid ounces	fl oz
L	liters	0.264	gallons	gal
m^3	cubic meters	35.71	cubic feet	ft^3
m^3	cubic meters	1.307	cubic yards	yd^3
MASS				
g	grams	0.035	ounces	oz
kg	kilograms	2.202	pounds	lb
Mg (or "t")	megagrams (or "metric ton")	1.103	short tons (2000 lb)	T
TEMPERATURE (exact)				
°C	Celcius temperature	1.8C + 32	Fahrenheit temperature	°F
ILLUMINATION				
lx	lux	0.0929	foot-candles	fc
cd/m^2	candela/m^2	0.2919	foot-Lamberts	fl
FORCE and PRESSURE or STRESS				
N	newtons	0.225	poundforce	lbf
kPa	kilopascals	0.145	poundforce per square inch	lbf/in^2

* SI is the symbol for the International System of Units. Appropriate

(Revised September 1993)

Table of Contents

CHAPTER 1: EXECUTIVE SUMMARY

In 1990, the Illuminating Engineer Society of North America (IESNA) promulgated a proposed new design standard for roadway lighting based on visibility. They called it Small Target Visibility (STV), and it was purported to be a superior to the existing illuminance- and luminance-based methods currently in use. The Texas Department of Transportation (TxDOT) was using an empirical method based on luminance and the collective experience of Department personnel around the state. Because roadway lighting is strongly associated with nighttime driving safety, it was felt that a serious look at this new methodology needed to be conducted to determine if the increased design effort attendant to implementing STV was offset by a measurable potential benefit accrued by nighttime accident reduction. In a nutshell, the researchers were asked to determine whether or not TxDOT should support the implementation of this new method at a substantially increased design cost.

To fully understand the theoretical thrust of the research, a brief explanation of the development of lighting design as it evolved to STV is in order. The first attempt at roadway lighting design focused on the output of the lighting fixtures, hereafter referred to as luminaires, and used illuminance as the salient design parameter. Later, it was recognized that drivers actually respond to the light that was reflected off objects in the road and off the pavement surface, i.e. luminance. Therefore, luminance became the standard for lighting design. Finally, lighting engineers took the problem to its next level of logical complexity by drawing the connection between luminance and the driver's eye and began searching for a method to design roadway lighting based on some component of visibility. STV is effectively the first attempt to relate the physics of roadway lighting performance to the biology of the human eye. From a physics perspective, visibility is a function of contrast. Contrast is merely the relationship between the amount of light reflected off a target and the amount of light reflected off its background (i.e. the pavement). In a static mode, this is easily calculable, but as roads support extremely dynamic conditions, the static calculation of contrast does little to relate the design to its corresponding operating condition. This is further complicated when the attempt to integrate human vision into the calculation is added. Visibility is infinitely random and infinitely variable. Thus, the best an engineer can do is hope to make a reasonable approximation to account for the immense range of human vision that will enter the lighted area in question. The validity of the design calculations are further questioned when the fact that many of the physical parameters used in the method are variable over time as well. The pavement's reflective characteristics will change with age. The luminaires will accumulate dirt and burn out thus changing their output characteristics. The amount of off-road lighting that contributes to visibility on the road changes as development along the lighted area changes. Finally, normal weather variations such as rain and ice totally invalidate the design calculations by changing the pavement's reflective characteristics from diffuse to specular. Thus, lighting engineers have set themselves a difficult goal to be able to accurately and mathematically model a lighted stretch of highway. To do so involves developing a complex computer simulation for each and every lighting installation, and this increases the level of design effort by at least an order of magnitude over current luminance or illuminance design. A large public agency, like TxDOT, must realize a distinct benefit of accident reduction due to better quality design to justify implementing such a labor intensive new methodology. Thus, this is the crux of this research project.

Procedure

The project was broken into a number of distinct areas of study.

- Over 120 articles and books on the subjects of visibility, lighting, roadway lighting design, human factors, and other related topics in three different languages were reviewed to establish the state-of-the-art and look for successful examples of lighting design changes resulting in nighttime accident reduction.
- A tort and liability review of current state and federal case law was completed to define Texas' potential liability if it decided to not implement a new national design standard for roadway lighting.
- A series of experiments were conducted at a test site on Interstate Highway 27 north of Abernathy, Texas to quantify the various parameters involved in visibility calculation and measurement. Computer programs were developed to compare measured visibilties with corresponding calculated visibilities.
- A calculation of propagated error due to design assumptions was completed to understand the effect of those assumptions on final calculated design parameters. This was merged with the field data to give the researchers a means to relate the efficacy of the design to model actual roadway conditions.
- A detailed study of pavement reflectance building on recent work in Canada was completed to relate the primary design parameter of background luminance to visibility. This was combined with photometric measurements made on several different pavements at the General Tire test site near Uvalde, Texas.
- Information Theory (IT) was applied to the roadway lighting design problem for the first time as a method to quantify safety improvements due to enhanced lighting design techniques.
- Coordination was made with the IESNA and the International Commission on Illumination (CIE), and an in-progress review of the experiments and the theory was conducted by Dr. Werner Adrian of Waterloo University in Ontario, Canada. This furnished an expert, peer review to ensure that the aspects being developed by this project were consistent with current practice. Dr. Adrian is regarded as the father of visibility research having completed most of the seminal work in an area in Germany in the 1970's.
- Assistance with the higher order mathematics was obtained from another international source, the University of Stuttgart, in Germany. Researchers at Stuttgart have developed a new level of mathematical analysis called Similarity Theory (ST). ST is related to IT and provided the Texas researchers with the theoretical tools needed to quantify several important light-related parameters.

Findings

The extensive literature review revealed just how dynamic the roadway lighting environment really is and just how many "simplifying" assumptions have been made to facilitate the calculation of lighting design parameters. The net effect of those assumptions is to reduce a complex dynamic environment to a sterile, static model that does not accurately reflect reality. The apparent result is a false sense of confidence regarding the "quality" of the resultant design. This project identified at least twenty assumptions that potentially introduce unrecognized error

into the final design solution. A good example of this type of assumption-based error is the assumption that the surface of the road is flat. This assumption is completely erroneous because all pavements are sloped to drain. The calculation of pavement luminance is a vector-based theory. Therefore, the introduction of an unaccounted angle impacts the actual observed luminance. A typical crown on "flat" stretches of straight road is 2%. The angle of the road's surface can increase to as much a 8% on superelevated curves on interstate exit ramps that are typically lighted. This assumption introduces an error of between 1% and 11% depending on the position on the road and luminaire mounting height. An average error of 4% can be used to correct this problem. Other errors lamp aging, luminaire dirt depreciation, spacing errors, and mounting errors (height and angle) accumulate to a total possible propogated error of over 200%. This is error induced in the static system only.

The second major finding of the literature review deals with the relationship between lighting and nighttime accident reduction. It is intuitive to believe that the engineer can improve the "safety" of a given highway location by carefully designed lighting installations. There has been much research done to try and prove this hypothesis. However, regardless of its ultimate interpretation, no study could conclusively prove a direct connection. In fact, an Australian study (Fisher, 1977) showed conclusively that there was an upper limit to the reduction of nighttime accidents by making upgrades to roadway lighting systems. Other studies of the same nature were unable to make the sought after connection and tended to blame the fact that enhanced lighting did not correlate to reduced nighttime accidents on bad data in police accident reports. This led the researchers to seek an alternative method to model the roadway lighting environment and explain the connection between the "quality" of the light and nighttime accidents. This led to the use of IT and ST as a theoretical basis for analysis.

Through IT, one can hypothesize that each roadway "scene" contains a finite quantity of information that is available to a driver for use in driving decision-making. The amount of information available is a direct function of visibility. Thus, an engineer should design the fixed pieces of the scene (i.e., the pavement, the lighting, and other elements) in a manner that maximizes the quantity of information. The bottomline is that to improve the quality of the lighting to the point where it will reduce accidents is to make a significant change in the quantity of available information. For example, the literature showed about a 40% reduction in nighttime accidents at uncontrolled intersections when lighting was installed. In IT terms, the scene changed from that of darkness, i.e. very little information content, to one where the amount of information available was greatly increased. Thus, the area in question became "safer." However, the Fisher study showed that as the engineers "tinkered" with the amount and quality of the light on existing lighting installations, nighttime accident rates fluctuated up and down. In some areas, they went up as the amount of light was increased. Both IT and the concept of contrast explain this phenomenon. Looking first at contrast, if the amount of light reflected off an object is equal to the amount reflected off its background, it becomes invisible. Therefore, the addition of too much light can have an inverse effect of safety. From the IT standpoint, changing the quality of the light did not appreciably increase the amount of information in the scene. Therefore, accident rates would not be expected to improve.

A field experiment at the test site was devised test this logic. A standard STV target was placed in the road, and the lights were turned out. A digital image was taken and the quantity of

information contained in the image (i.e. the roadway scene) was calculated using ST. This method creates a three dimensional curve based on calculating spatial frequencies in three directions. The volume under the curve represents the volume of information contained in the image. Taking a second image of the same scene after one half of the installed lighting was turned on yields a second curve, and this can be subtracted from the first curve to quantify the change in information by altering the scene. It was found that the mere addition of light increased the quantity of information by 80%. A third image was taken after the remaining lights were turned on, and it was found that the quantity of information only increased by 2%. Finally, the headlights of an automobile were added to the scene to further increase the illumination on the target, and no increase in information content was found. This verifies the previously unexplained results of the Fisher study, and establishes IT as a viable theoretical foundation for visibility measurement.

During a visit by Dr. Adrian to the Abernathy test site, it was noticed that the reflectance qualities of a small section of pavement varied laterally across the width of the pavement. This is due to the effect that traffic has on the pavement's surface in the wheel paths. STV classifies pavement reflectance into only four categories and about 80% of pavements fall into a single category. Since background luminance is driven by pavement reflectance, this finding is significant. The researchers expanded on data taken by Adrian on over 100 pavement samples taken in Canada using Adrian's photogoneometer. Data was also taken in Texas. The final analysis showed that the impact of traffic in the wheel paths is significant in asphaltic pavements and that both brightness and specularity increase over time. This invalidates an STV assumption that the pavement surface is both uniform in texture and diffuse in reflectivity. In fact, much further study is warranted to fully understand the actual impact of this effect. Again, the bottomline is simple. The pavement's reflectance is dynamic and must be considered as such in any design method that hopes to improve roadway lighting performance.

The tort and liability review was one of the bright points in the study. This portion of the project was commissioned to guide the Department's management group in an eventual STV implementation decision. The study found that the principle of Sovereign Immunity essentially protects the state from litigation if the IESNA promulgated STV as a new national design standard and Texas chose not to implement it. The fundamental concern was that TxDOT might be forced to implement STV to reduce its exposure to litigation based on the premise that the Department was not using the latest lighting design standard.

Recommendations

The comprehensive nature of this study gives the researchers great confidence in making the following recommendations.

- While the move to a visibility-based lighting design method is extremely desirable, Small Target Visibility is requires too many simplifying assumptions that introduce unrecognized error into the result. This makes it an approximation at best, and totally inaccurate at worst. If and when it becomes a national standard, the State of Texas should not implement it until the number of assumptions are reduced to a level where the calculations accurately model reality.

- Correction factors can be calculated for many of the visibility level (VL) input factors to account for dynamic changes over the installation's life cycle. This would permit a probabilistic design method to be developed based on changes over time of each of the identified design elements. Development of such a method is beyond the scope of this study but should be considered for future work in the area.
- The contribution of pavement reflectance to visibility-based design is not adequately recognized. This is surprising because background luminance is one of two fundamental design parameters. Before a reliable visibility-based design methodology can be developed, the change in pavement reflectance with respect to traffic, and its impact on contrast must be known. Additionally, the impact of driver observation angle change must also be fully understood before pavement reflectance can be accurately estimated.
- Information Theory and the calculation tools provided by Similarity Theory furnish a powerful and attractive tool for roadway lighting design. This method is particularly applicable to the area of safety lighting design where the placement of a relatively few luminaires can be critical to nighttime driving safety.
- The combination of digital imaging and IT-based processing algorithms can be successfully used to quantify a predictable function of visibility.

Finally, roadway lighting design should be based on a function of design speed just like every other feature on the roadway is designed. The researchers propose the following Nighttime Safe Stopping Sight Distance (NSSSD) model for future development of roadway lighting design. If we go back to the basics, it can be seen that the problem is one of identifying some method which will provide a driver with sufficient time to identify a critical target (i.e. one which will cause the driver to take some kind of evasive action) and maneuver the vehicle to a safe and appropriate point where an accident is avoided. Thus, if the worst possible case is assumed to be a situation which requires the driver to come to a complete stop before hitting the critical target, the physical functions can be broken down into the following four Driving Tasks.

Task 1. The driver must sample the driving environment for data that generates adjustments in driving behavior such as changes in speed and direction. This can be called sampling rate and has a probabilistic function associated with it. If a piece of data is sampled which would require a change to zero, the next three items will occur. This can be called sampling time.

Task 2. The driver must see and acquire an image (for purposes of this discussion, the image will be called the target) that generates the idea that the vehicle should be stopped. This can be called target acquisition time.

Task 3. The driver must process that target thought and react by stepping on the brake. This will be called reaction time and is generally taken to be 2.5 seconds (AASHTO, 1990).

Task 4. The vehicle must rapidly decelerate from its initial speed to zero. This will be called stopping time.

Thus, the critical dimension in the whole problem is time. Obviously, to convert from time to the required dimensions needed to design roadway lighting, we must move from a dynamic to static measurement. To get there, we must first know the initial velocity at which the driver is traveling when this chain reaction occurs. RP-8 states that 56 kilometers per hour (35 mph) is the top speed at which standard headlights provide sufficient lighting to conform to safe stopping

distance requirements. This seems to be somewhat at odds with nighttime speed limits on the average of 104 kilometers per hour (65 mph). Nevertheless, looking at the four tasks required for a driver to execute a safe stop, we can say that Task 4 is a function of initial velocity, the mass of the vehicle, and the coefficient of friction between the tires and the pavement. Calculating the braking distance is merely a physics problem that can easily be solved. Solving for the distance traveled during the reaction time in Task 3 is even simpler in that it is merely the velocity divided by 2.5 seconds. The problem becomes more complex when we try to solve for the distance traveled during target acquisition time. This is a function of velocity and visibility. Intuitively, the target's visibility is inversely proportional to the length of target acquisition time. The literature seems to indicate that the primary factor of nighttime visibility is contrast.

However, we would argue that target size is also extremely important. The implied assumption with STV is that if a lighting system can be designed around a small target, then anything larger will be more visible. The work done by Zwahlen and Schnell (1994) and Kahl and Fambro (1994) would indicate that the STV target may be too small to be of effective use to designers. Work by Freedman et al. (1993) indicates that the probability of detecting a target strongly depends on its type. Finally, the most important factor in safe night driving is Task 1. The amount of environmental information available to a driver is greatly reduced in the hours of darkness. Thus, to assume that a target of any size can be acquired and reacted to begs the initial assumption that the driver is going to look at the point where the target rests at point in time where the subsequent three tasks can be safely executed.

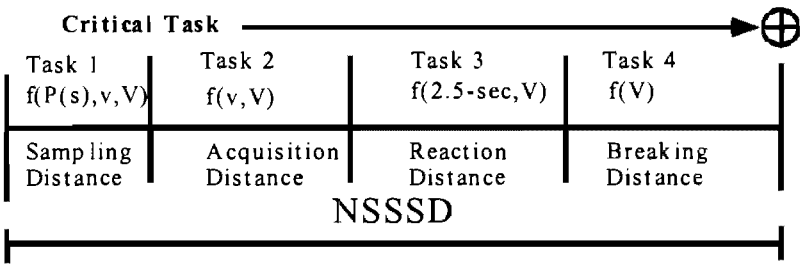

Where P(s) = Probability of sampling target
v = visibility
V = velocity

Figure 1.1. Nighttime Safe Stopping Sight Distance (NSSSD)

CHAPTER 2: LITERATURE REVIEW

To make the literature review coherent and to standardize the terms used by the various contributors to this report, the first document to be reviewed is *Mechanical and Electrical Equipment for Buildings, Seventh Edition* by Stein, Reynolds, and McGuinness. Chapter 18 of this handbook provides a very clear encapsulation of all the salient principles that must be understood by both the researchers and the readers of this and subsequent research reports. Thus it is felt that the next section will create a common foundation of knowledge on which to interpret the remaining information.

Light as Radiant Energy

The Illumination Engineering Society (IES) defines light as a form of energy that permits us to see. Light is considered to have a dual nature, the nature of a particle (photon) and the nature of a wave. The wavelengths of visible light are from 380 x 10^{-9} meters to 780 x 10^{-9} meters. A wavelength of 10^{-9} meters is usually referred to as a nanometer. So, the wavelengths are from 380 to 780 nanometer. Violet light is the shorter wavelength, higher energy 380 nanometer light, and the 780 nanometer wavelengths are the lower energy red lights. Green light falls between 500 and 600 nanometers. The previous measure of light wavelength was in Angstroms (10^{-10} meters), so violet light would be 3800 angstroms.

Light Incidence, Transmittance, Reflectance and Absorption

The luminous transmittance of a substance is a measure of its capability to transmit light through a material. The nomenclatures for luminance transmittance are listed below.

- Transmittance
- Transmission factor
- Coefficient of transmission
- Transmission coefficient.

These are used interchangeably. The transmittance is the ratio of the total transmitted light to the total incident light. Transmittance must be used cautiously because materials may be wavelength selective in transmitting light, so a spectral analysis of incident and transmitted light is sometimes called for if a material is selective in a wavelength of interest. For this study, the wavelengths of interest are restricted to visible light so we will easily recognize a wavelength selective filter. In general the transmission coefficient should refer to materials displaying non-selective absorption characteristics.

The ratio of reflected light to incident light is called one of the three names listed below.

- Reflectance
- Reflectance factor
- Reflectance coefficient

Reflectance is a measure of the light that bounces off a surface and is not transmitted. If half of

the incident light is bounced off the surface, the surface reflectance coefficient is 0.5 or 50%. If reflection of a beam of light takes place on a smooth surface, the reflection is known as specular and reflects away from the surface as a single beam of light. If the surface is very rough the reflections for a beam of light are scattered by the multifaceted surface. The light reflects in all directions away from the surface, and the surface is called diffuse.

The speed of light in a material, v_m, and the speed of light in free space, c_o, are related to the index of refraction, n, by the following.

$v_m = c_o/n$.

The index of refraction, n, is always greater than 1; therefore, v_m is always less than, c_o.

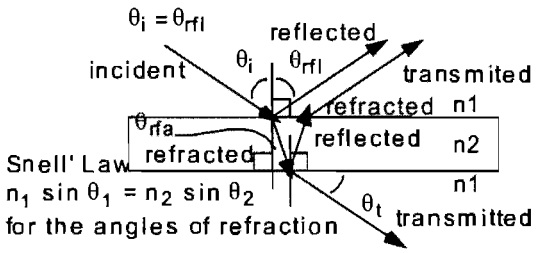

Figure 2.1. Specular Ray Tracing Model

Incidence radiation, I_o, @ Incidence angle, θ_i,
Reflected radiation, I_{rfl}, @ Reflected angle, θ_{rfl},
Transmitted radiation, I_t, @ Refracted angle, θ_{rfa},

The angle of incidence is equal to the angle of reflection, $\theta_i = \theta_{rfl}$.

Refraction takes place at a boundary where indices of refraction change. The incident angle and the refracted angle are related by Snell's Law, and reflect differences in speeds of light in the respective mediums.

Snell's Law: $n_1 \sin \theta_1 = n_2 \sin \theta_2$.
Transmission angle, θ_t,

Each time refraction takes place at a boundary, a portion of the incident light passes from medium, n_1, to medium, n_2, and the portion is transmitted. If the material is glossy some of the energy is converted from visible radiation to infrared radiation (heat) and lost (from the visible spectrum). The losses are absorption losses.

Absorption losses are exponential with distance such that

$I(x) = I_o e^{-kx}$,
Where I_o is the incident radiation entering the material,
x is the distance traveled through the material
k is the loss coefficient for the material
e is 2.718281...

Absorption losses are losses due to energy transformation from higher energy, visible light to lower energy, infrared non-visible light. Changing the radiation from the visible spectrum to the non-visible spectrum is thought of as a loss to the visible spectrum and a loss to an observer.

Diffuse reflections are due to first surface roughness and reflections at the boundary surface.

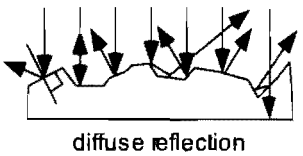

Figure 2.2. First Surface Diffuse Reflections

Diffuse transmissions are due to second surface roughness and refraction at the second surface boundary.

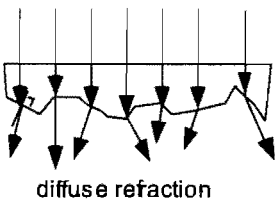

Figure 2.3. Second Surface Diffuse Refraction/Transmissions

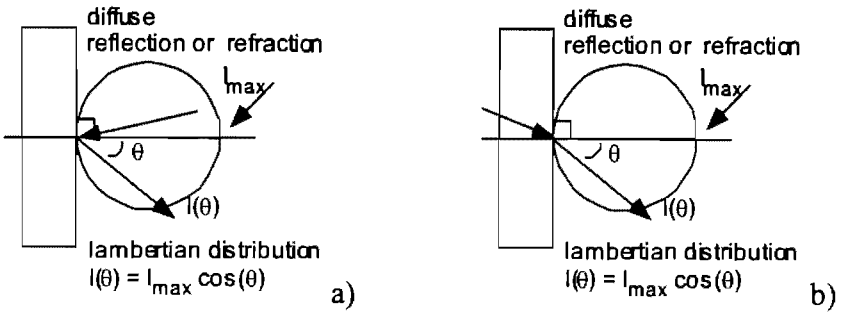

Figure 2.4. Lambertian Reflection or Refraction/Transmission Distribution

Lambertian distribution, $I(\theta) = I_{max} \cos(\theta)$, is a diffuse reflection distribution or refraction distribution due to the surface characteristics of a material. The roughness of the surface determines the reflection and refraction directions.

Surfaces are not flat, so the reflections, refractions, and transmissions have a partial specular characteristic and a partial diffuse characteristic as shown in Figure 2.5.

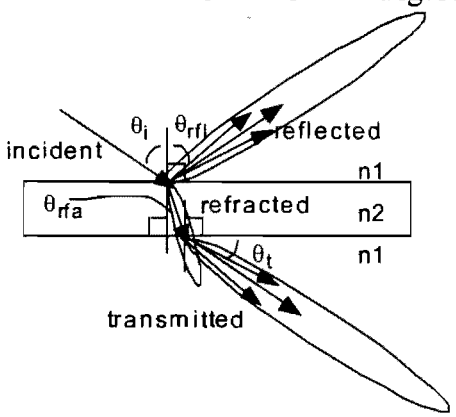

Figure 2.5. Reflection and Transmission Distributions

Most surfaces are somewhat smooth and somewhat rough so we get a diffuse reflection and a specular reflection. The reflectance is a measure of the total light reflected from the surface of any material. The reflectance does not depend on whether the surface is diffuse or specular; all the reflected light is measured. The ratio of incident light lost in a material is called the absorption coefficient. The absorbed light is not lost, it is simply changed from visible wavelengths to lower energy, non-visible wavelengths usually in the infrared. The sum of the transmitted, reflected, and absorbed light is equal to the incident light. The transmitted light may also be diffused after it passes through some material, but the total amount of light passing through the material is used in the transmission measurement to determine the transmission coefficient. Just as the total reflected light is used in the reflectance measurement to obtain the reflection coefficient.

Definitions

There are two basic systems of units used in lighting, American Standard (AS) and International System (SI) metric units. The IES uses SI units in their handbook and publications with AS units in brackets [AS].

Luminous Intensity: The AS unit for Luminous intensity is the candlepower (cp), and the SI unit is the candela (cd) and normally represented by the letter "I". A wax candle has a luminous intensity horizontally of approximately one candela (cp). A candela and a candlepower have the same magnitude. Luminous intensity is characteristic of the source only and independent of the visual sense of the eye.

Luminous Flux: The unit of luminous flux in both SI and AS units is the lumen [lm]. An isotropic radiator of one candela emanating from a sphere of one meter radius then one square meter of surface on the sphere has one lumen of flux passing across the boundary.

The human eye response to visible radiation is roughly a gaussian or normal bell curve with the center of the maximum visible sensitivity near 555 nanometer and 0.7 of the maximum visible range at approximately 505 nanometer and 595 nanometer. The relative sensitivity response of the eye is multiplied by the spectral output of a light source to determine the visibility of the light source with respect to a human eye. The output of the light source is measured in watts, the total power output of the light. The lumen is a measure of photometric power as perceived by the human eye, is frequency dependent, and a function of human physiology. A 500 watts (w) incandescent lamp amounts to approximately 45 watts measured radiometrically and about 10,000 lumens, so we have about 20 lm/w.

Illuminance: One lumen of luminous flux on one square foot produces one foot-candle (fc) of illuminance in AS units or one lumen of flux on one square meter produces one lux (lx) in SI units. Illuminance is normally represented with the letter "E." It is readily seen that one square foot is about an order of magnitude smaller than a square meter, so a lux is roughly an order of magnitude smaller than a foot-candle (10.764 lx =1 fc).

Illuminance Measurements: Due to the frequency response of the human eye, it takes roughly 10 times as much brightness of 400 nanometer blue light in the photopic region, to give a brightness of 1.00 at the 555 nanometer, yellow-green, wavelength. If an illuminance meter is to be useful, its response must be color corrected to the response of a human eye. Cadmium sulfide photo-cells roughly approximate the visible spectrum of a human eye and can be color corrected to match the spectral response of a human eye. The meter must also be correct for light incident at oblique angles to the glass surface shielding the photo cell; the oblique angle correction is known as cosine correction. A good illuminance meter will plainly indicate its color and cosine correction.

Luminance and Brightness: Light entering the eye gives us the sensation of brightness; however, brightness is a subjective measure because it depends on the object luminance (L) and on the state of adaptation of the eye. Brightness is referred to a subjective brightness, apparent brightness or brightness. The measurable, reproducible state of objective luminosity is its

luminance of photometric brightness. Luminance is the luminous intensity per unit projected area of a primary (emitting) or secondary (reflecting) light source. The SI unit is candela/square meter or a nit (cd/m^2 =nit); the AS unit is the foot-lambent (3.14 fL = 1 cd/f^2).

Luminance Measurement: Illuminance measurements (lux) are the most common measure of lighting levels; however, luminance (cd/m^2), a measure of brightness, is a measure of what we see. Luminance is a directional measure of light passing through a surface. A luminance meter is basically an illuminance meter with a hooded cell to block oblique light and calibrated in units of luminance.

The Eye as an Instrument/Photometric Sensor

Light entering the eye through the pupil is focused on the retina on the back surface of the eye. The retina contains light-sensitive cells called "cones," due to the shape of the cells, and light sensitive cells called "rods," also due to the cell shape. The cones are near the *fovea* in the center of the back of the eye with the rods being further out from the center. The cones respond rapidly to changes in lighting levels during day lighting and are responsible for color and detail vision. Rods are extremely light sensitive and responded to light levels 1/10,000 as bright a cone cell; however, rods lack color sensitivity and detail discrimination. Therefore, night vision (rod vision) is very coarse and all colors appear as shades of gray.

In central (*foveal*) vision, we have great detail and color sensitivity, central vision subtends about a 2 degree angle in the center of our visual field, from 2 to 30 degrees we have near field vision, from 30 to 60 degrees we have far field vision, and beyond 60 degrees we have peripheral vision. Near field vision has color and some detail, far field, and peripheral vision detects motion and has a high concentration of rod cells for low light conditions.

Visual Acuity

There are three components to visual acuity in any seeing task: the task, the lighting conditions, and the observer, and there are variables associated with each of the acuity component. Each of the visual acuity components have primary variables and secondary variables (Stein, et al, 1986)

1. Task: Primary Factors
    a. Size
    b. Luminance
    c. Contrast
    d. Exposure time

2. Task: Secondary Factors
    a. Type of object
    b. Degree of accuracy required
    c. Moving or stationary target
    d. Peripheral patterns

3. Lighting Conditions: Primary Factors
    a. Illumination level
    b. Disability glare
    c. Discomfort glare

4. Lighting Conditions: Secondary Factors
    a. Luminance ratios
    b. Brightness patterns
    c. Chromaticity

5. Observer: Primary Factors
    a. Condition of eyes
    b. Adaptation level
    c. Fatigue level

6. Observer: Secondary Factors
    a. Subjective impressions
    b. Psychological reactions

Contrast

Contrast (C) is a dimensionless ratio of luminance defined previous in equation 3. High contrast is critical in recognizing outline, silhouette, and size (Stein, et. al, 1986). It can be further described as follows.

$$C = (L_T - L_B)/L_B \quad (3)$$

Where: L_T = luminance of the task
L_B = luminance of the background, or as

$$C = (L_F - L_B)/L_B \quad (4)$$

Where: L_F = luminance of the foreground
L_B = luminance of the background.

Contrast is may be positive or negative and varies from $-1<C<0$ and $0<C<1$ and is generally independent of illumination, neglecting specularity (Stein, et. al, 1986). Note that in the second part, we demonstrated these equations (equations 3 and 5) as an absolute value of the ratio and defined contrast as a relative value.

Reflectance is also a measure of candela per square meter, so contrast may also be represented in terms of reflectance as shown in equation 5 as:

$$C = (R_T - R_B)/R_B \quad (5)$$

or

$$C = (R_F - R_B)/R_B \quad (6)$$

Where: R_T = Reflectance of the task
R_B = Reflectance of the background
R_F = Reflectance of the foreground.

Now that we have created a common framework for the technical thrust of this study, we can move on to the specifics of the study itself and how the literature lends itself to the objectives cited in the project abstract.

Luminance Evaluations

The calculation of the illuminance at a point, whether on a horizontal, a vertical or an inclined plane consists of two parts: the direct component and the reflected component (Lighting Design Practice Committee, 1974). The total of these two components is the illuminance at the point in question. Of the methods of determining the direct illumination component at a point, two methods: Inverse Square and Illumination Charts and Tables can be utilized for evaluating inclination effect. Variations in the formula involving the inverse-square law are used to determine the illuminance at definite points where the distance from the source is at least five times the maximum dimension of the source. In such situations the illuminance is proportional to the square of the distance from the source.
Illuminance on horizontal plane (E_h) is expressed as the following equation.

$$E_h = \frac{I\cos\gamma}{D^2} = \frac{I\cos^3\gamma}{H^2} \quad (7)$$

Where: I = Candlepower of the source in the direction of the point
D = Actual distance from the light source to the point
H = Vertical mounting height of the light source above the plane of measurement
γ = Angle between the light ray and a perpendicular to the plane at that point.

For horizontal plane: $\cos\gamma = {}^{H}/_{D}$

The surface luminance (L) is defined as the luminous flux per steradian emitted (reflected by a unit area of surface) in the direction of an observer. When the unit of flux per steradian is candela and the area is measured in square meters, the unit of luminance is candela per square meter . The surface luminance in general terms can be calculated if the reflectance coefficient $q(\beta,\gamma)$ and the illuminance value are known:

$$L = \frac{1}{\pi} E_h q(\beta,\gamma) \tag{8}$$

Where: $q(\beta,\gamma)$ = directional reflectance coefficient for angles of incidence of β and γ.

Although a simple concept of the quantity of light reflected by a surface is assessed from the reflectance coefficient, $q(\beta,\gamma)$, the distribution pattern will depend upon the surface characteristics and the angular relationship between the light source, the observation point, and the observation position. In principle, two types of reflectance are identified: diffuse and specular (or mirror). Snow is an example of diffuse surface, whereas a smooth, wet road is a good example of a specular surface. Most road surfaces are a mixture of both diffuse and specular reflectance.

The horizontal illuminance can be expressed as the following equation.

$$E_h = \frac{I(\phi,\gamma)\cos\gamma}{H^2} \tag{9}$$

Combining (6-3) and (6-4) the luminance can be written as the following equation.

$$L = \frac{q(\beta,\gamma)I(\phi,\gamma)\cos^3\gamma}{\pi H^2} \tag{10}$$

In practice, $q(\beta,\gamma)\cos^3\gamma$ can be expressed as a reduced luminance coefficient r and is given in a table for each road classification (see tables B1...B4 of National Standard Practice, 1990).

Target Luminance is a function of the vertical illuminance from each luminaire in the layout detected toward the target times the directional reflectance of the target toward the oncoming driver. The reflectance is 0.18 (IES, 1983). This yields the following equation.

$$L_t = 0.18\frac{L\sin\gamma\sin\phi\cos^2\gamma}{DZ^2} \tag{11}$$

Luminaire light distribution developed over the past fifteen years reflects the desire of the luminaire manufacturers to produce an optimal level of horizontal lux with acceptable uniformity in accordance with past versions of the Standard Practice.

Such luminaire light distributions yield reasonably good patterns of pavement luminance if used carefully (American National Standard Practice (1990). Accuracy of calculations of pavement luminance depends on two factors.

- If the photometric data used to determine the candlepower intensity at a particular angle correctly represents the output of the lamp and luminaire
- If the directional reflectance table represents accurately the reflectance of the actual surface

Since, in most cases, differences result in measured values less than the calculated values of the new, clean lamp and luminaire, the overall factor used to link calculated to measured levels is called the "Light Loss Factor" or LLF. The lighting design must incorporate a LLF in all calculations. Light Loss Factors that change with time after installation may be combined into a single multiplying factor for inclusion in calculations. It must be realized that a LLF is composed of still separate factors, each of which is controlled and evaluated separately. Many of these are controlled by the selection of equipment (Equipment Factor) and many others are controlled by planned maintenance operations (Maintenance Factor). A few factors, such as voltage regulation and weather, are beyond the control of the lighting system owner/operator and depend upon the actions of others.

REVIEW OF LITERATURE ON ACCIDENT CORRELATION TO ROADWAY LIGHTING IMPROVEMENT

The hypothesis that lighting a section of road must intuitively make it safer seems so logical that it almost begs to be accepted without evaluation. The question that really must be answered in this study is not whether roadway lighting enhances safety, but rather does the use of STV design methodology yield a safer nighttime driving environanometerent than the accepted illuminance/luminance (ILL/L) methods of design.

To understand the correlation between lighting and accidents, one must first identify those parameters that impact a driver's ability to avoid accidents. This is normally expressed through the components of stopping. In order to bring a vehicle to a safe stop from some speed, four things must occur in order.

1. The driver must sample the driving environment for data that generates adjustment in driving behavior such as changes in speed and direction. This can be called sampling rate and has a probabilistic function associated with it. If a piece of data is sampled which would require a change to zero, the next three items will occur. This can be called sampling time.
2. The driver must see and acquire an image (for purposes of this discussion, the image will be called the target) which generates the thought that the vehicle should be stopped. This can be called target acquisition time.
3. The driver must process that target thought and react by stepping on the brake. This will be called reaction time.
4. The vehicle must rapidly decelerate from its initial speed to zero. This will be called stopping time.

Stopping time is merely a function of physics and can be computed with great accuracy if the initial speed is known or can be estimated. Reaction time varies among individuals, but highway safety literature generally accepts this to be constant at 2.50 seconds. Acquisition time is a more complex parameter and is a function of both visibility (i.e. the driver being able to see the target) and other more random factors such as the driver's immediate attention when the target becomes visible or the ability of the driver to recognize the target as a hazardous image requiring an immediate reaction. If one were to assume that as the visibility of the target increases that the probability that an average driver will properly react to it also increases, then the aim of roadway lighting design for safety should be to create an environanometerent of enhanced visibility.

Safety Lighting

The Texas Department of Transportation Highway Illumination Manual (TxDOT, 1995) speaks to warrants for both continuous and safety lighting. In both cases, a ratio of night to day accident rates is used to identify cases where lighting of some form is justified. For continuous lighting (Case CL-4), a night to day accident ratio greater than 2.0 justifies the installation of this type of lighting. For safety lighting, the ratio is predictably less. A ratio greater than 1.25 justifies the installation of partial interchange/intersection safety lighting (Case SL-3), and a ratio greater than 1.5 justifies the installation of complete interchange/intersection safety lighting (Case SL-7). Thus Texas has created a warrant to light particular portions of the roadway when accident rates exceed a particular level. This contains the implicit assumption that adding light to a roadway will enhance nighttime traffic safety. This tracks well with the literature. Other authors have used a ratio of accident occurrence at night versus the accident rate during the day as an objective yardstick to both identify lighting requirements and to measure the efficacy of lighting upgrades after installation.

The Norwegian Institute of Transportation Economics conducted a study to validate the hypothesis that adding light enhanced traffic safety (Elvik, 1992). The study looked at the correlation between accidents and roadway lighting in 37 different studies in 11 different countries. The study identified three types of traffic environment as urban, rural, and freeways and grouped safety data according to these classifications. The author used Meta-Analysis to develop what he called a "criterion of safety" (CS effect) which is a ratio expressed as follows:

$$\text{CS effect} = \frac{\text{No. of night accidents after lighting/No. of night accidents before lighting}}{\text{No. of day accidents after lighting/ No. of day accidents before lighting}} \quad (12)$$

If the ratio is less than 1.00, then it could be concluded that lighting reduces the number of nighttime accidents. If it is greater than 1.00, then lighting increases the number of nighttime accidents. If lighting has no effect, then the ratio would be 1.00. This is an interesting approach in that it provides a means to prove or disprove the fundamental hypothesis. When one considers the effects of contrast on visibility, the argument that adding light to an area could conceivably make the contrast very small and essentially render objects invisible which would, in turn, cause the potential for accidents to increase. Elvik's system can be used to test this argument as well. This study found that roadway lighting reduced nighttime fatal accidents by 65% and nighttime injury accidents by 30%. It also calculated a reduction of "property-damage-only" accidents of

only 15%. It also found that these improvements vary by country and types of traffic environment. Elvik recognized that the studies he reviewed did not consider every conceivable source of error. He also found that there "are no doubt a large number of other variables with respect to which the effects of public lighting might be expected to vary." However, he was able to satisfy the statistical requirements for Meta-Analysis for regression to the mean, secular accident trends, and contextual confounding variables. He found that the two most significant variables were accident severity and accident type. Unfortunately, he was unable to confirm that lighting satisfying current warrants was either more or less effective than lighting which did not satisfy warrants. It should be noted that he found, in some cases, nighttime accident rates went up after public lighting was installed.

A study of the relationship between illumination and freeway accidents (Box, 1971) concluded that the addition of lighting reduced accidents by 40%. This study used a simpler ratio than equation 12 to determine the effect of adding lighting.

Safety ratio unlighted = No. of night accidents/No. of day accidents (13)

Safety ratio lighted = No. of night accidents/No. of day accidents (14)

Thus the unlighted ratio is compared to the lighted ratio, and if the unlighted ratio is found to be greater than the lighted ratio, it is concluded that lighting reduces accidents. If the reverse is true, then it is concluded that lighting increases accidents. Box concluded that freeway fixed lighting reduces accidents. It is interesting to note that his results for Interstate 20 in Dallas show a mean ratio of only 1.01 and confidence limits of 0.72 to 1.30. In fact, the best range in confidence limits was for Atlanta where the mean ratio was less than 1.00 that would indicate that lighting increases the number of accidents. The paper also speaks to the levels of illumination and concludes that it is not possible to determine an optimum level of illumination. He also concludes that those areas with the lowest illumination range had the best night/day accident ratios. This would lend credence to the argument that contrast may be the salient parameter in the visibility equation.

Roadways with typical in-surface illumination levels of 0.3 to 0.6 horizontal foot-candles (HFC) had the best accident rate ratios (Box, 1971). A great variation in luminaire output was found in the field. Data was analyzed for over 800 mercury lamps, and wide variations were found in lamp output. The erratic performance of systems invalidates any analysis of fine differences between various designs. The extent of variations may be enough to "wash-out" meaningful analysis of small variations in lighting design. As a group, lighted roadways had an average night/day rate ratio of 1.43 accidents of all kinds, and unlighted roadways had a ratio of 2.37. From Box's data, a lighting level of 0.3 to 0.6 HFC produced the best ratio of night/day accident rates. It is also interesting to note that he found that twenty-five percent of the urban traffic occurs at night and the primary accident problems involve collisions due to lack of adequate acceleration lanes. Therefore, on the issue of arbitrary target size, this study would seem to indicate a target that in some way models the rear end of a typical vehicle. That would support a similar finding that the target height should exceed 150 millimeters by Kahl and Fambro of Texas A&M University (Kahl and Fambro, 1994).

An Australian study (Fisher, 1977) went as far as to identify a point of diminishing returns with respect to the relationship between the costs of upgrading roadway lighting systems and the savings accrued by accident reduction. Fisher calculated a variable which he called the accident reduction factor (r).

$$r = \frac{\text{No. of night accidents after lighting/No. of day accidents after lighting}}{\text{No. of night accidents before lighting/No. of day accidents before lighting}} \quad (15)$$

His equation is surprisingly close to the Criterion of Safety used by the Norwegian Elvik. He found "r" to be significant at the 0.1% level. He also found that accident reduction was significant at the 5% level with respect to lighting. This means that the change in accidents as a result of pure chance rather than as a result of upgraded lighting could only happen in 1 instance out of 20. More importantly he found that only about 12 % of the variation in the data can be explained by the variation in light level. Thus this study seems to have a very sound statistical base, and its results are felt to be significant with regard to the basis of our own study. Fisher calculated an optimum lighting upgrade with respect to accident cost savings. The lighting upgrade in his study was the replacement of mercury lamps by high-pressure sodium lamps. He used a function for the lighting upgrade as expressed by the following equation:

$$U = \frac{\text{Lower hemisphere flux per unit area after upgrading}}{\text{Lower hemisphere flux per unit area before upgrading}} \quad (16)$$

He compared that to a cost function (SOC) which was the savings in accident costs over increased lighting costs due to the upgrade. Figure 2.6 is a copy of the graph from Fisher's paper and clearly shows the optimum benefit occurs at a point around 3.3 times the increase in flux per unit area. In other words to add more light does not amortize the additional cost of construction by a commensurate amount of accident cost savings. Fisher also puts a very pragmatic spin on the subject of lighting and roadway safety in the final paragraph of his paper when he states the following.

> "Lighting does reduce night accidents and is a valuable accident counter-measure. However, there are limits to its application, and it must be regarded as one of the many counter-measures available. Lighting explains only a very small part of the phenomenon of accidents, and there is a diminishing return as roadway lighting is expanded and upgraded."

A similar conclusion was reached by the Highway Research Board in a study on the effects of illumination on freeways (NCHRP, 1967). They found that there was no difference in the accident rate when illumination intensity was varied between 0.22 and 0.62 foot-candles. In fact visibility only increased 41.1% with this nearly 300% increase in illumination because of disability glare.

A University of Nebraska team evaluated the impact of lighting a rural at-grade intersection (Anderson, et al, 1984) and found that the addition of lighting generally reduced accidents. However, the greatest reduction among various designs was only about 14%, and in one case in the study the accident rate actually increased 6% after the addition of lighting. Six different

designs were studied and the variations in accident rate were less than 6% between differing designs. Between the two designs with the greatest difference in accident rate, the change in average horizontal illumination was 118% that produced a 6% improvement in accident performance. It should be recognized that the scope of this study was very limited, but it nevertheless shows that attempts to improve safety performance by varying design provide only marginal differences at best.

Taking the conclusions of the papers by Elvik, Box, Fisher, and Anderson, et al together, one can conclude that adding light to a road does enhance safety, and that the level of that light is hard to correlate with safety performance. By having a lower level of illuminance, an object will show higher contrast against both the background and the foreground when it is illuminated by the headlights of a vehicle. This paper cites a paper published in 1945 by C.I. Crouch that indicated that visual acuity rises with illumination level and then drops off as levels of glare and brightness reach a point where the observer experiences discomfort. This identifies a key biological constraint that must be considered in the design of roadway lighting systems. In essence, we have two dichotomous conditions to try and optimize in the design. On one hand, increasing the level of contrast makes an object more visible. This would lead an engineer to increase the light behind the object to create a situation of negative contrast and thus maximize visibility. However, the placement of the lighting to achieve this condition would create glare thereby reducing the observers visual acuity and making it harder to acquire and safely react to the presence of the object in the traveled way.

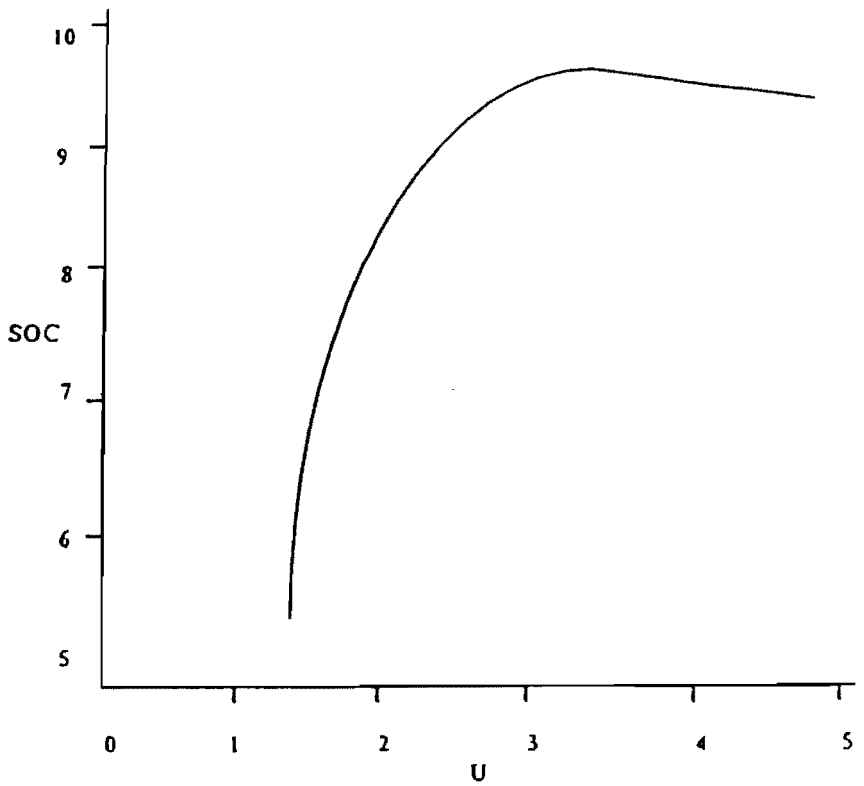

Figure 2.6. Fisher's Optimum Lighting Upgrade Analysis (Fisher, 1977).

This dilemma was addressed after a fashion by Jung and Titishov (1987). They used a standard 20 x 20 cm target, cut from a Kodak middle gray card (diffuse, 18% reflective standard) to conduct their contrast experiments. They discovered the fixed lighting has too many transient quantities that are difficult to characterize. In the case of luminance, there are only a few variables to characterize. The study considers luminance as reflected light in the luminance design standard and illuminance design standard as an incident light only design. It is difficult to reach agreement on standard values for visibility system parameters when the visibility factor is loaded with physical and human factors.

Jung and Titishov's solution is to concentrate on a less sophisticated parameter that can be computed easily at locations on the roadway using only dimensions and properties of the lighting system. Their parameter would be used in the same way as glare or illuminance to determine weaknesses in a roadway lighting system. They assume visibility of a small target is determined mostly by the negative contrast of a silhouette effect.

Jung and Titishov advocate backlighting the roadway to increase negative contrast while minimizing glare. In Jung and Titishov's opinion, the current illuminance and luminance standards are blocking development of backlighting because they do not reveal spots of bad visibility. According to them, it is necessary to perceive a critical object at a distance of about 90 m. Car headlights are not very effective at that distance so objects are seen by silhouette vision, i.e. negative contrast, if the objects are backlit.

Hall and Fisher (1978) examined the design of roadway lighting system by using empirically derived requirements of light technical parameters such as road luminance, luminance uniformity, and glare restriction. They also used a square target 200 mm x 200 mm with limited range of contrast. They found that lighting design based on a visibility matrix requires the introduction of simplifications. They caution that, "Inherent simplifications may not broaden our understanding but further rigidify our [technical] attitudes. For example, the thought that the [critical] task is the identification of simple objects on the carriageway is reinforced. This again prevents the consideration of the total environment, which includes the immediate surrounds of the carriageway. Indeed it may be argued that a visibility metric should include a weighting factor for spatial safety distribution over the carriageway." These authors go as far as to formally question the introduction of a contrast based visibility metric because of the difficulty of understanding the impact of inherent simplifications to the output of the design methodology.

Marsden (1976) studied road lighting, visibility, and accident reduction numerically and experimentally and focused to some extent on the issue of glare. For experimental investigation, disability glare is related to veiling luminance, which was measured with a Pritchard photometer. Horizontal illuminance near the road surface was measured by summing the outputs of photocells mounted on the ends of the vehicle. Vertical illuminance at road level was measured by a photocell mounted on the rear of the vehicle, and some instrumentation was mounted below the vehicle to record road reflectance data. They recorded all the information as well as the visual field of the driver on the tape. The tape was played in the laboratory and selected frames were frozen. An area of the shape can be defined (by operating brightening-up controls) for luminance analysis. This analysis was examined on the portion of the TV signal corresponding to the selected area. Analog processing gives the value of maximum, minimum, average and standard deviation of luminance within the selected area by using a calibration luminance scale on the picture.

Driver Parameters

Rackoff and Rackwell (1975) investigated the physiological components of driver reaction and target acquisition. They developed a vehicle-based television system to investigate driver eye movement pattern during night driving and to compare those patterns to daytime patterns on freeways and a rural highway. They determined the differences of visual search behavior at sites with high and low night accident rates and the effect of illumination on a driver's visual search. They discovered that nighttime visual search behavior is different from daytime visual search behavior, and the measure of visual search behavior is sensitive at sites with different accident rates relative to day and night conditions. The results demonstrate that the changes in visual search measures due to illumination not only demonstrate that illumination can affect visual search at the same sites, but also demonstrate that visual search behavior can be useful in associating the specific effects of various illumination designs on driver search patterns.

Walton and Messer (1974) discuss fixed roadway lighting from a driver visual workload measure of effectiveness of vehicle control. They were looking for a measure for determining when roadway lighting would be warranted. Their work compliments the concept discussed earlier with regard to target acquisition time, reaction time and stopping time.

Driving Tasks

Walton and Messer divide driving into three primary tasks, the information necessary to complete each task, and the priority level of each task. The tasks and priority levels are the positional level, the situational level, and the navigational level respectively. The positional level consists of speed and lane position and must be satisfied before any other task. The situational level is second and consists of changing speed, direction of travel, and position on the roadway. The navigational level consists of following a predetermined route from here to there and is the third level of priority after position and situation.

In a situation overload, a driver will shed lower priority tasks for high priority tasks. An environmental situation causing a driver to shed high priority tasks is not a suitable situation. Load shedding is not determined by the amount of work a driver must do but by the rate at which the tasks must be accomplished. An emergency situation will cause sudden load shedding. From an information supply standpoint, the size of the information supply to the driver is inversely proportional to the speed at which he is traveling. Fixed roadway lighting improves information processing capability of drivers by increasing the amount of information available for processing by making a larger proportion of the roadway visible.

In order to quantify the amount of information available due to fixed lighting, we first need to determine the total amount of information available to the driver under ideal lighted (i.e. day time) conditions. Then, we must determine the amount of information available in the same area at night without lighting, which then allows the computation of the contribution of the fixed lighting in terms of total information available to a driver. After the information contribution due to fixed lighting is assessed, it is then possible to determine the change in information available to a driver due to changes in fixed lighting.

Drivers are assumed to service information needs in a cyclic order dictated by priority of tasks. The cycle would be positional information search, situational information search, navigation information search and back to positional information search. From an information standpoint, the tasks involve sampling each task periodically with the period of the sample determined by the speed of the vehicle and complexity of the task. As a task becomes more complex the sample rate will increase.

The assumption of safe and effective vehicle positional control is based on redundant positional information of the roadway ahead and must be acquired each time the driver returns to a position information search and acquisition phase. During situational information search and navigation information search, the driver is assumed to be traveling without positional information. Information demand is the time required to complete a sequence of position, situation, navigation, and position information searches.

Positional Information

Most night time positional information is gathered from lane lines, edge lines, curb lies and position of other vehicles and a general view of the roadway. Much of the positional information under good (daylight) driving conditions can be obtained with peripheral vision. During nighttime driving the driver fixates on position markers rather than using peripheral vision. Time required to identify a task is about 0.2 seconds. The time for eye movement is from 0.1 to 0.3 seconds. So, the time required to sample a position source is about 0.3 seconds or more.

Situational Information

It is assumed that a driver scans situational areas to ensure safe operation when a potential hazard is visible about 25 % of the time, but if there are no hazards, the situational load drops. Increased complexity of the scene being viewed increases the mean fixation time of the situational information tasks.

Navigational Information

A driver can search for navigational information only after the positional and situational needs are fulfilled. Navigational information consists of reading signs and other navigation tasks. The complexity of the tasks is determined by a level of familiarity with the route and with the situation. New signs and situations require more time and increase stress levels. A word on a sign requires about 0.35 seconds to locate and read. Multiple unfamiliar signs are confusing and increase stress levels during navigation tasks. As navigational task time increases, positional and situational task times suffer. Road way lighting increases the positional information supply by increasing the visibility distance. Decreasing speed also increases visibility distance.

Walton and Messer's approach to warrant fixed roadway lighting is based on the driver's information needs to perform night driving tasks in a particular driving environment. Fixed roadway lighting is warranted when the information demand exceeds the information supply without fixed roadway lighting.

Adrian (1997) adds to the knowledge base with respect to driver physiology. He discusses rod vision and cone vision and the 2^{o} central field of view and blue shift in the eyes sensitivity. He also found that as the light levels decrease the spectral sensitivity of the eye changes, the sensitivity curve remains approximately the same shape. However, the peak of the curve shifts away from 550 nanometer, to a slightly bluer 520 to 530 nanometer. Low light level contrast sensitivity is shifted into the blue with higher contrast sensitivity in blue than in red.

Target Size and Composition

RP-8 (IES, 1990) specifies that size and composition of the "Small Target" to be 18 centimeters square and of 20% diffuse reflectance. This reference is silent as to the reasons why this particular target is chosen as the standard. Obviously, it is clearly an attempt to create a series of parameters that can be related to visibility and therefore, correlated to experimental and computed data with regard to quantifying visibility. A study led by Freedman (Freedman, et al, 1993) proved that the probability of detecting a target strongly depends on its type and that older drivers generally showed a significantly lower probability of target detection. Thus, the selection of a target's size, shape and composition should not be arbitrary. Other studies have used targets of different size than the STV target (the term target will be used to define a standard object used experimentally in these papers to relate to some other parameter of visibility, recognition, or other such factor). Roper (1953) used targets which were 40.64 centimeters square and which had a reflectance of 7.5%. Haber (1955) used a much larger target with a mean linear dimension of 91.4 centimeters and a reflectance of 15%. A German group (Waetjen, et al, 1993) used a target composed of a Landholt ring with a stroke width of 8.7 cm and a height of 43.5 cm. Jung and Titishov (1987) conducted their work with a 20-centimeter square target which had a reflectance of 18%. Zwahlen and Schnell (1994) used targets of varying reflectances that were 60.96 centimeters square and installed 30.48 centimeters above the pavement. They did further detailed studies on this type of target with a constant reflectance of 15.5%.

A team led by Janoff (Janoff, et. al, 1986) used a target composed of styrofoam hemisphere with a 0.15-m diameter skirt and an 18 % reflectance. The lighting system in controlled field conditions consisted of 200 watt high-pressure sodium (HPS) lamps mounted 30 ft high at spacings of between 68 and 88 ft. They chose 6 different lighting conditions: full lighting, 75 percent power, 50 percent power, every other luminaire extinguished, one side extinguished and no lighting and measured photometric data for each conditions. Subjects were required to drive the vehicle at the 55 miles per hour (88 kph) constant speed limit. The controlled field experiments results show that drivers tended to dislike reduced lighting on ramps or interchanges as opposed to reduced lighting on straight mainline roadway sections. They obtained a linear relationship between detection distance and horizontal illumination, pavement luminance and visibility index by using the six conditions.

Zwahlen and Yu (1990) studied two types of investigations to determine the distances at which the color and outside shape of targets can be identified at night under vehicle low-beam illumination for flat targets with three different outside shapes and with six different retroreflective color sheet coverings. First, the color and the shape recognition distances were investigated. Second, only the color recognition distance was determined. They used colors (red, green, yellow, orange, blue and white) and target shapes (circle, square and diamond) having the

same surface area (36 in^2) as independent variables. In both experiments the center, front of the vehicle is positioned above the centerline of the road, and the longitudinal centerline of the vehicle also positioned a 3-degree angle to the left of the road centerline. The results show that the color recognition distance was twice as long as the shape recognition distance. Also, they concluded that highly saturated red color of the retroreflective targets was the best. Hall and Fisher (1978) examined design of roadway lighting system by using empirically derived requirements of light technical parameters such as road luminance, luminance uniformity and glare restriction. They used a 200-mm square target with limited range of contrast. They found that lighting design based on visibility matrix gives better results than others. Finally, the 1990 Green Book (AASHTO, 1990) uses a target which is 150 millimeters in height as a standard from which to calculate stopping sight distance requirements for highway geometric curves. Thus it can be seen that target size and composition has been quite variable.

While roadway lighting can be installed for a variety of purposes, the consensus found in the literature seems to indicate that safety is the primary reason for making a capital investment in lighting systems. Thus, it would seem logical that the size and composition of the standard target used for design would be directly related to the dynamics of nighttime driving safety. A study done by Kahl and Fambro (1994) provides an excellent analysis of the comparison of targets to accidents. This pair correlated types of accidents with the size of the object involved and then compared it to the standard Green Book 150 millimeter target. They found that only 0.07 percent of reportable accidents were attributable to collisions with small objects in the road. They then concluded that the frequency and severity of these types of accidents did not justify the use of the 150-millimeter object height in the critical Stopping Sight Distance model. In fact, they found that only two percent of all accidents involved objects or animals in the roadway. In urban areas, 10.4 percent of the objects struck were less than 150 mm in height, and on rural roads only 1.8 percent were 150 mm or less in height. They also found that "more than 95 percent of the accidents resulted in low-severity injuries; therefore, a small object is not the most critical, hazardous encounter in the Stopping Sight Distance situation." They also make two recommendations that are of interest to the STV discussion

- The object height should be a function of and related to the smallest realistic hazard typically encountered on the roadway.
- The taillight height of an average vehicle (380 millimeters) is probably a good measure for the height of a typical hazard.

This would track well with the results of Zwahlen and Schnell (1994) who found that a 60.96 centimeter square target with 15.5% reflectance placed at 30.48 centimeters above the pavement could be spotted by subjects at an average distance of 104 meters with a standard deviation of 16.6 meters through the filter of a windshield. When this is compared to the STV model of the 18 centimeter target visible at 83 meters, there appears to be a potential that the STV target might be too small to be detected by the average observer, and that the use of it as a design standard does not directly equate to those hazard visibilities for which the lighting is being installed. The Zwahlen and Schnell target provides nearly three times the reflective surface at nearly the same distance (if one were to subtract the standard deviation from the mean distance) as STV. It should be noted that the Zwahlen and Schnell experiment was a static one in that the observer was not moving as would normally be the case in most roadway hazard situations. Also, the

observer's only data collection task was to search for the target. Jung and Titshov (1987), while using a target which was very close to that specified by STV, found that once "luminance levels meet standards for uniformity, spots of unsafe low contrast are clearly revealed..." They also seem to advocate the use of several standard values of reflectivity.

REVIEW OF THE LITERATURE ON PAVEMENT RELFECTANCE

Background on Pavement Luminance in Roadway Lighting Design

Until the 1983 IES/ANSI Standard Practice for Roadway Lighting (RP-8) was proposed, roadway lighting in North America was based on horizontal illuminance. In the 1983 RP-8, pavement luminance was introduced as the preferred basis of design with illuminance criteria included as an acceptable alternative (IES 1983). High mast and walkway/bikeway lighting systems were two exceptions where illuminance was presented as the only criterion for design. Along with pavement luminance, disability glare (veiling luminance) was also identified as a significant factor that affects the nighttime visual performance of a driver. At the time when RP-8 (IES 1983) was introduced, the IES/ANSI recognized that "luminance criteria do not comprise a direct measure of the visibility of features of traffic routes such as traffic and fixed hazards." However, they decided that "visibility" criteria proposed at the time were based on limited research and evaluation and therefore, cannot be adopted at that time. Nevertheless, RP-8 (1983) had a complete appendix (Appendix D) dedicated to visibility concepts for information purposes. This Appendix used the concept of *Visibility Index (VI)* developed based on research by Blackwell and Blackwell (1977) and Gallagher (1976) where the visibility of a gray-colored rubber traffic cone was considered as the target.

According to literature, the "Visibility" concept was first introduced in England by Waldram (1938) who identified the concept of "Revealing Power." He calculated the visibility for 24-inch square targets set on a grid pattern on the roadway and determined when a target became a dangerous obstacle for observers driving at 30 mph. Also in England, Smith (1938) conducted a study of the reflectance factors and revealing power of objects. He showed that 50 percent of the pedestrian clothing had a reflectance of less than 5 percent and 80 percent of the clothing had a reflectance below 15 percent. Based on these results, it was possible to show that a 10 percent reflectance target will always be darker than the pavement that can act as a background for a pedestrian wearing such clothes. Such a scenario provides negative contrast (pavement brighter than the target), and the target that is least visible on the roadway will be the one that is located where the pavement has the lowest luminance.

Based on research such as those mentioned above, CIE (International Commission on Illumination) adopted the following positions in its standard practice for roadway lighting design.

1. "Quality" of a lighting system is always higher when average pavement luminance is high.
2. "Quality" of a lighting system is always higher when "empty street" pavement luminance uniformity is excellent.
3. Glare needs to be considered in the design.

It was interesting to note that contrast was not considered as design criteria. Keck (1996) observed that CIE at the time felt that objects are almost always darker than the pavement, and therefore, by considering factors (1) and (2) above, would provide a simple design method.

In terms of reflective properties, all surfaces, including roadway pavement surfaces, are generally classified into three major groups. These are the ideally specular surface, perfectly diffuse surface and mixed reflection surface. The ideally specular surface reflects all the luminous flux received by a point at an angle of reflection equal to the angle of incidence. The reflected ray, normal to the surface at the point of incidence and the reflected ray all lie in the same plane. These surfaces form a similar geometric image. Some examples of almost ideally specular surfaces are mirrors, highly polished metal surfaces and liquid surfaces.

The perfectly diffuse (matte) surface reflects light as a cosine function of the angle from the normal, regardless of the angle of incidence. Since the luminance of a surface is equal to intensity divided by the projected area, and since the projected area is also a cosine function of the angle from the normal, the perfectly diffuse surface appears equally bright to an observer from any viewing angle. The luminance of the surface is independent of the luminance of the source of light but proportional to the illumination of the surface. These surfaces form no geometric image. Surfaces such as white matte finished paper or white painted walls appear to approximate closely with the perfectly diffuse surface. However, these surfaces behave as diffuse only if the angle of incidence is close to zero.

Most surfaces encountered in everyday life fall into the category of mixed reflection that is somewhere between the ideally specular and perfectly diffuse surfaces. These surfaces form no geometric image but act as a diffuse surface to some extent with some preference to direction of reflection. Therefore, the apparent brightness of such surface changes with the angle of incidence and the observer's viewing angle. King (1976) illustrated these surfaces with the luminous intensity distribution curves shown in Figure 2.7.

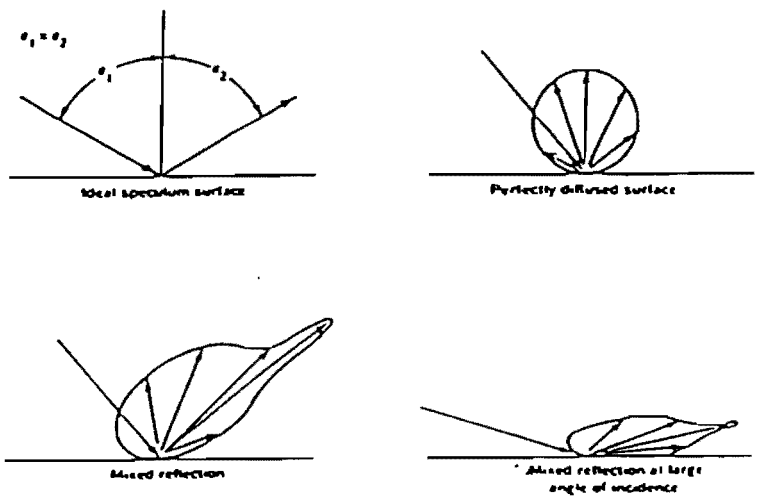

Figure 2.7. Luminous Intensity Distribution Curves for Different Types of Reflection (King 1976)

Pavement surfaces that encounter viewing angles between 86 and 89 degrees and incident angles between 0 and 87 degrees (both from the normal) exhibit characteristics of mixed reflection. Generally, a single luminaire over the pavement surface produces a single luminous patch that appears to the traveler to be shaped like a "T" on the surface of the roadway with the tail of the "T" always extending towards the observer irrespective of the observer's position on the roadway. This brightness (luminous) patch is almost completely on the observer side of the luminaire since very little of the light incident in the direction away from the surface is reflected back to the observer. The size, shape and the luminance of the patch depends to a great extent on the surface reflection characteristics of the pavement. Figure 2.8 illustrates the shape of a luminous patch produced by a luminaire on diffuse, smooth (specular) and wet surfaces.

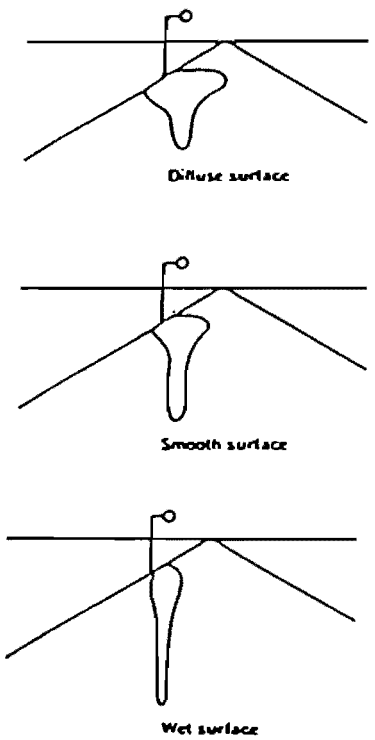

Figure 2.8. Luminous Patch Produced on Different Roadway Surfaces (King 1976)

In one of the earliest studies done on reflection characteristics of pavement surfaces, Christie (1954) of the Transportation and Road Research Laboratory (TRRL) in England found that a reduced range of data presented in a single family of curves is sufficient to calculate the luminance in important regions of a street lighting installation within an accuracy level of 15 percent. Christie adopted the point of view that brightness (luminance) in a lighting installation is built up from the bright patches produced by individual luminaires. This technique was used to assess the reflection characteristics of three types of pavement surfaces commonly used in England. The three surfaces were rolled asphalt with precoated chippings, "non-skid" rock asphalt and machine finished Portland cement concrete. After calculating the luminance factors, a family of curves for these surfaces was drawn. Since these curves do not present an immediate picture of how the surface is brightened, a perspective drawing showing the bright patch was developed using the luminance factor curves.

Comparing his brightness patch for the rolled asphalt surface with precoated chippings with results published by Waldram (1934), Christie concluded that the old surface (Waldram's test section) gave a much larger brightness patch than the new surface (Christie's test section). In comparing the rolled asphalt surface with the "non-skid" rock asphalt, Christie observed that the efforts to make pavement surfaces "non-skid" have seriously reduced their power to reflect light. Christie also found that in addition to coarse surfaces, fine textured surfaces with protruding small aggregates also produce short brightness patches. His explanation of this phenomenon was that within limits, what matters is the shape of the surface, not the size of its features (coarseness). He concluded that sharp projections necessary to prevent skidding tend to destroy the specular reflection of obliquely incident light that makes possible the formation of long patches. Christie also observed that in coarser surfaces where specular reflection is reduced, brightness has to depend more on diffuse reflectance than in the case of smoother surfaces. Since diffuse reflectance depends on the lightness of color, he said that the benefits of using light colored materials should be substantial. Christie also commented on how the type of luminaire can be changed to overcome problems involving smaller brightness patches. On skid resistant coarse surfaces, he suggested that high angle beam luminaires are not very satisfactory and medium angle luminaires with maximum intensity at 75 to 78 degrees are preferred.

Finch and King (1967) appear to have introduced the first direct reading reflectometer for roadway lighting purposes. Until then, reflective characteristics of pavements were evaluated using visual photometry and other photographic techniques. This device allowed full flexibility in changing all three angles relating to reflectivity. It operated on 115-volt AC power and it used a stray light rejection curve for the telephotometer where the light acceptance angle was approximately 3 minutes. The problem associated with this device is that it took approximately 3 hours to set up the equipment at site and another one hour to take one set of reflection data corresponding to a set of angles. If measurements were taken at 5-degree intervals for the vertical source inclination and the horizontal angle, it would result in 864 readings at one location and require 864 hours of data collection. King and Finch (1968) later developed a reflectometer for use in the laboratory where 12-inch diameter pavement cores were used to simulate the pavement. By automating the data collection procedure, they were able to make rapid automatic readings of directional reflectance factor thus enabling the collection of large volumes of data over a very short time. This device was able to simulate up to 600 feet of viewing distance. One significant feature of this reflectometer was that the color response was corrected to approximate that of the human eye.

Even after the development of their automated pavement reflectance measurement device, King and Finch (1968) observed that there was little application of it outside the research laboratory primarily due to the specialized nature and complexity of calculations involved. They suggested that one way to expand the use of reflectometry is to use a pavement surface classification system and proposed that the classification be based on directional reflectance properties of the pavement surface.

Towards the latter part of the 1970's, the University of Toronto (Jung et al. 1984) built a photometer for the road surface reflectance measurement based on concepts developed earlier by CIE (1976). This reflectometer features automated control of positioning, reading and recording data. It is capable of testing pavement cores 6 to 8 inches in diameter and at least 3 core samples

from a given pavement are required to classify the pavement type. Jung et al. (1984) conducted a study to measure reflectance properties of many types of pavements in Ontario. The measurements were made on 6-inch diameter cores taken from 36 different pavements where more than 400 core samples were processed. When factors such as traffic level and the position of the lane were considered, this accounted for about 100 different surface types.
Pavement surfaces were classified based on the average luminance coefficient Q_0, and the ratios S_1 and S_2 as defined by IES Roadway Lighting Committee (1976). Q_0 is considered as a measure of the overall brightness of the pavement as it appears to the viewer, whereas S_1 and S_2 describe the degree of specularity of the pavement surface. Over the years, two systems of four standard reflectance tables have been proposed for dry pavements. These two systems are indicated by "R-Series" and "N-Series" classifications. The proposed IES RP-8 Lighting Standard (1990) adopts the R-Series classification for its pavements and its features are indicated in Table 2.1.

Table 2.1. Road Surface Classifications Description

Class	Q_o	Description	Mode of Reflectance
R1	0.10	Portland cement concrete road surface. Asphalt road surface with a minimum of 15% of the aggregates composed or artificial brightener aggregates (labrodorite, quarzite)	Mostly diffuse
R2	0.07	Asphalt road surface with an aggregate composed of a minimum 60% gravel (size greater than 10 millimeters) Asphalt road surface with 10 to 15% artificial brightener in aggregate percent artificial brightener in aggregate mix. (Not normally used in North America)	Mixed (diffuse and specular)
R3	0.07	Asphalt road surface (regular and carpet seal) with dark aggregates (e.g. trap rock, blast furnace slag) rough structure after months in use (typical highway)	Slightly specular
R4	0.08	Asphalt road surface with a very smooth texture	Mostly specular

Theoretical Basis for "R-Series" Classification of Pavement Surfaces

The classification is based on specularity of the pavement as determined by a ratio, S1, and a scaling factor, Q_o, as determined by the overall "lightness" of the pavement. The normalized Q_o is given in table 2.1 for each of the pavements described. Greater accuracy in predicting pavement luminance can be achieved by evaluating specific pavements as to their S1 ratio and specific Q_o and then choosing the correct R-table.
The S1 ratio and specific Q_o for a pavement can be determined in one of two ways: (1) a core sample can be removed from the pavement and photometered by a qualified laboratory; (2) a field evaluation can be made.

The characteristics S1 and Q_o were adopted by CIE as basic quantities for evaluation of the reflection properties of a road surface (CIE Publication 30, 1976). The average luminance coefficient (scaling factor) Q_o is given by the following equation as a measure of the lightness of a road sample.

$$Q_0 = \frac{1}{\Omega_0} \int_0^{\Omega_0} q(\gamma, \beta) d\Omega \tag{17}$$

In the formula 8-1, Ω_0 is the relevant solid angle of incident light at a specified point on the road. Ω_0 is defined by a rectangular 'ceiling' at the mounting height *h* extending *3h* to the right and left to the specified point , *4h* toward the observer and *12h* behind the specified point. The special quantity S1 given by:

$$S1 = \frac{r(\tan\gamma = 2, \beta = 0)}{r(\gamma = 0, \beta = 0)} \tag{18}$$

The angles γ and β are as shown in Figure 2.9.

This function is derived from the angular distribution of the reduced luminance coefficient to indicate the shape of the reflection indicatrix:

$$r(\gamma, \beta) = q(\gamma, \beta)\cos^3\gamma \tag{19}$$

It was found that Q_o is highly correlated with the average luminance $\bar{L}$ on the road.

$$\bar{L} = \frac{1}{A} \int_0^A L_p \, dA \tag{20}$$

Where L_p is the luminance at point P

A is the relevant portion of the road area(usually restricted to one luminaire spacing.)

Based on calculations of 24 road surfaces, 24 luminous intensity distributions and 72 one sided lantern arrangements, the correlation coefficient between reflection characteristic Q_o and average luminance $\bar{L}$ was found to be 0.96 (Schmidt, 1986). Bodmann and Schmidt (1986) conducted field experiments to compare calculated and measured luminance characteristics. The reflection characteristics, Q_o were measured with the LTL, 200 portable road surface reflectometer.

The average luminance $\bar{L}$ was measured with the portable luminance meter. On average, the calculated values for $\bar{L}$ were found to be 31% higher than the measured values. The experimenters estimated the results as a reasonable estimate. If one takes into account maintenance factors such as the decrease of light output with age and deterioration of reflecting and transmitting materials of the luminaires, the agreement between calculated and measured luminance can be evaluated as perfect.

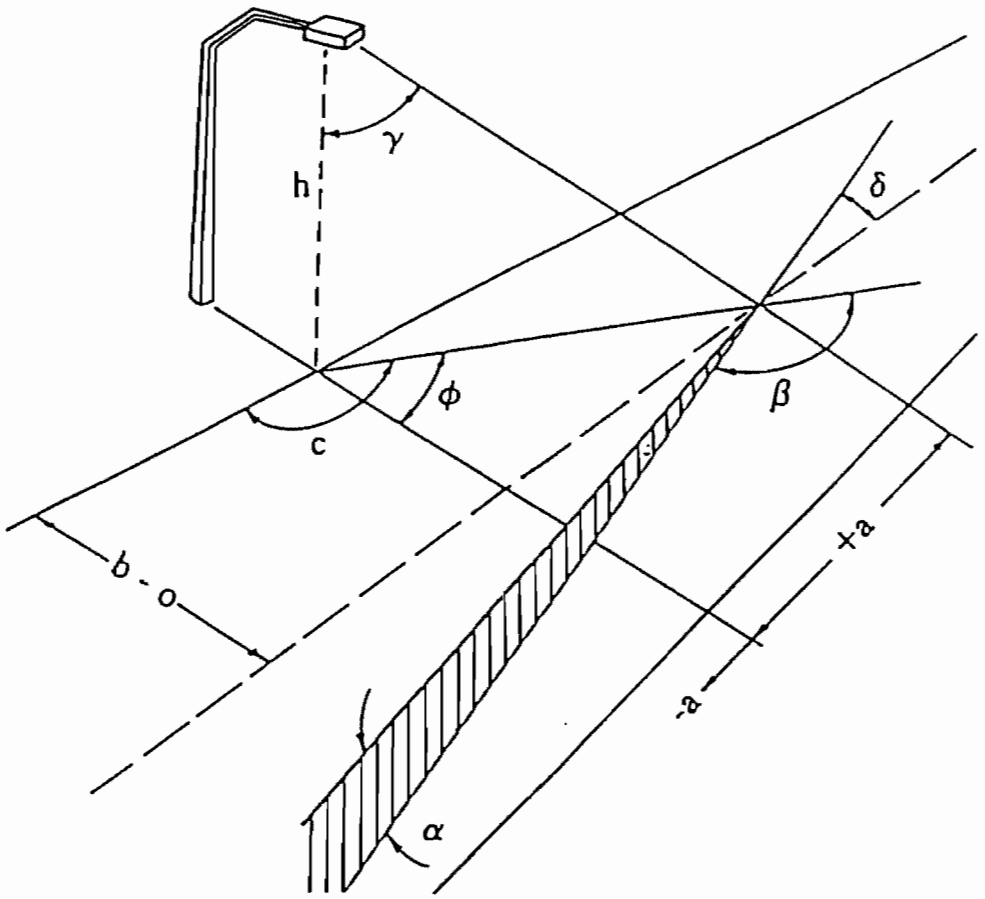

Figure 2.9. Schematic Diagram of Roadway Lighting

Table 2 identifies the values for the three reflectance parameters Q_0, S_1 and S_2. The N-Series classification was developed in Germany by Erbay (1 974). One note of caution by CIE was that variation of Q_0 within one pavement class might be very high, so the Q_0 value given within the standard must be scaled to correspond to the Q_0 of the actual surface being chosen.

Table 2.2. Reflectance Parameter Values for "R" and "N" Classifications (Jung et al. 1984)

Parameter	R-Series				N-Series			
	R1	*R2*	*R3*	*R4*	*N1*	*N2*	*N3*	*N4*
Q_0	0.10	0.07	0.07	0.08	0.10	0.07	0.07	0.08
S_1	0.25	0.58	1.11	1.55	0.18	0.41	0.88	1.61
S_2	1.53	1.80	2.38	3.03	1.30	1.48	1.98	2.84

Pavement Reflectance Studies

Results from this data quite clearly indicated a relationship between the S_1 ratio and the type of coarse aggregate used on the pavement surface. Table 2.3 outlines the range of Log (S_1) values obtained for three different types of coarse aggregates. Jung et al. (1984) attributed the different values to different levels of resistance to polishing under traffic.

Table 2.3. Relationship Between Coarse Aggregate on Pavement Surface and S_1 (Jung et al. 1984)

Coarse Aggregate	Range of Log (S_1)
Igneous or Trap Rock	-0.29 to -0.17
Limestone	-0.10 to -0.06
Blend of the Above Two Aggregates	-0.23 to -0.08

As for Q_0, a wide scattering of values was observed. Table 2.4 outlines the range of Q_0 values obtained for three different types of coarse aggregates. Jung et al. (1984) attributed the different values to different brightness levels of aggregate and on a concurrent increase in specularity of the surface. The appropriate value to be used in design depends on the road surface materials, their composition and changes to the pavement surface with time and traffic exposure. Jung et al. (1984) also noted that with time, asphalt pavements tend to brighten and Portland cement concrete tends to darken. They also observed that with coarse aggregates that are polishable due to traffic, there might be a shift in the specularity class, for instance from R2 to R3.

Table 2.4. Relationship Between Coarse Aggregate on Pavement Surface and S_1 (Jung et al. 1984)

Coarse Aggregate	Range of Log (S_1)
Dark Trap Rock	0.074 to 0.088
Bright Limestone	0.102 to 0.124
Blend of the Above Two Aggregates	0.086 to 0.097

Some of the notable observations made by Jung et. al, (1984) included changes in specularity between different lane wheelpaths and that asphalt pavements become more specular as reflected with increased values for Q_0, S_1, and S_2. In the end, it was reported that with regard to specularity only, the four pavement classes were regarded as sufficiently accurate for design purposes. However, the authors cautioned that due to high variability observed, Q_0 should be estimated more accurately by considering the surface course composition and the aggregate type. Nevertheless, based on their extensive measurements of pavement reflectivity, the authors published recommended (and amended) design values for different combinations of coarse aggregate type and mix design commonly used in Ontario, Canada.

Bodmann and Schmidt (1989) showed the marked variation in the reflection characteristics of road surfaces with time and traffic and highlighted some problems associated with the CIE recommended standard classes of pavement surfaces. They also pointed out that the decision on the class of surface to be used in the design is often based on assumptions and the standard r-table represents the individual road surface irrespective of temporal and local variations due to age and wear. Furthermore, the authors indicated that the classification of surfaces into four CIE

"R" classes is justified neither by test calculations nor by measurements on real streets. Based on these observations, the authors highlighted the positive aspects of the "C-Series" classification where only two standard surfaces are considered. The two classes of pavement surfaces are C1 and C2, C1 corresponds to the R1, and C2 corresponds to R2, R3 and R4 in the "R-Series" classification. The authors contend that the "C-Series " classification for dry road surfaces is more realistic and much more practicable. However, even under the "C" classification, the prediction of Q_0 remains a problem at the design stage.

Nielson et al. (1979) studied the reflectance characteristics of 41 different road samples, 24 of which were asphalt concrete, and the rest were hot rolled asphalt with coated chippings. The surface materials were cast into 30 cm x 35 cm rectangular specimens and were tested in the laboratory. In addition to the mix type indicated above, the maximum size of the aggregate, aggregate type and the climatic conditions were included in the experimental design. The results from this study can be summarized as in Table 2.5.

Table 2.5. Summary of Observations by Nielsen et al. (1979)

Factor(s) Investigated	Conclusions/Observations
Parameter Relationships	Q_0 and S_I are inversely correlated Retroreflection Q_R does not change significantly with the observation distance Specular reflection Q_S on dry roads increases with meeting distance to oncoming vehicle Specular reflection Q_S increases from dry to wet pavement by a factor of two For worn samples, Q_0 and Q_R are directly correlated.
Surface Wear	The brightness measured by Q_0 and Q_R develop slowly with wear Residual bitumen (after aggregate is polished) increases S_I Reflection properties increased slightly when summer tires are used, but improved during subsequent exposure to studded tires
Composition	Brightness of aggregate affects Q_0 and Q_R Brightness not affected by coarseness of aggregate

According to Bodmann and Schmidt (1986), if a decision has to be made as to whether or not a particular road lighting installation meets prescribed values, the tolerance $(1 \pm 0.1)\bar{L}$ can be recommended. Analysis of computer predicted luminances was conducted by (Janoff, 1993). The illuminance calculations performed in the past using computers were quite accurate when given all input parameters. However, in 1983 the roadway lighting standard changed based primarily on pavement luminance (Janoff, 1993). This change brought about more complex calculations. It also required the exact reflectance properties of the pavement surface. This made the computer programs accuracy very dependent on factors such as the r-tables, the formulae for computing pavement luminance, lighting geometry and the luminaire intensity distribution (Janoff, 1993). A standard practice based on visibility was proposed in 1990 (Janoff, 1993). The visibility level (VL) can be determined using photometers to measure target luminance, pavement luminance, and veiling luminance. A predictive computer program thus becomes an important factor to assist in the derivation of target, pavement, and veiling luminances for a road lighting design in progress. In 1992, the only predictive computer program available was STV. A study was performed to compare the target, pavement, and veiling luminances, as well as VLs, to measured values. This experiment consists of two

different targets. Each target was a 7 inch square, and one placed upstream of the closest luminaire and one downstream (Janoff, 1993). The targets consisted of three different reflectances: 5, 30, 80 percent. During this study there were 48 measured points. For accurate measurements all street lights were cleaned, aligned, and 12 new calibrated lamps were installed closest to the target locations. The results indicated that the predicted values did not match up with the measured values. There were significant differences between the target, pavement, and veiling luminances (Janoff, 1993). For example, during one experiment the veiling luminance (Lv) was measured and predicted at 275 feet for each target. The results are shown in Table 2.6.

Table 2.6. Veiling Luminance

Variable	Target Reflectance	Target Position	Measured	Predicted	Result Ratio
Lv	-	1	2.10	0.16	13.1
Lv	-	2	2.86	0.22	13.0

The measured value at target position one was 2.10 and the predicted value was 0.16. It was concluded that "... many of the problems may not be in the computational parts of STV, but rather in the (inaccurate) choice of r-tables, choice of nominal target reflectance, specification of proper candlepower distribution, or failure to include light reflected from pavement onto target." (Janoff, 1993).

An effect of headlights on luminance and visibility was studied experimentally. There are at least two relevant parameters to consider in roadway visibility. The first is headlight intensity in the direction of the road ahead and the other is the intensity in the direction of the eyes of the driver (Alferdinck et al, 1988). A study was performed to evaluate the increase of visibility due to the addition of vehicle lighting. A number of measurements were made under 20 different lighting conditions to determine increases in visibility. The reported measurements taken used 5, 30, and 80 percent target reflectances. The measurements were taken with and without headlighting. Measurements were taken first at 75 feet then every 50 feet up to 275 feet then they were taken every 100 feet up to 775 feet. The study concluded that at distances less than 275 feet there is a significant change in photometric visibility resulting from headlights (Janoff, 1992). However, at distances greater than 275 feet there is no effect of headlights on either small target visibility or recognition distances derived from subjective estimates provided by the drivers (Janoff, 1992).

Pavement Luminance and STV

The visibility-based method of roadway lighting design proposed by IES RP-8 (1990) defines visibility using the parameter *Visibility Level* (VL) which is defined as the following equation.

$$VL = \frac{\Delta L_{actual}}{\Delta L_{th}} \tag{21}$$

Where ΔL_{actual} is the actual luminance difference of a target to its background (i.e. ΔL_{actual} = Target Luminance - Background Luminance)
ΔL_{th} is the threshold luminance difference that makes an object just perceivable from the background

This *Visibility Level* model is based on work done by Adrian (1989). To determine ΔL_{th}, the observer is assumed to be a young adult (23 years) with normal eyesight whose fixation time is 0.2 seconds. The standard target used for STV is a perfectly diffuse 18cm x 18cm square with 20 percent reflectivity that reflects light in a Lambertian manner. The target is placed on the pavement such that it is vertical and perpendicular to a line from observer to the grid point.

A network of grid points is set up between adjacent luminaires, and for each lane of roadway there are 20 grid points for each lane between luminaires (Figure 2.10). The observer is positioned at a distance of 83.07 meters. The height of the observer is taken at 1.45 meters giving a downward direction of view of 1 degree at the location of the target. The following notable assumptions are made in the proposed STV design procedure:

- The pavement is a level surface
- The pavement surface is homogeneous
- The pavement surface is smooth, dry and its reflectance characteristics can be represented by one of four classes (R1 to R4) identified in the IES recommended practice (1990)
- Only the light from fixed luminaires is considered. No allowances are made for illumination from automobile headlights and from off-roadway sources

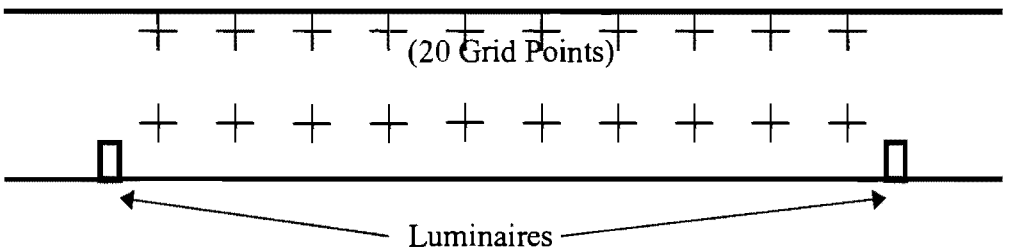

Figure 2.10. Network of Grid Points Between Luminaires Used to Calculate STV

The target luminance is calculated at the center of the target with only the light incident directly on the target from the luminaires being considered for its luminance calculation. The background luminance is considered as the average of the pavement luminance as viewed by the observer at a point adjacent to the center of the top of the target and at a point adjacent to the center of the bottom of the target. A simple calculation will show that the two points on the pavement whose luminances are averaged thus are approximately 12 meters (39 feet) apart.

Adrian et al. (Unpublished Data) recently studied the influence of light reflecting from the road surface on to the target on STV. Their results showed that this indirect portion of illuminance can contribute up to 15 percent of the total target illuminance. This will significantly alter the *Visibility Level* (VL) required to see the target under positive contrast.

CHAPTER 3: INFLUENCE OF PAVEMENT SURFACE CHARACTERISITICS ON LIGHT REFLECTANCE PROPERTIES (a thesis by Md. Mainul Hasa Khan)

Overview

Safe driving at night depends primarily on visibility and visual comfort. Since automobile headlights do not light a distance that is adequate for safe stopping at night, fixed roadway lighting plays an important part in safe driving at night. This thesis focuses on fixed roadway lighting only. The vehicle stopping sight distance consists of the following four components (40).

1. *Sampling Distance*, which is the distance at which the driver does adjustments in driving behavior, such as changes in speed and direction.
2. *Acquisition Distance*, which is the distance during which the driver decides that he, should stop the vehicle.
3. *Reaction Distance*, which is the distance at which the driver reacts by stepping on the brake (According to AASHTO green book, the reaction time is taken to be 2.5 seconds).
4. *Braking Distance*, which is the distance traveled while the vehicle decelerates from its initial velocity to zero.

The first two components are directly related to object visibility. The object must first be detected and then recognized by the driver before responding to it. Therefore, improved visibility should reduce accident rates at night.

The early designs on roadway lighting were based on the amount of light striking the surfaces of the pavement (i.e., illumination). However, it was later found that brightness of a pavement depends on the amount of light that is reflected from it. This led to the study of pavement surface reflection characteristics. Since then, it has been established that the ability to see an object at night is based not on the light that is emitted from the object, but on the difference in the brightness (or luminance) between the target and its background (contrast). Contrast is the main parameter of the visibility of a target. In roadway lighting design methods, pavement is considered as the background. Therefore, luminance distribution on the pavement surface is one of the most important measures used to evaluate the quality of roadway lighting.

Calculations of luminance of pavements are based on a two-dimensional array referred to as the r-table. R-tables can be developed for different pavement surfaces based on field measurements. However, for design purposes, CIE (International Commission on Illumination) classified dry pavement surfaces into four standard classes (R1 to R4) and assigned standard r-tables for each of these pavements.

The use of r-tables in the calculations of road surface reflectance properties has become questionable during the recent researches. So, it appears highly desirable to compare actual reflection properties of pavement surfaces with those derived from pure theoretical calculations. As a part of this research, data collected by the Roads and Transportation Association of Canada (RTAC) were analyzed (26). The RTAC measurements were taken using cores from existing

pavement surfaces and therefore represent reflection properties of pavement surfaces exposed to field traffic and weather conditions. The factors investigated in this research include pavement surface type, aggregates, age and traffic level with regard to pavement reflectance properties. Also a sensitivity analysis was conducted using a computer program that calculates pavement luminance and object visibility. For this analysis, in addition to the pavement type, factors such as luminaire geometry, luminous intensity of luminaire and target reflectivity were considered. Sensitivity analysis was also performed on standard pavements as recommended by CIE, taking both the average values of visibility parameters and values at individual points to observe the trend along the roadway.

This thesis is based on the research conducted and is divided into five chapters. In Chapter II present knowledge on different lighting issues that lead to the development of pavement reflectivity study is described in the form of literature review. A description of the research program is given in Chapter III. In Chapter IV, the results obtained from this research are analyzed to come to a conclusion. At the end, in Chapter V, conclusions derived from this research and recommendations for future researches on pavement reflectivity are presented.

Literature Review

General

The history of roadway lighting dates back to the 15th century, when the citizens of London and Paris began to carry lanterns at night. In 1866, the control of roadway lighting by government agencies began in Paris, when lanterns were hung on ropes stretched across the streets.

The first formal significant lighting research was initiated by Sweet in the 1910's. He conducted research on disability glare under the supervision of Railroad Warehouse Commission at Madison, Wisconsin. Subsequently, in 1914, an extensive research project was conducted in Philadelphia under the leadership of Preston Miller. Waldram of England continued this work in the late 1930's.

The first major roadway lighting installation that can be associated with the results of research was in Milwaukee, Wisconsin shortly before World War I. It was the first fully planned city street lighting system in the United States. The principal activity in street lighting during the 1920's was the design of lighting for business streets. Little attention was paid to the residential and public streets. In the 1930's began the era of traffic safety lighting when the number of night accidents began to increase. This resulted in the development of more efficient luminaires with controlled distribution.

Purpose of Roadway Lighting (14)

The primary purpose of roadway lighting is to provide the following.

1. A degree of safety to the road users.
2. A degree of driving comfort for night traffic, which is comparable to that experienced during daytime.
3. The traffic capacity of the road at night is equal to as much as possible to that of daytime.

In addition to the primary requirement of road safety, a roadway lighting system should ensure comfort for the driver. The visual comfort of the driver should not be regarded as a luxury, but as a means of allowing the driver the ability to drive with minimum stress. This would allow the best utilization of the traffic capacity of the road.

Some secondary purposes of roadway lighting are listed below.
1. Reduction of human misery and economic loss through accident.
2. Personal security.
3. Promotion of business.
4. Use of public facilities during the night.

Sources of Light

The sources of natural illumination are the sun, moon and stars. The sun is approximately 93×10^{6} miles away from the earth with a luminous intensity of 2.3×10^{27} candela. The moon is 240,000 miles away from the earth with a luminous intensity of 1.0×10^{7} candela of reflected light. The stars, because of their great distances from the earth, produce little illumination, although the illumination from some, especially at certain times of the year, is appreciable.

Daylight illumination is derived exclusively from the sun, and the sunlight is greatly modified by the atmosphere. Illumination on the earth's surface may reach approximately 10,000 fc in some places. In the shade of a building or a tree it is about 1000 fc, which is still far high compared to a few fc's from the modern-time luminaires.

The day light is very suitable for the very high eye adaptation level and the visibility level required to see an object is far more than required. But on a full moon, the maximum normal illumination measured was 0.0388 fc's. Therefore, it is necessary in some instances to have artificial lighting at night to attain a minimum level of brightness.

The nighttime illumination available to provide visibility of objects comes from four artificial sources
1. Fixed roadway lighting systems.
2. Vehicle head lighting systems and vehicle signals.
3. Traffic signal lights and lighted signs.
4. Extraneous off-roadway light sources.

Limitation of Vehicular Head Lights

This thesis focuses only on fixed roadway lighting. A research by Janoff (1992) showed that fixed roadway lighting systems produce better visibility of small targets placed on the road surface than standard low beam vehicular lighting (LBVL) systems. The headlights investigated in this study were installed in a 1986 Dodge Lancer, which used four 5.25-inch halogen lamps. For different target reflectances, visibility levels were calculated both for fixed lighting and fixed lighting in combination with LBVL at different observer-to-target distances (Figure 3.1). The figure shows that at distances more than 275 feet, there is generally no effect of headlights on

visibility. Janoff further studied the effect of LBVL on *detection distance,* (distance at which test subjects first saw the target on the road surface) and *recognition distance* (distance at which the test subject could determine the orientation of target). Janoff concluded that neither of these two measurements for the two lighting conditions yield any significant difference. Again target distances greater than 275 feet and high-speed vehicle, fixed roadway lighting is the preferred system to produce visibility.

Nielsen, Sorensen, Forsberg and Persson (1979) analyzed the effect of *retro-reflection coefficient (Q_R)* and *specular reflection coefficient (Q_S)* produced by vehicle lighting. Both these coefficients are defined as the ratio of the luminance at the point of measurement to the illuminance at the same point in a plane perpendicular to the direction of the incident light. Q_R corresponds the reflection of the driver's headlights from the pavement. Q_S corresponds to the reflection of the head lights of an oncoming vehicle from the pavement. It was found that Q_R does not change significantly with the observation distance whereas Q_S, on dry road surfaces, increases rapidly with the distance to oncoming vehicle. The average luminance coefficient for fixed roadway lighting (Q_0) and Q_R vary with the aggregate type on the pavement surface in a similar fashion.

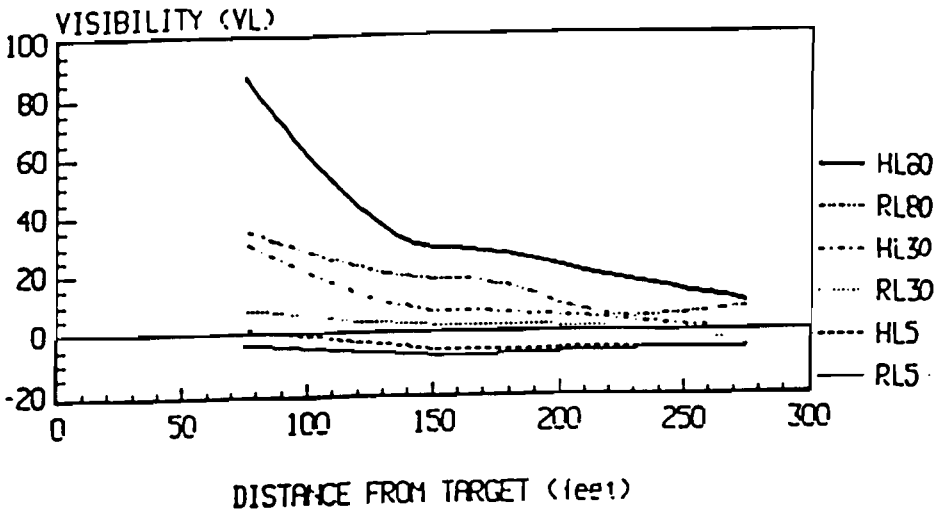

Figure 3.1. Effect of vehicular lighting and distance on visibility for 5,30 and 80 % target reflectance. (RL = Fixed roadway lighting only; HL = Fixed roadway + vehicular lighting) (*Janoff, 1992*)

Roadway Lighting as an Accident Counter Measure

The majority of information that the road user needs to carry out the nighttime driving task is of a visual nature. It is to be expected that at night such information will be less perceptible, and consequently the driver will be less effective than during the day. It is generally recognized that a single factor cannot be attributed to the cause of nighttime accidents. While the majority of accidents involve at least some degree of human error, other factors such as poor road design, adverse travel conditions and vehicular defects may also contribute to them.

The nighttime accident data is so much contaminated with various factors, which might influence accident occurrence, that it is very difficult to separate and compute them. In fact these factors are often complex and interacting. The main technique to analyze the influence of lighting on accidents has been the 'before' and 'after' study in which night accidents before and after a change in lighting are compared, using the day accidents as a reference. Another experimental technique is the comparison of accident rates for sites with road lighting with those sites without lighting. This method has been used in particular in studies of freeways in the USA. It assumes that lit and unlit sites are compatible.

Numerous studies have been done to determine the effects of public lighting on the number of accidents. Chapman and Hartmann (1969) and Linde (1970) have found that at low traffic levels, accident rates increase sharply compared to high traffic volumes. It has been seen that total traffic volume at night is only about one third of that by day. Thus on this account alone an increase in accidents is to be expected at night. The pattern of accident types is also not necessarily the same by night and by day. Fisher (1977) showed that the proportion of single vehicle accidents increased at night, especially in urban areas. The road user population may change at night, both in the kind of people using the roads and in the purpose associated with travel. The younger drivers have higher accident rates than the older drivers and this could be a contributing factor to the higher night accident rate.

Paul C. Box (1971) conducted a study to find a relationship between illumination and freeway accidents. He used the terms *unlighted safety ratio* as the ratio of nighttime accident to daytime accident in an unlighted condition. Similarly, *lighted safety ratio* indicates the situation in an lighted condition. The overall analysis showed that lighted roadways had an average night/day accident ratio of 1.43 while unlighted roadways had a ratio of 2.37. For individual results I-20 in Dallas showed that the ratio of *lighted safety ratio* and unlighted *safety ratio* is only 1.01 and studies in Atlanta showed that this ratio is less than 1.00 which indicate that inclusion of lighting had increased the number of accidents. Box found a great variation in luminaire output in field and concluded that illumination range of 0.3 to 0.6 horizontal fc increases the ratio of night/day accident.

Rune Elvic (1992) carried out a comprehensive study to see the effect of roadway lighting on accidents. He analyzed thirty-seven studies. The studies included were reported from 1948 to 1989 in eleven different countries from all over the world. His analysis showed that in eighty one percent of the cases, safety improved due to lighting and nineteen percent indicated that safety did not improve. This study also revealed that the effects of roadway lighting vary significantly with respect to accident severity. Lighting reduced nighttime fatal accidents about sixty five

percent, night time injury accidents by about thirty percent and night time property-damage-only accidents are reduced by fifteen percent. Elvik also recognized that era of the study, the country where the study was conducted and the traffic environment hardly affected the study results.

From the above accident studies and many more studies it may be concluded that hours of darkness present an elevated accident problem over day light hours. Nighttime accidents are relatively more numerous and more severe in their consequences and this disparity between night and day may be increasing in time. Basic psychological attributes of man suggest that the obvious cause is the inherent change in light level between day and night. Studies confirm that this is indeed a major factor but other factors such as changes at night in traffic flow and road user patterns probably have a significant effect. Thus the implementation of lighting in itself will not reduce the night accident problem to that of daytime. However, improvement in lighting level improves night vision radically and studies show road lighting to be responsible for significant accident savings.

So it is understood that more light does not necessarily solve the problem of reducing accident rates. It can be explained now with the concept of veiling luminance and contrast. Because veiling luminance, which has an adverse effect on visibility, increases with the level of light increase. Contrast does not depend on the amount of lighting emitted from the light source but on the reflective property of the object and the pavement.

Design Criteria

Since 1947, the Roadway Lighting Committee (RLC) of the Illuminating Engineering Society of North America (IESNA) has publishes Recommended Standard Practices (RP) for roadway lighting. Until RP-8 (1983) was proposed roadway lighting design in North America was based on horizontal illumination of the emitted light. Actually what the night time driver sees is not governed by the amount of light that falls on the pavement, but on the amount of light that is reflected from the pavement surface in the direction of the driver. It was realized that pavement luminance and veiling luminance criteria provide a better correlation with the visual impression of roadway lighting quality and in RP-8 (1983) pavement luminance (including veiling luminance) was introduced as an alternative to illumination criteria. For high mast and pedestrian walkways illumination was proposed to be the only criterion for design.

In the draft RP-8 (1998), the concept of *Small Target Visibility* (*STV*) is proposed for roadway lighting design. This came from the realization that only pavement luminance is not sufficient to see an object. It is necessary to have a difference in luminance of object and background for the object to be visible. This difference in luminance has to have a certain minimum value for visibility. This difference with respect to a threshold luminance value is termed *Visibility Level* (*VL*). *VL* is one of the metrics for *STV*. In the draft RP-8 (1998), recommended design criteria for high-speed roadways is based on luminance. As an alternative, both *STV* and luminance (with a lesser value than the first one) criteria may be fulfilled. For the urban environment, a pavement luminance criterion is recommended.

Small Target Visibility Method

As already mentioned in the previous section, Small Target Visibility is the last recognized concept in roadway lighting design. To understand this concept the following terms are explained in details. The concept of *STV* will be described consequently. Illumination is the measure of the amount of light flux falling on a surface. It is independent of the direction from which the light comes, the type of light source and the type of surface upon which it falls. Mathematically, illumination may be defined as the luminous flux density per unit area at a point on a surface.

$$E = \frac{d\varphi}{dA},$$

Where, E = Illumination
φ = Radiant flux
A = Lighted area.

If the luminous intensity (I) of a light source is known, the illumination (E) at a distance D is given by:

$$E = \frac{I}{D^2}.$$

Common units of illumination are lux, foot-candle, and lm/m^2.

In the draft RP-8 (1998) standard practice, illumination design criteria include: Average Maintained Horizontal Illumination ($E_{H,avg}$) and Illumination Uniformity Ratio ($E_{H,avg} / E_{H,min}$).

Though the design of roadway lighting initiated with the criteria based on horizontal illumination, it was soon realized that pavement luminance and veiling luminance criteria provide a better correlation with the visual impression of roadway lighting quality. Because what we see is not due to the amount of light emitted from the source, but the amount of light that is reflected from the pavement surface.From mathematical point of view, luminance flux density per steradian emitted (reflected/ transmitted) by a unit area of surface in the direction of the observer is defined as Luminance.

$$L = \frac{dI}{dA\cos\theta} \text{ (Flux leaving)}$$

$$L = \frac{dE}{d\omega\cos\theta} \text{ (Flux arriving)}$$

Where, I = Luminous intensity
E = Illumination
L = Luminance
θ = Angle between line of sight and normal to the surface considered
ω = Solid angle through which flux from a point source is radiated
A = Lighted area.

Luminance is the measure of the amount and concentration of light flux leaving a surface. The luminance of a surface depends on the direction from which the light strikes the surface, the direction from which the surface is viewed and the reflective properties of the surface. The source of radiation is not an issue and it is the luminance that controls the magnitude of the sensation that is received by the brain. Commonly used units of luminance are candela/m^2, lambert, and foot-lambert.

Luminance at a point P (Figure 3.2) is proportional to the horizontal illumination at that point.

$$L_b \propto E_H .$$

To equate the relationship a proportionality factor $q(\gamma, \beta)$ which is called directional reflectance coefficient is introduced.

$$L_b = q(\gamma, \beta) \times E_H .$$

But,

$$E_H = \frac{I(\gamma, \varphi)}{D^2} \times \cos\gamma .$$

Where, I is the intensity of the light source in that direction and D is the distance from the point of interest (P) to the light source.

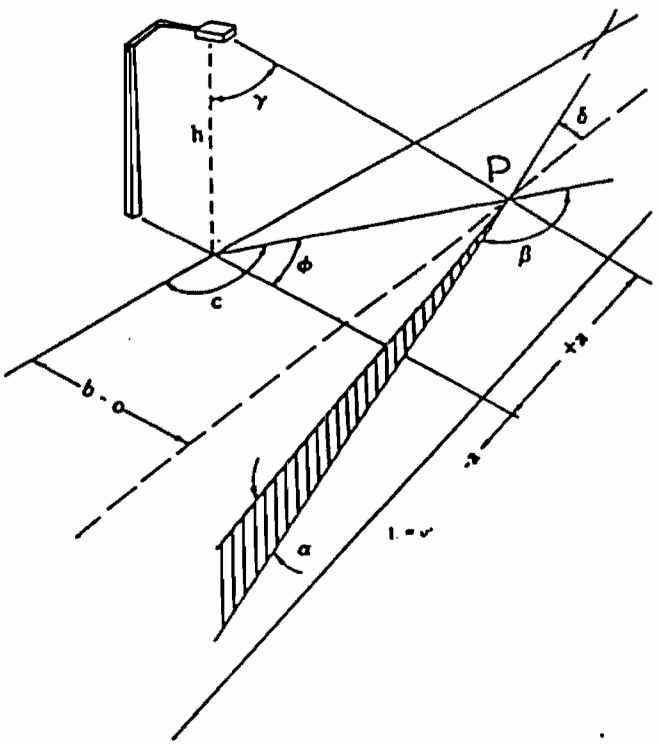

Figure 3.2. Angular relationships for calculating luminance for a single luminaire

Therefore, $L_b = \frac{q(\gamma,\beta) \times I(\gamma,\varphi)}{D^2} \times \cos\gamma$.

Substituting, $D = \frac{h}{\cos\gamma}$,

$$L_b = \frac{q(\gamma,\beta) \times I(\gamma,\varphi)}{h^2} \times \cos^3\gamma .$$

Introducing the light loss factor (LLF)

$$L_b = \frac{q(\gamma,\beta) \times I(\gamma,\varphi)}{h^2} \times \cos^3\gamma \times LLF .$$

When contribution of all the luminaires are taken into consideration, the following equation is formed.

$$L_b = \sum_{i=1}^{n} \frac{q(\gamma_i,\beta_i) \times I(\gamma_i,\varphi_i)}{h_i^2} \times \cos^3\gamma_i \times LLF_i$$

If SI units are used (L=cd/m^2 and I= cd), this value should be divided by π.

Since the purpose of a roadway lighting system is the improvement of nighttime roadway visibility, it would follow that the appropriate quantity and quality of fixed lighting should be designed on the basis of user-oriented visibility criteria. There are two visibility metrics, namely, *visibility index* introduced by Gallagher in 1975 (36, 37) and *visibility level* introduced by Adrian in 1989 (2).

Visibility Index (VI) of an object is the physical contrast multiplied by two correction factors. One factor is the relative contrast sensitivity (RCS) of an observer adapted to the luminance of the background. The second one is the disability glare factor (DGF), accounted for the loss in contrast due to glare. The *RCS* curve developed by Blackwell (1977) takes into account the effects of target size, observer age, target location and presentation time. The formula for *VI* is given by the following equation.

$VI = C \times RCS \times DGF,$

Where, C is the physical contrast defined as

$$C = \frac{L_t - L_b}{L_b} .$$

Here, L_t = Target Luminance
L_b = Background (pavement) luminance.

Luminance of a target is a function of the vertical illumination (E_v) from the luminaire in the layout directed toward the target and the directional reflectance of the target (ρ_t) toward the observer (Figure 3.2).

$$L_t = E_v \times \rho_t \sin\varphi ,$$

And, $$E_v = \frac{I(\gamma,\varphi)}{D^2} \times \sin\gamma ,$$

Where, I = Luminous intensity
D = Distance from the light source to the point
γ = (See Figure 3.2)
φ = (See Figure 3.2).

Therefore, $$L_t = \rho_t \times \frac{I(\gamma,\varphi)}{D^2} \times \sin\gamma \times \sin\varphi .$$

Substituting, $$D = \frac{(h - 0.5TH)}{\cos\gamma},$$

Where, h = Luminaire Mounting Height
TH = Target Height.

$$L_t = \rho_t \times \frac{I \times \sin\gamma \times \cos^2\gamma \times \sin\varphi}{(h - 0.5TH)^2} .$$

Visibility Level (VL) is defined as,

$$VL = \frac{L_t - L_b}{\Delta L}$$

The term in the denominator is termed as *Adrian's Delta L* and is the threshold luminance. It takes into account human factors such as driver age, observation time etc. ΔL is calculated in the following steps.

1. Determination of adaptation luminance which comprises of background luminance and discomfort glare. Adaptation luminance adjusts the eyes of the driver with the change of lighting level.
2. Determination of the sensitivity of the visual system as a function of adaptation luminance.
3. Adjustment in accordance with time of observation.
4. Adjustment for the age of the observer.
5. Adjustment for positive and negative contrast.

The previous equation may be re-written as this equation.

$$VL = \frac{(L_t - L_b)/L_b}{\Delta L / L_b} = \frac{C_{actual}}{C_{threshold}}.$$

Therefore, *VL* is equal to the ratio of actual and threshold contrast. Defined in this way, *VL* is simply the actual contrast with reference to the contrast required by the reference task. A *VL* of 5 means that for a given observer, a target's luminance contrast is 5 times the contrast needed for threshold perception. *VL* varies directly with target size and contrast, and inversely with the age of the observer. *VL* at a point does not bear any meaning and cannot describe a driving situation, but the average *VL* of a stretch of roadway in front of the driver could represent the quality of the lighting installation. Small Target Visibility (*STV*) is the weighted average *VL* calculated by incorporating the *VL*s of 20 standard targets per lane placed between two luminaires. The size of the targets is 18 cm square with a target reflectance of 50 %. The observer is assumed to look at an angle of 1° with the horizontal and each target is 273 ft. away from the observer.

Alternative Targets

To drive an automobile safely the operator must have sufficient lighting to evaluate information pertaining to the roadway, traffic and environmental conditions. The type and variety of visual tasks that must be evaluated include the following.

- Identification of the geometric conditions of the roadway, such as curves, grades, curbs, lane drops, and other physical features.
- Interpretation of operational controls such as signs, signals, markings, and channelization
- Identification of the potential hazards posed by objects on the pavement, such as potholes, bumps and other unexpected events.
- Justification of the speed, placement, and distances of other vehicles, pedestrians, and cyclists.

The size of the target may vary from a tractor-trailer to a small object lying on the road. The shape and composition also varies of the potential target. Published literature has suggested flat targets of different shape, size and composition. Lipinski, Keck, and Fies (1992) used some realistic objects such as a dog and a bicycle with different lighting arrangements. They measured the visibility level (*VL*) of these realistic tasks and compared them with *VL* of a small 18-cm square 20 % reflective target (Figure 3.3)

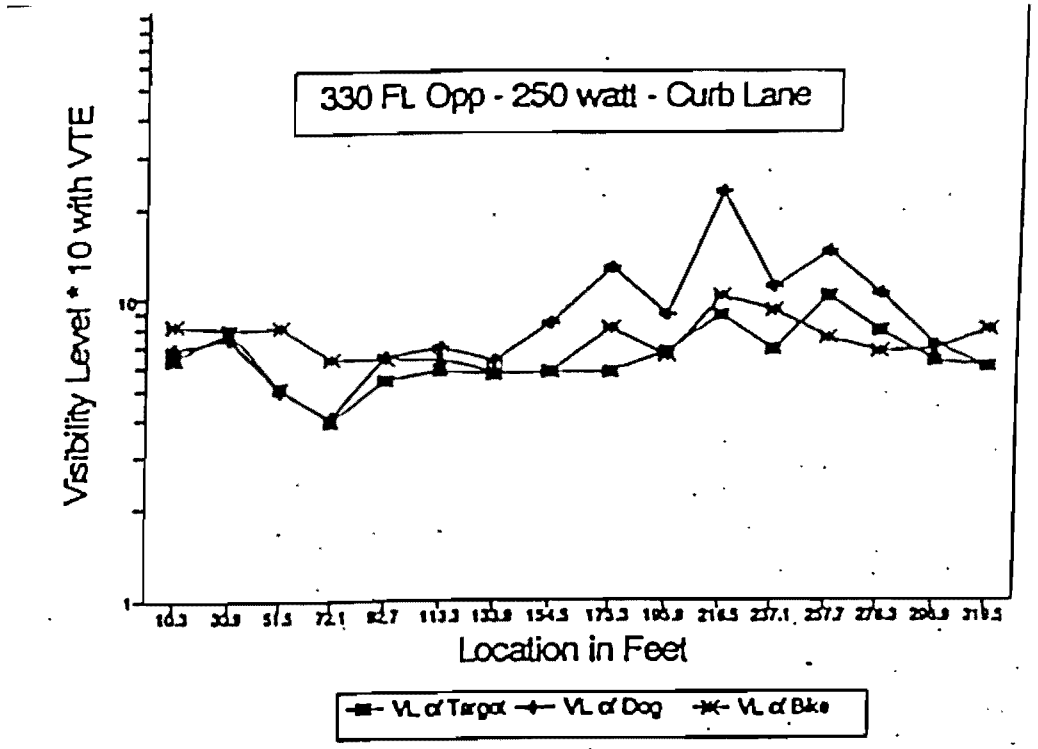

Figure 3.3. Comparison of VL of small target with some realistic objects. (*Lipinski et al., 1992)*

The results showed that the *VL* is lower for the small target, thus supporting the claim that small target visibility is a conservative measure of the visibility of realistic objects on the roadway.

Janoff and Havard (1997) conducted experiments with three target shapes including a flat target, a hemispherical target and a multifaceted target which was suggested by Lecocq(1993). This experiment produced a panel rating for a number of lighting installations. The visual performance task was then appraised as 'poor', 'fair' etc. by individual drivers and a mean panel rating (MPR) was calculated from the individual ratings.

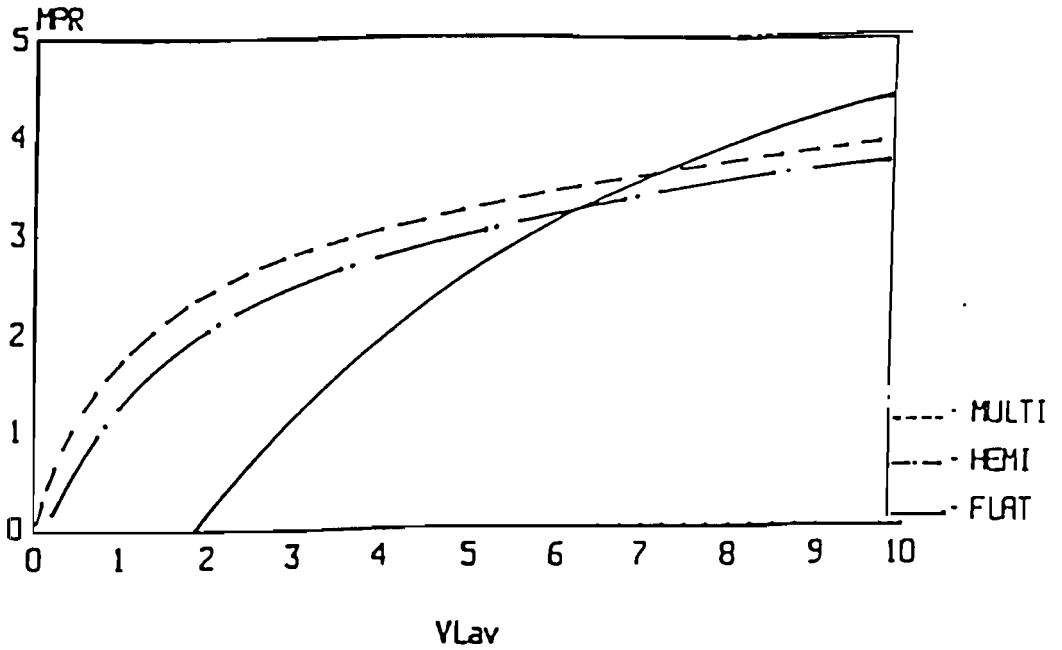

Figure 3.4. Visual performance task (in terms of Mean Panel Rating) for different types of targets (*Janoff and Havard, 1997*)

Results (Figure 3.4) show that the hemispherical and multifaceted targets behave rather similarly while the flat targets exhibit a different visibility pattern. These results seem to indicate that at lower levels of visibility, the hemispherical and multifaceted targets appear to be more visible to the test subjects, but as visibility increases, the flat targets appear to be more visible. The maximum visibility for the flat target was found to be greater than for other targets and the minimum visibility of flat target was found to be lesser than for other targets. It indicates that a much broader range of visibility for theflat target under the same set of lighting conditions prevails. Some indication was found that the hemispherical and multifaceted targets are less prone to disappear at contrast reversal locations on the roadway. This is based on the generally lower minimums exhibited by the flat targets and their lower *MPR*s at lower levels of visibility.

Safety in the driving task is the primary reason for the improvement of roadway lighting design. Therefore, the standard target used for design should be directly related to nighttime driving safety. A study done by Kahl and Fambro (1994) provides an excellent analysis of the comparison of targets to accidents. They found that only 0.07 percent of the reportable accidents were attributable to collisions with small objects and two percent of all accidents involved objects or animals on the roadway. 10.4 percent of the objects struck in urban areas and 1.8 percent of the objects struck in rural areas were less than 150 mm in height. They concluded that a small object is not the most critical standard target.

With regard to the reflectivity of objects, Smith (1938) showed that fifty percent of the pedestrian clothing has a reflectance coefficient of less than five percent and eighty percent of the clothing has a reflectance coefficient below fifteen percent.

Glare

The same luminaire that emits light and produces vision also emits rays of light directed to the eye of the observer, and as a result, produces a reduction in visual performance or a feeling of discomfort. This sensation produced by luminance within the visual field that is sufficiently greater than the luminance, to which the eyes are adapted to, is known as glare. In the roadway lighting scenario, glare can be a result of the lighting system, luminance of the pavement and the luminance of surrounding objects. Glare is subdivided into disability glare and discomfort glare.

Disability glare is the light within the eye that produces a veiling luminance (L_v) which is superimposed upon the retinal image of the object to be seen. This alters the apparent brightness of the object and the background against which it is viewed and causes a reduction in visual performance. L_v of a roadway lighting system can be calculated by using the following empirical formula derived for one single luminaire (35).

$$L_v = \frac{10E_v}{\theta^2 + 1.5\theta},$$

Where, E_v = Vertical illuminance in the plane of the pupil of the observer's eye.
θ = (See Figure 3.5).

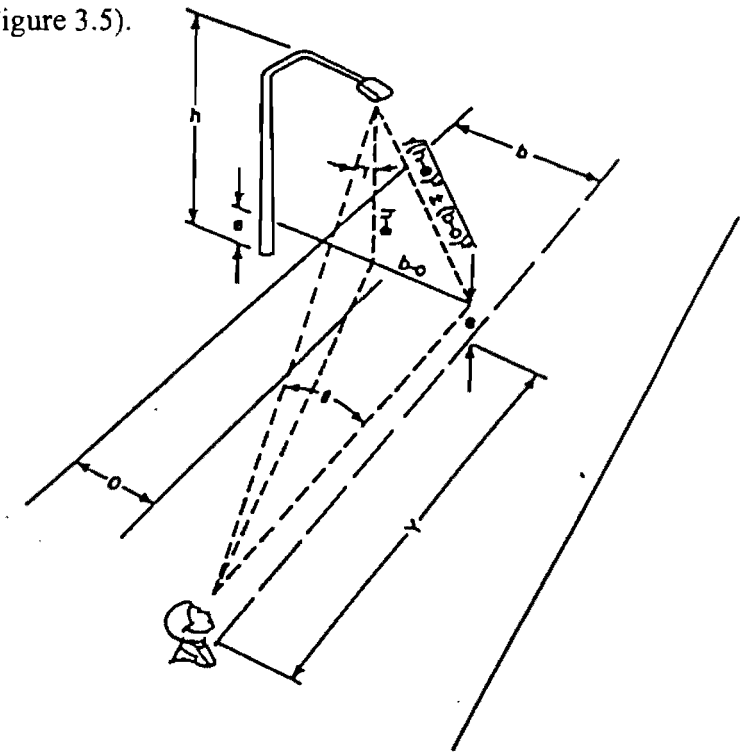

Figure 3.5. Angular relationship for calculating veiling luminance from a single luminaire

L_v can be measured at a particular location with a photo- electric telephotometer equipped with a special lens system in accordance with the above formula. Disability glare from the headlights of on coming cars can also be calculated and is considered in the proposed draft RP-8 (1998). Using an adaptation level for a rural county road of 0.034 cd /m^2 and a target contrast of 0.5, the

visibility of an object will be reduced by sixty five percent for veiling luminance resulting from the head lights of on coming vehicles (72).

Discomfort glare produces a sensation of ocular discomfort, which in its extreme form causes tears and pain. It may cause fatigue, which results in driving error. CIE has developed a graphical method of combining the discomfort glare from a number of luminaires, which results in a glare rating from 1 to 10. This is referred to as the *glare mark system*. In North America a method of combining the discomfort glare from a number of sources into a single factor called *Combined Brightness Effect (CBE)* has been developed (72). No field instrument has yet been invented to measure discomfort glare.

Light Loss Factor

The photometric data that is used in calculating illumination or luminance is obtained in laboratory conditions. But in the field, the performance of the luminaires deteriorates. Therefore, a multiplying factor, known as Light Loss Factor (*LLF*), is used in lighting calculations. This *LLF* is composed of separate factors, each of which is controlled and evaluated separately. Broadly *LLF* is divided into two categories. One is the *Maintenance Factor*, which is time dependent, and the other is the *Equipment Factor*, which does not depend on time. *Maintenance Factor* takes into account dirt accumulation on luminaire surface, lamp lumen depreciation and maintenance procedures. *Equipment Factor* relates mostly to the characteristics of the specific equipment selected. It takes into account factors such as temperature, voltage fluctuation, ballast variation, change in physical surroundings and surface depreciation resulting from adverse changes in metal, paint and plastic components which produce reduced light output.

Pavement Surface Reflection

The typical pavement surface is a mixture of aggregates and a binder with either Portland cement or asphalt acting as the binder. The type of aggregate used in pavement varies greatly and usually locally available materials are used. Sometimes, artificial aggregates are used to provide better skid resistance and light reflection characteristics. The light reflection properties of a pavement surface vary considerably with the types of materials use. Ketvirtis (1978) reported reflectances of ten percent and five percent for Portland cement concrete and asphalt concrete respectively. However, if a light color aggregate is used in the asphalt concrete, the reflectance may increase up to fifteen percent.

The pavement surface is generally a composite of particles, which are random in size and shape. The faces of these particles may reflect light either specularly or diffusely. Some particles may absorb light, and some are in the shadow due to their orientation (Figure 3.6).

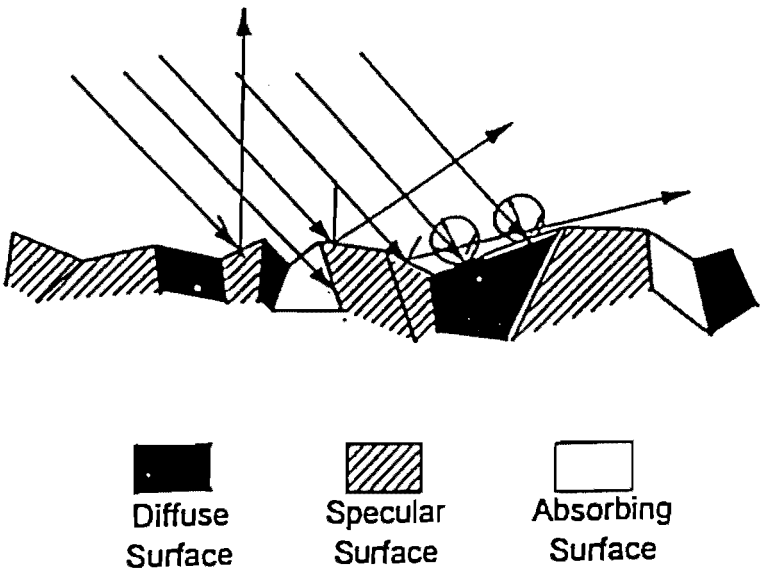

Figure 3.6. The reflection of light from small pavement particles

Mode of Reflection

The amount of light reflected from a particular surface depends upon the molecular condition or color of the surface and the wave length or color of the incident rays. Broadly, reflection by a surface can show three different modes (Figure 3.7).

1. Specular reflection: In ideal specular reflection, all luminous flux is reflected in an equal and opposite direction to the angle of incidence. The incident ray, the normal to the surface at the point of incidence and the reflected ray all lie in the same plane. Specular reflection is evident in smooth flat surfaces such as mirrors, highly polished metal surfaces and liquid surfaces.

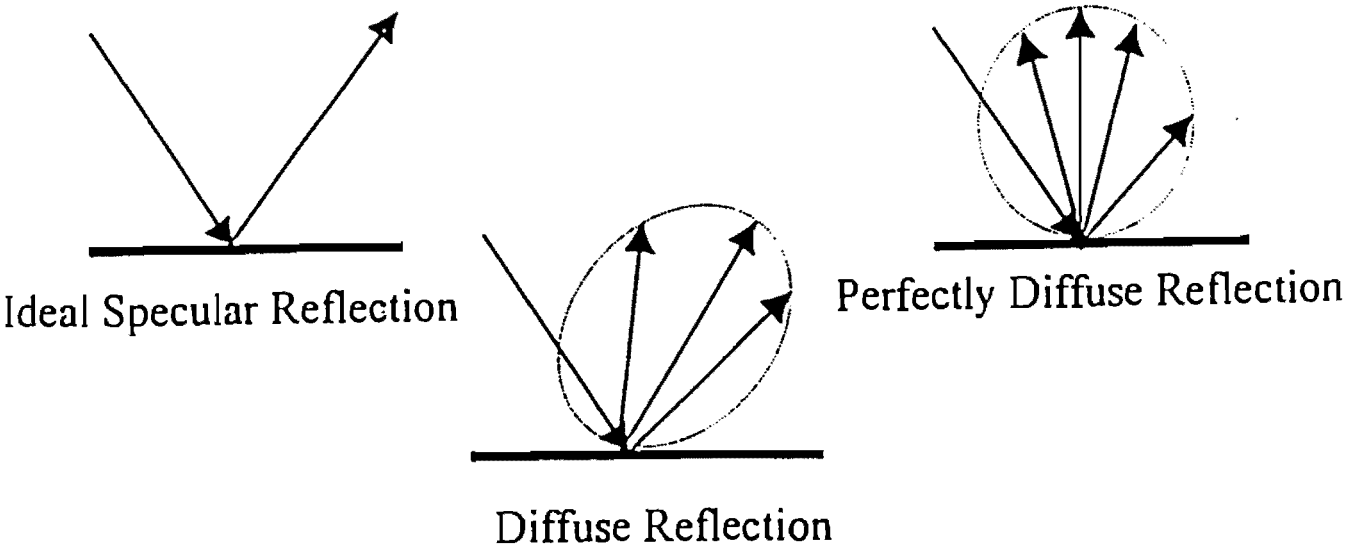

Figure 3.7. Luminous intensity distribution curves for different types of pavements

2. Diffuse reflection: If a material has a rough surface or is composed of minute crystals or pigment particles, the reflection is diffuse. Each single ray falling on an infinitesimal particle obeys the law of reflection, but as the surfaces of the particles are in different planes, they reflect light at many angles. Therefore, the reflection is independent of the angle of incidence. In a perfect diffuser, the intensity of reflected light varies only with the cosine of the angle between the normal of the surface and the direction of observation. This type of surface is known as a Lambertian surface. A Lambertian surface appears equally bright in all directions. Blotting paper, velvet, freshly fallen snow and heavily sandblasted opal glass achieve perfect diffuse reflection.

3. Mixed reflection: There is another type of surface that shows a reflection characteristic which is a combination of specular and diffuse reflection, resulting in light scattered in all directions, but a definite specular component also exists. Reflection from porcelain-enameled metal shows this tendency.

Reflection Indicatrix

When luminance factor q is plotted as a function of the angles γ and β in a direction opposite to the direction of light incidence, a three dimensional figure can be constructed as indicated in Figure 3.8. Such a figure is called a reflection indicatrix. This indicatrix can be formed by the locus of the points in any given direction (γ, β) from P. It is a line segment whose length is proportional to the luminance factor of the road surface at P when it is illuminated from the direction (γ, β) and viewed from O. The extent of the specular reflection caused by the surface is represented by the magnitude of the 'peak' of the indicatrix. For dry road surfaces a variety of reflection indicatrices are seen. They all have the shape of a *pear* with its apex at $\beta = 0$ and at large values of γ. Extreme cases of the indicatrix involve shapes with obtuse and sharp apex.

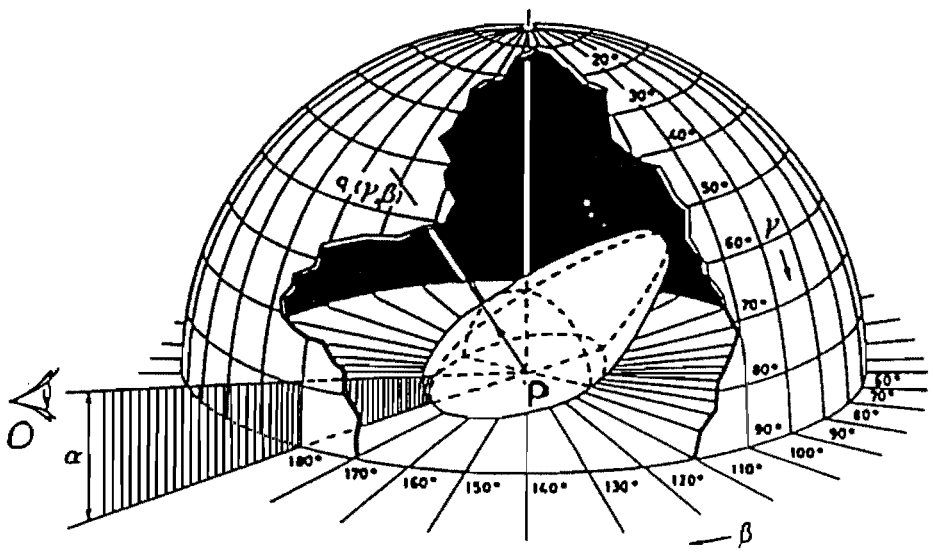

Figure 3.8. A typical reflection indicatrix

Basis for Roadway Classification Based on Reflectance Characteristics

For a single luminaire, the pavement luminance at a point is given by (Figure 3.2)

$$L_b = \frac{q(\gamma,\beta) \times I(\gamma,\varphi)}{h^2} \times \cos^3\gamma \, .$$

A reduced luminance coefficient $r(\gamma,\beta)$ is introduced where $r(\gamma,\beta) = q(\gamma,\beta)\cos^3\gamma$ so that,

$$L_b = \frac{r \times I}{h^2} \, .$$

The r-values can be shown as a two-dimensional array which is a function of the angles of γ and β. The array thus formed is called an r-table (see Figures 3.10-3.13).

An attempt has been made to approximate to the reflection properties of a road surface by employing a small number of characteristic quantities. It has been found that most surfaces can be reasonably well characterized by the *total reflection* and the *shininess*. Analogously, the terms *average luminance factor* (Q_0) and *specular factor* ($S1$ and $S2$) have been introduced to characterize road surfaces (21).

Where, $$Q_0 = \frac{\iint_\Omega q \, d\gamma \, d\beta}{\iint_\Omega d\gamma \, d\beta} \, ,$$

$$S1 = \frac{r(\beta = 0, \tan\gamma = 2)}{r(\beta = 0, \tan\gamma = 0)} \, ,$$

$$S2 = \frac{Q_0}{r(\beta = 0, \tan\gamma = 0)} \, .$$

It would seem at first sight to be obvious and reasonable to determine the average luminance factor Q_0 by averaging the values of q over a hemisphere, since a hemisphere can be considered as the locus of all possible positions of a luminaire which could make a contribution to Q_0. However the whole hemisphere is not needed in practice. The averaging of q therefore occurs over a part of the hemisphere denoted by Ω. Ω is the solid angle containing all directions in which the light from a luminaire at a height h above a flat road can strike the road within an area extending $4h$ beyond the luminaire (away from the observer), $12h$ before the luminaire and $3h$ on either side. Q_0 is very difficult to measure. But it may be approximated in an alternative way (see Figure 3.9). If the average illumination and the average luminance are measured for the part of

the road surface corresponding to the solid angle Ω used in the definition of Q_0, then Q_0 is given directly by the ratio of these two quantities (14).

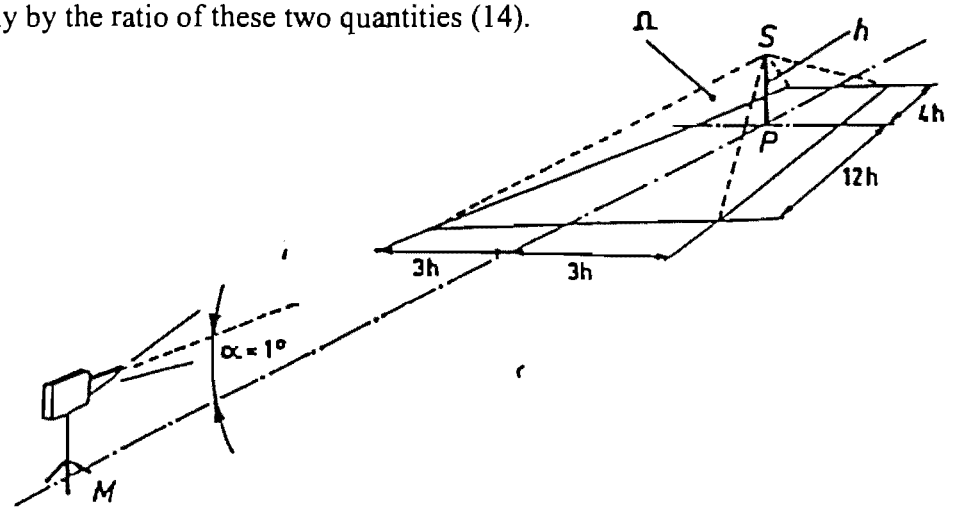

Figure 3.9. Simplified method for the determination of Q_0

The factors *S1* and *S2* are used to define the reflection character of the pavement. *S1* is the ratio of an r-value which is generally large for specular reflection (*r(0,2)*) to a factor which is generally large for diffuse reflection (*r(0,0)*). Thus *S1* is a measure of the degree of specular reflection. Similarly *S2* is the ratio between the average luminance factor to a value which is large for diffuse reflection.

It may be shown that there exists a strong correlation between *S1* and *S2* (74). *S1* and *S2 are* by no means independent parameters and consequently *S2* adds little or no information to that already carried by *S1* and vice versa. Investigations also show that Q_0 and *S2* are also strongly correlated. Therefore, it is logical to abandon *S2* from the criteria of characterizing road surfaces. Both Q_0 and *S1* can be measured by LTL 200 portable road surface reflectometer (13).

Roadway Reflection Classification Systems

CIE (Commission Internationale de I' Eclairage) is the most recognized international organization in the field of lighting. CIE successfully introduced two classification systems for dry road surfaces to facilitate luminance calculations at the design stage.

De Boer and Vermeulen developed the R-system in 1967. It comprises four classes RI, RII, RIII, RIV and the corresponding standard r- tables R1, R2, R3, R4. The r-tables for these surfaces are shown in Figures 3.10-3.13 along with the contour diagrams of the r-values. The contour diagrams were developed as an aid to this thesis and indicate the change of r-values. Here the observer looks along the Y-axis, while the light source is at an angle β with Y-axis at the origin. The r-values are symmetrical about the Y-axis. Getting the value of $r(\gamma,\beta)$ for a particular point on the pavement surface and the corresponding I-value from the photometric data one can readily calculate the pavement luminance at that point.

The C-system was developed by Burghout and optimized by Bommel. It comprises of two classes CI and CII and the corresponding r-tables are similar to R1 and R2, R3, R4 for C1 and C2, respectively.
Classes CI and RI cover bituminous concrete road surfaces with more than thirty- percent brighteners and cement concrete surfaces in good condition. All other dry road surfaces belong to the other classes. A general feature of different types of road surfaces is given in Table 3.1 and their parameters adopted by CIE are given in Table 3.2.

Erbay (1974) introduced another system where any pavement can be assigned a number, which is known as *Erbay Number.* This number is based on *S1* and *S2.*

Table 3.1. Road surface classification description (21)

Class	Q_0	Description	Mode of reflectance
R1	0.10	Portland cement concrete road surface. Asphalt road surface with a minimum of 15 % of the affregates composed or artificial brightener aggregates (labrodorite, quarzite)	Mostly diffuse
R2	0.07	Asphalt road surface with an aggregate composed of minimum 60 % gravel (size greater than 10 mm). Asphalt road surface with 10 to 15 % artificial brightener in aggregate mix. (Not normally used in North America)	Mixed (Diffuse and specular)
R3	0.07	Asphalt road surface (regular and carpet seal) with dark aggregate (e.g. traprock, blast furnace slag) rough structure after months in use (typical highway)	Slight specular
R4	0.08	Asphalt road surface with a very smooth texture	Mostly specular

Table 3.2. Parameters of the R-and C- classification systems (21)

Class	Limitation	Standard	S1	Q_0
RI	S1<0.42	R1	0.25	0.10
RII	0.42<S1<0.85	R2	0.58	0.07
RIII	0.85<S1<1.35	R3	1.11	0.07
RIV	S1≥1.35	R4	1.55	0.08
CI	S1<0.4	C1	0.24	0.10
CII	S1≥0.4	C2	0.97	0.07

Quality Criteria for Roadway Lighting

When the question of quality criteria for roadway lighting comes into picture one should actually be able to compare r-tables. Since each r-table consists of 396 data points, such a comparison is really difficult. As a simpler criterion the luminances may be chosen which occur in corresponding points on the pavement surface when applying the relevant pavement surfaces in a

roadway lighting installation. Since even comparing luminances in corresponding points of a grid is fairly complicated, the comparison procedure has been further simplified to a comparison of the quality criteria of roadway lighting which involve the pavement surface.
Luminance calculations for numerous roadway lighting installations have shown that Q_0 is highly correlated with the average luminance $\bar{L}$ on the road.

Where, L_p is the luminance at point P and A is the relevant portion of the road area, usually restricted to one luminaire spacing. $\bar{L}$ is measured with the portable luminance meter described by Morass and Renld (1967).

In addition to $\bar{L}$, CIE adopted two measures of luminance uniformity as quality criteria for roadway lighting.

1. The overall uniformity of luminance U_0 defined by the following equation.

$$U_0 = \frac{L_{\min}}{\bar{L}}$$

θ Lm Y	0	2	5	10	15	20	25	30	35	40	45	60	75	90	105	120	135	150	165	180
0	655	655	655	655	655	655	655	655	655	655	655	655	655	655	655	655	655	655	655	655
0.25	619	619	619	619	610	610	610	610	610	610	610	610	610	601	601	601	601	601	601	601
0.5	539	539	539	539	539	539	521	521	521	521	521	503	503	503	503	503	503	503	503	503
0.75	431	431	431	431	431	431	431	431	431	431	395	386	371	371	371	371	371	386	395	395
1	341	341	341	341	323	323	305	296	287	287	278	269	269	269	269	269	269	278	278	278
1.25	269	269	269	260	251	242	224	207	198	189	189	180	180	180	180	180	189	198	207	224
1.5	224	224	224	215	198	180	171	162	153	148	144	144	139	139	139	144	148	153	162	180
1.75	189	189	189	171	153	139	130	121	117	112	108	103	99	99	103	108	112	121	130	139
2	162	162	157	135	117	108	99	94	90	85	85	83	84	84	86	90	94	99	103	111
2.5	121	121	117	95	79	66	60	57	54	52	51	50	51	52	54	58	61	65	69	75
3	94	94	86	66	49	41	38	36	34	33	32	31	31	33	35	38	40	43	47	51
3.5	81	80	66	46	33	28	25	23	22	22	21	21	22	22	24	27	29	31	34	33
4	71	69	55	32	23	20	18	16	15	14	14	14	15	17	19	20	22	23	25	27
4.5	63	59	43	24	17	14	13	12	12	11	11	11	12	13	14	14	16	17	19	21
5	57	52	36	19	14	12	10	9.0	9.0	8.8	8.7	8.7	9.0	10	11	13	14	15	16	16
5.5	51	47	31	15	11	9.0	8.1	7.8	7.7	7.7										
6	47	42	25	12	8.5	7.2	6.5	6.3	6.2											
6.5	43	38	22	10	6.7	5.8	5.2	5.0												
7	40	34	19	8.1	5.6	4.8	4.4	4.2												
7.5	37	31	15	6.9	4.7	4.0	3.8													
8	35	28	14	5.7	4.0	3.6	3.2													
8.5	33	25	12	4.8	3.6	3.1	2.9													
9	31	23	10	4.1	3.2	2.8														
9.5	30	22	9.0	3.7	2.8	2.5														
10	29	20	8.2	3.2	2.4	2.2														
10.5	28	18	7.3	3.0	2.2	1.9														
11	27	16	6.6	2.7	1.9	1.7														
11.5	26	15	6.1	2.4	1.7															
12	25	14	5.6	2.2	1.6															

*All values have been multiplied by 10,000.

Q0 = 0.10; S1 = 0.25; S2 = 1.53

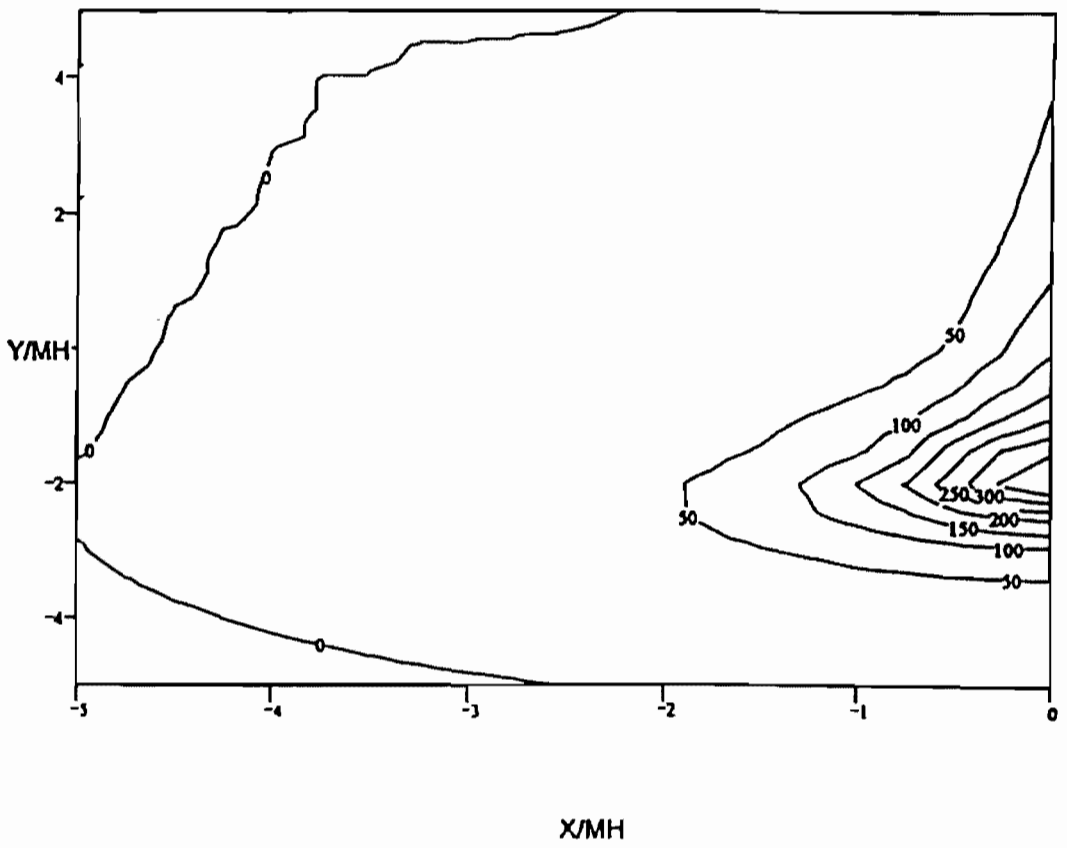

Figure 3.10. R-table and contour diagram of the r-values for standard R1 class

θ Lin Y	0	2	5	10	15	20	25	30	35	40	45	60	75	90	105	120	135	150	165	180
0	390	390	390	390	390	390	390	390	390	390	390	390	390	390	390	390	390	390	390	390
0.25	411	411	411	411	411	411	411	411	411	411	379	368	357	357	346	348	346	335	335	335
0.5	411	411	411	411	403	403	384	379	370	346	325	303	281	281	271	271	271	260	260	260
0.75	379	379	379	368	357	346	325	303	281	260	238	216	205	206	206	206	206	206	206	206
1	335	335	335	325	292	291	260	238	216	195	173	152	152	152	152	152	141	141	141	141
1.25	303	303	292	271	238	206	184	152	130	119	108	100	103	106	108	108	114	114	119	119
1.5	271	271	260	227	179	152	141	119	108	93	80	76	76	80	84	87	89	91	93	95
1.75	249	238	227	195	152	124	106	91	78	67	61	52	54	58	63	67	69	71	73	74
2	227	216	195	152	117	95	80	67	61	52	45	40	41	45	49	52	54	56	57	58
2.5	195	190	146	110	74	58	48	40	35	30	27	24	26	28	30	33	35	38	40	41
3	160	155	115	67	43	33	28	21	18	17	16	16	17	17	18	21	22	24	26	27
3.5	146	131	87	41	25	18	15	13	12	11	11	11	11	11	12	14	15	17	18	21
4	132	113	67	27	15	12	10	9.4	8.7	8.2	7.9	7.8	7.9	8.7	9.6	11	12	13	15	17
4.5	118	95	50	20	12	8.9	7.4	6.6	6.3	6.1	5.7	5.6	5.8	6.3	7.1	8.4	10	12	13	14
5	106	81	38	14	8.2	6.3	5.4	5.0	4.8	4.7	4.5	4.4	4.8	5.2	6.2	7.4	8.5	9.5	10	11
5.5	96	69	29	11	6.3	5.1	4.4	4.1	3.9	3.8										
6	87	58	22	8.0	5.0	3.9	3.5	3.4	3.2											
6.5	78	50	17	6.1	3.8	3.1	2.8	2.7												
7	71	43	14	4.9	3.1	2.5	2.3	2.2												
7.5	67	38	12	4.1	2.6	2.1	1.9													
8	63	33	10	3.4	2.2	1.8	1.7													
8.5	58	28	8.7	2.9	1.9	1.6	1.5													
9	55	25	7.4	2.5	1.7	1.4														
9.5	52	23	6.5	2.2	1.5	1.3														
10	49	21	5.8	1.9	1.4	1.2														
10.5	47	18	5.0	1.7	1.3	1.2														
11	44	16	4.4	1.6	1.2	1.1														
11.5	42	14	4.0	1.5	1.1															
12	41	13	3.6	1.4	1.1															

*All values have been multiplied by 10,000.

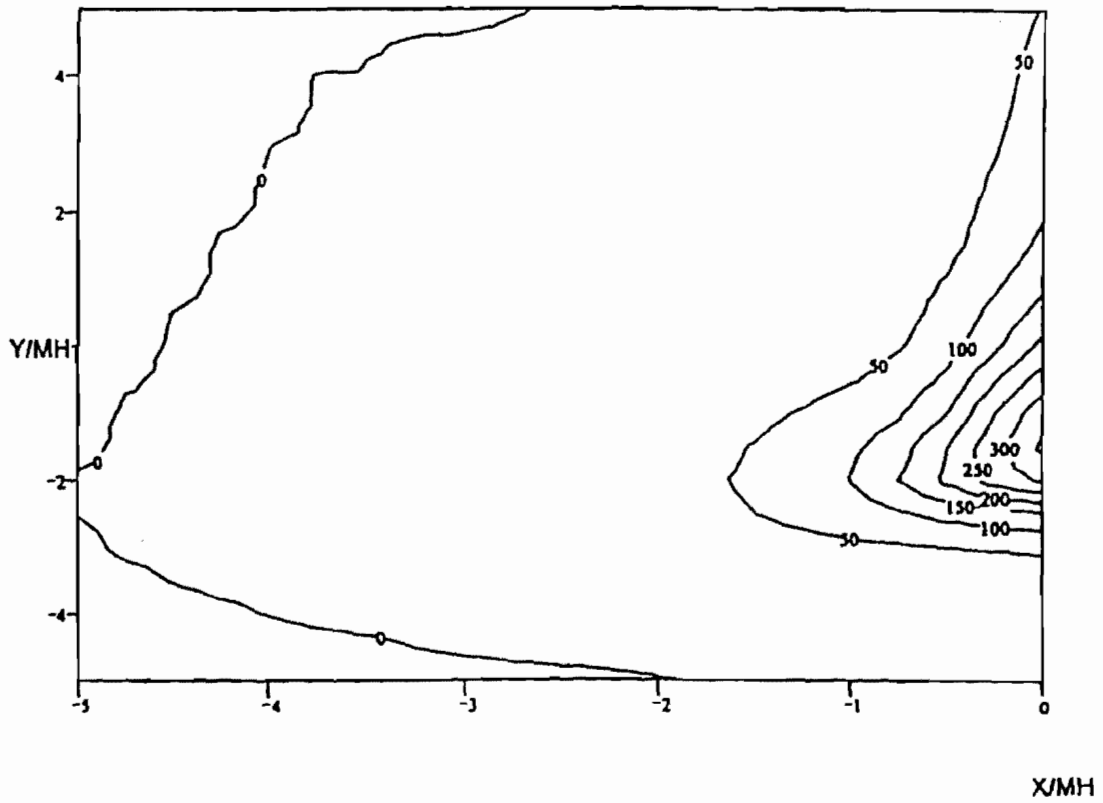

Figure 3.11. R-table and contour diagram of the r-values for standard R2 class

θ Lan Y	0	2	5	10	15	20	25	30	35	40	45	60	75	90	105	120	135	150	165	180
0	294	294	294	294	294	294	294	294	294	294	294	294	294	294	294	294	294	294	294	294
0.25	326	326	321	321	317	312	308	308	303	298	294	280	271	262	258	253	249	244	240	240
0.5	344	344	339	339	326	317	308	298	289	276	262	235	217	204	199	199	199	199	194	194
0.75	357	353	353	339	321	303	285	267	244	222	204	176	158	149	149	149	145	136	136	140
1	362	362	352	326	276	249	226	204	181	158	140	118	104	100	100	100	100	100	100	100
1.25	357	357	348	298	244	208	176	154	136	118	104	83	73	70	71	74	77	77	77	78
1.5	353	348	326	267	217	176	145	117	100	86	78	72	60	57	58	60	60	60	61	62
1.75	339	335	303	231	172	127	104	89	79	70	62	51	45	44	45	46	45	45	46	47
2	326	321	280	190	136	100	82	71	62	54	48	39	34	34	34	35	36	36	37	38
2.5	289	280	222	127	86	65	54	44	38	34	25	23	22	23	24	24	24	24	24	25
3	253	235	163	85	53	38	31	25	23	20	18	15	15	15	15	15	16	16	17	17
3.5	217	194	122	60	35	25	22	19	16	15	13	9.9	9.0	9.0	9.9	11	11	12	12	13
4	190	163	90	43	26	20	16	14	12	9.9	9.0	7.4	7.0	7.1	7.5	8.3	8.7	9.0	9.0	9.9
4.5	163	136	73	31	20	15	12	9.9	9.0	8.3	7.7	5.4	4.8	4.9	5.4	6.1	7.0	7.7	8.3	8.5
5	145	109	60	24	16	12	9.0	8.2	7.7	6.8	6.1	4.3	3.2	3.3	3.7	4.3	5.2	6.5	6.9	7.1
5.5	127	94	47	18	14	9.9	7.7	6.9	6.1	5.7										
6	113	77	36	15	11	9.0	8.0	6.5	5.1											
6.5	104	68	30	11	8.3	6.4	5.1	4.3												
7	95	60	24	8.5	6.4	5.1	4.3	3.4												
7.5	87	53	21	7.1	5.3	4.4	3.6													
8	83	47	17	6.1	4.4	3.6	3.1													
8.5	78	42	15	5.2	3.7	3.1	2.6													
9	73	38	12	4.3	3.2	2.4														
9.5	69	34	9.9	3.8	3.5	2.2														
10	65	32	9.0	3.3	2.4	2.0														
10.5	62	29	8.0	3.0	2.1	1.9														
11	59	26	7.1	2.6	1.9	1.8														
11.5	56	24	6.3	2.4	1.8															
12	53	22	5.6	2.1	1.8															

*All values have been multiplied by 10,000

Q0 = 0.07; S1 = 1.11; S2 = 2.38

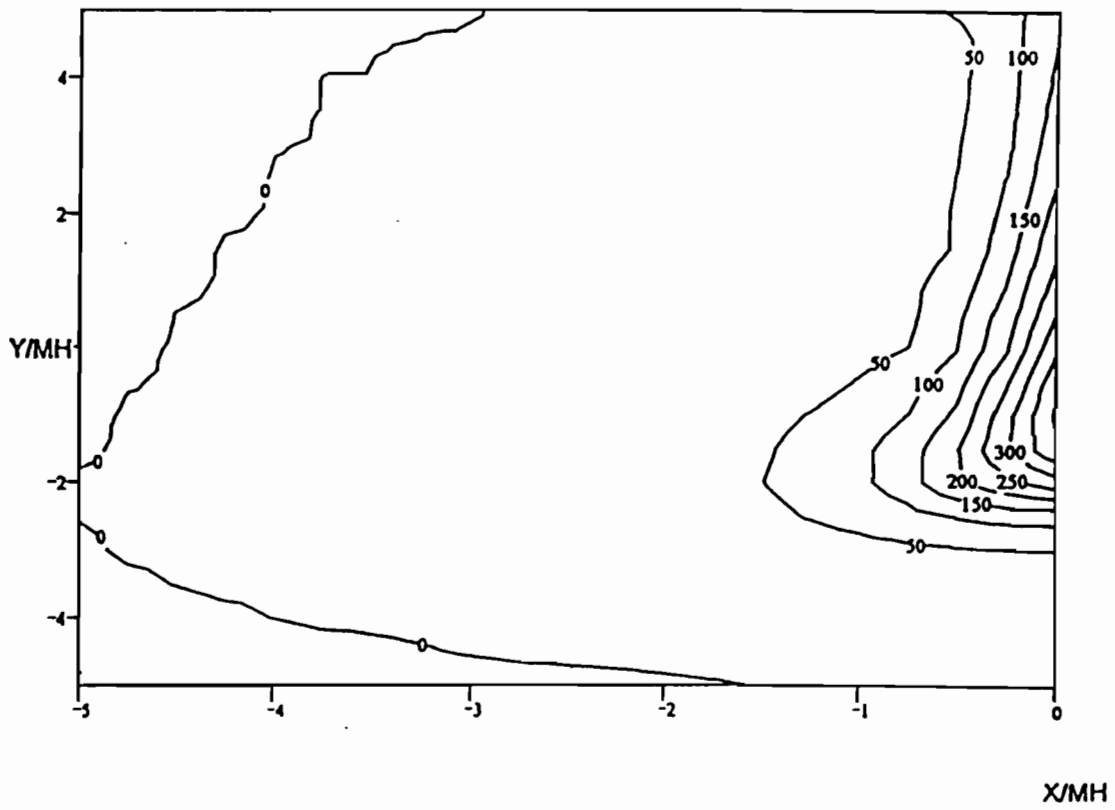

Figure 3.12. R-table and contour diagram of the r-values for standard R3 class

θ Un Y	0	2	5	10	15	20	25	30	35	40	45	60	75	90	105	120	135	150	165	180
0	264	264	264	264	264	264	264	264	264	264	264	264	264	264	264	264	264	264	264	264
0.25	297	317	317	317	317	310	304	290	284	277	271	244	231	224	224	218	218	211	211	211
0.5	330	343	343	343	330	310	297	284	277	264	251	218	198	185	178	172	172	165	165	165
0.75	376	383	370	350	330	304	277	251	231	211	198	165	139	132	132	125	125	125	119	119
1	396	396	396	330	290	251	216	198	185	165	145	112	86	86	86	86	86	87	87	87
1.25	403	409	370	310	251	211	178	152	132	115	103	77	66	65	65	63	65	66	67	68
1.5	409	395	356	284	218	172	139	115	100	88	79	61	50	50	50	50	52	55	55	55
1.75	409	396	343	251	178	139	106	88	75	66	59	44	37	37	37	38	40	41	42	45
2	409	383	317	224	145	106	86	71	59	53	45	33	29	29	29	30	32	33	34	37
2.5	396	356	264	152	100	73	55	45	37	32	28	21	20	20	20	21	22	24	25	26
3	370	304	211	85	63	44	30	25	21	17	16	13	12	12	13	13	15	16	17	19
3.5	343	271	165	63	40	26	19	15	13	12	11	9.8	8.1	8.8	8.8	8.4	11	12	13	15
4	317	238	132	45	24	16	13	11	9.6	9.0	8.4	7.5	7.4	7.4	7.5	7.9	8.6	9.4	11	12
4.5	297	211	106	33	17	11	9.2	7.9	7.3	6.6	6.3	6.1	6.1	6.2	6.5	6.7	7.1	7.7	8.7	9.6
5	277	185	79	24	13	8.3	7.0	6.3	5.7	5.1	5.0	5.0	5.1	5.4	5.5	5.8	6.1	6.3	6.9	7.7
5.5	257	161	59	19	9.9	7.1	5.7	5.0	4.6	4.2										
6	244	140	46	13	7.7	5.7	4.8	4.1	3.8											
6.5	231	122	37	11	5.8	4.6	3.7	3.2												
7	218	106	32	9.0	5.0	3.8	3.2	2.6												
7.5	205	94	26	7.5	4.4	3.3	2.8													
8	193	82	22	6.3	3.7	2.9	2.4													
8.5	184	74	19	5.3	3.2	2.5	2.1													
9	174	66	16	4.8	2.8	2.1														
9.5	169	59	13	4.1	2.5	2.0														
10	164	53	12	3.7	2.2	1.7														
10.5	158	49	11	3.3	2.1	1.7														
11	153	45	9.5	3.0	2.0	1.7														
11.5	149	41	8.4	2.6	1.7															
12	145	37	7.7	2.5	1.7															

O0 = 0.08; S1 = 1.55; S2 = 3.03

*All values have been multiplied by 10,000.

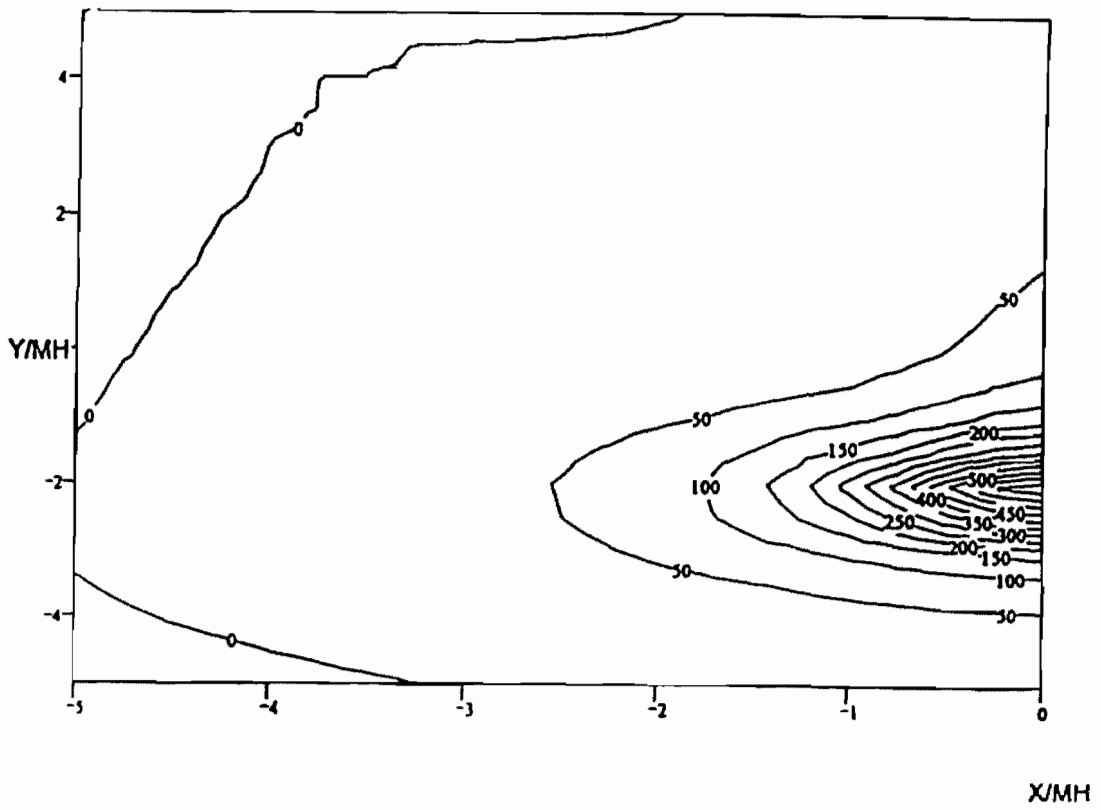

Figure 3.13. R-table and contour diagram of the r-values for standard R4 class

$$\bar{L} = \frac{1}{A}\int_0^A L_p dA,$$

2. The lengthwise uniformity along the observation line on the road U_l defined by,

$$U_0 = \frac{L_{min}}{L_{max}}$$

In accordance with CIE (1975) the following order of importance is attached to the quality criteria of roadway lighting as far as road surface luminance is concerned.

- $\bar{L}$ because of its large influence on adaptation, glare limitation, economy and energy consumption
- U_0 for the safety aspect of uniformity
- U_l for the comfort aspect of uniformity

Relationship between Reflection Properties and Composition of Surface Layer

The r-tables used by CIE contain the actually measured, reduced luminance coefficients of a road surface. In an investigation conducted by Schreuder, Schram, Burghout, Kreeft and Tom (1984) the r-tables have moreover been reduced in such a manner that the luminance coefficient at perpendicular light incidence q_p is equal to one. This has been done in order to eliminate possible differences in calibration between the various laboratories from which the r-tables originated. Data used in this investigation were available from 103 asphalt concrete road surfaces, including those containing pre-coated chipping, 5 cement concrete road surfaces and 57 surface dressings.

For asphalt concrete road surfaces, no systematic relationship was observed between $S1$ and q_p and also no relationship was found for the type of bituminous surfacing. Only Portland cement concrete road surfaces were found to appear solely in class CI. Therefore it may be concluded that the relationship between reflection and composition is determined only by the aggregate used. Also, the applied ratio between the quantities of bitumen and aggregate appears to influence the resultant reflection properties.

To find out the relationship between applied aggregate and the resultant reflection properties both the shapes and the size of reflection indicatrix should be taken into account. Therefore, pavement surfaces are compared according to the values of $\bar{L}$, U_0 and U_l. Investigations show that the relative performance in terms of $\bar{L}$, U_0 and U_l is independent of lighting arrangement, luminous intensity distribution of the luminaries and spacing to mounting height ratio (Burghout, 1979).

In asphalt concrete road surfaces where the usual aggregate has partly been replaced by white chipping, a clear relationship was found between the percentage of the total mineral aggregate, which consists of white chipping and $\bar{L}$ (Figure 3.14). At less than thirty percent white chipping contents $\bar{L}$ appears to increase steeply with increasing percentage of white chipping. The position of the points in the diagram appears to depend neither on the type of white chipping nor on the size of the aggregate grading of the chipping.

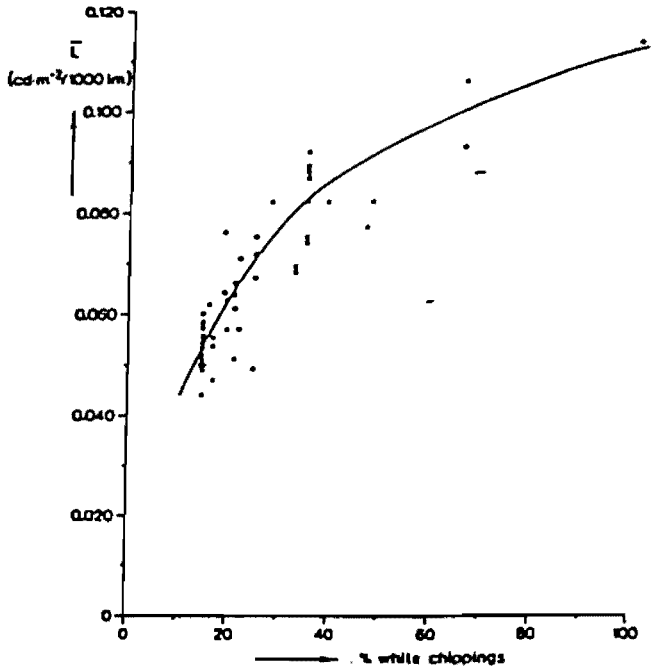

Figure 3.14. Mean luminance of an asphalt concrete road surface as a function of the percentage of the mineral aggregate which consists of white chipping (74).

A further analysis of the data show that asphalt road surfaces containing thirty percent or more white chipping will belong to class CI and thus have relatively good uniformity data. Asphalt concrete surfaces without white chipping hardly show a relationship between the applied quantity of chipping and $\bar{L}$.

The application of white chipping in the case of surface courses appears to show higher values of $\bar{L}$. It may be expected that the application of these chipping for surface dressings would lead to even better photometric results because the amount of chipping per unit area on the surface is greater than pre coated chipping.

Effects of Wear and Composition on Pavement Surface Reflection Properties

Bodmann and Schmidt (1988) carried out an experiment to see the temporal and local variations of road surface reflection. The selected streets differed in the age of the road surface and the volume of traffic but were similar in composition (bituminous concrete). Measurements of Q_0 and SI were taken at intervals of two to four months over a period of three years. With the results from five streets measured over the same period the average reduction was 3.5 percent for Q_0 and 12.6 percent for SI. Overall Q_0 appears to be more stable than SI. Streets of less age and less traffic show much stability in both Q_0 and SI values when compared with older streets and of more traffic volume. A single old street with higher traffic volume falls in different classes at different time. Furthermore Q_0 tends to increase during summer and decrease during winter.

The wheels of cars and trucks produce glossy stripes along the wheel paths. At the border and in the middle of the road the surface remains rough. A standard r-table does not take account of such a variety of appearances. Figure 3.15 (which is from the above mentioned study) shows that, for the row left of the center line on the lane which is contained in the glossy stripe, considerably higher SI values are measured as compared with those from the rest of the lane. Similarly, the Q_0 values are considerably higher for most points of the row.

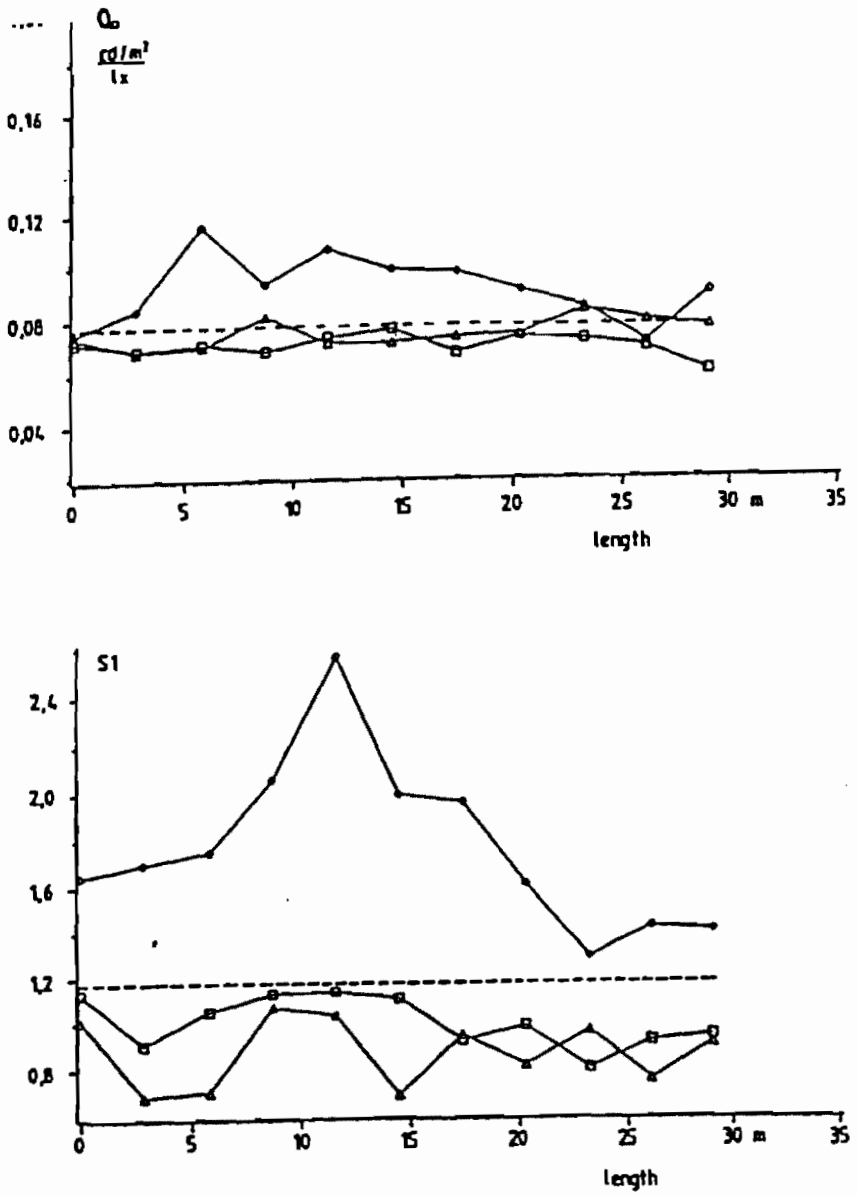

Figure 3.15. Local variations of Q_0 and $S1$ along a street (◆ points are along the wheelpath while ■ points are between wheelpath and ▲points are beside the edge of the road, but outside the wheelpath; ----- is the total means of measurements) (*Bodmann and Schmidt, 1988*)

The temporal development of Q_0 and $S1$ for new samples representing quartzite, basalt and a mixture of both minerals measured over an exposure period of 38 months is shown in Figure 3.16. The drastic change during the first 4 to 6 months reflects the erosion of bituminous films, whereas decrease in Q_0 and $S1$ thereafter may be explained due to grinding and cracking of mineral stones. At the end of the exposure period there was a temporary increase and then decrease of Q_0 and $S1$, which is due to the very hot summer of 1982.

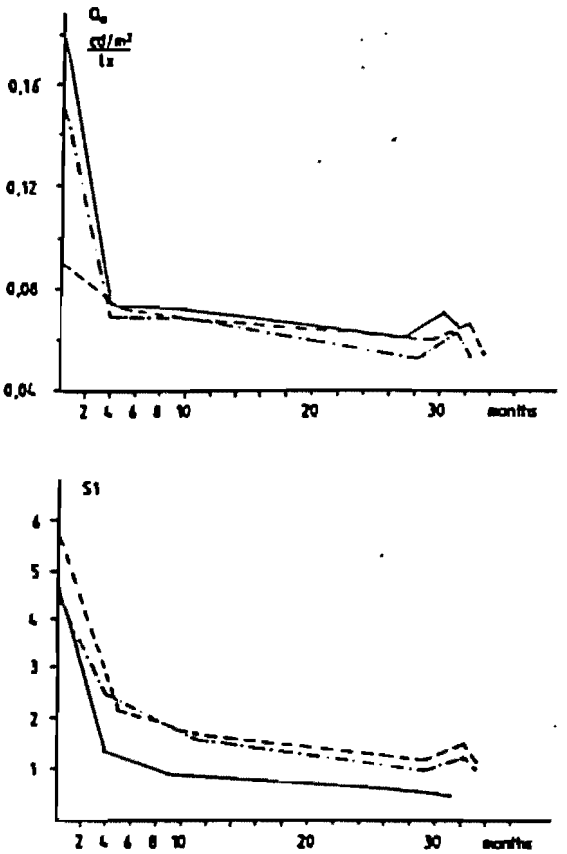

Figure 3.16. Temporal course of Q_0 and $S1$ of three road samples with increasing exposure period in a city street (*Bodmann and Schimidt, 1988*)

The impact of weathering on luminance characteristics $\bar{L}$, U_0 and U_l for the same samples are shown in Figure 3.17. In the initial state of the road samples $\bar{L}$ is high and U_0 is poor. With increasing exposure $\bar{L}$ decreases rapidly while U_0 and U_l arrive at a level that does not change very much with continuing exposure.

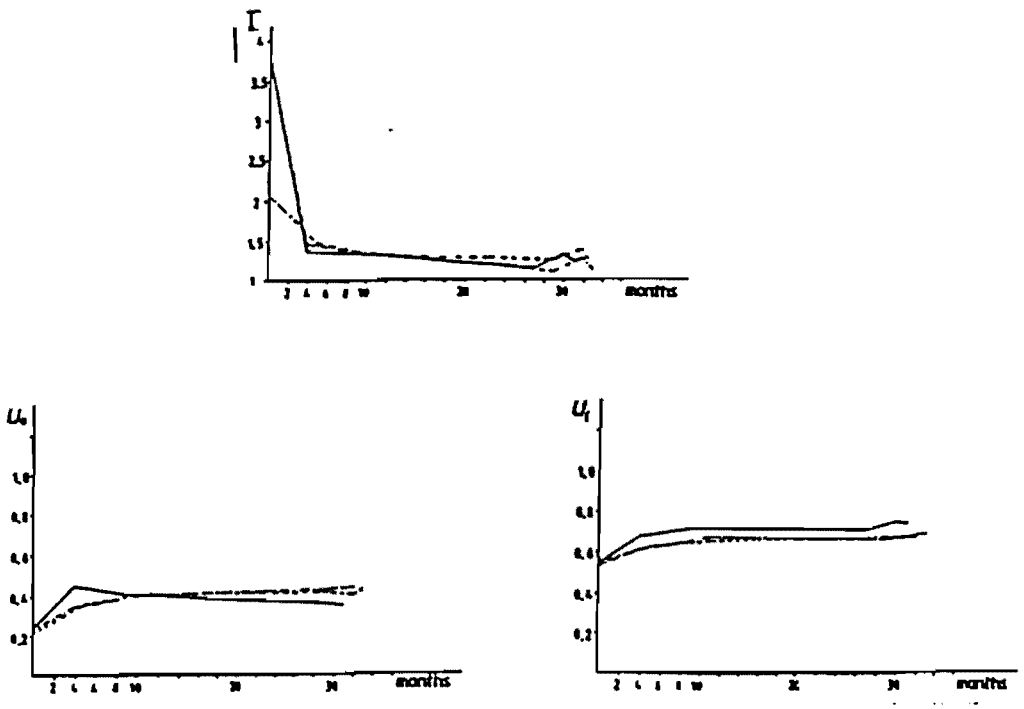

Figure 3.17. Temporal course of $\bar{L}$, U_0 and U_l calculated for a one sided lighting installation (*Bodmann and Schimidt, 1988*)

Measurement of Pavement Reflectance

King and Finch (1967) developed a pavement reflectometer for measuring the directional reflectance properties of pavement surfaces in the field. The reflectometer is basically a form of goniometer. It consisted of a lamp mounted on a curved rotating boom and a rigidly mounted telephotometer with provisions for angular position adjustments. The lamp was positioned to illuminate a given spot on the pavement from several vertical angles. The telephotometer was focused on the illuminated spot as the motor driven boom rotated the lamp through a 360° horizontal angle about the spot. The telephotometer output was fed to a strip chart recorder. During field measurements the entire reflectometer assembly was enclosed in a light proof covering in order to avoid interference from extraneous light sources. The directional reflectance factors obtained in such a way for an epoxy surface asphalt pavement is shown in Figure 3.18. Even with a high degree of automation data collection in the field is slow and cumbersome.

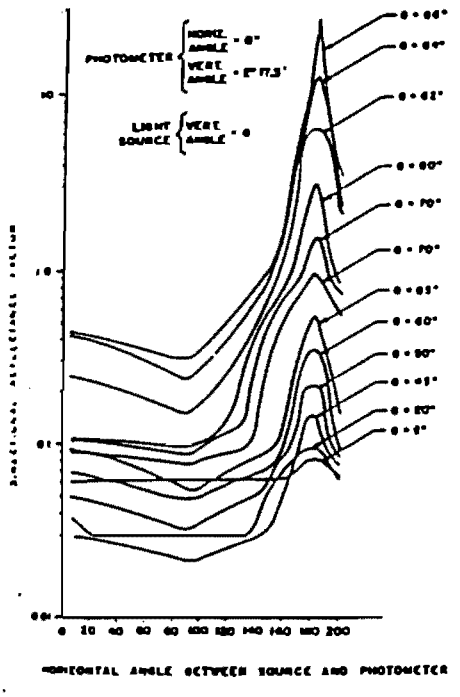

Figure 3.18. Directional reflectance factor for an epoxy surface asphalt pavement (*King and Finch, 1967*)

For large scale investigations a laboratory set up would be desirable. King and Finch then modified the above-described reflectometer, which was capable of simulating various light sources (1968). This reflectometer was also capable of simulating various vertical and horizontal angles as well as several driver-viewing distances (Figure 3.19).

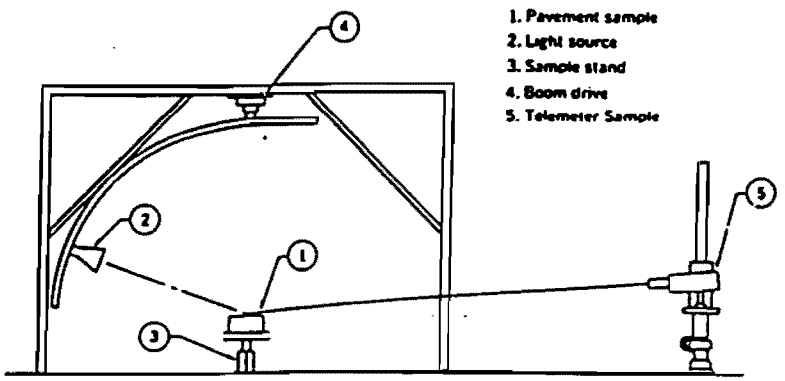

Figure 3.19. Sketch of the directional reflectance goniometer (*King and Finch, 1968*)

The telephotometer contained an oval-shaped aperture, which insured that only the surface of the pavement sample was being viewed during testing. Data were automatically recorded on paper punch tape for computer processing. Measurements were made on 12-inch core samples. Results for one sample (Type B traffic worn asphalt concrete) were revealed. Directional reflectance features were plotted against horizontal and vertical angles for different viewing distances. Because of very little difference between 50 feet and 100 feet viewing distance curves, these two could be combined into a single set of curves, as could be the curves for 400 feet and 600 feet viewing distances. For the purpose of comparisons, curves for 50 feet, 200 feet and 400 feet are shown in Figure 3.20. King and Finch (1976) once more continued their experiments on 11 samples, of which 5 were asphalt concrete and 6 were Portland cement concrete. Other than cleaning loose material from the surface, the samples were tested as received from the field. After automating the reflectometer as far as practicable, attention was then focused on the data recording and processing system. A combination of two methods of data recording was selected for final use. This consisted of a strip chart recorder and a digital recording system operating in parallel. The digital data processing system was chosen for speed and convenience of data processing, and the strip chart recorder was incorporated into the system to provide periodic visual checks on the data being gathered. The digital system printed the data directly on paper tape. The luminance values were then punched onto computer cards. A computer program (HILITES) determined the directional reflectance factors using the sample surface illumination and luminance values from the paper tape. These results are presented in tabular form. This tabular form is most useful for electronic data processing. However, to visualize the data, partial results for one asphalt and one Portland cement sample are shown in Figure 3.21. The directional reflectances are shown graphically as a function of horizontal and vertical angles. Inspection of test data showed the 0-180° horizontal angle portion of the curves to be a near mirror image of the 180-360° portion of the curves. Therefore, the corresponding values on each side of 180° were averaged.

(a)

(b)

(c)

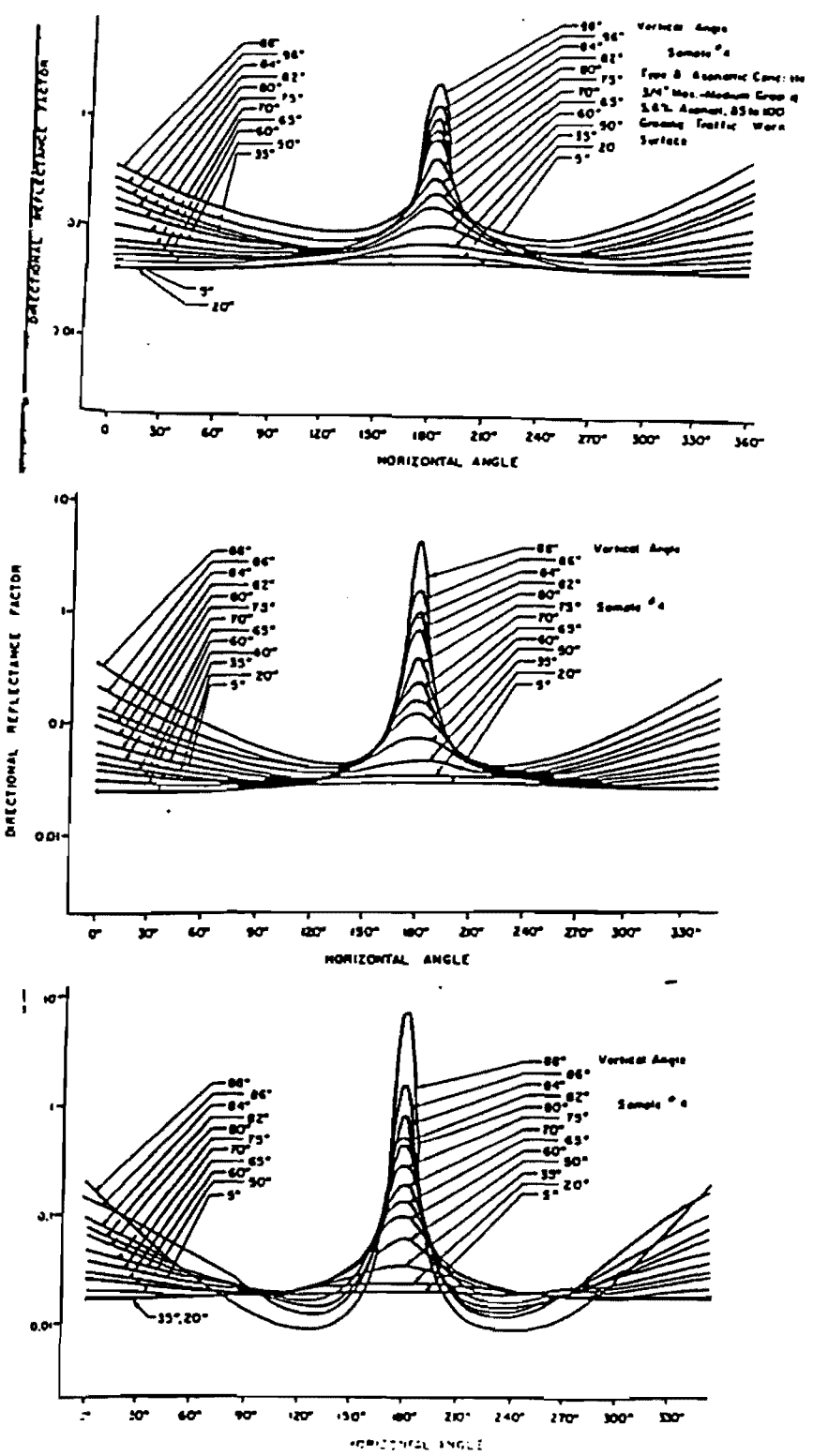

Figure 3.20. Directional reflectance factors for (a) 50, (b) 200 and (c) 400 feet viewing distance (*King and Finch, 1968*)

In 1984 Ronald N. Helms made a reflectometer to measure the reflectances of in-situ pavements. The research was concluded at the University of Colorado. The testing equipment consisted of gonio-reflectometer (to measure the complete hemispherical luminance feature data), Sand patch equipment (to measure the texture depth or macro structure of the pavement) and British portable tester (to measure the surface frictional properties of the surface). The gonio-reflectometer was composed to three sub systems -the reflectometer mechanism, the controller (which is a microcomputer and its peripherals) and the interface between the mechanism and the controller. However, problems were discovered in the reflectometer electronics that invalidated the test data.

(a)

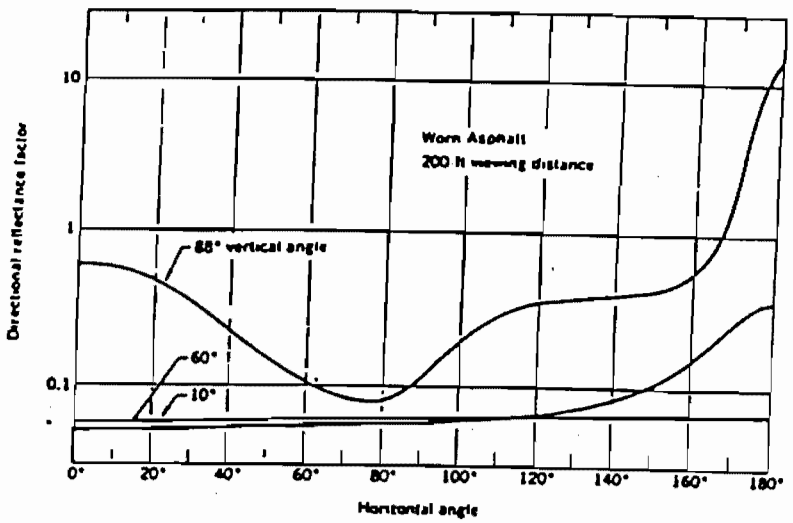

(b)

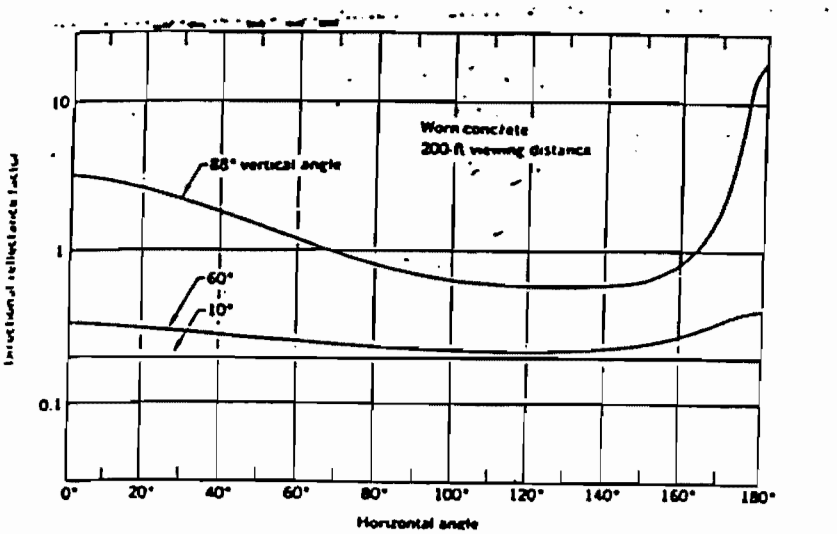

Figure 3.21. Directional reflectance factors for (a) asphalt and (b) Portland cement pavement surface (*King and Finch, 1968*)

Other Important Previous Research Work

It is very interesting to note that the concept of using the calculated visibility of a target as a criterion for evaluating the quality of a roadway lighting system originated in 1938 with J.H.Waldram even before the concept of illumination came into picture. He introduced the concept of *revealing power*. Waldram proposed an evaluation of targets with a range of reflectances chosen on the basis of the type of objects usually found on roadways. His idea was to use a mathematical model of the probability of each reflectance target at each grid point on the road to calculable a number, which he called the *revealing power*. Due to the lengthy calculations involved and lack of computers, the concept was never implemented.

A.W.Christie (1954) of the Transportation and Road Research Laboratory (TRRL) in England made some measurements at outdoors on the actual pavement surface. The experimental arrangement simulated an observer and a luminaire on a reduced scale. Christie adopted the point of view that luminance i.e. brightness in a lighting installation is built up from the bright patches produced by individual luminaries. According to him, each luminaire produces a bright patch on the surface of the pavement, which appears to be more or less T-shaped with a wide head stretching toward the observer (Figure 3.22).

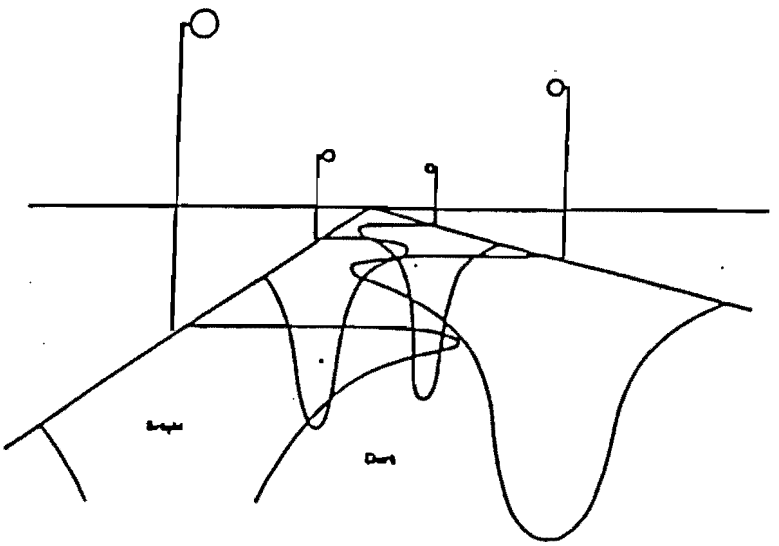

Figure 3.22. Perspective diagram of bright patches on lighted road

The exact shape depends on the nature of the surface and the light distribution of the luminaire. The appearance of the light does not depend on the relative position of the observer and luminaire, if they are not too close. This patch expands with the increase of the mounting height of luminaries. Christie assessed the reflection characteristics of three typical pavements used in England, namely rolled asphalt with pre coated chipping, non skid rock asphalt and machine finished concrete. After calculating the luminance factors, a family of reflection characteristic curves was drawn for each type within an accuracy of fifteen percent (with the approximations

made). But these curves did not present an immediate picture of how the surface is brightened by a street luminaire. So from this curves a perspective drawing showing the bright patch (in the form of a series of contours of equal luminance) formed by a simple type of luminaire under standard conditions were derived (Figure 3.23). It appears that in making the pavement surfaces skid resistant by having a protruding stone aggregate, have seriously reduced their power to reflect light. The shortness of the patches produced by street luminaries on many present day pavement surfaces is sometime said to be due to the coarseness of the surface. But very short patches are also obtained on pavements with a fine textured surface formed by protruding aggregate patches of small dimension (Figure 3.24). Actually to prevent skidding it appears that sharp projections are necessary and these tends to destroy the specular reflection of obliquely incident light which makes the formation of long patches possible. Therefore, it is clear that within limits it is the shape of the surface that matters and not the size of its features. Another reason for short patches in the modern pavements may be due to the fact that high-angle beam lighting are presently replaced by medium-angle-beam lighting. To compensate for the shortness of the patch produced, closer spacing of the luminaires is used.

(a)

(b)

(c)

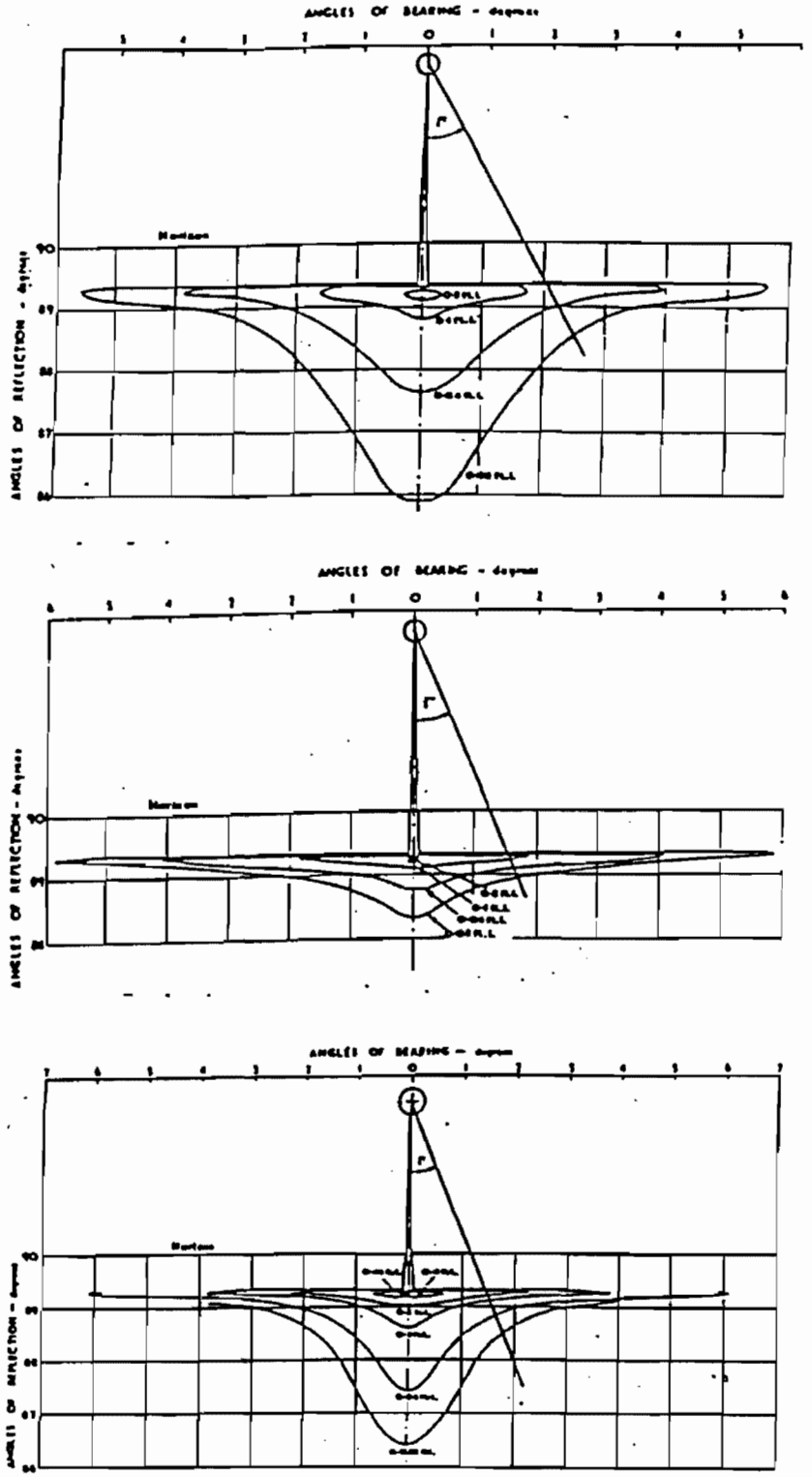

Figure 3.23. Iso-luminance contours in perspective for a (a) rolled asphalt with pre coated chipping; (b) non skid rock asphalt; (c) machine finished concrete under standard conditions (*Christie, 1954*)

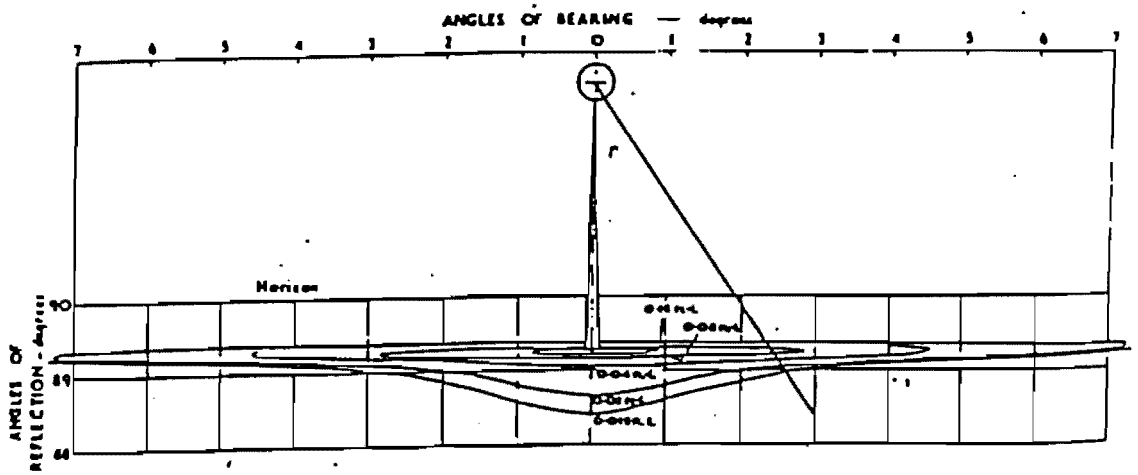

Figure 3.24. Standard iso luminance contours in perspective for bituminous sand carpet under standard conditions (*Christie, 1954*)

Nielsen, Sorensen, Forsberg and Persson in 1979 prepared eighty samples with differing aggregate compositions and subjected to accelerated wear in simulated summer and winter climates. They found that when all the conditions of wear are looked upon as a whole, Q_0 and $S1$are inversely correlated. They tested three type of samples where stone materials used were Diabas (comparatively light granite), quartzite (even lighter, natural stone) and Luxovite-Synopal and found out Q_0 values. They concluded that the brightness of the aggregate affects Q_0, which on the other hand are not affected by the coarseness of the aggregate as a whole. A light admixture influences Q_0 in the same way whether placed in the middle or top of the grading curve, while fine grained light admixtures have a lesser effect. A light admixture in pavements with coated chipping does not influence Q_0.

In 1980, Burghout and in 1984, a working group consisting of Schreuder, Schram, Burghout, Kreeft and Tom carried out long-term investigations to find out the relationship between light reflection and civil engineering properties of road surfaces. The r-tables used by CIE contain the actually measured, reduced luminance coefficients, of a road surface. In these investigations the r-tables were more over been reduced in such a manner that the luminance coefficient at perpendicular light incidence q_p is equal to one. This was done in order to eliminate possible differences in calibration between the various laboratories from which the r-tables originated. These values were called parameters and was denoted by the following equation.

$$P(x,y) = \frac{r(\tan\gamma = x, \beta = y^{\circ})}{q_p}$$

R-tables of 423 dry road surfaces from Eindhoven, Copenhegen and Berlin were investigated as a part of this study. A new parameter system called SCW-KEMA was introduced. It was concluded that, if one parameter system is considered *P(2.5,0)* or *P(2,0)* (which is the same as *S1* as per CIE) may be used. With regard to two parameter system the best option appeared to be a combination of *P (2; 0)* and *P (1; 90)*. Slight improvement is possible by adding *P (5; 5)*. The

gain in accuracy, however, seems hardly worthwhile in view of the complications associated with three-parameter system.

Three classification systems namely, SCW-KEMA, CIE-R, and CIE-N systems were analyzed. On the basis of the interaction of lighting installations and road surfaces it seems to be sufficient to distinguish only two groups of road surfaces. It was suggested to denote the two classes of road surfaces by C I and C II.

For CI, P *(2; 0)* < 0.4
For CII, *P (2; 0)* > 0.4

$\bar{L}$, U_0 and U_l can be determined with sufficient accuracy by distinguishing only these two groups of road surfaces. From a photometric point of view it is possible to define preferred road surfaces, viz. those of which,

$P(2;0) < 0.4$,
$q_p \geq 0.8$ cd/m^2/lux.

Jung, Kazakov and Titishov in 1984 built a photometer at the University of Toronto where the mounting height was held constant (Figure 3.25). It was used to measure the light reflectance properties of 36 different types of pavements in the province of Ontario, Canada. The laboratory measurements were carried out on 6-inch diameter samples. The measured pavement types were classified on the basis of their reflectance parameters (Q_0 ,$S1$,$S2$) which were calculated as average values from reflection metrics of at least three samples .

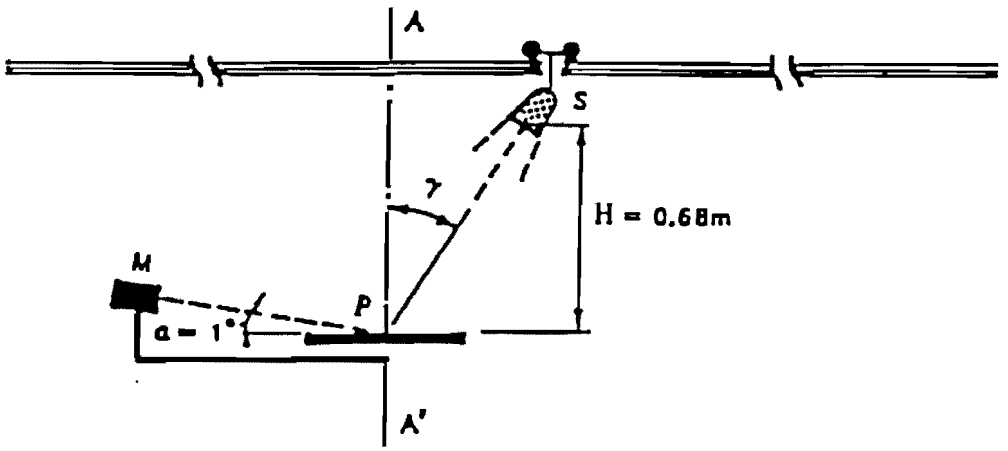

Figure 3.25. Sketch for the experimental set up for measurement of the reflection properties of road surfaces (*Jung et al., 1984*)

Figure 3.26 represents plot of log (*S1*) vs. log *(S2)* for Lindsay sections. The figure shows that for all Ontario test sections the plots are within the boundaries of the Erbay Atlas cloud indicated by the dashed line.

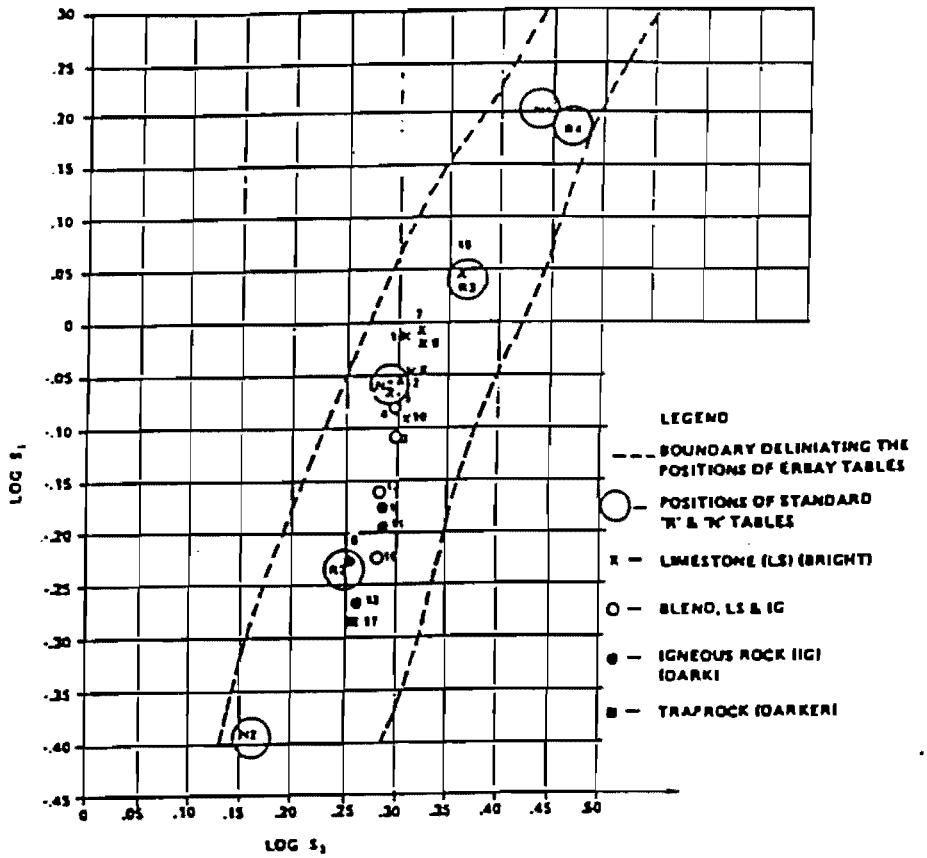

Figure 3.26. Specularity plot of (log *S1* vs. log *S2*) samples from Lindsay test section, Ontario (*Jung et al., 1984*)

Further Figure 3.26 reveals a relationship between *S1* and the type of coarse aggregate, ranging from hard trap rock and igneous stone to limestone. *S1* values are grouped as follows:

Coarse aggregate	Range of log (*S1*)
Igneous or trap rock	-0.29 to -0.17
Limestone	-0.10 to -0.06
Blend of the two	-0.23 to - 0.08

Figure 3.27 represent plot of log *S1* versus Q_0 for the same test sections. In general it shows a wide scattering of Q_0 values indicating large variations in brightness. It reveals the following grouping in terms of coarse aggregates.

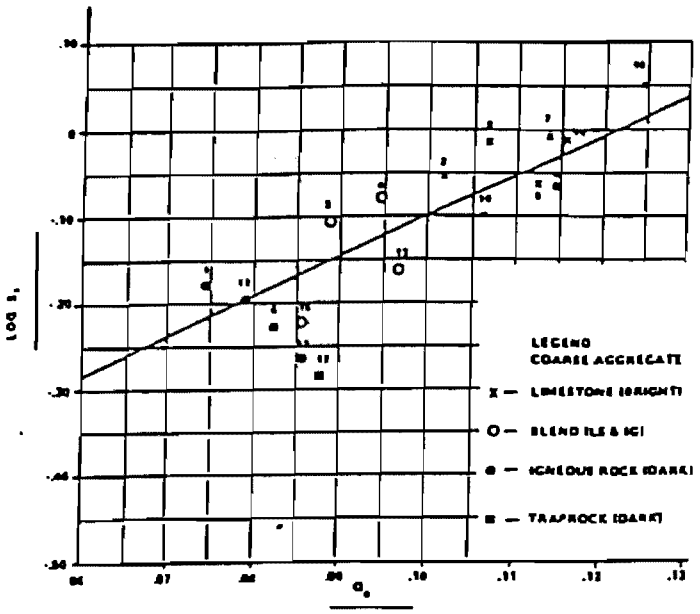

Figure 3.27. Specularity plot of (log *SI* vs. Q_0) samples from Highway 40 test section, Ontario *(Jung et al., 1984)*

Coarse aggregate	Range of Q_0
Dark trap rock	0.074 to 0.088
Bright limestone	0.102 to 0.124
Blend of the two	0.086 to 0.097

The effect of accumulated traffic on pavement surface reflectance properties was also investigated. With regard to the time of measurement a shift can be observed from lower specularity classes to higher ones. Also a shift of specularity was also observed when going from the driving lane to the outer passing lane. At the same time there was also an increase in brightness of the asphalt pavements with time or traffic accumulation, which is reflected in a shift of Q_0 values.

The influence on the light reflectance of the various observation angle α being different for the standard 1° was also studied, and it was found that all parameters tend to decrease with increasing α (39).

Bodmann and Schmidt (1989) conducted a very useful research to see the variation of the road surface reflection characteristics with time (also see section *Effects of Wear and Composition on Pavement Surface Reflection Properties*).

Visibility

The first successful attempt at developing a visibility criteria was the visibility index (*VI*) introduced in 1970 by Gallagher (also see section *Small Target Visibility Method*), which was base upon the research of Blackwell. Gallagher et al. used the bottom portion of an 18 inch traffic cone which was six percent gray or twenty nine percent white reflectant and established

the fact that the calculated visibility of an object was a very good prediction of the distance at which the drivers detected this target. Later in 1977, a study by Janoff showed that the VI was a better predictor of night time accident rates than was any of the other photometric measures that they evaluated .

In 1989, Adrian from the University of Waterloo, Canada offered a new visibility matrix based upon the works of Blackwell (1946), Aulthorn (1964) and his own. His visibility level (VL) was defined as simply the ratio of actual luminance to threshold luminance. The standard target proposed is known as *small target* and the concept is recognized as *Small Target Visibility* (*STV*) (also see section *Small Target Visibility Method*). The *VL* can be determined using photometers to measure target luminance, pavement luminance and veiling luminance. A predictive computer program then becomes an important factor for a road lighting design. The last computer program that is available is *STV* by Keck (1990) that is being updated as required. A study was performed by Janoff (1993) to compare the target, pavement and veiling luminances, as well as *VL*s, to actually measured values. This experiment consisted of two different targets. Each target was 7 inch square, and one placed upstream of the closest luminance and one downstream. The targets consisted of three different reflectances: 5, 30 and 80 %. The results indicated that the predicted values did not match up with measured values. There were significant differences between the target, pavement and veiling luminances . However, Janoff concluded that, perhaps with an accurate r-table for the surfaces under study, accurate reflectance values for the targets, accurate candle power distribution (including depreciation factors) and some derived field factors to account for light reflected from the pavement onto the target, a higher degree of relationship can be derived between measured and predicted values.

In 1997, Adrian, Gibbons and Laura Thomas made an amendment in calculating *STV* and studied the influence of light reflected from the road surface on the target luminance. The reflected light from a total of seventy-two pavement sections was used for each target luminance calculation. Based on the calculation, it was decided that road sections further than 6 multiples of target size from the target need not to be included in the calculation because they contribute less than five percent of the total target luminance. A similar calculation was performed for β angles and it was then decided to perform the calculation for $\beta = \pm 45°$. As seen from the calculation the light reflected from the pavement to the target can contribute up to fifteen percent of the total target luminance. This amount will change the *VL* of the target and *VL* can be reduced as much as half the *VL* where no reflection for the pavement is considered.

Adrian and Gibbons (1997) also investigated the influence of observation angle (α) on road surface reflection characteristics. The measurement took place at the University of Waterloo using a goniometer and samples were provided by the University of Toronto. Impact of the change of α was observed on pavement luminance, each curve showed a trend toward a horizontal line (Figure 3.28). This represents a trend toward Lambertian reflection at high levels of α (approximately 20°). For α<20°mixed reflection becomes the reflection mode. For this region of α an analytical model of reflection was suggested. If a pavement type behaves like Lambertian surface γ would be the only angle, which would influence the luminance of the surface.

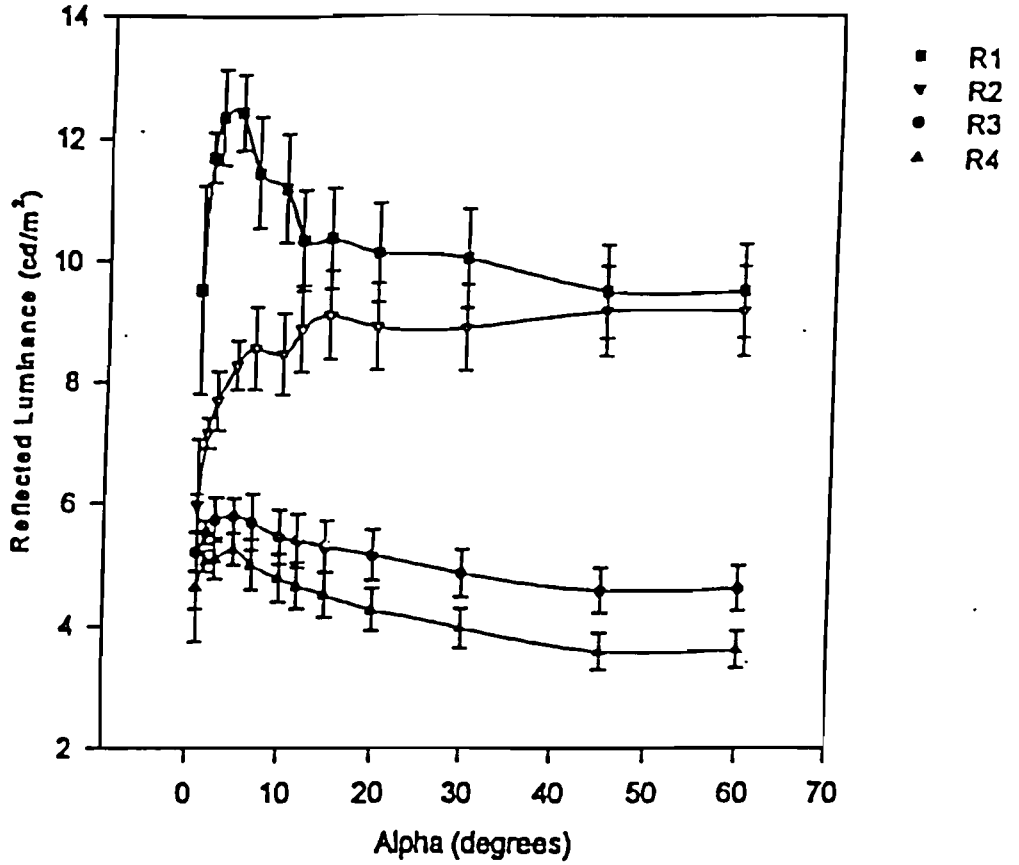

Figure 3.28. The influence of observation angle for four standard pavements where β=0° and γ=0° (*Adrian et al., 1997*)

Research Program

Introduction

For this research, reflectance data from a total of 151 samples in nine provinces in Canada were used (26). These samples were measured for the reflectance characteristics using the automated reflectance measuring facility at the University of Toronto and the results were first published by the Roads and Transportation Association of Canada (RTAC). These reflectance data were analyzed to investigate the effect of various factors related to pavement reflectance. The reflectance parameters used were average luminance coefficient (Q_0) and specularity factor (SI). The computer program '*STV*', developed by M.E. Keck was used to perform a sensitivity analysis to predict the influence of a number of parameters on pavement luminance and visibility level. From the Canadian pavement reflectance data, r-tables for four common pavement types with similar levels traffic were selected for further analysis. The sensitivity analysis also included four standard pavements.

The computer program '*STV*' calculates the average pavement luminance and weighted average visibility level for a section of road as well as the individual values of these parameters at locations assigned by the user. It assumes that the observer looks at the roadway at an angle of 1° from the horizontal. To calculate *VL*, it uses the visual acuity of a 23-year-old person. The target

luminance is calculated at the center of the target. Pavement luminance is calculated as the average of the luminance values at the base of the target (with no target in place) and at the point on the pavement which the observer can see immediately above the target. The input data include the luminaire photometric data and pavement reflectance data. As a part of this research, pavement luminance values were calculated both with and without the target in place. Two luminaires were considered in a single sided 140-ft. spacing and 30-ft. mounting height arrangement for a 19-ft. wide road with R3 classification. For a target located just upstream of the luminaire near the observer, the difference in background luminance with and without the target in-place was found to be 14 %.

Research Plan

The research work was conducted in two phases. A detailed description of the work is outlined below.

Phase 1: Sensitivity Analysis using *STV* program:

1. Analysis of visibility parameters such as Pavement Luminance, Visibility Level and Uniformity Ratio (ratio of maximum to minimum pavement luminance) for standard pavements: This analysis included both the average and individual values of visibility parameters at target points between two luminaires according to *STV* concept.
2. Analysis of visibility parameters at standard target points between two luminaries using r-tables from Canadian pavements: The purpose of this analysis was to make a comparison of visibility parameters using both standard and measured r-tables.

Phase 2: Analysis of Canadian Pavement Reflectance Data:

This analysis included the effect of Average Luminance Coefficient (Q_0) and Specularity Factor (SI) on different engineering characteristics of pavement. These characteristics include cumulative traffic, age, texture depth and aggregates type.

The standard pavements selected are those adopted by CIE and are limited to dry pavements only. A sensitivity analysis was conducted on both the average and individual values of the Visibility Level and Pavement Luminance for the four standard types of pavements using the *STV* software. The variables used were luminaire geometry arrangement, luminous flux of lamp and target reflectance. While analyzing a certain parameter, all other parameters were kept constant.

A four-lane roadway with 12-ft lanes was used for the analysis. The luminaire used was ge-7318 produced by GE Lighting Systems. A light loss factor of 0.65 was selected to reflect an average condition. The lighting arrangement used is shown in Figure 3.29. The luminaires were assumed to have no tilt and rotation (see Figure 3.29). A row of ten identical luminaires was considered. It was assumed that the height of the driver's eye is 1.45 meters above the road surface and the size of the target is 18 cm square.

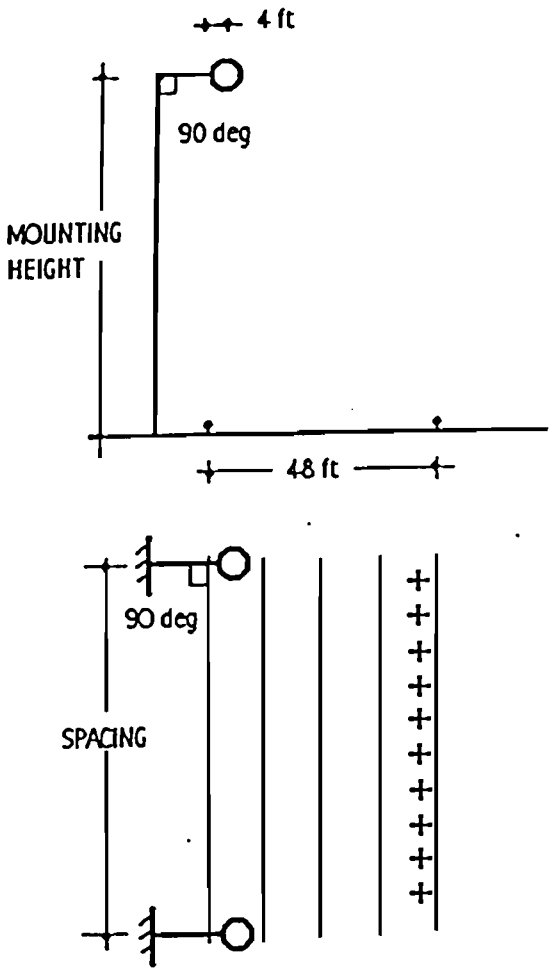

Figure 3.29. Schematic of luminaire geometry used in the analysis

For the sensitivity analysis, luminaire spacings of 100,150 and 200 ft. were considered. Mounting heights were taken as 20,30 and 40 ft. The luminaire arrangements were single sided, opposite and staggered. Two luminuous flux of 25,000 lumen and 40,000 lumen were used. A target reflectance of 50 percent was used. Table 3.1 shows the *STV* value, pavement luminance and uniformity ratio for the different combinations of data.

R3 is the standard r-table applicable to most types of pavement constructed in the United States. Therefore, the analysis of visibility parameters at individual points between two luminaires was performed on the standard R3 pavement and with the same configuration as in Figure 3.29. Though visibility parameters were obtained for the *STV* locations (twenty points in two rows per lane) for analysis purposes, ten target locations were selected between the two luminaires with the first and the last one at S/20 from the luminaires along the roadway and S/10 in-between. Here S denotes the spacing between the two consecutive luminaires. The targets were 3 ft away from the east edge of the roadway. Figure 3.30 shows the schematic with target locations.

Sensitivity analysis was also conducted on actual pavements using '*STV*' software. Pavement reflectance data from 151 core samples with 6 and 8 inch. diameters were obtained for various types of pavements from all over Canada. These pavement surfaces included open graded and dense friction course asphalt cement pavements, concrete pavements and seal coats. Samples

were taken from both on and between wheel paths to account for change in reflection properties due to traffic wear. Several types of coarse aggregates accounting for different mineralogical types, colors and textures were used in these pavements. R-tables were constructed by the Canadian researchers for each sample and Q_0, *S1* and *S2* values were calculated from the r-tables. Each pavement sample was also assigned an Erbay number and the appropriate R classification according to the CIE system. Four pavement types were selected to represent the four standard types of pavements. These were concrete, open graded, and seal coat and dense friction course classified as R1, R2, R3 and R4 respectively. Concrete and dense friction course samples were obtained from New Brunswick and the other two were obtained from

Table 3.3. Average visibility parameters obtained by the '*STV*' program for standard pavements (SS= Single Sided, OP= Opposite, ST= Staggered)

PVMT. CLASS	SPACING(ft.)	MOUNTING HEIGHT(ft)	LUMINOUS FLUX (lm)	LUMINAIRE ARRANGEMENT	VISIBILITY LEVEL	PAVEMENT LUMINANCE (cd/m^2)	UNIFORMITY RATIO
R1	100	30	25000	ST	4.32	1.83	3.2
	150	20	25000	ST	5.57	1.38	17.7
	150	30	25000	SS	4.25	1.22	6.3
	150	30	25000	OP	5.32	2.43	1.8
	150	30	25000	ST	4.29	1.21	5.9
	150	30	40000	ST	4.85	1.94	5.9
	150	40	25000	ST	2.94	1.06	3.3
	200	30	25000	ST	5.57	0.91	7.1
R2	100	30	25000	ST	4.17	1.38	3
	150	20	25000	ST	5.54	1.03	23.2
	150	30	25000	SS	4.44	0.92	8.8
	150	30	25000	OP	4.83	1.84	2.2
	150	30	25000	ST	4.46	0.92	7
	150	30	40000	ST	5.02	1.47	7
	150	40	25000	ST	3.12	0.81	3.5
	200	30	25000	ST	5.46	0.69	9

Table 3.3. Continued

PVMT. CLASS	SPACING(ft.)	MOUNTING HEIGHT(ft)	LUMINOUS FLUX (lm)	LUMINAIRE ARRANGEMENT	VISIBILITY LEVEL	PAVEMENT LUMINANCE (cd/m^2)	UNIFORMITY RATIO
R3	100	30	25000	ST	4.49	1.38	3.9
	150	20	25000	ST	5.86	1.03	24.9
	150	30	25000	SS	4.43	0.92	13.5
	150	30	25000	OP	4.58	1.84	3
	150	30	25000	ST	4.88	0.92	9.4
	150	30	40000	ST	5.5	1.47	9.4
	150	40	25000	ST	3.37	0.82	4.5
	200	30	25000	ST	5.5	0.69	12.9
R4	100	30	25000	ST	4.46	1.54	3.4
	150	20	25000	ST	6.49	1.15	20.1
	150	30	25000	SS	4.39	1.03	18.5
	150	30	25000	OP	4.19	2.05	3.6
	150	30	25000	ST	5.21	1.03	8.3
	150	30	40000	ST	5.88	1.64	8.3
	150	40	25000	ST	3.5	0.92	3.9
	200	30	25000	ST	5.52	0.77	11.7

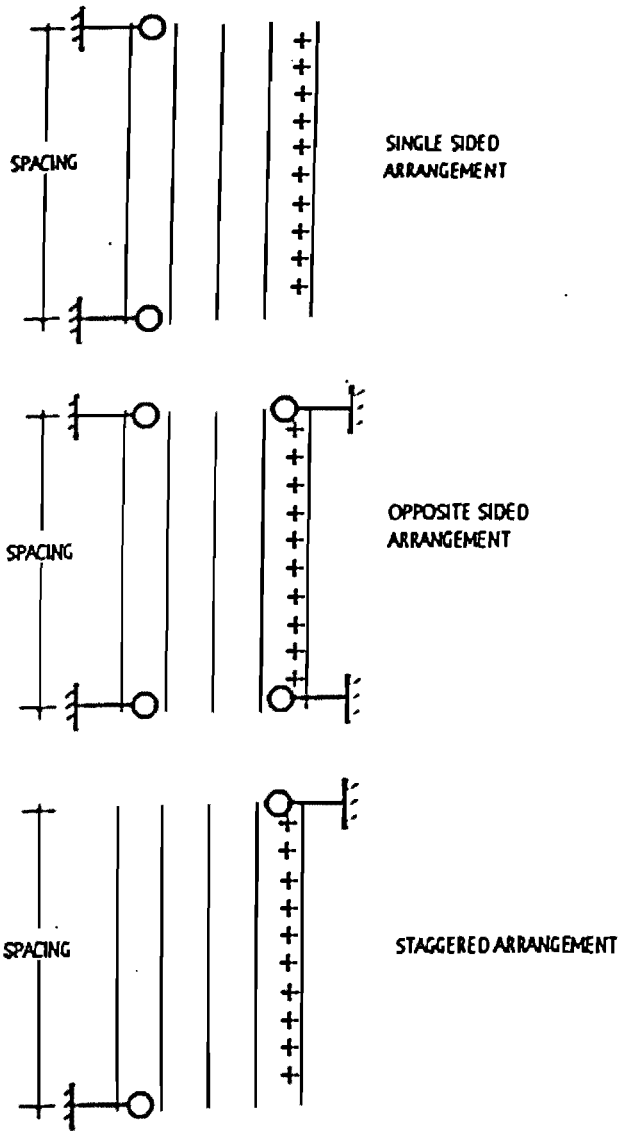

Figure 3.30. Different luminaire arrangements and target locations used in analysis

British Columbia. The visibility parameters at ten target locations were calculated for both standard and actual pavements using the '*STV*' computer program and these results were compared.

Reflectance characteristics of pavements with coarse aggregate such as sandstone, granite, limestone, graywacke, gneiss and trap rock were analyzed and the values of reflectance parameters were plotted. It was ensured that samples to be compared had nearly the same level of cumulative traffic. In calculating the cumulative traffic, lane traffic distribution factors of 80-20 % for four-lane roads and 50-40-10% for six-lane roads were used. Annual percent growth rate for traffic was taken as 2 %.

Analysis Of Results

In the previous chapter, the research effort was described in detail. In this chapter, results obtained from the research are discussed. First, results from the sensitivity analysis are presented for both standard and actual pavements. Then results from the analysis on reflectance of actual pavements are presented.

Sensitivity Analysis Using *'STV'* Program

Sensitivity analysis was conducted using the CIE standard r-tables with the aid of *'STV'* software. Both the average and individual values of pavement luminance and visibility level at different target locations were considered. Uniformity ratio (maximum / minimum pavement luminance) was calculated for the roadway design area. Subsequently, sensitivity analysis was also conducted using measured r-tables.

Standard Pavement Reflectance Data

Figure 3.31 shows the effect of changing the luminaire spacing on visibility parameters. Increasing the spacing decreases the average pavement luminance and increases *VL* in all pavement types. A 50 % reflectance target is possibly seen in positive contrast (target brighter than the pavement). As indicated earlier in Section *Small Target Visibility Method*, the contrast is given by the equation

$$C = \frac{L_t - L_b}{L_b}.$$

Therefore, the contrast will increase if the background (pavement) luminance decreases. A change in contrast is several times more effective in changing visibility than an equal change in adaptation. As shown in Figure 3.31, the visibility should increase with an increase in spacing for positive contrast situations. Moreover, increasing spacing reduces glare and the adaptation level, which tends to increase *VL*. This also changes the luminance uniformity ratio, which has no direct effect on *VL*. Since Q_0 is the average luminance coefficient, the following equation is true.

Luminance = $Q_0 \times$ *Illumination.*

A single luminaire type was used in all cases. Therefore, illumination for a particular point should not change with pavement type and pavement luminance depends on Q_0 only. For low (100 ft) and high (200 ft) spacing it seems that the pavement type has little effect on *VL*. But for 150 ft spacing R1 pavement (Q_0=0.1) shows the lowest *VL* and highest pavement luminance because it reflects more light. The R4 pavement (Q_0 = 0.08) shows the opposite trend. It is also interesting to note that since theoretically R2 and R3 have the same average luminance coefficient Q_0, they show exactly the same pavement luminance values regardless of luminaire spacing.

If mounting height is changed while keeping all other parameters constant, then both contrast and pavement luminance varies with it (Figure 3.32). It is logical to think that a higher mounting height results in lower average pavement luminance, but it is also accompanied by lower target luminance because target has higher reflectivity than the pavement in the background. The change in target luminance is higher than the change in pavement luminance. In this situation, the threshold luminance value does not change much and the result is a lower *VL*. On the other hand, uniformity ratio also decreases drastically and it may be favorable for visibility. The effect on pavement type when mounting height is changed, similar to that of changing the spacing. The

luminance curves for R2 and R3 almost overlaps, because they have the same average luminance coefficient values.

If the number of luminaires per unit length of roadway remain the same, the average pavement luminance will not change (Figure 3.33). It means that for the same spacing, single sided and the staggered arrangements will give the same pavement luminance while in the opposite arrangements with number of luminaires doubled, pavement luminance increased by 100 % (also see Figure 3.30). For R1 pavements that have the highest luminance coefficient, the pavement luminance should be the highest and for R2 and R3 it should be the lowest. But the change in luminaire arrangement causes a significant change in the luminances of both target and background. Under the single sided arrangement, *VL* does not seem to change very much with change of pavement type. For staggered arrangement, *VL* increases from R1 to R4. But for the opposite arrangement, the reverse trend is observed. The target luminance does not change with pavement type. Higher pavement luminance results in lower threshold luminance (ΔL) which dominates over the increase in pavement luminance and results in higher *VL*. The opposite arrangement is seen to have the highest *VL* and lowest uniformity and thus performs the best. But the number of luminaires is twice that of other two arrangements if the spacing were to remain the same.

Figure 3.34 shows that higher the luminous flux (lamp lumen), higher the average pavement luminance and higher the *VL*, but the uniformity ratio remains the same. Pavement luminance changes proportionately at each point. Therefore, the ratio of maximum to minimum luminance must remain constant. Contrast is also constant since the luminance of the target and the background increase proportionately. Again, Q_0 is the highest for R1, the lowest for R2, R3 and in-between for R4 class and so will be the pavement luminance.

The above analysis reveals that *STV* is an optimization process. Higher *VL* is achieved by either increasing the spacing, decreasing the mounting height, changing the luminaire arrangement to opposite or increasing the luminous flux. Pavement luminance and uniformity ratio should also be considered for better lighting design due to adaptation. Therefore each variable in the luminaire arrangement should be evaluated and it should be determined. Therefore if the required criteria for *VL*, pavement luminance and uniformity ratio are met while minimizing the number of luminaires per unit length of road.

Figure 3.35 shows the effect of luminaire spacing on visibility parameters. For the staggered arrangement, is the point of the maximum pavement luminance lies near the north fixture (see Figure 3.30) for the200 ft. spacing because of less distance from the luminaire. The analysis was performed on R3 pavement only and the same I-table was used for each luminaire spacing. Therefore, at a particular point, the higher the illumination, higher will be the pavement luminance. Since horizontal illumination is inversely proportional to the square of the distance from the luminaire to the point consider, lower the distance, higher the horizontal illumination and hence higher the pavement luminance. As the luminaire spacing is reduced, the point of maximum luminance shifts to the south fixture. For a spacing of 100 ft., most of the points near the south fixture have high pavement luminance because of less distance from the luminaire. Therefore, these points are in negative contrast whereas for a spacing of 200 ft., the reverse is true. For spacings in-between, uniform *VL* with negative contrast is observed.

Figure 3.36 shows the effect of mounting height on *VL* and pavement luminance when all other parameters were held constant. The point of maximum pavement luminance is seen to shift from the north fixture to the south fixture when mounting height is increased. This may be explained by the minimum distance between the lamp and the point on the pavement surface and by the calculation method for pavement luminance in the *STV* method. These curves may shift depending on the roadway width, but the trend will remain the same. As the mounting height is increased the luminance values become more uniform, because the effect of change in pavement luminance becomes less, due to higher distance from luminaire to target location. For a mounting height of 40 ft., *VL* is the highest (negative contrast) near the south fixture and for a mounting height of 20 ft., *VL* is the highest near the north fixture. *VL* appears to be fairly uniform for a mounting height of 30 ft.

For opposite and staggered arrangements, the mid-point between luminaires get the maximum amount of light, thus resulting in maximum pavement luminance as well (Figure 3.37). But the single-sided arrangement shows a uniform trend and lower values than the other two arrangements. It also shows all-positive contrast, which may be explained by the lower values of pavement luminance. For the single-sided arrangement, the effect due to distance is much less than for the other two arrangements. This is more pronounced because of a 4 lane (48 ft) road. On the other hand, the all-negative contrast for the staggered arrangement may be described by the higher values of pavement luminance. Opposite arrangement show both types of contrast.

Figure 3.38 shows that higher lamp lumen gives higher pavement luminance and higher *VL*. As described in the previous paragraph, for the staggered arrangement, the point of maximum pavement luminance is at the mid-point. Both pavement luminance and *VL* patterns are similar for both lamp lumen values. This may be because increase in luminous flux has the same effect on both target luminance and background luminance.

So far, the analysis was conducted on a target of 50 % reflectance. In Figure 3.39, target reflectance of 50 % was compared with 20 % target reflectance. Since target reflectance has nothing to do with pavement luminance, higher target reflectance results in a lowering of negative-contrast *VL*, which would be result in a more conservative design than for a target reflectance of 20 %.

In Figure 3.40, threshold luminance is calculated for an opposite luminaire arrangement. The *VL* and target and pavement luminances were calculated for each target and the threshold luminance value ΔL was back calculated for each point. The straight lines show the average threshold luminance value for all ten target locations. It is seen that at least two targets are invisible, considering the threshold luminance. Each point on the curve shows the value of the difference in luminance between target and background (L_t-L_b). The ratio of (L_t-L_b) and ΔL will give the *VL* for each target. According to the *visibility level* concept, there is no difference between positive and negative threshold luminance, as long as the magnitude remains the same. So, higher the luminance difference between target and the background above the threshold value (positive and negative) the more it is visible. In fact, this threshold luminance will vary from one target location to another and it will also depend on the luminaire arrangement.

Actual Pavement Reflectance Data

After conducting the sensitivity analysis on standard pavement surfaces '*STV*' software was used to calculate the visibility parameters using measured reflectance data. Once this was done, results obtained from measured data were compared with those obtained from standard pavements.

Figure 3.41 shows the pavement luminance (L_b) and visibility level (VL) patterns for a typical four-lane highway with staggered luminaire arrangement (150-ft. spacing and 30 ft. mounting height) for a 25000-lumen luminaire using standard r-tables. The luminance curve for R1 is the flattest because it is the most diffused of surfaces. The luminance curve for R4 is the steepest because it is the most specular of surfaces. The more specular pavement surfaces shows maximum pavement luminance at the middle of the two luminaires, because this point gets the maximum amount of light for less distance when compared to other points along the roadway. On the other hand, the diffuse surfaces do not reflect light in particular directions and shows a more uniform trend in pavement luminance. All these cases result in negative-contrast visibility and R1 give the lowest values in most target locations. R3 and R4 seem to result in a more uniform trend.

Figure 3.42 shows the same curves, but with a different Q_0 values where standard r-tables are modified (scaled) using Q_0 values from measured data. Figure 3.42 shows a similar pattern to that in Figure 3.41 because the ratio of standard and measured Q_0 is only used as a scaling factor. It linearly transforms the r- values from standard r-tables. Pavement luminance is directly proportional to the Q_0 values of the pavements. Therefore, it follows that the ratio of the luminance values at any target location for these two curves for each pavement class is equal to the ratio of the Q_0 values. Therefore, pattern for the pavement luminance and visibility level curves drawn from standard and modified r-tables for each pavement class is 'parallel'.

Figure 3.43 was drawn from measured reflectance data. In this analysis Portland cement concrete, open-graded asphalt concrete, seal coat and dense asphalt concrete friction course pavements represent R1, R2, R3 and R4 classes of pavements respectively, as classified according to their *S1* values. Figure 3.43 does not show a significantly different pattern from the previous two. Table 3.4 shows the reflectance parameters of these pavements.

Table 3.4. Measured (actual) reflectance parameters of four selected pavements

Pavement Type	**R-Class**	Q_0	*S1*
Portland Cement Concrete	R1	0.113	0.354
Open Graded Asphalt Concrete	R2	0.045	0.794
Seal Coat	R3	0.049	1.229
Dense asphalt concrete Friction Course	R4	0.086	1.579

The main point of interest is the comparison between Figures 3.41 through 3.43. Such a comparison is made in Figures 3.44 and 3.45. Figure 3.44 shows the pavement luminance pattern from standard, scale and actually measured r-tables for each of the above mention pavement classes. Figure 3.45 shows the VL patterns for the same pavement classes. When visibility parameters from standard and scaled r-tables are used, they show the same trend as already mentioned. Higher Q_0 values result in higher pavement luminance. In fact, this is the adopted

way by CIE of calculating the pavement luminance and visibility level values for a certain pavement using standard r-tables. In this procedure the only information required on the pavement are the pavement reflectance class (R1, R2, R3 or R4) and the corresponding Q_0 value. Due to linear scaling, the pattern for both of these curves shows the same trend, but the question is the reliability and accuracy of the 'scaling' technique. Table 3.5 shows the percent difference for average pavement luminance and the weighted average visibility level for all of these pavements.

Table 3.5. Comparison of pavement luminance (cd/m^2) for different pavements

	Standard r-table	Scaled r-table	Measured r-table	% Difference Actual-Standard	% Difference Actual-Scaled
Portland Cement Concrete	1.21	1.37	1.56	22.4	12.2
Open Graded Asphalt Concrete	0.92	0.59	0.4	130	47.5
Seal Coat	0.92	0.64	0.44	109	45.5
Dense Asphalt Concrete Friction Course	1.03	1.10	1.11	7.2	0.9

Table 3.6. Comparison of visibility level for different pavements

	Standard r-table	Scaled r-table	Measured r-table	% Difference Actual-Standard	% Difference Actual-Scaled
Portland Cement Concrete	4.3	4.5	5.2	17.3	13.5
Open Graded Asphalt Concrete	4.5	4.3	4.9	8.2	12.2
Seal Coat	4.9	4.4	4.7	4.3	6.4
Dense Asphalt Concrete Friction Course	5.2	5.4	5.5	5.5	1.8

The difference in pavement luminance calculated using actual and scaled r-tables is as much as 47.5 % and the difference in visibility level is as much as 13.5 %. The difference in pavement luminance for actual and standard r-tables is as much as 130 % and the difference in visibility level is as much as 17.3 %. Since the trends of these curves are quite similar and the 'scaled' curve has just shifted to either side of the 'measured' curve, there may be some calibration value that can be used to relate standard or scaled pavements with actual pavements. Again, finding out Q_0 and *SI* values for all the pavements where lighting design is to be performed is not practical. Therefore, the practical use of the scaling technique is questionable.

Analysis of Canadian Pavement Reflectance Data

With the passage of time and traffic, the reflectance properties of pavement will change. In this analysis, the pavement reflectance parameters Q_0 and $S1$ were related to age of pavement and cumulative traffic. As seen from Figure 3.46, data for points along the wheel path are so scattered that a general conclusion is not feasible. In calculating the cumulative traffic volume, the lane traffic distribution factors and annual traffic growth rate were assumed. Also, because of lack of data, equivalent single axle loads could not be calculated and effects from all kinds of vehicles (considering AADT) were grouped together, even though different vehicle types have different effects on pavement surface. Yet a general trend emerged showing increasing parameter values with increasing cumulative traffic. This trend is expected because with traffic the pavement gets polished and becomes more specular, resulting in a higher $S1$ value. With increasing traffic, both asphalt and concrete pavements appear to brighten and therefore, Q_0 would increase with cumulative traffic. This trend is more pronounced in concrete pavements. In Figure 3.47, which relates to samples, taken from between the wheel path show the same trends for Q_0. But for $S1$, asphalt surface shows decreasing values with increasing cumulative traffic volume. Actually between- wheel path samples are less likely to experience polishing effect by traffic and specularity for asphalt pavements seems to decrease with weathering action.

These may illustrate the effect of age on pavement reflectance (Figure 3.48). Asphalt pavements show an increasing trend of both Q_0 and $S1$ with time, while concrete pavements show a uniform trend and does not appear to change much with time. Actually, asphalt surface is more vulnerable to traffic wear which increases its brightness and specularity while Portland cement concrete surface is more stable. Since trucks are the type of vehicles that have greatest impact of wear on pavement, another graph was drawn (Figure 3.49) similar to the previous one, but taking the cumulative truck traffic. Although, as expected, Q_0 and $S1$ values show increasing trend for asphalt pavements the trend for concrete pavement is not quite clear. There is a possibility that Portland cement concrete pavements may darken with time due to tire particle deposit (Q_0 decreases) and the decrease in $S1$ may be due to weathering action.

Intuitively, it can be said that Q_0 and $S1$ values must have a relationship with the texture depth of pavement. With increasing time and traffic, texture depth decreases and the pavement becomes more specular resulting in an increase of $S1$ and Q_0 for asphalt pavements.

Data were available regarding the specularity factor $S2$ and nearest Erbay Number for each sample. The analysis was done on Q_0 and $S1$ only. In Figure 3.51, $S2$ and Erbay Number was considered to see if they give any additional information that is not already provided by Q_0 and $S1$. A regression analysis was made with all the data points and the coefficient of correlation (R^2) for the relationship between parameters were calculated. The results for open graded pavements are shown in Figure 3.52. These results indicate that only Q_0 and $S1$ are significantly independent.

An analysis was also conducted for different types of coarse aggregates used in the different pavement surfaces (Figure 3.52). Graywacke and granite were coarse aggregates used in dense friction course pavement. Granites are composed pre- dominantly of quartz and potassium feldspar and as a result, are light-colored compared to graywacke and as a result, has a higher Q_0 value than the graywacke aggregate. Comparing the specularity factors of samples from wheel path and between the wheel path, the former shows a higher value, because of polishing action in

the wheel path. Table 3.7 shows different values of Q_0 and SI for pavements with different coarse aggregate types both for wheel path and between-wheel path samples.

Table 3.7. Reflectance parameters for different coarse aggregates used in pavements

	Q_0		SI	
Coarse Aggregate Type	**WP**	**BWP**	**WP**	**BWP**
Graywacke	0.075	0.064	0.82	0.72
Granite	0.09	0.085	0.67	0.64
Argillite+Slate+Granite	0.087	0.076	1.105	1.06
Quartzite (SandStone)	0.09	0.089	0.73	0.69
Granite+(Metamorphic)LimeStone	0.092		0.82	
Graywacke	0.054	0.051	0.35	0.35
Granite+Gneiss	0.103	0.077	0.1	0.12
Granite	0.43	0.24	0.65	0.67
Alluvial Deposit	0.076	0.079	0.082	0.083
Glacial Deposit	0.37	0.43	1.81	1.84

Conclusions and Recommendations

Conclusions

The main conclusions that came out from the analysis of the reflectance characteristics of standard pavement surfaces and the real pavement surfaces are listed below.

1. The concept of '*STV*' as a measure of visibility is an optimization process. The lighting geometry parameters such as spacing, mounting height and luminaire orientation, and luminaire photometric parameters, such as luminous flux may be changed to achieve the required *VL*, pavement luminance and luminance uniformity ratio. However, These parameters may have opposing effects on the lighting parameters indicated above. One has to select the best lighting installation that meets the design criterion by trial and error, which is impossible without a computer-based application.
2. For negative contrast, in typical lighting arrangements, 50 % target reflectance give a more conservative design (less magnitude of *VL*) than a 20 % target reflectance. Since typical roadway lighting installation results in negative contrast using 50 % target reflectance as a design criterion will lead to higher installation costs. Furthermore, targets such as pedestrian clothing have reflectance values even below 20 % and a target with a reflectance value higher than 50 % may be uncommon.
3. The use of standard r-tables to measure pavement luminance and visibility level for a pavement by scaling the standard r-table with the measured Q_0 value may not be accurate. The results obtained by using measured, standard and scaled r-tables show an appreciable difference. Furthermore, to implement this scaling technique one has to know the Q_0 value for the particular class of pavement for which lighting designs is performed. Unless the designer has a library of Q_0 and SI values for all possible pavement types, this may not be a practical scenario. A feasible alternative to standard r-tables is not likely in the present context.

4. Characterization of the reflectance properties of a pavement surface only requires Q_0 and *S1*. *S2* and Erbay number are highly correlated to *S1* and are therefore redundant.
5. No clear relationship of cumulative traffic with Q_0 and *S1* was evident since the data points are scattered. But there is a tendency for both Q_0 (brightness) and *S1* (specularity) to increase with the increase in cumulative traffic for both asphalt and concrete pavements. For this analysis, no data was available to calculate EASL's to account for the weighted traffic wear on pavement surfaces. Q_0 and *S1* values are seen to be more or less constant for concrete pavements which reveals that concrete is less vulnerable to traffic wear.
6. The different climatic conditions of the Canadian provinces appeared to have a significant effect on the reflectance parameters of the pavements. Both the Q_0 and *S1* values vary between the wheel path and out side the wheel path and also vary with time. But r-tables do not take into account the variations of these factors. A particular pavement may have more than one level of reflectance at different locations on the pavement. Therefore assuming only one standard r-table for a particular pavement will not give result that reflect the actual situation.

Recommendations

In view of the results obtained from the research, the following recommendations are made for future researches.

1. Standard r-tables should either be modified or the range of standard pavements expanded in such a way that it takes into account the overall and local variation of pavement surface reflectance characteristics.
2. An important relationship may exist between the reflective properties of a pavement and cumulative traffic volume and texture depth of the pavement. A relationship or a mathematical model would be helpful in accurately predicting the reflective properties of pavements.
3. A relationship between the visibility parameters of pavements calculated using actual and standard r-tables is likely to exist. A calibration methodology to update design parameters may be feasible.
4. While calculating pavement luminance for the calculation of visibility level, the computer program '*STV*' assumes that there is no target in place. Calculations done in this research show an appreciable difference between luminances calculated with and without target in-place. Therefore modifications to '*STV*' to incorporate target-in-place would result in more accurate prediction of *VL*.

CHAPTER 4: DIGITAL IMAGE PROCESSING AND SPATIAL FREQUENCY ANALYSIS OF TEXAS ROADWAY ENVIRONMENT(a thesis by Zhen Tang)

Fourier Analysis

In the late 1960's, Blakemore and Campbell suggested that the neurons in the visual cortex might process *spatial frequencies* instead of particular features of the visual world. In English, this means that instead of piecing the visual world together like a puzzle, the brain performs something akin to the mathematical technique of *Fourier Analysis* to detect the form of objects. While this analogy between the brain and the mathematical procedure is at best a loose one (since the brain doesn't really "do" a Fourier Analysis), whatever the brain actually does when we see an object is easier to understand within this context.

In our research, our equipment collects the light from a certain solid angle and records the light intensities from different directions onto different locations (pixels) on the image plane, with information of each direction into each *pixel* accordingly. It means, there is no *spatial frequency* involved until our researcher look at these video clips. However, once we look at them, we might be doing *Fourier Analysis* with our eyes and brains as Blakemore and Campbell suggested. It is only natural to go further to directly carry out the *Fourier Analysis* and examine the result with the help from the mathematical software and computers we possess. Thus, a review of the basic concepts of Fourier Analysis will be very helpful starting point.

Fourier Theory Fundamental

Fourier series

Fourier analysis was initially developed by the Physicist Joseph Fourier to study heat transfer problems. Fourier recognized that any (Figure 4.1: Figure for $f_p(x)$) function, $f_p(x)$, whose graph displays a periodicity, T, can be considered to be an infinite sum of sinusoidal functions.

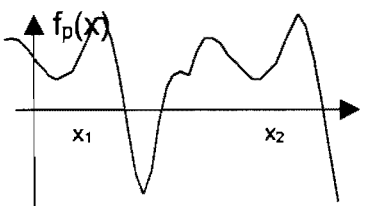

Figure 4.1. Figure for $f_p(x)$

The Fourier series may be represented as the sum of a series of sine functions, cosine functions, complex exponential functions or any of several other sinusoidal representations (Wilson (1995), Baher (1990), and Lathi (1989)).

Series Representation of a Limited Function:

Consider a uniform and finite periodic function $f_p(x)$ with period p defined over a range of its variable x between x_0 and x_1. This function may be represented at any point over its range by a series of circular functions where n is an integer.

$$T = x_1 - x_0$$

$$\omega = \frac{2\pi}{T}$$

$$f_p(x) = \frac{A_0}{2} + \sum_{n=1}^{\infty} (A_n \cos(n\omega x) + B_n \sin(n\omega x))$$

$$A_0 = \frac{2}{T} \int_{x_0}^{x_1} f_p(x) dx$$

$$A_n = \frac{2}{T} \int_{x_0}^{x_1} f_p(x) \cos(n\omega x) dx$$

$$B_n = \frac{2}{T} \int_{x_0}^{x_1} f_p(x) \sin(n\omega x) dx$$

$$f_p(x) = \sum_{n=0}^{\infty} C_n \cos(n\omega x - \theta_n)$$

$$f_p(x) = \sum_{n=-\infty}^{\infty} D_n e^{in\omega x}$$

$$D_n = \frac{1}{T} \int_{x_0}^{x_1} f_p(x) e^{-in\omega x} dx$$

Where: x is in an x-unit (in spatial case it should be a length unit)
T is the period of the function,
ω is an angular frequency in radiance per x-unit,
θ_n , is a phase shift angle, and
A_n B_n C_n & D_n are amplitudes of the frequencies at $\omega_n = n\omega$.

When we choose $f_p(x) = \sin 2\pi x$, the waveform can be obtained in Matlab as shown in Figure 4.2 in addition, the corresponding spectrum is shown in Figure 4.3. Obviously, the period of $f_p(x)$ is T = 1 LU (Length Unit). Thus, frequency $f = \frac{1}{T} = 1$ LU^{-1} or angular frequency $\omega = \frac{2\pi}{T} = 2\pi \frac{rad}{LU}$ and $b_1 = 1$ represent the only nonzero component in the spectrum.

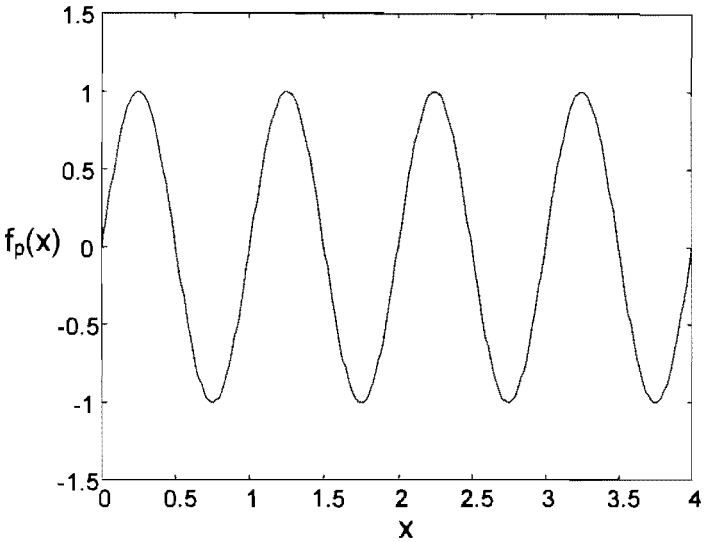

Figure 4.2. A single frequency wave. ($f_p(x) = \sin 2\pi x$)

The Fourier series of any periodic function may be represented in either the x-domain(spatial or time domain) as a function of f(x) or in the ω-domain as a function of frequency F(ω).

$$f_p(x) = \sum_{n=0}^{\infty} F_n(\omega)$$

When the function is represented in x-space it is usually a reasonably continuous function in x. In ω-space, the function is represented as an infinite series of amplitudes, A_n, B_n, C_n, or D_n, at discrete frequencies, ω_n, with discrete phase shifts θ_n. The discrete frequencies are determined only by the period, T, of the periodic function. Each frequency contains a portion of the total energy or power in the function f(x). The total energy in the function f(x) is the sum of the amplitudes in each discrete frequency.

$$E_{f(x)} = \sum_{n=0}^{\infty} |C_n|^2$$

$$E_{f(x)} = \sum_{n=-\infty}^{\infty} \left| D_n e^{i(n\omega x + \theta_n)} \right|^2 = \sum_{n=-\infty}^{\infty} |D_n|^2$$

The Fourier series moves a function back and forth between dual domains, frequency domain, ω, and position domain, x, with different aspects of the function represented uniquely in each domain.

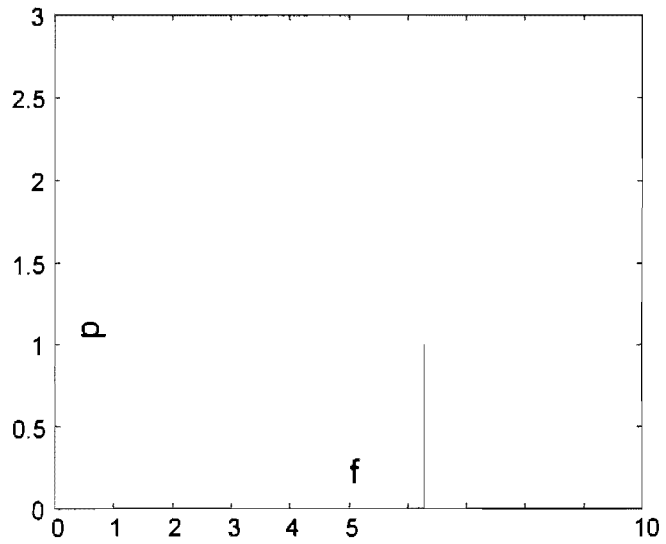

Figure 4.3. The spectrum of the single frequency wave.

Shortly following the development of Fourier series of periodic signals the problem of non-periodic functions was addressed. It has been noted that Fourier series of periodic functions have discrete frequency content and an infinite sum of the discrete frequencies. The discrete frequencies are associated with the period as the following.

$\omega_n = n2\ \omega\ /T;\ n= 0, 1, 2,3,\ldots$

$\omega_0 = 0{\times}2\ \omega\ /T;$ Constant term, The non-oscillating term,

$\omega_1 = 1{\times}2\ \omega\ /T;$ the fundamental frequency, first oscillating term

$\omega_2 = 2{\times}2\ \omega\ /T;$ the first harmonic, second oscillating term

$\omega_3 = 3{\times}2\ \omega\ /T;$ the second harmonic, third oscillating term

It can be seen, as the period, T, decreases, ω_1 becomes larger and $(\omega_2 - \omega_1)$ grows larger, and the distance between ω_{n+1} and ω_n increases. As the period, T, increases, ω_1 becomes smaller and ω_1 and ω_2 grow closer together. As, T, becomes very large, ω_1 and ω_2 move close together until, as, T, goes to infinity, the frequency becomes continuous. We have a non-periodic, f(x), in the space domain and a continuous function, F(ω), in the frequency domain. This leads us to a tool known as *Fourier analysis*.

Fourier Analysis in One Dimension

A mathematical tool of great utility in the analysis of both linear and nonlinear phenomena is *Fourier analysis*. This tool is widely used in the study of electrical networks and communication systems.

Let us look at one-dimensional functions first. Any function, $f(x)$ (not limited to periodic function) may be considered to be composed of the superposition of a series of continuous periodic functions of suitable amplitudes and frequencies. Now a periodic function u can be represented by $F(u)e^{jxu}$, so that the original function, considered as a summation of periodic functions, becomes the following.

$$f(x) = \int_{-\infty}^{\infty} F(u)e^{jxu}du$$

$$F(u) = \frac{1}{2\pi}\int_{-\infty}^{\infty} f(x)e^{-jxu}dx$$

The function, which gives the amplitudes *F(u)* of the periodic terms of frequency u, is called the Fourier Transform of Equation (4.1-7). Whenever *f(x)* or *F(u)* can be determined, the other can be computed from the Fourier Transform relationship. This concept is of extraordinary power in many problems of analysis in optics as well as in various other fields.

Since the Fourier transform *F(u)* is a frequency domain representation of a function *f(x)*, the *u* characterizes the frequency of the decomposed cosinusoids and sinusoids and is equal to the number of cycles per unit of *x* (Bracewell (1965)). If a function or waveform is not periodic, then the Fourier transform of the function will be a continuous function of frequency (Brigham (1988)).

Discrete Fourier Transform

Because a digital computer works only with discrete data, numerical computation of the Fourier transform of *f(x)* requires discrete sample values of *f(x)*. In addition, a computer can compute the transform *F(u)* only at discrete values of *u*, that is, it can only provide discrete samples of the transform.

Suppose that a continuous function $f(x)$ is discretized into a sequence by taking N samples Δx units apart.

$$\{f(x_0), f(x_0 + \Delta x), f(x_0 + 2\Delta x), \ldots, f(x_0 + [N-1]\Delta x)\}$$

It will be convenient in subsequent developments to use x as either a discrete or continuous variable, depending on the context of the discussion.

$$f(x) = f(x_0 + x\Delta x) \text{ .1-15)}$$

Where x now assumes the discrete values $0,1,2,\ldots,N-1$.
In other words, the sequence $\{f(0), f(1), f(2),\ldots, f(N-1)\}$ denotes any N uniformly spaced samples from a corresponding continuous function. With this in mind, the discrete Fourier transform pair that applies to sampled function is given by the following equation.

$$F(u) = \frac{1}{N}\sum_{x=0}^{N-1} f(x)\exp[-j2\pi ux/N]$$

for $u = 0,1,2,\ldots,N-1$, and

$$f(x) = \sum_{u=0}^{N-1} F(u)\exp[j2\pi ux/N]$$

for $x = 0,1,2,\ldots,N-1$.

In the two-variable case the discrete Fourier transform pair is

$$F(u,v) = \frac{1}{MN}\sum_{x=0}^{M-1}\sum_{y=0}^{N-1} f(x,y)\exp[-j2\pi(ux/M + vy/N]$$

for $u = 0,1,2,\ldots,M-1$, $v = 0,1,2,\ldots,N-1$, and

$$f(x,y) = \sum_{u=0}^{M-1}\sum_{v=0}^{N-1} F(u,v)\exp[j2\pi(ux/M + vy/N]$$

for $x = 0,1,2,\ldots,M-1$, $y = 0,1,2,\ldots,N-1$.

These equations can be used to compute transforms and inverse transforms of appropriately-sampled data.

The discrete Fourier transform and its inverse are periodic with period N. Thus, only the N values of each variable in any one period are required to obtain f(x, y) from F(u, v). Or, only one period of the transform is necessary to specify F(u, v) completely in the frequency domain.

Let us consider the one-variable case. By translation property of discrete Fourier transform, the magnitudes of the transform values from (N/2)+1 to N-1 are reflections of the values in the half period to the left of the origin. Thus the actual highest frequency is N/2.

Fast Fourier Transform

The number of complex multiplications and additions required to implement certain equations is proportional to N^2. Proper decomposition of this equation can make the number of multiplication and addition operations proportional to $N\log_2 N$ The decomposition procedure is called the *fast Fourier transform* (FFT) *algorithm*. The reduction in proportionality from N^2 to $N\log_2 N$ operations represents a significant saving in computational effort. The Fourier transform command in Matlab is implemented this way as most other mathematical software is.

Fourier Analysis of Digital Images

The *Fourier transform*, in essence, decomposes or separates a waveform or function into sinusoids of different frequency which sum to the original waveform. It identifies or distinguishes the different frequency sinusoids and their respective amplitudes (Brigham (1988)).

Frequency Domain Representation of Digital Images

Physical laws suggest that any conceivable object that can yield an image may always be represented by a series or by a simple or multiple Fourier integral. The amplitudes of the terms of the series or the integrand of the integral usually can be regarded as describing the spatial frequencies, which leads to a complete representation of the same object in a different domain rather than the spatial. There have been plenty of great examples in contemporary optics and mathematics.

It is often useful to think of functions and their transforms as occupying two domains. These domains are referred to as the upper and the lower domains in older texts, ``as if functions circulated at ground level and their transforms in the underworld" (Bracewell (1965)). They are also referred to as the function and transform domains, but in most physics applications, they are called the time and frequency domains respectively. Operations performed in one domain have corresponding operations in the other. For example, the convolution operation in the time domain becomes a multiplication operation in the frequency domain, The reverse is also true. Such theorems allow one to move between domains so that operations can be performed where they are easiest or most advantageous.

The earlier contents of this section prepare us for the most often used transform in our research, the two-dimensional fast Fourier transform on a discrete matrix (the digital image). The result of this transform is a discrete matrix whose elements represent the frequency domain amplitudes.

Using Matlab

As a powerful mathematics software package, Matlab provides very convenient function to perform the two-dimensional discrete Fourier transform and inverse, respectively FFT2 and IFFT2. The following example will show the transform of a 128-by-128-pixel picture at the center of which there is a white square hole in a black background into its frequency space counterpart.

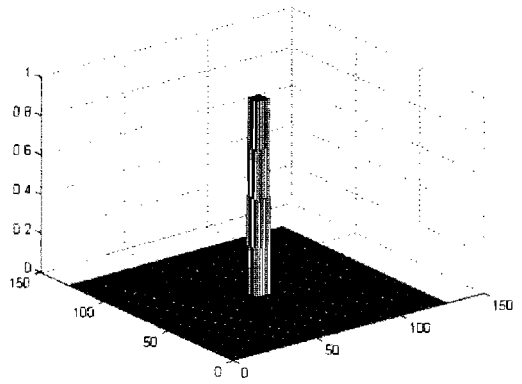

Figure 4.4. D view of a square hole

Using the command FFT2 transforms the real space 2-D matrix into a complex 2-D matrix that is not as easily understood. Figure 4-4 shows the real part of each element of the matrix while Figure 4-5 shows the modulus.

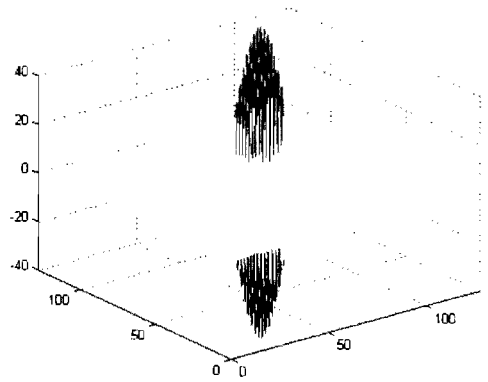

Figure 4.5. D view of the real part of the square hole's FFT.

Occasionally, people are also interested in the square of the modulus as power spectrum.

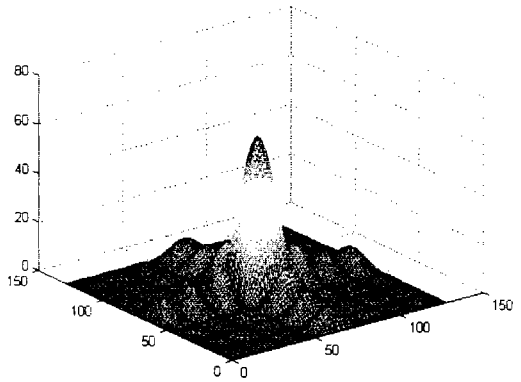

Figure 4.6. 3-D view of the absolute value of the square hole's FFT.

Let us look at a picture of the earth.

Figure 4.7. Earth (64 x 64, Gray Level)

The Fourier transform of this image is shown in the frequency domain.

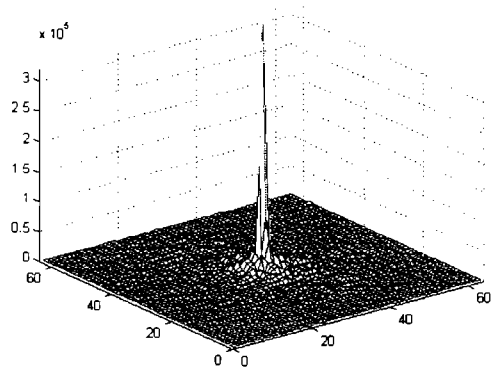

Figure 4.8. Absolute FFT result

It is common to illustrate Fourier spectra of images as intensity functions. The dynamic range of Fourier spectra usually is much higher than the typical display method is able to reproduce faithfully, in which case only the brightest (largest values) parts of the spectra are visible on the display screen. A useful technique that compensates for this difficulty consists of displaying the following function instead of $|F(u,v)|$, where c is a scaling constant and the logarithm function performs the desired compression.

$$D(u,v) = c\log[1 + |F(u,v)|]$$

The use of this equation greatly facilitates visual analysis of Fourier spectra, as shown in Figure 4.8 and 4.9.

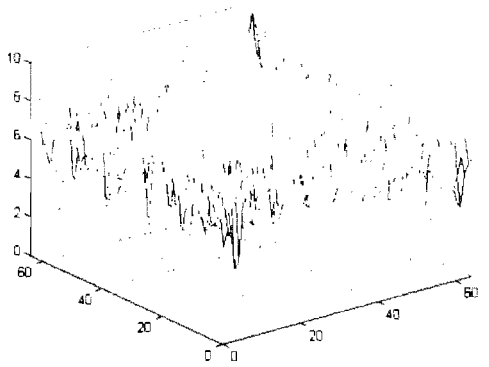

Figure 4.9. Log scaled 3-D view of Fig. 4.6

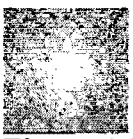

Figure 4.10. 2-D intensity illustration of the log scaled Fourier spectrum

Looking at Volume Under FFT Curve

Initially, we started doing FFT on an image, getting the absolute value for each element of the FFT matrix and drawing it in the 3-D view. The results look much alike. First, there is an extremely tall spike representing the zeroth term of the Discrete Fourier Transform (DC component) at the center of the frequency plane. Then, there is the low-frequency and mid-frequency range in which usually much more common height spikes can be found comparing to the high frequency range. Usually in the high-frequency range, there is nothing but relatively flat component representing noise. However, for some highly periodically featured pictures, there could be some unique features shown in this range. We try our best to investigate hoping to find something useful.

The Idea

We assume that the volume under certain frequency range will tell us the amount of information in which we are interested. We followed the following steps to find out.

1. Prepare two images into black and white ones with 256 gray levels.
2. Subjectively judge which of the two has more amount of valuable information.
3. Find the size of the image.
4. Take the FFT of the image.

5. Divide the area of the 2-D FFT into bands starting from the zeroth term,

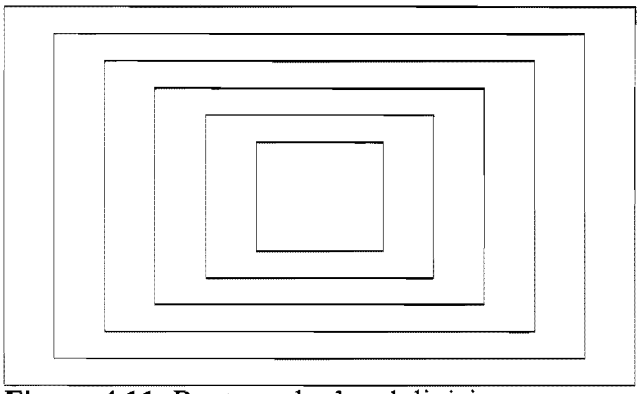

Figure 4.11. Rectangular band division

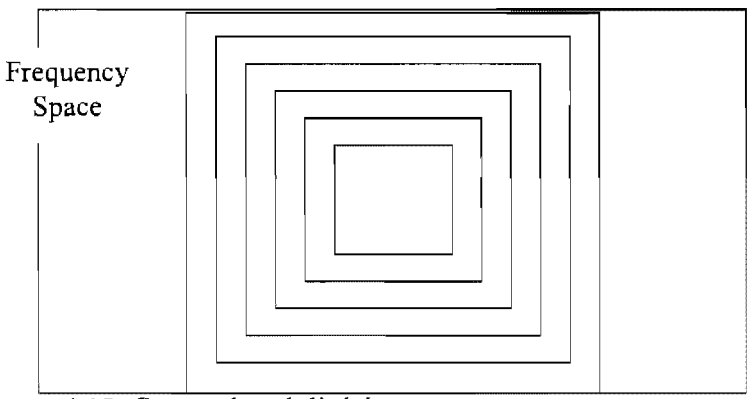

Figure 4.12: Square band division

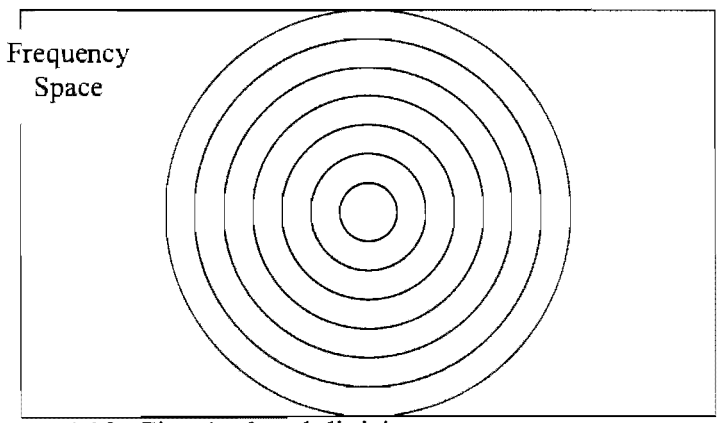

Figure 4.13: Circular band division

6. Sum the magnitudes of the FFT pixels inside each ring to get the volume of that ring.

7. Import the sums to Microsoft® Excel 97.
8. Combine different rings to analyze the relation between the combined volume under FFT curve and amount of valuable information according to the subjective result.

Choice of Division

Now let us discuss which method we should use to make the division in the discrete Fourier transform (DFT) result.

Basically there are two choices, circular division and rectangular division. The reason was that the DFT given by the software is in the form of a matrix, usually a two-dimensional one for a two-dimensional image. From this point of view, the rectangular division is sort of 'intrinsic', and thus easy to compute. On the contrary, to make a circular division, we have to locate the center of the matrix, calculate the distance between this center and each element of the matrix. With the distance falling into our pre-determined grids, we then say this element belongs to group n instead of the next groups. Obviously, circular division will involve much more computing.

Initially, rectangular division was chosen. Rectangular bands can be easily found according to the columns and rows as (shown in Figure 4.11). Several early calculations and curves were generated this way. (For example, the light on and light off images to be introduced later.)

As the study progressed, the author concluded that by symmetry about axis $\omega_x=0$ and axis $\omega_y=0$ the extra columns of the matrix (as shown in Figure 4.12) should be neglected. In other word, the author wants to have equal $\Delta\omega_x$ and $\Delta\omega_y$. Thus, the division becomes square instead of rectangular shape brought by the camera. The extra columns of frequency components are outside of the visual bandwidth and may be without significant changes in the image quality. This division method is also used on very small square images cut from large images.

On the other hand, the author is looking forward to finding the distribution of the Fourier transform along the modulus frequency without regarding any direction. By this standard, circular would definitely be the choice. At this point, it is only natural to bring the symmetry to the next step. Can the division be symmetrical in any direction (circular as shown in Figure 4.13)? We know that rectangular or square divisions are easy to calculate. However when the matrix becomes very large in size, for example 720 by 480 pixels, it is found that circular division can do as well. (Figure 4.13). In addition, circular division provides better way to understand the stuff.

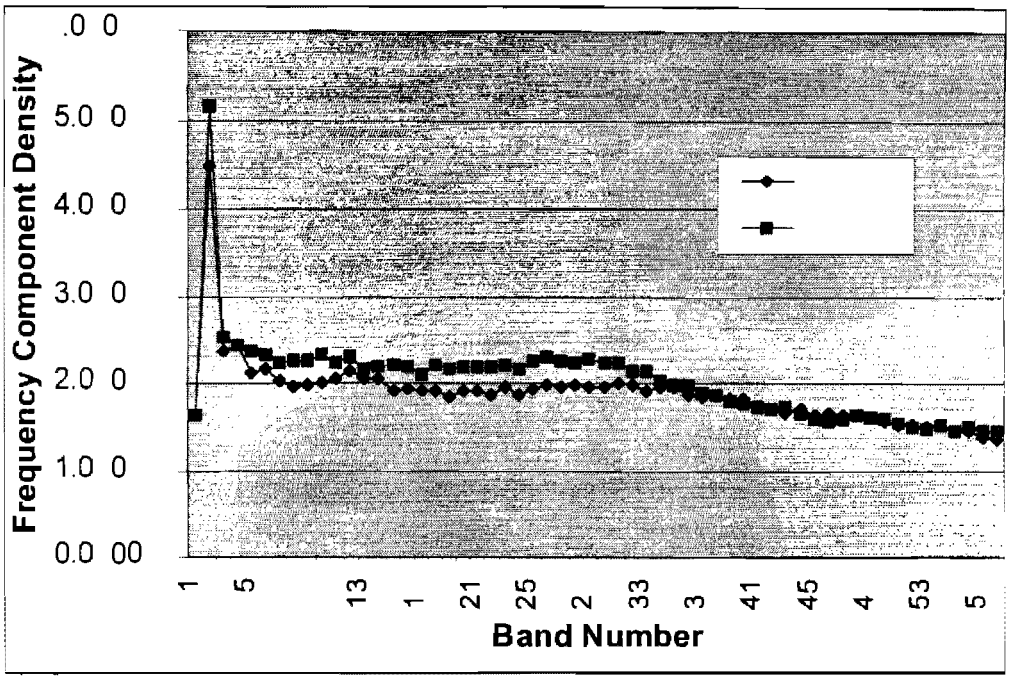

Figure 4.14: Comparison between circular and square division

Thus, for a large size image with more than 400 by 600 pixels, we will use the circular division as the better option. However, in situations where the images' sizes are less than 100 pixels, we choose to use square division as the only choice because the difficulty in dividing and the deviation brought by the circular division in such small matrices.

Separating the Zeroth Term (the DC component)

After examining the equations of 2-D discrete Fourier transform, it is obvious that the center of the frequency domain should be the result of summing all the gray-level values of every pixel in the picture. It describes how bright the picture looks from a far distance rather than describing any feature of the picture that is detailed. The author borrows the electrical term, 'DC component', to refer to this value. Usually when a large size picture is involved, this 'DC component' tends to get extremely large comparing with other frequency components. What we want to make sure is that this value will not get in the way of our examining other potentially useful values.

The initial calculation puts the DC component along with other low frequency components in the center block (the first band) and finds the summation in that part. To avoid the effect of this DC component, the author chose to simply neglect the center block of our divisions.

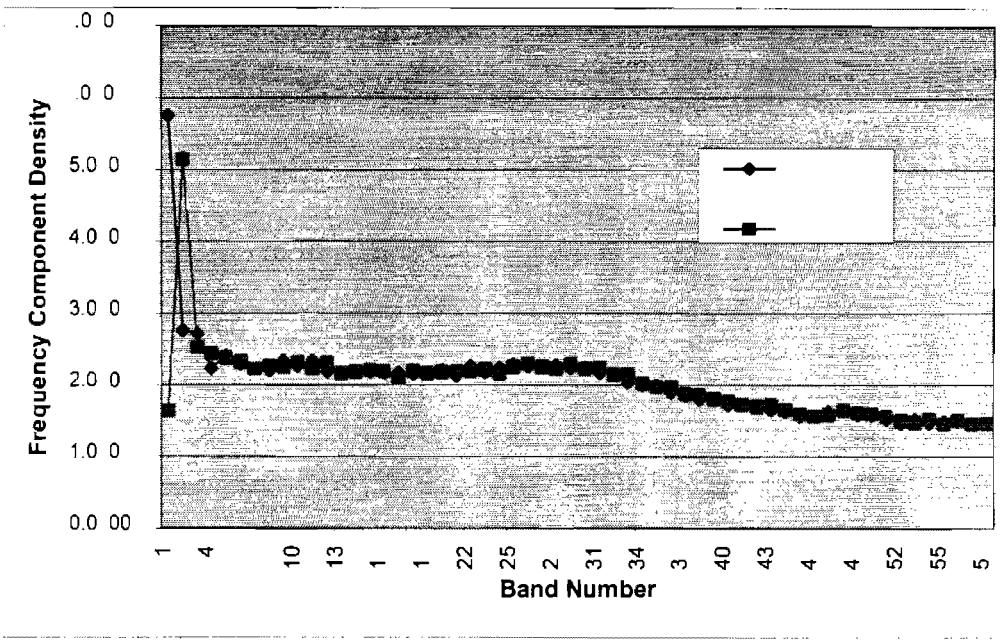

Figure 4.15: Comparison between separating and not separating the DC value

However after examination of the result of MATLAB® command FFT2 (Discrete Fast Fourier Transform in 2-D) and FFTSHIFT (Shifts DC component to center of spectrum, for matrices, swaps the first and third quadrants and the second and fourth quadrants for visualizing the Fourier transform with the DC component in the middle of the spectrum.), the author found that the output frequency matrix is not symmetrical when the input matrix has even numbers of rows and columns although it does require even numbers of rows and columns for the sake of easier and faster calculation. In most cases, a discrete image has even number of rows and even number of columns. Thus, there is no center element in the output matrix. There are four elements that are closest to the ideal center. In the initial calculations, the author avoided the problem by including the DC component in the first band (the lowest frequency band).

Currently, the author believes that the DC component of the transform should be separated from the matrix because it has a special property. It describes the background luminance that tells relatively how bright one image is among a series of such images. The author found that the MATLAB® software chooses to put the DC component of the transform on one of the four centermost location and managed to modify the program to do the separation without greatly changing the distribution of frequency component among other frequency bands (see Figure 4.15).

Defining the Frequency Range

Now that our available frequency domain rings start only at the second, there comes the question, 'Exactly what frequency range should we look at?'

Common sense tells us that in the high frequency range, noise usually takes up most of the activity instead of the real image. Nevertheless, at first we will not exclude any other frequency range. We will see some reasoning to take out some part of the frequency range in the chapter that deals with the STV. For right now, we will include every ring starting with the second ring and watch the result carefully.

STV Image Analysis

Researchers have been studying the visibility of small targets on highway. They have developed special hardware to perform the experiments in the real environment. They have also developed equations to do the visibility calculation. What we present here hopefully will be another perspective to look at the problem.

Frequency Component Analysis

Ten Image Sections with Targets

Ten images are carefully cut down from images taken of targets at different locations on the near side of the road lamps. Each of them is of size 64 by 64 pixels, with the target located at the center and some pavement as the background.

First, we judge the visibility of these target by looking at a pair of these cut images and subjectively judge in which one the target can be seen better. This method is known as 'subjective bubble sorting'.

Figure 4.16. Original left side location # 1

Figure 4.17. Original left side location # 2

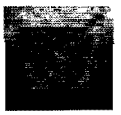

Figure 4.18. Original left side location # 3

Figure 4.19. Original left side location # 4

Figure 4.20. Original left side location # 5

Figure 4.21. Original left side location # 6

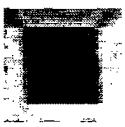

Figure 4.22. Original left side location # 7

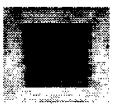

Figure 4.23. Original left side location # 8

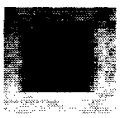

Figure 4.24. Original left side location # 9

Figure 4.25. Original left side location # 10

Steps of 'subjective bubble sorting': (Distance between eyeballs and computer screen is 2 ft.)

Table 4.1. Subjective Bubble Sorting

Step number	Finding	Ranking Adjustment Starting with low visibility
0	None	1, 2, 3, 4, 5, 6, 7, 8, 9, 10
1	2<1	2, 1, 3, 4, 5, 6, 7, 8, 9, 10
2-7	3>1, 4>3, 5>4, 6>5, 7>6, 8>7	2, 1, 3, 4, 5, 6, 7, 8, 9, 10
8-11	9<8, 9<7, 9<6, 9>5	2, 1, 3, 4, 5, 9, 6, 7, 8, 10
12-14	10<8, 10<7, 10>6	2, 1, 3, 4, 5, 9, 6, 10, 7, 8

We should be aware that human judgement error exists in such methods.

Sampling Theorem

A bandlimited signal is a signal, f(t), which has no spectral components beyond a frequency B Hz; that is, F(s) = 0 for |s| > B. The sampling theorem states that a real signal, f(t), which is bandlimited to B Hz can be reconstructed without error from samples taken uniformly at a rate R > 2B samples per second. This minimum sampling frequency, R_N= 2B Hz, is called the Nyquist rate or the Nyquist frequency. The corresponding sampling interval, T = 1/2B (where t = nT), is called the Nyquist interval. A signal bandlimited to B Hz which is sampled at less than the Nyquist frequency of 2B, i.e., which was sampled at an interval T > 1/2B, is said to be undersampled.

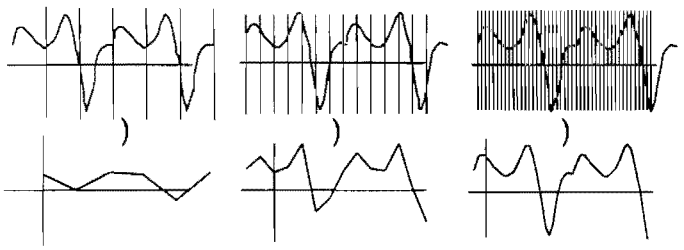

Figure 4.26. f(x)sampled a) below the Nyquist, b) below the Nyquist, c) at or above the Nyquist rate and the reconstructed $f_R(x)$'s from the Nyquist samples

Human eye resolution and cut-off frequency

An interesting question emerged from examining the above images. What does the driver see instead of the video camera? To answer this question, first we need to find out what resolution a human eye has. It is related to the cutoff frequency. In other word, we will be able to decide what frequency range is effective in the frequency domain representation of a digital image. If that frequency is lower than the maximum frequency, we can remove all of the higher frequency components. Further more, we can use inverse FFT to reconstruct a digital image that shows what a human eye should see.

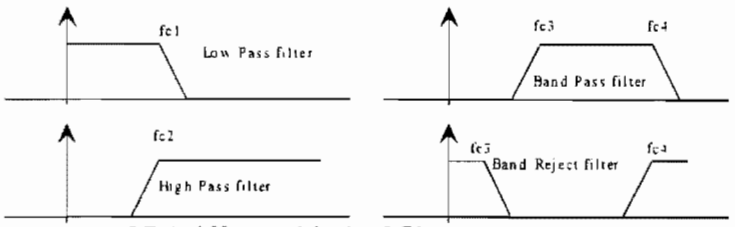

Figure 4.27. Different kind of filters

The resolutions of human eyes vary. However, it is said that roughly most people have a bar-gap resolution of a minute of arc. We will try to determine the upper cutoff frequency of human eye based on this resolution value and the measurement among our images.

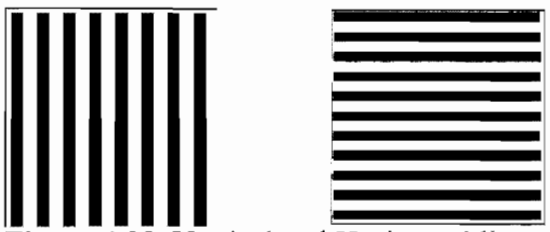
Figure 4.28. Vertical and Horizontal lines

Consider a line segment of 18 centimeters (Because this is the length of a side of the standard square target) located at 83 meters away from the observer. We can estimate the span of the line segment from the observer's (eyeball or camera) point of view as the following equation.

$$\frac{18cm}{8300cm} \bullet \frac{180^\circ}{\pi} \bullet \frac{60'}{1^\circ} = 7.46 \text{ minute of arc}$$

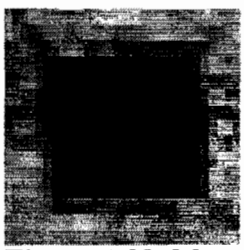
Figure 4.29. Magnified original left side location # 10

Then we measure the target in the image to be 22 pixels. This gives us the following equation.

$$\frac{22pel}{7.46'} = 2.9 \text{ pixel per minute of arc}$$

Obviously, we now are able to find in our particular example the one minute of arc human bar-gap resolution is equivalent to about 3 pixels. Meanwhile, the resolution of the digital video

camera is 1 pixel by definition. The number of pixels per min of arc is related to digital video camera's magnification or zooming. In a video cam that has a "zooming" capability, the images should be taken at same zooming settings.

We can claim that under the settings we picked for these images, an average human eye has a sample rate as low as approximately one third of the camera.

$$R_{human} = \frac{1}{3} R_{camera}$$

This implies that the cutoff frequency of eye will be one third of that of the camera.

$$B_{human} = \frac{1}{3} B_{camera}$$

With this knowledge in hand, we can examine the Fourier transform equations and estimate the corresponding frequency limit. We know that the frequency domain representation of a 30 by 30 pixel image is a 30 by 30 matrix with constant term located at center. That gives B_{camera}=[-15, 15]. From (6.3-3), we have B_{human} =[-5, 5].

In an FFT of a digital image with 30 by 30 pixels, the effective frequency component representing a typical human eye gain under the same situation will be from the center to the 5th ring introduced and illustrated in Figure 4.12. If the image size is 480 by 480, the frequency component within 80 rings (ring introduced and illustrated in Figure 4.13) from the center should be considered what human eyes get.

Following are the result of the reconstructed images with higher frequency component outside of the 5th ring removed.

Figure 4.30. Filtered left side location # 1

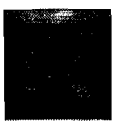

Figure 4.31. Filtered left side location # 2

Figure 4.32. Filtered left side location # 3

Figure 4.33. Filtered left side location # 4

Figure 4.34. Filtered left side location # 5

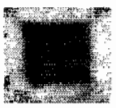

Figure 4.35. Filtered left side location # 6

Figure 4.36. Filtered left side location # 7

Figure 4.37. Filtered left side location # 8

Figure 4.38. Filtered left side location # 9

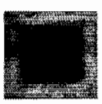

Figure 4.39. Filtered left side location # 10

The following points can be seen when figures 4.30 through 4.39 are compared with figures 4.16 through 4.25 :

- The resolution of the video cam is greater than that of the human eye.
- The images may be filtered to determine the cutoff spatial frequency intrinsic of individual human eye. Suppose the images' frequency components are filtered one ring at a time from the highest ring. When the observer first detects a change of content judging only by his eyes, we say he has a cutoff frequency related to that ring number.
- For most people, filtering the component above the 5^{th} ring does not significantly reduce the resolution for their eyes.

FFT Analysis of the Images

Ten Cut-around-the-target Images

For 20 of the cut target images, we perform the calculations. We pick square division due to the limited pixels within the digital image. A plot of the FFT calculation result is shown in Figure 4.40. It also has a size of 30 by 30 pixels. The square at location (16, 16) represents the DC value. The bright squares at adjacent locations represent the frequencies that have relatively larger component. We also find that these high value points are mainly located around the center or on the axes of the f_x=0 and f_y=0. Because of these missing frequency component at off-axis frequency space, our choice of the square division method introduced earlier becomes a very

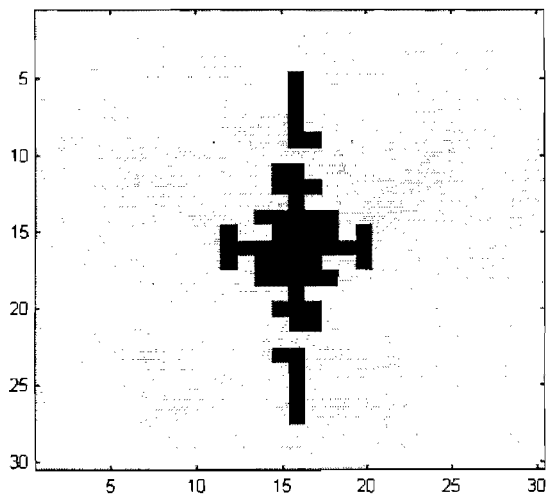

good approximation of circular division.
Figure 4.40. Frequency domain left side location #7

First, let us look at a 3-D plot of the frequency component distribution of the series of target images (30 by 30 pixel) of the ten left locations.(Figure 4.41) There are two general features. First, the later locations have higher components than the early ones. Second, the frequency

component is mainly distributed within the first 5 ring. For higher frequencies, it is hard to say whether the value is more related to signal or noise.

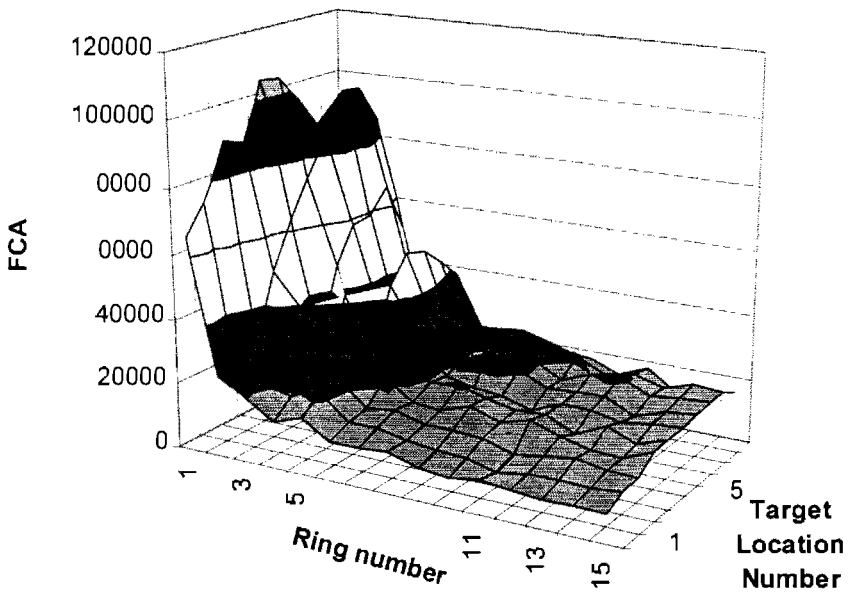

Figure 4.41. Frequency component distribution of 10 targets on the left side in 3-D plot

In Figure 4.41, the first column (ring number = 1) shows the zeroth terms (DC values) of the Discrete Fourier Transform that represent the background luminance (the (16, 16) point in Figure 4.40). The second column shows the summation of the first ring (adjacent 8 points in Figure 4.40) and so on. The first columns appear to be dynamically equivalent to an STV type evaluation. Figure 4.42 is the same data presented in a two-dimensional graph.

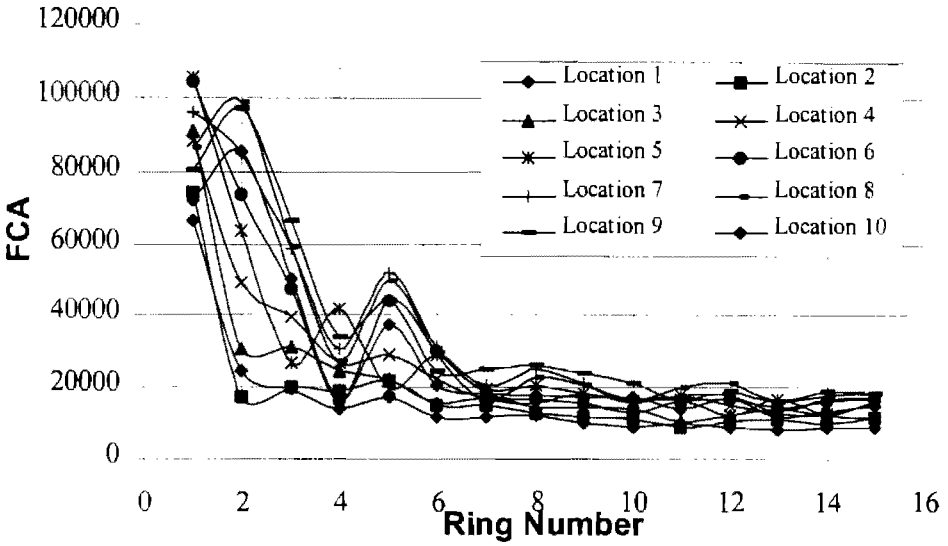

Figure 4.42. Frequency component distribution of 10 targets on the left side in 2-D plot

The second observation provides us another justification for us to neglect the higher frequency components.

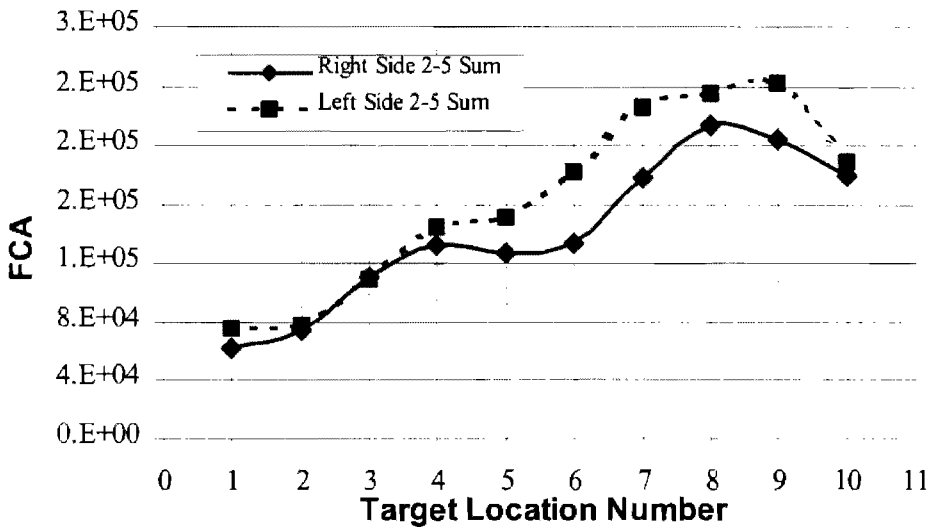

Figure 4.43. Frequency Component Comparison of Left and Right Targets

The results of the frequency component analysis of both left side and right side are shown in Figure 4.44. What we can see from this plot are the following observations.

- The frequency component analysis values at further locations are usually higher than those at nearer locations.
- The frequency component analysis values of the left side of the road are usually higher than those of the right side.

- The highest frequency component analysis value of either side does not occur at the furthest location.
- The lowest frequency component analysis value of either side occurs at the nearest location.

Now we can compare with VTC(Video Target Contrast) and n-point VTC results shown in the following two plots.

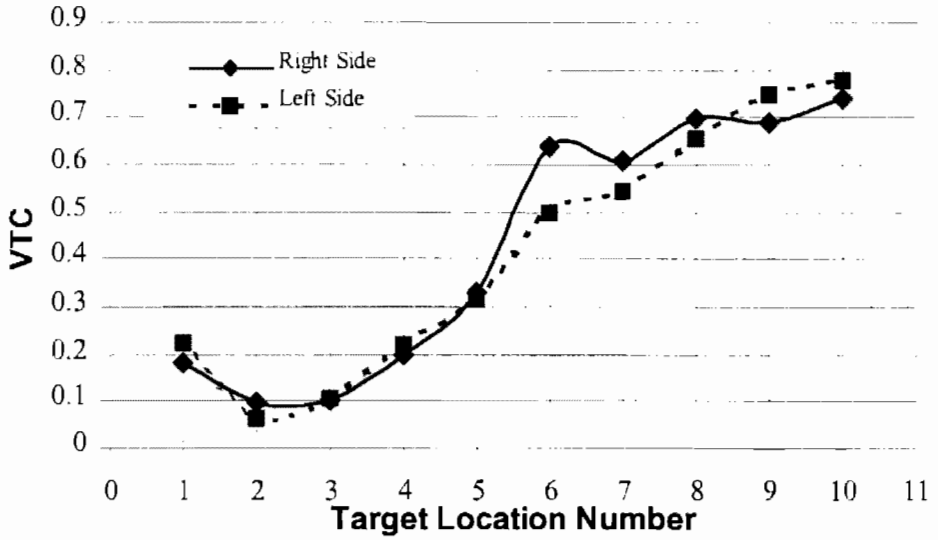

Figure 4.44. VTC Comparison of Left and Right Target

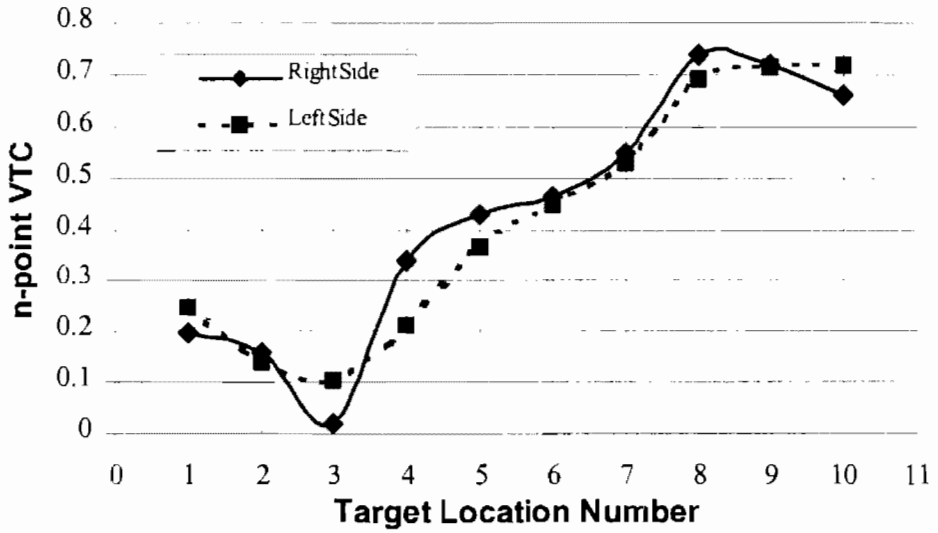

Figure 4.45. n-point VTC Comparison of Left and Right

To compare these data better, we normalize all series of results to make them fit into interval [0, 1] so that they can be shown in a single graph. From both the left side comparison and the right side comparison, we can see the dynamic relations of the results given by different methods

agree generally. They almost have the same slope. The differences occur at the beginning and end. The shape of the curve of our frequency component analysis is closer to the n-point VTC (VTCn) curve.

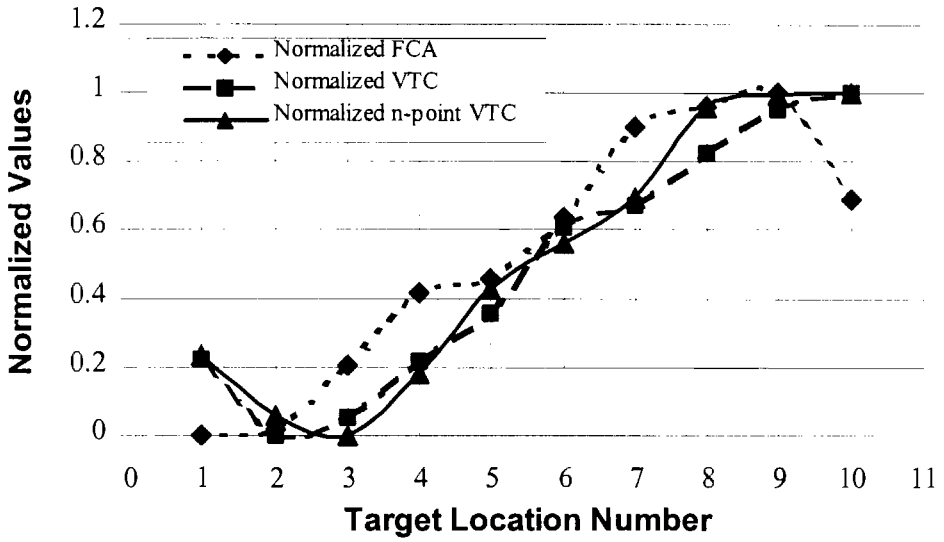

Figure 4.46. Comparison of Methods (left side targets)

As seen from Figures 4.45 and 4.46, visibility distribution obtained by using the FCA method shows dynamically same response with visibility obtained by using the VTC method. FCA visibility values are almost mach with the VTC visibility values at the target locations 2nd, 5th, 6th, 8th and 9th for left side and at the target locations 2nd, 5th, 7th, 8th and 9th for the right side. For the rest of the target locations there is acceptable difference between the methods.

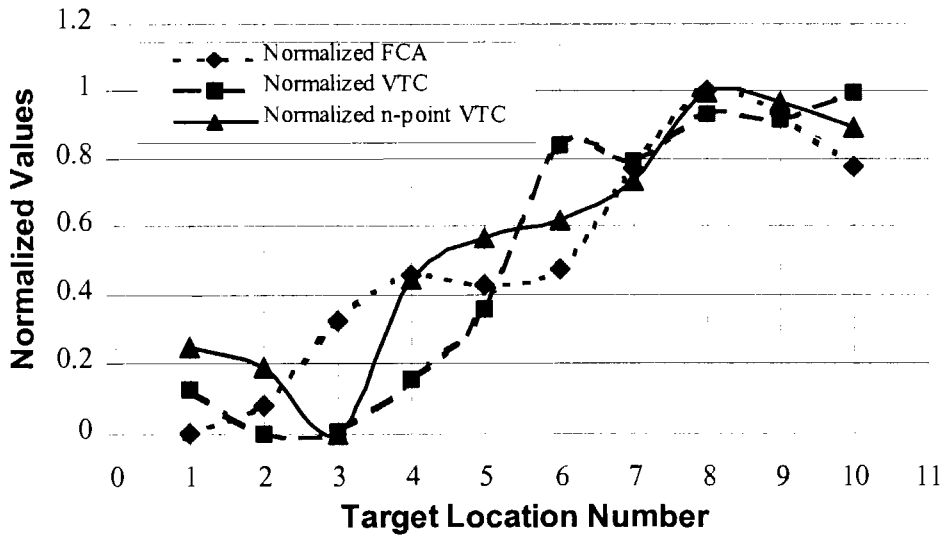

Figure 4.47. Comparison of Methods (right side targets)

Lights Off and Lights On Images

Digital images acquired under dramatically different lighting conditions prove to be great tools to learn the relation between image content and the corresponding frequency component. All the plots in this section are were calculated using rectangle division method introduced earlier. The zeroth term of the Discrete Fourier Transform was included in the first band. Thus it contributes to the first point in the distribution curve.

Image Acquisition

In a typical night time roadway situation we would like to compare the information available to an observer under no light conditions, off road lighting conditions, partial roadway lighting conditions, and under full roadway lighting conditions.

All the images were made using an analog CCD video camera and a digital CCD video camera. The images were transferred to computer disk and Fourier transforms of the images were calculated. The analog and digital video images were compared to determine the similarities and differences in the digital and analog images then Fourier transforms of both types of images were calculated and compared. Either image represents the scene very well so we used the most convenient image capture and transfer technology available to us. The image capture and transfer technology was in the mid price range state-of-the-art electronics. More expensive technology would not improve the analysis significantly.

Understanding Frequency Domain

No Light Condition

The series starts with the image under no light conditions. As shown in Figure 4.48, there is no light for the CCD camera to record, the scene is black. However, the Fourier transform of the CCD image shows some high frequency components and the amplitude of the components increase with increasing frequency. That shows that the elements of the digital image matrix are not simply all zeros. Otherwise, we would have nothing in the spatial frequency domain. Upon a very close inspection of the no light CCD image matrix, it was discovered that the gray scale pixels were indeed different from "dead black" or 0.

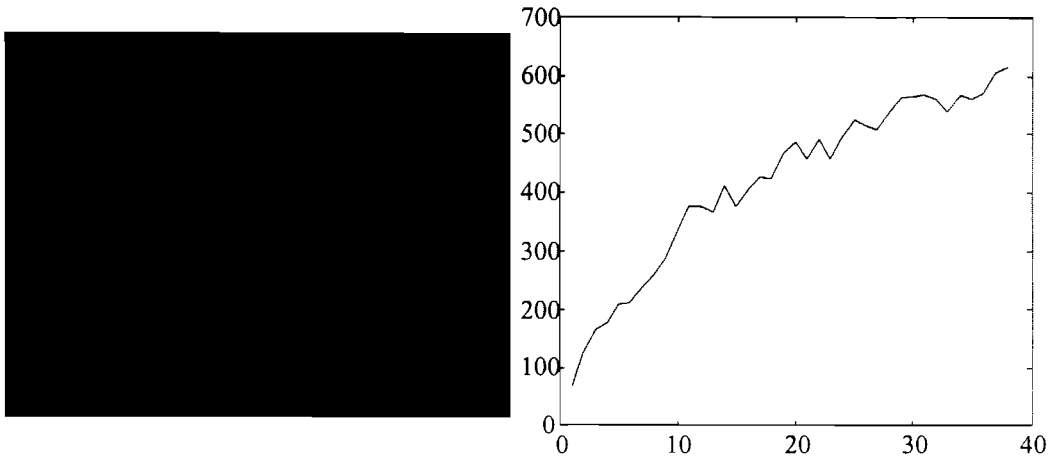

Figure 4.48: No light image(and frequency component distribution)

We know that the CCD camera has 256 levels of gray available and all the cells in the CCD array are not registering 0 for no light. The fact that the CCD has a dark current always present in each cell of the CCD array determines that some of the cells will be read at a level above 0. The values above 0 are distributed randomly throughout the CCD array.

There are two choices to fix the dark current problem. We can cool the CCD array to –40°F, which is very expensive. Or, we can determine what the Fourier transform of the dark current looks like and filter the dark current out of the Fourier transforms. We characterized the dark current frequency response, as shown above, to determine the dark current's contribution to the Fourier transform. The dark current's contribution was very small compared to the Fourier transform of images under other conditions. Therefore, we choose not to filter it out, but filtering it out is an easy task if it becomes necessary.

Off road lighting conditions

After the zero light condition had been established the off road lighting conditions were imaged. The site we used for our roadway lighting conditions was adjacent to a lighted rest stop on U. S. Interstate 27, north of Abernathy, Texas. The off road lighting was too low for the CCD video camera to clearly image the site, however the oncoming automobile head lights, and other light sources in the field of view of the camera were ready for imaging.

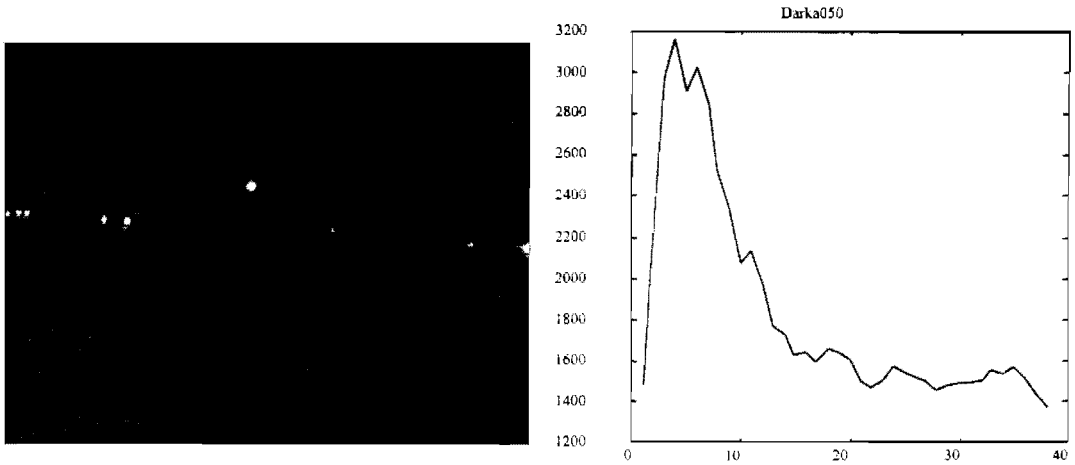

Figure 4.49: Off road lights image (and frequency component distribution)

In Figure 4.49, the spatial frequency content in the high spatial frequency region has increased slightly but the low frequencies have remained small. There is an increase in the amplitudes of the frequencies from range 4 to 14 due to the auto and other point source lights. The point sources produce enough light for the camera to image themselves but not enough energy to illuminate any portion of the site. The contribution of the off road lighting from the rest stop lighting is visible in the original image and calculated in the Fourier transform, but the details are not visible in Figure 4.49 due to the resolution of the reproduction in the paper. The rest stop off road lighting was just at the threshold of the CCD's low light imaging limit. Under such circumstance, the human observers were in their lower mesoptic vision region. The average background luminance and the low frequencies from range 1 to 3 are very small because there is almost no contrast in the image.

We also imaged the off road lighting conditions with an STV target in the field of view. It was a standard 20% reflective, 18-cm x 18-cm target. Two fixed LED diodes were mounted on the target to make it locatable in the CCD's field of view and for future luminance calibration techniques. In Figure 4.50, the LED's are clearly visible in the low middle center of the image and the auto headlights have moved. The single unmoving source in all the frames is an outdoor light at a farm house The addition of the LED's and the changes in both locations and intensities of the auto head lights have changed the Fourier transform slightly. The more intense auto headlights in the middle right increase the amplitude of the midrange frequencies, but the higher frequency components still remain very low.

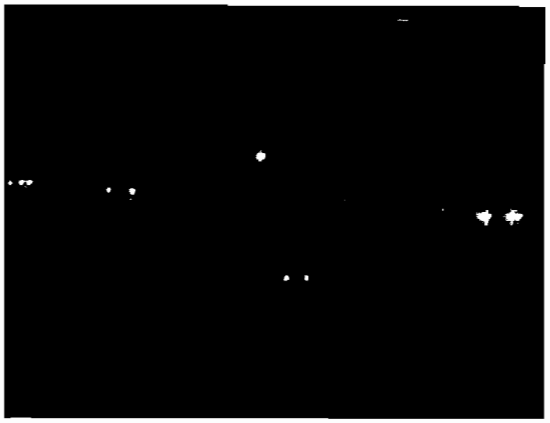

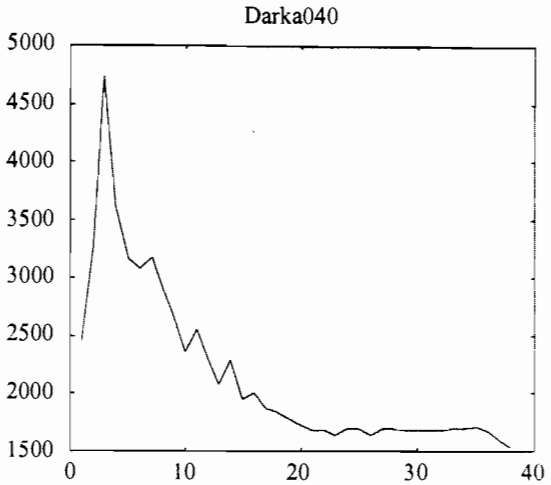

Figure 4.50: Off road lights and LEDs image(and frequency component distribution)

Lighting Conditions

Under partial roadway lighting conditions the roadway lights behind the STV target were energized to determine the frequency response to this contribution of partial illumination of the site. As can be seen in Figure 4.51, there is an image of the top portion of the STV target and a portion of the roadway surface and its surrounding area are illuminated.

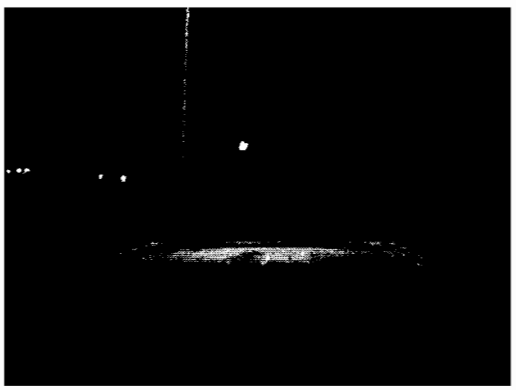

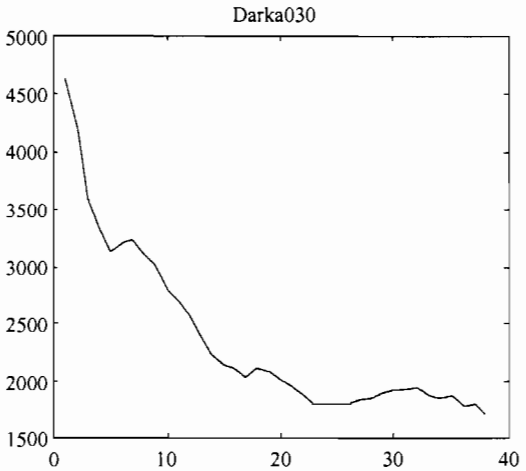

Figure 4.51: Partial roadway lighting image (and frequency component distribution)

From the Fourier analysis of the scene the lower range frequencies, from range 1 to 3, have increased because the average background luminance has increased, but it has not increased a great deal. The mid frequencies, from range 4 to 14, have also changed slightly reflecting the more detail available in the image. The high frequency content has increased slightly.

Under full roadway lighting conditions shown in Figure 4.52, all the details of the roadway are clearly visible, the STV target is clearly visible along with the auto headlights. From the Fourier analysis it can be seen that the lower range frequencies, from range 1 to 3, have increased significantly reflecting the large increase in the background luminance of the image. The midrange frequencies, from range 4 to 14, have increase significantly reflecting the availability of much more detail of the scene in the video image. The high frequencies, from range 15 to about 35 have also increased significantly showing the increase in available detail in the higher frequency ranges.

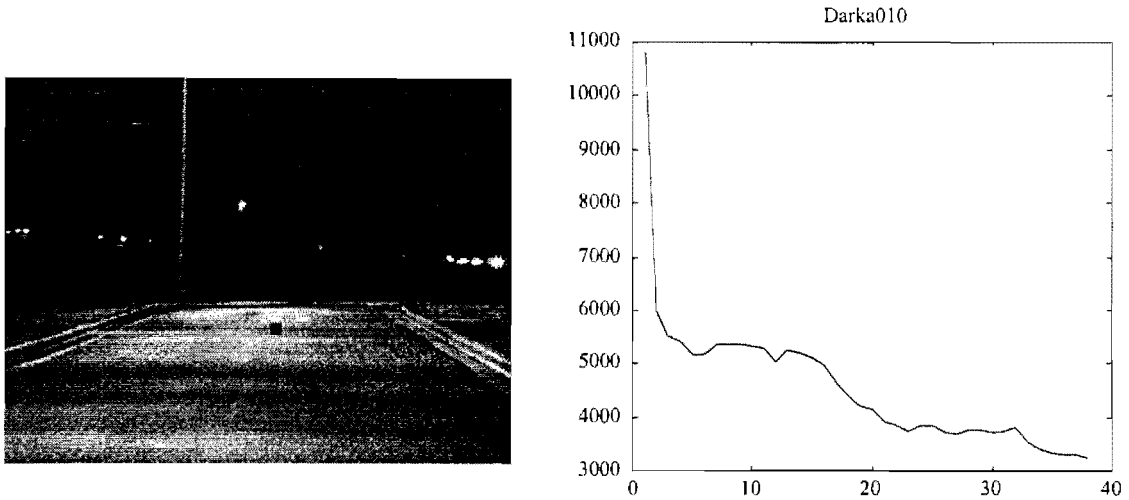

Figure 4.52: Full roadway lighting image
(and frequency component distribution)

Conclusion

The graphs of in the previous figures were all scaled but they are still hard to compare. When all the graphs are placed in the same scale as shown in Figure 4.53, we can see the changes in spatial frequency content from a lights off to a lights on situation. The changes represent the differences in the information available to an observer as more light is added to the scene. As more light is added to the scene the average background luminance of the scene increases as shown in the region, from range 1 to 4. From range 4 to 38, as more light is added to the scene, the amplitudes of the higher frequencies increase, reflecting the added detail available to an observer.

The curve associated with Figure 4.52, has the largest partial volumes above each partial area. The total volume, the sum of all the partial volumes, is a measure of the total information available to the observer. An observer has a visual transfer function with a cutoff frequency of about one minute-of-arc (1') or less, so an observer cannot resolve the higher frequencies past about, range 12 to 13 (according to the calculation in earlier section). As the background average luminance increases from a few cd/m^2 to thousands of cd/m^2 , the range 1 to 4, an observers visual response changes from sotopic to mesoptic to photopic. So the absolute value of the background luminance from the Fourier transform determines the visual lighting level response and the higher frequencies determine the details available to the observer.

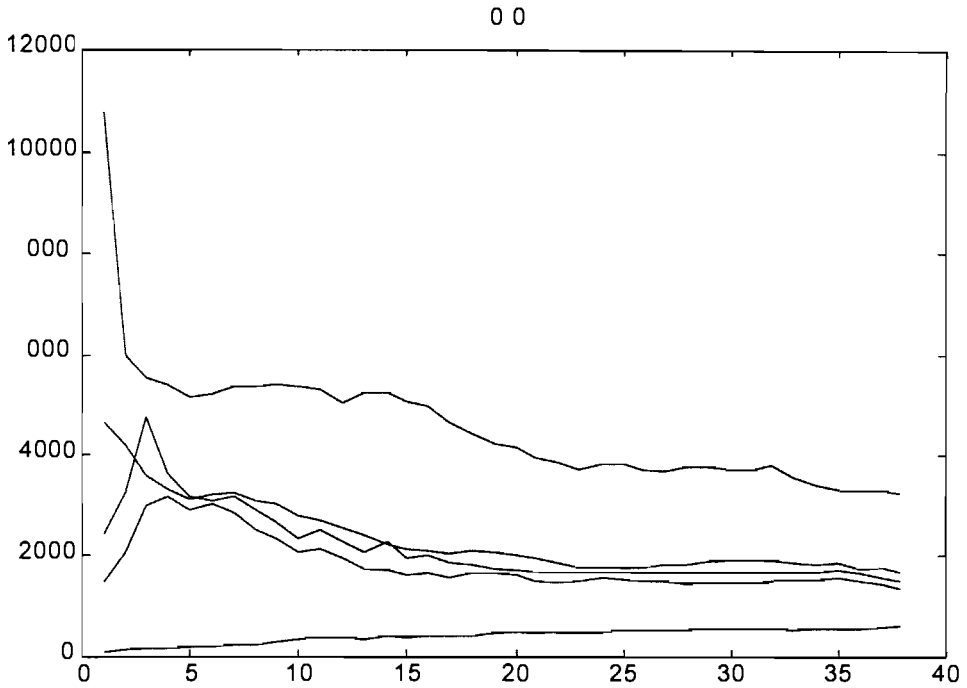

Figure 4.53: Frequency component distribution (comparison of variable lighting situations)

Now it should be noted that in order to change the scene noticeably to an observer the modulation transfer function (MTF) must change by at least 10% or the changes in the scene are not noticeable to an observer (Williams (1989)). We also believe that if MTF is kept unchanged, then the information provided by the scene must change by at least 10% for a clear recognition. From Figure 4.53, it is clear that there is a greater than 10% change from no light to some lights and there is a greater than 10% change from some light to full roadway lighting. The fully lighted roadway has almost a maximum background luminance. In order to increase the MTF by 10% the background luminance and all the higher frequency components must be increased or decreased by 10%. Since an observer's eyes operate over eight orders of magnitude in background luminance differences, from night vision to day time vision, 10% may not be discernable in mesoptic vision. However, we are satisfied when the changes in the spatial frequency are discernable to the observer.

Daylight and night pictures

Figures 4.54 and 4.55 show how the field-of-views in day and night conditions are considerably different.

Note the Daylight pictures have a horizontal illuminance of 60-kLux, the night images have a min of 10-Lux and a max of 50-Lux. For example, the two LED's attached to the target were turned on both in the daylight picture and the night picture. They can be clearly seen in the night picture. Because the illuminance caused by an LED has about 5000-mcd that is in the same order

of magnitude with the nighttime environment. However in the daylight picture when the environment is much brighter, the LED's can't be seen at all. This is because the camera divides the luminance into 256 levels from brightest to dimmest for each image. The day and night images are different in scale by 3 orders of magnitude. So it is necessary to adjust the relative amplitudes of the day and night images to place them on the same scale.

Figure 4.56 shows the raw frequency component distribution. It can be seen that the frequency component values in the two curves, daylight picture (60-kLux) and night picture (50-Lux), take the same shape in the lower frequency range and differ in the mid frequency and high frequency ranges. In those ranges, the night picture curve has lower values than the daylight one. In figure 4.57, the curve of the night picture is divided by a thousand to have the correct order of magnitude according to the illuminance measurement result. The daylight image is shown fully in the photopic region of vision while the roadway lighting image is in the mesoptic region. The 3 orders of magnitude difference makes the night time image unresolvable with respect to the daylight image if they are on the same scale. To show them in a better way, a logarithm of figure 4.57 is calculated and plotted in Figure 4.58.

Figure 4.54: Daylight road and target

Figure 4.55: Night road and target

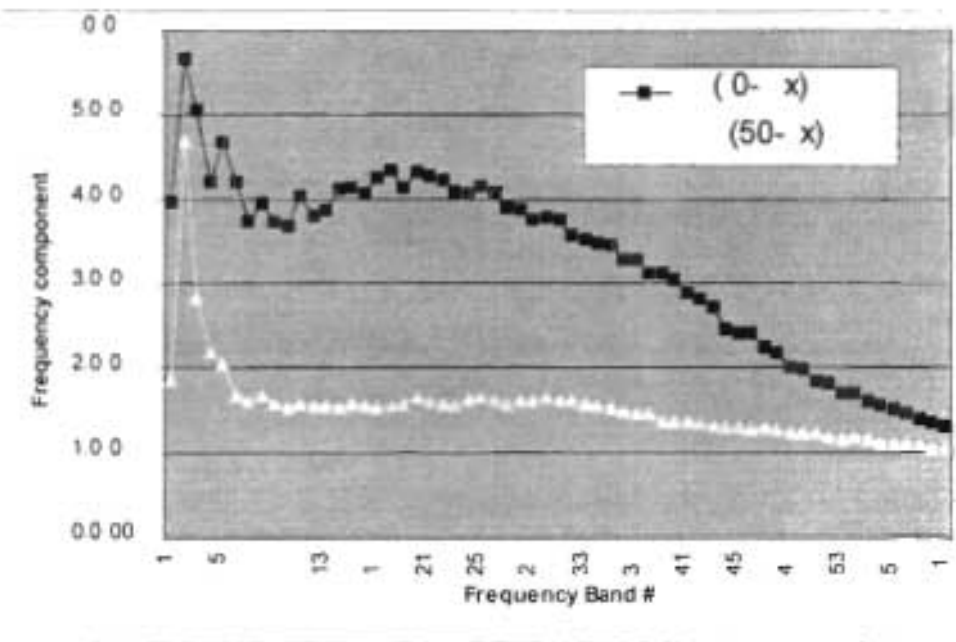

Figure 4.56: Comparison of frequency component distributions.

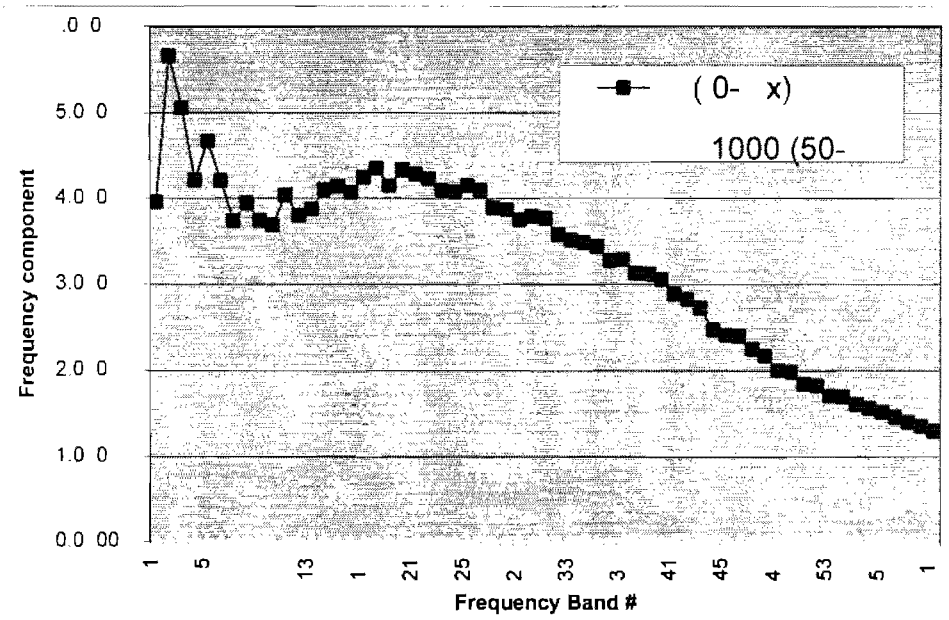

Figure 4.57: Comparison of re-scaled frequency component distribution.

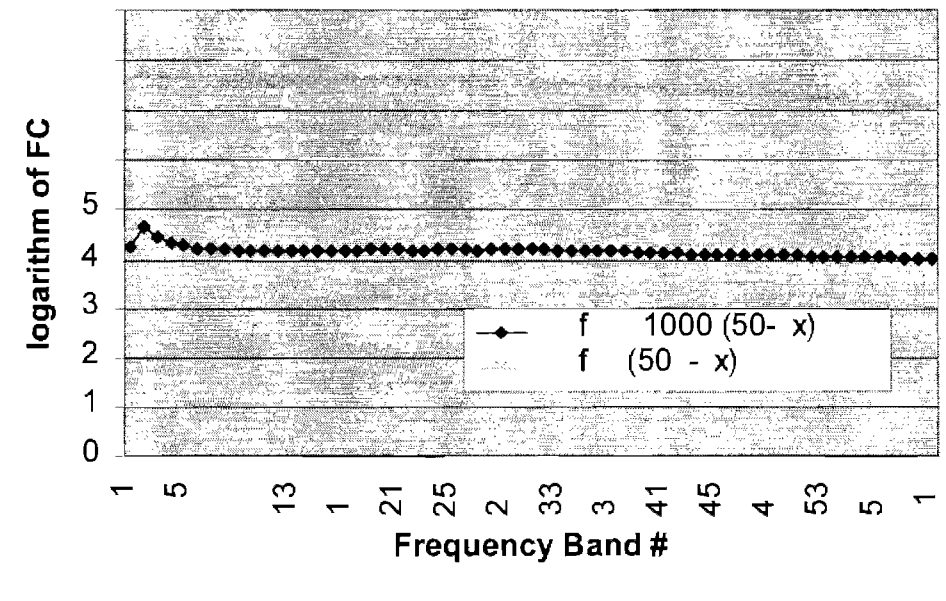

Figure 4.58: Figure 4.57 shown in logarithm.

Dynamic versus Static Roadway conditions

It has been shown in previously sited literature that when the measures of a roadway lighting situation is reported accidents, the STV model design method and the Luminance model design method are basically equivalent.

The STV calculation is specifically based on a static model. The visibility level of each of 20 targets is calculated. The visibility of each target is calculated using a calculated luminance of the STV target, the calculated point background luminances immediately above and below the STV target and the eye adaptation to the average luminance of the target and the background of interest. The background of interest is an ideal patch of roadway surface. Then all the visibility levels for the 20 targets are averaged in some manner to determine the goodness or the badness of a particular lighting situation. (A discussion of an STV calculation is made in chapters 7 and 10 of this paper and in RP-8.)

Contrast is a calculation based on the target luminance and background luminance around a target of interest. The STV model uses contrast and the eye adaptation to an average background luminance level. STV is a calculation based on Contrast, Contrast is a calculation based on Luminance, and the eye adaptation is a calculation based on average background luminance(DL4).

The roadway lighting for a driver is a dynamic situation with the eye adaptation being determined by the dynamic background luminance as the driver passes along the roadway around the roadway lights. The eye adaptation to the average background luminance must be determined as a dynamic situation as the driver passes through the luminance patterns generated by the lighting design.

In the STV model the eye adaptation is treated as though the eye is adapted to each target luminance when the luminance of a particular location is experienced as a transient situation. The transient situation should be viewed as a derivative rather than a constant and eye adaptation should be characterized as an average adaptation to the roadway background luminance rather than the adaptation for a specific single target.

The lights on lights off images of figures 4-48 to 4-52 show the average background luminance, the DC value plus the first few low frequency components of the Fourier transform, increasing as lighting is added to a scene. Under the no light situations of figures 4-49 and 4-50, the average background luminance is very low and the eye adaptation level will be determined by the very low average background luminance. As the lights are turned on in figure 4-51, the average background luminance takes a large jump then in figure 4-52 as the whole scene is illuminated the average background luminance takes another large jump.

The driving situation may be viewed as dynamic changes in the scene, or as dynamic changes in the spatial frequencies of the scene as an observer advances on a particular target. Figure 4.58 represents a dynamic roadway situation as an observer approaches a target on a roadway. Image number five has noise introduced into the image due to a video capture artifact. The noise is completely perodic and can be seen in the Fourier transform of image five as a general amplitude

increase in the higher frequency spectrum of the Fourier Spectrum of image five and as a high frequency noise spike in the tale of the Fourier spectrum. Image number six is equivalent to an STV scene with the observer 83-meters from the target and looking 1^{o} down angle at a 20% reflective target.

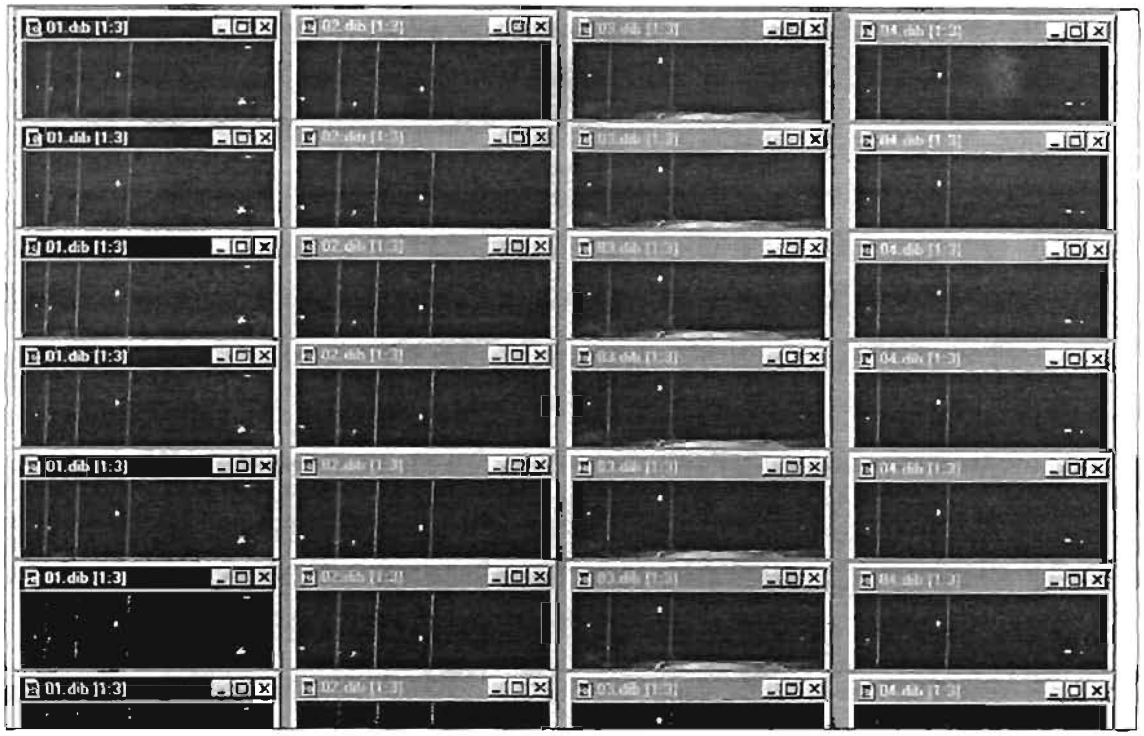

Figure 4.58 Dynamic Roadway images of 20% STV targets, and perodic noise in image #5

The graphs in figure 4.59 and 4.60 show the spatial frequency analysis of the several images set of in sequence as the observer approaches the targets. The graph of Figure 4.59 includes the DC and low frequency band component. Figure 4.60 has had the DC and low frequency component removed and the graphs have been rescaled so details of the midfrequency and high frequency ranges may be shown.

In Figure 5.59 the amplitudes of the Fourier spectrum increases in the midrange frequencies. For the observer the change in the spatial frequency content is larger than 10% form the first (distant) observation to the twelfth (close) observation. The change in frequency spectrum from one image to the next image gives a derivative of the spatial frequencies of adjacent images. The change in spatial frequencies of the several observations yields multiple derivatives or a slope of the change of spatial frequencies with respect to observer position.

In a dynamic situation the change in observer position would be a change in position with respect to time or simplu an observer velocity. So the observer sees a change in spatial frequencies with respect to time as the observer approaches the target. The slope of the derivative is determined by the observer's velocity with respect to the target.

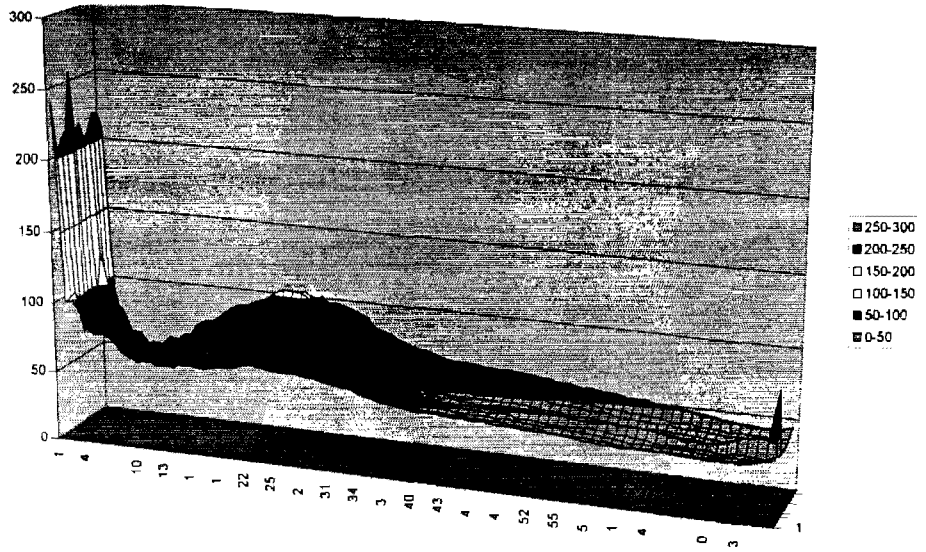

Figure 4.59 Fourier spectrum of dynamic roadway image observation

With the graph rescaled in figure 4.60 the high frequency noise and the high frequency spike of image number five is clearly visible on the right side of the graph. The changes in the Fourier spectrum amplitudes is also clearly visible and a change of the Fourier spectrum of 10% or more may clearly be seen. The change in the Fourier spectrum in a dynamic situation with a moving observer may be seen in the slope of the spatial frequency change from observation 1 to observation 12. An acceleration in spatial frequencies or a change in the slope of the change in the spatial frequencies may also be observed from one image to the next as an observer approaches the target.

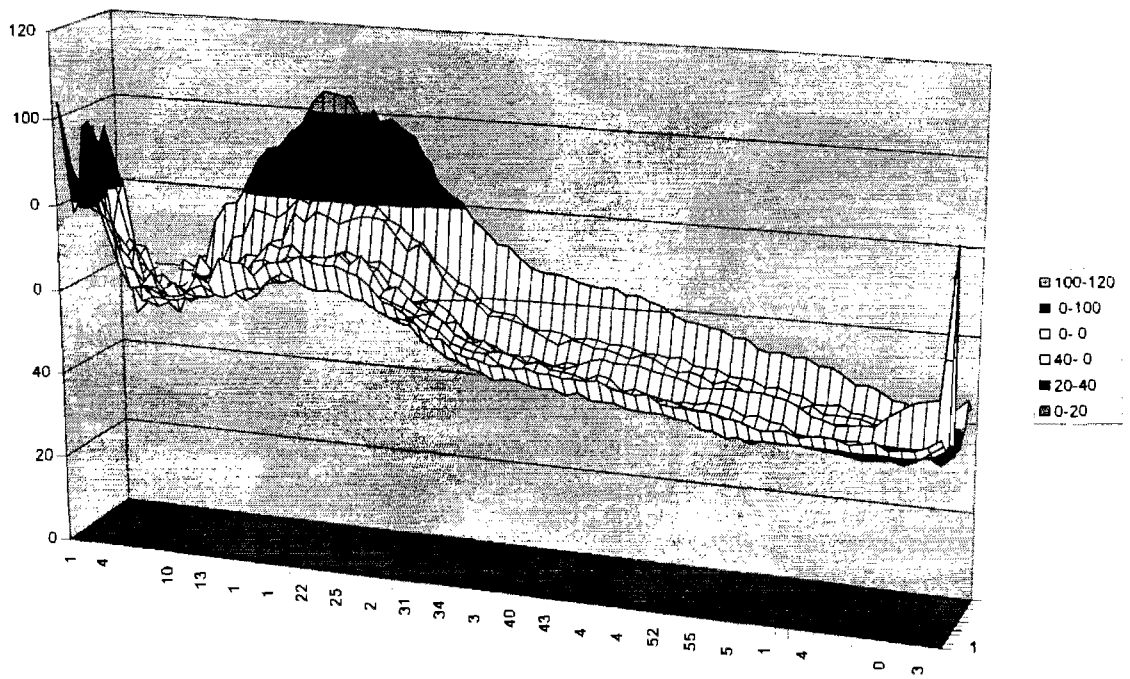

Figure 4.60 Fourier spectrum of dynamic roadway image observation with DC term removed

In Figure 4.58 the right side of the graph shows the average background luminance (DC luminance term) and the very low frequency portion of the Fourier spectrum. From a visibility level perspective the mesoptic adaptation level of the observer is going to be determined by the dynamic average of the background luminance.

As an observer passes through a roadway lighting situation the observers adaptation level will be determined by the observers adaptation time constant and by the observers speed through the roadway lighting situation. From a dynamic perspective the observer mesoptic adaptation level will be determined by the time average DC luminance the observer experiences as the roadway lighting situation is traversed. With the noise spike from the image capture artifact removed the observer average relative background luminance and low frequency terms is about 225 on the scale shown. When the images are calibrated to the average background luminance level of the scene the mesoptic region of the observer may be determined.

Conclusion

Theoretically the frequency component analysis does provide another perspective to look at the STV problem.

The spatial frequency content of a scene must change at least 10% or there is no discernible change in the scene for an observer. Starting from a "lights off" condition to a "lights partially on" gives a change of image of more than 10%. Changing from a "lights partially on" to a "lights on" condition gives more than a 10% change in the spatial frequency. From one "lights on" condition (Luminance design) to another "lights on" condition (STV design) does not appear to change the Fourier frequency spectrum the necessary 10% for an observer to notice a change in a scene.

The example images we studied show that the relative visibility levels of the 20 target images revealed by the frequency component analysis dynamically match the STV results. In other word, we can roughly reproduce the same behavior of the different target locations.

We believe that dynamically FCA and VTC are equivalent in revealing the visibility in the specified circumstances.

In order to be comparable, standardized image acquisition method should be carefully designed and carried out. We are interested in maintaining fixed focal length, fixed tilt of camera, constant lighting, etc. Frequency analysis method can be use as an alternative visibility calculated method.

Contrast is a calculation based on luminance. STV is a calculation based on luminance and eye adaptation to an average background luminance (DL4).

Point luminance and average luminance are the measurement needed to calculate both contrast and STV.

The observers visual response is determined by the average dynamic background luminance the observer experiences traveling down the roadway. Calculating STV based on a static roadway condition assumes steady state mesoptic visibility adaptation levels optomized for each STV target location. The dynamic mesoptic visibility adaptation level for a moving observer will only match STV calculations in one or two locations of the STV calculation.

The observer will see a dynamic change in spatial frequencies in a dynamic situation when the observer focuses on an approaching target and the change in spatial frequency spectrum is larger than 10% due to dynamic observation of the target.

CHAPTER 5: EXPERIMENTAL SYTEM FOR LUMINANCE AND ILLUMINANCE MEASUREMENTS

Experimental investigation was performed on the west side rest area north of Abernathy on I-27 interstate. Experimental activities began at the test side around 10 p.m. to absolutely sure that there was no sunlight what so ever, be it a soft glow on the horizon or a reflecting cloud, so that the data would be incontrovertible. One set of experiments was completely finished at the same night to avoid potential change in conditions over the intervening day. A measurement experiment, which could not be completed the same night, was abandoned and redone at the next opportunity.

The STV model used during the experimentation was a static model and did not take into account dynamic changes in contrast due to the relative motion of a small target observer. The small target was also used for dynamic model during the experimentation. Static and dynamic experimental visibility measurements were completed for three different sizes of target (18x18, 25x25 and 36x36) with two different reflective surfaces (%20 and %50).

During the experiments, a luminance and an illuminance probes were used to measure luminance and illimunance of the roadway lights, respectively. A photometer was used to display the measurement values from luminance and illuminance probes and 3-CCD video camera was used to record images of the targets. The targets and luminance-illuminance-photometer stand were used as experimental equipment.

Experimental Field

All visibility experiments (static and dynamic) were performed on a one-lane road on the west side rest area north of Abernathy on I-27 as seen in Figure 2.1. Figure 2.1 shows the dimensions and orientation for the test field. To fulfill the requirements of the experiment, we chose an experimental location that met the following requirements.

- easily accessible and safe at night,
- far away from the glow of city lights (30 miles),
- easily closed off to traffic,
- a predetermined number of lights,
- easily measurable off-road lighting from one side only.

In the test field, 250 Watts General Electric luminaire heads (M400R2 Luminaire, Catalog number M4RR25S9M4GMS3072) with 250 HPS (Sylvania) lamps were replaced to the poles (Pole 8A through 12A). The field between the poles 10A and 11A was chose as a target locations' field and was marked according to the STV method properties. In the target locations' field, two lines were marked along the roadway lane by assuming one lane12 ft wide. In addition, ten target locations were marked on the each line (total twenty target locations on both lines) as seen in Figure 4.9.

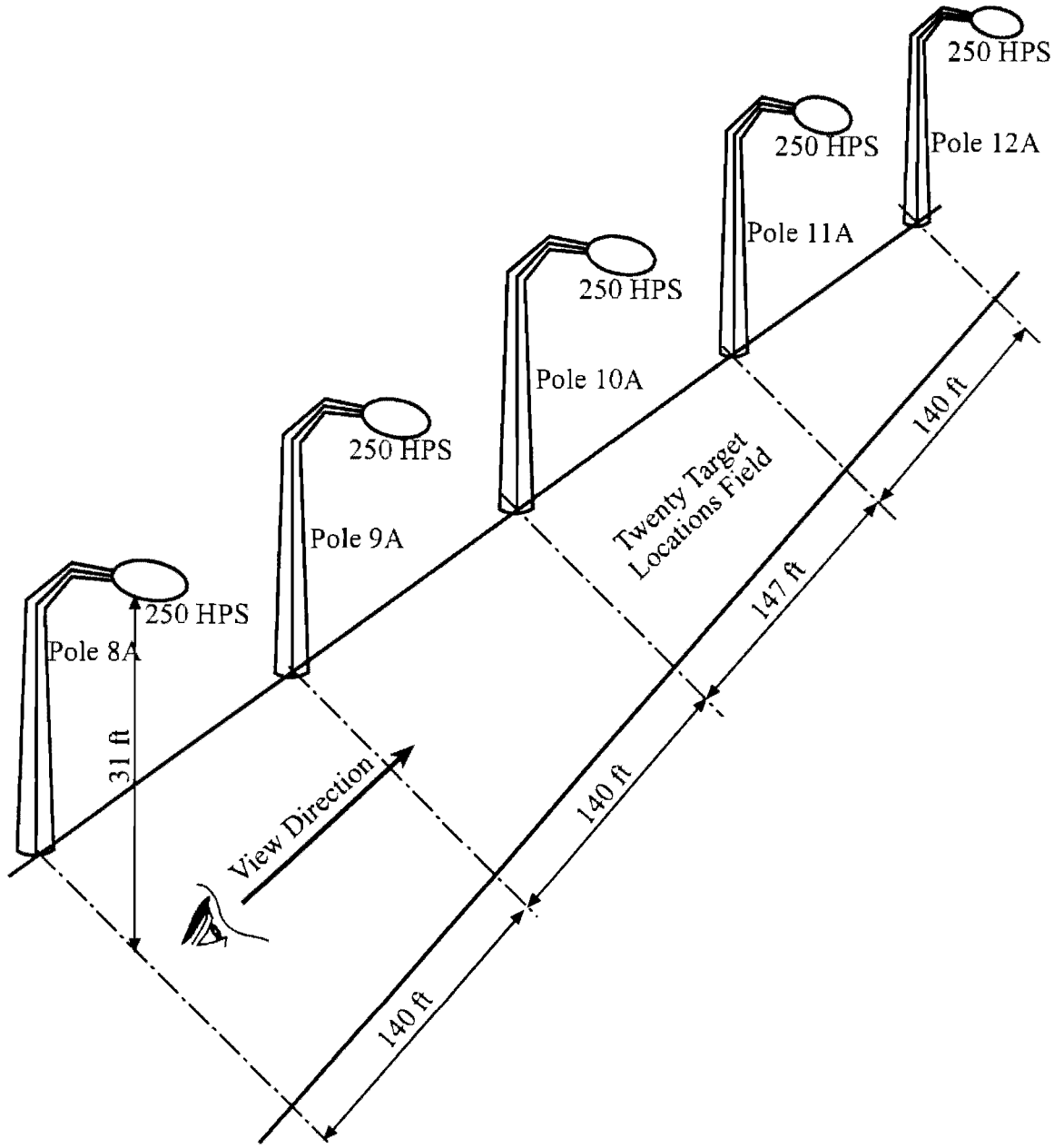

Figure 5.1 Dimensions and orientation of the experimental field.

Measurement Devices and Equipment

Photometer, luminance probe, illuminance probe, and 3CCD video camera were used as measurement devices for experiments. The target and luminance-illuminance-photometer stand were used as experimental equipment.

Photometer

Tektronix designs J17 Photometers as a hand held digital light measurement device as seen in Figure 2.2. The interchangeable J1800 series sensor heads (luminance and illuminance probes, etc), designed for use with the J17 photometer, provide the ability to make photometric, radiometric, and calorimetric measurements. As a photometric device, illuminance measurement can be read for white, blue, and yellow colors independently. It can be connected to a computer by using RS_232 pin connection. This device can be operate between –15 C and 55 C, and 48 hours at 97% relative humidity (30 C to 60 C).

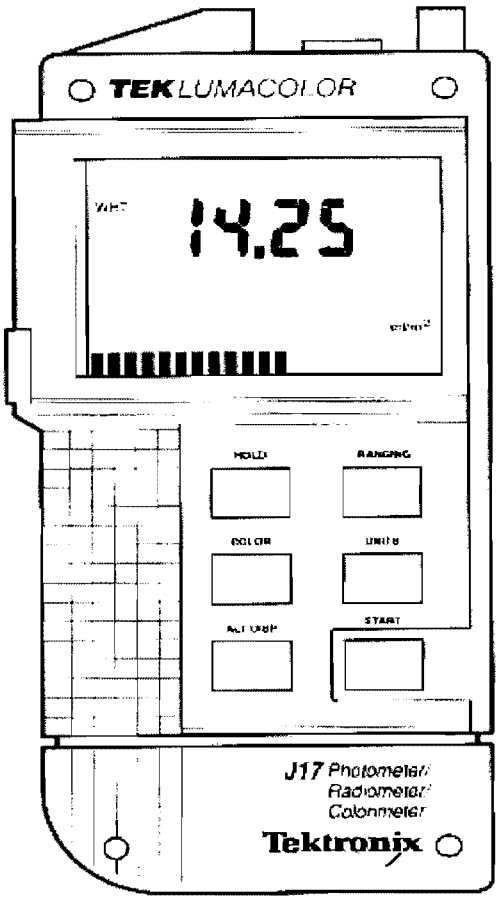

Figure 5.2 Photometer.

Luminance Probe

Tektronix designs J1803 Luminance probe for use in making display or lighting luminance measurement in cd/m^2 and footlamberts as seen in Figure 2.3. The Luminance probe has an acceptance angel of approximately eight degrees. As long as the entire acceptance angel is uniformly filled by the light source, the luminance probe-to-surface distance is not critical, and the reading will be the same regardless of any distance. This device can be operated between – 15 C and 55 C, and 48 hours at 97% relative humidity (30 C to 60 C).

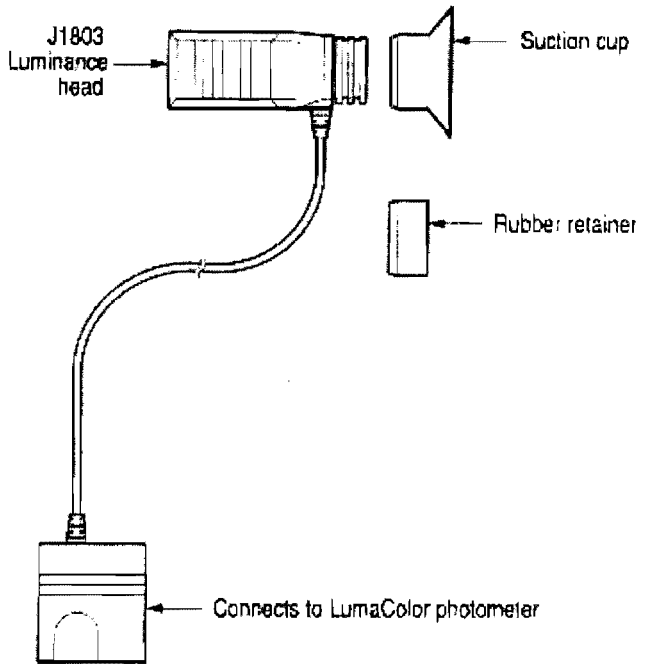

Figure 5.3 ***Luminance probe.***

Illuminance Probe

J1811 Illuminance probe (Figure 5.4) are designed by Tektronix for use illuminance measurement applications such as highway illuminance, office lighting, aircraft lighting, safety and emergency lighting and light trespass. The Illuminance probe is also accurately cosine corrected to simulate an ideal 180–degree field-of-view detector, and includes a build in leveling indicator. This device provides lighting illuminance measurement in lux (lm/m^2) or foot-candles. Luminous intensity in candelas may be obtained by multiplying the illuminance reading (measurements) by the square of the measurement distance. This device can be operate between –15 C and 55 C, and 48 hours at 97% relative humidity (30 C to 60 C).

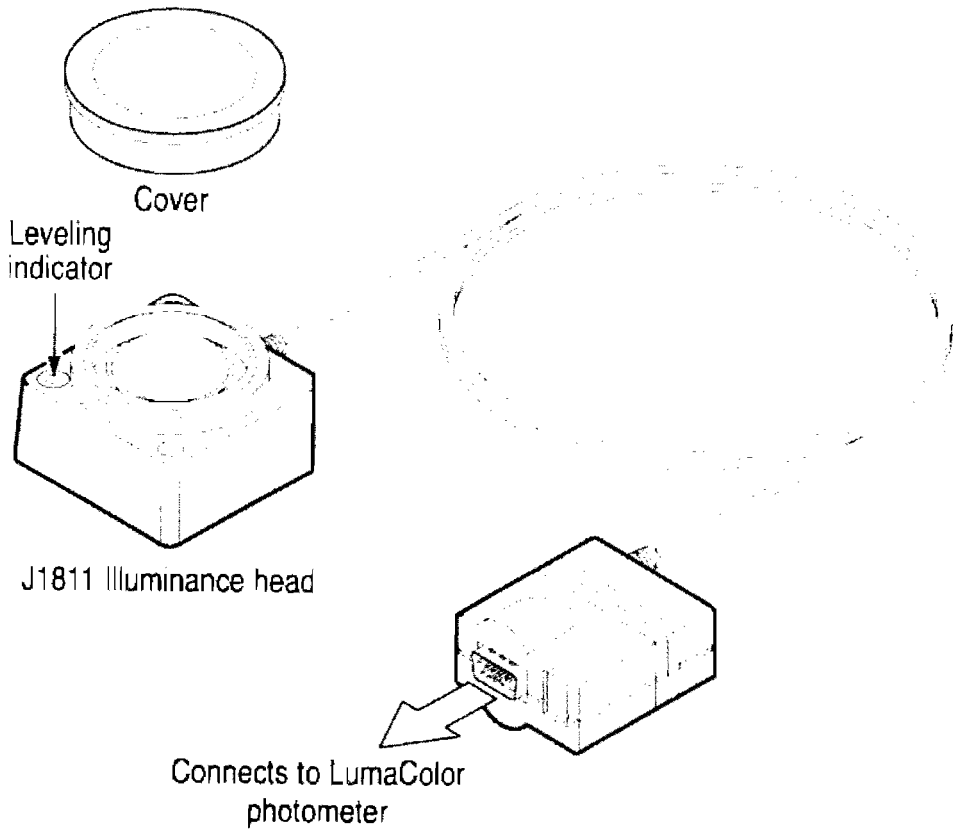

Figure 5.4 Illuminance probe.

Video Camera

A 3CCD (Charge Coupled Device 1/3") SONY video camera was used with a Hi8 video tape to record the target images. The 3CCD camera system employs high density three-chip precision, and each CCD image includes a total of 410,000 pixel. An image is separately projected by the lens into three primary colors; red, green and blue (RGB). Same technical properties of the 3CCD video camera are given as follow.

Video recording system	: Rotary two heads, helical scanning FM system
Video signal	: NTSC color, EIA standards
Usable cassette	: 8 mm video format cassette (Hi8 or standard 8 mm)
Image device	: 3CCD (Charge Coupled Device 1/3")
Viewfinder	: Electronic viewfinder (monochrome)
Lens	: Combined 12 x power zoom lens f =5.5 to 66 mm, F1.6 to 1.8, 40 to 480 mm when converted into a 35-mm still camera. Filter diameter 52 mm, TTL autofocus system, and Inner focus wide macro system
Minimum illuminance	: 4 lx (F1.6)
Illuminance range	: 4 lx to 100,000 lx (0.37 to 9.294 foot-candles)

Main characteristic differences of Hi8 video system from a 8 mm video system are as follows.

- Hi8 increases the FM carrier frequency range of luminance signal between 4.2 - 5.4 MHz to 5.7 - 7.7 MHz. This is improved horizontal resolution more than 400 lines.
- The Hi8 video system, covering a wide frequency range, uses metal evaporated tape to obtain a high-quality video signal for recording and playback. The metal evaporated tape is useful for video systems because it has large magnetic energy that admit high-density recorder.
- Hi8 video camera recorder must use Hi8 videocassettes for higher-quality pictures.
  A PC computer with a video image capture card was used as a data acquisition.

Target

A target was built by connecting two aluminum pieces to each other at 90 degrees to make the foundation of the target. Two other aluminum holders were designed to mount red LED at 45 degrees from the vertical line. These two LEDs were replaced inside the cylindrical hole to protect the target surface from their light. They were used to find exact boundaries of the target. An 18 x 18 cm, %20 reflective gray scale paper was placed on the vertical surface of the aluminum foundation as a reflective surface as seen in Figure 2.5.

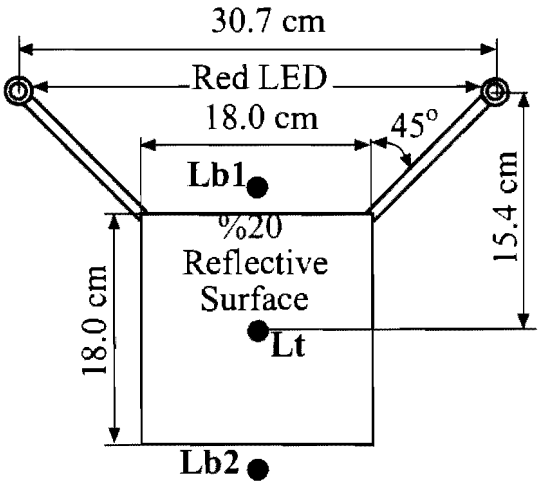

Figure 5.5 STV Target.

Luminance-Illuminance-Photometer Stand

Luminance-illuminance-photometer stand which consists of a metal base (height 10 in), three connectable rods that attach to the base (length 2.5 ft.), and a platform that attaches the top of any rod or stand alone. The platform is useable for all required luminance and illuminance measurements. Illuminance measurements required a recess to lay the sensor both sky-ward and round-ward (horizontal mounting) and two holes to hold the sensor at 90 degrees to the platform surface to measure illuminance in the north, east, south, and west directions (vertical mounting). The Luminance probe was mounted on the protractor to measure luminance directly from the

poles. The Luminance probe lies on the platform in the directions of north, east, south, and west to measure horizontal luminance. See Figure 5.6.

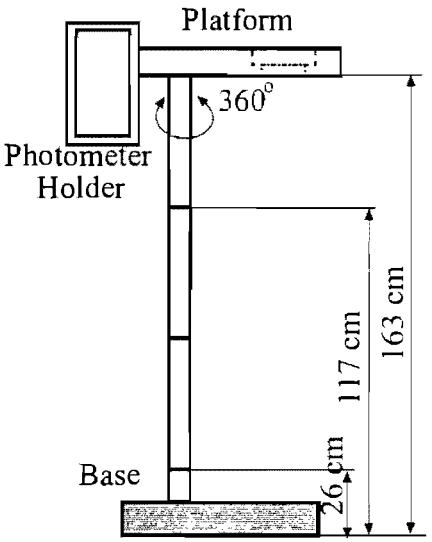

Figure 5.6 Luminance-illuminance-photometer stand.

Static Experimental Procedure

Two types of experimental measurement were performed to complete experimental study. One is measurement of luminance and illuminance and the other is measurement of visibility of the small target.

Luminance and Illuminance Measurements Procedure

During the experimentation, luminance and illuminance were measured using the luminance probe (luminance head) and the illuminance probe (illuminance head) with the photometer. These measurements were recorded in the line 1 and in the line 2 at three levels, 26 cm, 117 cm, and 163 cm. At each level, luminance and illuminance values were measured in the north, east, south, and west directions. In addition to this, illuminance was recorded directly from the luminaire head (fixture).

LUMINANCE MEASUREMENTS PROCEDURE

Luminance measurements were performed using the luminance head with the photometer and the luminance-illuminance-photometer stand in the following steps.

1. Luminance probe was connected to the photometer with the cable. For calibration purpose, luminance probe light entrance was closed until zero reading obtained from the photometer.
2. The stand was assembled to obtain first measurement height. In these condition, the luminance probe height was 26 cm above from the road surface.

3. The luminance probe was fixed to the arm of the protractor, facing outward. The stand was placed on the first target location on the line 1.
4. The bottom edge of the protractor was placed on the platform and held it in place while the arm of the protractor was manipulated. The arm of the protractor was aimed toward the luminaire head (pole 10A). The luminance probe was moved up, down, right and left until a maximum measurement value was achieved. The maximum value and angel of ascent were recorded. To assure accurate values, the luminance probe was only moved either up and down or left to right at one time.
5. The platform was rotated so that the protractor/luminance probe pointed at the light of luminaire head (pole 11A). The operation stated in step 4 was then repeated.
6. The protractor/luminance probe was placed on its side on the platform and it is oriented to the north, east, south, and west and the measurements from each direction were recorded.
7. Step 4 through 6 was repeated for the rest of the target locations on the line 1 and line 2.
8. Two and three rods were added to the stand for a total height of 117 cm and 163 cm, respectively.
9. The steps above were repeated to complete luminance measurements at the different height on the experimental field.

ILLUMINANCE MEASUREMENTS PROCEDURE

Illuminance measurements were performed using the illuminance head with the photometer and the luminance-illuminance-photometer stand in the following steps.

1. Illuminance probe was connected to the photometer with the cable. For calibration purpose, illuminance probe light entrance was closed until zero reading obtained from the photometer.
2. The stand was assembled to obtain first measurement height. In these condition, the illuminance probe height was 26 cm above the road surface.
3. The illuminance probe was placed face up on the platform to measure skyward illuminance.
4. The stand was directly placed on the first target location on the line 1. Technician was stayed about six feet away, opposite the light source as not to interface with the ambient light. The measurement was recorded.
5. The stand was moved to the second target location and illuminance measurement was recorded.
6. Step 4 was repeated for the rest of the target locations on line 1 and line 2.
7. The illuminance probe was placed face down on the platform to measure downward illuminance (reflection).
8. Step 4, 5 and 6 were repeated for the rest of the target locations on line 1 and line 2.
9. The illuminance probe was placed into the two holes, so that it was perpendicular to the surface of the platform, and the stand was placed on the line 1 at the first target location.
10. The illuminance probe was oriented to the north, east, south, and west and readings were recorded.
11. Step 10 was repeated for the rest of the target locations on line 1 and line 2.

12. Two and three rods were added to the stand for a total height of 117 cm and 163 cm, respectively.
13. The steps above were repeated to complete illuminance measurements at the different height on the experimental field.

CHAPTER 6: LUMINANCE AND ILLUMINANCE

Luminance and illuminance measurements were performed between the installations on two STV lines (line 1 and line 2). Each line has 10 measurement (target) locations, therefore there are 20 measurements locations between the installations. Luminance and illuminance were measured at three different height above the roadway surface (26 cm, 117 cm and 163 cm) for each measurement location.

Luminance Measurements

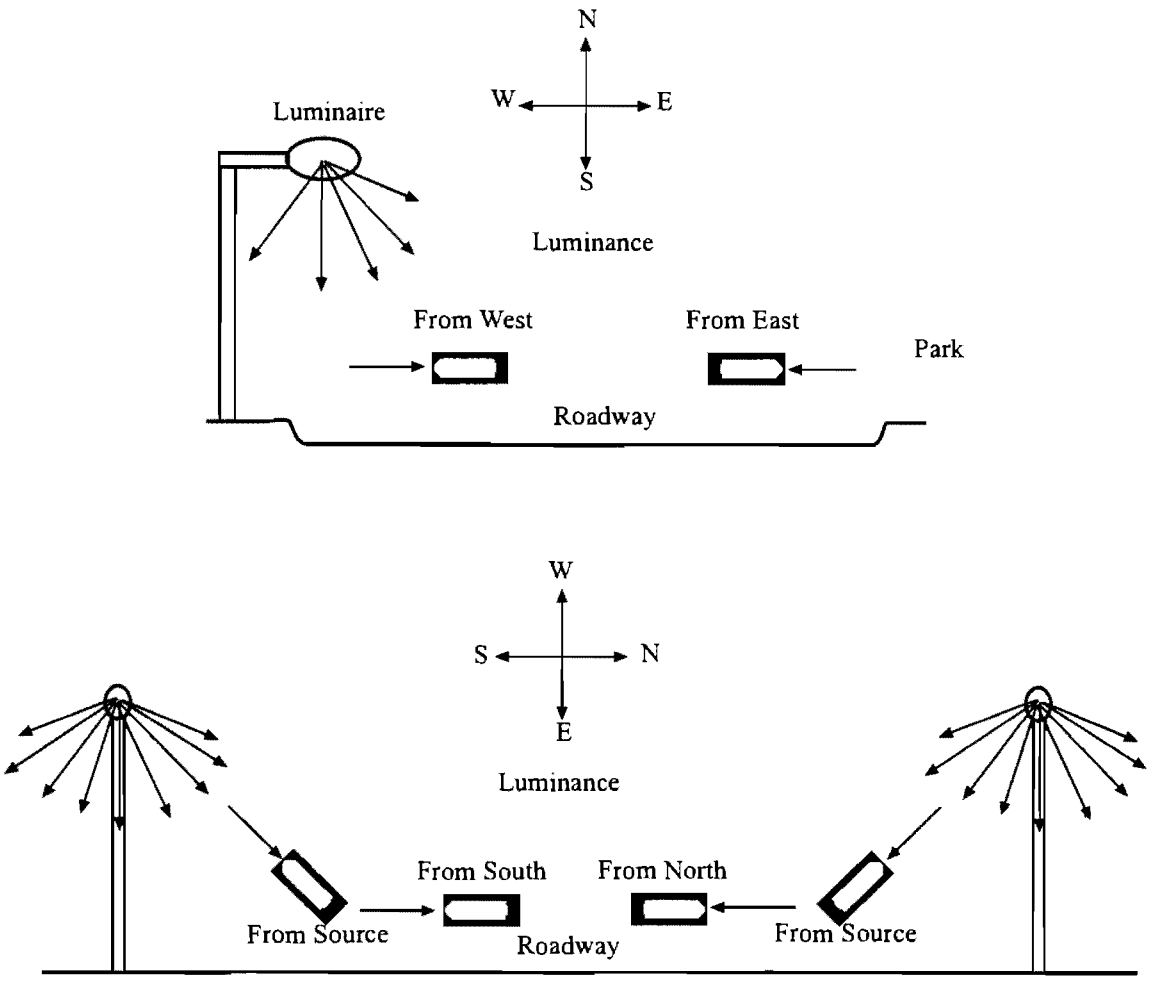

Figure 6.1 Luminance measurement directions between the installations.

Luminance measurements were performed at three heights in the south, north, east west, north source and south source directions as seen in Figure 3.1. For this purpose, the luminance head (J1803) was placed on the platform (Figure 2.6). To measure luminance in the south, north, east and west directions, the luminance head was oriented parallel to these directions. To measure luminance in the source direction, the luminance head was attached to the protractor and then the

protractor was placed on the platform. The protractor was used to direct the luminance head towards the south and the north luminaire sources.

Final Luminance Measurements

For final luminance measurements, the light fixtures on the poles 8A, 9a, 10A, 11A and 12A were replaced with the new fixtures manufactured by General Electric Company (M400R2 Luminaire, Catalog Number: M4RR25S9M4GMS3072). Old lamps were also replaced with new ones.

Luminance Distribution at 26 cm

Figures 6.2 and 6.3 show the luminance distributions obtained directly from the south and north luminaire (source), respectively. The measurements are performed at 26 cm above from the roadway surface for the line 1 and 2. Figure 6.2 shows those luminance values of the south luminaire decrease when measurement location is far from the south luminaire for both of the lines. On the other hand, luminance values of north luminaire increase when measurement location gets closer to it as seen in Figure 6.3. The Luminance values on the line 2 are generally higher than the luminance values on the line 1. This is related to the photometric data distribution of the luminaire.

Figures 6.4 and 6.5 show the luminance distribution in the south and north directions. There are slight differences between the luminance values on the line 1 and 2. When these values are compared with the source luminance values (Figure 6.2 and 6.3), it can be seen that, the luminance values measured in the south and north direction are negligible.

Figures 6.6 and 6.7 show the luminance distribution in the east and west directions. There are no luminance values recorded from east and west directions for the line 1 and 2. East side of the roadway was parking area (rest area) which was lighted. At the tent measurement location, luminance value is almost eighty times greater than the values measured at other locations. Because in that direction there is a light source replaced for the purpose of lighting the parking area.

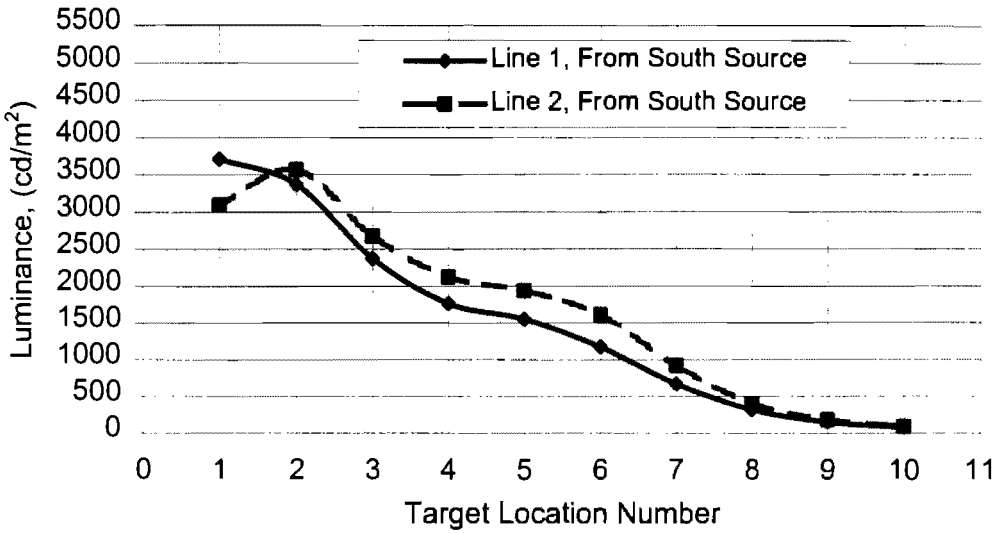

Figure 6.2 Luminance distribution, in the south source direction, between the installation at 26 cm height above the roadway surface on the lines 1 and 2.

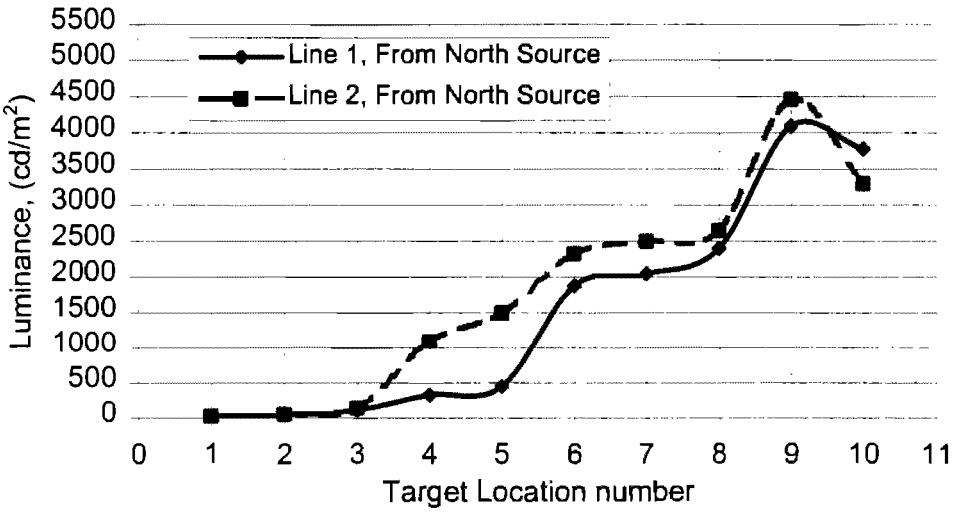

Figure 6.3 Luminance distribution, in the north source direction, between the installation at 26 cm height above the roadway surface on the lines 1 and 2.

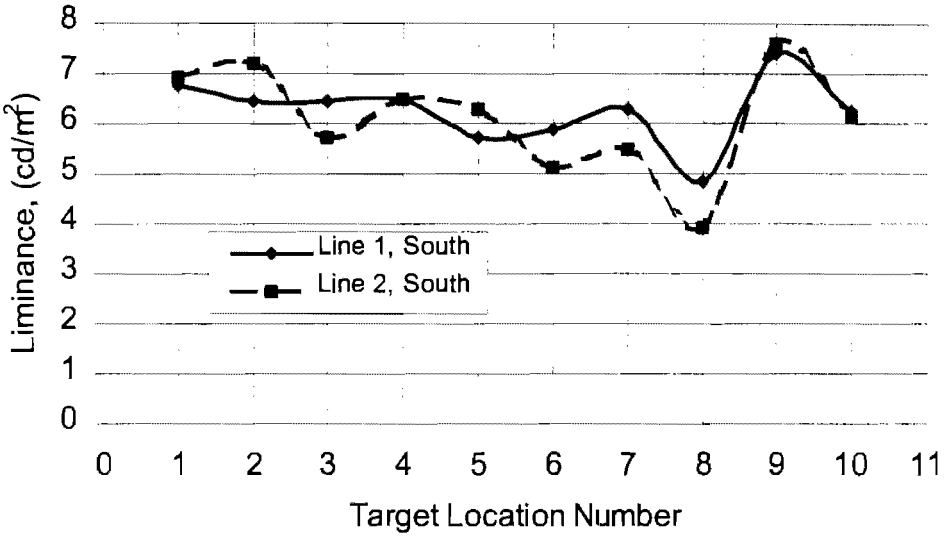

Figure 6.4 Luminance distribution, in the south direction, between the installation at 26 cm height above the roadway surface on the lines 1 and 2.

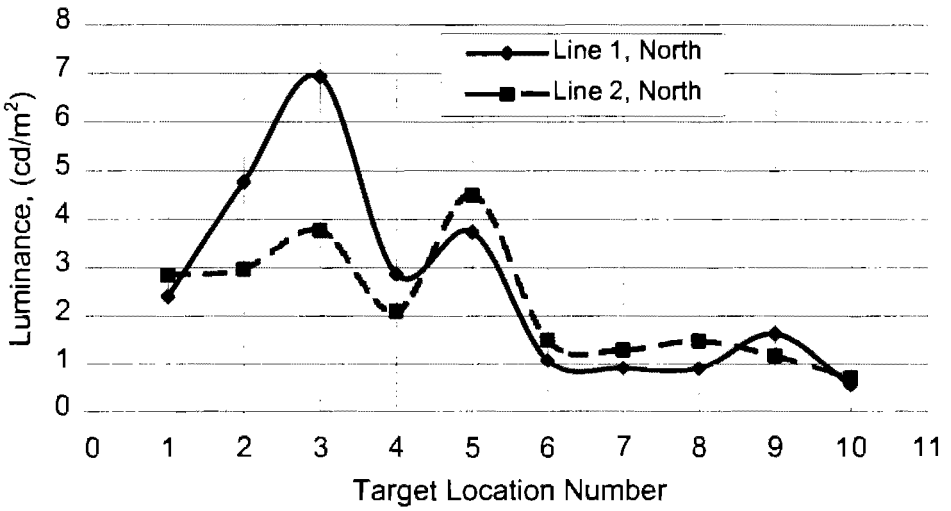

Figure 6.5 Luminance distribution, in the north direction, between the installation at 26 cm height above the roadway surface on the lines 1 and 2.

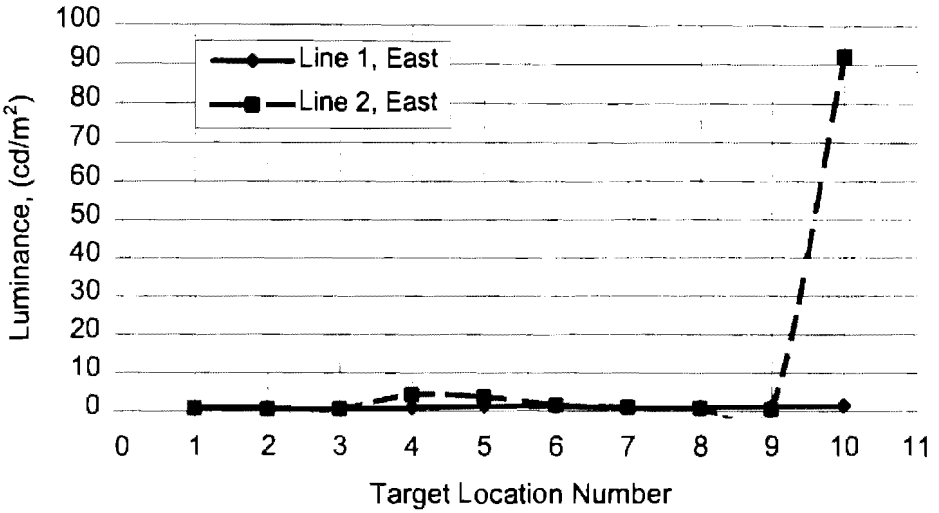

Figure 6.6 Luminance distribution, in the east direction, between the installation at 26 cm height above the roadway surface on the lines 1 and 2.

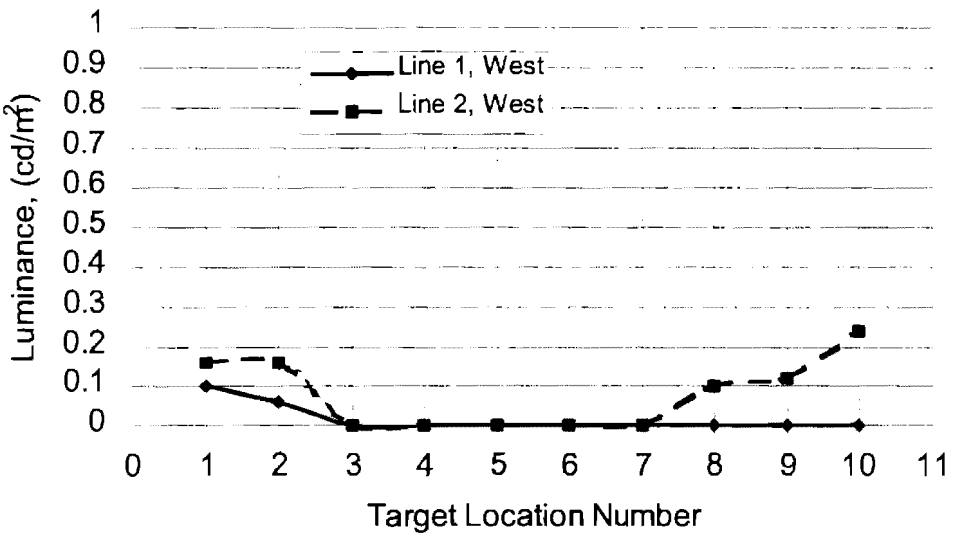

Figure 6.7 Luminance distribution, in the west direction, between the installation at 26 cm height above the roadway surface on the lines 1 and 2.

Luminance Distribution at 117 cm

Figures 6.8 and 6.9 show the luminance distributions obtained directly from the south and the north luminaire, respectively. The measurements are performed at 117 cm above from the roadway surface for both of the lines. These figures also show the same characteristics as in Figures 6.2 and 6.3.

Figures 6.10 and 6.11 show the luminance distributions in the south and the north directions. They also show the same characteristics as in Figures 6.4 and 6.5.

Figures 6.12 and 6.13 show the luminance distributions in the east and the west directions. There are no luminance values recorded from east and west directions except for the 5^{th} and the 10^{th} measurement locations in Figure 6.12 for both of the lines. East side of the experimental field is parking area which is lighted. At the 5^{th} and 10^{th} measurement locations, luminance values are recorded. Because at that direction there is a light source replaced for the purpose of lighting the parking area.

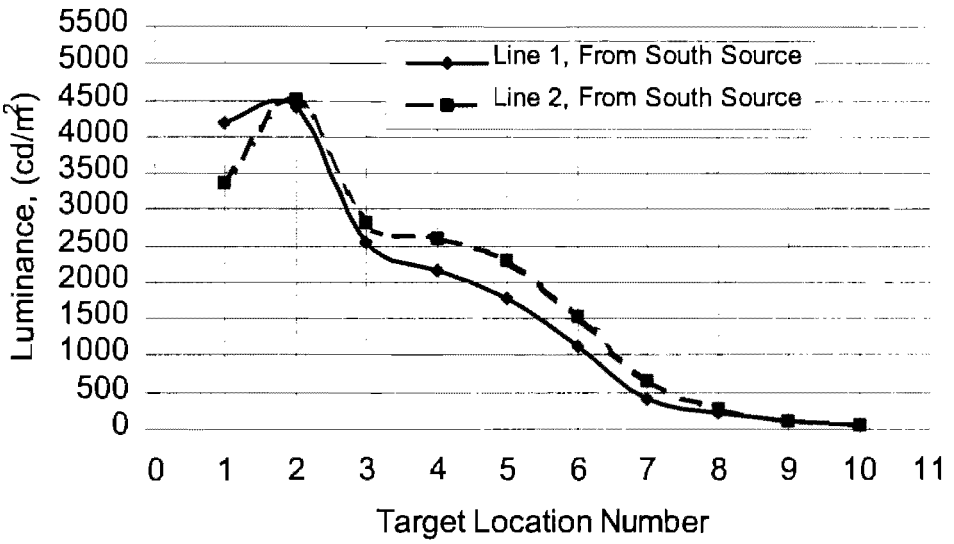

Figure 6.8 Luminance distribution, in the south source direction, between the installation at 117 cm height above the roadway surface on the lines 1 and 2.

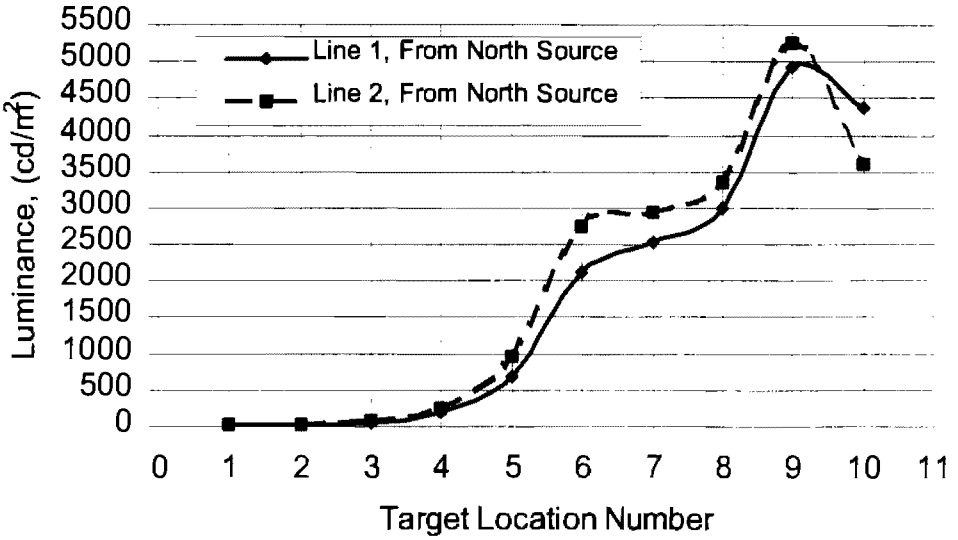

Figure 6.9 Luminance distribution, in the north source direction, between the installation at 117 cm height above the roadway surface on the lines 1 and 2.

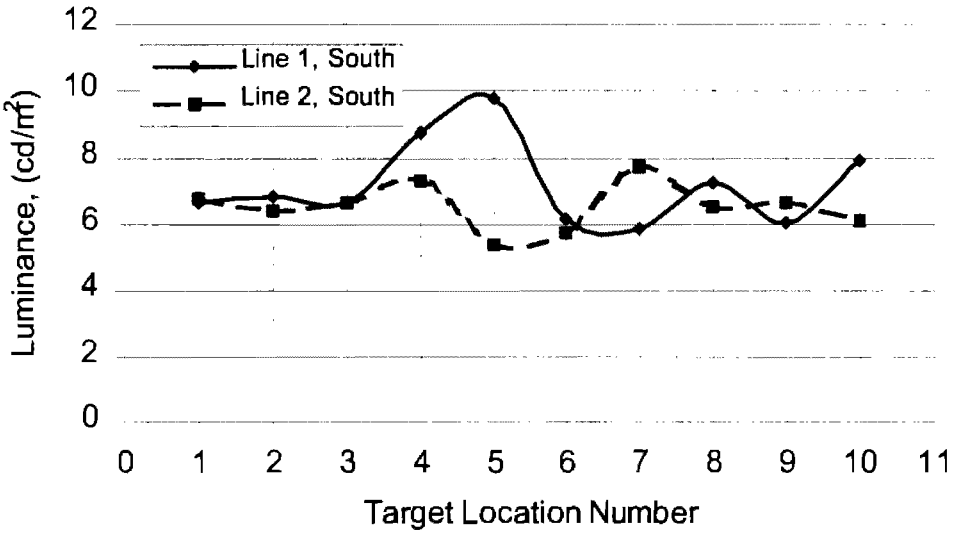

Figure 6.10 Luminance distribution, in the south direction, between the installation at 117 cm height above the roadway surface on the lines 1 and 2.

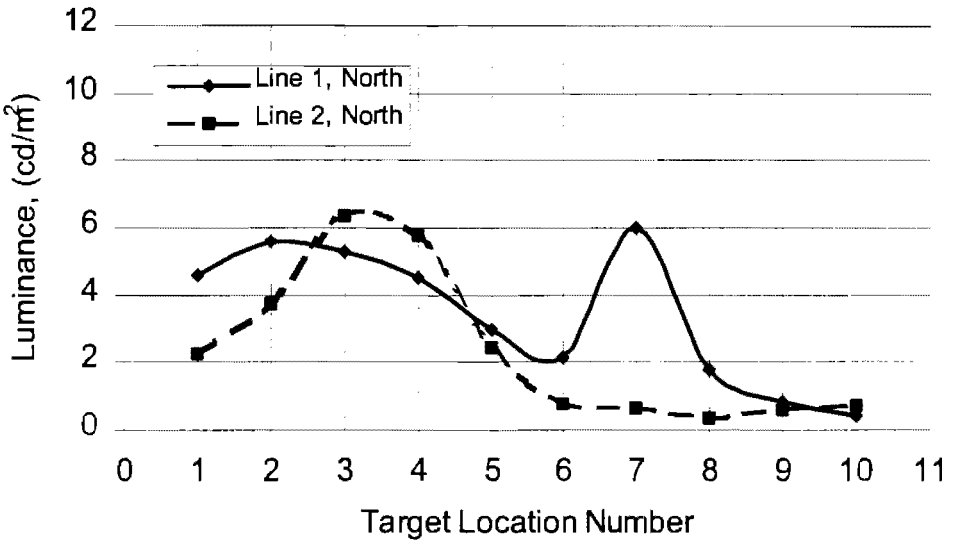

Figure 6.11 Luminance distribution, in the north direction, between the installation at 117 cm height above the roadway surface on the lines 1 and 2.

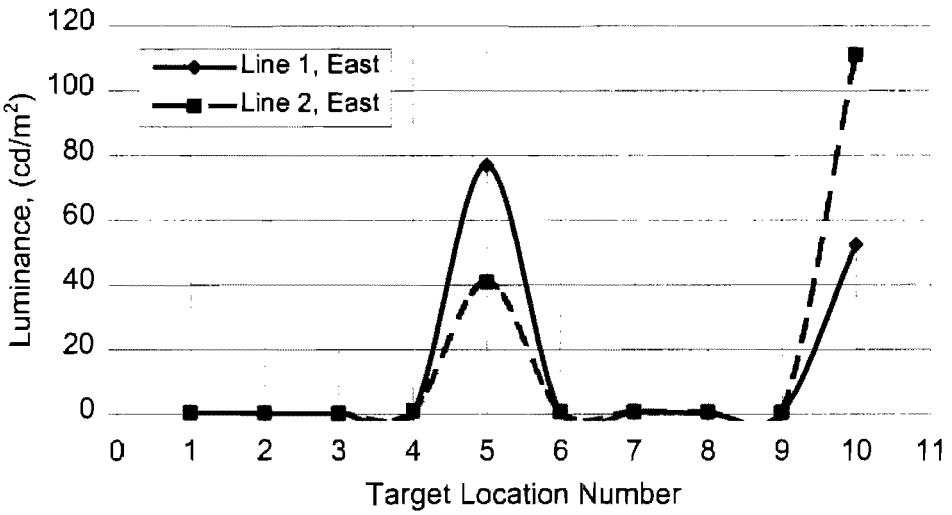

Figure 6.12 Luminance distribution, in the east direction, between the installation at 117 cm height above the roadway surface on the lines 1 and 2.

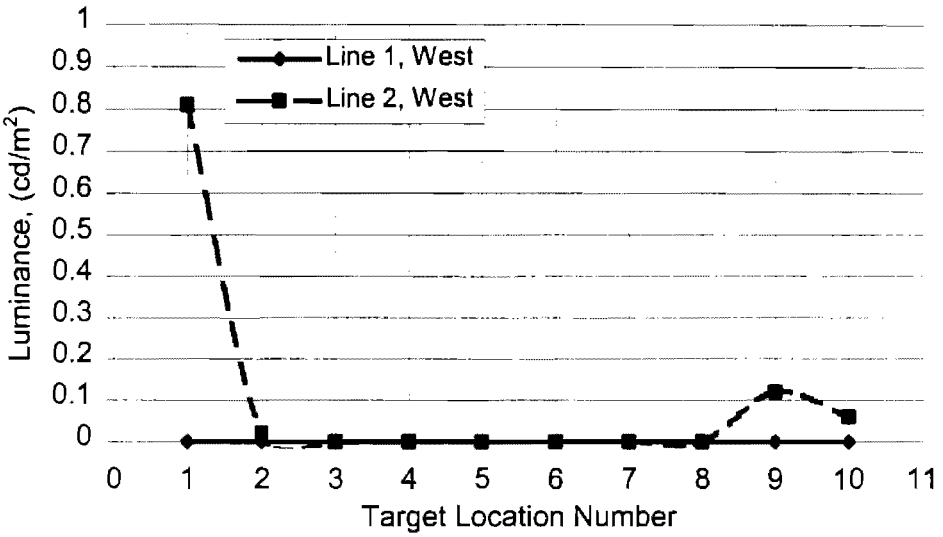

Figure 6.13 Luminance distribution, in the west direction, between the installation at 117 cm height above the roadway surface on the lines 1 and 2.

Luminance Distribution at 163 cm

Figures 6.14 and 6.15 show the luminance distributions obtained directly from the south and north luminaires, respectively. The measurements are performed at 163 cm above from the roadway surface for the line 1 and 2. Figures 6.14 and 6.15 show the same characteristics with Figures 6.3 and 6.4.

Figures 6.16 and 6.17 show the luminance distribution in the south and north directions. They also show the same characteristics with Figures 6.10 and 6.11.

Figures 6.12 and 6.13 show the luminance distribution in the east and west directions. They also show the same characteristics with Figures 6.12 and 6.13.

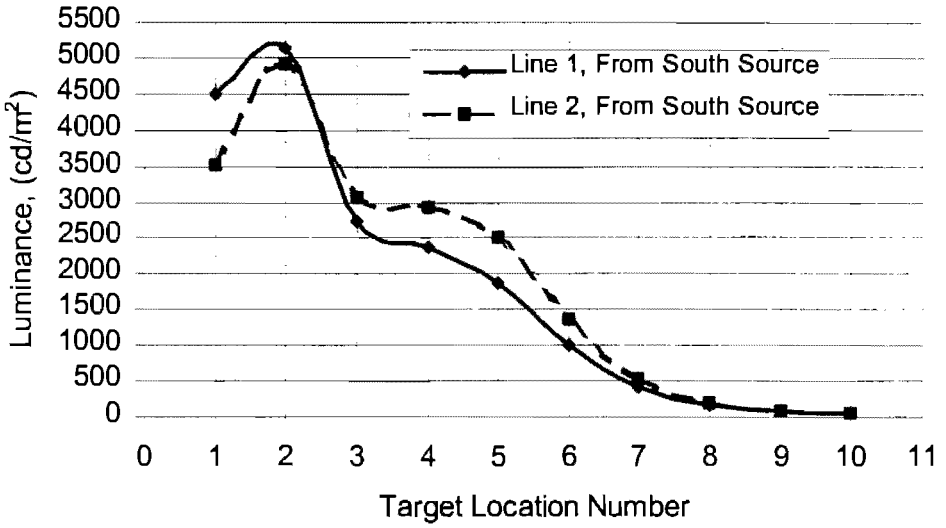

Figure 6.14 Luminance distribution, in the south source direction, between the installation at 163 cm height above the roadway surface on the lines 1 and 2.

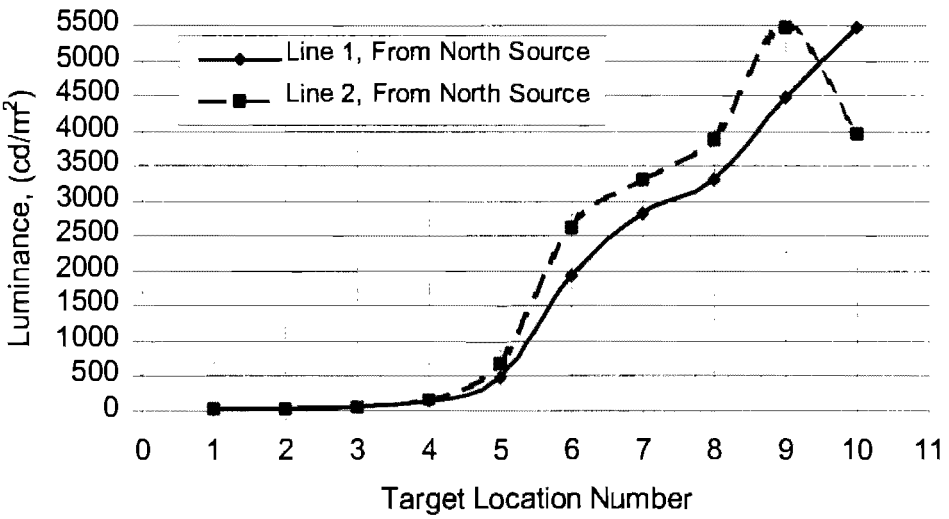

Figure 6.15 Luminance distribution, in the north source direction, between the installation at 117 cm height above the roadway surface on the lines 1 and 2.

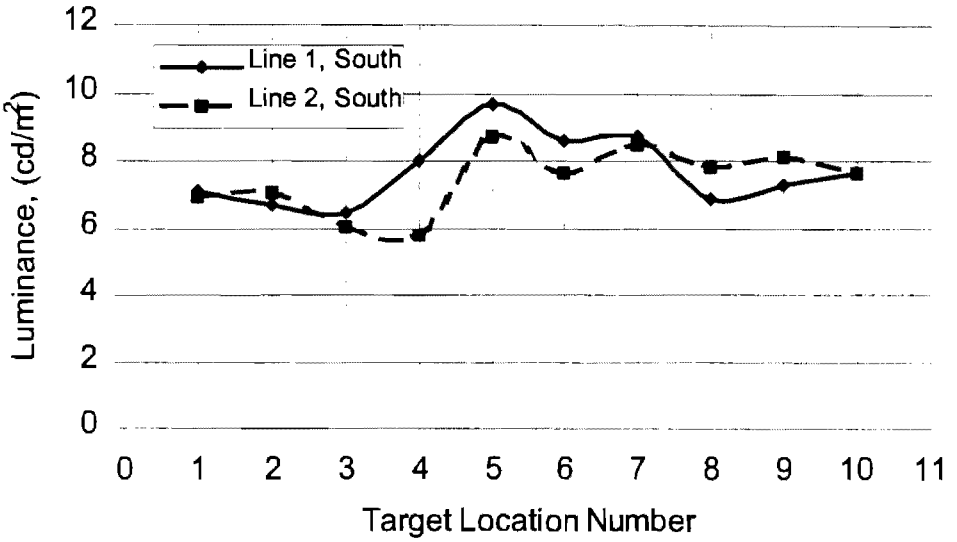

Figure 6.16 Luminance distribution, in the south direction, between the installation at 163 cm height above the roadway surface on the lines 1 and 2.

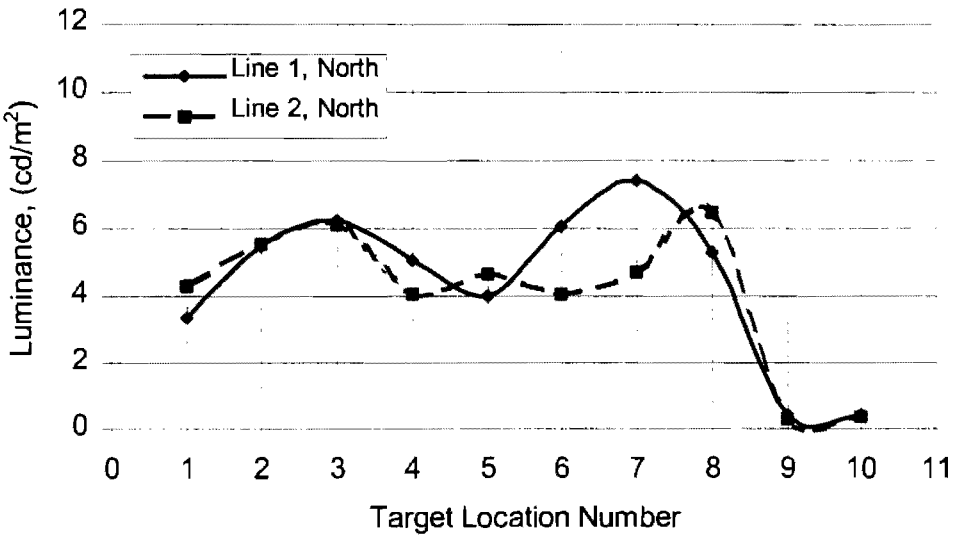

Figure 6.17 Luminance distribution, in the north direction, between the installation at 163 cm height above the roadway surface on the lines 1 and 2.

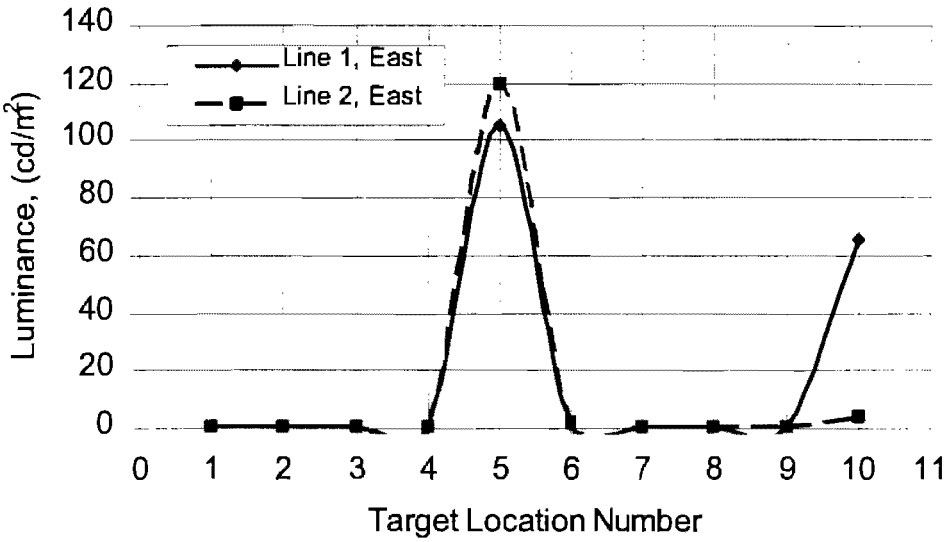

Figure 6.18 Luminance distribution, in the east direction, between the installation at 163 cm height above the roadway surface on the lines 1 and 2.

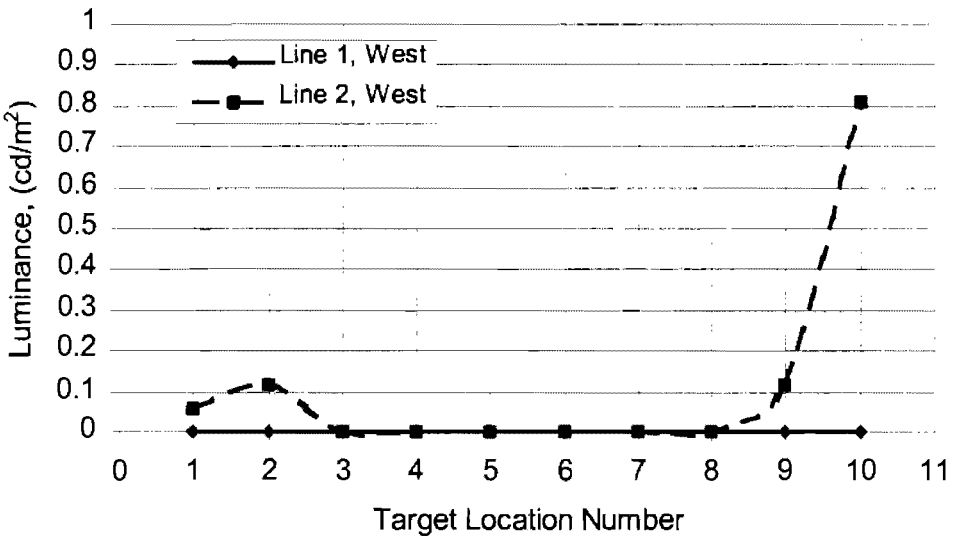

Figure 6.19 Luminance distribution, in the west direction, between the installation at 163 cm height above the roadway surface on the lines 1 and 2.

Luminance Measurement Compression

Figures 6.20 and 6.21 show the luminance distributions on the line 1 and line 2 obtained directly from the south luminaire, respectively. Figures 6.22 and 6.23 show the luminance distributions on the line 1 and line 2 obtained directly from the north, respectively. The measurements are

performed for the line 1 and 2 at heights of 26 cm, 117 cm and 163 cm above the roadway surface in the figures. As seen from the figures, luminance distribution characteristics of the luminaires show same type of pattern at all three heights. But luminance values of the south and the north luminaires change slightly with the height. Since light measurement values changed inverse proportionally with the square of the direct distance between the measurement device and the luminaire (the heights of 163 cm has less direct distance). Also, of course luminance distribution characteristic related to the photometric data distribution of the luminaire. There is no difference in luminance values between the 6^{th} and 10^{th} locations. This characteristic is related to the photometric data distribution.

Figures 6.24 and 6.25 show the luminance distributions in the south direction on the lines 1 and 2, respectively. Figures 6.26 and 6.27 show the luminance distributions in the north direction on the lines 1 and 2, respectively. Figures 6.28 and 6.29 show the luminance distributions in the east direction on the lines 1 and 2, respectively. Finally, Figures 6.30 and 6.31 show the luminance distributions in the north direction on the lines 1 and line 2, respectively. The measurements are performed for the lines 1 and 2 at heights of 26 cm, 117 cm and 163 cm above the roadway surface in the figures. As seen from the figures (6.24-6.31), the luminance values in the south, north, east and west directions are very less (approximately 0.2% of the source) than the luminance values recorded directly from the related luminaires (sources). In Figures 6.28 and 6.29, high luminance values are recorded at heights of 117 cm and 163 cm at the 5^{th} and 10^{th} measurement locations. Because at these locations the luminance head directly pointed to the rest area (park) light because of the measurement location. The luminance in the east direction can still be neglected when it is compared to the source luminance at the same location.

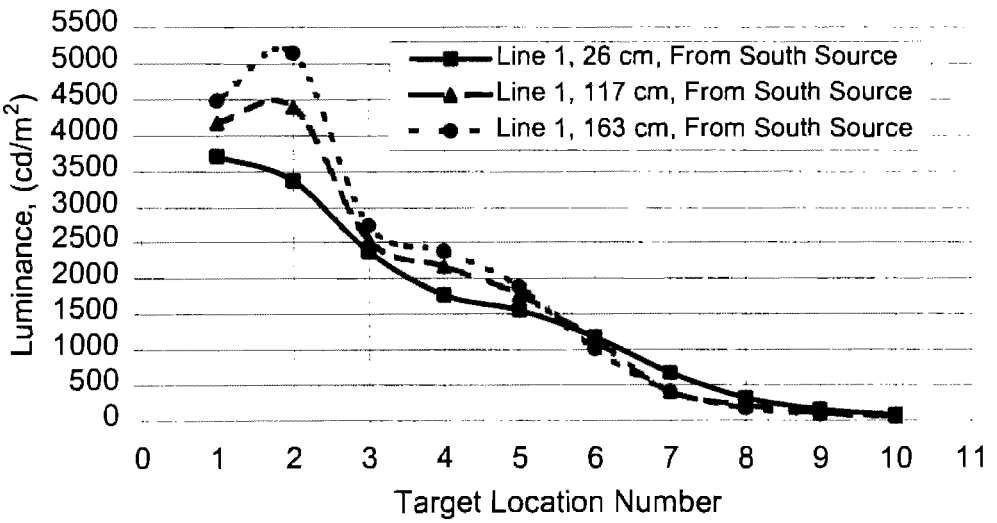

Figure 6.20 Luminance distribution, in the south source direction, between the installation at 26, cm, 117 cm and 163 cm height above the roadway surface on the line 1.

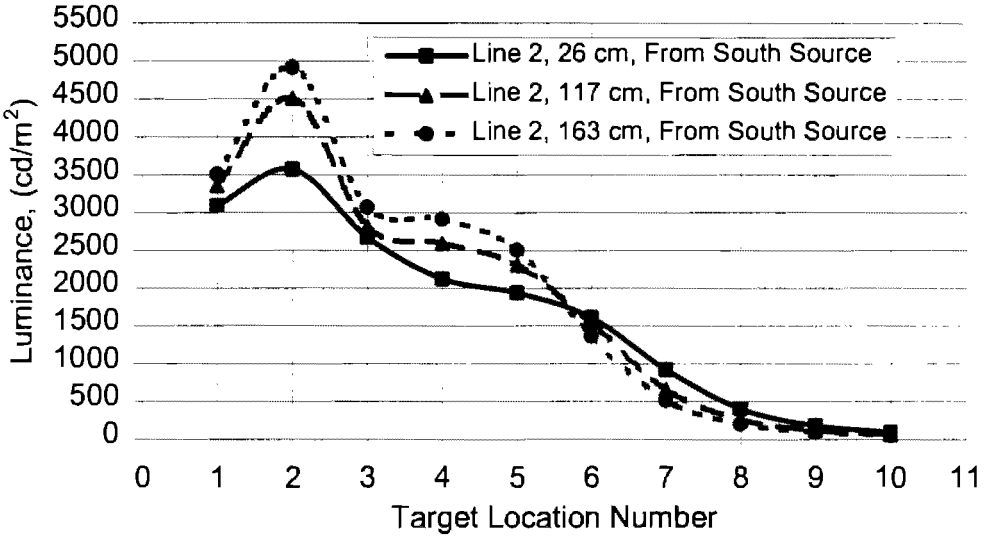

Figure 6.21 Luminance distribution, in the south source direction, between the installation at 26, cm, 117 cm and 163 cm height above the roadway surface on the line 2.

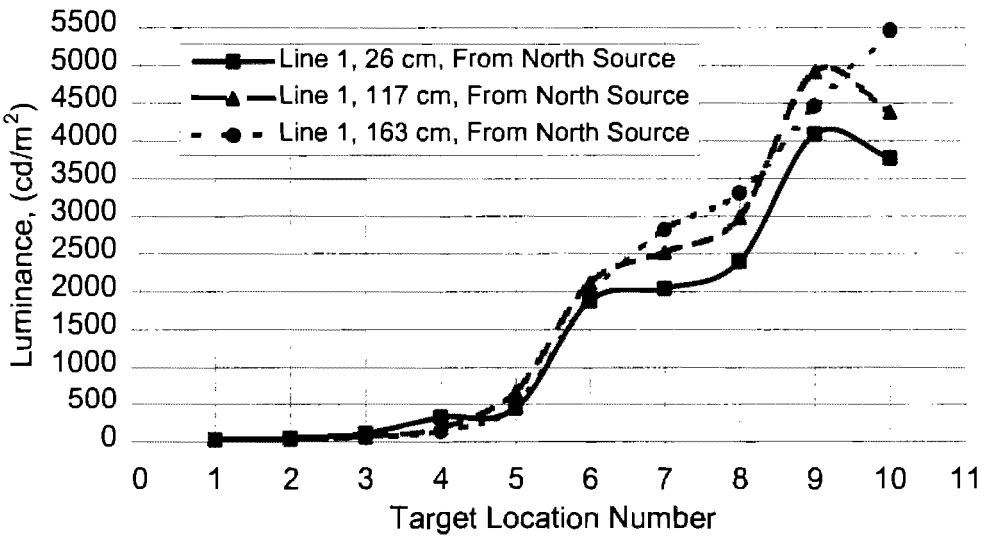

Figure 6.22 Luminance distribution, in the north source direction, between the installation at 26, cm, 117 cm and 163 cm height above the roadway surface on the line 1.

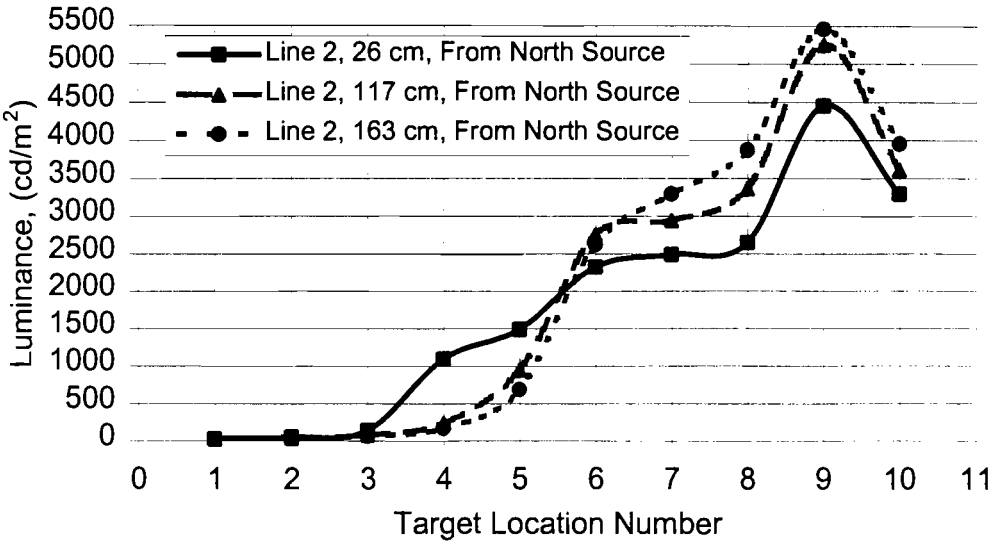

Figure 6.23 Luminance distribution, in the north source direction, between the installation at 26, cm, 117 cm and 163 cm height above the roadway surface on the line 2.

First Luminance Measurement

The luminance measurements were performed first time in the experimental field without changing any conditions. Under these circumstances, luminance measurements were performed in the north source, south source, north, south, east and west directions. The plots were only indicated in the north and south source directions.

Figures 6.24 and 6.25 show the luminance distributions in the south source direction on the lines 1 and 2, respectively. Figures 6.26 and 6.27 show the luminance distributions in the north source direction on the lines 1 and 2, respectively. As seen from the figures, the luminance distribution values are higher values obtained at the height of 163 cm. The measurement difference between the heights is larger when the measurement location close to poles. Because luminance effect reduces with the inverse proportionally square of the distance between the source and measurement point as well as photometric data distribution.

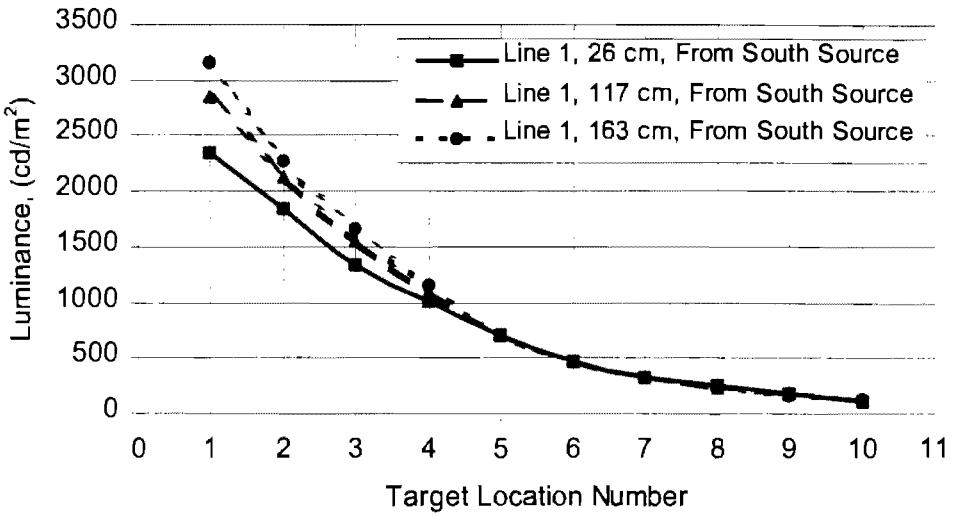

Figure 6.24 Luminance distribution, from south source, at 26 cm, 117 cm and 163 cm height above the roadway surface on line 1.

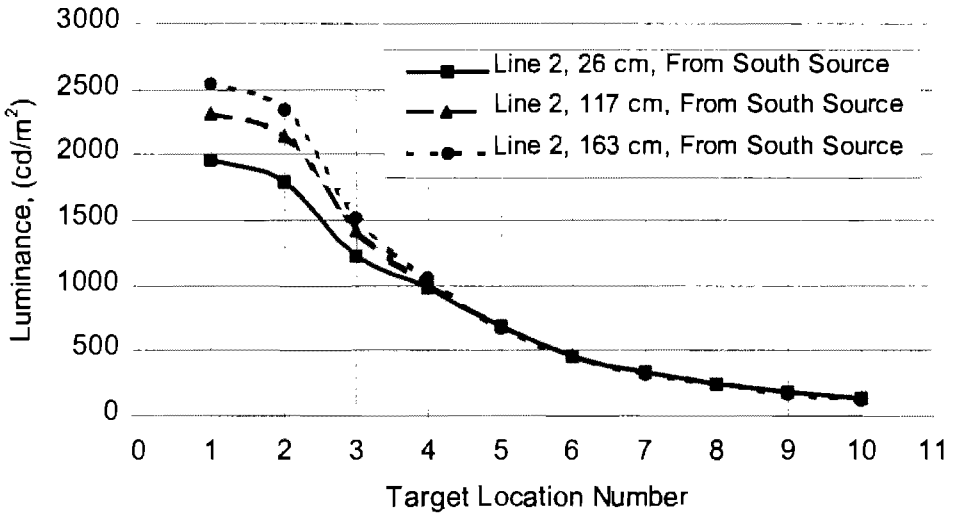

Figure 6.25 Luminance distribution, from south source, at 26 cm, 117 cm and 163 cm height above the roadway surface on line 2.

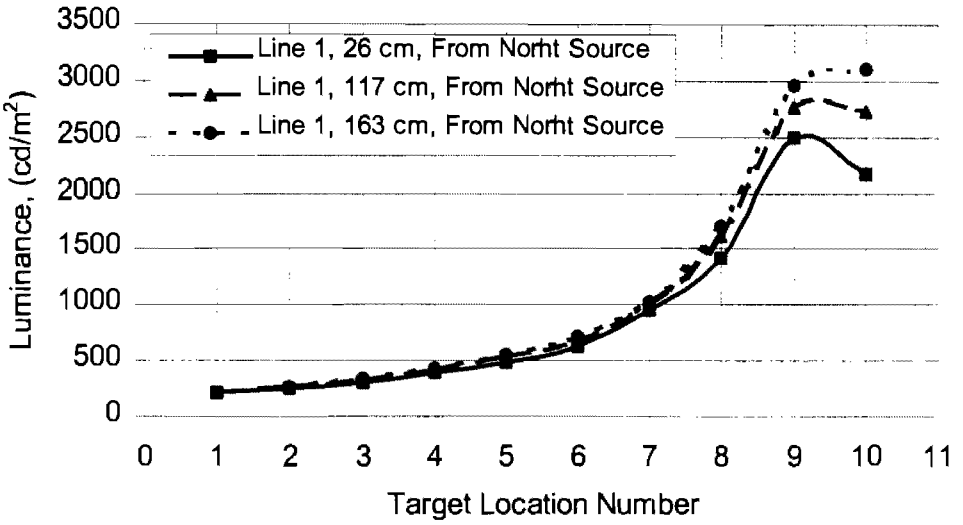

Figure 6.26 Luminance distribution, from north source, at 26 cm, 117 cm and 163 cm height above the roadway surface on line 1.

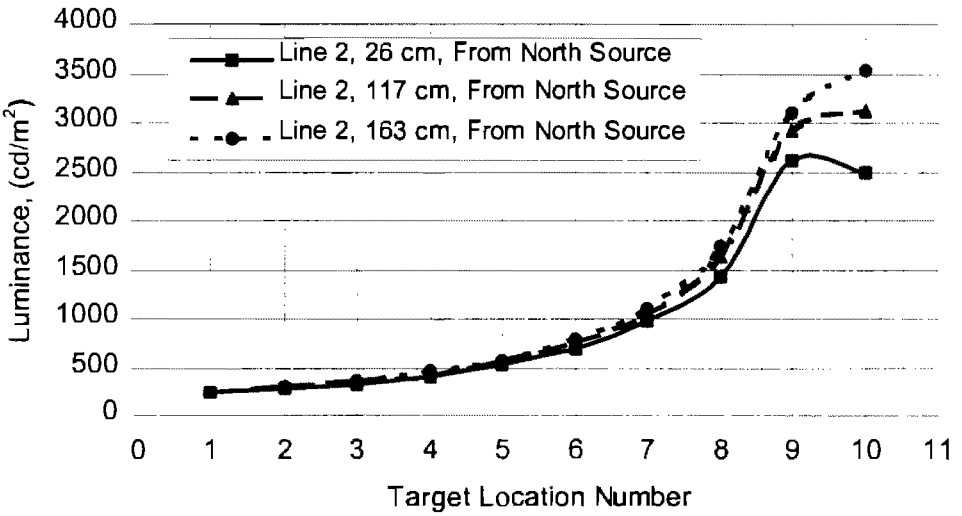

Figure 6.27 Luminance distribution, from north source, at 26 cm, 117 cm and 163 cm height above the roadway surface on line 2.

Luminance Measurements with Clean Lenses

The luminance measurements were performed second time in the experimental field by replacing the new lamp and cleaning the lens of the lamps. Under these circumstances, luminance measurements were again performed in the north source, south source, north, south, east and west directions. The plots were only indicated in the north and south source directions.

Figures 6.28 and 6.29 show the luminance distributions in the south source direction on the lines 1 and 2, respectively. Figures 6.30 and 6.31 show the luminance distributions in the north source direction on the lines 1 and 2, respectively. As seen from the figures, the luminance distribution values are higher values obtained at the height of 163 cm. The measurement difference between the heights is larger when the measurement location close to poles. Because luminance effect reduces with the inverse proportionally square of the distance between the source and measurement point as well as photometric data distribution.

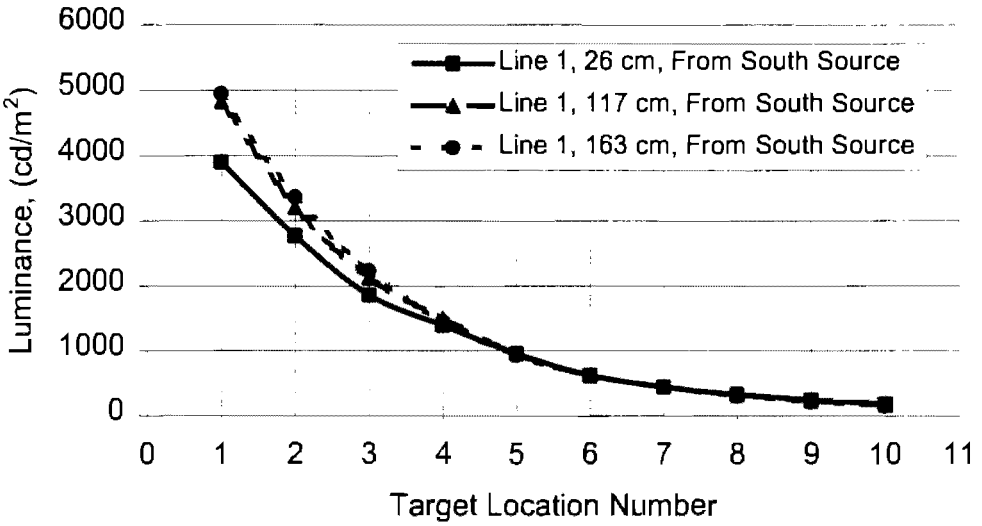

Figure 6.28 Luminance distribution, from south source, at 26 cm, 117 cm and 163 cm height above the roadway surface on line 1.

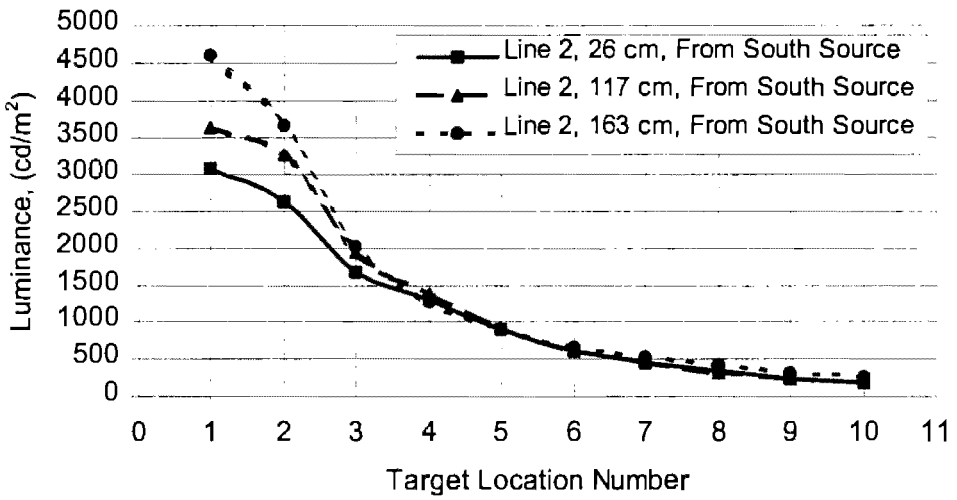

Figure 6.29 Luminance distribution, from south source, at 26 cm, 117 cm and 163 cm height above the roadway surface on line 2.

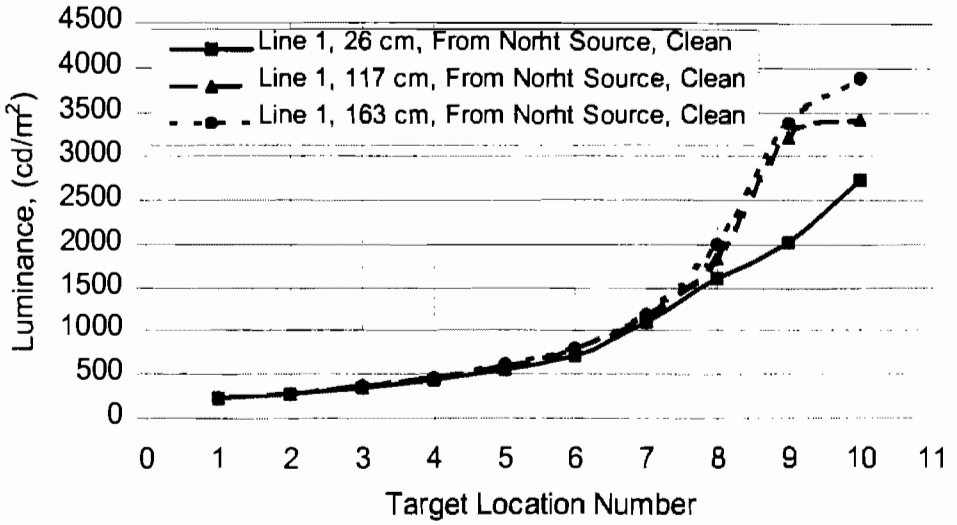

Figure 6.30 Luminance distribution, from north source, at 26 cm, 117 cm and 163 cm height above the roadway surface on line 1.

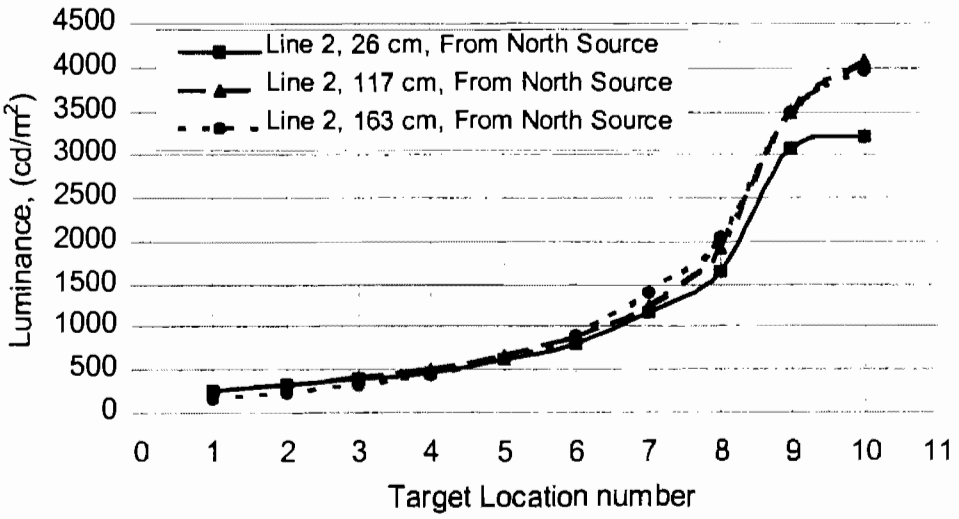

Figure 6.31 Luminance distribution, from north source, at 26 cm, 117 cm and 163 cm height above the roadway surface on line 2.

Comparison Between the First and Clean Measurements

Figures 6.32, 6.33, 6.34 and 6.35 show the illuminance distribution between the installation at the height of 26 cm, 117 cm and 163 cm, respectively. The figures indicate that measurements with the clean lenses are better than the lenses as it was (without cleaning). The big measurement changes can be noticed at the locations that are closer to the poles. When the measurement location getting far from the poles the change becomes smaller.

As it was explained previously, luminance value reduces with the inverse proportionally square of the distance between the source and measurement locations (Luminance/Distance^2). Also, of course photometric data distribution effects the luminance distribution on the roadway.

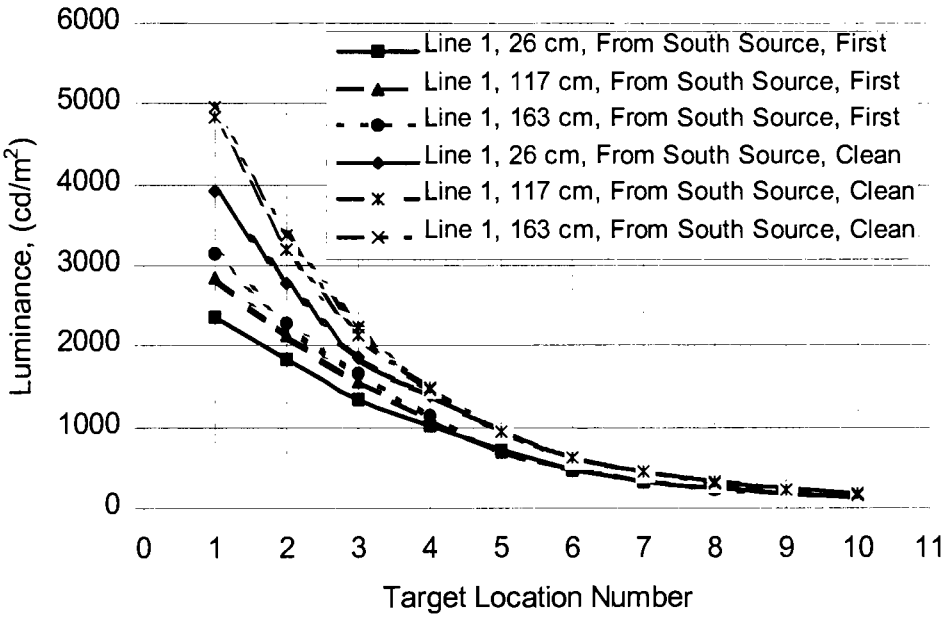

Figure 6.32 Luminance distribution from south source at 26 cm, 117 cm and 163 cm heights above the roadway surface on line 1.

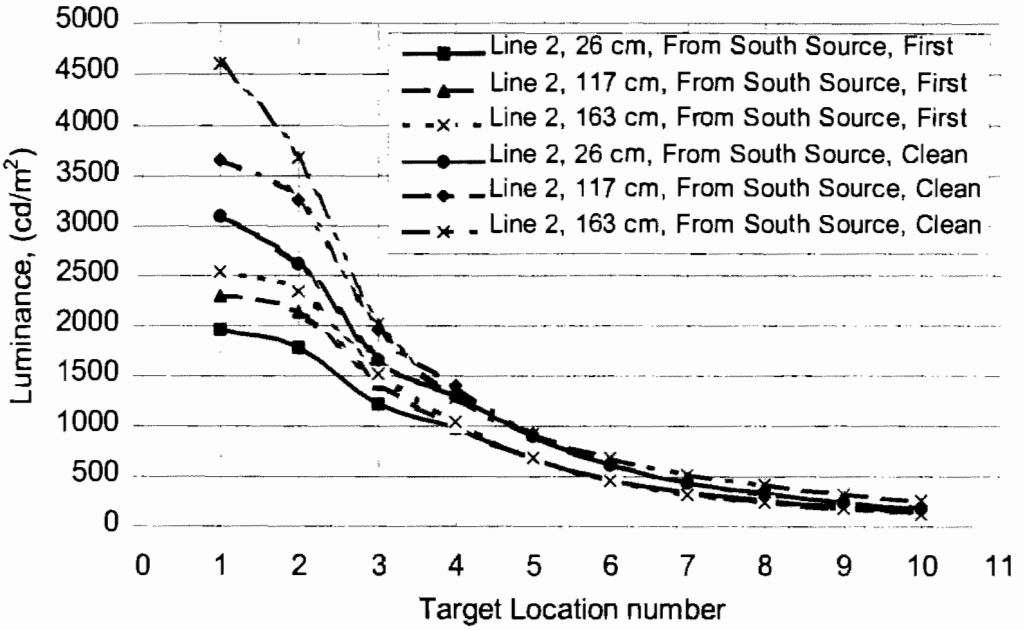

Figure 6.33 Luminance distribution from south source at 26 cm, 117 cm and 163 cm heights above the roadway surface on line 2.

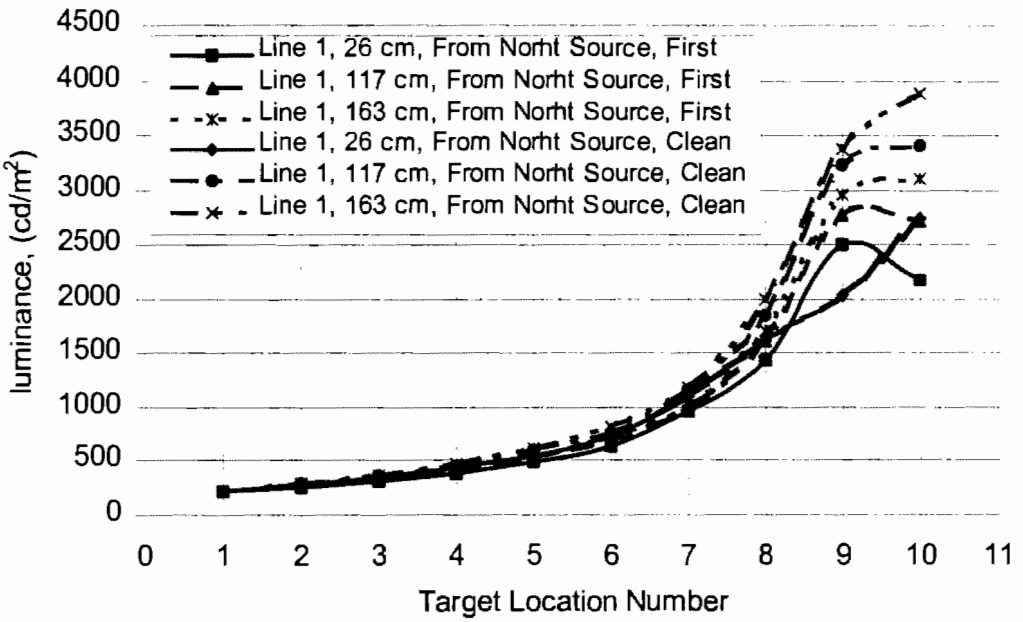

Figure 6.34 Luminance distribution from north source at 26 cm, 117 cm and 163 cm heights above the roadway surface on line 1.

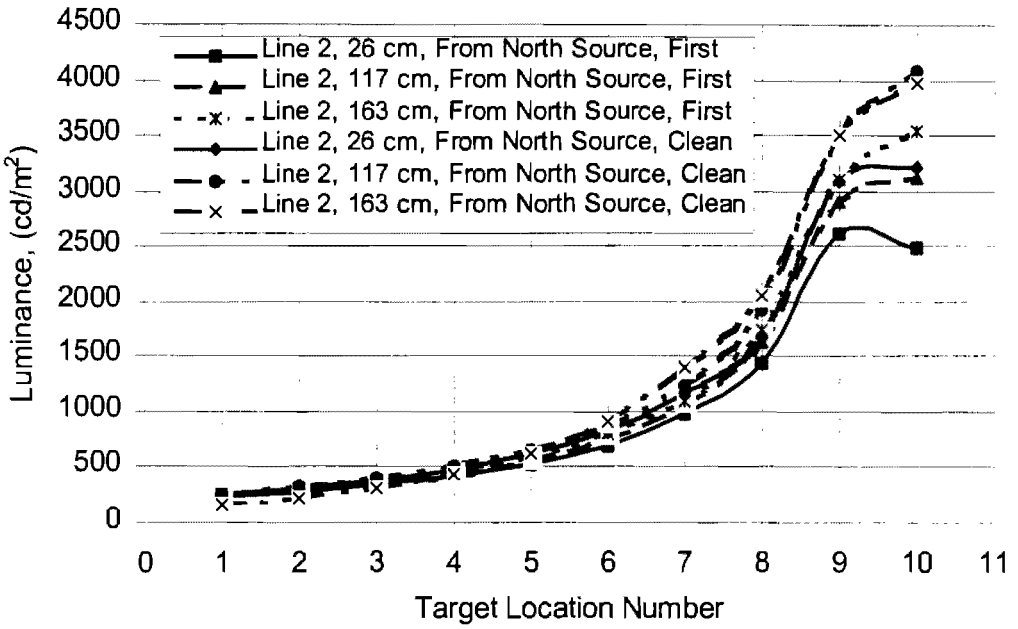

Figure 6.35 Luminance distribution from north source at 26 cm, 117 cm and 163 cm heights above the roadway surface on line 2.

Illuminance Measurements

Illuminance measurements were also performed at the three heights above the roadway surface in the sky, south, north, east, west and ground directions as seen in Figure 3.36. For this purpose, the illuminance head (J1811) was placed on the platform (Figure ??) to measure illuminance in the sky, south, north, east, west and ground directions.

Final Illuminance Measurement

For final illuminance measurements, the light fixtures on the poles 8A, 9a, 10A, 11A and 12A were replaced with the new fixtures manufactured by General Electric Company (M400R2 Luminaire, Catalog Number: M4RR25S9M4GMS3072). Old lamps were also replaced with new ones.

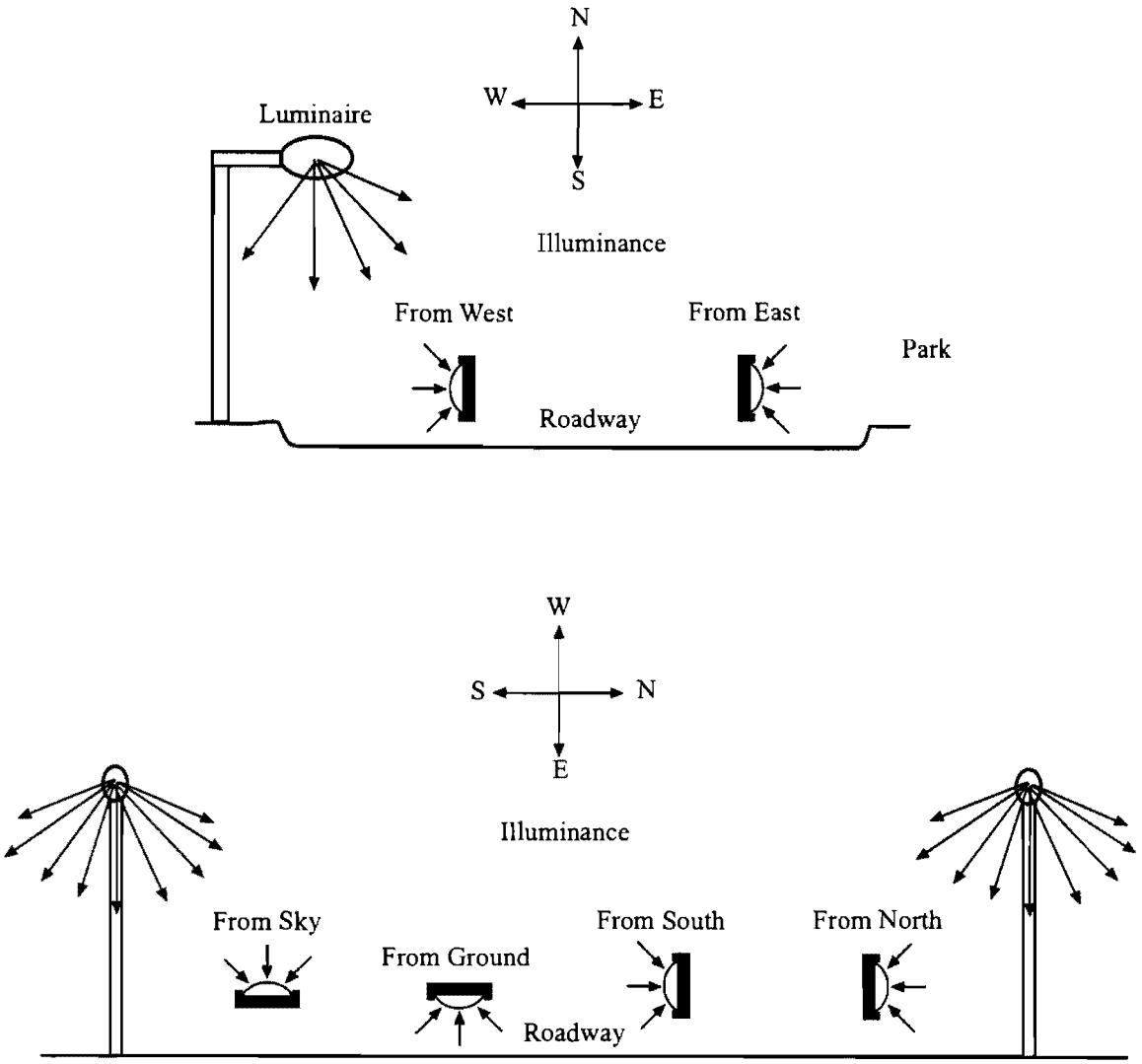

Figure 6.36 Illuminance measurement directions between the installations.

Illuminance Distribution at 26 cm

Figures 6.37 show the illuminance (horizontal illuminance) distributions obtained in the sky direction between the installations. The measurements are performed at the height of 26 cm above the roadway surface for the lines 1 and 2. Figure 6.37 shows that the illuminance values in the sky direction are quickly reduce between the 1st and 4th measurement locations. The illuminance values slightly change between the 4th and 7th measurement locations. Finally, the illuminance values rapidly increase between the 7th and 10th measurement locations. At the first and tenth measurement locations are the closest locations to the luminaires. Therefore, the highest illuminance values are measured at those locations. At the middle of the experimental field, the minimum illuminance values are measured because of the longer distance from the luminaires. The figure also shows that there is significant illuminance difference between the lines 1 and 2. This difference related to the photometric data distribution of the luminaires.

Figures 6.38 and 6.39 show the illuminance (vertical illuminance) distribution in the south and the north directions, respectively. As seen from the figures, the illuminance rapidly increases between the 10^{th} and 9^{th} measurement locations in Figure 6.40, and the 1^{st} and 2^{nd} measurement location in Figure 6.39. The first and tenth measurement locations are the closest locations to the luminaires then the vertical illuminance is less than 2^{nd} and 9^{th} measurement locations. The illuminance values are reduces when the measurement locations get far from the luminaires. Because the illuminance values varies inverse proportionally with square of the direct distance between the luminaire and measurement locations.

Figures 6.40 and 6.41 show the illuminance (vertical illuminance) distribution in the east and the west directions, respectively. As seen in Figure 6.40, the illuminance distributions for both of the lines are almost constant in the east direction. The illuminance distributions for the both of the lines in the west direction (Figure 6.41) start from the high illuminance value and than reduce to the lower value at the middle of the installation then finally increase to the higher value again. Reason for the distribution that the first and the tent measurement locations are the closest locations to the luminaires. The illuminance values on the line 2 are higher than on the line 1. Because the illuminance had has better angle on the line 2.

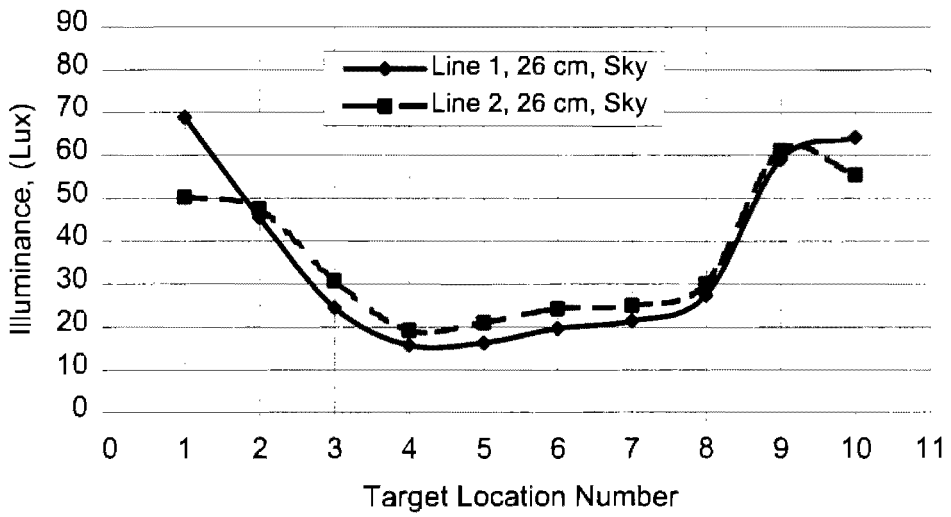

Figure 6.37 Illuminance distribution, in the sky direction, between the installation at 26 cm height above the roadway surface on the lines 1 and 2.

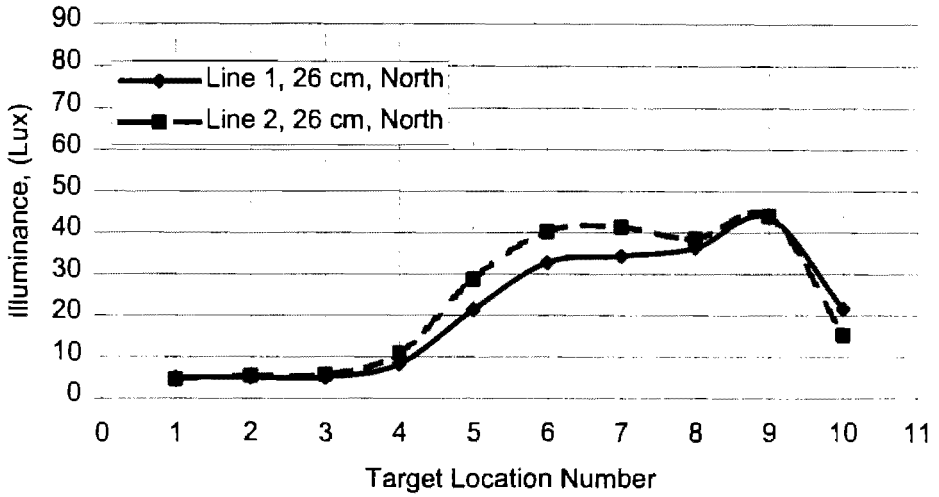

Figure 6.38 Illuminance distribution, in the north direction, between the installation at 26 cm height above the roadway surface on the lines 1 and 2.

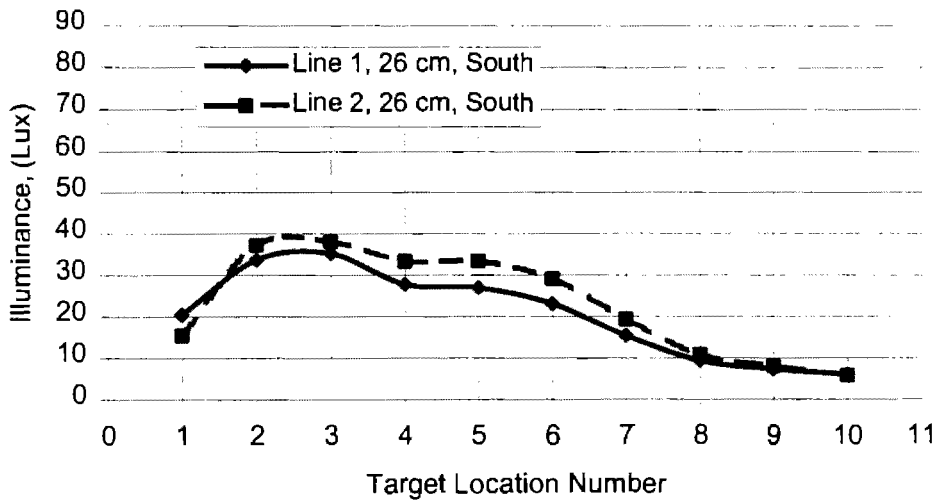

Figure 6.39 Illuminance distribution, in the south direction, between the installation at 26 cm height above the roadway surface on the lines 1 and 2.

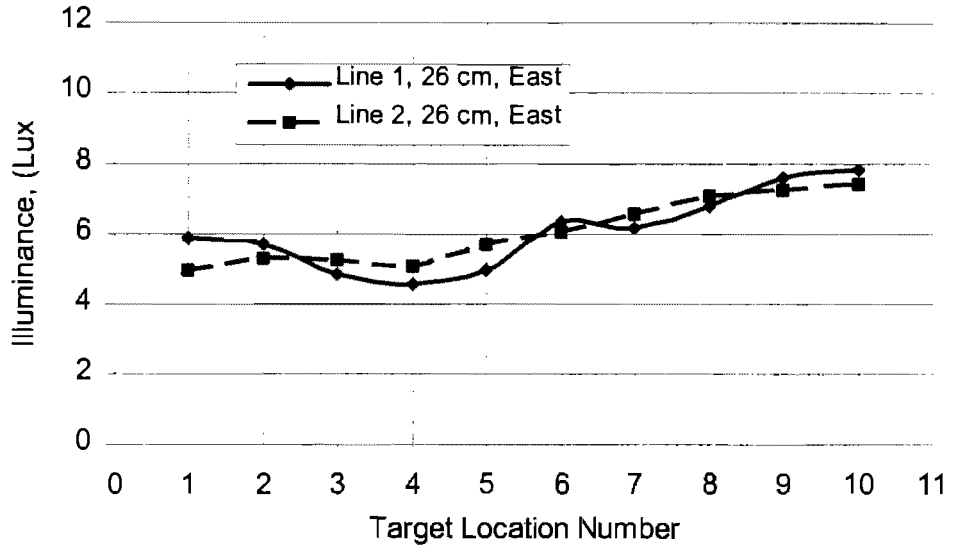

Figure 6.40 Illuminance distribution, in the east direction, between the installation at 26 cm height above the roadway surface on the lines 1 and 2.

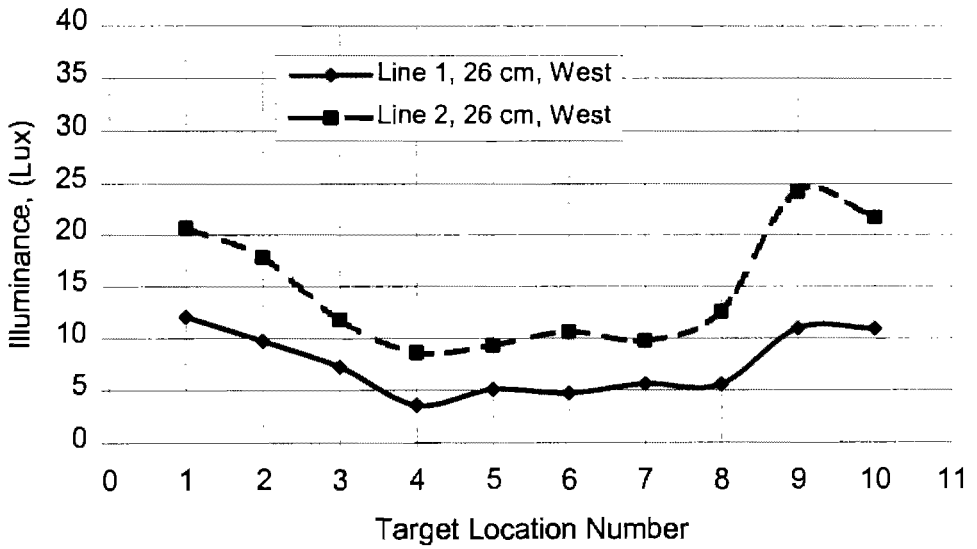

Figure 6.41 Illuminance distribution, in the west direction, between the installation at 26 cm height above the roadway surface on the lines 1 and 2.

Illuminance Distribution at 117 cm

Figures 6.42 show the illuminance (horizontal illuminance) distributions obtained in the sky direction. The measurements are performed at the height of 117 cm above the roadway surface for the lines 1 and 2. Figure 6.42 shows same type of illuminance distribution as in Figure 6.37.

Figures 6.43 and 6.44 show the illuminance (vertical illuminance) distribution in the south and the north directions, respectively. The measurements are performed at the height of 117 cm above the roadway surface for the lines 1 and 2. Figure 6.43 and 6.44 show same type of illuminance distribution as in Figure 6.38 and 6.39.

Figures 3.45 and 3.46 show the illuminance (vertical illuminance) distribution in the east and the west directions, respectively. The measurements are performed at the height of 117 cm above the roadway surface for the lines 1 and 2. Figure 3.45 and 3.46 show same type of illuminance distribution as in Figure 3.40 and 3.41.

Figures 6.47 shows the illuminance (reflectance) distribution at the height of 117 cm above the roadway surface in the ground directions. As seen from the figure, the illuminance distributions for the both of the lines in the ground direction start from the high illuminance value and than reduce to the lower value at the middle of the installation then finally increase to the higher value again. Reason for the distribution that the first and the tent measurement locations are the closest locations to the luminaires then more light hits to the roadway surface and more light reflect from it. The illuminance values on the line 2 are higher than on the line 1 because of the photometric data of the luminaires.

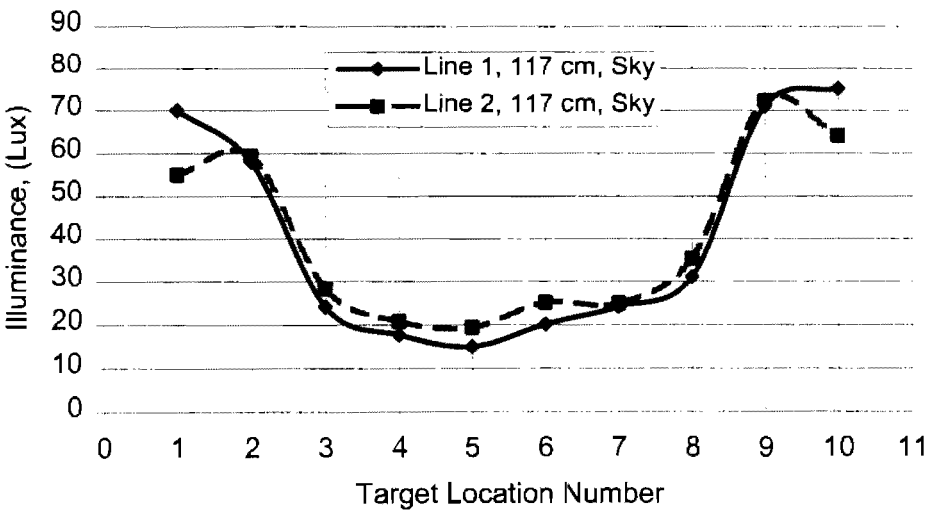

Figure 6.42 Illuminance distribution, in the sky direction, between the installation at 117 cm height above the roadway surface on the lines 1 and 2.

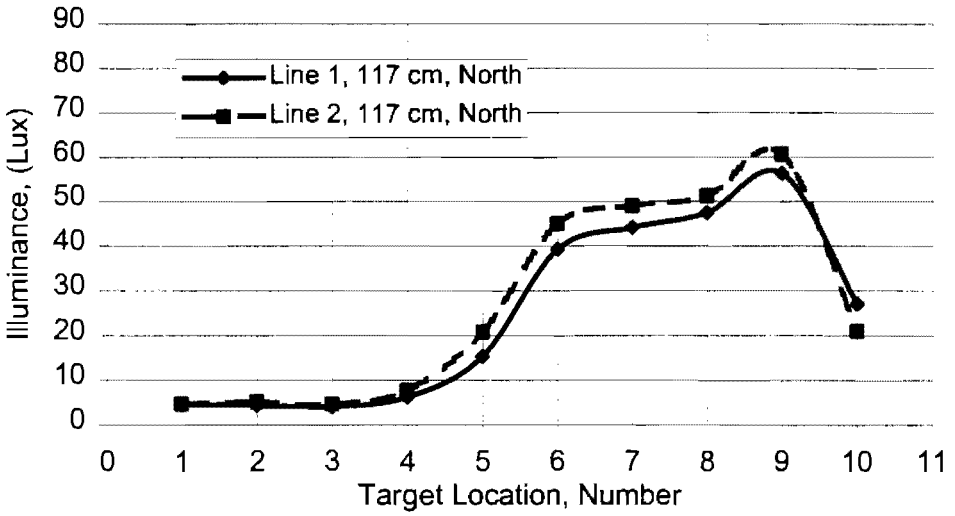

Figure 6.43 Illuminance distribution, in the north direction, between the installation at 117 cm height above the roadway surface on the lines 1 and 2.

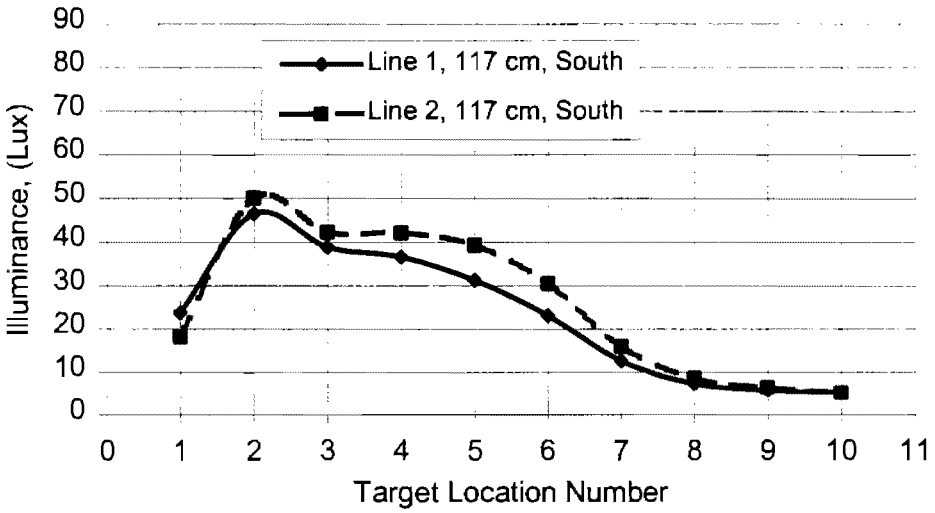

Figure 6.44 Illuminance distribution, in the south direction, between the installation at 117 cm height above the roadway surface on the lines 1 and 2.

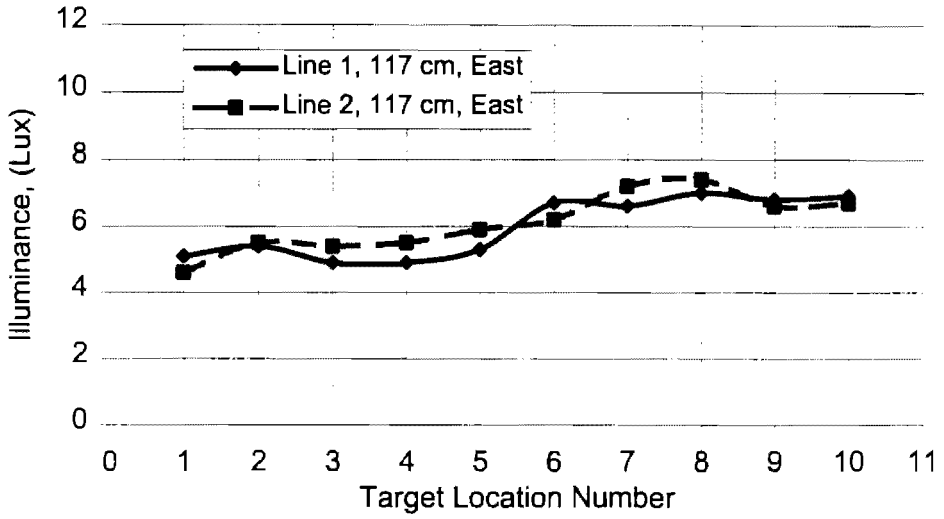

Figure 6.45 Illuminance distribution, in the east direction, between the installation at 117 cm height above the roadway surface on the lines 1 and 2.

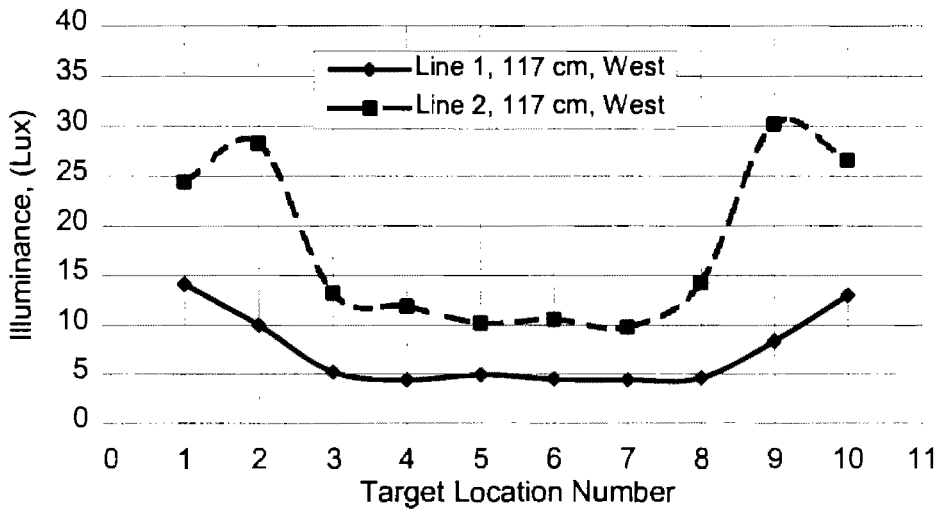

Figure 6.46 Illuminance distribution, in the west direction, between the installation at 117 cm height above the roadway surface on the lines 1 and 2.

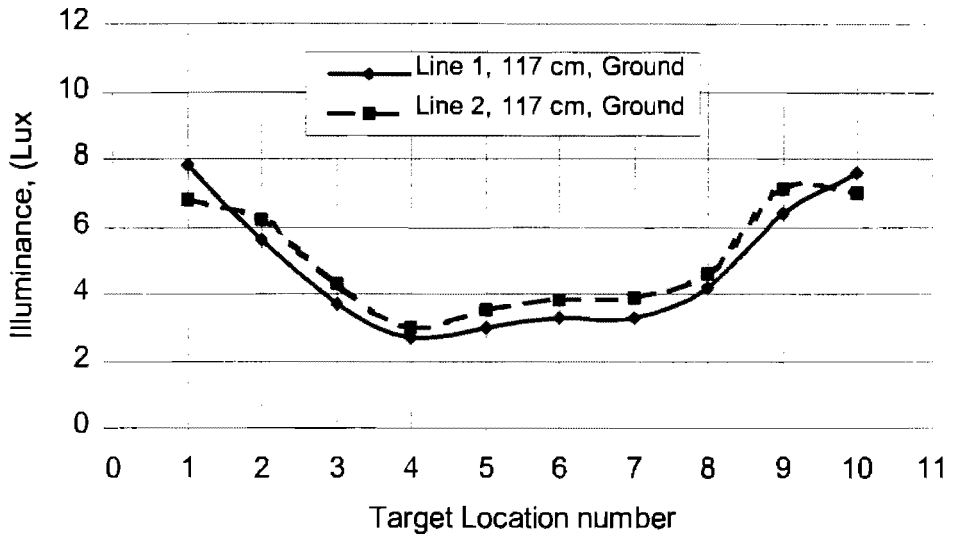

Figure 6.47 Illuminance distribution, in the ground direction, between the installation at 117 cm height above the roadway surface on the lines 1 and 2.

Illuminance Distribution at 163 cm

Figure 6.48 show the illuminance (horizontal illuminance) distributions obtained in the sky direction. The measurements are performed at the height of 163 cm above the roadway surface for the lines 1 and 2. Figure 6.48 shows same type of illuminance distribution as in Figure 6.37.

Figures 6.49 and 6.50 show the illuminance (vertical illuminance) distribution in the south and the north directions, respectively. The measurements are performed at the height of 163 cm above the roadway surface for the lines 1 and 2. Figures 6.49 and 6.50 show same type of illuminance distribution as in Figure 6.38 and 6.39.

Figures 6.51 and 6.52 show the illuminance (vertical illuminance) distribution in the east and the west directions, respectively. The measurements are performed at the height of 163 cm above the roadway surface for the lines 1 and 2. Figure 6.51 and 6.52 show same type of illuminance distribution as in Figure 6.40 and 6.41.

Figures 6.53 shows the illuminance (reflectance) distribution at the height of 163 cm above the roadway surface in the ground directions. Figure 6.53 shows same type of illuminance distribution as in Figure 6.47.

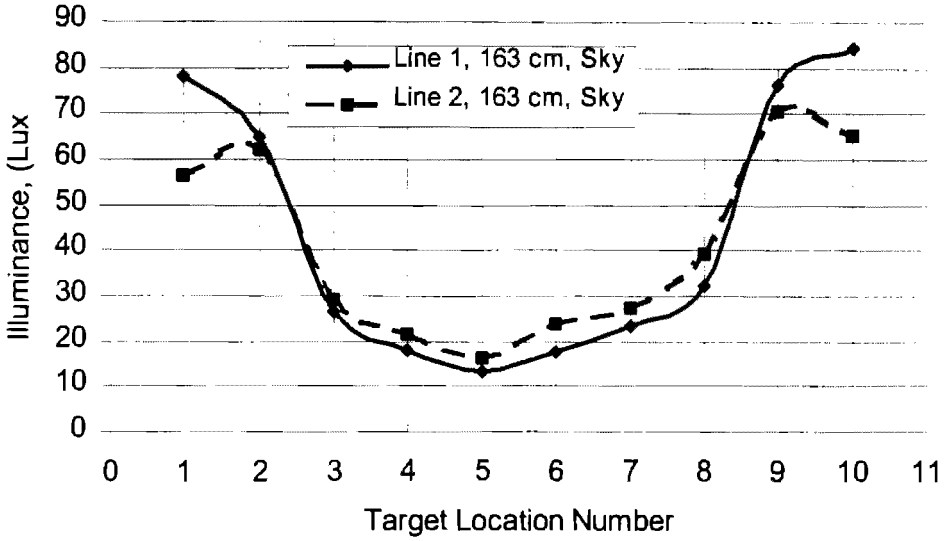

Figure 6.48 Illuminance distribution, in the sky direction, between the installation at 163 cm height above the roadway surface on the lines 1 and 2.

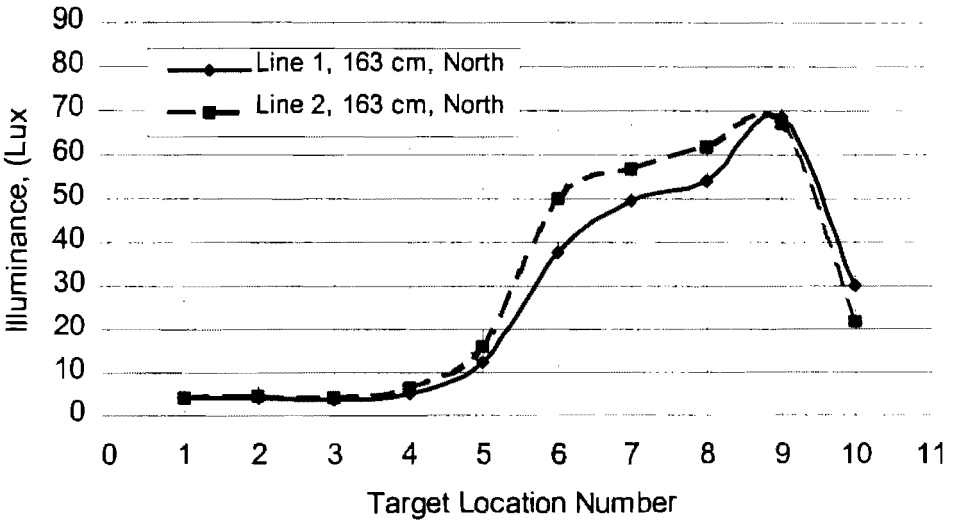

Figure 6.49 Illuminance distribution, in the north direction, between the installation at 163 cm height above the roadway surface on the lines 1 and 2.

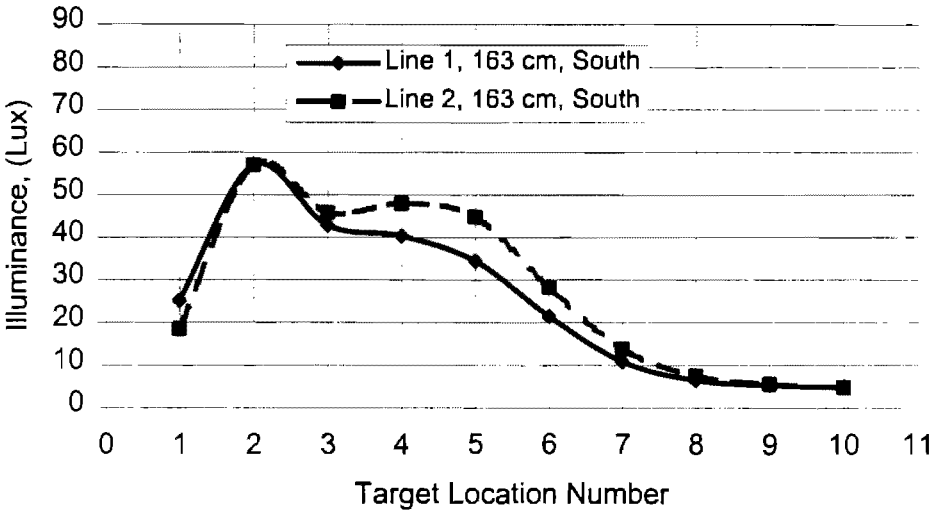

Figure 6.50 Illuminance distribution, in the south direction, between the installation at 163 cm height above the roadway surface on the lines 1 and 2.

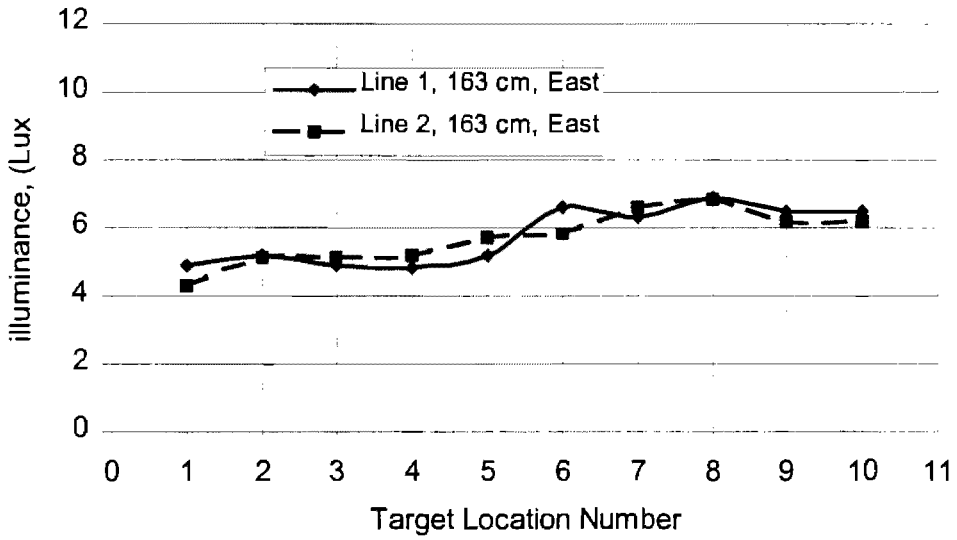

Figure 6.51 Illuminance distribution, in the east direction, between the installation at 163 cm height above the roadway surface on the lines 1 and 2.

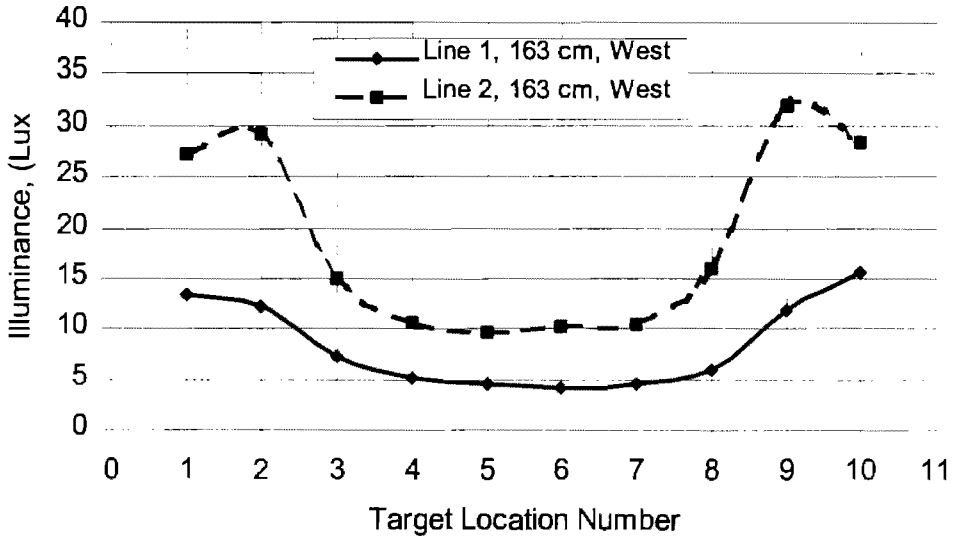

Figure 6.52 Illuminance distribution, in the west direction, between the installation at 163 cm height above the roadway surface on the lines 1 and 2.

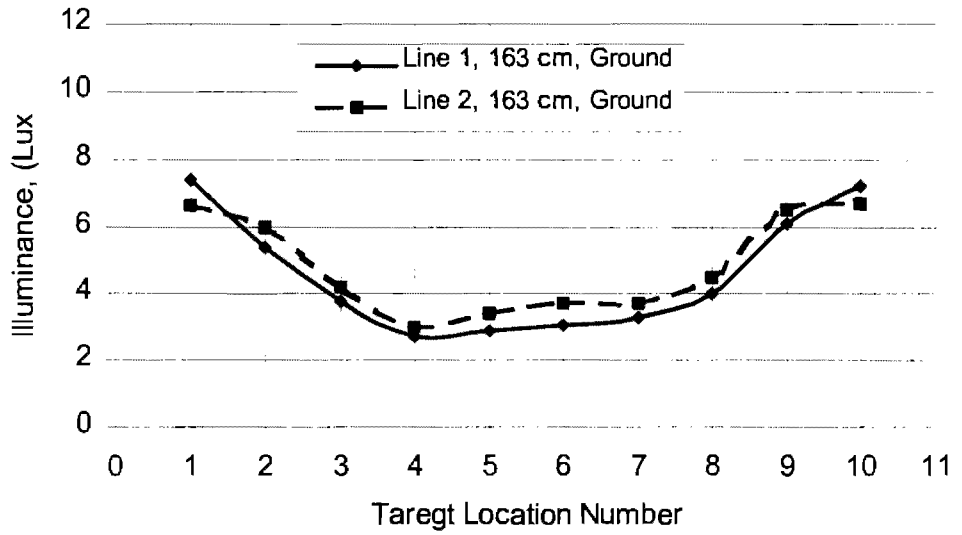

Figure 6.53 Illuminance distribution, in the ground direction, between the installation at 163 cm height above the roadway surface on the lines 1 and 2.

Illuminance Measurement Compression

Figures 6.54 and 6.55 show the illuminance (horizontal illuminance) distributions on the lines1 and 2 in the sky direction, respectively. The illuminance measurements are performed for the lines 1 and 2 at the heights of 26 cm, 117 cm and 163 cm above the roadway surface. As seen from the figures, illuminance distribution of the luminaires shows same type of pattern at all

three heights. But illuminance values in sky direction change slightly with the measurement's height. Since illuminance changes inverse proportionally with the square of the direct distance between the measurement device and the luminaire. Hence, the illuminance at the height of 163 cm has highest values.

Figures 6.56 and 6.57 show the illuminance distributions in the north direction on the lines 1 and 2, respectively. Figures 6.58 and 6.59 show the illuminance distributions in the south direction on the lines 1 and 2, respectively. As seen from the figures, the illuminance distribution values are higher values obtained at the height of 163 cm. As it is explained, this measurement height provides closer distance than the other measurement heights. Of course, this distribution is also related to the photometric data of the luminaires.

Figures 6.60 and 6.61 show the luminance distributions in the east direction on the lines 1 and 2, respectively. These figures show that the illuminance distribution in the east direction is not depends on the measurement heights. Because there is no luminaire using for the purpose of lighting the roadway in the east direction. There is light for lighting the parking area.

Figures 6.62 and 6.63 show the luminance distributions in the west direction on the lines 1 and 2, respectively. Figure 6.62 shows that the illuminance distribution on the line 1 in the west direction does not depend on the measurement heights. But, the illuminance distribution on the line 2 in the west direction depends on the measurement heights. Because roadway lights is in the west side of the roadway and measurement device has better visual angle for the line 2 than for the line 1.

Figures 6.64 and 6.65 show the luminance distributions in the ground direction on the lines 1 and 2, respectively. There is no illuminance difference between the two measurement height (117 cm and 163 cm).

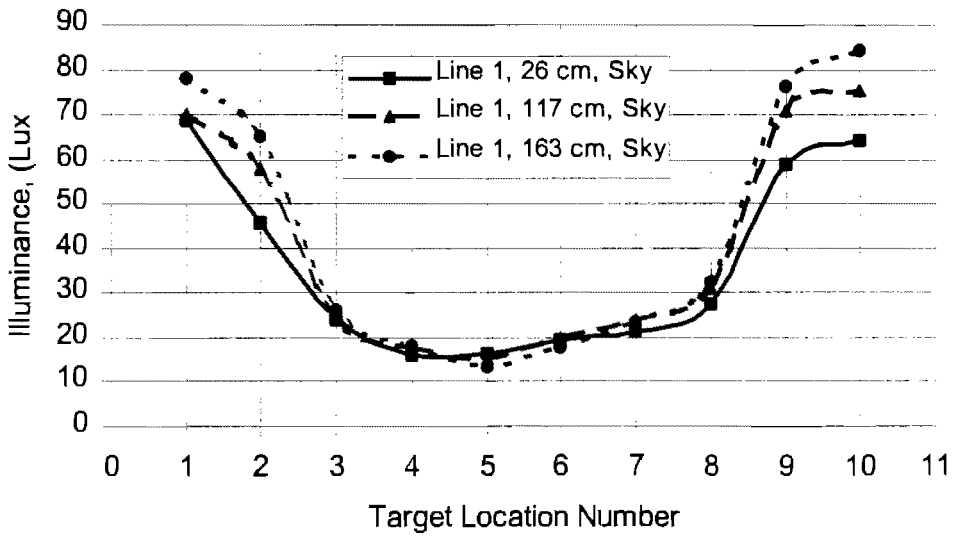

Figure 6.54 Illuminance distribution, from sky direction, between the installation at 26, cm, 117 cm and 163 cm height above the roadway surface on line 1.

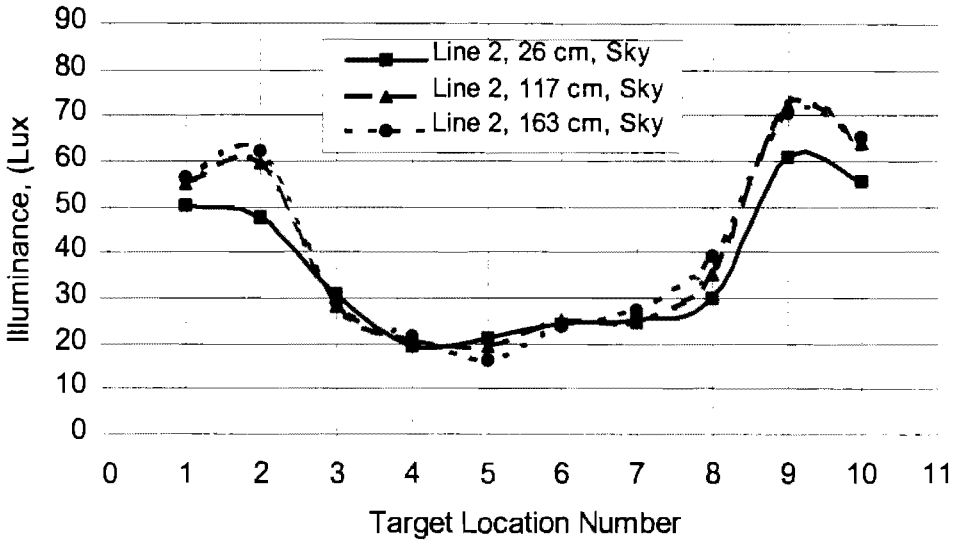

Figure 6.55 Illuminance distribution, from sky direction, between the installation at 26, cm, 117 cm and 163 cm height above the roadway surface on line 2.

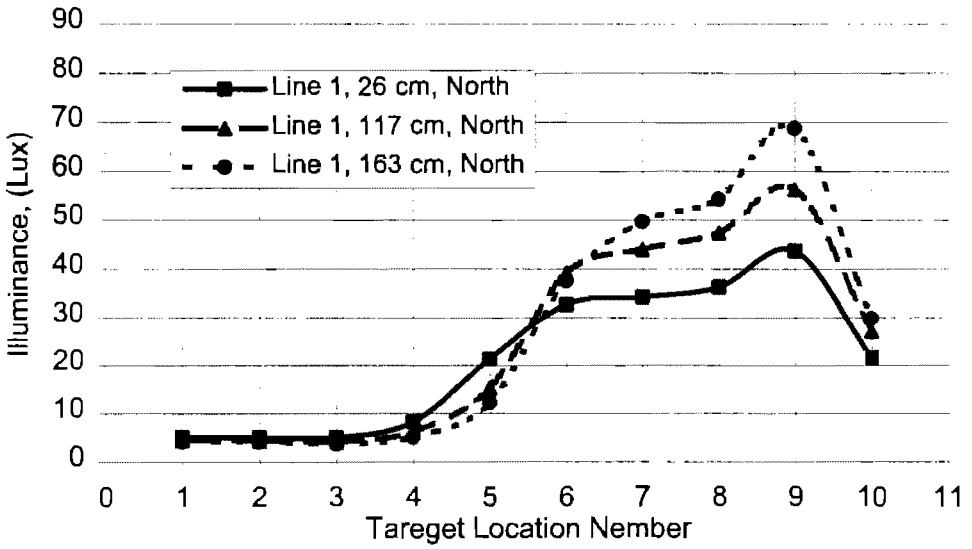

Figure 6.56 Illuminance distribution, from north direction, between the installation at 26, cm, 117 cm and 163 cm height above the roadway surface on line 1.

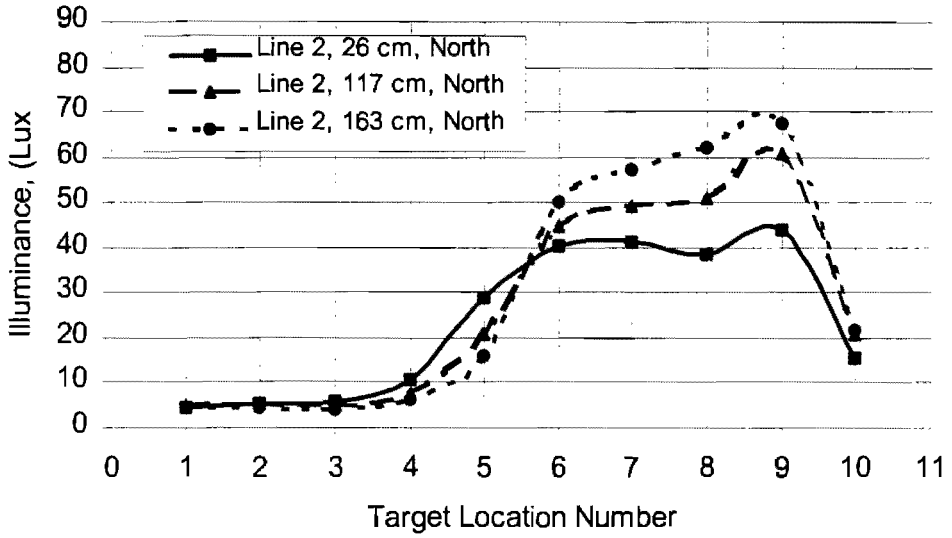

Figure 6.57 Illuminance distribution, from north direction, between the installation at 26, cm, 117 cm and 163 cm height above the roadway surface on line 2.

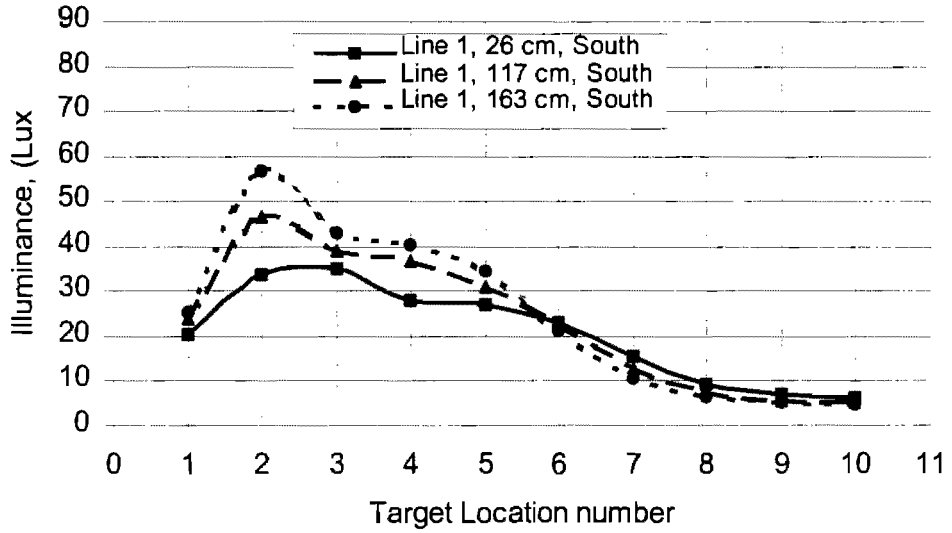

Figure 6.58 Illuminance distribution, from south direction, between the installation at 26, cm, 117 cm and 163 cm height above the roadway surface on line 1.

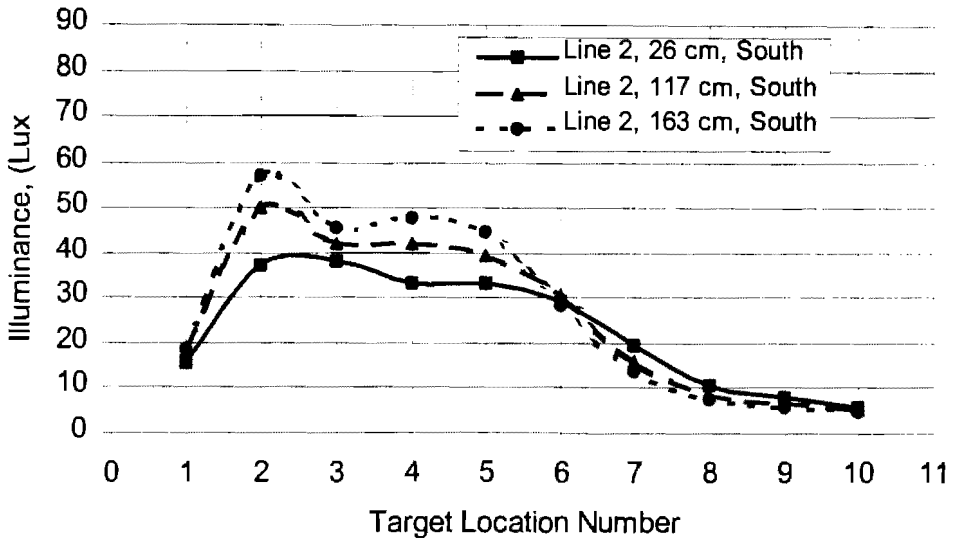

Figure 6.59 Illuminance distribution, from south direction, between the installation at 26, cm, 117 cm and 163 cm height above the roadway surface on line 2.

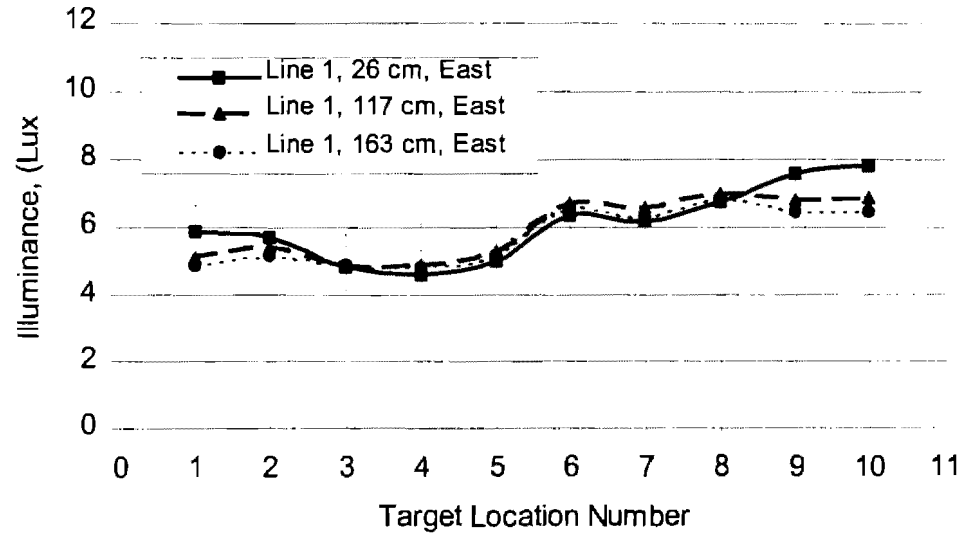

Figure 6.60 Illuminance distribution, from east direction, between the installation at 26, cm, 117 cm and 163 cm height above the roadway surface on line 1.

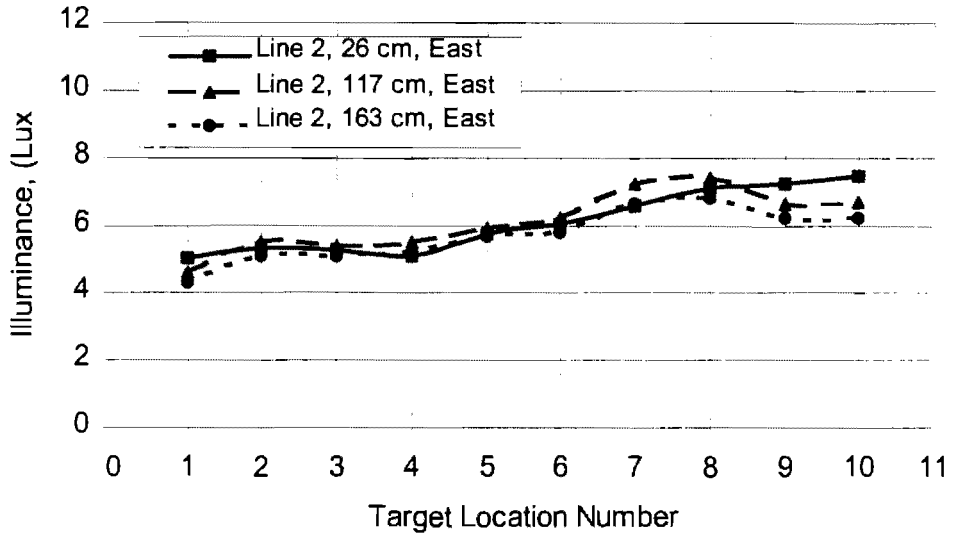

Figure 6.61 Illuminance distribution, from east direction, between the installation at 26, cm, 117 cm and 163 cm height above the roadway surface on line 2.

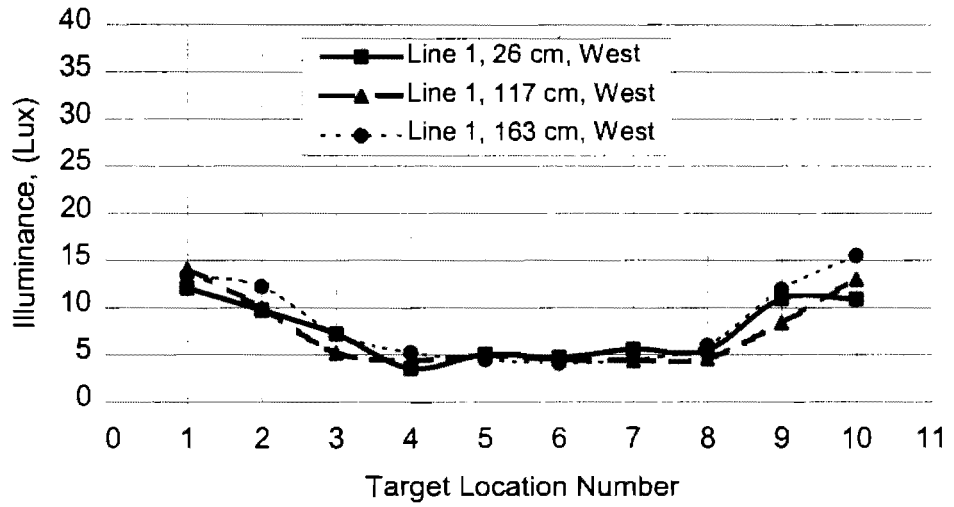

Figure 6.62 Illuminance distribution, from west direction, between the installation at 26, cm, 117 cm and 163 cm height above the roadway surface on line 1.

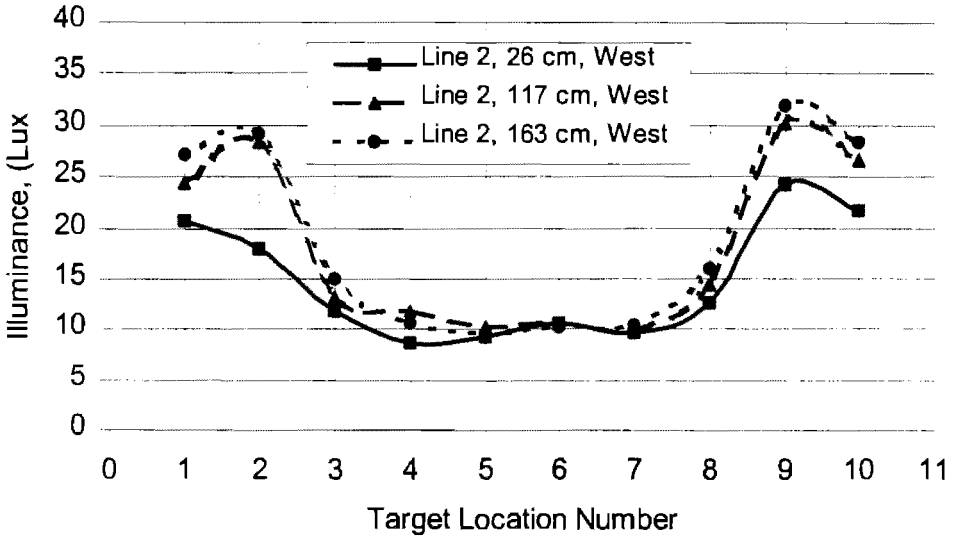

Figure 6.63 Illuminance distribution, from west direction, between the installation at 26, cm, 117 cm and 163 cm height above the roadway surface on line 2.

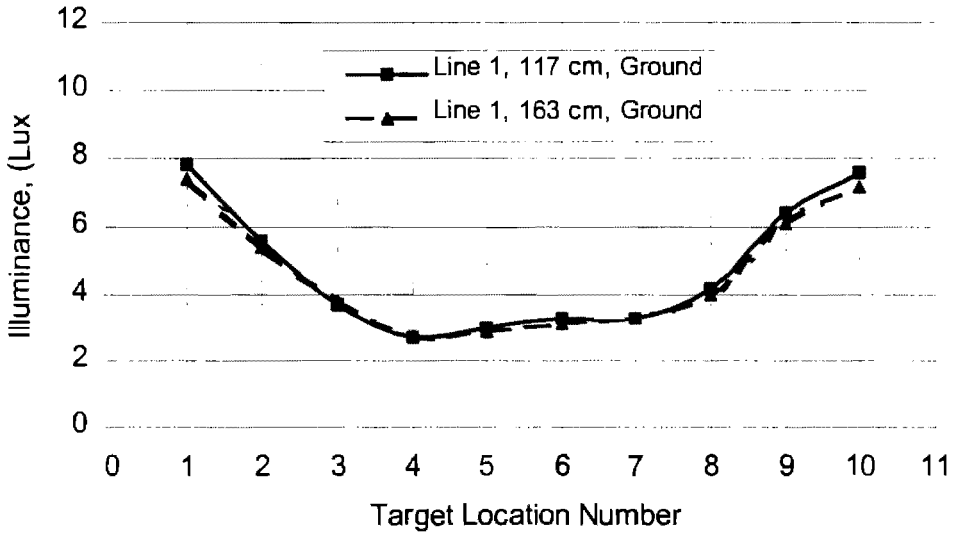

Figure 6.64 Illuminance distribution, from ground direction, between the installation at 26, cm, 117 cm and 163 cm height above the roadway surface on line 1.

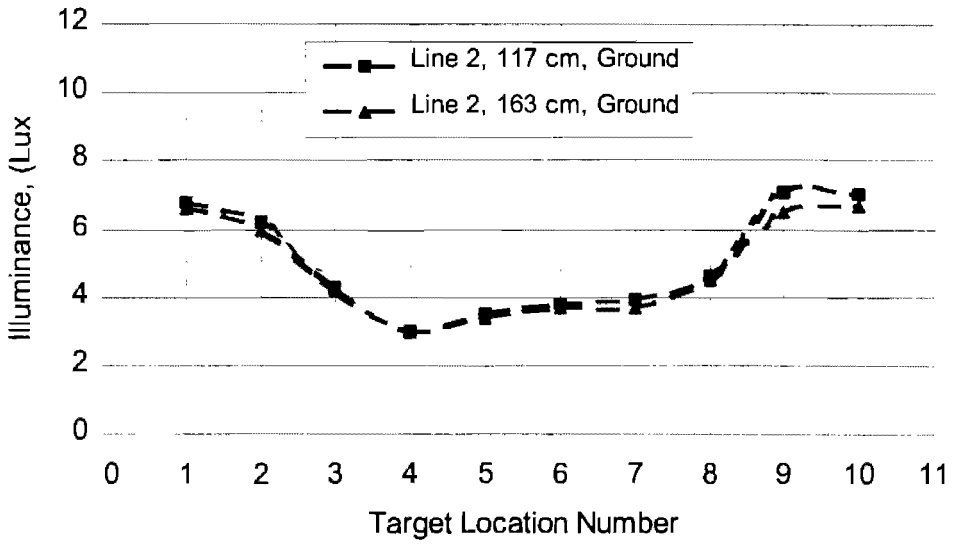

Figure 6.65 Illuminance distribution, from ground direction, between the installation at 26, cm, 117 cm and 163 cm height above the roadway surface on line 2.

First Illuminance Measurements

The illuminance measurements were performed first time in the experimental field without changing any conditions. Under these circumstances, illuminance measurements were performed in the sky, north, south, east and west directions. The plots were only indicated in the sky, north and south directions. Plots were not indicated in the east and west directions because there is not light source in these directions.

Figures 6.66 and 6.67 show the illuminance (horizontal illuminance) distributions on the lines1 and 2 in the sky direction, respectively. The illuminance measurements are performed for the lines 1 and 2 at the heights of 26 cm, 117 cm and 163 cm above the roadway surface. As seen from the figures, illuminance distribution of the luminaires shows same type of pattern at all three heights. But illuminance values in sky direction change slightly with the measurement's height except the measurement points that are close to the sources.

Figures 6.68 and 6.69 show the illuminance distributions in the north direction on the lines 1 and 2, respectively. Figures 6.70 and 6.71 show the illuminance distributions in the south direction on the lines 1 and 2, respectively. As seen from the figures, the illuminance distribution values are higher values obtained at the height of 163 cm. As it is explained, this measurement height provides closer distance than the other measurement heights. Of course, this distribution is also related to the photometric data of the luminaires. In the north direction (Figures 6.68 and 6.69), illuminance measurements at the 8^{th} and 9^{th} locations are much lower than the other measurements at the same locations because dirt lens effects the photometric data distribution. In the south direction (Figures 6.70 and 6.71) show that there is almost no difference between three measurements, even though measurements were made at the 26 cm height that is higher than the other two because dirt creates non uniformity distribution on the lamp lenses then it translates non uniform photometric data distribution also.

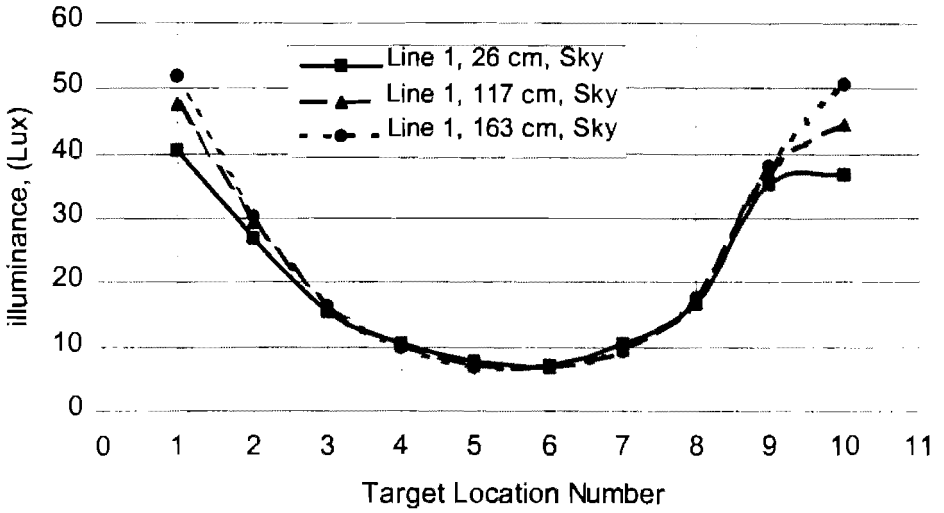

Figure 6.66 Illuminance distribution, from sky direction, at 26 cm, 117 cm and 163 cm height above the roadway surface on line 1.

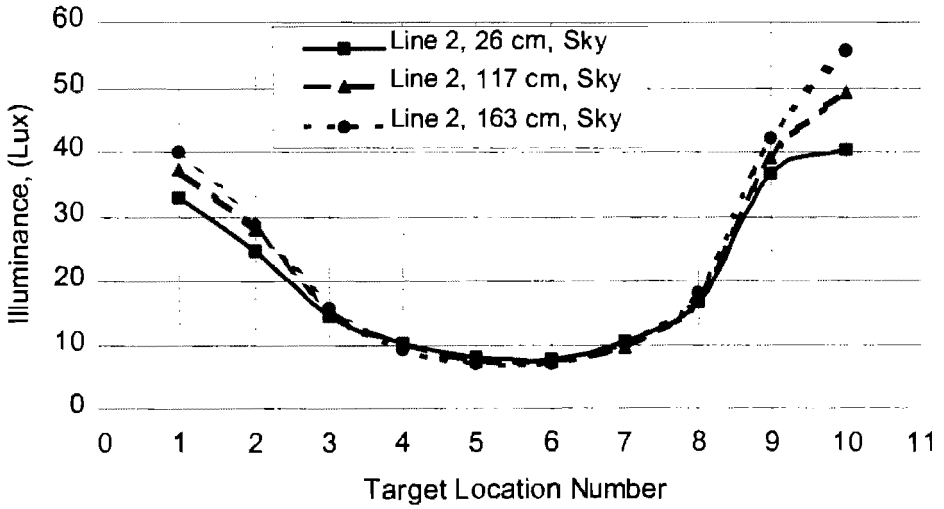

Figure 6.67 Illuminance distribution, from sky direction, at 26 cm, 117 cm and 163 cm height above the roadway surface on line 2.

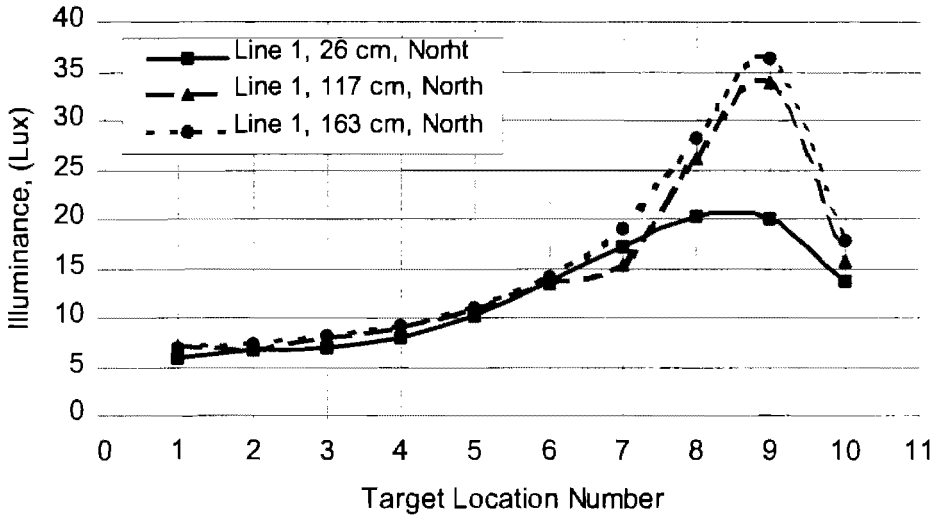

Figure 6.68 Illuminance distribution, from north direction, at 26 cm, 117 cm and 163 cm height above the roadway surface on line 1.

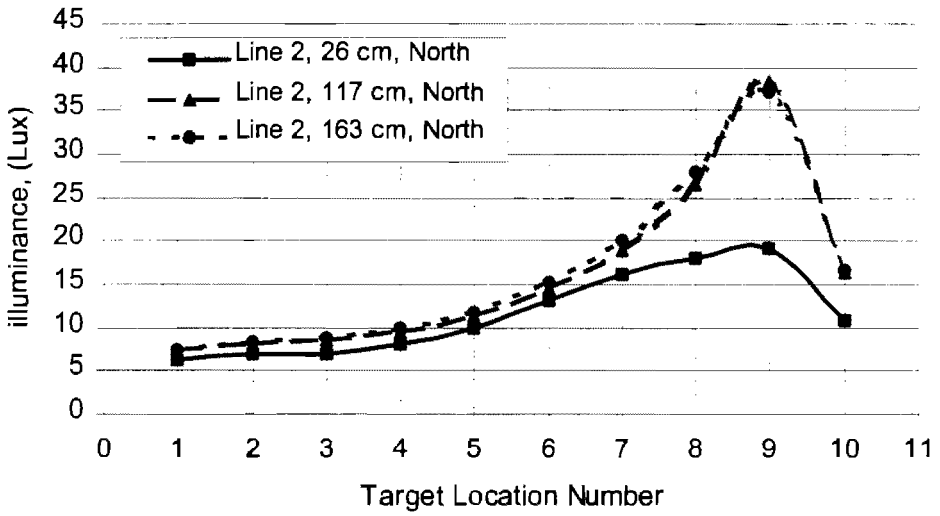

Figure 6.69 Illuminance distribution, from north direction, at 26 cm, 117 cm and 163 cm height above the roadway surface on line 2.

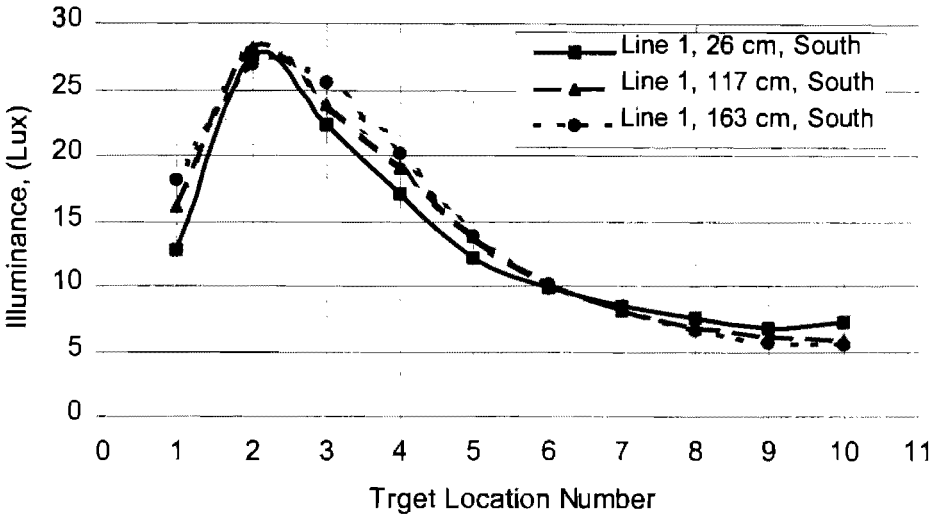

Figure 6.70 Illuminance distribution, from south direction, at 26 cm, 117 cm and 163 cm height above the roadway surface on line 1.

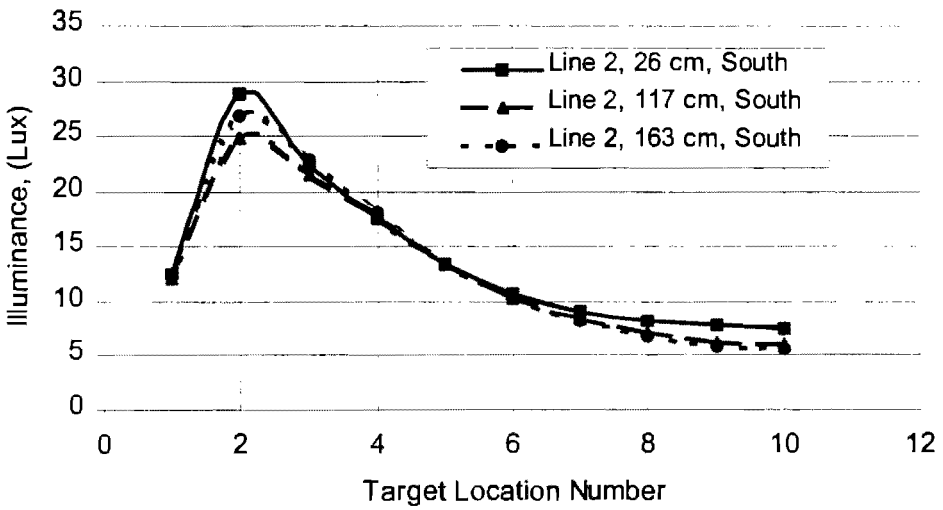

Figure 6.71 Illuminance distribution, from south direction, at 26 cm, 117 cm and 163 cm height above the roadway surface on line 2.

Illuminance Measurements with Clean Lenses

The illuminance measurements were performed second time in the experimental field by replacing the new lamp and cleaning the lens of the lamps. Under these circumstances,

illuminance measurements were again performed in the sky, north, south, east and west directions. The plots were only indicated in the sky, north and south directions.

Figures 6.72 and 6.73 show the illuminance (horizontal illuminance) distributions on the lines1 and 2 in the sky direction, respectively. The illuminance measurements are performed for the lines 1 and 2 at the heights of 26 cm, 117 cm and 163 cm above the roadway surface. As seen from the figures, illuminance distribution of the luminaires shows same type of pattern at all three heights. But illuminance values in sky direction change slightly with the measurement's height except the measurement points that are close to the sources. The measurement values at the 163 cm shows less than the other two measurements. These values are suppose to be grater then the other measurement values as seen for measurements at the 117 cm height which are greater than the measurements at 26 cm height. This is because of the photometric data distribution.

Figures 6.74 and 6.75 show the illuminance distributions in the north direction on the lines 1 and 2, respectively. Figures 6.76 and 6.77 show the illuminance distributions in the south direction on the lines 1 and 2, respectively. As seen from the figures, the illuminance distribution values are higher values obtained at the height of 163 cm in the north direction measurements. In the south direction measurements show that measurement values obtained at the 163 cm are less values. Reason for this, the lens of the lamp could not clean good and it effects the photometric data distribution on the roadway.

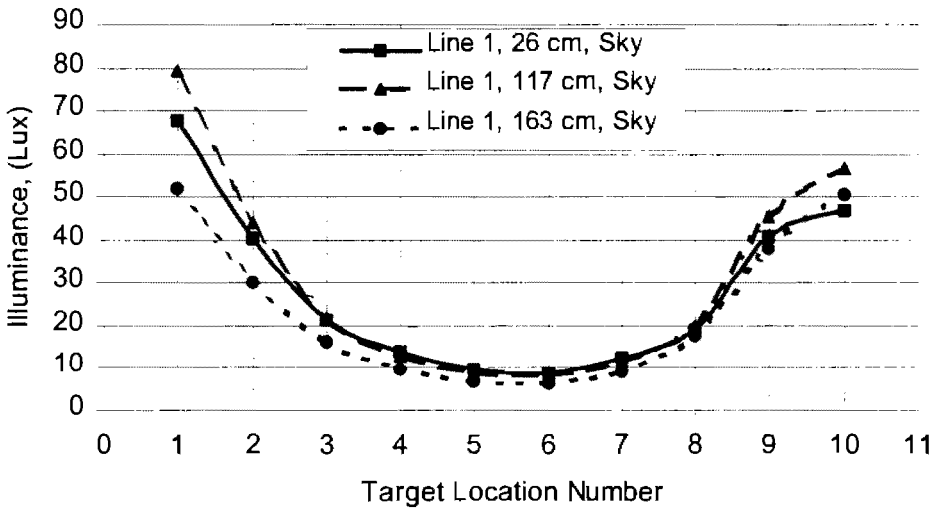

Figure 6.72 Illuminance distribution, from sky direction, at 26 cm, 117 cm and 163 cm height above the roadway surface on line 1.

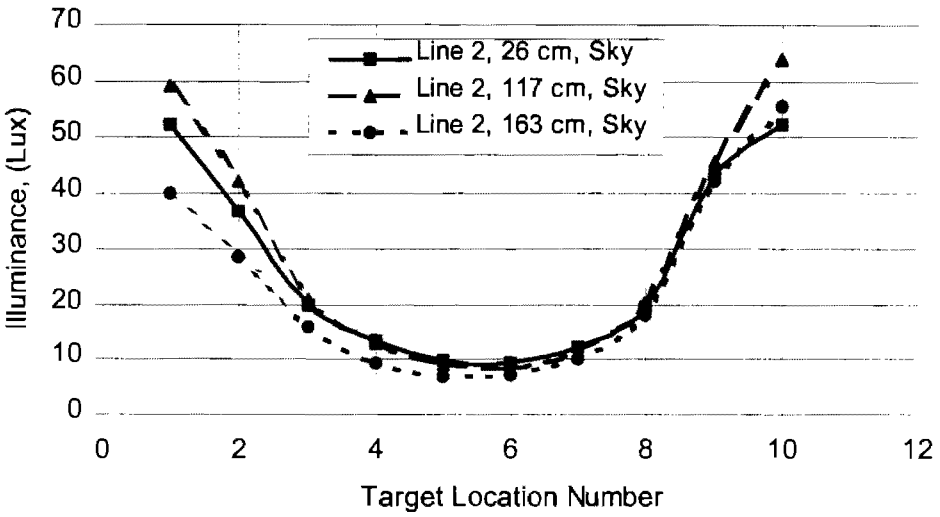

Figure 6.73 Illuminance distribution, from sky direction, at 26 cm, 117 cm and 163 cm height above the roadway surface on line 2.

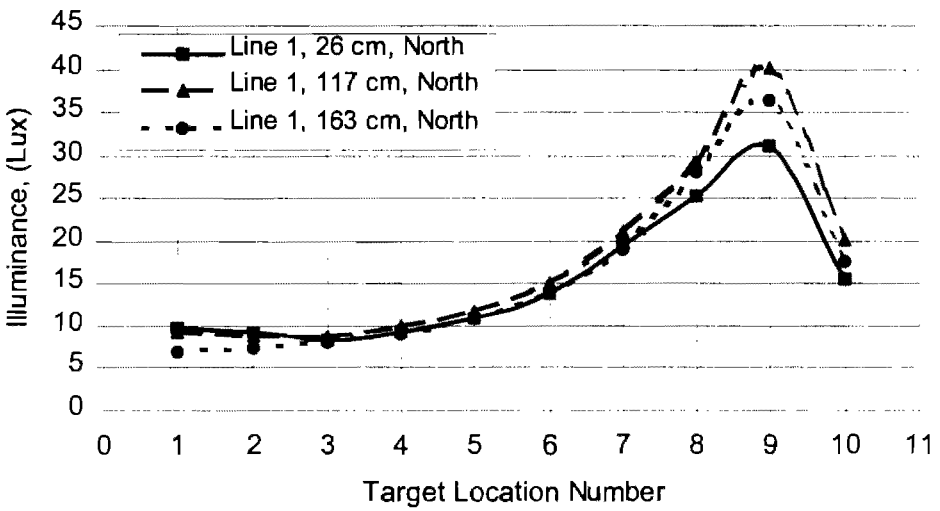

Figure 6.74 Illuminance distribution, from north direction, at 26 cm, 117 cm and 163 cm height above the roadway surface on line 1.

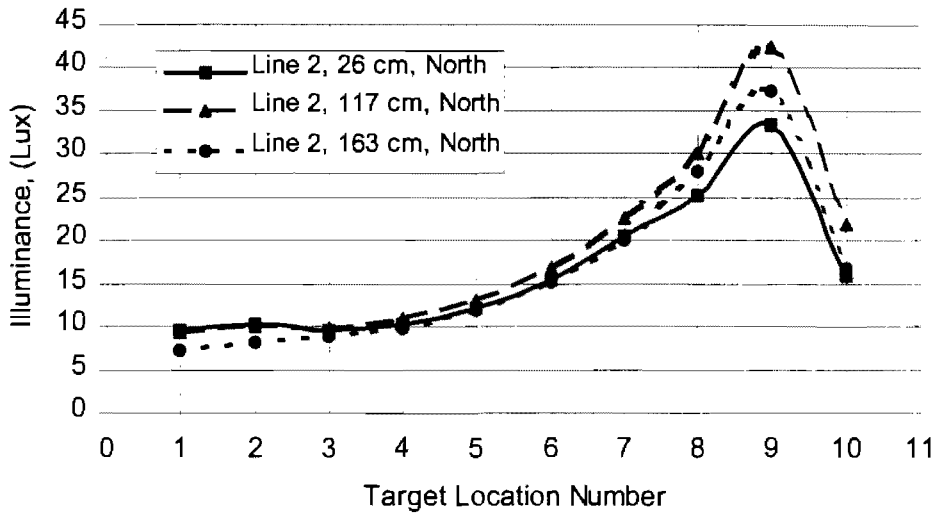

Figure 6.75 Illuminance distribution, from north direction, at 26 cm, 117 cm and 163 cm height above the roadway surface on line 2.

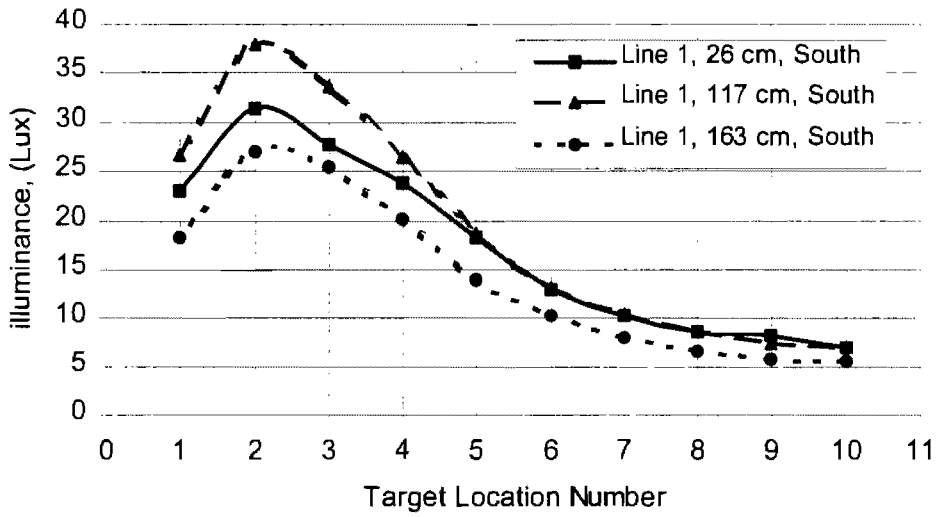

Figure 6.76 Illuminance distribution, from south direction, at 26 cm, 117 cm and 163 cm height above the roadway surface on line 1.

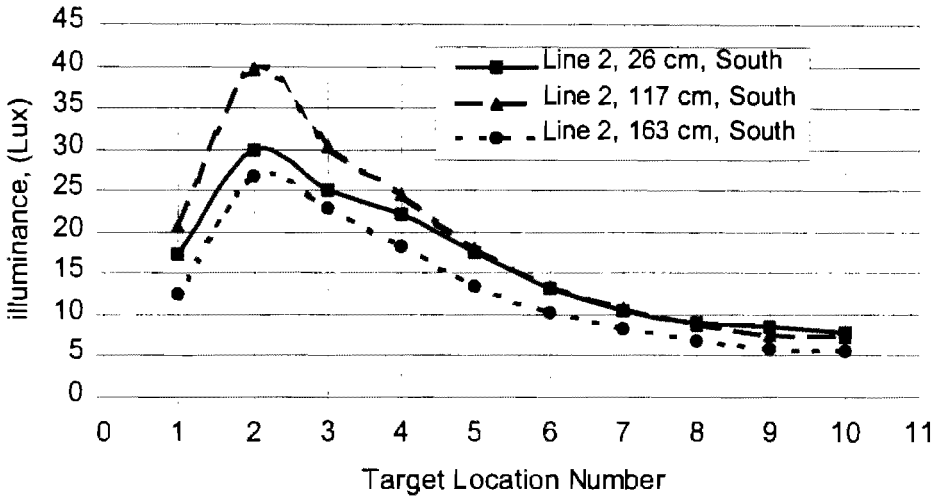

Figure 6.77 Illuminance distribution, from south direction, at 26 cm, 117 cm and 163 cm height above the roadway surface on line 2.

Comparison between the First and Clean Measurement

Figures 6.78, 6.79 and 6.80 shows the illuminance distribution between the installation at the height of 26 cm, 117 cm and 163 cm, respectively. The figures indicate that measurements with the clean lenses are better than the lenses as it was (without cleaning). The big measurement changes can be noticed at the locations that are closer to the poles the biggest changes were at the closest location to the poles. When the measurement location getting far from the poles the change becomes smaller and smaller. As seen from the figure there is slightly illuminance change at the middle of the poles. Because illuminance reduces inverse proportionally with square of the distance.

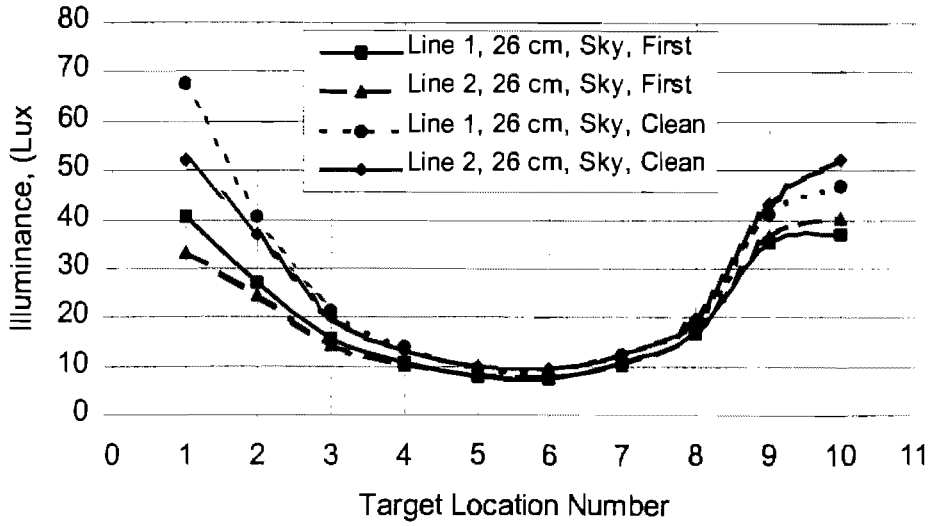

Figure 6.78 Illuminance distribution from sky direction at 26 cm height above the roadway surface on lines 1 and 2.

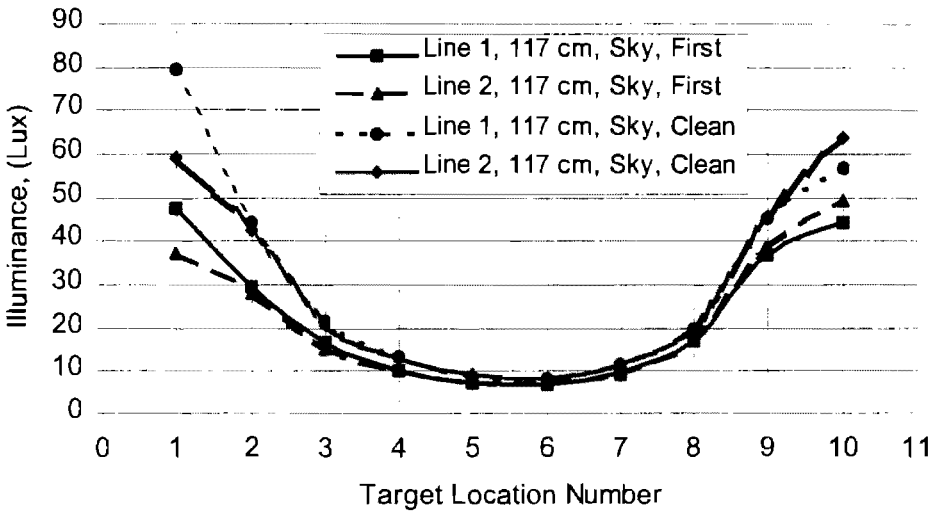

Figure 6.79 Illuminance distribution from sky direction at 117 cm height above the roadway surface on lines 1 and 2.

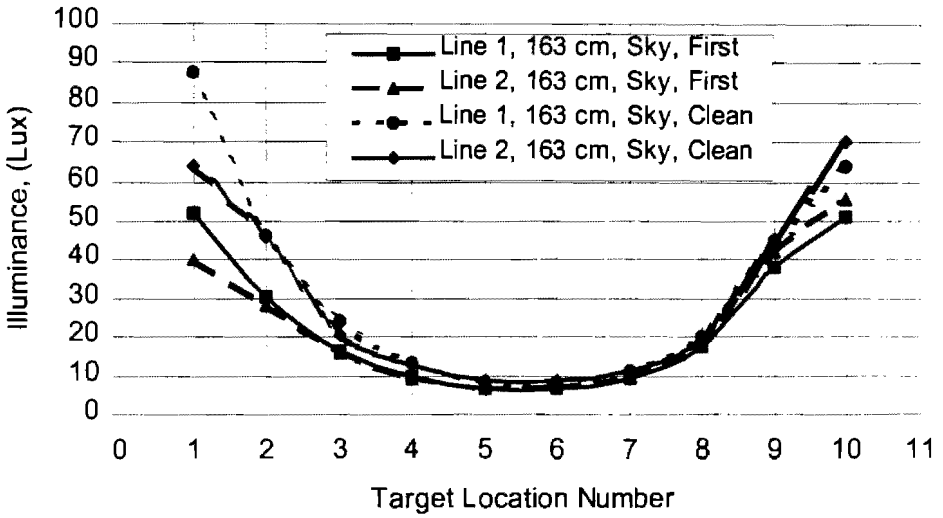

Figure 6.80 Illuminance distribution from sky direction at 163 cm height above the roadway surface on lines 1 and 2.

CHAPTER 7: LUMINANCE, ILLUMINANCE AND STV CALCULATIONS

Illuminance and luminance calculations are performed using GE program that is called ALADAN. The program is downloaded from GE web page and the following data are entered to the program to obtain luminance and illuminance distribution between the installations.

Pole Configuration :	Left Side Only
Mounting Height:	31
Lane Width:	12
Lane Quantity:	1
Curb overhang:	0
Luminaires/Pole:	1
Luminaire Tilt:	0
Photometric ID:	7318
Initial Lumen:	27500
Light Loss factor:	1.0
Linear units:	Ft
Light units:	FC
Calculation Type:	IES
Output:	Illuminance or Luminance
Pavement R:	R1 through R4
Spacing to be:	Fixed at 147

X Coord	Y Start	Spacing	Qty
0	7.35	14.7	10

	Start	Incr	Qty
X	3	6	2
Y	7.35	14.7	10

After entering all the above data which specifies our experimental field properties click the calculation button to calculate the luminance or the illuminance output in two forms: graphical and table.

Luminance Calculation

The Aladan program is used to calculate luminance distribution with respect to pavement type R1, R2, R3 and R4.

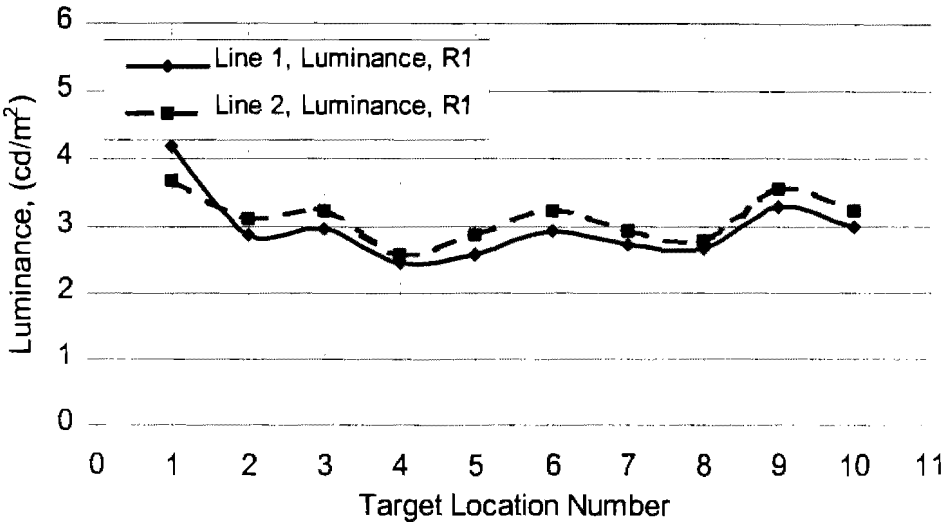

Figure 7.1 Luminance distribution for R1 type of pavement on lines 1 and 2.

As seen from Figure 7.1, luminance distribution starts with high value at the first target location then it reduces to value 2.5 at the fourth target location and is almost stays constant until tenth target location on line 1. Luminance distribution on line 2 is similar to the line 1 but the values slightly less that line 1 because target locations on the line 2 are farther than the target locations on the line 1 and also the photometric data distribution is effect. The Aladan program also calculates the following values for R1 pavement:

Average luminance (cd/m^2):	3.04,
Minimum luminance (cd/m^2):	2.45,
Maximum luminance (cd/m^2):	4.19,
Uniformity (overall average/minimum):	1.24,
Uniformity (overall maximum/minimum):	1.71,
Coefficient of variance:	0.14,
Maximum gradient (parallel to axis):	1.46.

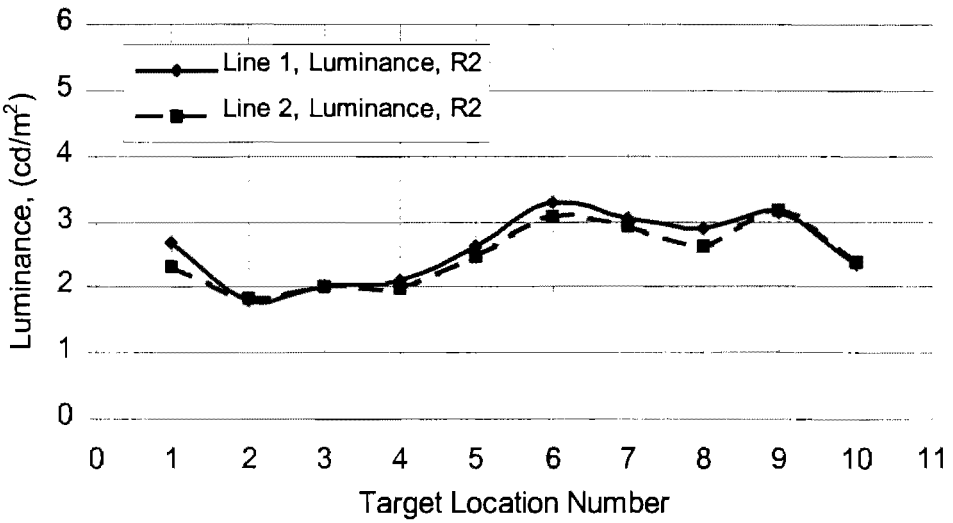

Figure 7.2 Luminance distribution for R2 type of pavement on lines 1 and 2.

Figure 7.2 shows the luminance distribution for R2 pavement on lines 1 and 2. The luminance values between the installation starts with high value at the first target location then it reduces to value 1.81 at the second target location and than it increase to the value 3.28 and reduces to the value 2.35 at the tenth target location. Luminance distribution on line 2 is similar to the line 1 but the values slightly less that line 1. The Aladan program also calculates the following values for R2 pavement:

Average luminance (cd/m^2):	2.54,
Minimum luminance (cd/m^2):	1.81,
Maximum luminance (cd/m^2):	3.28,
Uniformity (overall average/minimum):	1.40,
Uniformity (overall maximum/minimum):	1.81,
Coefficient of variance:	0.18,
Maximum gradient (parallel to axis):	1.48.

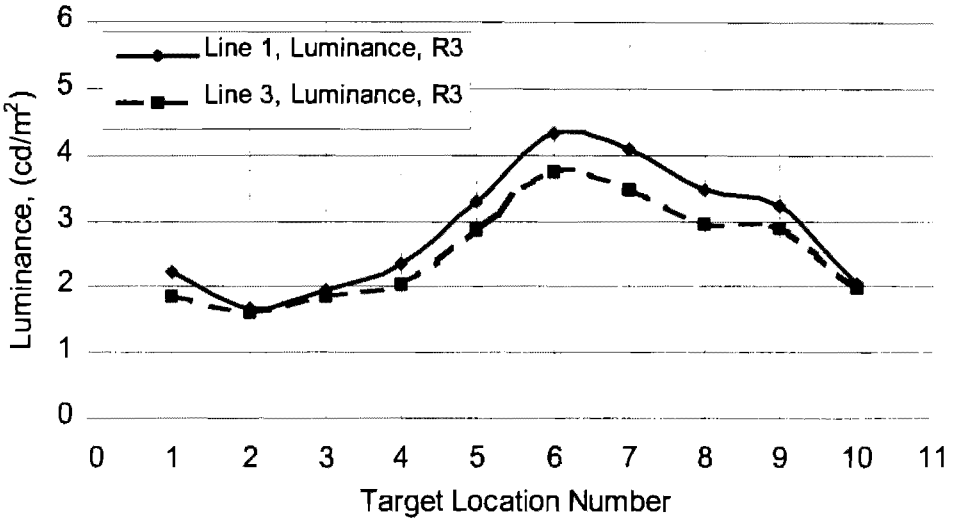

Figure 7.3 Luminance distribution for R3 type of pavement on lines 1 and 2.

Figure 7.3 shows the luminance distribution for R3 pavement on lines 1 and 2. The luminance values between the installation starts with the value 2.0 at the first target location then it reduces to the value 1.61 at the second target location and than it increase to the value 4.33 at the sixth target location and it reduces to the value 2.0 at the tenth target location. Luminance distribution on line 2 is similar to the line 1 but the values slightly less that line 1. The Aladan program also calculates the following values for R3 pavement:

Average luminance (cd/m^2):	2.69,
Minimum luminance (cd/m^2):	1.61,
Maximum luminance (cd/m^2):	4.33,
Uniformity (overall average/minimum):	1.68,
Uniformity (overall maximum/minimum):	2.70,
Coefficient of variance:	0.31,
Maximum gradient (parallel to axis):	1.58.

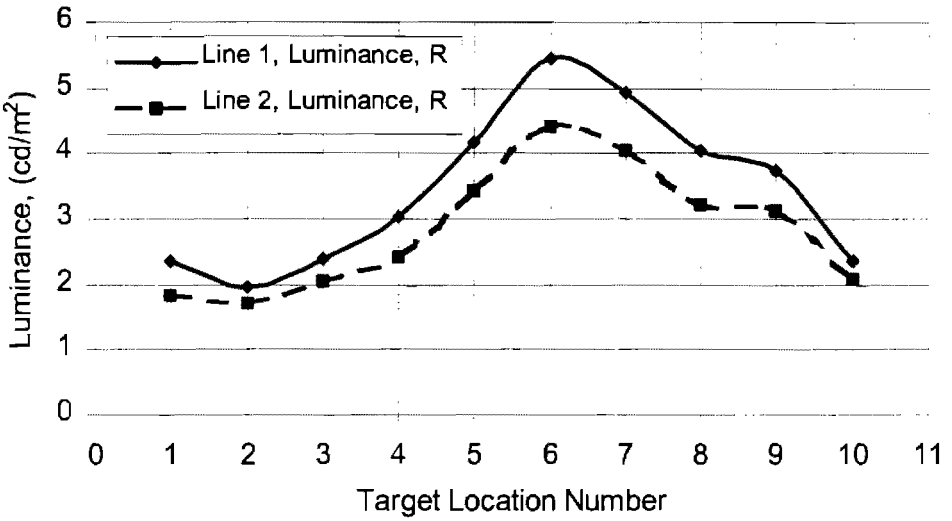

Figure 7.4 Luminance distribution for R4 type of pavement on lines 1 and 2.

Figure 7.4 shows the luminance distribution for R4 pavement on lines 1 and 2. The luminance values between the installation starts with the value 2.35 at the first target location then it reduces to the value 1.70 at the second target location and than it increase to the value 5.44 at the sixth target location and it reduces to the value 2.25 at the tenth target location. Luminance distribution on line 2 is similar to the line 1 but the values slightly less that line 1. The Aladan program also calculates the following values for R4 pavement:

Average luminance (cd/m^2):	3.14,
Minimum luminance (cd/m^2):	1.70,
Maximum luminance (cd/m^2):	5.44,
Uniformity (overall average/minimum):	1.84,
Uniformity (overall maximum/minimum):	3.19,
Coefficient of variance:	0.34,
Maximum gradient (parallel to axis):	1.59.

Luminance Comparison

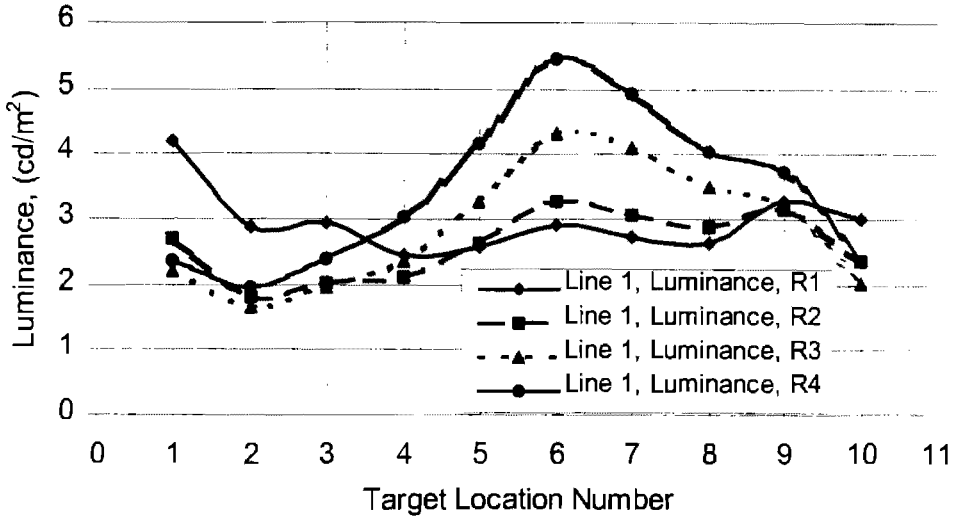

Figure 7.5 Luminance distribution for R1, R2, R3 and R4 on the line 1.

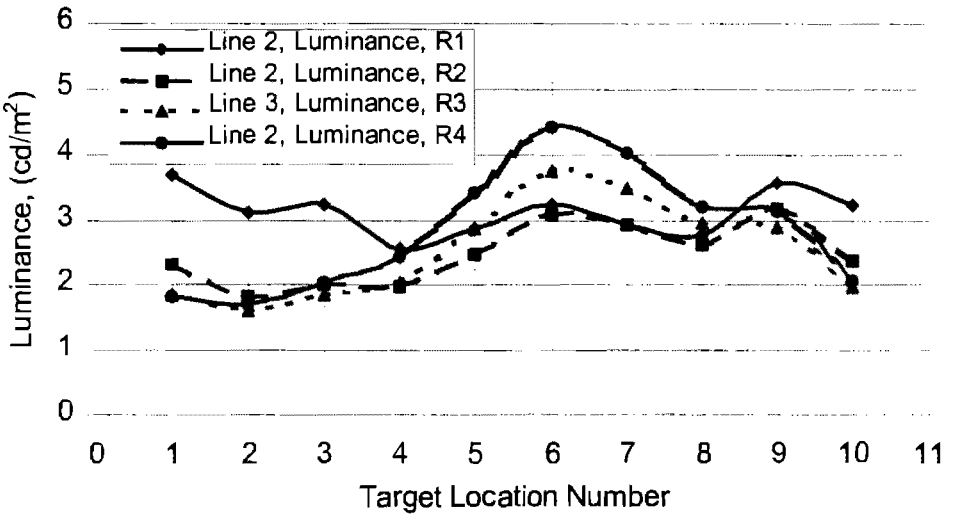

Figure 7.6 Luminance distribution for R1, R2, R3 and R4 on the line 2.

Figure 7.5 and 7.6 show the luminance distribution for R1, R2, R3 and R4 pavement on the lines 1 and 2, respectively. As seen from Figure 7.5, the best pavement is R4, R1 is the second good pavement, R3 is the third pavement and R2 is the worst pavement according to luminance distribution for the line 1. For line 2 (Figure 7.6), the best pavement is R1, R4 is the second good pavement, R3 is still the third pavement and R2 is still the worst pavement. Table 7.1 shows that the averege luminance values for both lines and overall average four pavements. According to the overall average numbers (Line 1+Line 2)/2), R4 is the best pavement, R1 is the second best pavement, R3 is the third pavement and R2 is the worst pavement to provide luminance.

Table 7.1 Arithmetic average of the luminance values

	R1	R2	R3	R4
Line 1	2.958	2.597	2.862	3.440
Line 2	3.116	2.483	2.527	2.831
Overall Average	3.04	2.54	2.69	3.14

Illuminance Calculation

Illuminance calculation is not depend on the pavement type, it is depend on luminaire and its mounted properties like, height of the pole, overhang, tilt, location, rotation, etc. Figure 7.7 shows illuminance distribution on the pavement between the installation for the GE7318 luminaire. As seen from the figure, calculated illuminance distribution by using Aladan software that is the same type of distribution with experimentally measured illuminance. Illuminance is maximum at locations that are close to luminaire and minimum at the middle of the installations.

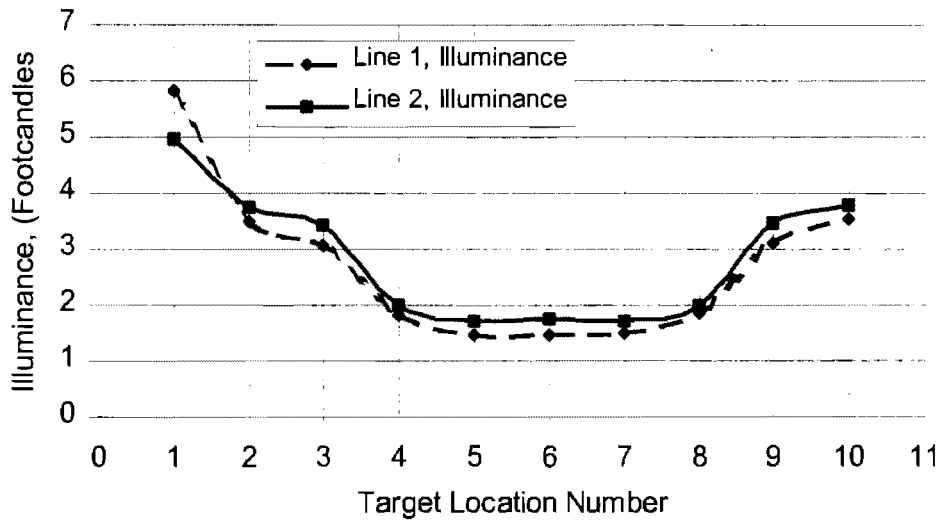

Figure 7.7 Illuminance distribution on the lines 1 and 2.

The program also calculates the following.

Average illuminance (Footcandles): 2.79,
Minimum illuminance (Footcandles): 1.47,
Maximum illuminance (Footcandles): 5.82,
Uniformity (overall average/minimum): 1.9,
Uniformity (overall maximum/minimum): 3.96,
Coefficient of variance: 0.44,
Maximum gradient (parallel to axis): 1.72.

STV Calculation

The first successful attempt at developing a visibility criteria was the visibility index (*VI*) introduced in 1970 by Gallagher' which was base upon the research of Blackwell. Gallagher et al. used the bottom portion of an 18 inch traffic cone which was six percent gray or twenty nine percent white reflectant and established the fact that the calculated visibility of an object was a very good prediction of the distance at which the drivers detected this target. Later in 1977, a study by Janoff showed that the *VI* was a better predictor of night time accident rates than was any of the other photometric measures that they evaluated .

In 1989, Adrian from the University of Waterloo, Canada offered a new visibility matrix based upon the works of Blackwell (1946), Aulthorn (1964) and his own. His visibility level (*VL*) was defined as simply the ratio of actual luminance to threshold luminance. The standard target proposed is known as *small target* and the concept is recognized as *Small Target Visibility* (*STV*). The *VL* can be determined using photometers to measure target luminance, pavement luminance and veiling luminance. A predictive computer program then becomes an important factor for a road lighting design. The most recent computer program available is *STV* by Keck (1990) that is being updated as required. A study was performed by Janoff (1993) to compare the target, pavement and veiling luminances, as well as *VL*s, to actually measured values. This experiment consisted of two different targets. Each target was 7 inch square, and one placed upstream of the closest luminance and one downstream. The targets consisted of three different reflectances: 5, 30 and 80 %. The results indicated that the predicted values did not match up with measured values. There were significant differences between the target, pavement and veiling luminances . However, Janoff concluded that, perhaps with an accurate r-table for the surfaces under study, accurate reflectance values for the targets, accurate candle power distribution (including depreciation factors) and some derived field factors to account for light reflected from the pavement onto the target, a higher degree of relationship can be derived between measured and predicted values.

In 1997, Adrian, Gibbons and Laura Thomas made an amendment in calculating *STV* and studied the influence of light reflected from the road surface on the target luminance. The reflected light from a total of seventy-two pavement sections was used for each target luminance calculation. Based on the calculation, it was decided that road sections further than 6 multiples of target size from the target need not to be included in the calculation because they contribute less than five percent of the total target luminance. As seen from the calculation the light reflected from the pavement to the target can contribute up to fifteen percent of the total target luminance. This amount will change the *VL* of the target and *VL* can be reduced as much as half the *VL* where no reflection for the pavement is considered.

The appropriate quantity and quality of fixed lighting should be designed to provide comfortable seeing for nighttime drivers. Since the purpose of a roadway lighting system is the improvement of nighttime visual tasks. Visual tasks can be specified in terms of quantities that are measurable in the object space. Some of these quantities are given as follows.

1. Luminance of the object.
2. Luminance of the background.
3. Contrast (calculates using item 1 and 2).

4. Size.
5. Time.
6. Temporal frequency characteristics.
7. Location relative to the line of sight.
8. Movement in the field of view.
9. Non-uniformities of luminance in the object and the background.

Visibility of any target is related to the above variables: additionally, cognitive factors such as attention, expectation and habituation will effect recognition of objects. The lighting designer directly considers first four variables that listed above. The designers assumed that both the object (target) and the background luminance are uniformly distributed, and the following assumptions were made.

Luminance. Increasing luminance increases visibility.
Contrast. Increasing contrast increases visibility. Given a dark object on a bright background or a bright object on a dark background, seeing improves.
Size. Increasing visual size of any object increases visibility.
Time. Given the more time to see a target, likelihood of target acquisition becomes better.

An object may be seen because it differs either in luminance or in color: that is, there may be either a luminance (brightness) contrast or a chromatic contrast. Both types of contrast depend on the reflectance properties of the scene and of the incident illumination and the illumination level. In this report, luminance contrast (contrast) will be considered.

Contrast, or more accurately luminance contrast, between an object and its adjacent background is defined in several ways (IES Lighting Handbook, Reference Volume, Section 3, 1981).

$$C = \frac{L_d - L_b}{L_b} \tag{7.1}$$

or

$$C = \frac{L_g - L_t}{L_t} \tag{7.2}$$

$$C_{mod} = \frac{L_{max} - L_{min}}{L_{max} + L_{min}} \tag{7.3}$$

Where, C = Contrast
C_{mod} = Contrast modulation
L_d = Luminance of the detail
L_b = Luminance of the background
L_g = The greater luminance
L_t = The lesser luminance.
L_{max} = The maximum luminance
L_{min} = The minimum luminance.

Equation (7.1) produces positive and negative contrast values $(-1 < C < \infty)$ that are related to luminance values of an object luminance and its adjacent background luminance. If objects are darker than their background, contrast range is between –1 and 0. If objects are brighter than their background, contrast range is between 0 and ∞.

Equation (7.2) always produces positive contrast values $(0 \le C < 1)$ because the equation considers subtracting smaller luminance value from the greatest luminance value weather objects is darker or brighter than their backgrounds.

Equation (7.3) is a alternative to Equations (7.1) and (7.2) which is often called contrast but it usually, and more properly, called contrast modulation. It applies to periodic patterns. The equation also produces contrast modulation numbers between 0 and 1 $(0 \le C_{mod1} < 1)$. C_{mod1} does not track negative contrast with respect to detail of interest. If contrast modulation value is 0.8 (high contrast), it means such objects are well visible. If contrast modulation value is less than 0.2 (low contrast), it means such objects are barely visible (ref book).

In general, Equation (4.1) consider negative contrast but it does not consider positive contras at the same scale with negative contrast. Equation (7.2) and (7.3) just consider positive contrast. In that purpose, Equation (7.3) can slightly be modified then negative values of contrast modulation can easily be discussed.

$$C_{mod2} = \frac{L_d - L_b}{L_d + L_b} \tag{7.4}$$

Now as the background and the detail invert we see C_{mod2} go from positive values to negative values with well-defined limits, $-1 \le C_{mod2} \le 1$.

STV Calculation Method

In the draft RP-8 (1998), the concept of *Small Target Visibility* (*STV*) has been proposed for roadway lighting design. This came from the assumption that only pavement luminance is not sufficient to see an object. It is necessary to have a difference in luminance of object and background for the object to be visible. This difference in luminance has to be above a certain minimum value for visibility. This difference with respect to a threshold luminance value is termed *Visibility Level* (*VL*). Threshold VL values has been excepted by IES Committee, and published in RP_8 as seen in Table 3. *VL* is one of the metrics for *STV*. In the draft RP-8 (1998), recommended design criteria for high-speed roadways is based on luminance.

Theoretical STV calculation has been obtained for a specific lighting situation using the *Keck* software and following the methodology is published in the RP-8. The program (Keck program) calculates theoretical visibility level distribution between the luminaires by assuming ideal conditions on the roadway. For visibility level calculation, only fixed roadway lighting luminaires are considered for the purpose of providing roadway and pedestrian lighting in the calculations (Figure 7.8). For a roadway lighting installation meets the criteria of RP-8, and the following conditions are assumed and published in RP-8.

1. The observer is located on a line parallel to the centerline of the roadway that passes through the calculation points.
2. The observer located on the line at the distance 83.07 meters from the point.
3. With a 1° downward view from the horizontal, as the defined observation geometry, the fixation line meets the road at 83.07 meters at 1.45 meters eye position from the road.
4. The point's luminance on the pavement is assumed, and the target's luminance is assumed. The target is located at the intersection of two grid lines as seen in Figure 4.9.
5. The pavement is assumed level and the surface is assumed uniform and homogeneous.
6. The target's surface is assumed to be perfectly diffuse, vertical and perpendicular to a line from the observer to the grid point, and the light is reflect in a Lambertian manner (Figure 4.10).
7. The pavement surface is assumed to be smooth, dry and to have directional light reflectance characteristics, which are expressed in terms of a reduced luminance coefficient.
8. Only fixed lighting luminaires installed for the purpose of providing roadway and pedestrian lighting are considered in the calculations.
9. The distribution of those luminaires is assumed to be representing by a table of luminous intensities.

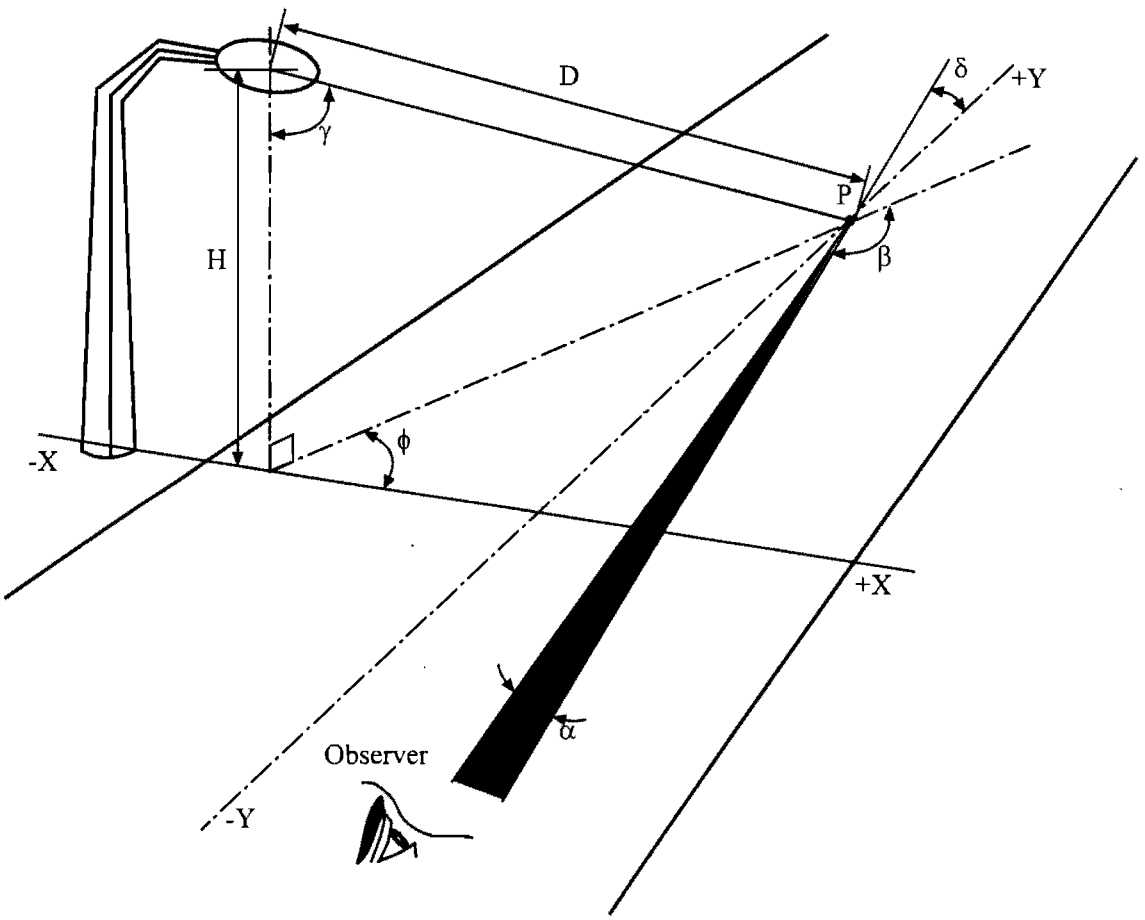

Figure 7.8 Single luminaire.

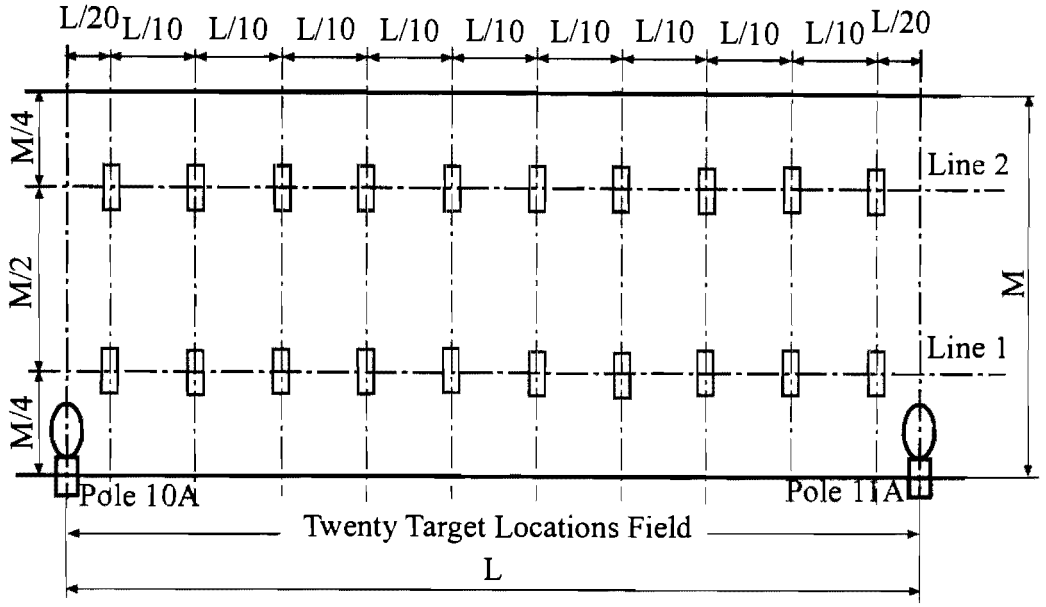

Figure 7.9 Target location orientation between the installation.

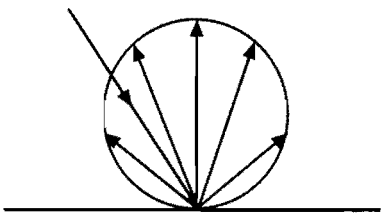

Figure 7.10 Perfectly diffuse reflection.

The above assumptions define the observer location with respect to the calculated point, object (target) and pavement reflection types, object and pavement luminance calculations, and pavement geometric and structural properties. The accuracy of calculations for pavement luminance, and STV not only depends on the above assumptions, but also depends upon the following conditions.

1. The lighting design calculation must include a Light Loss Factor (LLF).
2. Whether or not the photometric data used to determine the candlepower intensity at a particular angle correctly represents the output of the lamp and luminaire.
3. Whether or not the directional reflectance tables (r-tables) provides accurately directional reflectance coefficients of the actual surface.

The visibility level formula is defined in RP-8 and elsewhere, as shown in the following equations.

$$VL = \frac{L_t - L_b}{DL_4} \tag{7.5}$$

$$VL = \frac{L_t - L_b}{L_b} \times \frac{L_b}{DL_4} \tag{7.6}$$

where $C = \frac{L_t - L_b}{L_b}$ was defined as a contrast or visibility, then Equation (4.6) yields

$$VL = C \times \frac{L_b}{DL_4} \tag{7.7}$$

RP-8 uses Equation (7.5) to calculate *VL* distribution between the installation.

Illuminance Calculations Methods

Illuminance is the measure of the amount of light flux falling on a surface. It is independent of the direction from which the light comes, the type of light source and the type of surface upon which it falls. Mathematically, illuminance may be defined as the luminous flux density per unit area at a point on a surface.

$$E_h = \frac{d\varphi}{dA}, \tag{7.8}$$

Where, E_h = Horizontal illuminance from one individual luminaire
φ = Radiant flux
A = Lighted area.

If the luminous intensity ($I(\phi,\gamma)$) of a light source is known, the horizontal illuminance (E_h) at a distance D is given by:.

$$E_h = \frac{I(\phi,\gamma) \times Cos(\gamma) \times LLF}{D^2} \tag{7.9}$$

Where, I : Intensity at angle γ and ϕ
D : Distance between the luminaire and calculated point
LLF : Light loss factor.

$$D = \frac{H}{Cos(\gamma)} \tag{7.10}$$

Where, H = Luminaire mounting height above the pavement surface.
Finally, substituting Equation (7.10) into the equation (7.9) the horizontal illuminance yields

$$E_h = \frac{I(\phi,\gamma) \times Cos^3(\gamma) \times LLF}{H^2}. \tag{7.11}$$

The total horizontal illuminance is the sum of the values calculated for all contributing luminaires then the Equation (7.11) yields

$$E_h = \sum_{i=1}^{n} \frac{I_i(\phi_i, \gamma_i) \times Cos^3(\gamma_i) \times LLF_i}{H_i^2}. \qquad (7.12)$$

Recommended average maintained roadway illuminances are given in table 7.2 with respect to roadway and pavement classifications (RP-8).

Table 7.2 Recommended average maintained roadway illuminances (IES Roadway Lighting committee; Proposed American Standard Practice for Roadway Lighting).

Roadway Classification	Area Classification	Pavement Classification, Lux (Footcandles)		
		R1	R2, R3	R4
Freeway	Commercial	6 (0.6)	9 (0.8)	8 (0.7)
	Intermediate	4 (0.4)	6 (0.6)	5 (0.5)
	Residential			
Expressway	Commercial	10 (0.9)	14 (1.3)	13 (1.2)
	Intermediate	8 (0.7)	12 (1.1)	10 (0.9)
	Residential	6 (0.6)	9 (0.8)	8 (0.7)
Major	Commercial	12 (1.1)	17 (1.6)	15 (1.4)
	Intermediate	9 (0.8)	13 (1.2)	11 (1.0)
	Residential	6 (0.6)	9 (0.8)	8 (0.7)
Collector	Commercial	8 (0.7)	12 (1.1)	10 (0.9)
	Intermediate	6 (0.6)	9 (0.8)	8 (0.7)
	Residential	6 (0.6)	6 (0.6)	5 (0.5)
Local	Commercial	6 (0.6)	9 (0.8)	8 (0.7)
	Intermediate	5 (0.5)	7 (0.7)	6 (0.6)
	Residential	3 (0.3)	4 (0.4)	4 (0.4)

Pavement Luminance Calculation Method

Though the design of roadway lighting initiated with the criteria based on horizontal illumination, it was soon realized that pavement luminance and veiling luminance criteria provide a better correlation with the visual impression of roadway lighting quality. Because what we see is not due to the amount of light emitted from the source, but the amount of light that is reflected from the pavement surface. From mathematical point of view, luminance flux density per steradian emitted (reflected/ transmitted) a unit defines area of surface in the direction of the observer as Luminance.

Luminance is the measure of the amount and concentration of light flux leaving a surface. The luminance of a surface depends on the direction from which the light strikes the surface, the direction from which the surface is viewed and the reflective properties of the surface. The source of radiation is not an issue and it is the luminance the producer of light intensity and reflectivity that controls the magnitude of the sensation that is received by the brain.

Luminance at a point P (Figure 7.8) is proportional to the horizontal illumination at that point.

$$L_b \propto E_h \tag{7.13}$$

Where, L_b = Pavement luminance from one individual luminaire at point P.

To equate the relationship a proportionality factor $r(\beta,\gamma)$ which is called directional reflectance coefficient is introduced.

$$L_b = \frac{r(\beta,\gamma)}{MF} \times E_h \tag{7.14}$$

Where, r = Reduced coefficient of reflectance at angles γ and β.
MF = Multiplying factor used by the r-table (often 10,000)

Substituting Equation (7.11) into the Equation (7.14) and multiply with $(1/\pi)$ to obtain SI units (Lb = cd/m^2 and I = cd), the equation (7.14) yields

$$L_b = \frac{1}{\pi} \times \left(\frac{r(\beta,\gamma) \times I(\phi,\gamma) \times Cos^3(\gamma) \times LLF}{MF \times H^2} \right). \tag{7.15}$$

The total luminance is the sum of the values calculated for all contributing luminaires then the Equation (7.15) yields

$$L_b = \frac{1}{\pi} \times \left(\sum_{i=1}^{n} \frac{r_i(\beta_i,\gamma_i) \times I_i(\phi_i,\gamma_i) \times Cos^3(\gamma_i) \times LLF_i}{MF \times H_i^2} \right). \tag{7.16}$$

Recommended maintained roadway luminances are given in table 4.3 with respect to roadway classifications (RP-8).

Table 7.3 Recommended maintained roadway luminance (IES Roadway Lighting committee; Proposed American Standard Practice for Roadway Lighting).

Roadway Classification	Area Classification	Cd/m^2	$\frac{L_{avg}}{L_{min}}$	$\frac{L_{max}}{L_{min}}$	$\frac{L_v}{L_{avg}}$
Freeway	Commercial	0.6	3.5	6.0	0.3
	Intermediate	0.4	3.5	6.0	0.3
	Residential	–	–	–	–
Expressway	Commercial	1.0	3.0	5.0	0.3
	Intermediate	0.8	3.0	5.0	0.3
	Residential	0.6	3.5	6.0	0.3
Major	Commercial	1.2	3.0	5.0	0.3
	Intermediate	0.9	3.0	5.0	0.3
	Residential	0.6	3.5	6.0	0.3
Collector	Commercial	0.8	3.0	5.0	0.4
	Intermediate	0.6	3.5	6.0	0.4
	Residential	0.4	4.0	8.0	0.4
Local	Commercial	0.6	6.0	10.0	0.4
	Intermediate	0.5	6.0	10.0	0.4
	Residential	0.3	6.0	10.0	0.4

Target Luminance Calculation Method

Luminance of a target is a function of the vertical illuminance (E_v) from the luminaire in the layout directed toward the target and the directional reflectance of the target (r_t) toward the observer (Figure 7.8). Figure 7.8 shows angular relationships between the luminaire, the surface of a vertical target and the observer. The reflectance of the target surface is assumed to be diffuse (Lambertian) for target luminance calculation.

$$L_t = E_v \times r_t \times Sin(\phi), \tag{7.17}$$

Where, L_t = Target luminance

E_v = Vertical illuminance at point P

r_t = Target reflection factor $r_t = R_c \times Cos(1^\circ)$

R_c = Surface reflection coefficient of a target (for 20%reflective surface R_c=0.2 and for 20% reflective surface R_c = 0.2).

$$E_v = \frac{I(\phi,\gamma) \times Sin(\gamma) \times LLF}{D^2} \tag{7.18}$$

$$D = \frac{(H - 0.5 \times TH)}{Cos(\gamma)} \tag{7.19}$$

Where, TH = Target height

0.5 = Diffuse reflectance factor.

Substituting Equation (7.18) and (7.19) into the Equation (7.17) and multiply with (1/π) to obtain SI unit, then the equation (7.10) yields

$$L_t = \frac{1}{\pi} \times \left(\frac{I(\phi,\gamma) \times Sin(\gamma) \times Sin(\phi) \times Cos^2(\gamma) \times r_t \times LLF}{(H - 0.5 \times TH)^2} \right) \qquad (7.20)$$

Substituting r_t into the Equation (4.20), final equation yields

$$L_t = \frac{1}{\pi} \times \left(\frac{I(\phi,\gamma) \times Sin(\gamma) \times Sin(\phi) \times Cos^2(\gamma) \times R_c \times Cos(1^0) \times LLF}{(H - 0.5 \times TH)^2} \right) \qquad (7.21)$$

The total luminance from the target surface is the sum of the values calculated for all contributing luminaires then the Equation (4.21) yields

$$L_t = \frac{1}{\pi} \times \sum_{i=1}^{n} \left(\frac{I_i(\phi_i,\gamma_i) \times Sin(\gamma_i) \times Sin(\phi_i) \times Cos^2(\gamma_i) \times R_c \times Cos(1^0) \times LLF}{(H_i - 0.5 \times TH)^2} \right) \qquad (7.22)$$

The Roadway reflectance (r-Tables)

CIE (Commission Internationale de I' Eclairage) is the recognized international organization in the field of roadway lighting. CIE successfully introduced roadway classification systems for dry pavements to facilitate luminance calculations at the design stage.

De Boer and Vermeulen developed the R-system to classify roadway surfaces (pavements) in 1967. It comprises four classes of pavements RI, RII, RIII and RIV, and their corresponding standard *r*- tables R1, R2, R3 and R4. *r*-tables include *r* values (directional reflection coefficients) with respect to β and γ angles. Here the observer looks along the Y-axis (Figure 7.8), while the light source is at an angle β with Y-axis at the origin. The *r*-values are symmetrical about the X-axis. Getting the value of $r(\beta,\gamma)$ for a particular point from the *r*-table on the pavement surface and the corresponding I-value from the photometric data one can readily calculate the pavement luminance at a point. The r-tables are used directly in the calculation of STV for background luminance but target luminance appears to come exclusively from the light source with no contribution from the pavement luminance.

Table 7.4 *r*-table of *r* values for standard *R1* type of pavement (All values have been multiplied by 10,000).

δ tan Y	0	2	5	10	15	20	25	30	35	40	45	60	75	90	105	120	135	150	165	180
0.00	655	655	655	655	655	655	655	655	655	655	655	655	655	655	655	655	655	655	655	655
0.25	619	619	619	619	610	610	610	610	610	610	610	610	610	601	601	601	601	601	601	601
0.50	539	539	539	539	539	539	521	521	521	521	521	503	503	503	503	503	503	503	503	503
0.75	431	431	431	431	431	431	431	431	431	431	395	386	371	371	371	371	371	386	395	395
1.00	341	341	341	341	323	323	305	296	287	287	278	269	269	269	269	269	269	278	278	278
1.25	224	224	224	215	198	180	171	162	153	148	144	144	139	139	139	144	148	153	162	180
1.75	189	189	189	171	153	139	130	121	117	112	108	103	99	99	103	108	112	121	130	139
2.00	162	162	157	135	117	108	99	94	90	85	85	83	84	84	86	90	94	99	103	111
2.50	121	121	117	95	79	66	60	57	54	52	51	50	51	52	54	58	61	65	69	75
3.00	94	94	86	66	49	41	38	36	34	33	32	31	31	33	35	38	40	43	47	51
3.50	81	80	66	46	33	28	25	23	22	22	21	21	22	22	24	27	29	31	34	38
4.00	71	69	55	32	23	20	18	16	15	14	14	14	15	17	19	20	22	23	25	27
4.5	63	59	43	24	17	14	13	12	12	11	11	11	12	13	14	14	16	17	19	21
5.00	57	52	36	19	14	12	10	9.0	9.0	8.8	8.7	8.7	9.0	10	11	13	14	15	16	16
5.50	51	47	31	15	11	9.0	8.1	7.8	7.7	7.7										
6.00	47	42	25	12	8.5	7.2	6.5	6.3	6.2											
6.50	43	38	22	10	6.7	5.8	5.2	5.0												
7.00	40	34	18	8.1	5.6	4.8	4.4	4.2												
7.50	37	31	15	6.9	4.7	4.0	3.8													
8.00	35	28	14	5.7	4.0	3.6	3.2													
8.50	33	25	12	4.8	3.6	3.1	2.9													
9.00	31	23	10	4.1	3.2	2.8														
9.50	30	22	9.0	3.7	2.8	2.5														
10.0	29	20	8.2	3.2	2.4	2.2														
10.5	28	18	7.3	3.0	2.2	1.9														
11.0	27	16	6.6	2.7	1.9	1.7														
11.5	26	15	6.1	2.4	1.7															
12.0	25	14	5.6	2.2	1,6															

Q0 = 0.10: S1 = 0.25: S2 = 1.53

Table 7.5 *r*-table of *r* values for standard *R2* type of pavement (All values have been multiplied by 10,000).

δ tan Y	0	2	5	10	15	20	25	30	35	40	45	60	75	90	105	120	135	150	165	180
0.00	390	390	390	390	390	390	390	390	390	390	390	390	390	390	390	390	390	390	390	390
0.25	411	411	411	411	411	411	411	411	411	411	379	368	357	357	346	346	346	335	335	335
0.50	411	411	411	411	403	403	384	379	370	346	325	303	281	281	271	271	271	260	260	260
0.75	379	379	379	368	357	346	325	303	281	260	238	216	206	206	206	206	206	206	206	206
1.00	335	335	335	325	292	291	260	238	216	195	173	152	152	152	152	152	141	141	141	141
1.25	303	303	292	271	238	206	184	152	130	119	108	100	103	106	108	108	114	114	119	119
1.50	271	271	260	227	179	152	141	119	108	93	80	76	76	80	84	87	89	91	93	95
1.75	249	238	227	195	152	124	106	91	78	67	61	52	54	58	63	67	69	71	73	74
2.00	227	216	195	152	117	95	80	67	61	52	45	40	41	45	49	52	54	56	57	58
2.50	195	190	146	110	74	58	48	40	35	30	27	24	26	28	30	33	35	38	40	41
3.00	160	155	115	67	43	33	26	21	18	17	16	16	17	17	18	21	22	24	26	27
3.50	146	131	87	41	25	18	15	13	12	11	11	11	11	11	12	14	15	17	18	21
4.00	132	113	67	27	15	12	10	9.4	8.7	8.2	7.9	7.6	7.9	8.7	9.6	11	12	13	15	17
4.50	118	95	50	20	12	8.9	7.4	6.6	6.3	6.1	5.7	5.6	5.8	6.3	7.1	8.4	10	12	13	14
5.00	106	81	38	14	8.2	6.3	5.4	5.0	4.8	4.7	4.5	4.4	4.8	5.2	6.2	7.4	8.5	9.5	10	11
5.50	96	69	29	11	6.3	5.1	4.4	4.1	3.9	3.8										
6.00	87	58	22	8.0	5.0	3.9	3.5	3.4	3.2											
6.50	78	50	17	6.1	3.8	3.1	2.8	2.7												
7.00	71	43	14	4.9	3.1	2.5	2.3	2.2												
7.50	67	38	12	4.1	2.6	2.1	1.9													
8.00	63	33	10	3.4	2.2	1.8	1.7													
8.50	58	28	8.7	2.9	1.9	1.6	1.5													
9.00	55	25	7.4	2.5	1.7	1.4														
9.50	62	23	6.5	2.2	1.5	1.3														
10.0	49	21	5.6	1.9	1.4	1.2														
10.5	47	18	5.0	1.7	1.3	1.2														
11.0	44	16	4.4	1.6	1.2	1.1														
11.5	42	14	4.0	1.5	1.1															
12.0	41	13	3.6	1.4	1.1															

Q0 = 0.07; S1 = 0.58; S2 = 1.80

Table 7.6 *r*-table of *r* values for standard *R3* type of pavement (All values have been multiplied by 10,000).

6 tan Y	0	2	5	10	15	20	25	30	35	40	45	60	75	90	105	120	135	150	165	180
0.00	294	294	294	294	294	294	294	294	294	294	294	294	294	294	294	294	294	294	294	294
0.25	326	326	321	321	317	312	308	308	303	298	294	280	271	262	258	253	249	244	240	240
0.50	344	344	339	339	326	317	308	298	289	276	262	235	217	204	199	199	199	199	194	194
0.75	357	353	353	339	321	303	285	267	244	222	204	176	158	149	149	149	145	136	136	140
1.00	362	362	352	326	276	249	226	204	181	158	140	118	104	100	100	100	100	100	100	100
1.25	357	357	348	298	244	208	176	154	136	118	104	83	73	70	71	74	77	77	77	78
1.50	353	348	326	267	217	176	145	117	100	86	78	72	60	57	58	60	60	60	61	62
1.75	339	335	303	231	172	127	104	89	79	70	62	51	45	44	45	46	45	45	46	47
2.00	326	321	280	190	136	100	82	71	62	54	48	39	34	34	34	35	36	36	37	38
2.50	289	280	222	127	86	65	54	44	38	34	25	23	22	23	24	24	24	24	24	25
3.00	253	235	163	85	53	38	31	25	23	20	18	15	15	14	15	15	16	16	17	17
3.50	217	194	122	60	35	25	22	19	16	15	13	9.9	9.0	9.0	9.9	11	11	12	12	13
4.00	190	163	90	43	26	20	16	14	12	9.9	9.0	7.4	7.0	7.1	7.5	8.3	8.7	9.0	9.0	9.9
4.50	163	136	73	31	20	15	12	9.9	9.0	8.3	7.7	5.4	4.8	4.9	5.4	6.1	7.0	7.7	8.3	8.5
5.00	145	109	60	24	16	12	9.0	8.2	7.7	6.8	6.1	4.3	3.2	3.3	3.7	4.3	5.2	6.5	6.9	7.1
5.50	127	94	47	18	14	9.9	7.7	6.9	6.1	5.7										
6.00	113	77	36	15	11	9.0	8.0	6.5	5.1											
6.50	104	68	30	11	8.3	6.4	5.1	4.3												
7.00	95	60	24	8.5	6.4	5.1	4.3	3.4												
7.50	87	53	21	7.1	5.3	4.4	3.6													
8.00	83	47	17	6.1	4.4	3.6	3.1				Q0 = 0.07: S 1 = 1. 11: S2 = 2.38									
8.50	78	42	15	5.2	3.7	3.1	2.6													
9.00	73	38	12	4.3	3.2	2.4														
9.50	69	34	9.9	3.8	3.5	2.2														
10.0	65	32	9.0	3.3	2.4	2.0														
10.5	62	29	8.0	3.0	2.1	1.9														
11.0	59	26	7.1	2.6	1.9	1.8														
11.5	56	24	6.3	2.4	1.8															
12.0	53	22	5.6	2.1	1.8															

Table 7.7 *r*-table of *r* values for standard *R4* type of pavement (All values have been multiplied by 10,000).

6 tan Y	0	2	5	10	15	20	25	30	35	40	45	60	75	90	105	120	135	150	165	180
0.00	264	264	264	264	264	264	264	264	264	264	264	264	264	264	264	264	264	264	264	264
0.25	297	317	317	317	317	310	304	290	284	277	271	244	231	224	224	218	218	211	211	211
0.50	330	343	343	343	330	310	297	284	277	264	251	218	198	185	178	172	172	165	165	165
0.75	376	383	370	350	330	304	277	251	231	211	198	165	139	132	132	125	125	125	119	119
1.00	396	396	396	330	290	251	216	198	185	165	145	112	86	86	86	86	86	87	87	87
1.25	403	409	370	310	251	211	178	152	132	115	103	77	66	65	65	63	65	66	67	68
1.50	409	396	356	284	218	172	139	115	100	88	79	61	50	50	50	50	52	55	55	55
1.75	409	396	343	251	178	139	108	88	75	66	59	44	37	37	37	38	40	41	42	45
2.00	409	383	317	224	145	106	86	71	59	53	45	33	29	29	29	30	32	33	34	37
2.50	396	356	264	152	100	73	55	45	37	32	28	21	20	20	20	21	22	24	25	26
3.00	370	304	211	95	63	44	30	25	21	17	16	13	12	12	13	13	15	16	17	19
3.50	343	271	165	63	40	26	19	15	13	12	11	9.8	9.1	8.8	8.8	9.4	11	12	13	15
4.00	317	238	132	45	24	16	13	11	9.6	9.0	8.4	7.5	7.4	7.4	7.5	7.9	8.6	9.4	11	12
4.50	297	211	106	33	17	11	9.2	7.9	7.3	6.6	6.3	6.1	6.1	6.2	6.5	6.7	7.1	7.7	8.7	9.6
5.00	277	185	79	24	13	8.3	7.0	6.3	5.7	5.1	5.0	5.0	5.1	5.4	5.5	5.8	6.1	6.3	6.9	7.7
5.50	257	161	59	19	9.9	7.1	5.7	5.0	4.6	4.2										
6.00	244	140	46	13	7.7	5.7	4.8	4.1	3.8											
6.50	231	122	37	11	5.9	4.6	3.7	3.2												
7.00	218	106	32	9.0	5.0	3.8	3.2	2.6												
7.50	205	94	26	7.5	4.4	3.3	2.8													
8.00	193	62	22	6.3	3.7	2.9	2.4													
8.50	184	74	19	5.3	3.2	2.5	2.1													
9.00	174	66	16	4.6	2.8	2.1														
9.50	169	59	13	4.1	2.5	2.0														
10.0	164	53	12	3.7	2.2	1.7														
10.5	158	49	11	3.3	2.1	1.7														
11.0	153	45	9.5	3.0	2.0	1.7														
11.5	149	41	8.4	2.6	1.7															
12.0	145	37	71	2.5	1.7															

Q0 = 0.08; S1 = 1.55; S2 = 3.03

Veiling Luminance Calculation Method

The luminaire used for roadway lighting emit light directly to the eye of the observer, and as a result produces a reduction in visual performance or a feeling of discomfort. This sensation produced by intense source luminance within the visual field that is sufficiently greater than reflected luminance, to which the eyes are adapted, is known as *glare*. Glare produces a veiling luminance (L_v) that is superimposed upon the retinal image of the object to be seen. This alters the apparent brightness of the object and the background against which it is viewed and causes a reduction in visual performance. L_v can be calculated by using the following empirical formula derived for one single luminaire.

$$L_v = \frac{K}{\theta^n} = \frac{10 \times E_v}{\theta^n} \qquad (7.23)$$

$$n = 2.3 - 0.7 \times Log_{10}(\theta) \quad \text{for} \quad \theta < 2$$

$$n = 2.0 \quad \text{for} \quad \theta \geq 2$$

Where, E_v = Vertical illuminance in the plane of the pupil of the observer's eye (Equation (7.18)).

θ = (See Figure 7.11).

Total veiling luminance is the sum of the veiling luminance of all of individual contributing luminaires. Then Equation (7.23) yields

$$L_v = \sum_{i=1}^{m} \frac{K_i}{(\theta^n)_i} = \sum_{i=1}^{m} \frac{10 \times (E_v)_i}{(\theta^n)_i} \qquad (7.24)$$

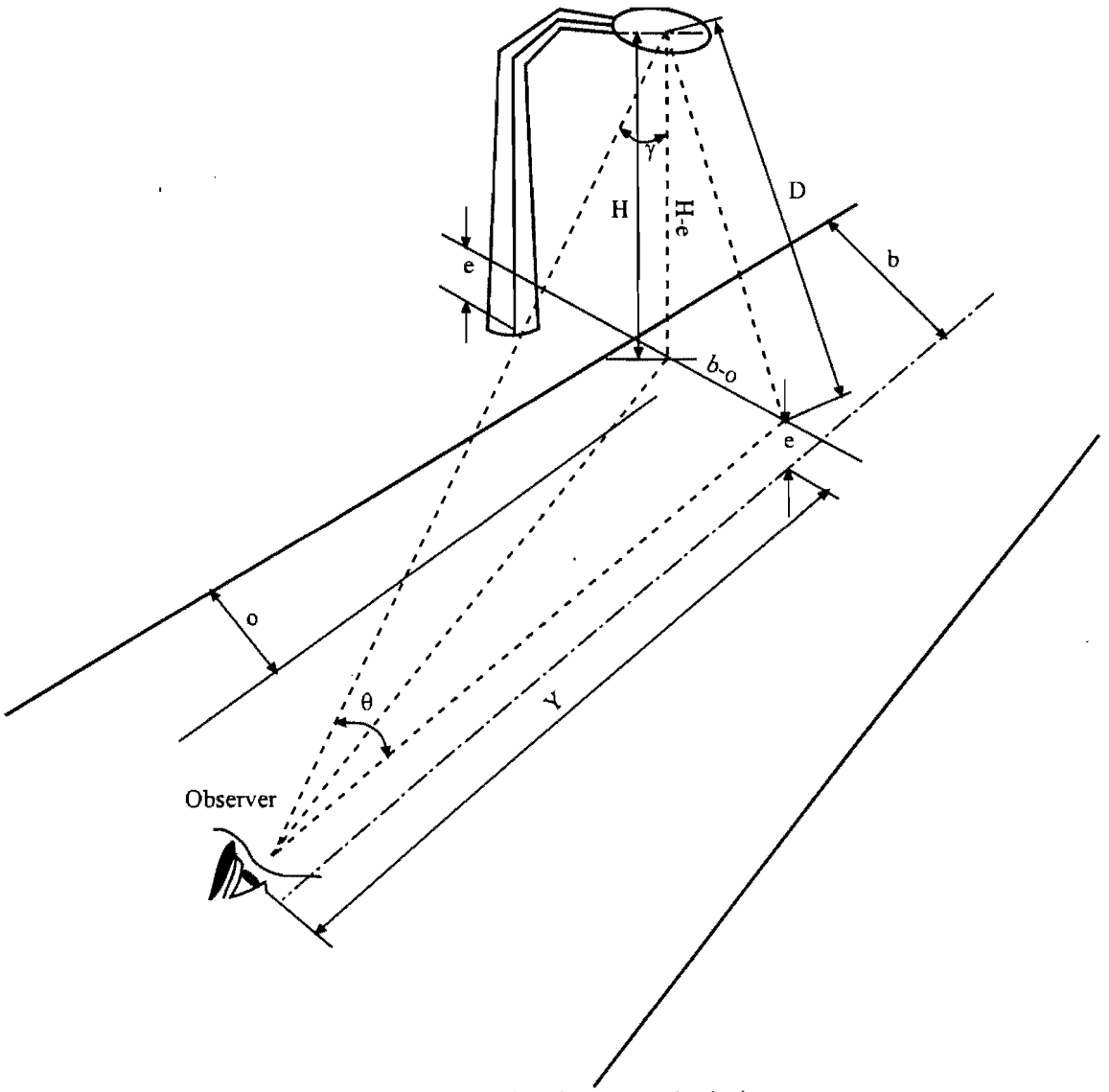

Figure 7.11 Angular relationship for veiling luminance calculation

$$D = \sqrt{(H-e)^2 + (b-o)^2}$$

Light Loss Factor

The photometric data that is used in calculating illumination or luminance is obtained under laboratory conditions. But in the field, the performance of the luminaires deteriorates. Therefore, a multiplying factor, known as Light Loss Factor (*LLF*), is used in lighting calculations. This *LLF* is composed of several separate factors, each of which is controlled and evaluated separately. Broadly *LLF* is divided into two categories. One is the *Maintenance Factor*, which is time dependent, and the other is the *Equipment Factor*, which does not depend on time. *Maintenance Factor* takes into account dirt accumulation on luminaire surface, lamp lumen depreciation and maintenance procedures. *Equipment Factor* relates mostly to the characteristics of the specific equipment selected. It takes into account factors such asambiant temperature, voltage fluctuation, ballast variation, change in physical surroundings and surface depreciation resulting from adverse changes in metal, paint and plastic components which produce reduced light output.

Small Target Visibility Calculation Steps

Contrast definition as given before is a combination of object and background luminances. The Small Target Visibility definition uses the contrast definitions, but STV always assumes targets (objects) are darker that their background and uses the following formula for visibility calculation.

$$C = \frac{L_t - L_b}{L_b} \tag{7.25}$$

If the visibility level is defined with the following formula

$$VL = \frac{L_t - L_b}{L_b} \times \frac{L_b}{DL_4} = C \times \frac{L_b}{DL_4} \tag{7.26}$$

Until this point, target luminance and background luminance calculation methods are given, then visibility of the target (object) can be able to calculate. At this calculation stage, calculation methods of target (Equation (7.21)) and background luminance (Equation (7.15)) already explained. Veiling luminance calculation method is also given.

Equation (7.26) shows that *VL* is a ratio with contrast, background luminance and DL_4. After this calculation stage, DL_4 calculation steps will be introduced step by step. All these steps will show what is the function of DL_4. Before starting to calculate DL_4, lets make some assumption as follows.

1. The observer is 60 years old with normal eyesight whose fixation time is 0.2 seconds.
2. The target is an 18x18 cm square flat surface perpendicular to both the road surface and the observer's line of sight.

3. The target reflects light in a Lambertian manner with a reflectance of 50%.

Step 1: Calculate adaptation luminance.

$$L_a = L_b + L_v$$
$$LL_a = Log_{10}(L_a)$$
$$A = \arctan\left(\frac{\text{Target size}}{\text{Distance observer to target}}\right) \times 60$$

Where, L_a = Adaptation luminance
A = Visual angle in minutes.

Step 2: Calculate the sensitivity of the visual system as a function of adaptation luminance.

$$L_a \geq 0.6 \quad \Rightarrow \quad \left\{\begin{array}{l} F = (Log_{10}(4.1925 \times L_a^{0.1556}) + (0.1684 \times L_a^{0.5867}))^2 \\ L = (0.05946 \times L_a^{0.466})^2 \end{array}\right\}$$

$$L_a > 0.00418 \text{ and } L_a < 0.6 \quad \Rightarrow \quad \left\{\begin{array}{l} F = 10^{(2\times((0.0866\times LL_a^2)+(0.3372\times LL_a)-0.072))} \\ L = 10^{(2\times((0.319\times LL_a)-1.256))} \end{array}\right\}$$

$$L_a \leq 0.00418 \quad \Rightarrow \quad \left\{\begin{array}{l} F = 10^{((0.346\times LL_a)+0.056)} \\ L = 10^{((0.0454\times LL_a^2)+(1.055\times LL_a)-1.782)} \end{array}\right\}$$

Step 3: Calculate some constant to obtain DL_1 using the following equations.

$$B = Log_{10}(A) + 0.523$$
$$C = Log_{10}(L_a) + 6.0$$
$$AA = 0.36 - \left(\frac{0.0972 \times B^2}{B^2 - 2.513 \times B + 2.789}\right)$$
$$AL = 0.355 - \left(\frac{0.1217 \times C^2}{C^2 - 10.4 \times C + 52.28}\right)$$

$$AZ = \frac{V \times (AA^2 + AL^2)}{2.1}$$
$$DL_1 = 2.6 \times \left(\frac{V \times F}{A} + V \times L\right)^2$$

Step 4: Calculate the M from the following one of three empiric equation. Then determine the value of a negative contrast adjustment factor (FCP). If LL_a is less than -2.4, FCP is not accurate.

$$LL_a > -2.4 \text{ and } LL_a < -1.0 \Rightarrow \left\{ M = 10^{(-10^{-(0.075\times((LL_a+1)^2)+0.0245)})} \right\}$$

$$LL_a \geq -1.0 \Rightarrow \left\{ M = 10^{(-10^{-(0.125\times((LL_a+1)^2)+0.0245)})} \right\}$$

$$LL_a \leq -2.4 \Rightarrow FCP = 0.5 \text{ (}TGB\text{ and }FCP\text{ need not be calculated)}$$

$$TGB = -0.6 \times L_a^{-0.1488}$$

$$FCP = 1.0 - \left(\frac{M \times A^{TGB}}{2.4 \times DL_1 \times \frac{AZ+2}{2}} \right)$$

Step 5: Adjust DL_1 in accordance with the observation time which is a constant, 0.2 seconds.

$$DL_2 = DL_1 \times \frac{AZ+T}{T}$$

Where, T = Observation time.

Step 6: Calculate the adjustment for the age of the observer and then adjust DL_2 accordingly. In the calculations the age is always 60 and therefore adjustment is always 1.

$$\text{Age} \leq 64 \Rightarrow FA = \frac{(TA-19)}{2160} + 0.99$$

$$\text{Age} > 64 \Rightarrow FA = \frac{(TA-56.5)}{116.3} + 1.43$$

$$DL_3 = DL_2 \times FA$$

Where, FA = Adjustment constant
TA = Observer age 60.

Step 7: Calculate the adjustment if the target is darker than the background (negative contrast).

$$L_t < L_b \Rightarrow DL_4 = DL_3 \times FCP$$

Otherwise $DL_4 = DL_3$

Step 8 (Final Step): Calculate Visibility Level (*VL*).

$$VL = \frac{L_t - L_b}{DL_4}$$

Summary of Data: Large *VL* values are not counted as heavily in the calculation of the summary values used in Table 7. In order to compensate for this saturation in recognition times (0.2 seconds). The calculated summary values are described as follow.

1. Negative VL values are converted to positive and calculate RWVL values.

$$RWVL = 10^{(-0.1 \times ABS(VL))}.$$

2. Average the *RWVL* values.
3. Convert the averaged *RWVL* values to weighted average *VL (WtAvgVL)*.

$$WtAvgVL = -10 \times Log_{10}(RWVL)$$

Table 7.8 Recommended maintained values of target VL

CLASIFICATION OF ROADWAY AREA	STV CRITERIA *WtAvgVL*
Freeway "A"	3.2
Freeway "B"	2.6
Expressway	3.8
Other Roadways-Undivided	3.8
Other Roadways-Undivided	2.6

Visibility Level Calculation

Small target visibility calculation method is introduced in a previous section. Here, application of the method to an object will be introduced. Roadway lighting designers assumed an object (target) is always darker that the background as seen in Figure 7.12. This assumption is always produce negative visibility or contrast for an object as defined in the previous section ($C = (L_t - L_b) / L_b$).

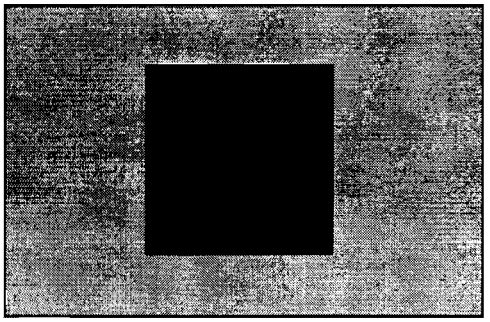

Figure 7.12 STV assumption for contrast distribution.

As seen from the visibility equation, target and background luminances should be known to obtain the visibility of the target. Target and the background luminances are calculated using Equations (7.21) and (7.15), respectively. Target luminance is calculated at the middle of the target and background luminance is calculated at the immediate middle points of the upper and lower boundaries of the target as seen in Figure 7.13. L_{b1} and L_{b2} (Figure 7.13) are separately calculated using equation (7.15) and the pavement luminance L_b is calculated by taking arithmetic average of L_{b1} and L_{b2} as follow.

$$L_b = \frac{L_{b1} + L_{b2}}{2} \tag{7.27}$$

Where, L_{b1} = Background luminance at the upper boundary of the target (Figure 7.13)
L_{b2} = Background luminance at the lower boundary of the target (Figure 7.13).

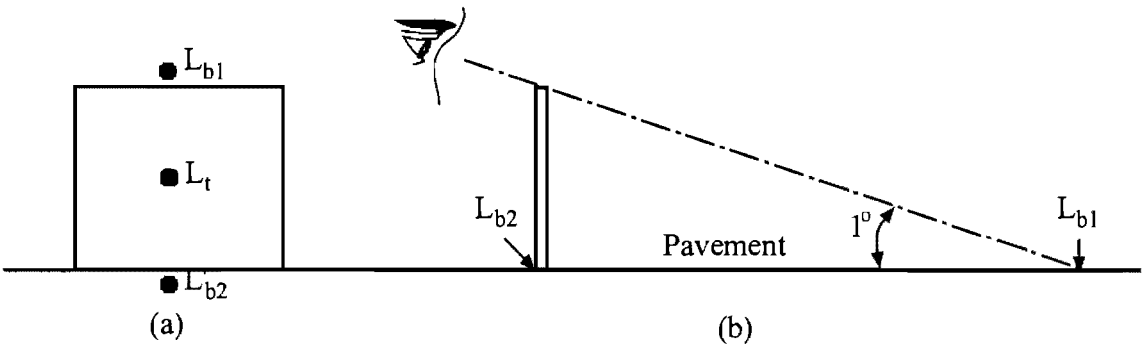

Figure 7.13 Luminance calculation locations on the target; a) front seeing , b) side seeing.

Visibility Level Program (Keck's Program)

The Roadway Lighting committee of the IES decided to create a new criterion for designing and evaluating the roadway lighting system. The decision was done by committee action. The computer program, developed by Merle E. Keck, used in calculating the visibility Level of the lighting systems. In this program, he used the target, observer, target locations and dimensions as provided by the IES Roadway Lighting Committee in its 1990 proposed revision of the ANSI/IES RP-8.

The program keeps the observer age (64 years), the observation time (0.2 seconds) and the size of the target (18x18 cm flat target) constant for all calculations. The compute program calculates the visibility level of a set of small target, in terms of the adaptation level, contrast and glare produced by the lighting system. Twenty target locations (grid points) are created between two installations. Targets are located at the intersection points of the grids. The Visibility Level (*VL*) of each target is evaluated with the observer location at the same distance and angle relative to each target. The program also calculates waited average visibility level. This prevents the average from being distorted by a few targets having an excessively high or low value. Output of the program includes *VL* values for each individual target and pavement luminance values for each target locations (grid points).

The program is used to calculate *VL* values for our experimental field. In the field, the roadway lighting system is already designed. In this portion of the study, the roadway lighting design properties (geometric, pavement and luminaire) are loaded to the program to obtain theoretical *VL* values distribution between the installation. The geometric properties of the experimental field are given as follows.

1. Luminaire photometric data = Ge7318.ies
2. Initial Lumen = 27500 lm
3. Pavement type = R3
4. Road wide = 12 ft
5. Number of luminaire = 4
6. Distance between the installation = 147 ft.

The above values and also some additional values are loaded to a computer to obtain visibility level (*VL*) for area of interest by following the steps below there are (use capital letters),

1. Type "D" to chose the driver.
2. Type "1".
3. Enter project number.
4. Enter number of luminaires type (there is one type of in our experimental field then we entered "1").
5. Enter the specific luminaires photometric data file name. We entered "Ge7318.ies".
6. Enter LLF. We entered "0.65".
7. Enter initial lumens of the specific luminaire. We entered "27,000".
8. Enter pavement type (R1, R2, R3, and R4). We entered R3
9. Leave default number there (0.07).
10. Enter unite. We entered "FT".
11. Enter sensitivity. We levied default "0.01".
12. Enter target surface reflectance value. We entered "0.2" for %20 reflective surface and "0.5" for %50 reflective surface.
13. Enter automatic grid and manual grid options. We entered manual "NSTD".
14. Enter "N or Y".
15. Enter left edge of the road. We entered "0".
16. Enter road wide. We entered "12".
17. Enter number of luminaires. We entered "4".

18. Hit to "Enter". Then enter the coordinates x, y and z, height of the poles, orientation, tilt, rotation and type of the luminaires. We entered as follows.
19. Enter "N or Y".
20. If you want to continue manual hit to "Enter".
21. We enter "2".
22. Enter the location of the first (west) grid point. We entered "3".
23. Enter the location of the last (east) grid point. We entered "9".
24. Enter the number of grid points across the street. We entered "2".
25. Enter the y-value for first row of the grid point. We entered "147.36".
26. Enter your chose "1 or 2". We entered "2".
27. Enter number of rows of grid points. We entered "10".
28. Enter location of the last row of points. We entered "279.65".
29. Enter "N or Y".
30. Enter one of the number you want to do.

This program was run for 20% and 50% reflective surface target with four different types of pavements. For each individual run, all the loaded values were kept constant except target surface reflection value (item 12) and pavement type (item 8). The results of the program (visibility level, *VL*) were plotted and also compared.

20% Reflected Target

The program calculates all negative visibility values between the installation for 20% reflective surface target with four different pavements. Taking absolute values of the program outputs performed the plots.

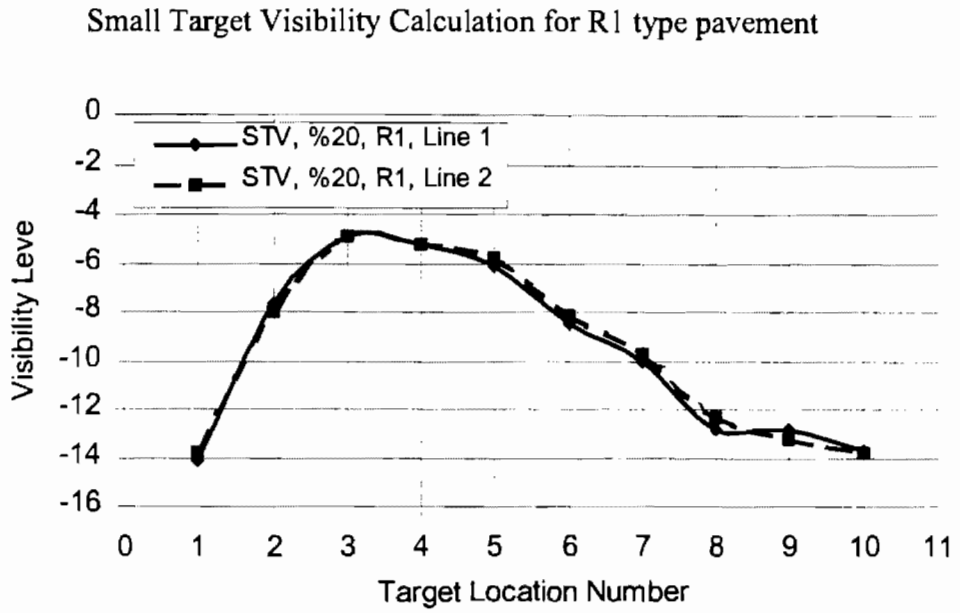

Figure 7.14 Visibility level distribution for 20% target, *R1* pavement, and line 1 and 2 between the installation.

As seen from Figure 7.14, *VL* distribution between the installation is same for line 1 and 2. The target has lowest visibility level values at the target locations 3rd, 4th and 5th. But visibility level values at those points are still greater than the recommended *VL* values, 3.8, (Table 7.8). It means, the 20% reflected target is visible between the installation on the lines 1 and 2. This installation is good installation for *R1* pavement.

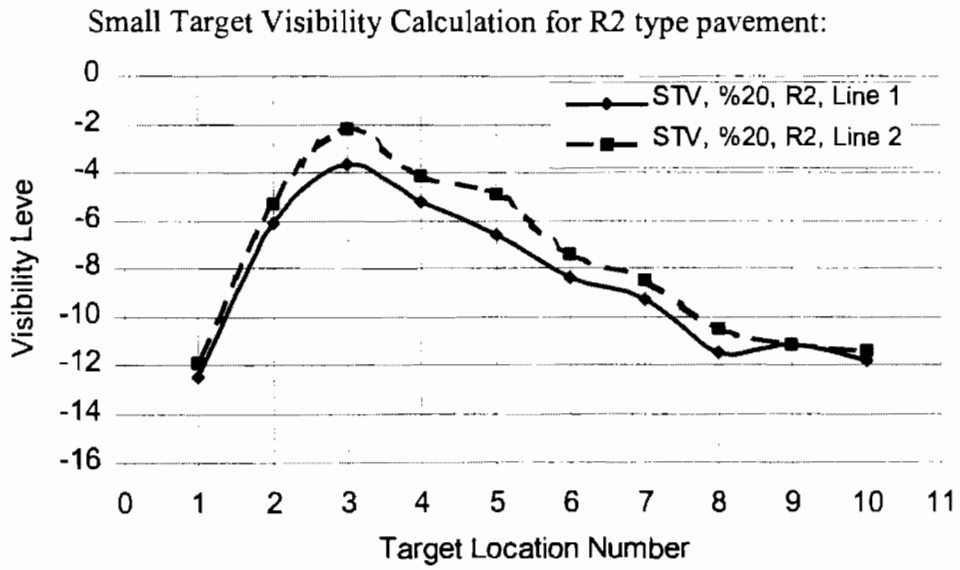

Figure 7.15 Visibility level distribution for 20% target, *R2* pavement, and line 1 and 2 between the installation.

As seen from Figure 7.15, *VL* distribution on the line 1 and 2 are slightly different between the installation. The target has lowest visibility level values at the target locations 3rd and 4th. Target is still visible at those target locations except at the target location 3rd on the line 2. At that point target visibility level value is less than the recommended *VL* values, 3.8, (Table 7.8). So, this installation also needs to be improve for *R2* pavement.

Small Target Visibility Calculation for R3 type pavement:

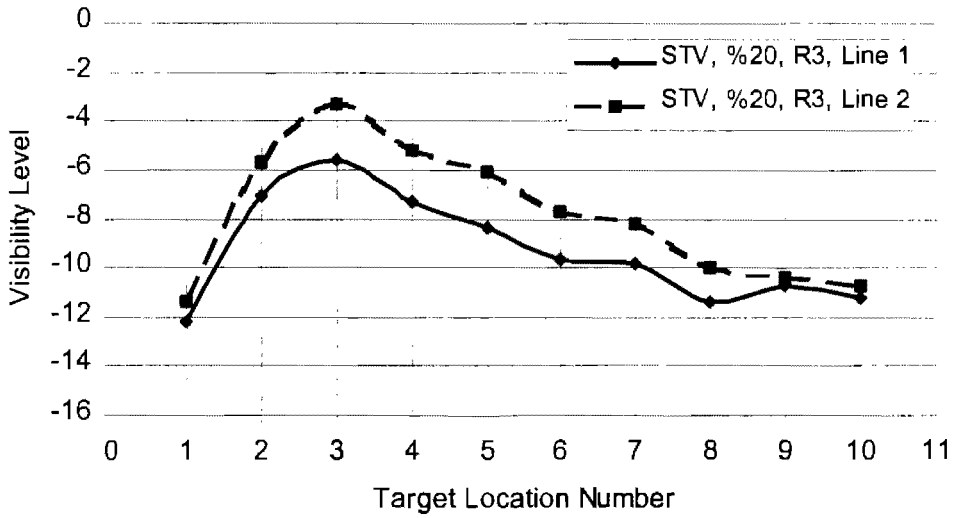

Figure 7.16 Visibility level distribution for 20% target, *R3* pavement, and line 1 and 2 between the installation.

As seen from Figure 7.16, *VL* distribution on the line 1 and 2 are slightly different between the installation. The target has lowest visibility level values at the target locations 3rd. Target is still visible at this target locations except at the target location 3rd on the line 2. At that point target visibility level value is less than the recommended *VL* values, 3.8, (Table 7.8). So, this installation also needs to be improving for *R3* pavement.

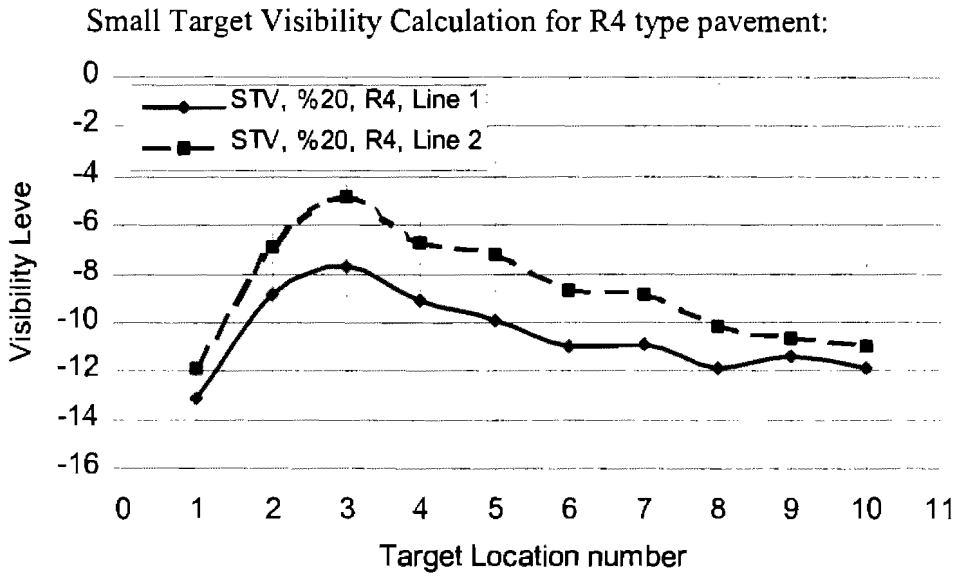

Figure 7.17 Visibility level distribution for 20% target, *R4* pavement, and line 1 and 2 between the installation.

As seen from Figure 7.17, *VL* distribution on the line 1 and 2 are slightly different between the installation. The target has also lowest visibility level values at the target locations 3rd. But target is still visible at that target location whose *VL* value is greater than the recommended *VL* value, 3.8, (Table 7.8). This installation provides enough light between the installation for *R4* pavement.

50% Reflected Target

The program calculates negative and positive visibility values between the installation for 50% reflective surface target with four different pavements. Again, taking absolute values of the program outputs performed the plots.

Small Target Visibility Calculation for R1 type pavement:

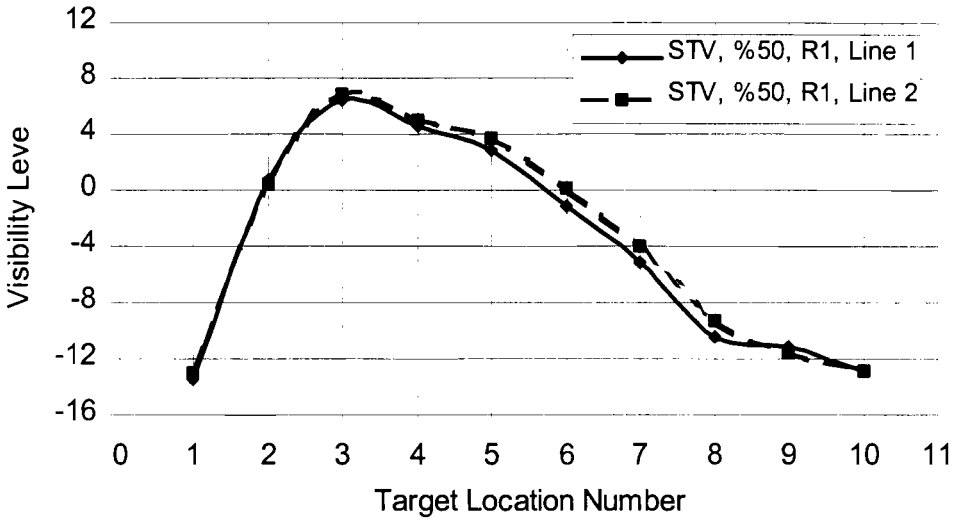

Figure 7.18 Visibility level distribution for 50% target, *R1* pavement, and line 1 and 2 between the installation.

As seen from Figure 7.18, *VL* distribution on the line 1 and 2 are almost the same between the installation. The target has lowest visibility level values at the target locations 2^{nd}, 5^{th}, 6^{th} and 7^{th}. Target is still visible at those target locations except the target is at the target locations 2^{nd}, 5^{th} and 6^{th} on both lines. At those locations target visibility level value is less than the recommended *VL* values, 3.8, (Table 7.8). So, this installation needs to be improving for *R1* pavement.

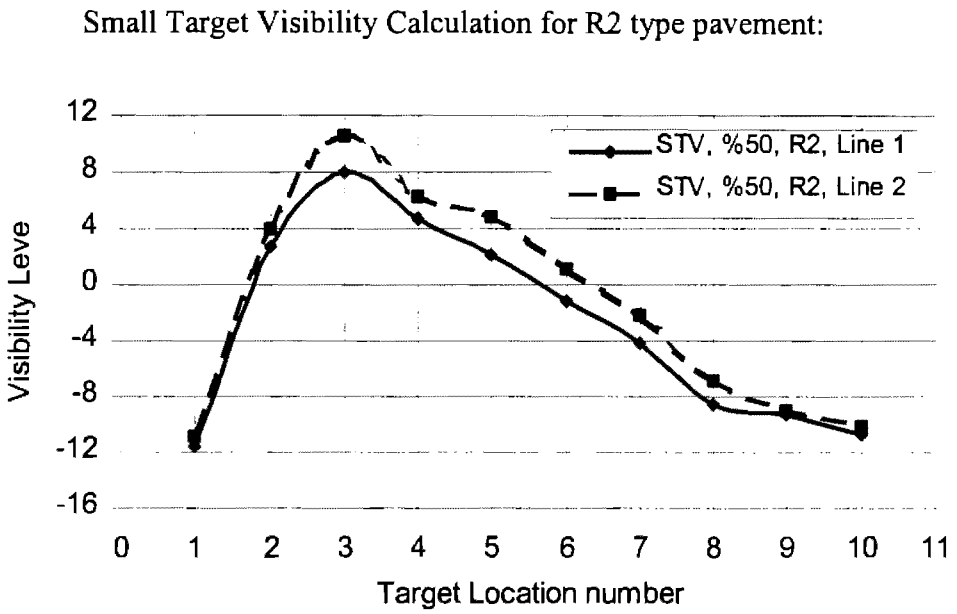

Figure 7.19 Visibility level distribution for 50% target, *R2* pavement, and line 1 and 2 between the installation.

As seen from Figure 7.19, *VL* distribution on the line 1 and 2 are slightly different between the installation. The target has again lowest visibility level values at the target locations 2nd, 5th, 6th and 7th. Target is invisible at the target locations 2nd and 5th on the line 1, 6th on both lines and 7th on the line 2. At those locations target visibility level value is less than the recommended *VL* values, 3.8, (Table 7.8). So, this installation also needs to be improving for *R2* pavement.

Small Target Visibility Calculation for R3 type pavement:

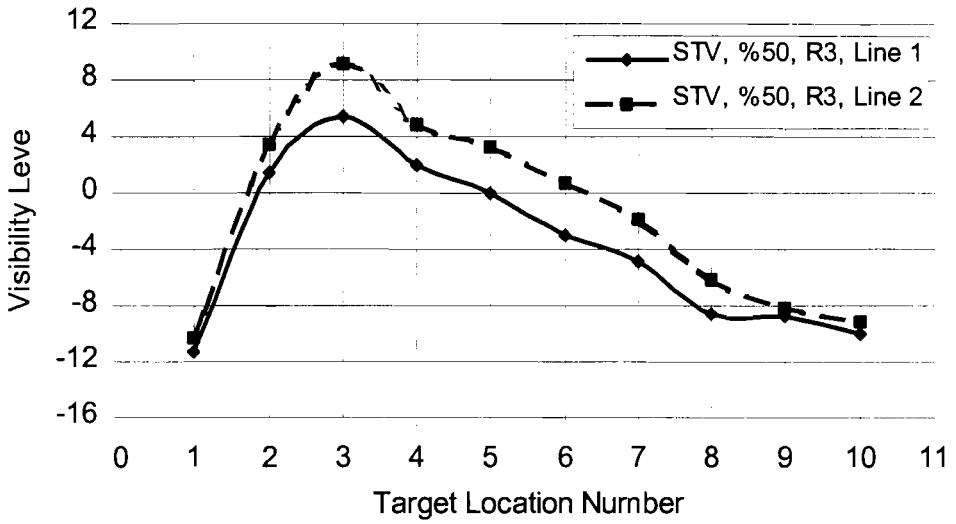

Figure 7.20 Visibility level distribution for 50% target, *R3* pavement, and line 1 and 2 between the installation.

As seen from Figure 7.20, *VL* distribution on the line 1 and 2 are different between the installation. The target has lowest visibility level values at the target locations 2nd, 4th, 5th, 6th and 7th. Target is invisible at the target locations 2nd, 5th, 6th on both lines, 4th on the line 1 and 7th on the line 2. At those points target visibility level value is less than the recommended *VL* values, 3.8, (Table 7.8). So, this installation also needs to be improving for *R3* pavement.

Small Target Visibility Calculation for R4 type pavement:

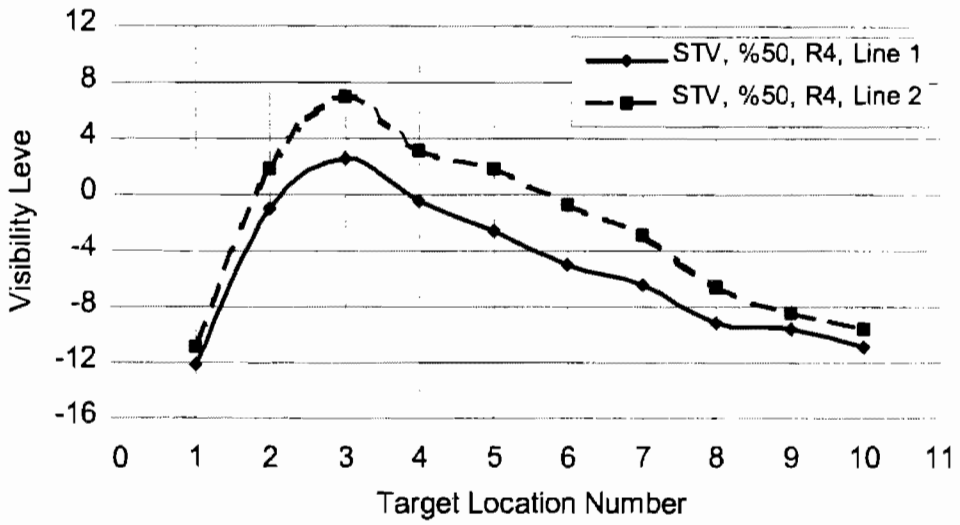

Figure 7.21 Visibility level distribution for 50% target, *R4* pavement, and line 1 and 2 between the installation.

As seen from Figure 7.21, *VL* distribution on the line 1 and 2 are different between the installation. The target has lowest visibility level values at the target locations 2nd, 3rd, 4th, 5th, 6th and 7th. Target is invisible at the target locations 2nd, 4th, 5th on the both line, 3rd on the line l, 6th and 7th on the line 2. At those locations target visibility level value is less than the recommended *VL* values, 3.8, (Table 7.8). So, this installation also needs to be improving for *R4* pavement.

Visibility Level of 20% and 50% Target Comparison

Arithmetic average of the *VL* values of 20% and 50% reflective surface targets are separately calculated for each type of pavement for the lines 1 and 2 (Table 4.9 and 4.10). Also the overall average of visibility level is calculated for the R1, R2, R3 and R4 pavement by using the formula as the following equation.

$$Overall\ average = \frac{Line\,1 + Line\,2}{2}.$$

Table 7.9 Arithmetic average of *VL* values for 20% reflective target.

	R1	R2	R3	R4
Line 1	9.58	8.63	9.34	10.58
Line 2	9.49	7.75	7.87	8.7
Overall Average	9.535	8.19	8.605	9.64

Table 7.10 Arithmetic average of *VL* values for 50% reflective target.

	R1	R2	R3	R4
Line 1	6.86	6.31	5.53	5.96
Line 2	6.68	6.6	5.71	5.28
Overall Average	6.77	6.155	5.62	5.62

20% Target with Four Different Pavements:

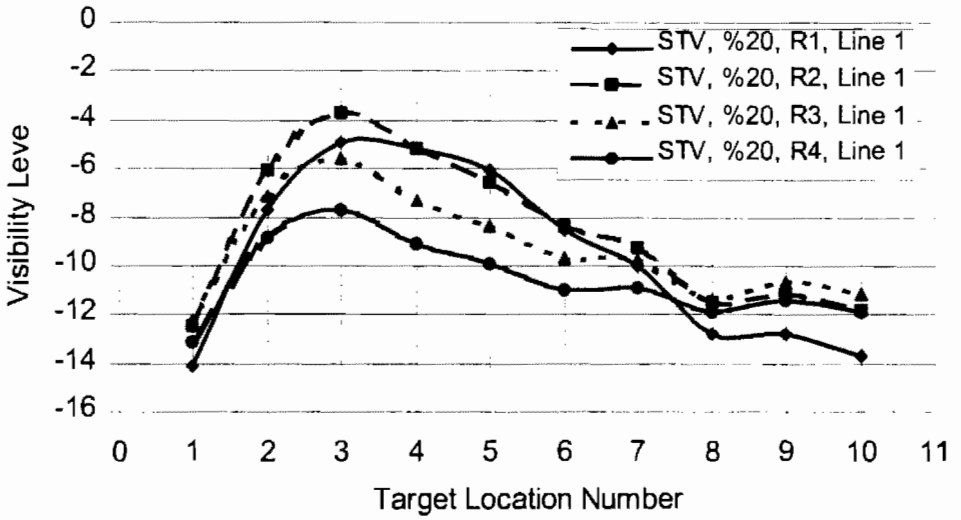

Figure 7.22 Visibility level distribution for four different pavements on the line 1 between the installations.

Arithmetic average value of the *VL* values for the pavement types *R1, R2, R3* and *R4* on the line 1 is 9.58, 8.63, 9.34 and 10.58 (Table 4.9), respectively. According to the average values and Figure 4.22, *R4* type of pavement is the best, *R1* and *R3* are second and almost the same and *R2* is the worst pavements to create visibility level values for 20% target on the line 1.

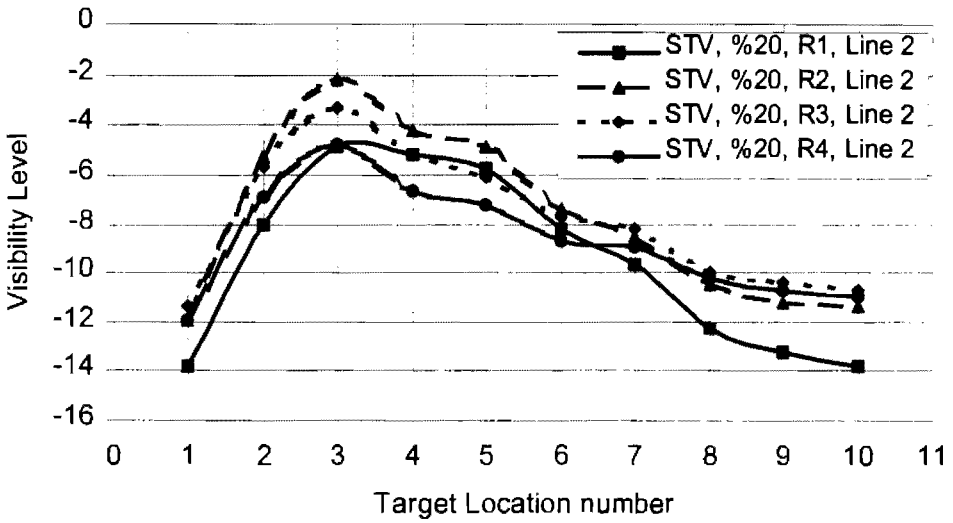

Figure 7.23 Visibility level distribution for four different pavements on the line 2 between the installations.

Arithmetic average value of the *VL* values for the pavement *types R1, R2, R3* and *R4* on the line 1 is 9.46, 7.75, 7.87 and 8.7 (Table 4.9), respectively. According to the average values and Figure 4.23, *R1* type of pavement is the best, *R4* is the second and *R2* and *R3* are the worst and almost the same pavements to create visibility level values for 20% target on the line 2.

From Figure 4.22 and 4.23, *R4* type of pavement is provides better VL values on the line 1 but it provides second good *VL* values on the line 2. On the line 2, *R1* type of pavement provides the better *VL* values. *R1* and R3 type of pavements provide second good *VL* values on the line 1 but *R3* is the worst pavement to provide VL values on the line 2. *R2* type of pavement is the worst pavement to provide *VL* values for 20% reflective target. According to the overall average luminance values (Table 7.9), R1 and R4 are the best pavement and R3 is the second best pavement and R2 is the worst pavement to provide visibility level values for 20% reflective target.

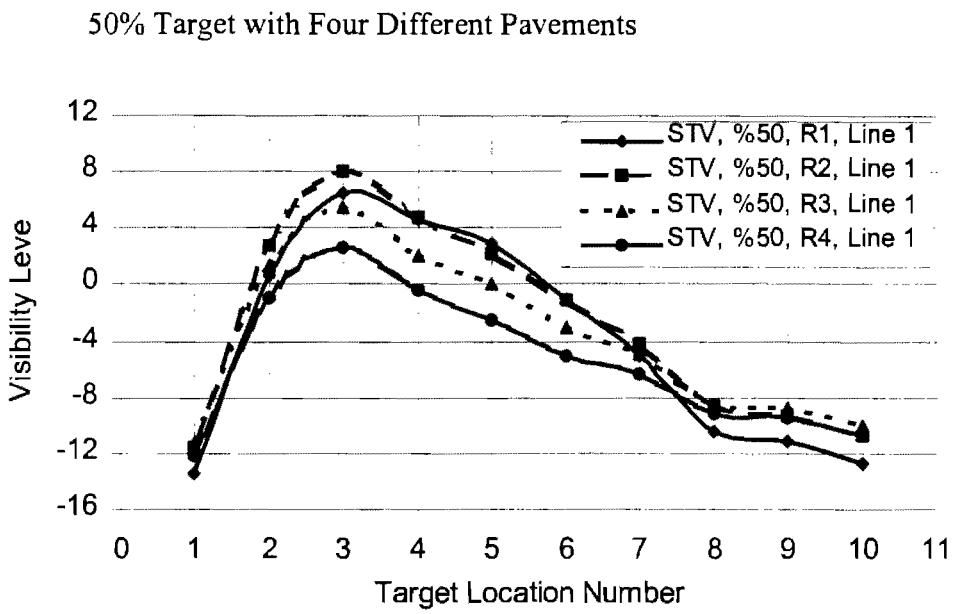

Figure 7.24 Visibility level distribution for four different pavements on the line 1 between the installations.

Arithmetic average value of the *VL* values for the pavement types *R1, R2, R3* and *R4* on the line 1 is 6.86, 6.31, 5.53 and 5.96 (Table 7.10), respectively. According to the average values and Figure 7.24, *R1* type of pavement is the best, *R2* is second, *R4* is third and *R3* is the worst pavements to create visibility level values for 50% target on the line 1.

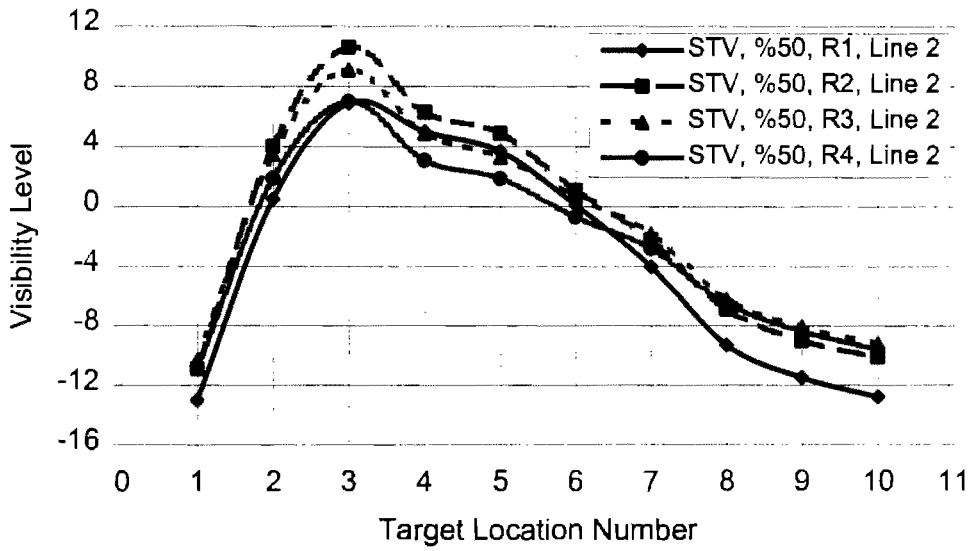

Figure 7.25 Visibility level distribution for four different pavements on the line 2 between the installations.

Arithmetic average value of the *VL* values for the pavement types *R1, R2, R3* and *R4* on the line 1 is 6.68, 6.6, 5.71 and 5.28 (Table 7.10), respectively. According to the average values and Figure 7.25, *R1* and *R2* types of pavements are the best, *R3* is second and *R4* is the worst pavements to create visibility level values for 50% target on the line 2.

From Figure 7.24 and 4.25, *R1* and *R2* types of pavements provide better *VL* values on the line 1 and 2 for 50% reflective target. *R3* and *R4* types of pavements are the worst pavements to provide visibility value for 50% reflective target and they switch the order for line 1 and 2. According to the overall average luminance values (Table 7.10), R1 is the best pavement, R2 is the second best pavement, and R3 and R4 are the worst pavement to provide visibility level values for 50% reflective target.

20% and 50% Target Comparison for R3 Pavement:

In this section, 20% and 50% reflective surface targets are only compared for *R3* type of pavement. Since, our experimental field has R3 type of pavement and experiments were performed for 20% and 50% reflective targets

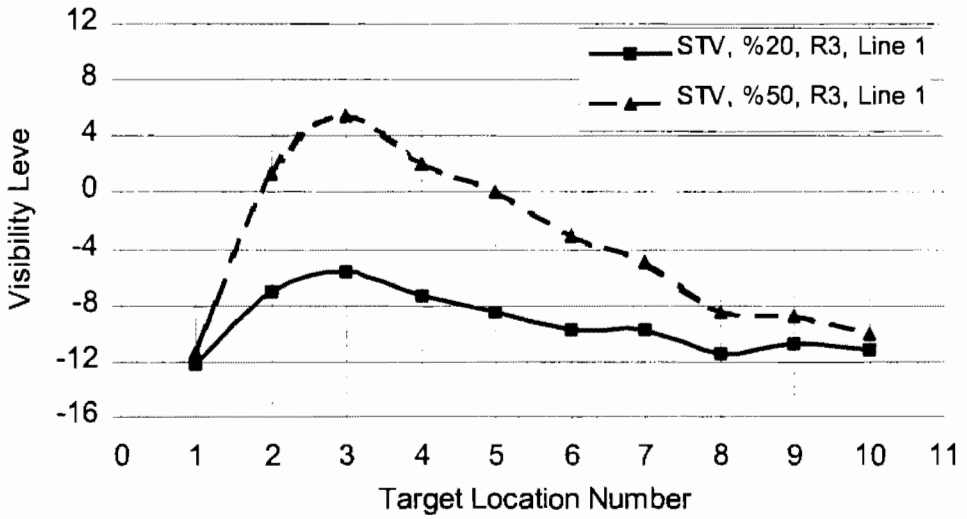

Figure 7.26 Visibility level distribution on the line 1 between the installations

As seen from Figure 7.26, visibility level of 20% and 50% reflective targets are extremely different from each other except target locations 1st, 3rd 9th and 10th for R3 type of pavement on line 1. On the line 1, if the target 20% reflective it is visible at the any target locations between the installation. If the target is 50% reflective it is invisible at the target locations 2nd, 4th, 5th and 6th.

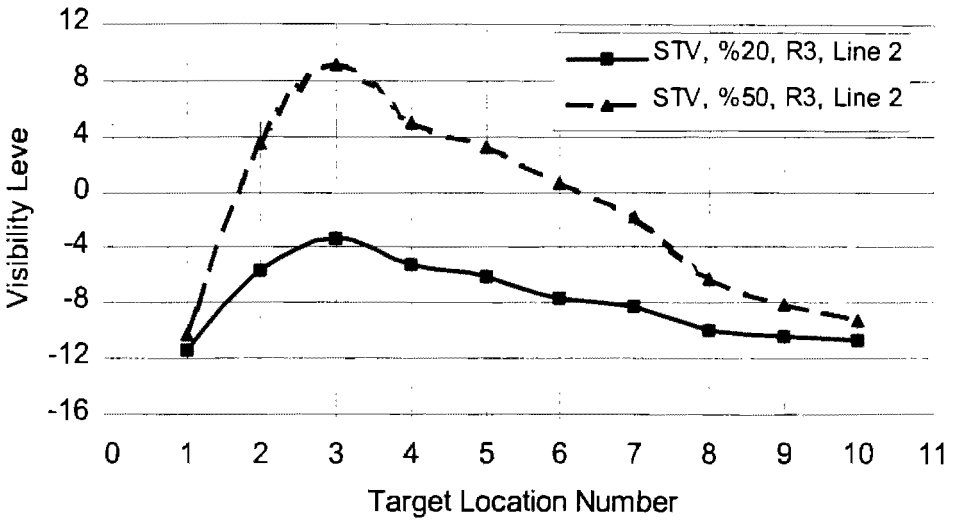

Figure 7.27 Visibility level distribution on the line 2 between the installations.

Figure 7.27 shows that visibility level of 20% and 50% reflective targets are extremely different from each other except target locations 1st, 2nd, 4th, 9th and 10th for R3 type of pavement on line 2. On the line 2, if the target 20% reflective it is visible between the installation except at target location 3rd. If the target is 50% reflective it is invisible at the target locations 2nd, 5th, 6th and 7th.

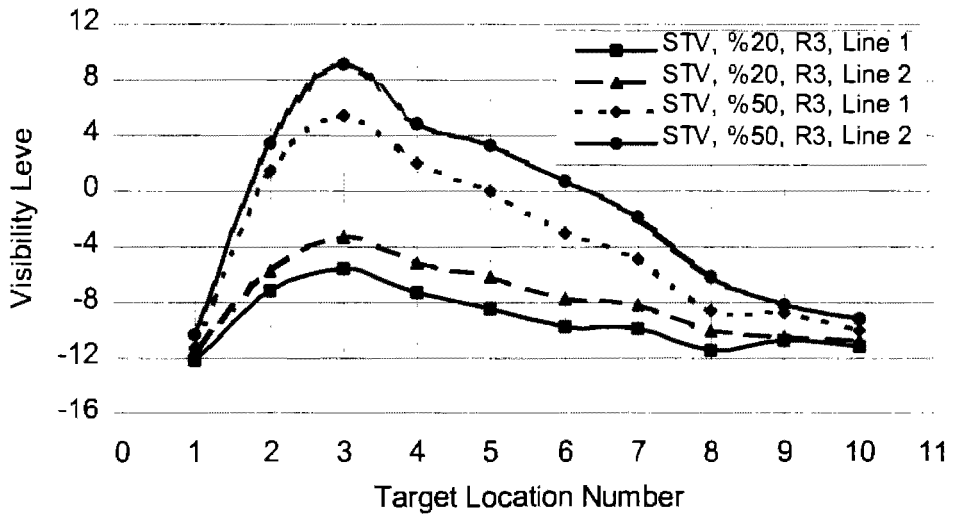

Figure 7.28 Visibility level distribution on the line 1 and 2 between the installations.

Figure 7.28 shows visibility distribution of 20% and 50% reflective target for *R3* type of pavement on line 1 and 2 between the installation. Theoretical calculations show that the 20% reflective target is visible at the any target locations for *R3* type of pavement between the installation. Theoretical calculations also show that the 50% reflective target is invisible at the target locations 2nd, 5th and 6th on both lines, 4th on the line 1 and 7th on the line 2 for *R3* pavement between the installation. As a result, if there is 20% target on the *R3* pavement, the

target is visible any target location between the installation according to the existence light installation. If there is 50% target on the *R3* type of pavement, the target is approximately invisible 30% distance between the installation according to the existence light installation. Therefore, the light installation should be examined, and recalculated for 50% reflective target.

Luminance Illuminance And STV Comparison

In this section, the calculated luminance, the illuminance (using Aladan program), and the visibility level (using Keck's program) values will be compared by using the geometric properties of the experimental field.

Theoretical Comparison

In this section, the luminance method, the illuminance method, the STV method and the experimental method are compared using the experimental field properties. The Keck program is ran to obtain STV values (visibility level) distribution, the GE program (Aladan) is run to obtain luminance and illuminance distribution.

Keck program is ran for R3 pavement and the following the average value of the visibility level is calculated. *WtAvgVL* (weighted average visibility level) = 7.9. Table 2.7 shows the recommended maintained values of target VL (visibility level). In the table recommended *WtAvgVL* value is presented for expressway 3.8. Calculated *WtAvgVL* value is more than twice of the recommended VL values. It means that, according to RP-8 regulation, this roadway has enough light for visual aspect.

Figure 7.29 shows the visibility level distribution with the threshold value. Figure 7.29 is obtained by dividing the normalized visibility level values to the recommended *WtAvgVL* value of 3.8 for commercial expressway. From the figure, the visibility level values are above the threshold line, except at the third target location on the line 2. It means that according to the STV method, the target is visible at any point between the installation except at the third target location on line 2.

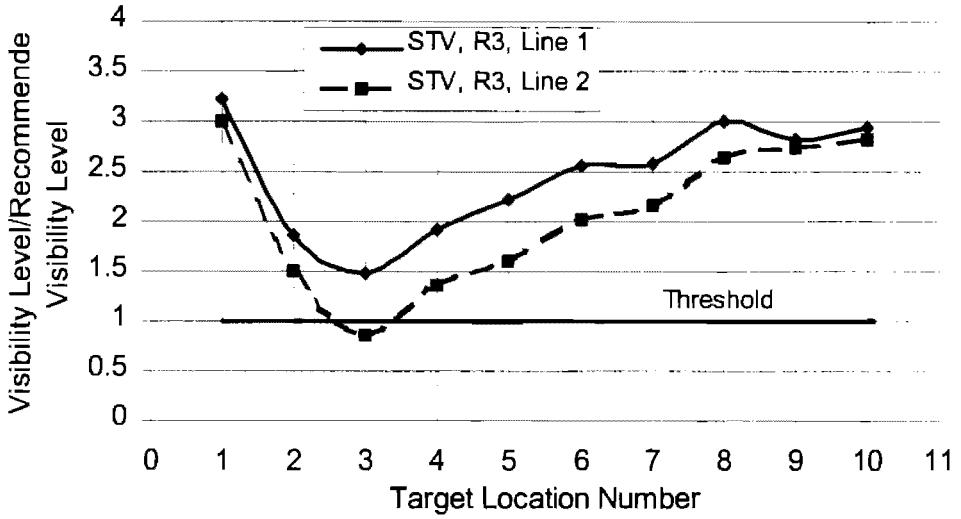

Figure 7.29 Distribution of the ratio of the visibility level to the recommended average visibility level.

The Aladan program is ran to obtain the following luminance results for R3 type of pavement. Table 7.3 shows the recommended maintained roadway luminance values. In the table roadway luminance value is presented for expressway (commercial) 1.0. Calculated roadway luminance value is 1.75 and it is 1.75 times greater than recommended luminance value. It means that, this roadway has enough light for comfort visual aspect.

Figure 7.30 shows the luminance distribution with the threshold value. Figure 7.30 is obtained by dividing the calculated luminance values to the recommended Luminance value of 1.0 for commercial expressway. From the figure, the normalized luminance values are above the threshold line, except at the third target location. It means that according to the Luminance method, the target is visible at any point between the installation.

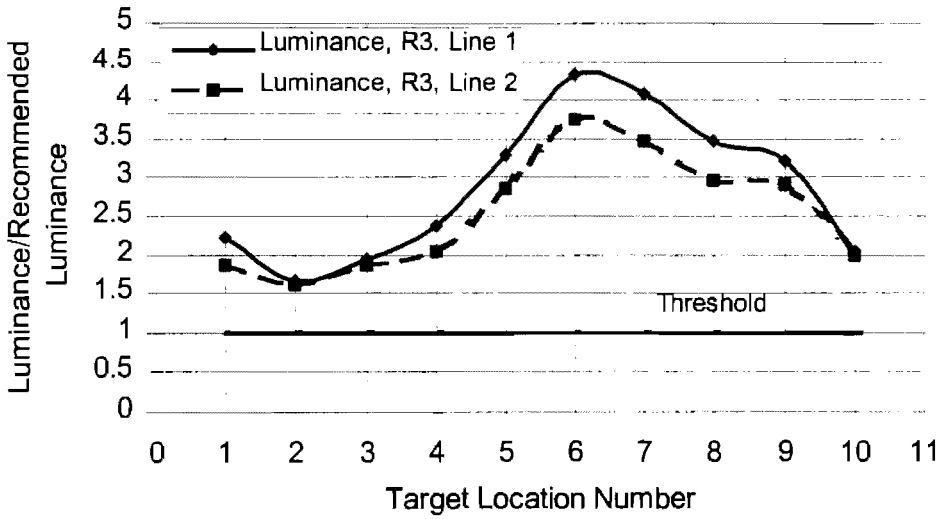

Figure 7.30 Distribution of the ratio of the luminance to the recommended luminance value.

The Aladan program is ran to obtain the following illuminance results for R3 type of pavement. Table 7.2 shows the recommended average maintained roadway illuminance values. In the table roadway luminance value is presented for expressway (commercial) 1.3 (Footcandles). Calculated roadway luminance value is 1.81 and it is 1.39 times greater than recommended luminance value. It means that, this roadway has enough light for comfort visual aspect.

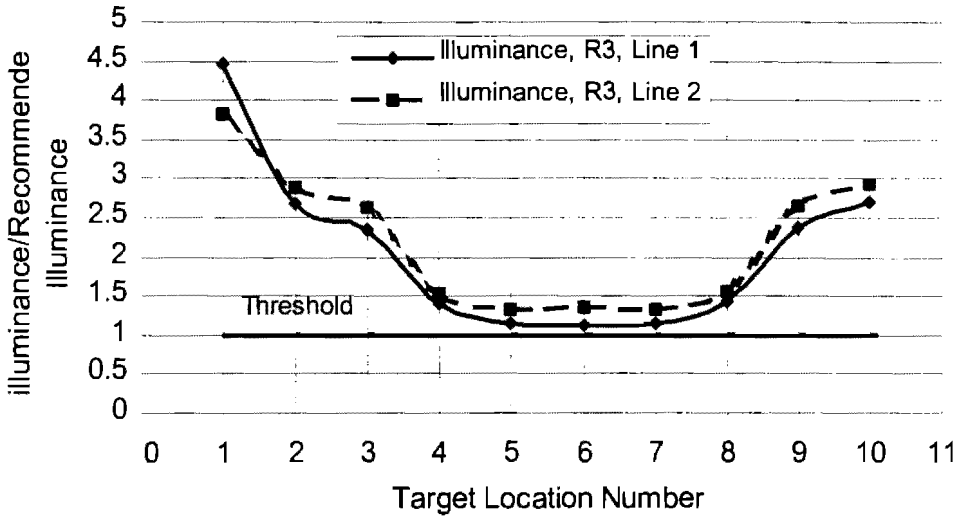

Figure 7.31 Illuminance distribution divided by recommended average luminance value.

Figure 7.31 shows the illuminance distribution with the threshold value. Figure 7.31 is obtained by dividing the illuminance values to the recommended illuminance value of 1.3 (Footcandles) for commercial expressway. From the figure, the normalized illuminance values are above the threshold line at the any target locations. Overall average of the illuminance shows that there is enough light on the roadway to provide comfort visual aspect.

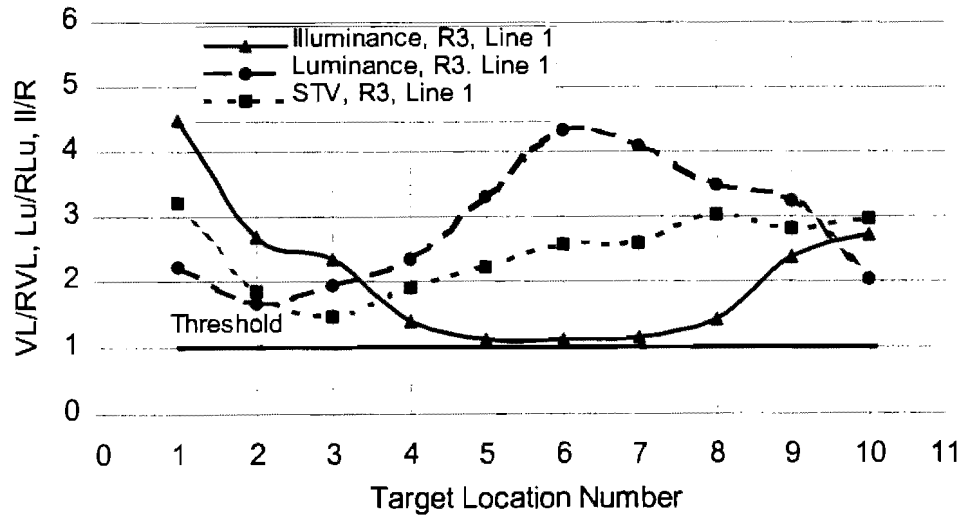

Figure 7.32 Visibility distribution of the STV, luminance, and illuminance methods on the line 2.

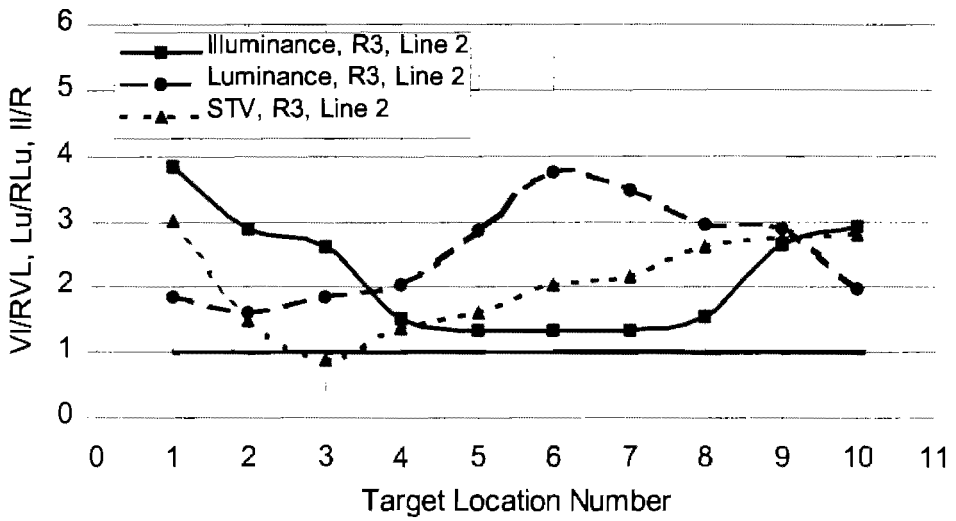

Figure 7.33 Visibility distribution of the STV, luminance, and illuminance methods on the line 2.

Figures 7.32 and 7.33 show comparison of the STV, luminance, and illuminance methods on the lines 1 and 2, respectively. The figures again show the illuminance method is more conservative method than the other two theoretical methods. When the calculated values of these three methods for the experimental field are divided to their recommended values, the ratios are obtained at the each target locations (Figures 7.32 and 7.33). When the calculated average values were concerned, the three theoretical methods gives average values greater than recommended values. However, when the calculated values for each target location are divided to the recommended average values, the all three methods gives ratios more than 1 (it means there is enough light to provide comfort visibility) target is visible.

Table 7.11 indicates recommended average and calculated values of STV, luminance and illuminance methods. The ratio is calculated by dividing calculated values to the recommended values. As seen from the table, the STV method gives ratio of 2.08, the luminance method gives ratio of 2.69, and the illuminance method gives ratio of 2.14. However, the three methods theoretically show that the roadway has enough light to provide comfort visual aspect. According to the ratios the STV and the illuminance methods are the most conservative methods than the luminance method.

Table 7.11 Recommended and Calculated STV, luminance, and illuminance values.

	Recommended	Calculated	Ratio
STV	3.8	7.9	2.08
Luminance (cd/m2)	1.0	2.69	2.69
Illuminance (Footcandles	1.3	2.79	2.14

Experimental Comparison

To compare the experimental illuminance values to the calculated illuminance values, the unit of the both measurements was converted to the unit "Footcandles". Aladan program already calculates the illuminance with the unit of Footcandles. Experimental system measures the illuminance with the unit of "Lux" that can be converted to the Footcandles by multiplying with the constant of 0.0927. After the converting the units to Footcandles the following figures are plotted.

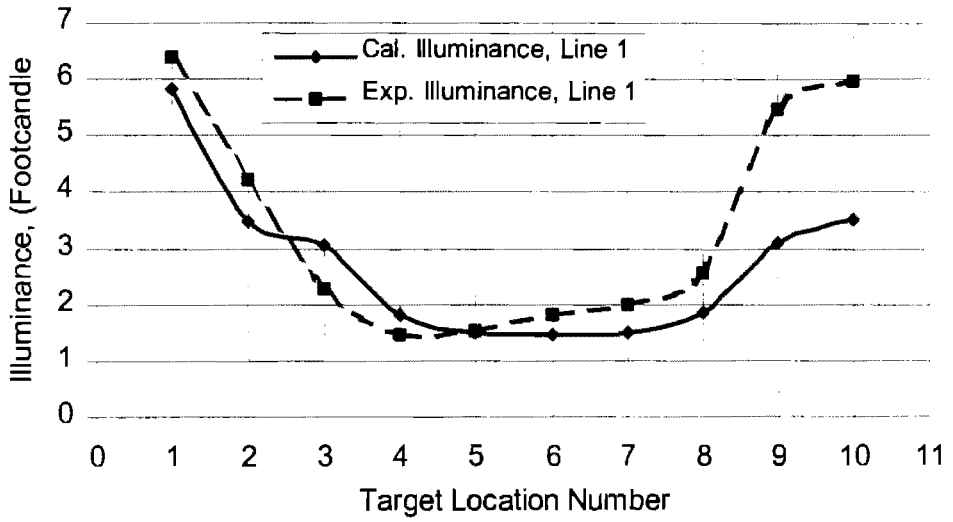

Figure 7.34 Comparison of experimentally and numerically obtained illuminance distribution on line 1.

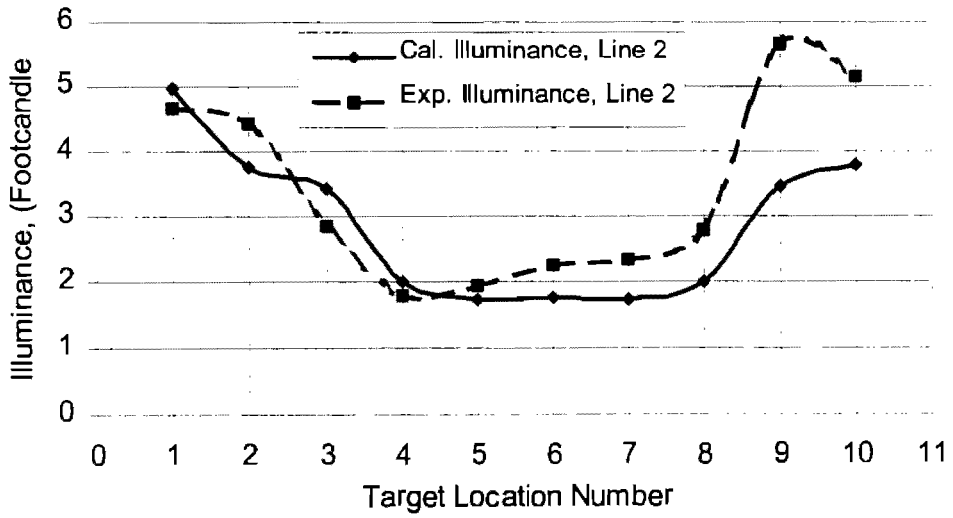

Figure 7.35 Comparison of experimentally and numerically obtained illuminance distribution on line 2.

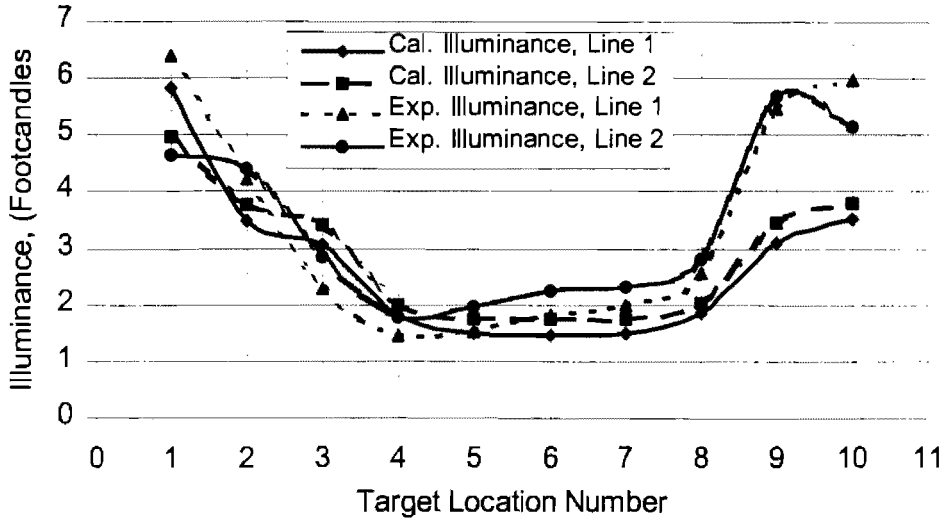

Figure 7.36 Comparison of experimentally and numerically obtained illuminance distribution on lines 1 and 2.

Figures 7.34 and 7.35 show the comparison of numerical and experimental illuminance distributions on the lines 1 and 2, respectively. Figure 7.36 shows the comparison of numerical and experimental illuminance distributions in one figure. As seen from the figures, Illuminance distribution obtained using both methods shows good dynamic agreement each other. Until 6^{th} target location, there is maximum 20% difference between both methods, but after 6^{th} target location, the difference between the measurements reaches to 80% difference. This large percentage difference can be able to explain with the maintenance errors such as, rotation angle, tilt angle, etc.

CHAPTER 8: RECORDING AND ANALYZING VIDEO IMAGES

In this section, two types of experiments were involved: static experiments (video image recording) and dynamic experiments

Recording Of Static Video Images

Video images were recorded using 3CCD SONY video camera in the following steps:

1. Target was placed at the first target location on the line 1 as seen in Figure 7.9.

2. The video camera was placed at a distance of 83-meters and a height of 1.45 meters above the pavement (Figure 8.1).

3. The target was placed at the center of the camera frame to obtain a one-degree down angle, and the video image was recorded for approximately 12 seconds.

4. A constant 83-meter distance was maintained for each target of interest at all target locations and steps 1 through 3 were repeated until video images of the target were recorded at all the target locations on line 1 and line 2 as seen in Figure 8.2.

5. The video images were loaded into the computer using a video editing system and video capture card. The picture analysis program was developed in our laboratory using Visual Basic used to analyze the images.

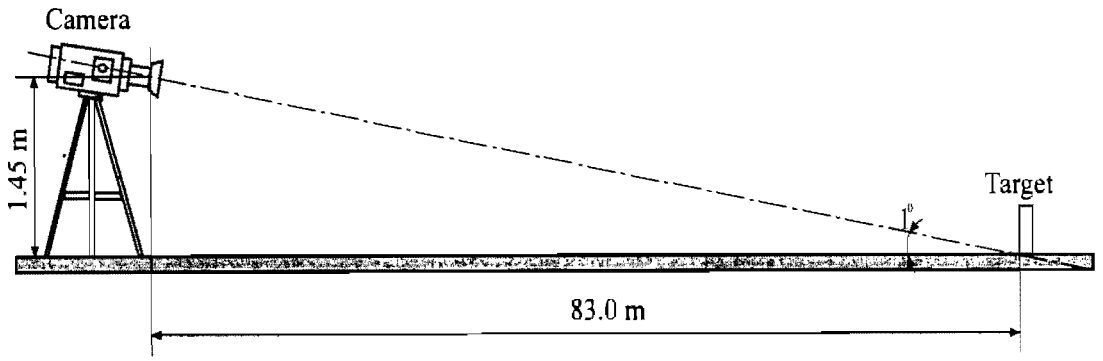

Figure 8.1 camera and target orientation.

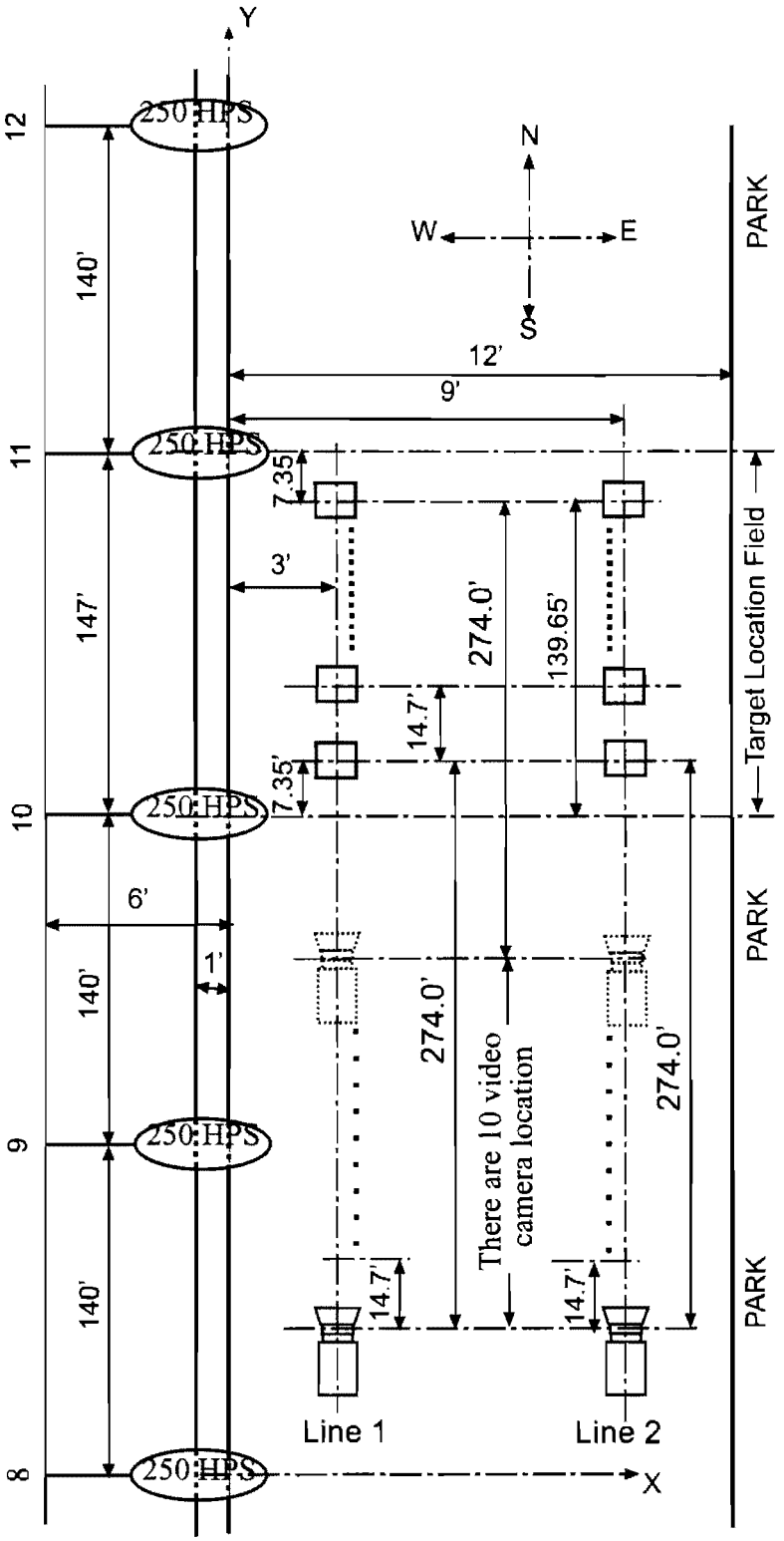

Figure 8.2 Orientation of the video camera and target for static video recording system.

Recording of Dynamic Video Images

Visibility measurements will be performed dynamically in the experimental field for two different reflective surfaces and three different sizes of square targets.

Reflective surface:
1.20%
2.50%

Target size:
1.18 x 18 cm (324 cm^2) standard small target (STV)
2.25.45 x 25.45 cm (2*324 = 648 cm^2) target
3.36 x 36 cm (4*324= 1296 cm^2) target

The experimental field will be designed according to the RP-8 (American national Standard Practice for Roadway Lighting), and dynamic experiments will be performed for three different sizes of targets and two different reflective surfaces. The two identical targets will be placed one on each STV line, and the video camera will be moved to the target in twelve equal steps. The furthest distance between the video camera and the targets is 425.4 feet, an intermediate measure is 273 feet (83 meters and 1 degree don angel) the closest distance between the video camera and the targets is 102 feet and each step is 29.4 feet (Figure 8.3). Experimental measurements will perform in following steps.

1. Mark the experimental field according to the RP-8.
2. Mark the twelve stationary location of the video camera.
3. Place the two identical targets on the first target locations on the STV left and right lines.
4. Place the video camera at the furthest distance (425.4 feet) from the target.
5. Center the targets in the video image and record the video image of the targets in the frame.
6. Move the video camera one step closer to the target (29.4 feet) with the target location held constant and record the image of the targets again.
7. Continue to record the images of the targets for the 12 dynamic camera location.
8. Place the targets at the second target location on the STV lines and place the video camera at 425.4 feet and follow steps 4 through 8 for recording the video images of the targets.
9. Continue steps 4 through 8 until recording images of the targets for every target locations (10 target locations).
10. Repeat steps 1 through 9 to record the video images of the two different reflective target surfaces and three different target sizes (total of six sets of experiments).

The measurements will contain 120 images for each target size and target reflectance. During the dynamic experiments, the camera will be at a height of 1.45 meters from the ground, and the images of the target will be placed in the middle of the video camera frame at the each of the measurements points.

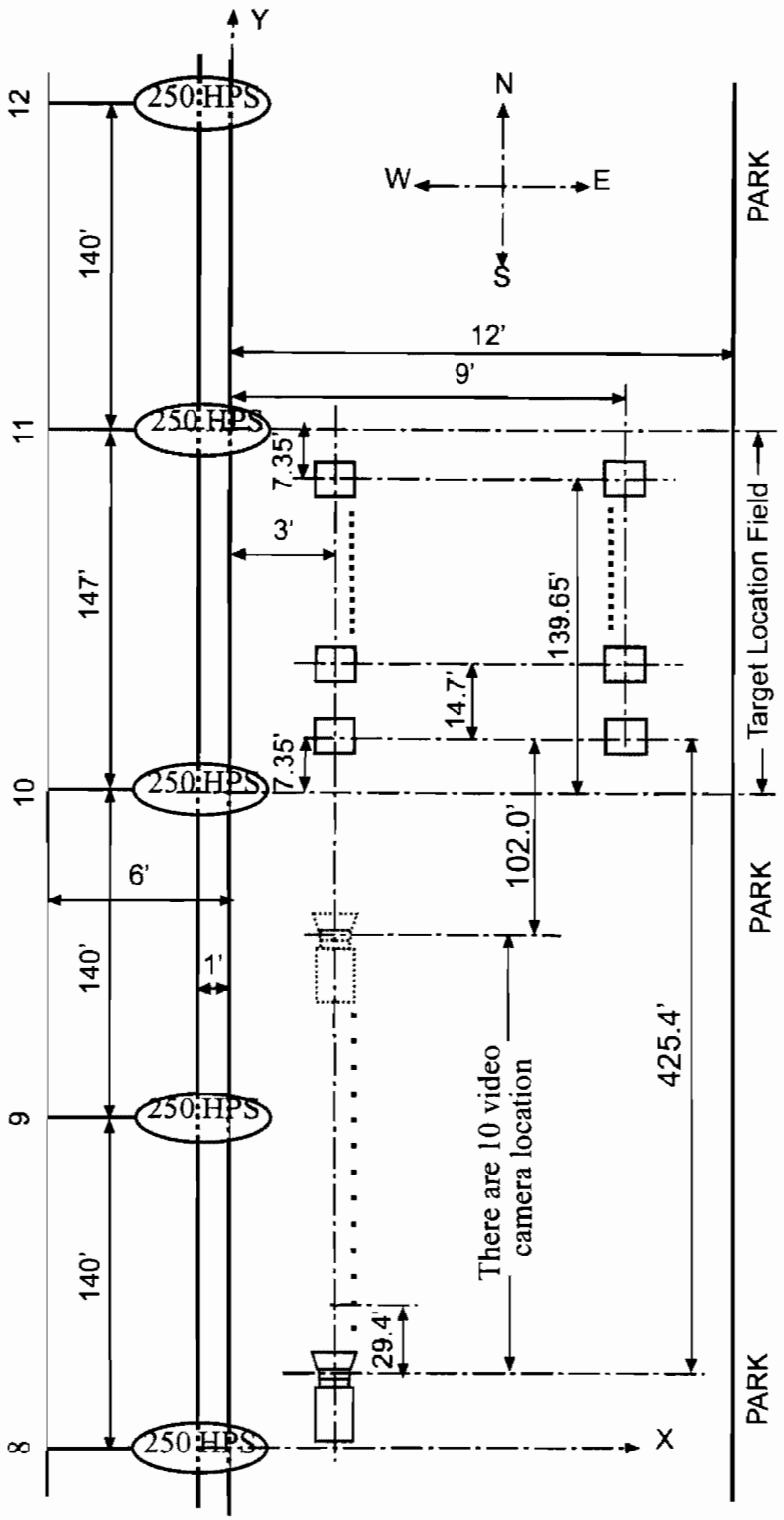

Figure 8.3 Dynamic Visibility Measurement and Experimental Orientations.

Visibility Analysis from Images

Three different calculation methods were performed to determine the contrast of an STV target: VTC, VTC *n* points, VTCa. These experiments were performed after all the luminaire heads were replaced with new 250 Watt luminaires.

Rackoff and Rackwell (1975) developed a vehicle-based television system to investigate driving vision patterns during nighttime driving. The system compared vision patterns during nighttime driving to vision patterns during daytime driving on freeways and a rural highway. The system also determined differences in vision patterns at sites with high and low nighttime accident rates and the effect of illuminance on a driver's vision pattern. The researchers found nighttime vision patterns were different from daytime vision patterns. The changes in vision patterns due to the amount of illuminance prove that illuminance can affect a driver's ability to see effectively.

Janoff *at. al.* (1986) tried to determine if roadway lighting can be reduced or eliminated at night when traffic volume is much lower than design capacity without significantly reducing drivers' abilities to control their vehicles safely and effectively. Researchers used a Styrofoam hemisphere with a 6-in (0.15-m) diameter skirt with an 18% reflecting surface. The research team obtained a linear relation between the detection distance and horizontal illuminance and the pavement luminance and contrast index by using six different lighting methods as parameters: every luminaire lit, 75 % of the luminaires lit, 50% of the luminaires lit, every other luminaire lit, luminaires on only one side of the road lit, and no luminaires lit. Results of the controlled field experiments show that drivers felt more negative toward reducing the lighting on all ramps and interchanges than the lighting on straight mainline roadway sections.

Zwahlen and Yu (1990) performed two investigations to determine the distances at which the color and shape of a target can be identified at night under vehicle low-beam illuminance. The targets were flat and one of three shapes and one of six colors. First, distances for color and shape recognition were investigated. Second, distance for color recognition only was investigated. The target colors were red, green, yellow, orange, blue or white. The target shapes were a circle, square or diamond and had a surface area of 36 in^2. Results of the investigations show that the distance for color recognition was twice as far as the distance for shape recognition. Researchers found the saturated red retroreflective targets to be most visual of all the target colors.

Hall and Fisher (1978) examined the design of a roadway lighting system by using empirically derived requirements of light technical parameters such as road luminance, luminance uniformity, and glare restriction. The researchers used a square target (200 mm x 200 mm) with a limited range of contrast. They found that lighting design based on a contrast matrix yields good results.

Marsden (1976) studied road lighting contrast and accident reduction, both numerically and experimentally. During the experimental investigation the disability glare was related to veiling luminance, measured with a Pritchard photometer. Horizontal illuminance near the road surface was measured by summing the outputs of photocells mounted on each end of the vehicle. Vertical illuminance near the road surface was measured by a photocell mounted on the rear of

the vehicle. Some instrumentation was also mounted below the vehicle to record road reflectance data. Researchers recorded all this information and the visual field of the driver with a video recorder. The video was played in the laboratory and could be frozen on a selected frame. Certain areas on the frame could be defined (by operating brightening-up controls) for luminance analysis. This analysis was examined on the portion of the TV signal corresponding to the selected area. Analog processing gave the value of maximum, minimum, average and standard deviation of luminance within the selected area by using a calibration luminance scale.

In previous studies researchers used humans to detect the distance at which shape, color and contrast are recognized. Experimental results fluctuated because every human eye detects shapes and colors at different distances. Additional information at the site of the experiment such as weather conditions and sensitivity of the experiment equipment effected the results. One of the most important issues for experimental research is eliminating those site effects as much as possible.

In this study a 3-CCD video camera was used instead of a human eye. The 3-CCD camera was mounted 83 m away from and 1.45 m above an 18 cm x 18 cm, 20% reflective target. The target was located in the middle of the camera frame and satisfied the 1 degree angle (STV requirement). All information (global information) was recorded on a video camera. The video was played in the laboratory and selected frames, including the target, could be frozen and loaded into the computer for analysis.

Pixel Analysis Program

A *3CCD* SONY video camera was used with a Hi8 video tape to record the target images. The *3CCD* camera system employs high density three-chip precision, and each *CCD* image includes a total of 410,000 pixel. An image is separately projected by the lens into three primary colors; red, green and blue (*RGB*). An experimental system was designed according to rules of RP-8 (1). Video images were recorded at the 83-meter distance and 1.45 meter above the small target. The small target image was placed at the center of the camera frame to satisfy one-degree down angle (Cuvalci, *at. al*, 1998).

Programs were developed to read and analyze photometric data from the video tape. The analyses were examined including the portion of the frame with the target. In the selected portion, a pixel analysis was performed to investigate the contrast of the STV target. These pixels included global information such as luminance, illuminance, and reflection information. Through the pixel analysis, contrast distributions were obtained between the roadway lights. Therefore, the measurement and analysis system was independent from an individual's eye response.

The small target images were loaded in a computer using a video editing system. From the images, the picture analysis program using the following formula as a percent calculated the visibility values.

The visibility values were converted to percentages according to the following conditions.

- If a white object was on a white background or a black object was on a black background, then visibility percentage was zero.
- If a white object was on a black background then contrast is infinity, and a black object was on a white background then visibility percentage is 1.

Co-ordinate Definition

After loading the video images of the small target to the computer, each image was loaded to the screen one by one by the picture analysis program (Figure 5.4). When the image is on the screen, the mouse clicks on the red *LED* of the small target to calculate *x1, x2, y1* and *y2* co-ordinates. At the same time, the program transfers the small target from the picture with enough background to another picture box. Then, the center of the small target (center of the reflective surface) was calculated by the following algorithm:

$$Dis = \left[(x1 - x2)^2 + (y1 - y2)^2 \right]^{1/2}$$

$$Ratio = Dis / 30.7$$

$$Xc = (x1 + x2) / 2$$

$$Yc = (y1 + y2) / 2 + Ratio * 15.4$$

Where 30.7 cm is the distance between the two red LED, and 15.4 cm is the distance between the center of the small target and red LED. To obtain the boundaries of the small target, the distance between the center and the boundaries were multiplied with *Ratio* and than the obtained values were added or subtracted to the center co-ordinate of the small target.

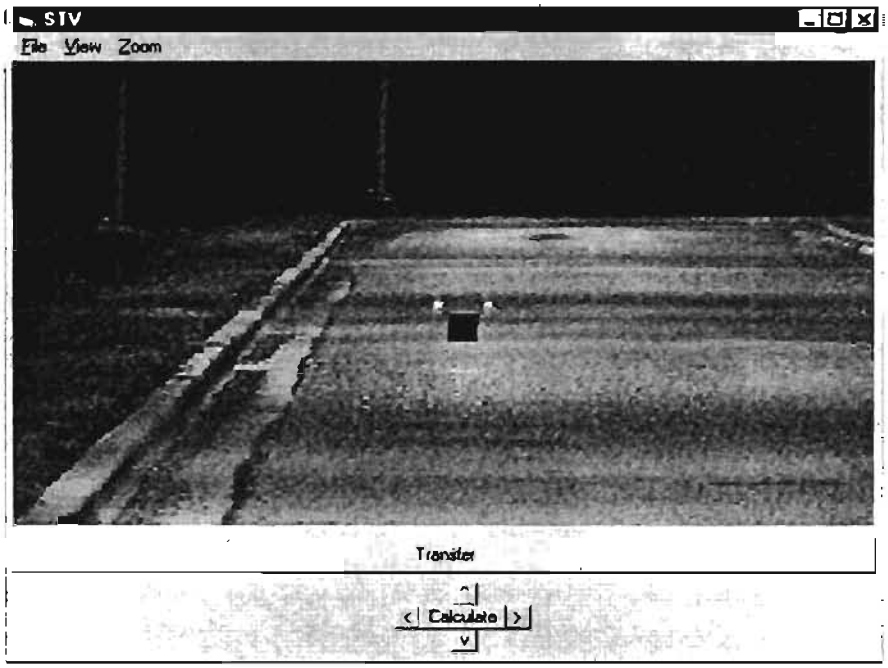

Figure 8.4 Picture with the small target.

Target Zoom

From the picture, the small target was transferred to another picture box with a background. During the transformation, the color image was zoomed for better recognition the boundaries of the small target, and at the same time, it was constructed to a black and white picture. To obtain the black and white picture, each pixel of the color picture was separated into three main colors; red, green, and blue. The arithmetic average of the main colors ($(R+G+B)/3$) was calculated for each pixel and recorded at the same pixel to obtain grain scale picture as follows:

$$c = colorRGB$$
$$Blue = Int(c / 65536)$$
$$c = c - Blue * 65536$$
$$Grean = Int(c / 256)$$
$$Red = c - Grean * 256$$

In the zoom box a frame was defined at the original target size and data (pixel) reading co-ordinates (sample lines) for visibility calculations that was marked on the background and on the reflective surface. If the locations of the sample lines were not in the right places, the frame will move up, down, right and left by using the arrow buttons to adjust the small target in the frame as seen in Figure 8.5. The adjustment provides the right co-ordinate to read data.

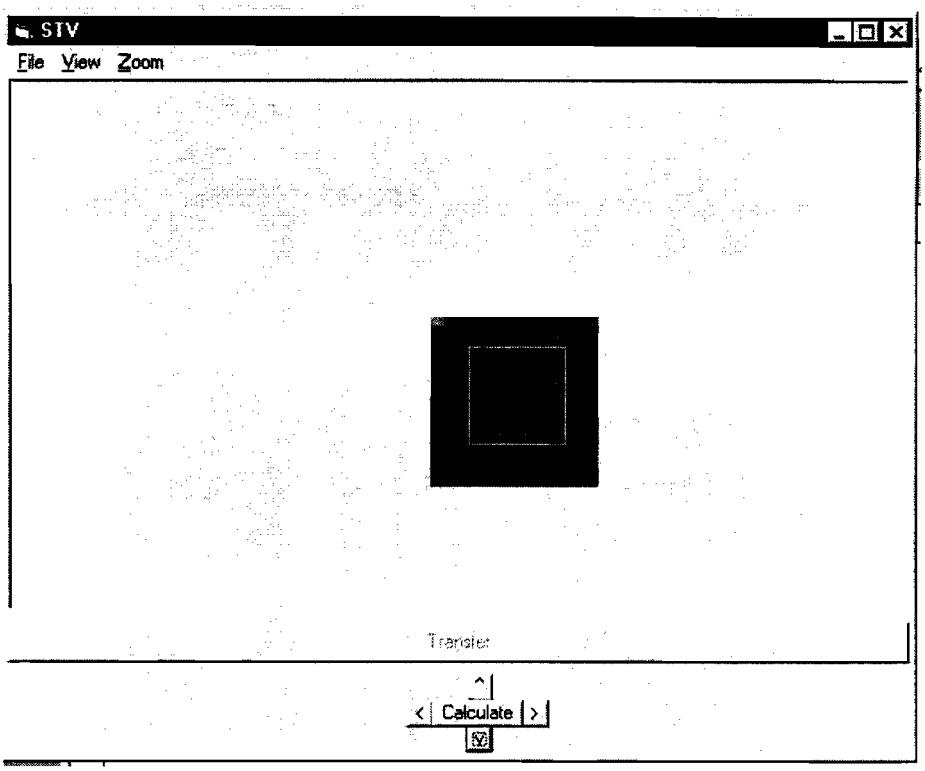

Figure 8.5 Zoom box.

The program reads the pixel values at the marked points as seen in Figure 8.5 and calculates visibility by using Equation (7.1). The spectral density of the target with background is also calculated and presented in Figure 8.6. The pixel distribution of the picture with target presents as seen in Figure 8.7. From the Figure 8.7, pixels around the target borders and red LED sharply changed from one value to another. This pixel change around the target borders also presents luminance change proportionally between the target and the background. The picture analysis program flow chart was shown in Figure 8.8 and it is run as follows.

1. Load (open) a image with target.
2. Click on the red LEDs (order is not important) to find border of the target.
3. Program grapes the color target with the enough background and transfers the color image to black and white image.
4. Chose fine replacement to find target border very sensitively by using up, down, right and left arrows.
5. The program reads equal number of pixel values inside and outside of the target borders.
6. Calculate the visibility by clicking on the calculation button.
7. The program gives the calculated visibility values also if you want you can see spectral and pixel distribution by clicking the related buttons.
8. Load a new picture from the file to continue the visibility.

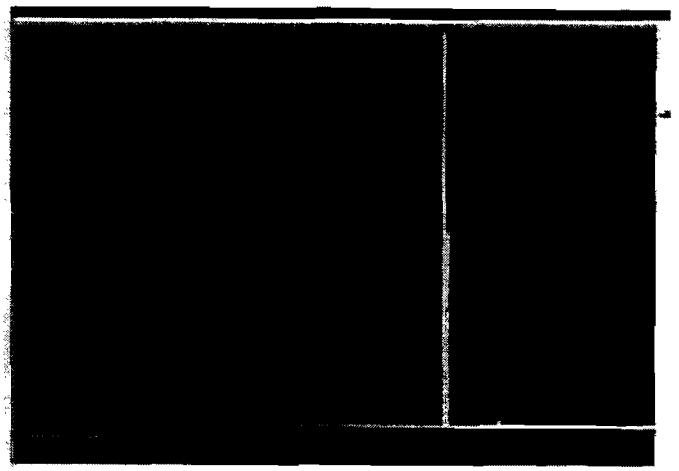

Figure 8.6 Spectral density.

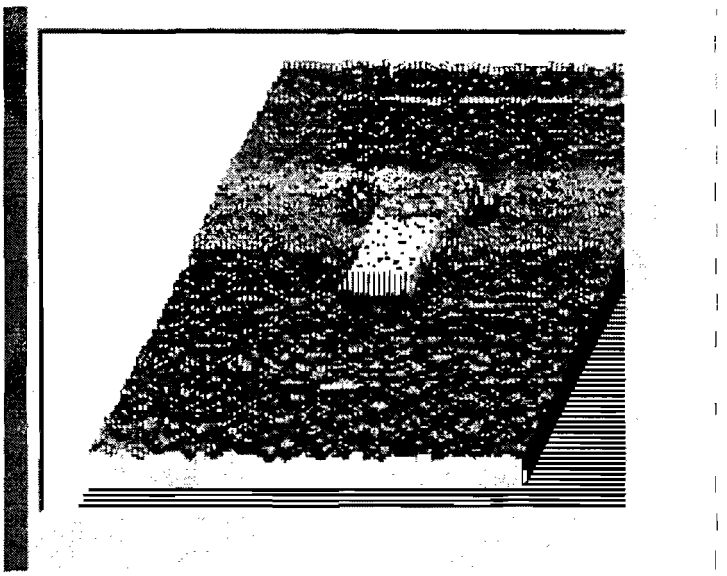

Figure 8.7 Pixel distribution of the picture with target.

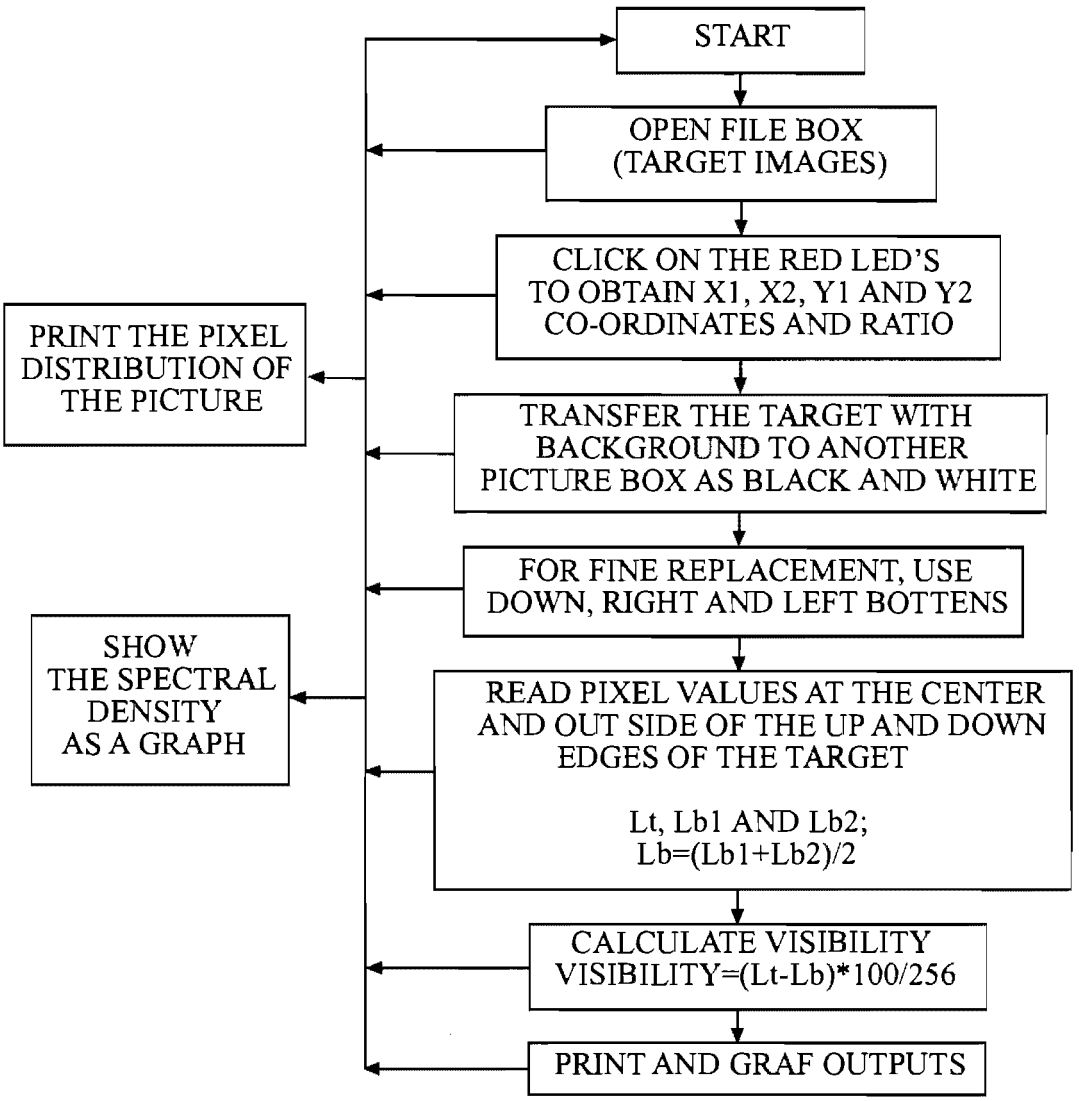

Figure 8.8 Flow chart of the picture analysis program.

Contrast Calculation Methods

As mentioned before, three different calculation methods were performed to determine the contrast of an STV target: VTC, VTC *n* points, VTCa. Figure 8.9a shows the VTC method, and Figure 8.9b shows the VTC *n* points and VTCa methods. In the figure, Pb's and Pt's are the pixel values. Of course these values proportionally related to the luminance values at that points.

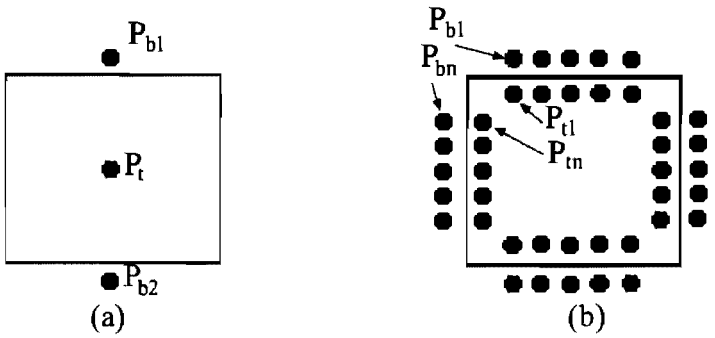

Figure 8.9 STV and contrast model.

Video Target Contrast (VTC) Method

Image analysis program calculates the contrast of the target using STV calculation method. As explained previously, STV method uses the luminance at the center of the target and mathematical average of the immediate outside luminance of the upper and lover boundaries to calculate the contrast as seen in Figure 8.9. In this section, pixel values (Figure 8.9a) will be use for contrast calculation instate of using luminance values. In general, pixel values are proportionally related to the luminance values. Furthermore, Equation (7.1) will be rearrange as a Video Target Contras (VTC) such as

$$VTC = \frac{P_t - P_b}{P_b} \tag{8.1}$$

where VTC : Video Target Contrast
P_t : Pixel value at the center of the target
P_b: Average pixel value of the target $P_b=(P_{b1}+P_{b2})/2$.

In this section, the image program uses Equation (8.1) to calculate the VTC of the target for each recorded image. Therefore, there are total 20 images recorded and analyzed for both of the lines between the installation. Figure 8.10 shows VTC distribution for 20% target. As seen from the figure, target has negative visibility except 2nd target location between the installation. From the image analysis if the VTC of the target is between the –0.2 and 0.2, the target is not visible (invisible). Therefore, Figure 8.10 show the target is invisible at the 2nd and 3rd target locations for both of the lines. Target visibility increases after 3rd target location to the 10th target location. It is also visible at the 1st target location. In general, the target has better visibility values on the line 1 that it is on the line 2.

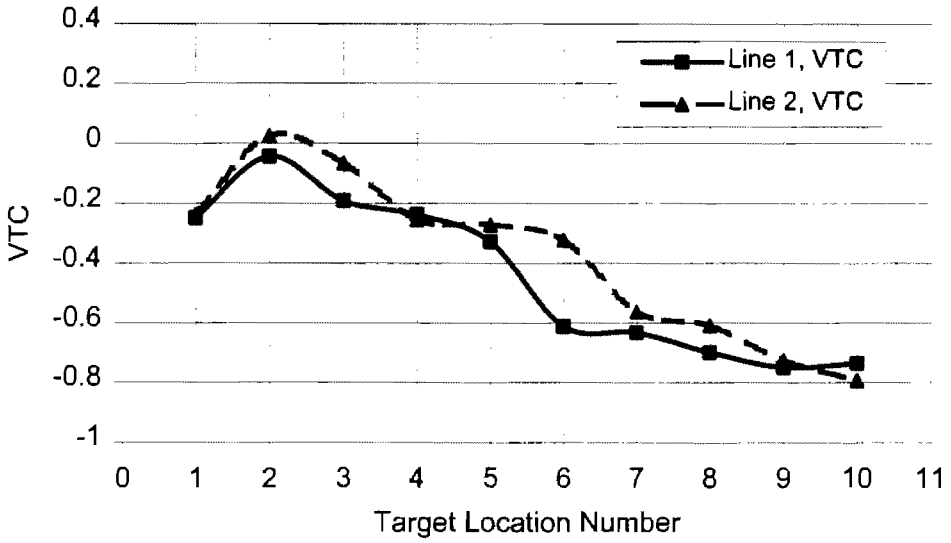

Figure 8.10 VTC distribution calculated from images for 20% reflective target on the lines 1 and 2.

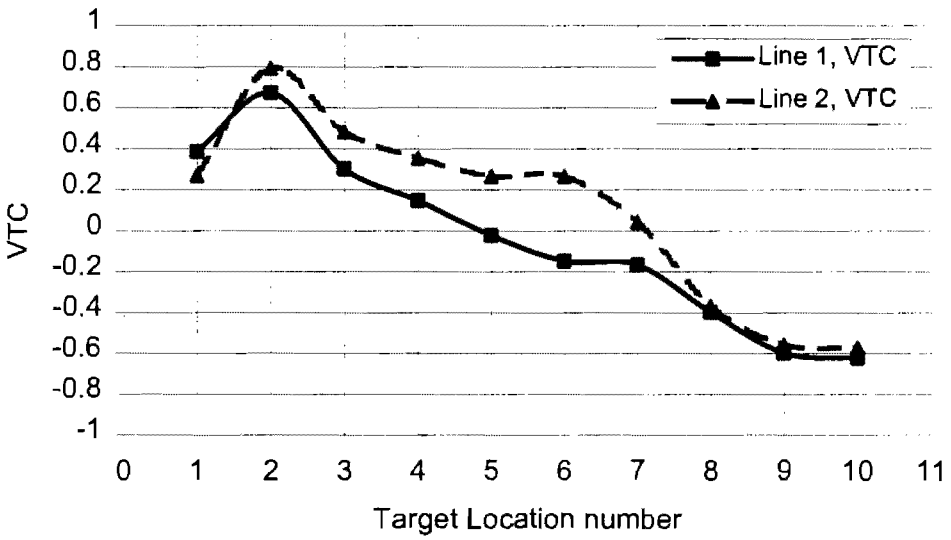

Figure 8.11 VTC distribution calculated from images for 50% reflective target on the lines 1 and 2.

Figure 8.11 shows VTC distribution of the 50% target. As seen from the figure, target has positive and negative visibility values. Figure 8.11 show the target is invisible at the 4^{th} trough 7^{th} target locations on the line 1 and 7^{th} on the line 2. At the rest of the target locations, the target is visible. In general, when the target is on the line 2, it has better visibility values than it is on the line 1.

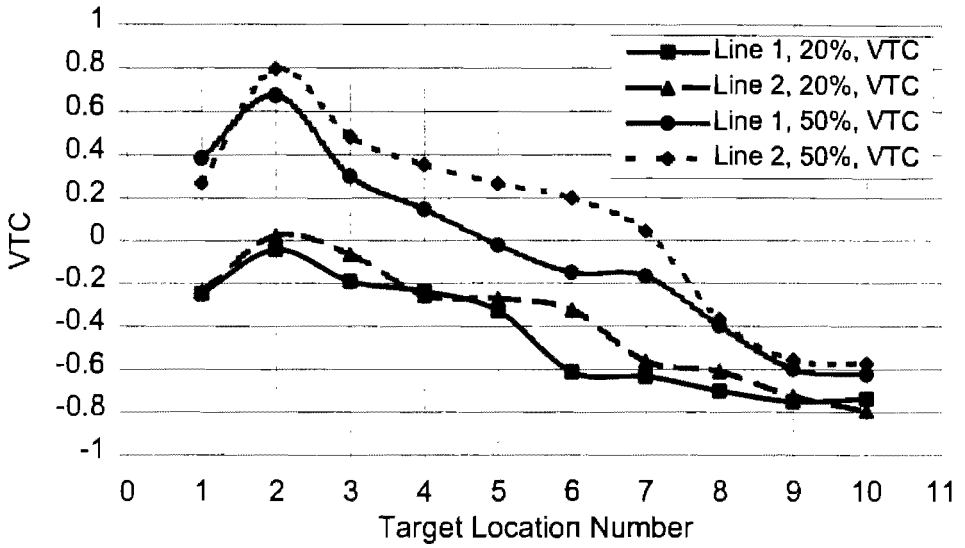

Figure 8.12 VTC distribution comparison for 20% and 50% reflective target on the lines 1 and 2.

Figure 8.12 show the contrast comparison of the 20% and 50% targets. Twenty percent target invisible at the 2nd and 3rd target locations, but fifty percent target invisible at the5th , 6th and 7th target locations. Therefore, 20% target gives better visibility result than fifty percent target. On the other hand 20% target more visible than 50% target under experimental field conditions.

Video Target Contrast *n* Points (VTCn) Method

In this section, Equation (8.1) is modified to calculate the contrast of the target. The center pixel value of the target is calculated by taking arithmetic average of the inside pixel values along the borders of the target (Figure 8.9b). The background pixel value of the target is calculated by taking arithmetic average of the outside pixel values along the borders of the target (Figure 8.9b). Therefore, the contrast equation is as the following.

$$VTCn = \frac{P_t - P_b}{P_b} \tag{8.2}$$

$$P_t = \frac{\sum_{i=1}^{n} P_{ti}}{n} \quad \text{and} \quad P_b = \frac{\sum_{i=1}^{n} P_{bi}}{n} \tag{8.3}$$

where $VTCn$: VTC n point
P_t : Average pixel value of the target
P_b: Average pixel value of the background.

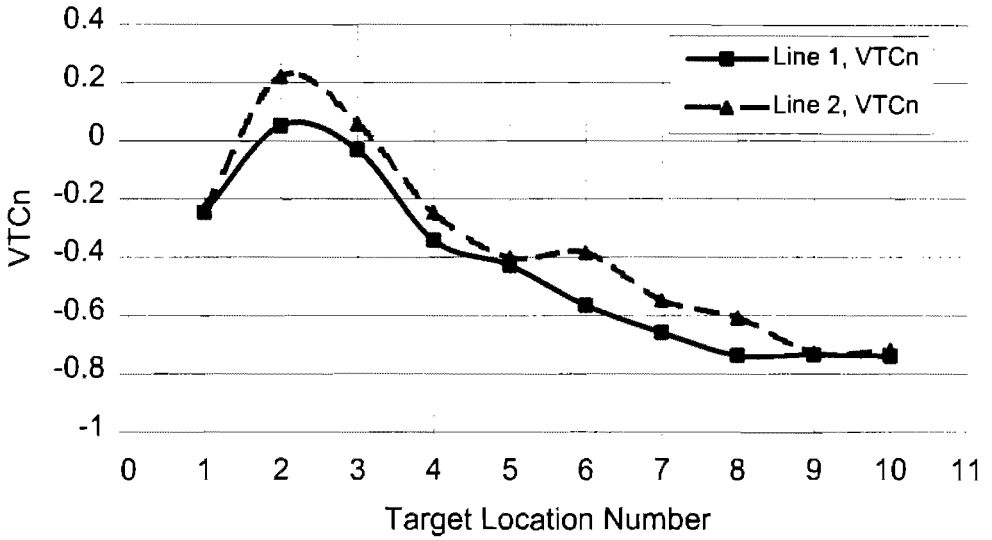

Figure 8.13 VTCn distribution calculated from images for 20% reflective target on the lines 1 and 2.

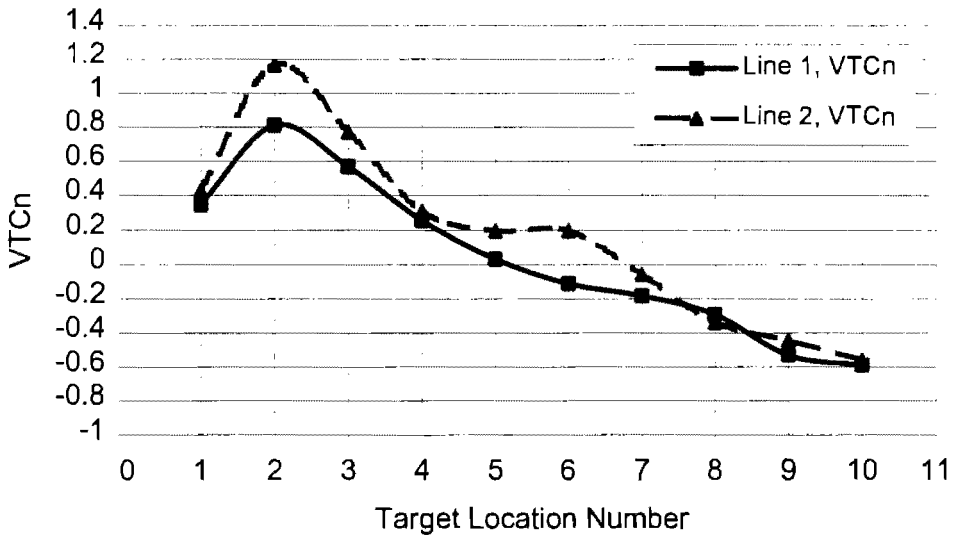

Figure 8.14 VTCn distribution calculated from images for 50% reflective target on the lines 1 and 2.

Video Target Contrast Average (VTCa) Method

In this section, Equation (8.1) is again modified to calculate the contrast of the target. For this purpose, contrast is calculated for each individual pixel (P_{ti} and P_{bi}) along the border of the target using the following formula as shown below.

$$C_i = \left| \frac{P_{ti} - P_{bi}}{P_{bi}} \right| \tag{8.4}$$

where C_i : Contrast at any point along the target border
P_{ti} : Pixel value at any point inside of the target border
P_{bi} : Pixel value at any point outside of the target border.

VTCa is defined arithmetic average of the contrast along the target boundaries yields the following equation.

$$VTCa = \frac{\sum_{i=1}^{n} |C_i|}{n} = \frac{\sum_{i=1}^{n} \left| \frac{P_{ti} - P_{bi}}{P_{bi}} \right|}{n} \tag{8.5}$$

where C_a is VTCa.

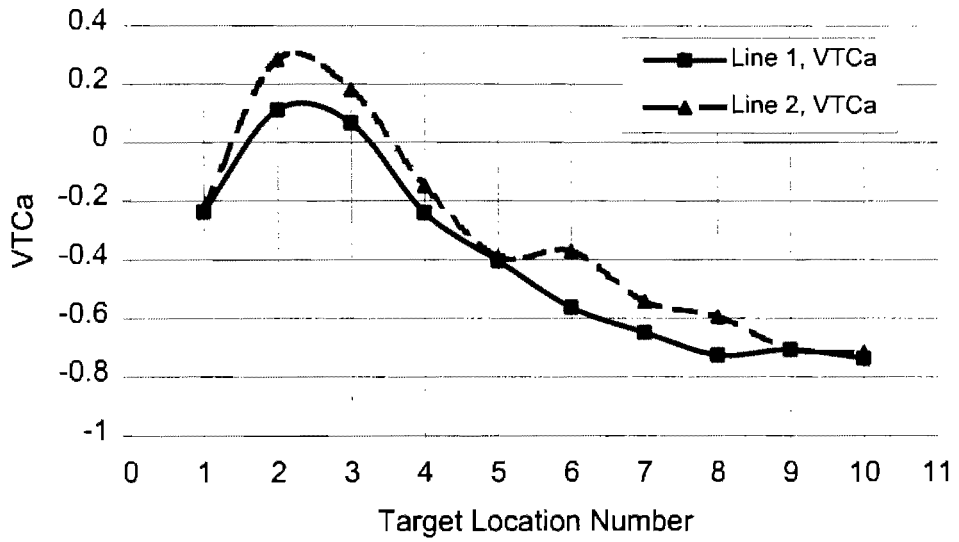

Figure 8.15 VTCa distribution calculated from images for 20% reflective target on the lines 1 and 2.

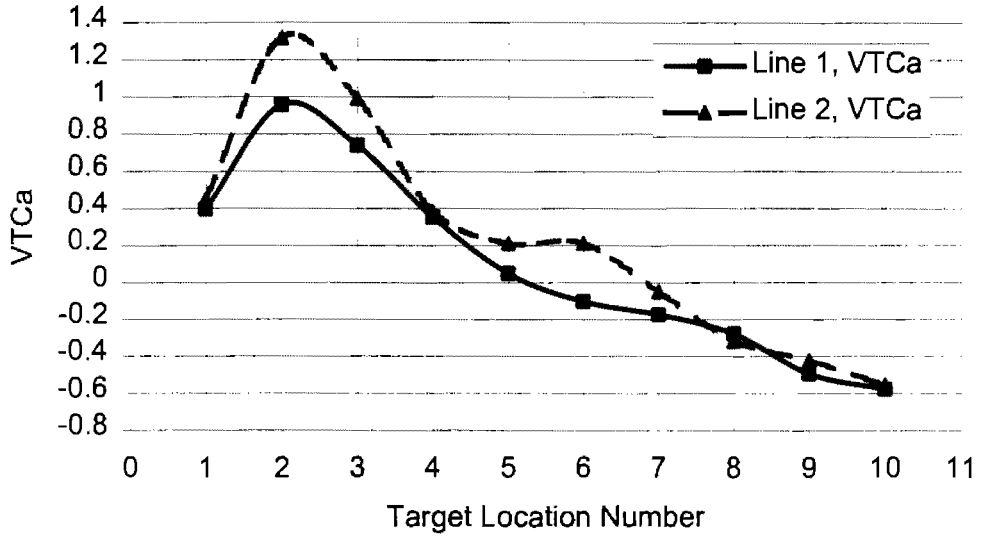

Figure 8.16 VTCa distribution calculated from images for 50% reflective target on the lines 1 and 2.

Comparison of Three Methods

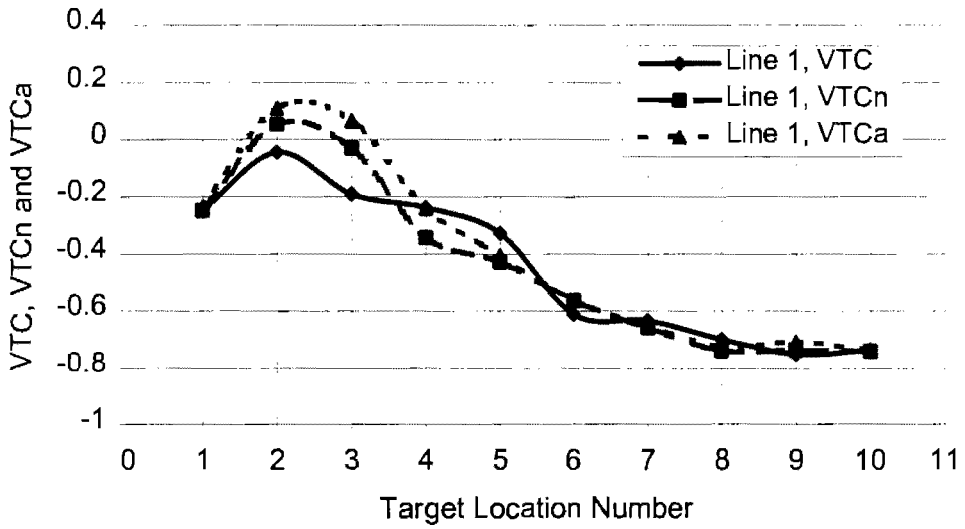

Figure 8.17 Contrast distribution of three methods for 20% target for on line 1.

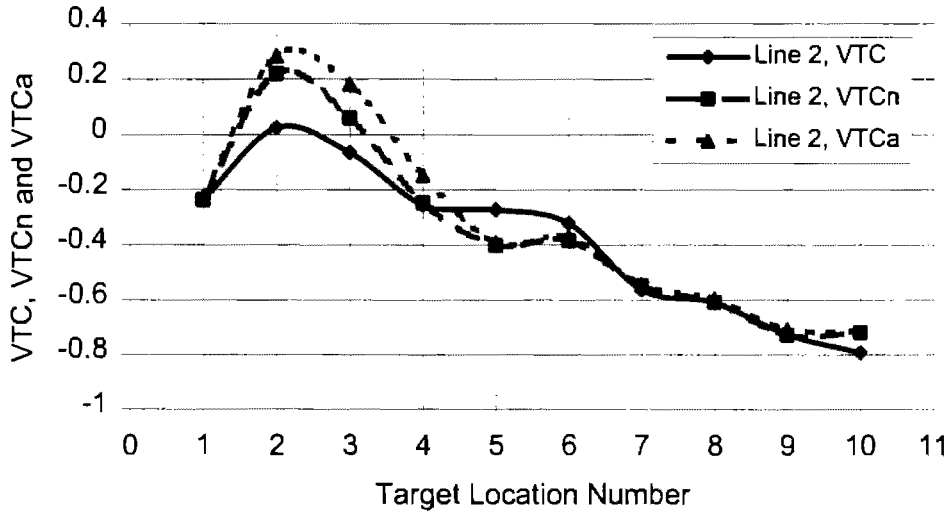

Figure 8.18 Contrast distribution of three methods for 20% target on line 1.

Figure 8.17 and 8.18 shows contrast values obtained using the three different methods for 20% target on line 1 and 2, respectively. As seen from the figures, after 6th and 1st target locations there are almost no contrast difference between the methods. But there is contrast difference between 2nd and 6th target locations.

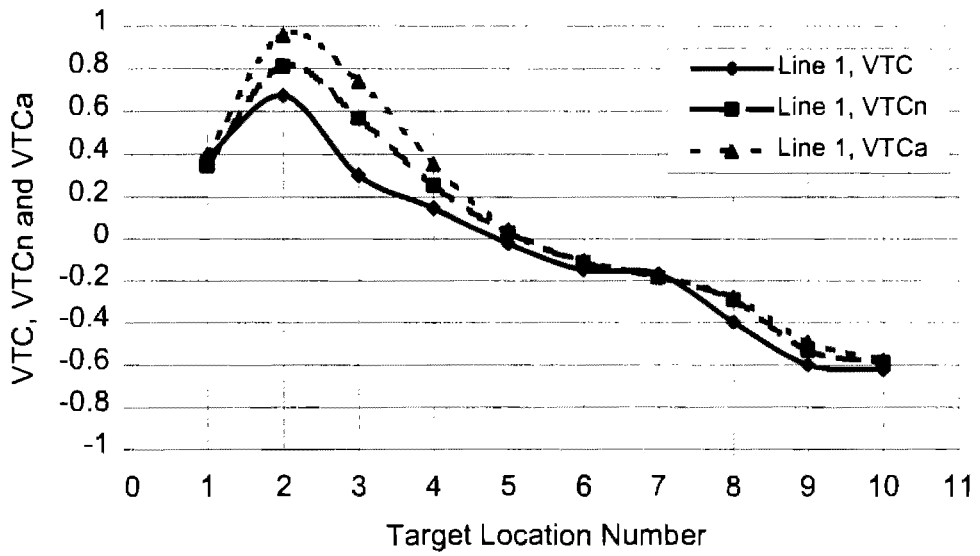

Figure 8.19 Contrast distribution of three methods for 50% target on line 1.

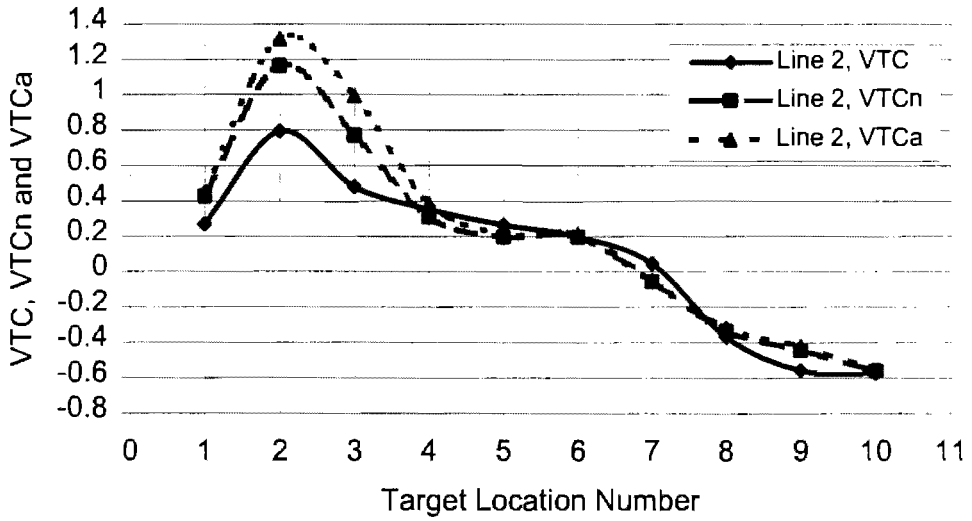

Figure 8.20 Contrast distribution of three methods for 50% target on line 1.

Figure 8.19 and 8.20 shows contrast values obtained using the three different methods for 50% target on line 1 and 2, respectively. As seen from the figures, between the 5th and 10th target location there is almost no contrast difference between the methods. But there is contrast difference between 1st and 4th target locations.

Contrast value difference between the methods is related to the sensitivity of the methods. VTC method only uses three values to calculate VTC whose values are at the center of the target and center of the immediate outside of the upper and lower borders. When only one value was taken center of the target, it means pixel (luminance) distribution on the target surface is uniform. But it is not in reality. Same assumption was made for the background pixel values. Only two values were taken one of them from middle of the upper border and the other from middle of the lower border. Average of these two values represents background luminance of the target. Again, pixel distribution along the upper and lower borders assumed uniform and pixel distribution along the two side borders was completely ignored or same distribution was assumed for upper and lower boundaries. In reality, pixel distribution is not uniform on the target surface, and along the boundaries, because photometric data of luminaires and roadway surface (background) are not uniform. Also, side borders of the target contribution to contrast of the target can not be ignored. This method which is the same method in terms of using luminance values with visibility level calculation (VL). VTCn method is more conservative and more realistic methods than VTC method. This method considers a lot of pixel values along the immediate inside and outside of the target boundaries. Therefore, the method considers pixel distribution along the upper and lower boundaries, also for the two side boundaries. Why around the boundaries because pixel differences at those locations creates contrast of the target, so, this method more realistic and better than VTC method.

VTCa method is more conservative and more realistic methods than VTC method and VTCn method. This method considers a lot of pixel values along the immediate inside and outside of the target boundaries as VTC *n* point method. Difference between the VTCn method and VTCa

method is that the target and background luminance calculates by taking average of the luminance (pixels) inside and outside of the target borders (Equation (8.3)), respectively, but VTCa method calculates the contrast for the each pixel combination (pixel inside and outside of the border), then calculates the VTCa by taking arithmetic average of the each calculated contrast for each pixel combinations (Equation (8.5)). As a result, this method gives contrast for each pixel reading locations along the boundaries of the target. Hence, it makes the VTCa method more realistic method than the other two for experimental study under the STV requirements.

Dynamic VTC

In this section, two targets are placed at the first target locations on the lines 1 and 2. The video is camera placed the maximum distance 425.9 ft from the targets and is moved 12 times toward the targets with 29.4 ft increments. Distance between the video camera and the targets is 102 ft when the video camera is placed at the first measurement location. Figures 8.21 through 8.30 show VTC distributions related to the observer (video camera) distance. As seen from Figure 8.21, the targets are visible at the any distance on the lines 1 and 2, but the better VTC is calculated when the observer was at the maximum distance. Reason for this, as we know visual acuity depends on contrast difference between the background and object, so longer observer distance creates low visual angle (less than 1 degree), on other hands large background. The large background provides better visibility for objects.

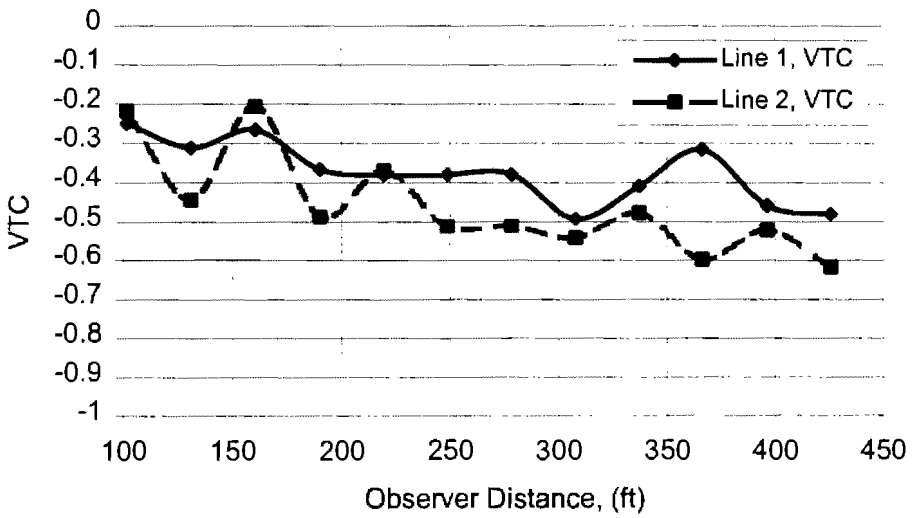

Figure 8.21 Dynamic contrast distribution for first target location on lines 1 and 2.

Figure 8.22 show same visibility distribution with respect to distance when the targets are placed at the second target locations on the lines 1 and 2. In the figure, targets have negative VTC when the observer was placed the distance longer than 175 ft. Targets have positive VTC when the observer locates closer than 175 ft. Targets are not visible between the distance 175 ft and 400 ft. As we know, if VTC between -0.2 and 0.2, target is not visible.

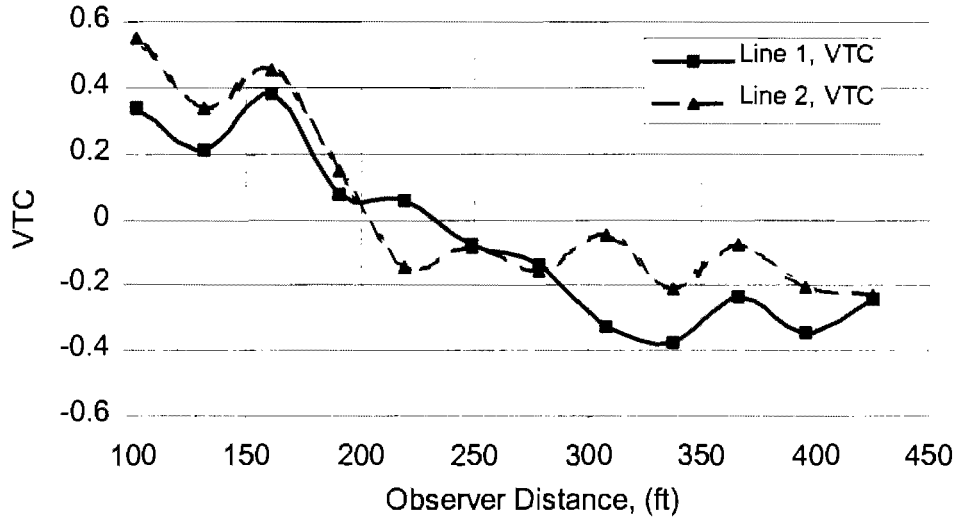

Figure 8.22 Dynamic contrast distribution for second target location on lines 1 and 2.

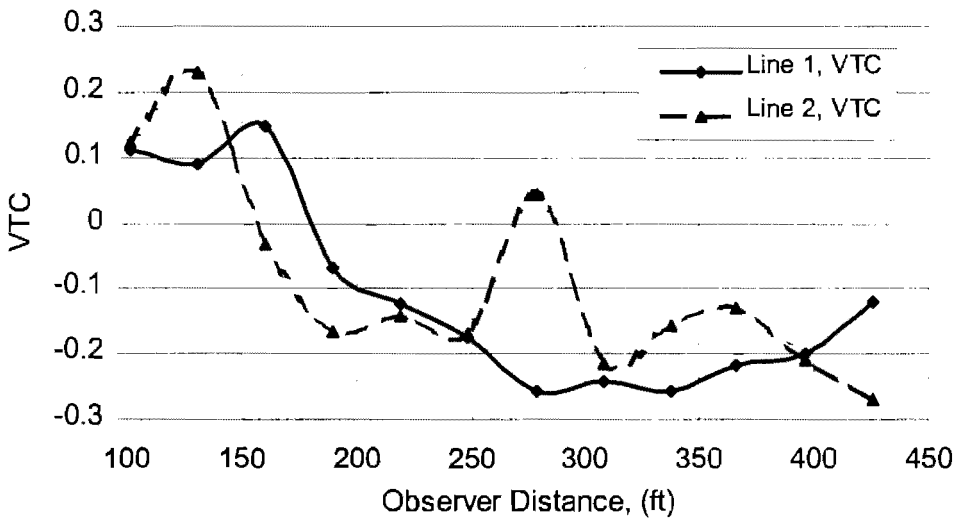

Figure 8.23 Dynamic contrast distribution for third target location on lines 1 and 2.

Figure 8.22 shows that the target is not visible at the distance longer than 175 ft. But the target is visible on the line one at the distance longer tan 280 ft. When the target was placed at the third target location (Figure 8.23), it is almost provides same behavior when the target replaced at the second target location (Figure 8.22).

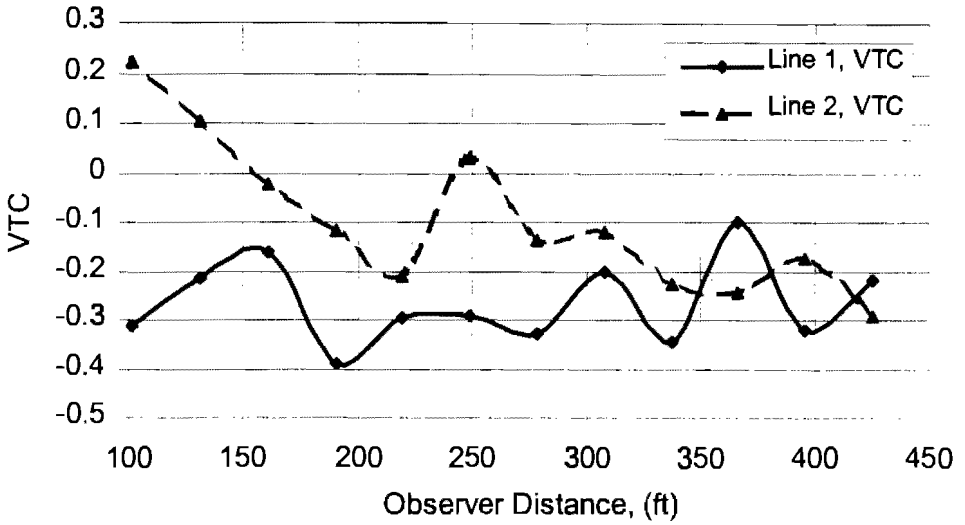

Figure 8.24 Dynamic contrast distribution for fourth target location on lines 1 and 2.

Figure 8.24 shows that the target is not visible when was placed on the line 1 except the distance more than 330 ft, but it is almost visible every where on the line 2.

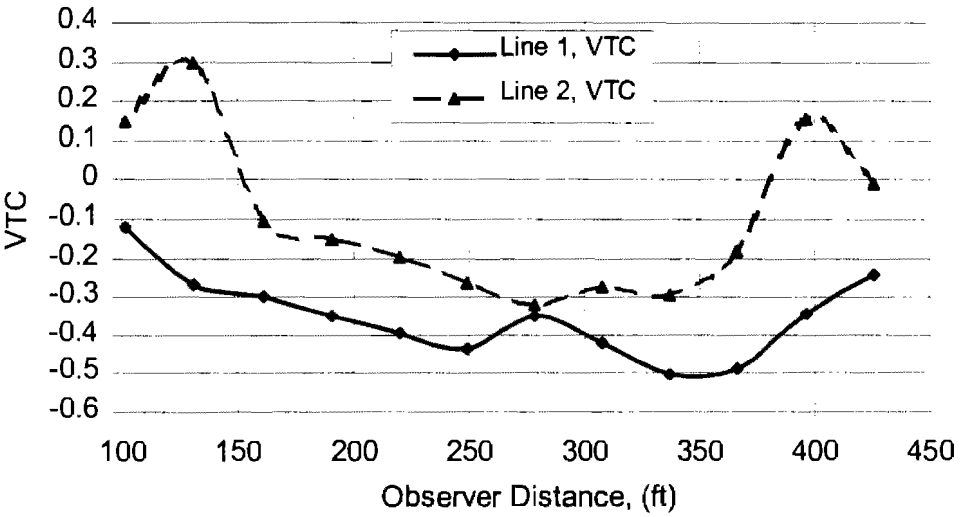

Figure 8.25 Dynamic contrast distribution for fifth target location on lines 1 and 2.

As seen from Figure 8.25, target is visible on the line 1 but it is not visible at the distances closer than 225 ft and longer than 370 ft.

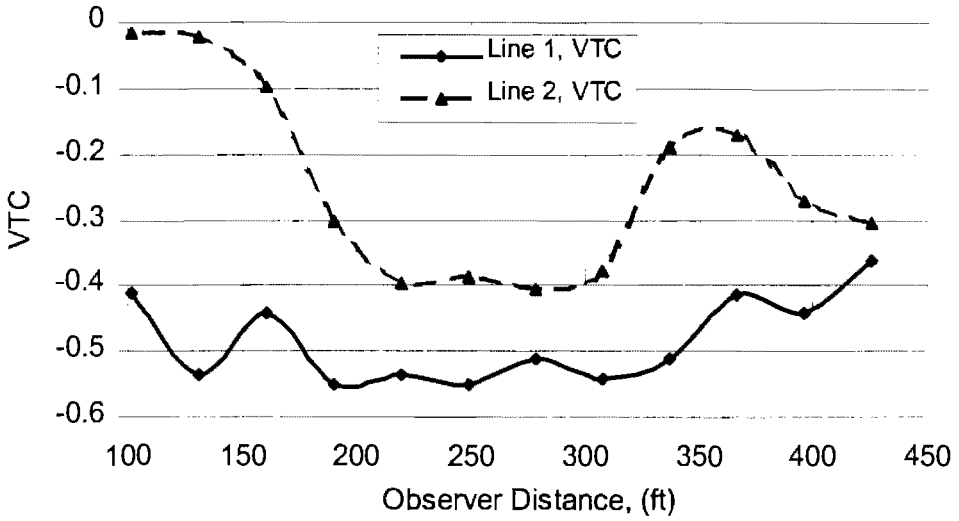

Figure 8.26 Dynamic contrast distribution for sixth target location on lines 1 and 2.

When the target is placed at the sixth target location, VTC values is not fluctuate between the positive and negative regions. Target is only invisible when the observer distance is closer than 175 ft.

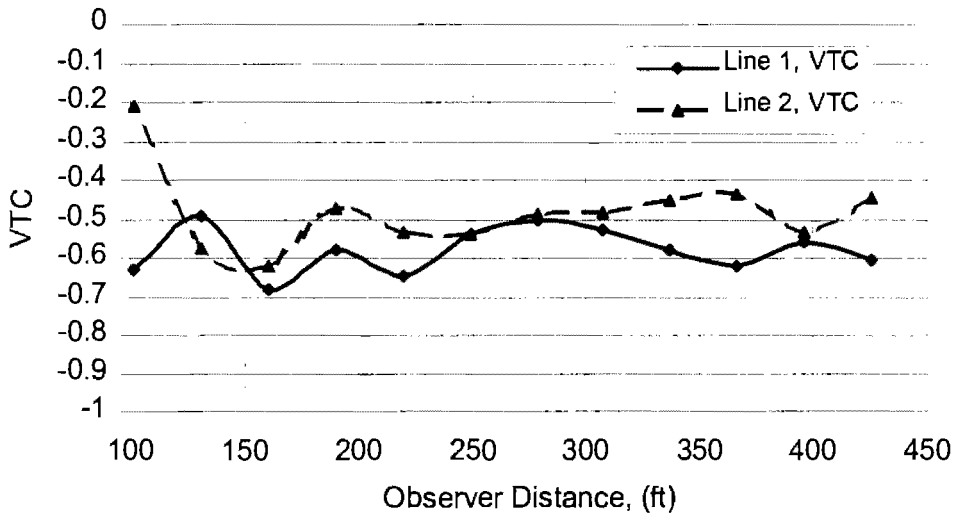

Figure 8.27 Dynamic contrast distribution for seventh target location on lines 1 and 2.

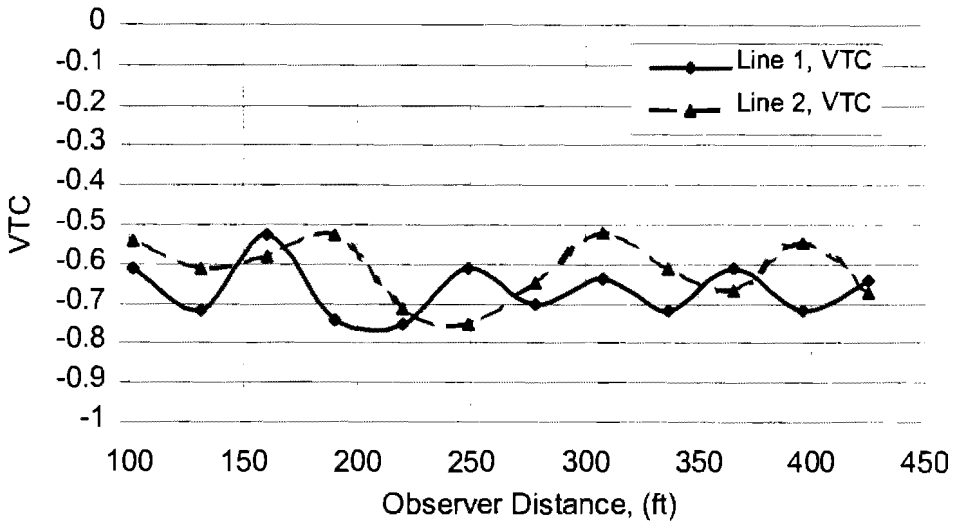

Figure 8.28 Dynamic contrast distribution for eighth target location on lines 1 and 2.

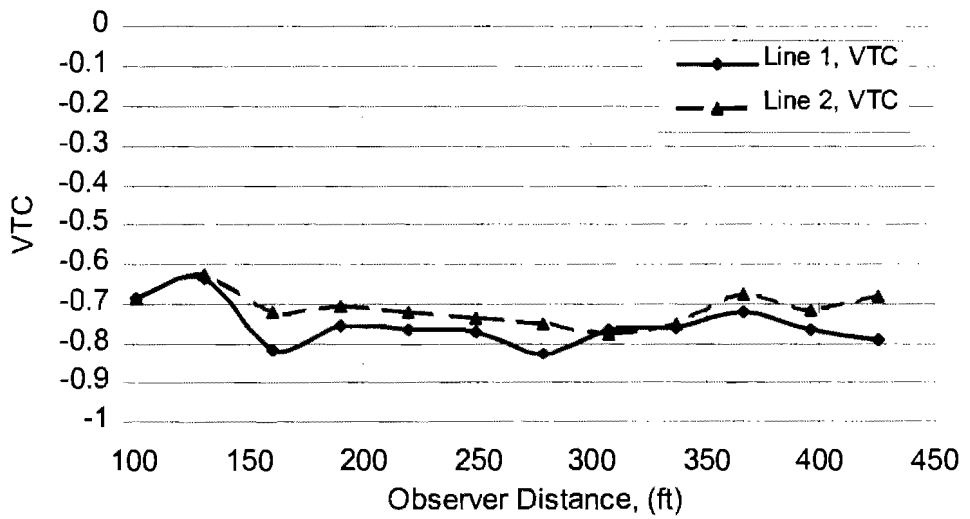

Figure 8.29 Dynamic contrast distribution for ninth target location on lines 1 and 2.

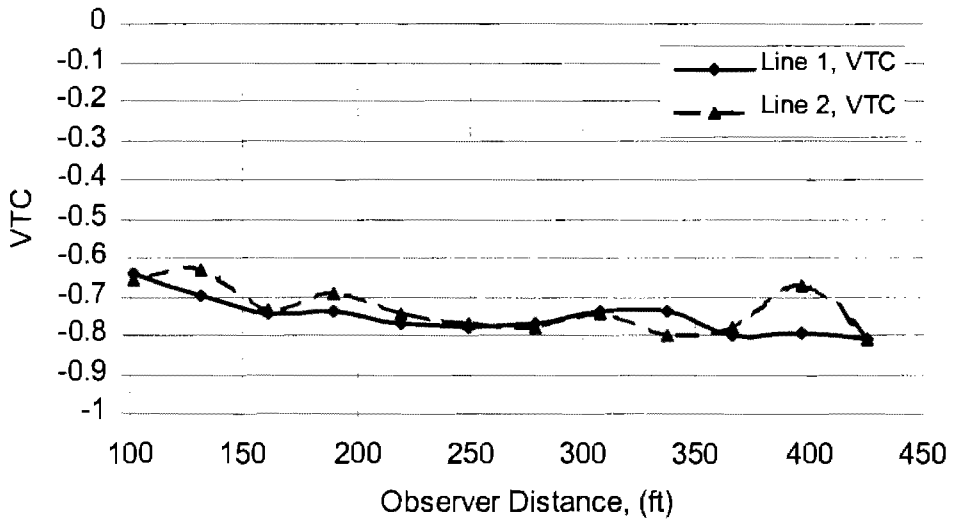

Figure 8.30 Dynamic contrast distribution for tenth target location on lines 1 and 2.

As seen from Figure 8.27 through 8.30, the target is visible and it has only negative VTC values when it is placed at the seventh thorough the tenth target locations.

Figures 8.21 through 8.25 show the same kind of dynamic behavior, the targets have negative and positive VTC values related to the observer location. VTC distribution related to the distance is not fluctuate between the negative and positive values when the targets are placed at the seventh, eighth, ninth and tenth target locations (Figure 8.26 through 8.30). Also, VTC distribution almost stays constant related to the distance.

In general, the figures show that observer has better visual acuity when observer gets far from the target. Reason for that longer distance creates small angle that provides better background luminance (large background). When the observer gets close to the target, observer visual angle gets larger that is provides small background. This experiments also give same result with regular VTC like target has worse VTC when it is at the first, second and third target locations, and after the third target location, its VTC value increases until tent target location. Figure 8.31 indicates that average VTC values distribution that is obtained by taking the averege of the twelve absolute values of the VTC for each target locations. The figure show dynamically the same distribution with the regular VTC. As seen that when target average VTC value is high at the first target location then it gets lower at the second and third target locations, after that it increases rest of the target locations.

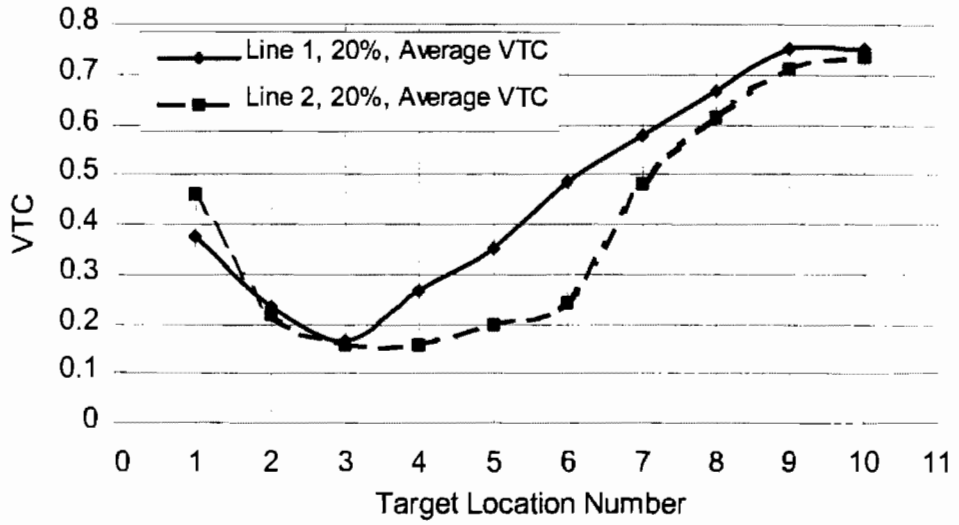

Figure 8.31 Average VTC distribution for tenth target location on lines 1 and 2.

Figure 8.32 through 8.43 show VTC distribution related to the target location under constant observer distance. For this experiments, targets are placed at the first target location and the video camera is placed at a constant distance (ex, 425.9 ft). After recording image of the targets, targets are placed at the second target locations on the line s 1 and 2 then the video camera distance is keep constant 425.9 ft. Experiment are performed until tent target locations. After that the targets images are recorded for twelve different constant distance and the following figures are plotted. Figure 8.32 through 8.43 show VTC of the target changes with respect to target location. It means target location itself creates VTC properties (target and background luminance)

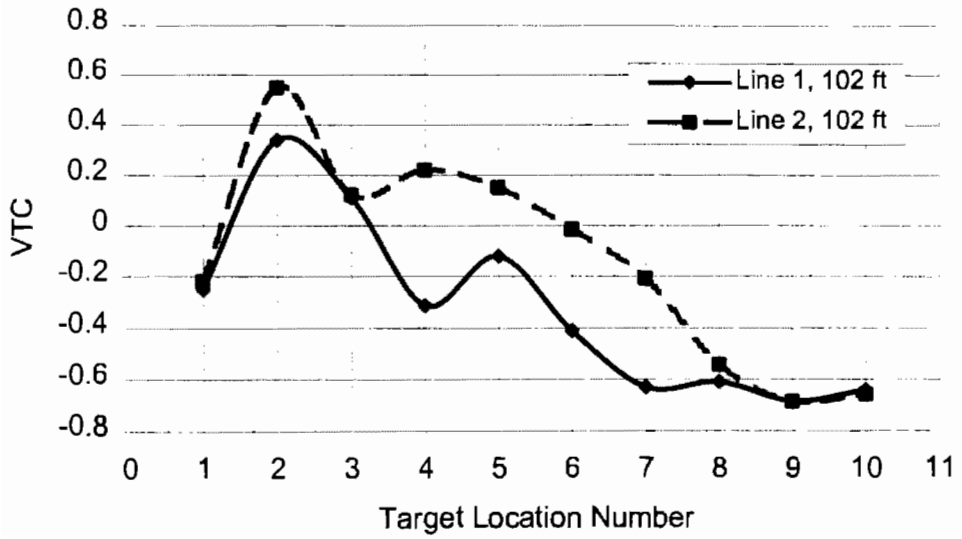

Figure 8.32 VTC distribution for constant distance 102 ft on lines 1 and 2.

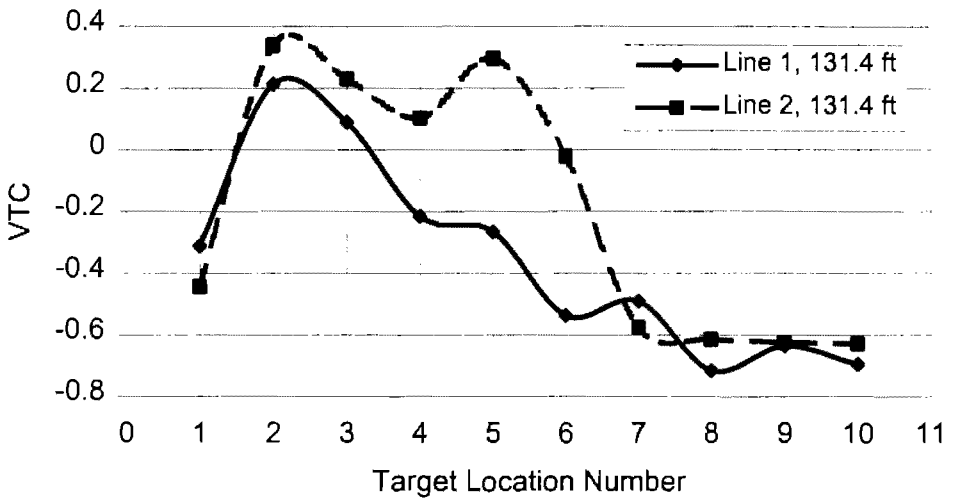

Figure 8.33 VTC distribution for constant distance 131.4 ft on lines 1 and 2.

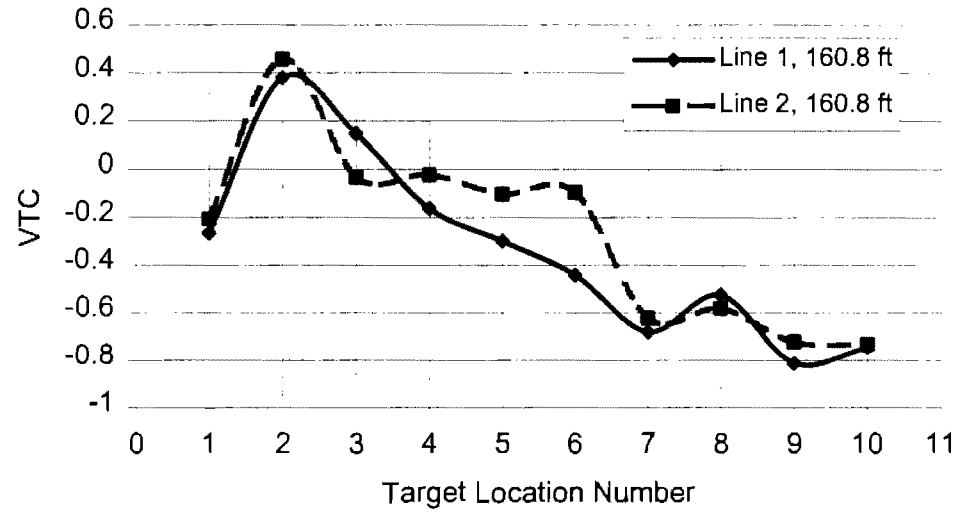

Figure 8.34 VTC distribution for constant distance 160.8 ft on lines 1 and 2.

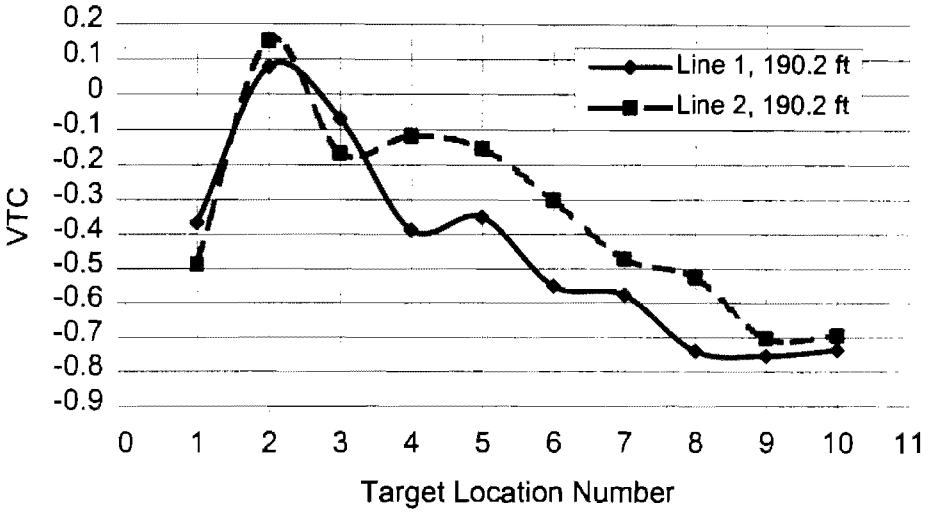

Figure 8.35 VTC distribution for constant distance 190.2 ft on lines 1 and 2.

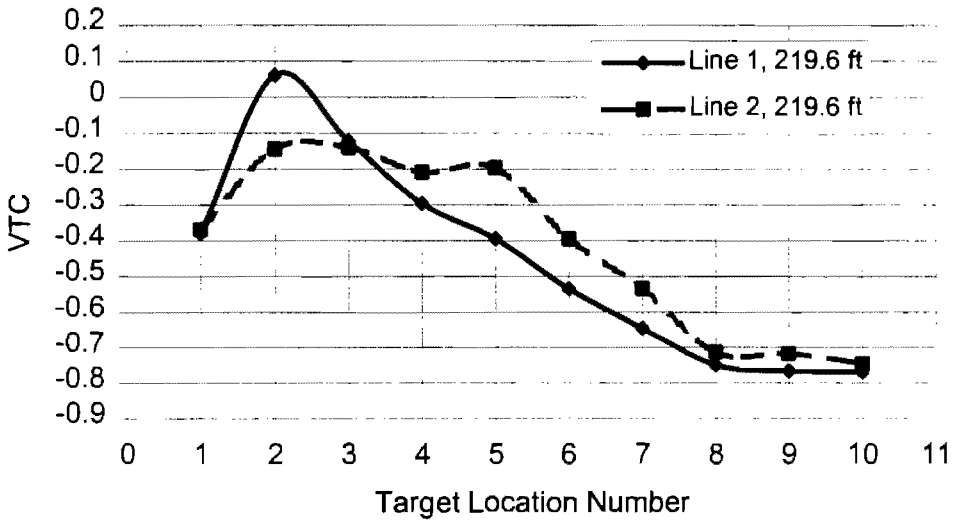

Figure 8.36 VTC distribution for constant distance 219.6 ft on lines 1 and 2.

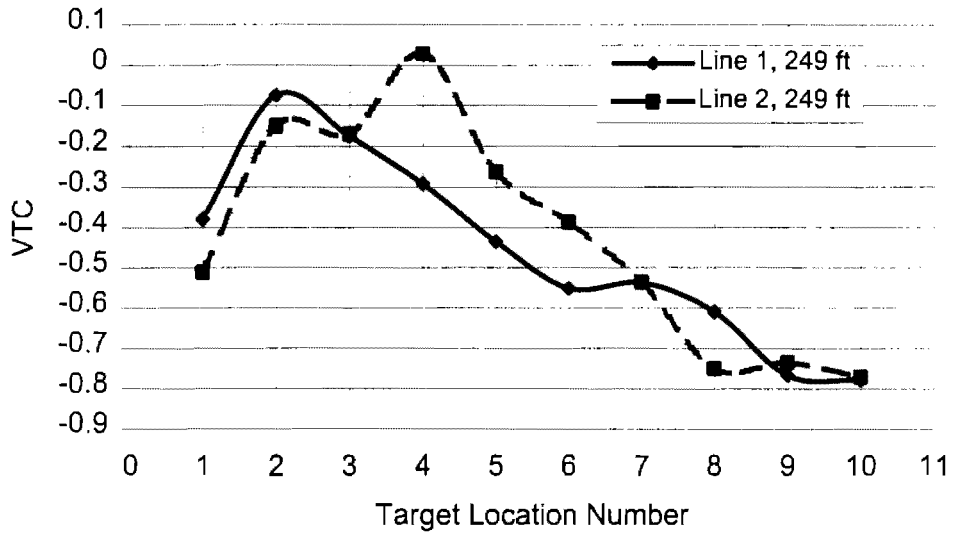

Figure 8.37 VTC distribution for constant distance 249 ft on lines 1 and 2.

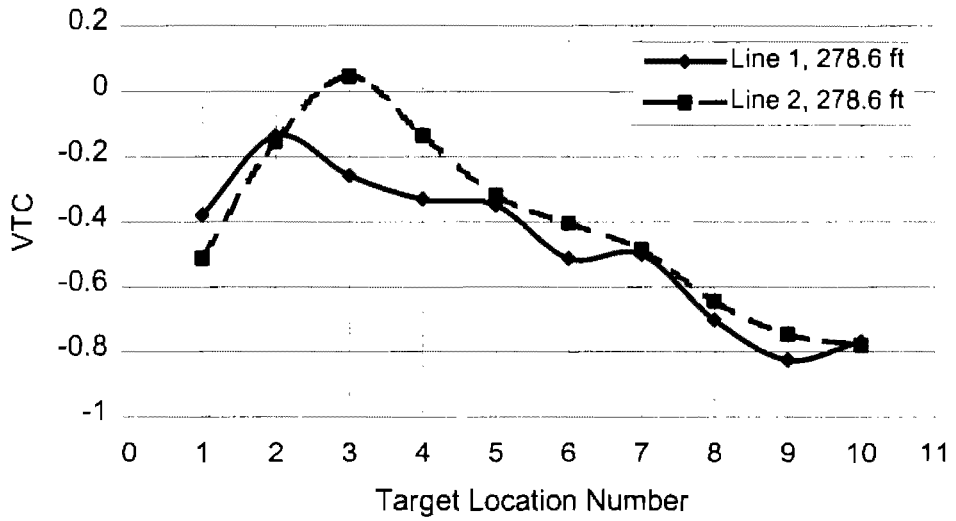

Figure 8.38 VTC distribution for constant distance 278.6 ft on lines 1 and 2.

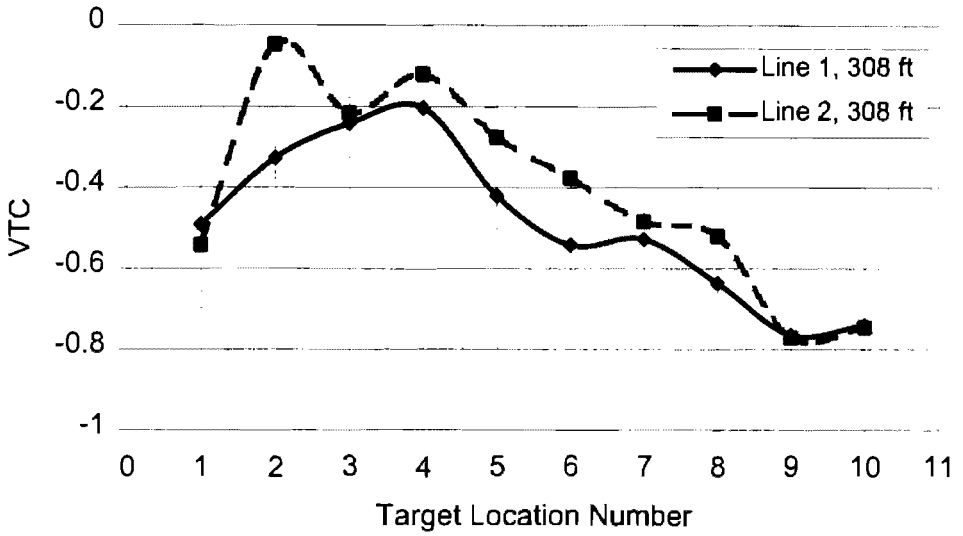

Figure 8.39 VTC distribution for constant distance 308 ft on lines 1 and 2.

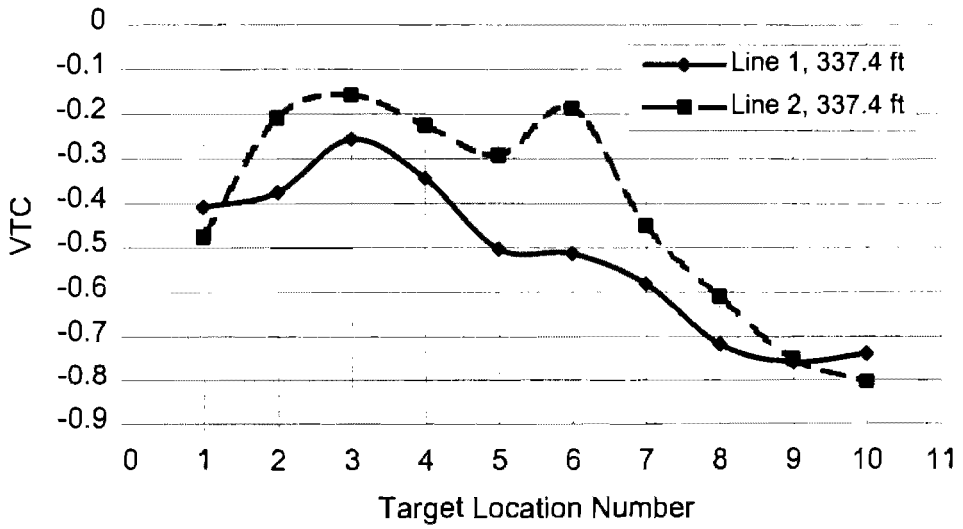

Figure 8.40 VTC distribution for constant distance 337.4 ft on lines 1 and 2.

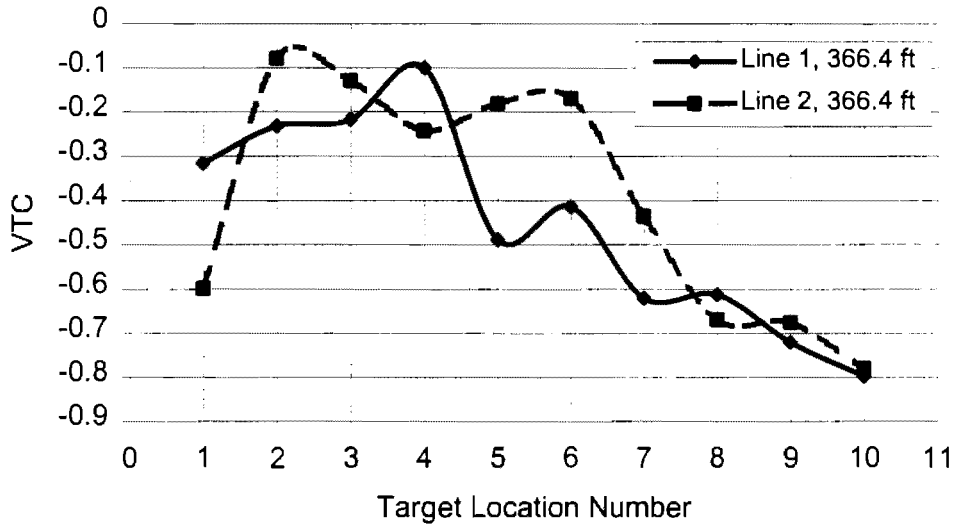

Figure 8.41 VTC distribution for constant distance 366.4 ft on lines 1 and 2.

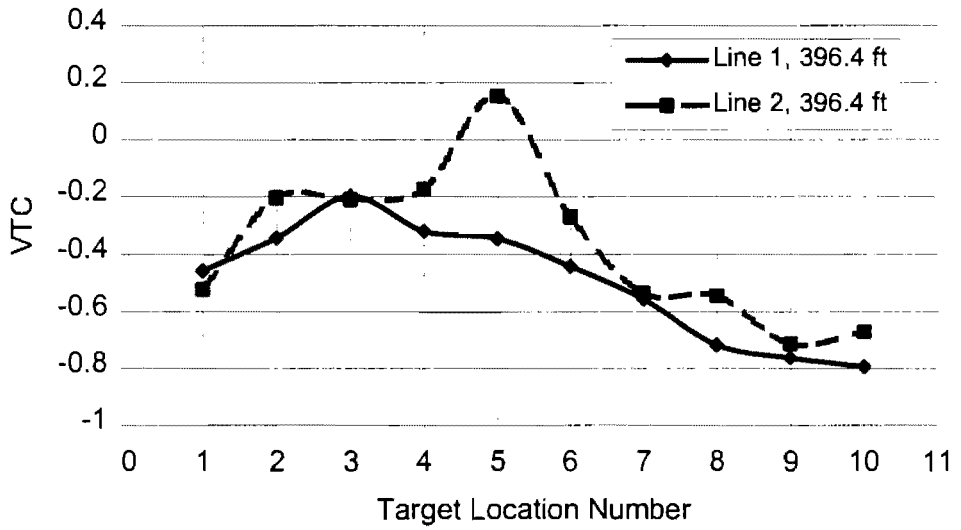

Figure 8.42 VTC distribution for constant distance 396.4 on lines 1 and 2.

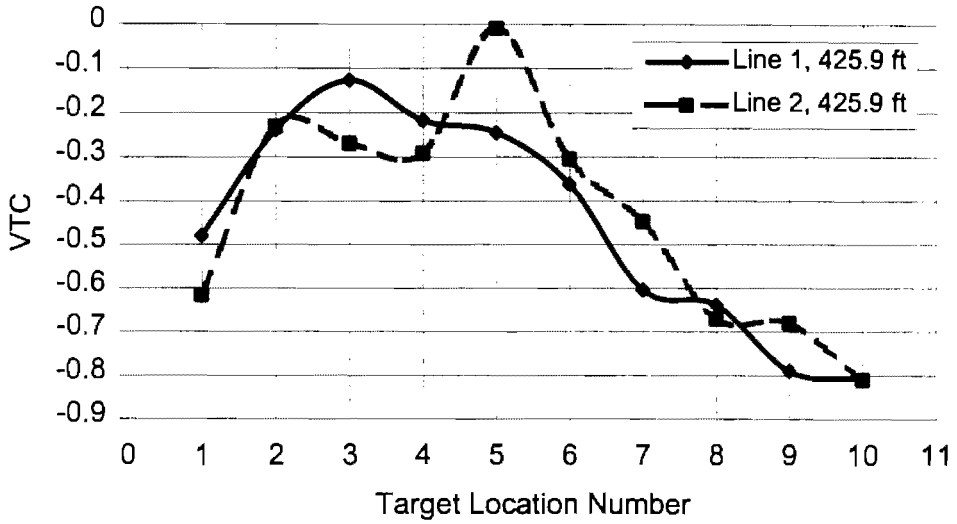

Figure 8.43 VTC distribution for constant distance 425.9 ft on lines 1 and 2.

Video Target Contrast Comparison

In this section, Luminance, Illuminance and STV methods will be compared with the Video Target contrast method. For the comparison, the luminance values is divided to its recommended value, the illuminance values is divided to its recommended value, the STV values is divided to its recommended value, and the VTC values is divided to its calibrated value. Results were called "normalized luminance (N. Luminance), normalized illuminance (N. Illuminance), normalized STV (NSTV) and normalized VTC (NVTC)".

Normalize of VTC

Normalization of the VTC, Calculated VTC values from images were divided to the value that obtained by calibration the video zoom. For this purpose, four people who have very good vision controlled the target image through the video camera and without video camera. Video camera zoom was set according to this calibration. The image, which is not visible, the VTC value was calculated and it was taken as a reference VTC number. All the other VTC numbers were divided to the reference number to obtain the threshold line for VTC values. Above the threshold is visible, otherwise it is not.

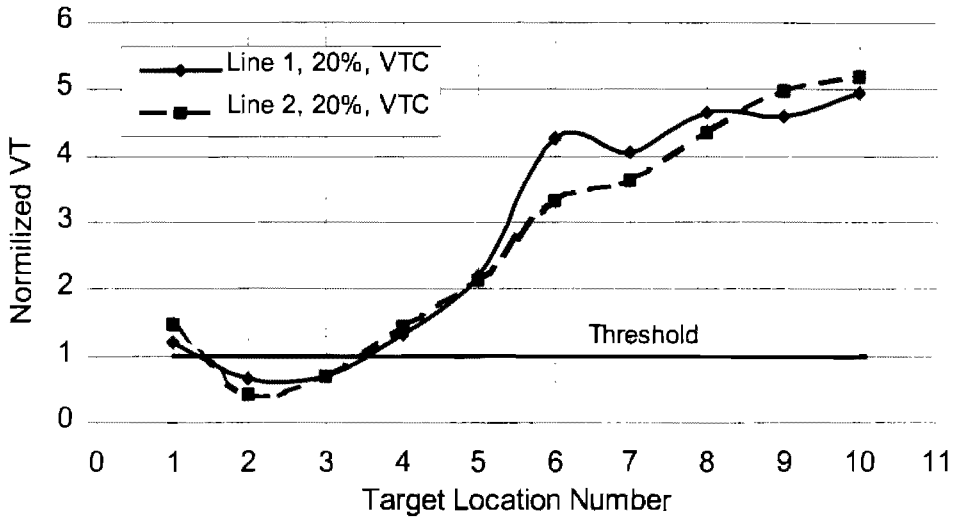

Figure 8.44 Normalized VTC distribution for lines 1 and 2.

As seen from the figure, target is not visible at the second and third target locations (down the threshold line). The target is visible at the rest of the target locations (above the threshold line).

Normalized VTC and Luminance Methods Comparison

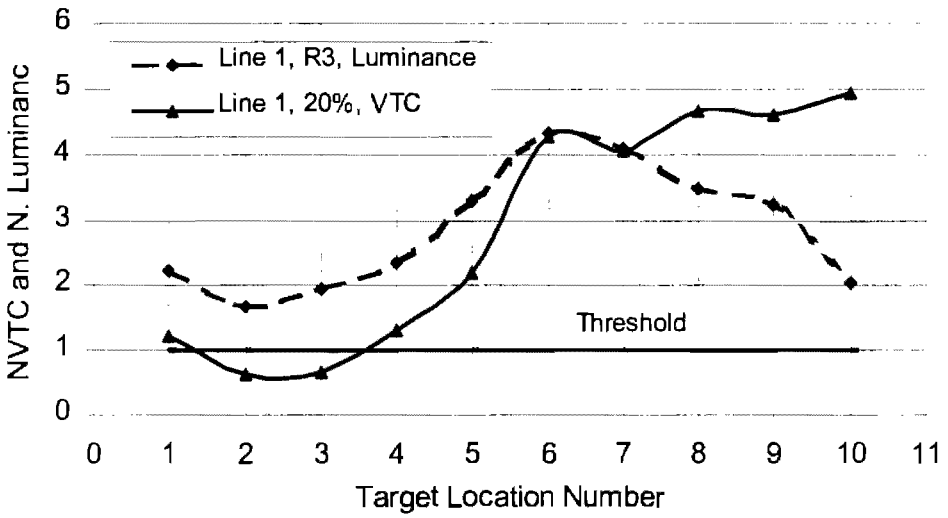

Figure 8.45 Comparison of the luminance and STV contrast methods on line 1.

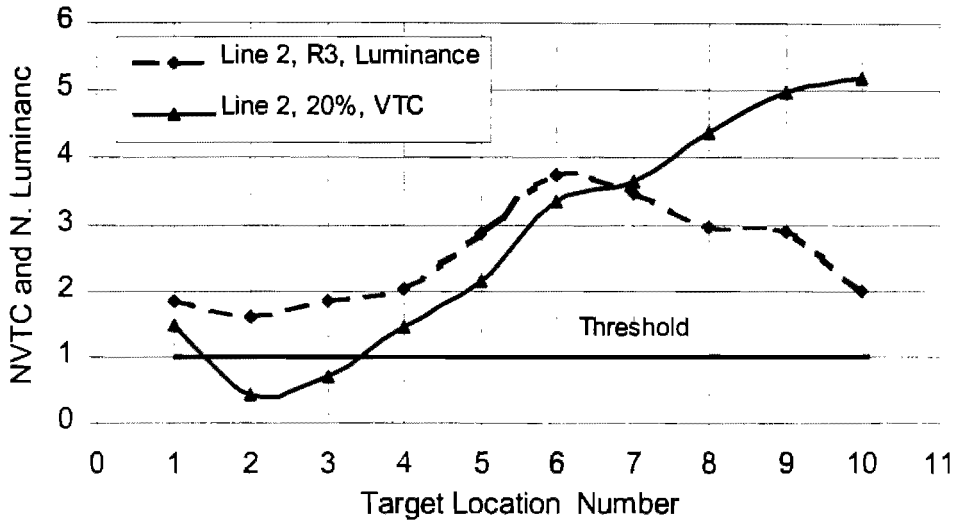

Figure 8.46 Comparison of the luminance and STV contrast methods on line 2.

Figure 8.46 and 8.46 shows the N. Luminance and NVTC distribution on the lines 1 and 2. Both figures, the normalized luminance and normalized VTC values indicates the same dynamic behavior. Both methods show high value at the first target location and the lover value at the second target location; values increase until sixth target location, after that when the luminance values increases between the sixth and tent target locations, the VTC values decrease at the same locations. The luminance value is only equal to the threshold value at the second location (Figures 8.45 and 8.46). It means that the target should be visible at the any point between the installations. VTC methods show the value lower than the threshold value at the second location as well as at the third location. It means that according to the VTC method, target is not visible at the second and third target locations. As a result; there are dynamically very close relation between both methods except the locations sixth through tenth. However even at these locations, both methods shows that the target is visible.

Normalized VTC and Illuminance Methods Comparison

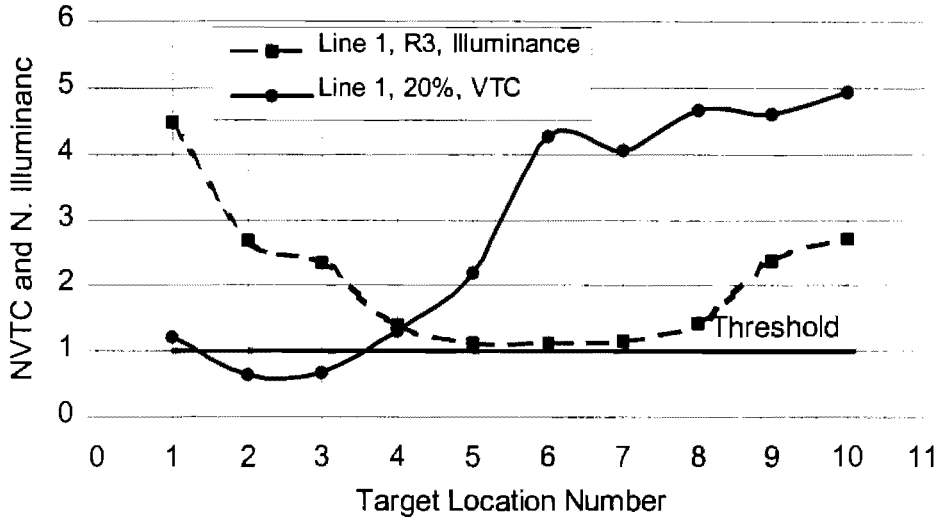

Figure 8.47 Comparison of the illuminance and STV contrast methods on line 1.

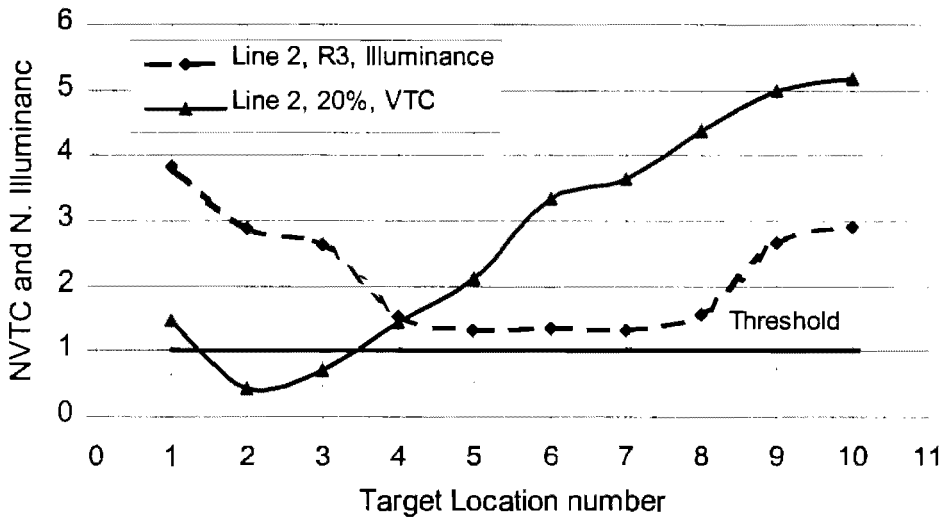

Figure 8.48 Comparison of the illuminance and STV contrast methods on line 2.

Figure 8.47 and 8.48 shows the illuminance and STV contrast distribution on the lines 1 and 2. Both figures, dynamic changing of the normalized illuminance and VTC values are completely different. The illuminance value starts with high value and continuously reduces until fourth target location. But the values are still above the threshold value. At the same distance, VTC values goes under the threshold value at the second and third locations and it stays above the threshold value at the rest of the locations. But the illuminance values stay constant between the fourth and eighth target locations. After that they increases until the tent target locations. According the illuminance method, target should be visible at the any point between the

installations. Additionally, illuminance and VTC distributions do not have same kind of dynamical behavior.

Normalized VTC and STV Methods Comparison

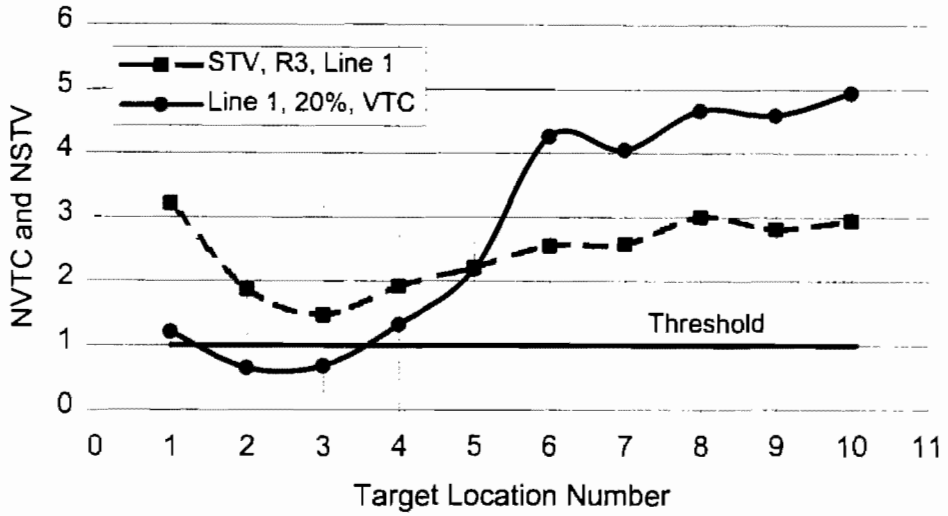

Figure 8.49 Comparison of the VTC and STV methods on line 1.

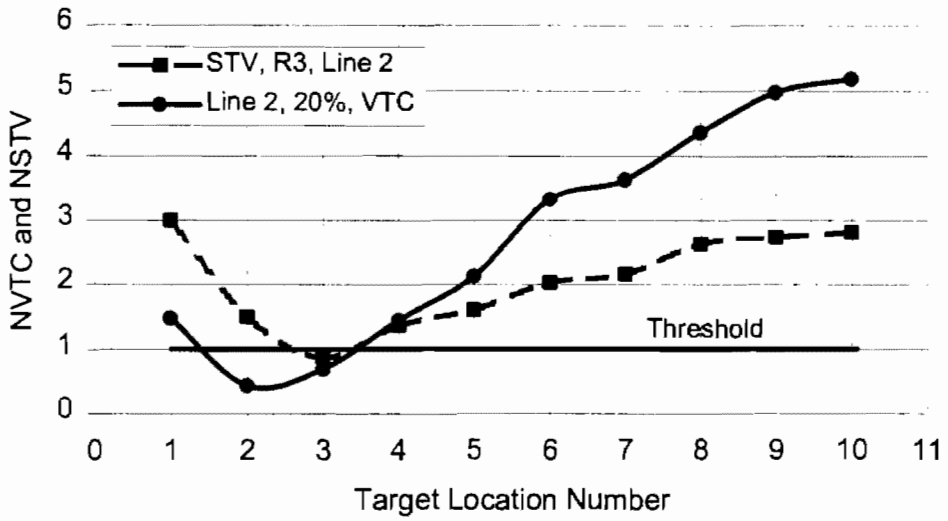

Figure 8.50 Comparison of the VTC and STV methods on line 2.

Figure 8.49 and 8.50 shows the normalized visibility level (VL) and VTC distribution on the lines 1 and 2. Both figures show that the dynamic changing of the VL and VTC values is the same. The VL values start with high value and continuously reduces until third target location. But the values are still above the threshold value on the line 1 except the NSTV value at the third

location on the line 2 is lower than the threshold value. At the same locations, VTC values goes under the threshold value at the second and third locations. The NSTV and VTC values are stay above the threshold level between the fourth and tent target locations. There is only one NSTV values under the threshold level at the third target location on the line 2. However, there are two VTC values at the second and third target locations under the threshold line on the lines 1 and 2. As a result; there are very close relation between the both methods dynamically except the third target location.

As a result, VTC method is the experimental method and it could be the reference for the theoretical methods. Because this values are the actual values recorded at the experimental field. The recorded target images can be seen in Figures 8.51 through 8.70 for only line 1. As seen from the images, the target is not visible when it vas at the second and third target location. When average ratios of the three methods (Table 7.11) was compared each other, the STV (ratio=2.08) and Illuminance (ratio=2.14) methods are the most conservative methods than the luminance (ratio=2.69) method. VTC method is dynamically more compatible with the STV and luminance methods (Figures 8.45, 8.46, 8.49 and 8.50). But according this both method, target should be visible at any point between the installation, but it is not visible at the second and third target locations according to the experimental analysis (VTC).

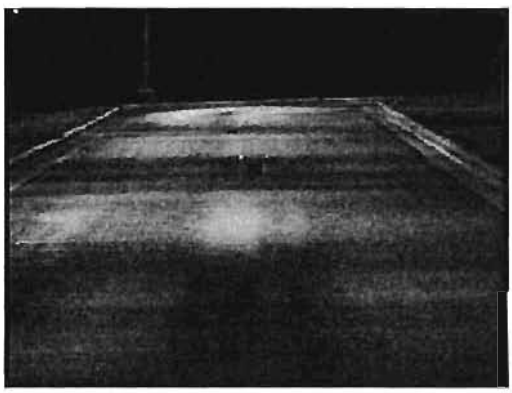

Figure 8.51 20% target image at the first target location on line 1.

Figure 8.52 20% target image at the second target location on line 1.

Figure 8.53 20% target image at the third target location on line 1.

Figure 8.54 20% target image at the fourth target location on line 1.

Figure 8.55 20% target image at the fifth target location on line 1.

Figure 8.56 20% target image at the sixth target location on line 1.

Figure 8.57 20% target image at the seventh target location on line 1.

Figure 8.58 20% target image at the eighth target location on line 1.

Figure 8.59 20% target image at the ninth target location on line 1.

Figure 8.60 20% target image at the tenth target location on line 1.

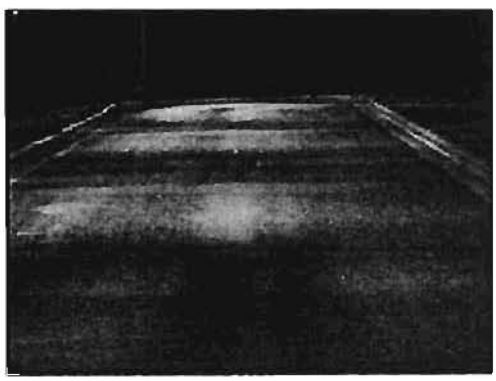

Figure 8.61 20% target image at the first target location on line 2.

Figure 8.62 20% target image at the second target location on line 2.

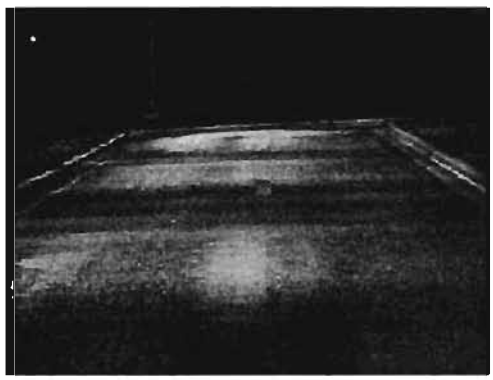

Figure 8.63 20% target image at the third target location on line 2.

Figure 8.64 20% target image at the fourth target location on line 2.

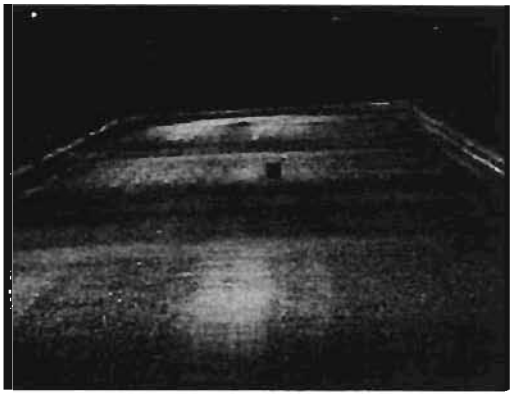

Figure 8.65 20% target image at the fifth target location on line 2.

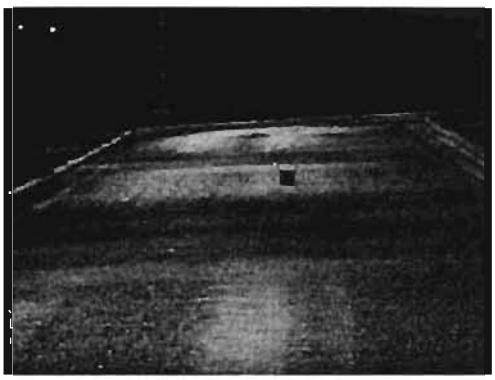

Figure 8.66 20% target image at the sixth target location on line 2.

Figure 8.67 20% target image at the seventh target location on line 2.

Figure 8.68 20% target image at the eighth target location on line 2.

Figure 8.69 20% target image at the ninth target location on line 2.

Figure 8.70 20% target image at the tenth target location on line 2.

Normalized VTC and STV Method Comparison for 50% Target

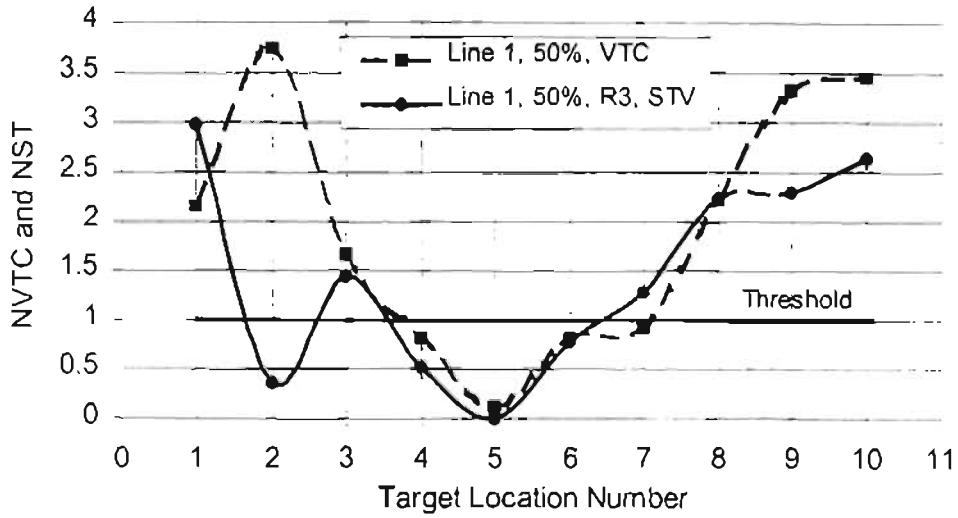

Figure 8.71 Comparison of the illuminance and STV contrast methods on line 1.

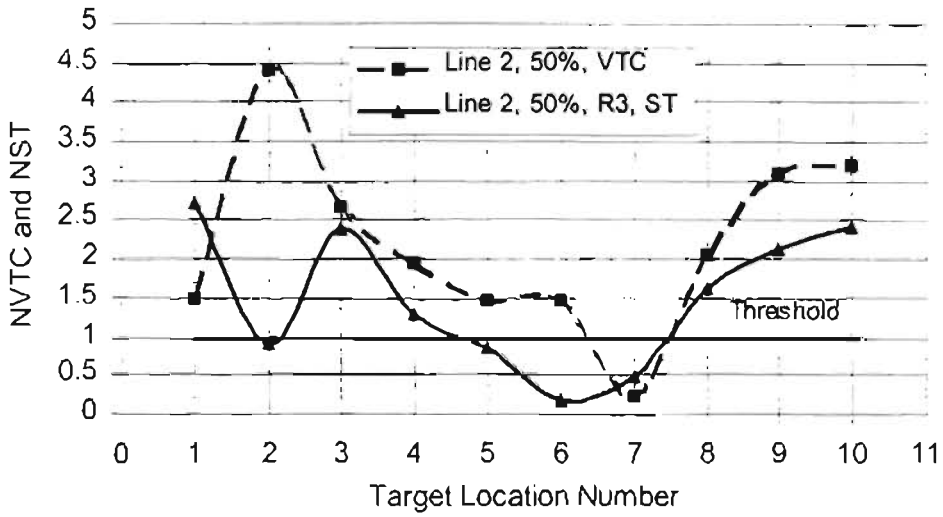

Figure 8.72 Comparison of the illuminance and STV contrast methods on line 2.

Figure 8.71 and 8.72 were obtained by dividing VTC and STV values to their threshold values and show the NVTC and NSTV distribution on the lines 1 and 2. Both figures, dynamic changing of the normalized NVTC and NSTV values are completely different until the third target location. As seen from the figures, while VTC values increase from the target location one to two then it is decreases from the target location two the three, STV values degreases from the target location one to two then it is increases from the target location two the three. At the target location two, target is visible according to the VTC but it is not visible according to the STV. The target is invisible at the fourth, fifth and sixth targets locations on the line 1 according to

both methods. But the target is not visible at the fifth, sixth and seventh targets locations on the line 2 according to the STV method but it is only invisible at the seventh target location on the line 2 according to the VTC method. As a result; this two method does not dynamically related each other until the third target location, especially there is big value difference at the second target location, but after there is nut much difference except the tenth target location, also both results are dynamically compatible. The images of the 50% targets are given Figures 8.73 through 8.92. From the Figure 8.74, the target is very clearly seen that it is visible but according to the STV it is not.

According to this comparison, STV method does not also give good result for 50% target. This method needs to be improving to obtain realistic STV distribution.

Figure 8.73 50% target image at the first target location on the line 1.

Figure 8.74 50% target image at the second target location on the line 1.

Figure 8.75 50% target image at the third target location on the line 1.

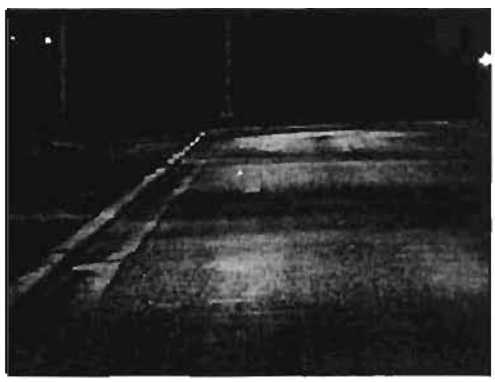

Figure 8.76 50% target image at the fourth target location on the line 1.

Figure 8.77 50% target image at the fifth target location on the line 1.

Figure 8.78 50% target image at the sixth target location on the line 1.

Figure 8.79 50% target image at the seventh target location on the line 1.

Figure 8.80 50% target image at the eighth target location on the line 1.

Figure 8.81 50% target image at the ninth target location on the line 1.

Figure 8.82 50% target image at the tenth target location on the line 1.

Figure 8.83 50% target image at the first target location on line 2.

Figure 8.84 50% target image at the second target location on line 2.

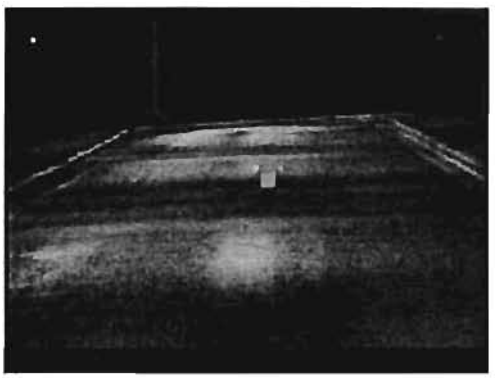

Figure 8.85 50% target image at the third target location on line 2.

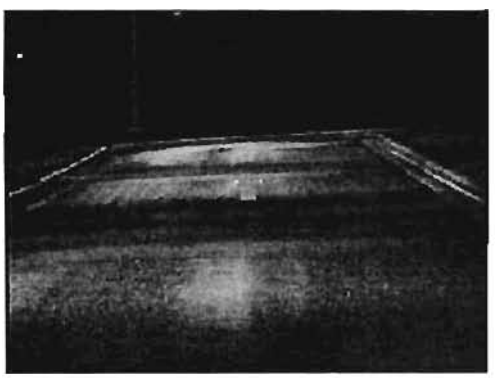

Figure 8.86 50% target image at the fourth target location on line 2.

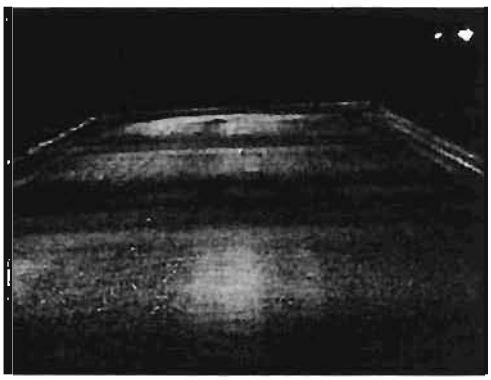

Figure 8.87 50% target image at the fifth target location on line 2.

Figure 8.88 50% target image at the sixth target location on line 2.

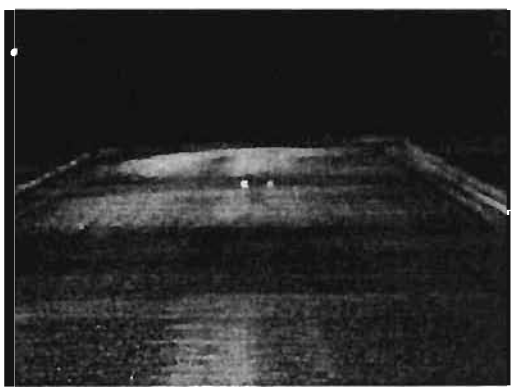

Figure 8.89 50% target image at the seventh target location on line 2.

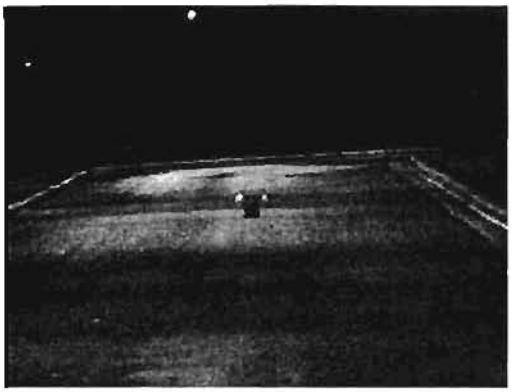

Figure 8.90 50% target image at the eighth target location on line 2.

Figure 8.91 50% target image at the ninth target location on line 2.

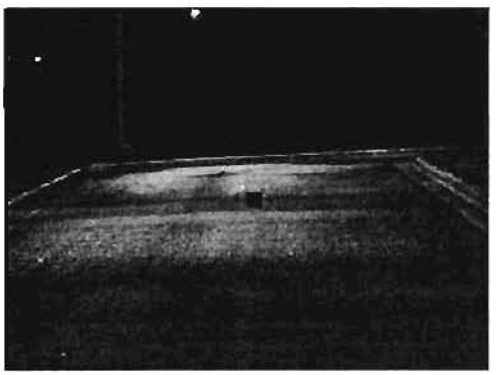

Figure 8.92 50% target image at the tenth target location on line 2.

CHAPTER 9: ANALYSIS OF THE STV AND VTC METHODS

In this section, some of the RP-8 assumptions will be examined by using recording images in the experimental field.

Pixel Distribution

Before plotting the pixel distribution along the immediate outside and inside of the target that is obtained from recording images in the experimental field. The 20% reflective surface target placed on the white background in the laboratory (Figure 6.1) and its images recorded. After that the pixel distribution inside and outside of the target borders were plotted to provide base information of pixel distribution. Figure 6.2 and 6.3 provides pixel distributions of the along the target borders. Figure 6.2 indicates pixel distribution outside of the target borders (background). As seen from the figure, pixel distribution on the background is very close the constant distribution (2.1% fluctuation). Figure 6.3 indicates pixel distribution inside of the target borders. As seen from the figure, pixel distribution on the target surface is also very close the constant distribution (3% fluctuation). The pixel fluctuation on the target surface bigger than the background pixel fluctuating because target sits 90 degree on the surface which is create the background luminance and there is no extra light was used to provide light for the target surface.

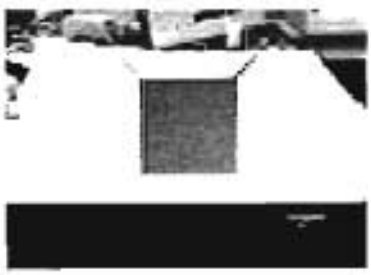

Figure 9.1 Test target in the laboratory.

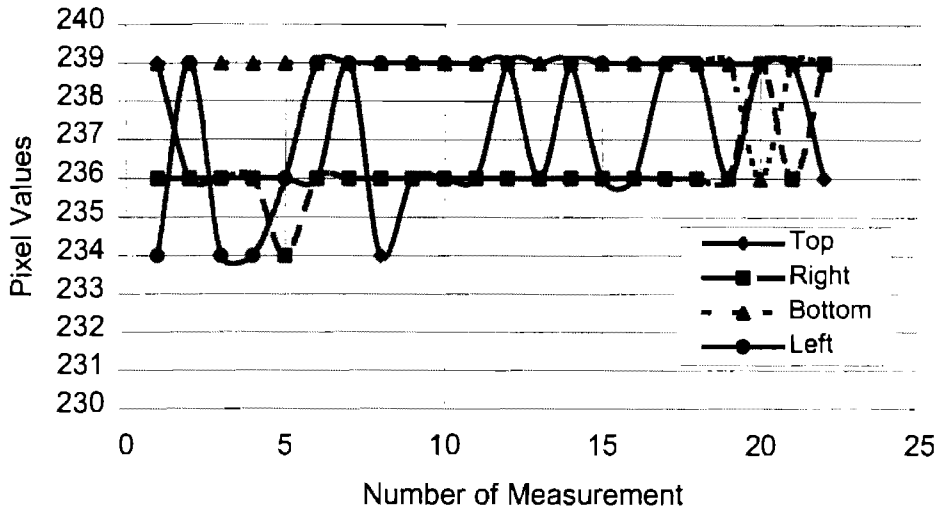

Figure 9.2 Pixel distribution of the test target along the outside of the boarder of the target.

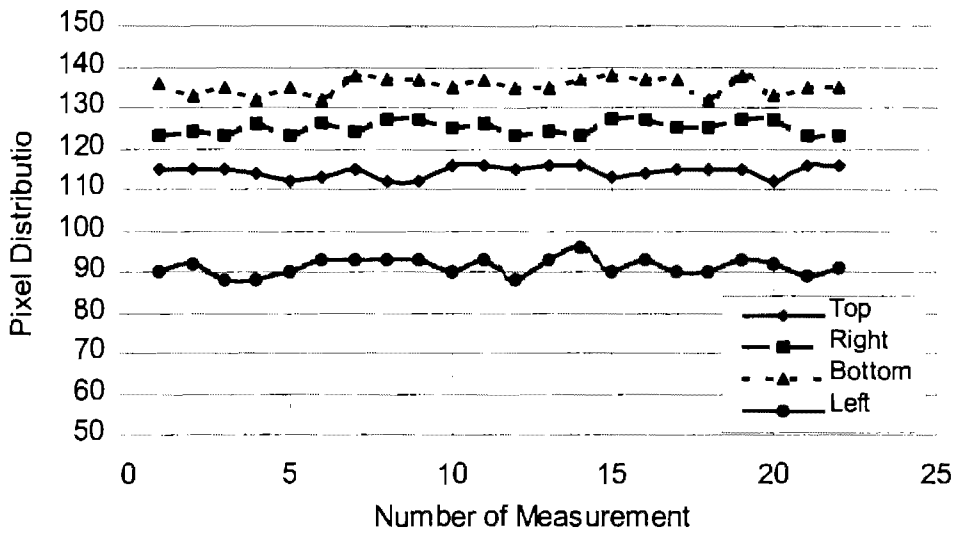

Figure 9.3 Pixel distribution of the test target along the inside of the boarder of the target.

Figure 9.4 shows that the pixel distribution along the immediate outside of the target boundaries for the second target location that provides worse STV contrast value. The pixel values along the top boundary fluctuates between 74 and 104, along the bottom boundary fluctuates between 55 and 65, along the right boundary fluctuate between 54 and 77, and along the left boundary fluctuate between 55 and 103. The background pixel (luminance) distribution is related to the pavement reflectance properties (uniformity, etc.) and the photometric data of luminaire. But pixel fluctuation at the background (top and bottom) is directly related to the pavement

reflectance properties. The pixel fluctuation along the right and left boundaries is also related to the photometric data.

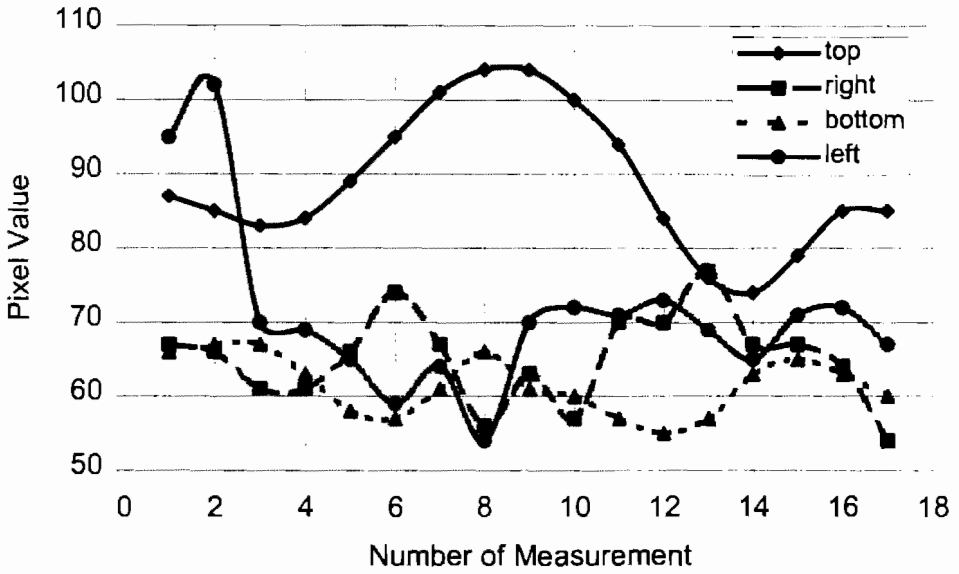

Figure 9.4 Pixel distribution outside of the boundaries of the target for the target location 2.

Figure 9.5 shows that the pixel distribution along the immediate inside of the target boundaries for the second target location that provides worse STV contrast value. The pixel values for the top boundary fluctuates between 77 and 97, for the bottom boundary fluctuates between 68 and 85, for the right boundary fluctuate between 76 and 98, and for the left boundary fluctuate between 76 and 98. The target has very smote surface with 20% reflectivity. But as seen from the figure, pixel distribution even fluctuates on the target surface because of non-uniform pavement reflection.

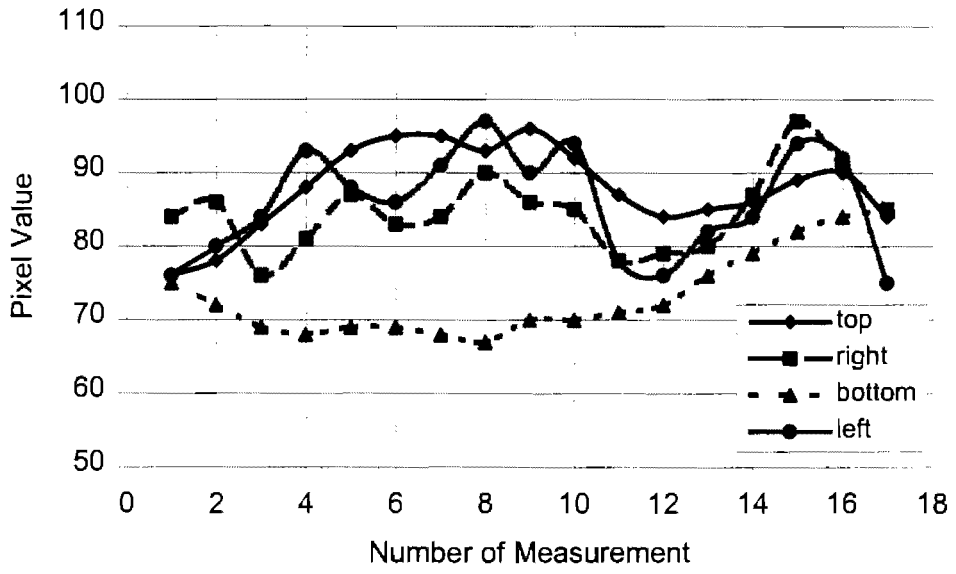

Figure 9.5 Pixel distribution inside of the boundaries of the target for the target location 2.

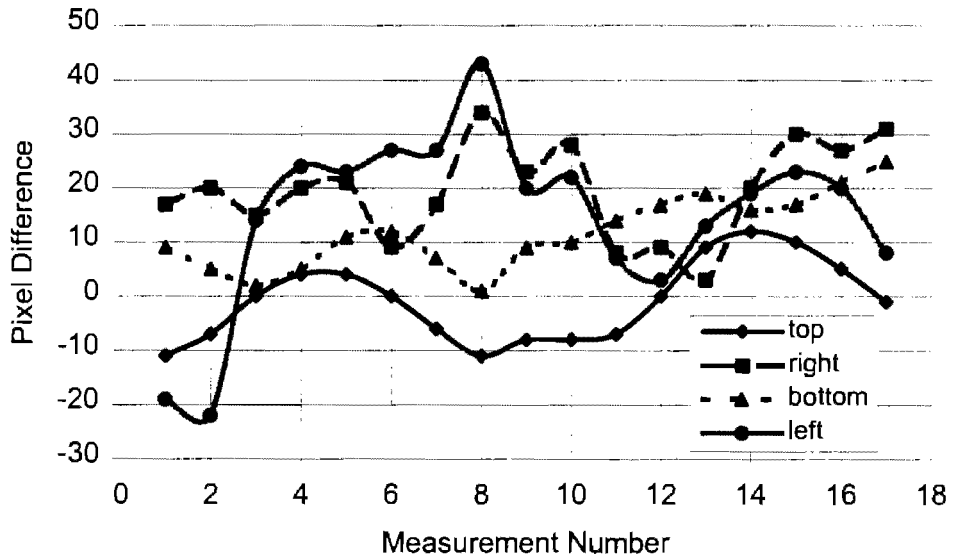

Figure 9.6 Pixel difference distribution between the inside and the outside boundaries of the target for the target location 2.

Figure 9.6 shows that the pixel difference (L_t - L_b) as calculated in STV formula, distribution along the target boundaries for the second target location that provides worse STV contrast value. The pixel difference values for the top boundary fluctuates between -11 and 12, for the bottom boundary fluctuates between 0 and 25, for the right boundary fluctuate between 2 and 34, and for the left boundary fluctuate between -22 and 43. As seen from the figure, along the top and left boundaries difference of the pixel distribution fluctuates between the negative and

positive values (classic army camouflage techniques). Along the other two boundaries, difference of the pixel distribution fluctuates between the positive values.

Figure 9.7 shows that the pixel distribution along the immediate outside of the target boundaries for the ninth target location that provides better STV contrast value. The pixel values along the top boundary fluctuates between 75 and 95, along the bottom boundary fluctuates between 140 and 170, along the right boundary fluctuates between 117 and 163, and along the left boundary fluctuates between 86 and 145.

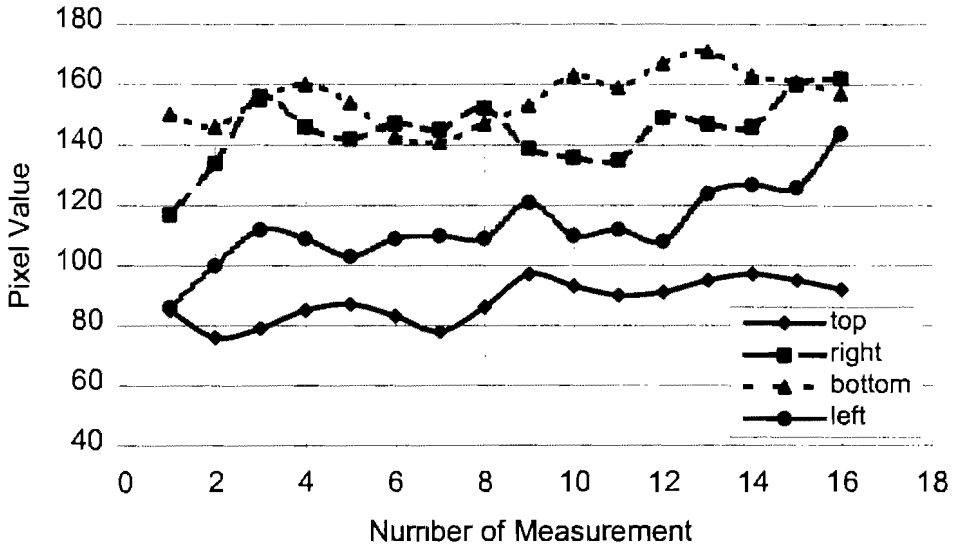

Figure 9.7 Pixel distribution outside of the boundaries of the target for the target location 9.

Figure 9.8 shows that the pixel distribution along the immediate inside of the target boundaries for the ninth target location. The pixel values along the top boundary fluctuates between 28 and 48 along the bottom boundary fluctuates between 28 and 68, along the right boundary fluctuates between 32 and 68, and along the left boundary fluctuates between 26 and 44.

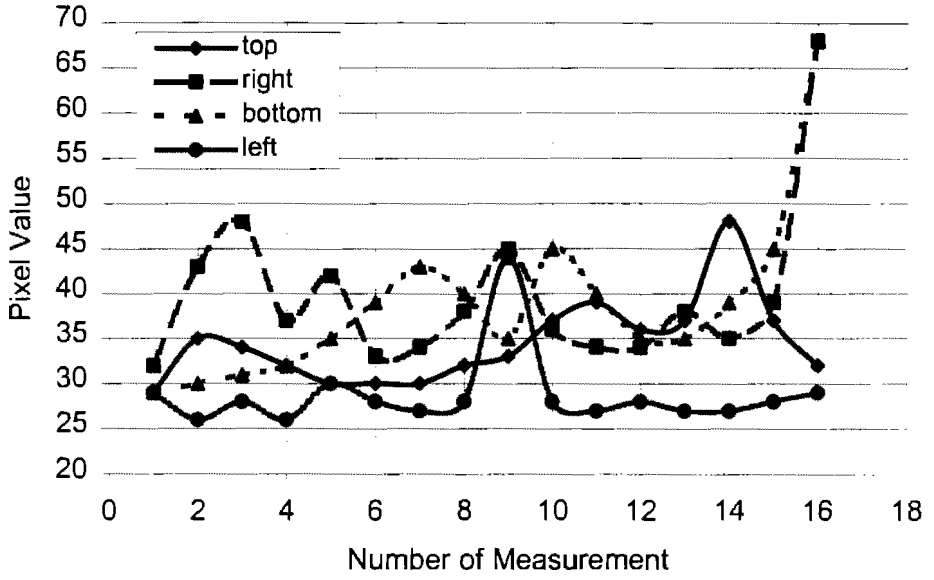

Figure 9.8 Pixel distribution inside of the boundaries of the target for the target location 9.

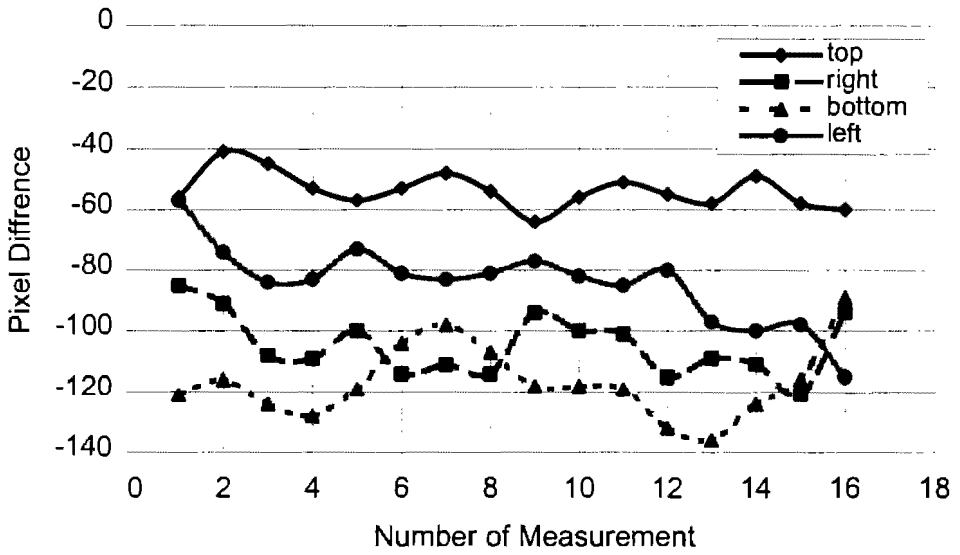

Figure 9.9 Pixel Difference distribution between the inside and the outside boundaries of the target for the target location 9.

Figure 9.9 shows that the pixel difference (L_t - L_b) distribution along the target boundaries for the ninth target location. The pixel difference values along the top boundary fluctuates between -75 and -40, along the bottom boundary fluctuates between -135 and -90, along the right boundary fluctuate between -120 and -85, and for the left boundary fluctuate between -55 and -115. As

seen from the figure, along the all boundaries, difference of the pixel distribution fluctuates between the negative values.

STV methods assume that, the background luminance and the target luminance distributions are constant along the boundaries. As seen from Figure 9.4 through 9.9, the pixel distributions along the boundaries are not constant neither the background pixels (luminances) and the target pixels (luminances). STV method also does not consider the luminance distribution along the right and the left boundaries. But the figures show that luminance is not also constant along the right and left boundaries.

According to the STV contrast method, Figures 9.4 through 9.6 show pixel distributions for worse case, and Figures 9.7 through 9.9 also show pixel distribution for the best case. These two cases indicated that the pixel (luminance) distribution could not be taking constant along the inside and outside of the boundaries. Let us calculate (L_t - L_b) by taking constant pixel distribution. From the Figure 9.4, the following pixel values can be obtained for extreme cases;

For the Outside of the Boundaries:

The Pixel values for the top boundary:	74 or 104
The pixel values for the bottom boundary:	55 or 65
The pixel values for the right boundary:	54 or 77
The pixel values for the left boundary:	55 or 103

For the Inside of the Boundaries:

The Pixel values for the top boundary:	77 or 97
The pixel values for the bottom boundary:	68 or 85
The pixel values for the right boundary:	76 or 98
The pixel values for the left boundary:	76 or 98

Again, STV takes one data at the middle of the target as the target luminance value and takes average of the two background values as the background Luminance.

Case 1

Assume STV method reads 74 and 55 as the background pixels and 97 as the target pixel. So,

$$L_t - L_b = 97 - \left(\frac{74+55}{2}\right) = 32.5$$

Case 2

Assume STV method reads 104 and 65 as the background pixels and 97 as the target pixel. So,

$$L_t - L_b = 97 - \left(\frac{104+65}{2}\right) = 12.5$$

Case 3

Assume STV method reads 74 and 55 as the background pixels and 68 as the target pixel. So,

$$L_t - L_b = 68 - \left(\frac{74+55}{2}\right) = 3.5$$

As seen from these cases, these values should be divided to the DL_4 value for obtaining the visibility level values which will be linearly proportional each other because these values will be divided to the same number (DL_4). Case 1 gives 9.5 times greater (L_t - L_b) values that Case 3 and 2.9 times greater than case 2. When the single values are taking as the target and background luminances, the way of different (L_t - L_b) values could be calculated. On the other words, visibility level values can be calculated much different than it should be.

In the previous section, STV method has been investigated. Mainly, STV method assumes homogeneous the target and the background luminance distributions and it also assumes that the target is darker than its background. In the reality these assumptions can not be satisfied like there is no homogeneous background luminance distribution (Figure 9.4) because pavement is not homogeneous. Also, the target is not always darker than its background. Target can have the background luminance distribution as seen Figure 9.10. In this luminance distribution, top of the target has negative (L_t-L_b) value and bottom of the target has positive (L_t-L_b) value. Let us give an example;

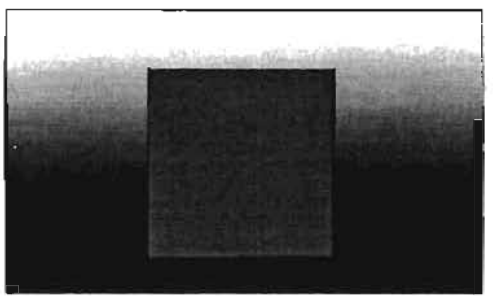

Figure 9.10 A target with its background.

Target Luminance (L_t)	=	52 cd/m^2
Background luminance at the top (L_{bt})	=	70 cd/m^2
Background luminance at the bottom (L_{bl})	=	34 cd/m^2

$$L_t - L_b = 52 - \frac{70+34}{2} = 52 - 52 = 0$$

When we consider (L_t-L_b) calculation separately for top and bottom border results yield
For top boundary:

$$L_t - L_b = 52 - 70 = -18$$

For bottom Boundary:

$$L_t - L_b = 52 - 34 = 18$$

As seen from the calculations, when the average of the background luminance is taken as a background luminance (L_t-L_b) becomes zero. But when the each boundary is considered separately to calculate the (L_t-L_b), it will be –18 for top boundary and 18 for bottom boundary, it means that the target has positive contrast for the top and negative contrast for the bottom, but

both boundary providers the same visual acuity. According to the STV calculation this target is not visible, there is no contrast difference between the target boundaries and their backgrounds. Actually, there is contrast difference as seen from calculation, STV method just cancels out negative and positive contrast values.

STV method calculates the visibility level values by using the formula as mentioned before is

$$VL = \frac{L_t - L_b}{L_b} \times \frac{L_b}{DL_4} = C \times \frac{L_b}{DL_4}$$

where $C = \frac{L_t - L_b}{L_b}$. The sign of the VL values depend on the sign of the C. Let us study sign and value of the C by assuming the following luminance distributions as examples:

Example 1:

Figure 9.11 shows homogeneous luminance distribution around the target. Luminance points are marked according to the STV method.

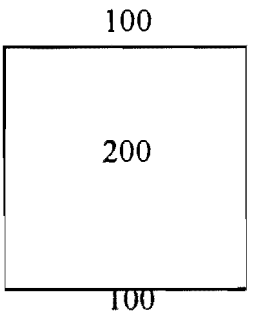

Figure 9.11 Luminance distribution.

$$C_1 = \frac{L_t - L_b}{L_b} = \frac{200 - 100}{100} = \frac{100}{100} = 1.0$$

Example 2:
Figure 9.12 again shows homogeneous luminance distribution around the target. Luminance points are also marked according to the STV method.

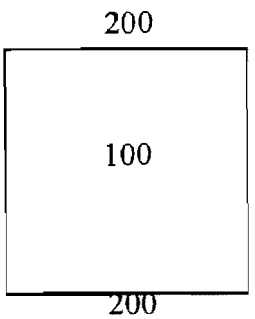

Figure 9.12 Luminance distribution.

$$C_2 = \frac{L_t - L_b}{L_b} = \frac{100-200}{200} = \frac{-100}{200} = -0.5$$

Examples 1 and 2 should give the same absolute contrast value, but it is not.

Example 3:

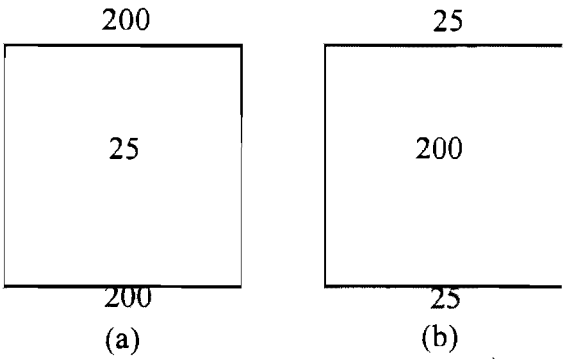

Figure 9.13 Luminance distributions (a and b).

$$C_3 = \frac{L_t - L_b}{L_b} = \frac{25-200}{200} = \frac{-175}{200} = -0.875$$

$$C_4 = \frac{L_t - L_b}{L_b} = \frac{200-25}{25} = \frac{175}{25} = 7.0$$

Examples 3 and 4 should also give the same absolute contrast value, but it is not. There is very big difference between the C_3 and C_4 because of the definition.

Contrast Modulation

In the section entitled *Video Target Contrast Average (VTCa) Method,* it is mentioned as a better method than the other two for calculating VTC. In this section this method will be compared with the method of Video Target Contrast Average Modulation ($VTCa_{mod}$) Method. Contrast modulation formula is described with the formula (7.4). The formula will be modified for the experimental system as the following.

$$C_{im} = \left| \frac{P_{ti} - P_{bi}}{P_{ti} + P_{bi}} \right| \qquad (9.1)$$

where C_{im} : Contrast modulation at the point i along the target borders
P_{ti} : Pixel value at the point i inside of the target borders
P_{bi} : Pixel value at the point i outside of the target borders.

$VTCa_{mod}$ is defined arithmetic average of the contrast along the target boundaries as the following formula.

$$VTCa_{\text{mod}} = \frac{\sum_{i=1}^{n} |C_{im}|}{n} = \frac{\sum_{i=1}^{n} \left| \frac{P_{ti} - P_{bi}}{P_{ti} + P_{bi}} \right|}{n}. \tag{9.2}$$

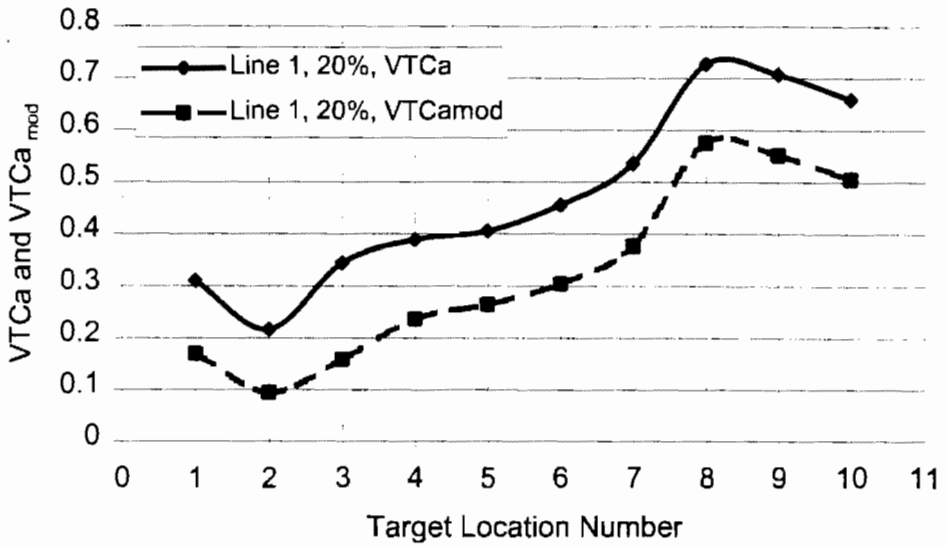

Figure 9.14 VTCa and $VTCa_{mod}$ values distribution for 20% target on the line 1.

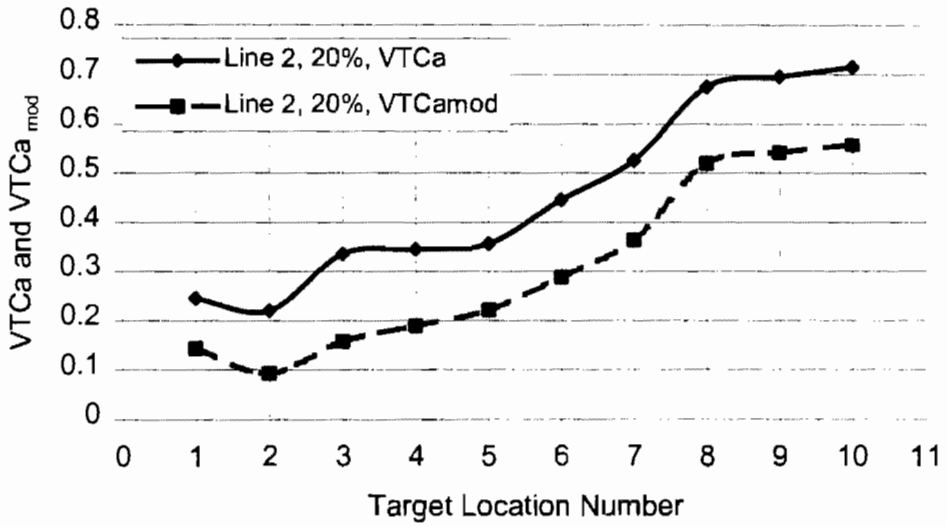

Figure 9.15 VTCa and $VTCa_{mod}$ values distribution for 20% target on the line 2.

Figures 9.14 and 9.15 indicate that the VTCa and $VTCa_{mod}$ values distribution for 20% target on the lines 1 and 2, respectively. The $VTCa_{mod}$ method is more conservative methods than the

VTCa (Equation 8.5) because P_{ti} term is added to the denominator of the $VTCa_{mod}$ formula (Equation 9.2). Both distributions are almost parallel each other between the installation except between the target locations 2 and 4 as well as 7 and 8 because of the nature of the equations.

Figures 9.16 and 9.17 show that the VTCa and the $VTCa_{mod}$ values distribution for 50% target on the lines 1 and 2, respectively. The $VTCa_{mod}$ method is again more conservative methods than the VTCa. Both distributions dynamically show the same kind of characteristics but when the values compared there are extremely considerable difference between both distributions, especially between the target locations one and five. As seen from the figure, when the contrast change moderately, the VTCa values drastically change between the target locations one and five but the $VTCa_{mod}$ is not change drastically in the same section. Let us look the following examples to better understanding the drastic changing.

Example 1:

Target luminance: 50 cd/m^2
Background luminance: 25 cd/m^2

$$\frac{L_t - L_b}{L_b} = \frac{50-25}{25} = 1.0$$

$$\frac{L_t - L_b}{L_t + L_b} = \frac{50-25}{50+25} = 0.333$$

Example 2:

Target luminance: 200 cd/m^2
Background luminance: 25 cd/m^2

$$\frac{L_t - L_b}{L_b} = \frac{200-25}{25} = 7.0$$

$$\frac{L_t - L_b}{L_t + L_b} = \frac{200-25}{200+25} = 0.777$$

From the examples, when the target luminance changes from 50 cd/m^2 to 200 cd/m^2 (background luminance is constant), $\frac{L_t - L_b}{L_b}$ changes seven times and $\frac{L_t - L_b}{L_t + L_b}$ changes just 2.33 times.

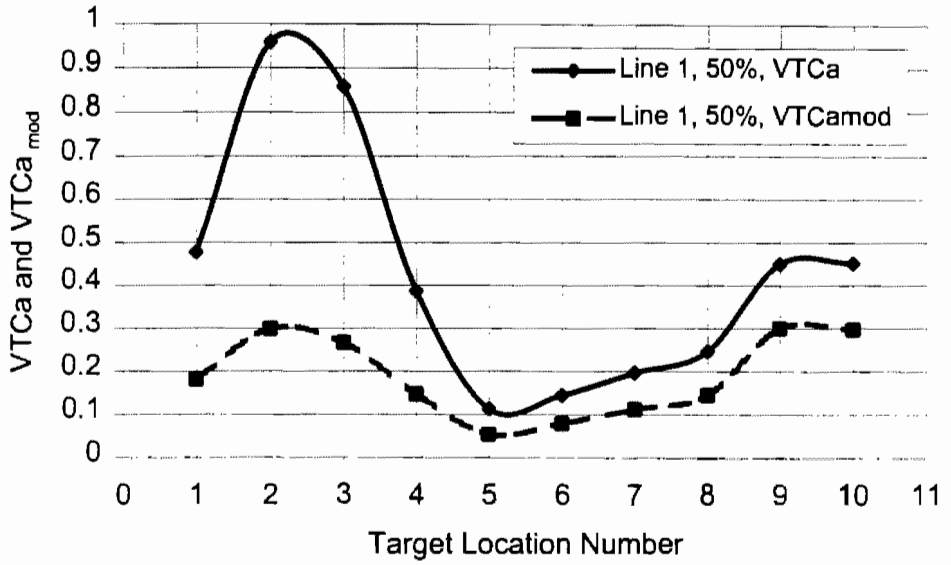

Figure 9.16 VTCa and $VTCa_{mod}$ values distribution for 50% target on the line 1.

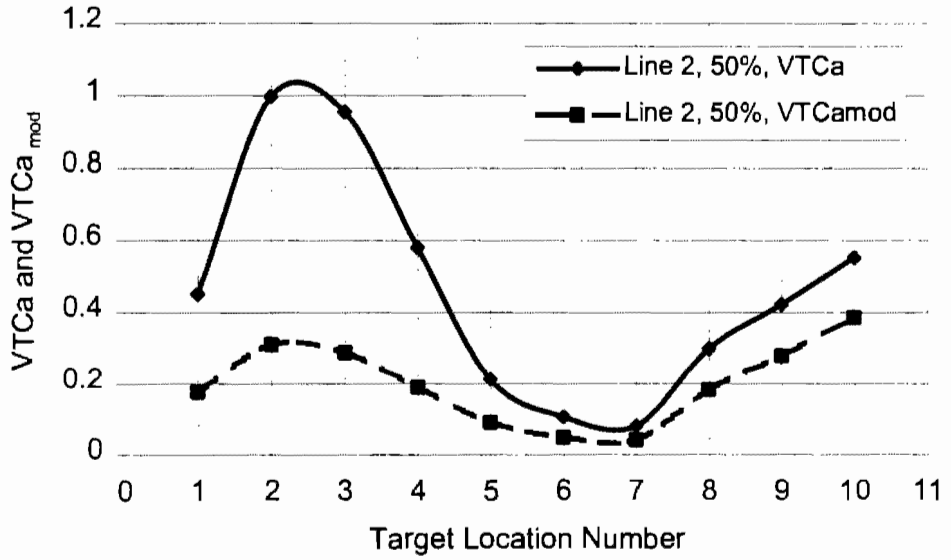

Figure 9.17 VTCa and $VTCa_{mod}$ values distribution for 50% target on the line 2.

CHAPTER 10: CONCLUSION

Illuminance measurements were compared with the calculated illuminance values that were obtained from Aladan software. Both methods gives same dynamic illuminance distribution but until 6^{th} target location, there is maximum 20% difference between both methods; after 6^{th} target location, the difference between the measurements reaches to 80% difference. This large percentage difference can be able to explain with the maintenance errors such as, rotation angle, tilt angle, etc. also photometric data distribution.

Comparison of the STV, luminance, and illuminance methods on the lines 1 and 2 show that the STV and illuminance methods are more conservative method than the other one theoretical method. But these three methods provides ratios (calculated value/recommended value) more than 1.It means that there is enough light to provide comfort visibility (target should be visible at any location between the installation).

STV result is dynamically very compatible with the luminance results, except the target locations between the 6^{th} and 10^{th}. Between the target location 6^{th} and 10^{th}, while the STV value increases, the luminance values decreases. But those values are still above the threshold value.

Pixel analysis program was developed to measure the Video Target Contrast (VTC) distribution. To calculate the VTC values, the program compares the pixel values inside (on the target surface) and outside (on the background) of the target borders. The output of the program was compared with the STV, Luminance and Illuminance outputs. The results show that, VTC output is dynamically the same with STV and Luminance outputs. Three different VTC method were developed: VTC, VTCn and VTCa Methods. Results shows that VTCa methods is the best experimental methods. Because it is consider VTC value for each pixel number combinations (target pixel number and its background pixel number) along the target boundaries. VTC method is the same method with STV method such as STV and VTC methods consider just three points to calculate visibility of the target: Fist one is at the middle of the target surface and average of the two background luminance that are immediate outside of the upper and lover target boundaries.

For the theoretical applications, the three points may be enough to calculate visibility because the method assumes perfect conditions available on the target surface and its background. In additional, the STV method does not consider to calculate visibility both right and left border of the target. The recorded images show the following.

- The pixel distribution along the target boundaries on the target and the background is not uniform. When the method chooses only one point for visibility calculation it can be minimum as well as maximum luminance (pixel) value. So, the result can be much different as seen in the given examples.
- In the recording figures, VTC values change from negative to positive (negative and positive contrast) along the target boundaries, but STV assume it is negative or positive.
- The right and the left boundaries of the target is really effect the target visibility, but STV method does not count it.

STV method shows that the 20% target has only negative visibility level values. Experimental system shows that it has positive VTC value at the second target location on line 2, it has positive VTCn value at the second target location on the line 1 as well as second and third target locations on the line 2, and it has positive VTCa values at the second and third target locations on the lines 1 and 2.

STV methods shows that target visible at the any point between the installations but CTV, CTVn and CTVa methods show that the target is not visible at the second and third target locations.

STV method considers waited average visibility level (WtAvgVL) value to evaluate the light distribution on the roadway. It says that if WtAvgVL value grater that recommended WtAvgVL value (WtAvgVL is 3.8 for expressway), the roadway has enough light to provide comfort visual aspect. But in reality, it is not right to compare visibility with WtAvgVL values, the method should compare the VL values with recommended VL values at each individual target location. Because visibility is the local variable, it is not global variable.

STV method is not gives good result because of above variables.

STV values for 50% target is more interesting than 20% target. STV method gives invisible value for 50% at the second target location, but VTC shows (image) the target at the second target location is very clearly visible. STV and VTC methods show completely opposite dynamics between the first and third target locations. It also proves that STV method does not give correct answer for visibility distribution.

Dynamic STV values shows that the target is generally more visible when the distance between the target and observer is the longer (experiments were approximately performed until 430 ft), because longer distance provides lover (lover than 1 degree) observer angel which creates larger background for the target (obstacle). The target will be seen smaller from the longer distance therefore, it most probably increases the adaptation time. So, the visibility should consider together.

Future Research

The program used for calculating VTC values through the pixel analysis method. Calculation of the VTC values can be the same either using pixel values or luminance values. Because VTC values is the ratio of the pixel or luminance values. When the image is calibrated the pixel values will be linearly converted to the luminance values. Therefore, the result will be the same. But if the pavement luminance or any other source luminance value want to be known through the image analysis, the image has to be calibrated. After the calibration, the three dimensional luminance distributions on the roadway can be map between the installations. Also the luminance values of the any source in the images can be calculated.

The new theoretical model can be created to calculate visibility distribution by using the experimentally obtained results.

CHAPTER 11: BUDGET ERROR REPORT: CORRECTIONS IN PAVEMENT LUMINANCE CALCULATIONS DUE TO ROADWAY CROWN, SUPERELEVATION GEOMETRY AND ILLUMINAIRE DESIGN

Abstract

Calculation methods are usually performed for ideal conditions to determine the illuminance and luminance but other design limitations should be considered in the real world. Many, hard predictable, factors enter the design equation, as for example, the pavement is not level, aging lamps lamp reflector and refractor is not centered, the lamp is off center and tilted, lamp's ballast issues, voltage fluctuation, photodetectors response, ambient temperature factors, reliability of illuminaires, etc. These factors decrease the lamp unit performance and naturally decrease an object visibility..As human eye is a complex device it is difficult to accurately design an outdoor illumination system just simply based on numerous theoretical assumptions. Most roads are crowned about 2% in the straight path and curves can have superelevation up to 8%. This fact renders the typical design assumption invalid in all cases. This paper seeks to develop a general analytic undestanding of the problem. and shows that an error of up to 4% is introduced into the calculated pavement luminance if crown and superelevation are not considered by the roadway lighting designer. Using the presented factors, the average illuminance difference can be over 123% and this makes some highway design methods, for example, STV, difficult to justify.

Introduction

The luminance of a source or the light reflected from the surface is defined as an intensity of the source or a surface in the direction of an observer per unit area. The superelevation of the road surface will cause that the projected area is reduced by a factor that is proportional to the angle of the tilt. Variations of formulas can be used by a civil engineer to calculate the illuminance and luminance. The simplest approach is to calculate the illuminance, E_h of a horizontal plane,

$$E_h = \frac{I(\Phi,\gamma)\ \cos\gamma}{D^2} = \frac{I(\Phi,\gamma)\ \cos\gamma^3}{H^2} \qquad (10.1)$$

Where: I is the candlepower of the source in the direction of the point
D is the distance from the light source to the point
H is the vertical mounting height of the light source
γ is an angle between the light ray and a horizontal plane of the point(Figure 6.1).

The surface illuminance, L, is the luminous flux reflected by a unit area surface in the direction of an observer and is defined as

$$L = \frac{1}{\pi} E_h\ q(\beta,\gamma) \qquad (10.2)$$

Where: $q(\beta,\gamma)$ is the directional reflectance coefficient for angles of incidence of β and γ.

Combining the two above equations the luminance is the following equation in practice for a civil engineering design, the directional reflectance coefficient, $q(\beta,\gamma)\cos^3\gamma$, is given in tables

for each road classification in the National Standard Practice, 1990. The equations used for the standard luminance calculation assume a flat road surface.

$$L = \frac{q(\beta,\gamma) I(\Phi,\gamma) \cos^3 \gamma}{\pi H^2} \tag{10.3}$$

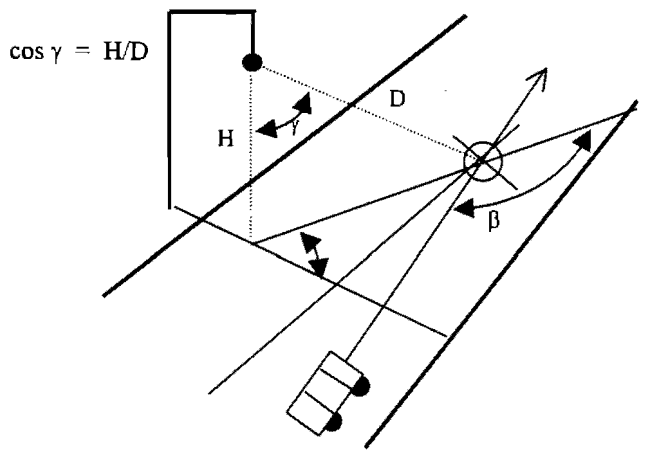

Figure 10.1: Geometry of roadway lightning design.

This assumption is always wrong for highways. The roadway designer must include cross-slopes for drainage (i.e. crown), and superelevation on horizontal curves used at freeway ramps. These areas of the roadway are typically lighted. Therefore, pavement geometry with respect to luminaire geometry should be considered.

Typical Texas Roadway Lighting Case

The equation (3) can be rewritten while including the factor for angle δ as in the following equation.

$$L = q(\beta,\gamma,\delta) \cos^2 \gamma \bullet \cos(\gamma,\delta) \bullet \frac{I(\Phi,\gamma)}{\pi H^2} \tag{10.4}$$

Separating the superelevation factor, the equation (4) can be rewritten for angle ε standing alone and to be represented by corr(δ,γ) intensity decrement it can be numerically expressed.

$$L = q(\beta,\gamma,\delta) \cos^2 \gamma \bullet \frac{I(\Phi,\gamma)}{\pi H^2} \; corr(\gamma,\delta) \tag{10.5}$$

In Figure 10.2, a typical straight stretch of a highway has 2% crown. The transition stretch has an average 2% crown for the inner lane of the curve and 0%crown for the outer lane at its beginning. The outer lane is then lifted while both lanes are continuously tilted until they meet the curve's superevelvation of 8%.

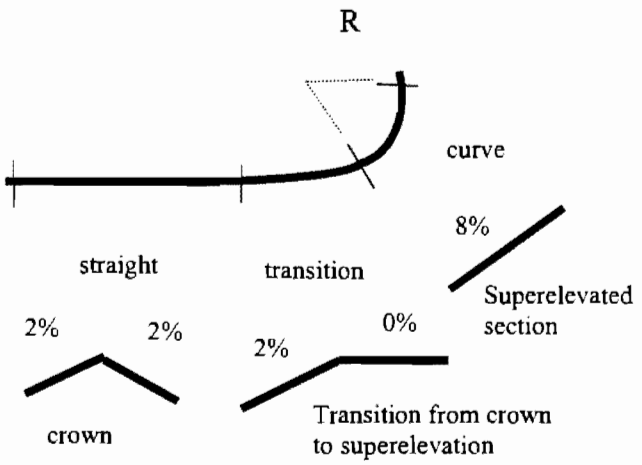

Figure 10.2: Typical stretch of a highway.

A typical Texas roadway shown in Figure 10.3 has a luminaire pole installed fifteen feet from the outside edge of pavement. Each lane is twelve feet wide. Two basic luminaires used on Texas highways have wattages of 250 Watts and 400 Watts. The pole mounting height is 40 feet for a 250 Watt luminaire and 50 feet for a 400 Watt unit. The mounting arm is 8 feet long.

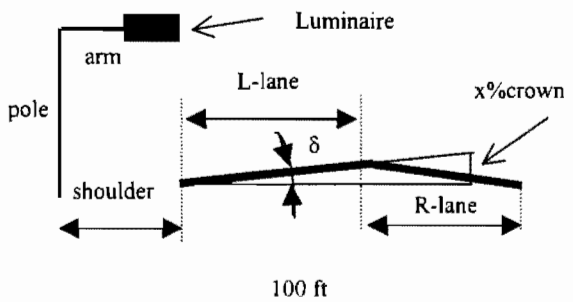

Figure 10.3: Typical roadway lighting arrangement.

Superelevation Correction (Sc)

Below there are two specific examples for the West Texas road which has its crown of 2% in the straight path and 8% for the ramp. The angle (δ) between the road surface and the horizontal level is 1.146° for a 2% crown and 4.57° for an 8% superlelevation.

Figure 10.4 shows the cross-sectional geometry of one light illuminating the surface of the highway. The luminance of the road surface is corrected by the cosine of the angle between the vertical axis and the slope of the road.

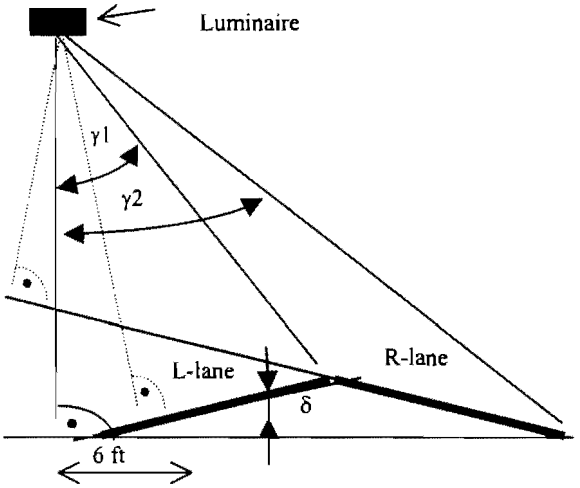

Figure 10.4: Geometry of one road light.

The factor, corr(δ,γ), can be tabulated for all the road width of 0 to 24 ft. For example the angle γ at 6 ft from the luminaire vertical axis and 50 ft pole is 6.9°, Figure 10.4.

$$tg\ \gamma = \frac{6\,ft}{50\,ft} \quad \rightarrow \quad \gamma = 6.9°$$

The percentage change in cos (δ,γ) is calculated using the following equation:

$$100\%\,[\,1 - \frac{\cos\gamma}{\cos(\gamma - \delta)}] = 100\%[1 - \frac{\cos 6.9°}{\cos(6.9° - 1.14°)}] = 0.22\%$$

Then the factor, corr(δ,γ), is the following equation:

$$corr(\gamma, \delta) = abs[\,1 + \frac{0.23\%}{100\%}] = \pm 1.0022$$

The light beam below the luminaire has almost zero correction. The factor for the 2%superelevation of the 24 ft-wide highway starts at the left side for γ = 0° with ±1.000 19727 for 50ft pole. It reaches its maximum of ±1.00455 on the right side of the highway path at 12 ft distance. The 8% ramp has its SC factor much higher. For practical purposes one can assume the SC factor to be ±1.01 to decrease (deteriorate) the calculated luminance.

It can be calculated that the failure to consider the effect of 2% of the pavement surface introduces an error of as much as 1%. This level of error can be significant mostly for an 8% superelevation. The equations shown in this report are in a general form and there is a need for further improvement and accuracy. Then they can be used to develop correction factor tables for

any set of roadway geometric characteristics. These tables can then be used by roadway lighting designers to increase the accuracy of the design for any specific project.

Aging of Lamps (Mf*Lld)

Aging lamps is known; however, the lamp evaluation does not consider accurately the several hundreds or thousands hours of usage. The light loss factor (maintenance factor), LLF, is used in a lighting calculation. The time, temperature, and voltage variations, dirt accumulation on the luminaire surfaces, lamp filament deterioration, maintenance procedures, equipment and ballast variation. Some factors are beyond control of the lightning provider, for example, voltage regulation, weather, emission control of the atmosphere.

When a filament illuminaire burns tiny vapor is deposited on the glass container walls. The time dependent depreciation effects must be considered in the initial design. Regular maintenance is important regarding the energy conservation and it is covered by the maintenance factor (MF). The information about chosen lamp intensity depreciation is available from the manufactures tables and graphs. Based on the elapsed time per year the lamp lumen depreciation (LLD) is determined. Saltner (1960) reported the aging test of luminaires. The maximum spread was up to ±6% for fluorescent lamps. Also brand new luminaires can be used for measurements after 100 hours of burning (1988), but his measurement is rather laboratory value but not when brand new lamp is installed on a pole.

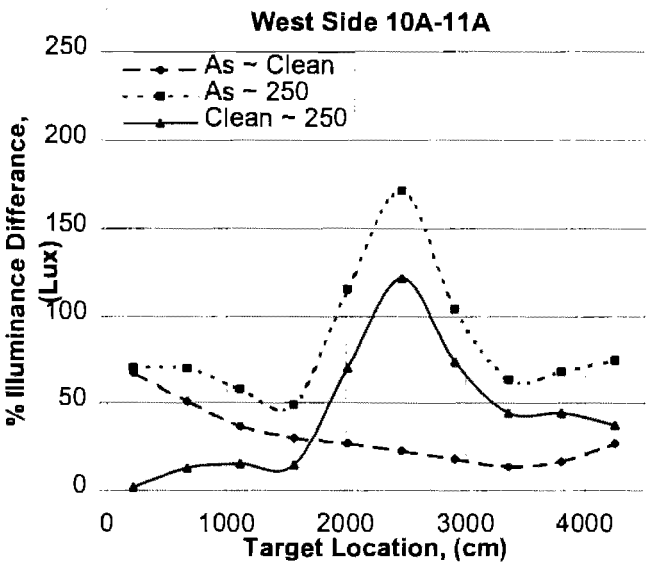

Figure 10.6: Target illuminance vs. target location and cleanliness of the lamps.

Lamp Reflector And Refractor (LRR)

The lamp reflector and refractor have its tolerance from the manufactures. Each manufacturer part has its variation in the aluminum material from the light source of which it is made despite manufacturing specifications require an accurate specular aluminum reflector sheet. Even a small degree of specularity can significantly influence the performance. Franklin (1974) found that the total efficiency difference is up to 9 percent.

Luminaire Dirt Depreciation (LDD)

Dirt accumulated on a luminaire causes a loss of the light output. It has been experimentally seen that the output loss is a non linear function. The RP-8 proposed standard describes five categories of the ambient environment. Assuming about 4000-4300 hours of usage a year and life cycle of 8000 hours, the luminaire dirt depreciation has a factor of 0.9 to 0.7 or even less for moderate ambient environment.

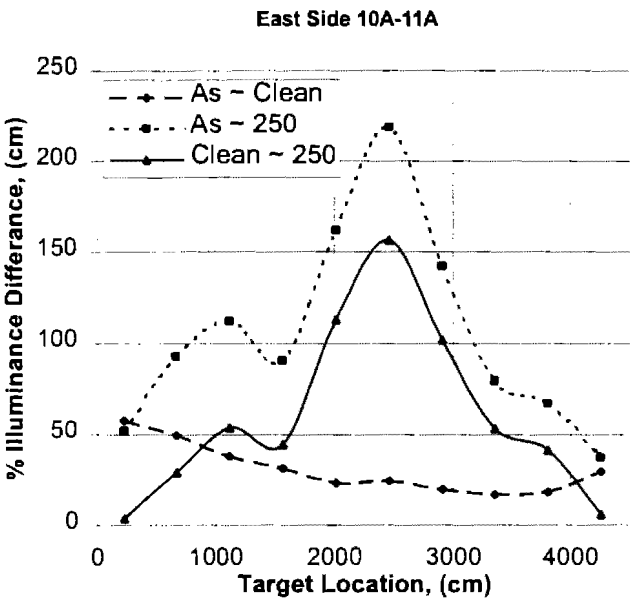

Figure 10.7 Target illuminance vs. target location and cleanliness of the lamps.

The experimental investigations shown in Figures 10.6 and 10.7 were performed on a single lane road on the West side of a rest area north of Abernathy, Texas between Abernathy and Halecenter on Interstate Highway 27. An array of 10 targets was placed between two poles. Figure 10.6 shows percentage change of illuminance on the west STV line between the poles 10A and 11A. Figure 10.7 shows percentage change of illuminance on the east STV line between the poles 10A and 11A. In Figures 10.6 and 10.7 labeled 'As 250' means during its original conditions the measurements were taken– entering the experimental field first time without doing any improvement in the field Labeled 'Clean' means after the original conditions, when we removed the lenses of luminaires, cleaned them, and then, put them back. Labeled '250' - we replaced 5 luminaires with the new 250 watts luminaire.

West STV line (west side)

Figure 10.6 shows the original luminaires with clean lenses provide an average of 30 percent better illuminance than the luminaire with original lenses while the new luminaires approximately provide average of 45 percent better illuminance than the original luminaire with clean lenses. The new 250 watts luminaires approximately resulted in an average of 80 percent better illuminance than the original luminaire with original lenses.

East STV line (west side)

In Figure 10.7 the original luminaires with clean lenses provided an average of 45 percent better illuminance than the luminaire with original lenses. New luminaires resulted in about of 60 percent better illuminance than the original luminaire with clean lenses. The new 250 watts luminaires performed on an average of 100 percent better illuminance than the luminaire with original lenses.

The STV measurements demonstrate the significance of a condition of an illuminaire - the illuminance and visibility change before and after cleaning the unit. The above measurement show variation from 30 to 100 percent. Assuming an average of 30% change (factor 0.3) that is used in Table 10.2 seems to be a very conservative assumption.

Lamp Off Center and Tilted (LCT)

Tilt is the angular position of the luminaire around an axis through the light center and along the 90-270 degree horizontal axis. When the luminaire is level, the tilt is zero degrees. On roadway mounted units the tilt was as high as ±5°. The luminaire can off center. The lateral displacement can be larger than is the arc displacement in halogen lamps. The lamp data sheet (1974) usually shows a ±3% variation. A one degree of an incidence angle will cause a 5% error at 70 degrees and 10% at 80 degrees (1988). The high-pressure sodium lamps also performed with at least ±3% variation in specific direction.

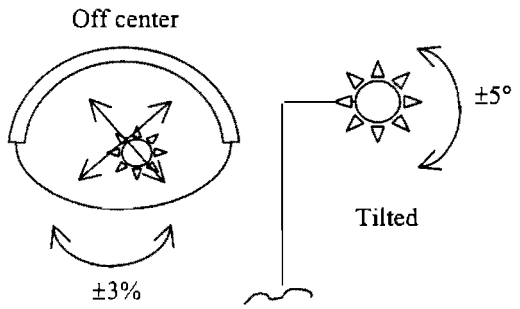

Figure 10.8: Lamp off center and tilted.

Voltage Fluctuation and Lamp's Ballast (VF)

There is an expected guaranteed level from the utility company. The ANSI (American National Standards Institute) permits the flux lamp to fluctuate by ±10% for mercury lamps, ±20% for high pressure sodium lamps and ±15% for metal halide lamps. Generally the voltage changes in RMS terms and influences the luminous output The ballast performance is variable too. A good

practice is to assume that the utility power fluctuates up to ±6% (1997). The lamp ballast is used to improve the power factor of the illumination unit and to lower the power surges to a utility system. The 92.5% is the minimum that the lamp output can be lower with the CBM ballast (by the Certified Ballast Manufactures Associations). There are three basic electromagnetic HPS ballast types; non-regulating, lead-type regulators and lag-type regulators. If the wrong ballast is installed, it can waste energy, increase operating costs, shorten lamp life, produce lower than desired light levels and result in lamp cycling when voltage dip occur. Non-regulating ballasts produce large changes in light output as line voltage changes, for example, a 1% line voltage change will cause a 2.5% light output change. Lead-type regulating ballasts give at 1% voltage change a light output decrease by 1.5%. Lag-type regulating ballasts, a 1% voltage change will result of 0.8% change in light output (GE, 1997). This parameters are assumed when new system is running under nominal conditions when a proper match between the luminaire type and its rating with matching ballast, is maintained through the life of the lighting system. Assuming voltage fluctuation up to ±6%, the light output can change up to ±9%.

The real problem starts when a not certified ballast is used. It has been seen that the energy conserving ballasts or non certified ballast can lower the output to 60% of lamp rated lumens (Lewin, 1998). That means the illuminaire generally runs at lower voltage than nominal.

One can conclude that the photometric results are directly associated with the type of a luminare. Each high pressure ballast has its own fingerprint The design information is provided by the manufactures. Due to normal lamp manufacturing tolerance, new HPS lamps may vary from its nominal design voltage as much as 15% and the lamp lumen output may vary also by 15% (GE, 1997). When the lamp ages, it runs at higher voltage. The whole design process is called volt-watt trace fingerprint.

Photodetectors Response (PR)

The actual lighting measurements cannot be neglected while one determines the design error. Generally the spectral sensitivity of photodetectors is different of our eye sensitivity. At night human eye is more sensitive to lower frequencies, blue light, detected by rods, while during the day the cons detect mostly the red light. In Figure 10.9, the comparison between the selenium cell and photopic response function is shown. The standard detector does not have the matching curve for a human eye. The calibration is established by comparing the detector to a known source while adding color filters. When matched, the error is believed to be no more than ±3%, however, when measured for the relative spectral response for several color corrected detectors, the error was massive over 50%. The $V(\lambda)$ and $V'(\lambda)$ represent the eye sensitivity for day and night respectively. The curves differ at shorter wavelengths and the error can be up to 2%.

Lamp Output Vs. Temperature (LOTE)

The mercury lamps are temperature dependent because the output of a fluorescent lamp depends on the ambient temperature vs. the coldest spot of an arc. However, they still have transparent arc tube, and the own arc is semitransparent to its own radiation. The IES recommends for laboratory conditions to held temperature ±2°F, then the 5 percent output range can be accomplished. The mercury lamp is calibrated for 25 °C ambient temperature and everything

above or below, the luminous output decreases or increases about 1 – ½ percent per 1°C. HID lamps are not sensitive to ambient temperature; however, the high-pressure sodium lamps are far most sensitive to returned radiant power. The high-pressure sodium lamps are opaque to their emitted light and the power is absorbed by the arc tube, evaporated luminous material and the end caps (Lewin, 1998). This effect in practice must be pinpointed to specific reflector design. In this publication it has been assumed that a difference in luminous flux will not be higher than 5%.

Luminous Detectors (LDE)

In illumination design, the lamps are treated with a high level of respect and enthusiasm. What has been usually left behind is the meter calibration process. Kostkovski estimates up to 4.1% fluctuation of results relative to SI unit. The laboratory "expensive" light meters are certified to about ±5% (Lewin, 1998). As stated above, the NBS value is much tougher. The inexpensive portable light meters are not accurate with the specs error of up to ±15% (Kostkowski , 1974). The selenium cell is the obvious choice for the light detector design, however, the unit's linearity is not high, the cell is sensitive to damage by high temperature and also fatigue.

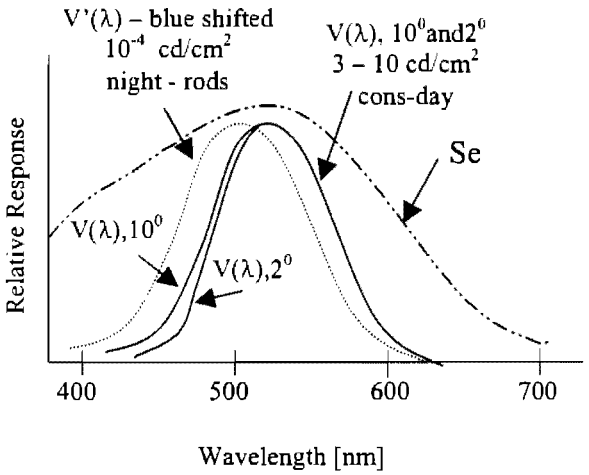

Figure 10.9: Relative response of a human eye and a Se Photodetector .

Burned Illuminaire (BI)

It is a common factor to assume that some of the illumination units are not functioning. It is a good engineering practice to assume that 96% of functioning desirable, 94% is acceptable and 92% tolerable. The factor of 1.06 was used in Table 10.2 for error summary.

Luminance, Illuminance and STV Methods

The luminance and illuminance methods are simple traditional goniometer techniques, where a single intensity reading is collected, such as luminance and illuminance. Numerous authors have done some experimental studies to design roadway lighting by taking single intensity

measurements. The early designs on roadway lighting were based on the amount of the light striking the surfaces of the pavement (i.e., illumination). However, it was later found that brightness of a pavement depends on the amount of the light that is reflected from it (luminance). This led to the study of pavement surface reflection characteristics. Since then, it has been established that the ability to see an object at night is based not on the light that is emitted from the object, but on the difference in the brightness (or luminance) between the target and its background (contrast). Contrast is the main parameter of the visibility of a target. In roadway lighting design methods, pavement is considered as the background, and therefore, luminance distribution on the pavement surface is one of the most important measures used to evaluate the quality of roadway lighting. Calculations of luminance of pavements are based on a two-dimensional array referred to as the r-table. R-tables can be developed for different pavement surfaces based on field measurements. However, for design purposes, CIE (International Commission on Illumination) classified dry pavement surfaces into four standard classes (R1 to R4) and assigned standard r-tables for each of these pavements.

STV method is used both as illuminance and luminance method. Illuminance method calculates amount of light hitting the target and the pavement. Luminance method calculates amount of the light reflected from the target and pavement. The visibility level, V_L can be written as the following equation.

$$V_L = \frac{L_t - L_b}{L_b} * \frac{L_b}{DL_4} \tag{10.6}$$

Where: L_t is the target luminance
L_b is the background luminance
DL_4 is a function of sensitivity of visual systems, observation time, and the age of the observer.

The contrast, C, can be represented as the following equation.

$$C = \frac{L_t - L_b}{L_b},$$

The visibility is shown as the following equation.

$$V_L = C * \frac{L_b}{DL_4} \tag{10.7}$$

STV methods generally calculate the visibility, V_L at 20 location between two poles. The conditions of lighting systems are assumed good. The target can become invisible during "right conditions" of the target luminance and the background luminance. It is not the insufficient lighting but rather the combination of background and target luminance that matches. Table 10.2 lists the variation of factors that changes the illuminance and luminance while the roadway lighting system is aging. The error over 123% is possible. The designer might spend significant resources to build a nearly perfect illumination system, however, when it is built the numerous mostly unpredictable factors may take place.

Does The STV Method Significantly Improve the Design of Roadway Lighting?

Table 10.2 indicates that an error can be over 123%. One can introduce the error variation to the visibility equation of (7), and create the following equation.

$$V_L = C * \frac{L_b \pm (L_B * 1.23)}{DL_4} \tag{10.8}$$

This equation shows that the small target visibility can be greatly influenced numerous variation of non design factors. The objective is to compare the information contents that is needed for each target to be visible to a human eye.

Table 10.2: Errors coming from different factors of the roadway lightning design

	Aging of Lamps	Lamp Reflector and Refractor	Luminaire Dirt Depreciation	Lamp Ballast	Voltage Fluctuations	Photodetector Response	Luminous Detectors
	MF*LLD	LRR	LDD	LBA	VF	PR	LDE
Estimated deviation	±6%	±9%	-30%	9%	±10-20%	±2%	±5-15%
Mult. factor	1.06	1.09	1.3	1.09	1.10	1.02	1.05

	Lamp Out	Luminous Flux vs. Temp.	Super-elevation Error	**TOTAL ERROR**
		LOTE	SC	
Estimated deviation	96% desirable 94% acceptable 92% tolerable	±5%	4%	1.06 * 1.09 * 1.3 * 1.09 * 1.10 * 1.02 * 1.05 * 1.06 * 1.05 * 1.04 =
Mult. factor	1.06	1.05	1.04	**2.23**

Conclusion

The real world looks different in design methods than that performed for ideal conditions to determine the illuminance and luminance. Many, hard predictable, factors enter the design equation, as for example, the pavement is not of equal level, aging lamps lamp reflector and refractor is not centered, the lamp is off center and tilted, lamp's ballast issues, voltage fluctuation, photodetectors response, ambient temperature factors, reliability of illuminaires, etc. These factors decrease the lamp unit performance by several percent and naturally they decrease the object visibility. It can be calculated that the failure to consider the effect of 2% of the pavement surface introduces an error of as much as 1%. This level of error can be significant mostly for an 8% superelevation. The equations shown in this paper are in a general form and can be used to develop correction factor tables for any set of roadway geometric characteristics. These tables can then be used by roadway lighting designers to increase the accuracy of the design for any specific project. A collection of other problems was presented in this paper. The human eye is a complex device and it is difficult to accurately design an outdoor illumination system just simply based on numerous theoretical assumptions. Table 10.2 lists the variation of factors that changes the illuminance and luminance. The variation can be up to 123%. When this

variation is introduced to the visibility equation, the equation shows that the visibility can be greatly influenced by an error. The information contents on the graph would suggest that STV methods would not have significant gain over classic luminance and illuminance designs of the roadway lighting, and this makes some highway design methods, for example, STV to be too complicated, expensive and without larger significance to the roadway designs.

BIBLIOGRAPHY

Adrian, W.K., (1997). "A Method to Predict Visual Performance in Mesoptic Lighting," *Report for EPRI Lighting Research Office*, Electric Power Research Institute, Palo Alto, California.

Adrian, W. (1989). "Visibility of Targets: Model for Calculation," *Lighting Research and Technology,* Vol 22 (NO4), Great Britain.

Adrian, W.K.(1997) "Amendments in Calculating STV: Influence of Light Reflected from the Road Surface on the Target Luminance." Unpublished Data.

Adrian, W.K.,(1997). "A Method to Predict Visual Functions and Visual Performance in Mesopic Lighting Levels," Report Prepared for the EPRI Lighting Research Office.

Adrian, W..K., and Gibbons, Ronald B., (1996). "Influence of Observation Angle on Road Surface Reflection Characteristics," *Proceedings Paper #70*, 1996 Annual Conference Illuminating Engineers Society of North America, New York, New York.

Adrian, W.K. and Topalova, R.V., (1990). "Visibility Under Transient Adaptation," *Transportation Research Record 1327,* Transportation Research Board, Washington, D.C., pp. 47-48.

Alferdinck, J.W. and Padomos, P., (1988). "Car Headlamps: Influence of Dirt, Age, and Poor Aim on Glare and Illumination Intensities," *Lighting Research and Technology,* 20(4), pp. 195-198.

American Association of State Transportation and Highway Officials, (1990). *A Policy on Geometric Design of Highways and Streets,* AASHTO, Washington, D.C.

Anderson, Kyle A.,Hoppe, W..J., McCoy, P.T., and Price, R.E.,(1984). "Cost- Effectiveness Evaluation of Rural Intersection Levels of Illumination," *Transportation Research Record N995,* Transportation Research Board, Washington, D.C., pp. 47-48.

Basset, M.G. (1983) "Automated Facility for Measurement of Pavement Sample Reflectance Characteristics," *Transportation Research Record 904,* Transportation Research Board, Washington, D.C., pp. 87-91.

Basset, M.G.(1988). " Measurement of Reflection Properties of Wet Pavement Samples," *Journal of the Illuminating Engineering Society,* Illuminating Engineers Society of North America, New York, New York, pp. 99-104.

Basset, M.G., and Jung F. W., (1985). "Pavement Reflection Studies," *Transportation Research Circular N297* ,Transportation Research Board, Washington, D.C., pp. 12-13.

Blackwell, H.R., (1946). "Contrast Thresholds of the Human Eye," *Journal of the Optical Society of America,*36 (11).

Blackwell, O.M., and Blackwell H.R., (1977). "A Proposed Procedure for Predicting Performance Aspects of Roadway Lighting in Terms of Visibility," *Journal of the Illuminating Engineering Society,* Illuminating Engineers Society of North America, New York, New York, pp. 148-166.

Bodmann, H.W., and Schmidt, H.J., (1989). "Road Surface Reflection and Road Lighting: Field Investigations," *Lighting Research and Technology,* 20(4), pp. 159-170.

Box, P.C., (1972). "Comparison of Accidents and Illumination," *Highway Research Record 416,* Transportation Research Board, Washington, D.C., pp. 1-9.

Box, P.C.,(1971). "Relationship Between Illumination and Freeway Accidents," *Journal of the Illuminating Engineering Society 66(5),* pp. 365-393.

Box, P.C., (1989). "Major Route Accident Reduction by Improvements," *ITE 1989 Compendium of Technical Papers,* pp. 307-310.

Campbell, K. (1991). "Accident Typologies for Collision Reduction," *VTI Report 372A, Part I,* Linkoping.

Campbell, K. (1993). "Recent Research in Developing Accident Typologies," *Proceedings of Human Factors Research in Highway Safety,*

Christie, A.W., (1954). "Reflection Characteristics of Pavement Surfaces," *Highway Research Board Bulletin No. 89,* Transportation Research Board, Washington, D.C. pp. 21-37.

CIE, (1981). "An Analytic Model for Describing the Influence of Lighting Parameters Upon Visual Performance," *CIE Report No. 19/2,* International Commission on Illumination.

CIE, (1976). "Calculation and Measurement of Luminance and Illuminance in Road Lighting," *CIE Publication 30,* International Commission on Illumination.

Clear, Robert, and Berman, Sam, Target Size, (1985). "Visibility, and Roadway Performance, 1985," *Journal of the Illuminating Engineering Society,* 5(2), Illuminating Engineers Society of North America, New York, New York, pp. 167-180.

De Clercq, G., (1985). "Fifteen Years of Road Lighting in Belgium," *International Lighting Review 36(1),* pp. 2-7.

Ellis, K. L., (1976). "Measurement of Directional Reflectance of Pavement Surfaces and Development of Computer Techniques for Calculating Luminance," *Journal of the Illuminating Engineering Society,* 5(2), Illuminating Engineers Society of North America, New York, New York, pp. 118-126.

Ellis, R.D., and Herbsman, Z., (1996). "Illumination Guidelines for Nighttime Highway Work," *NCHRP Research Results Digest,* No. 216, Transportation Research Board, Washington, D.C.

Elvik, R., (1992). "Meta-Analysis of Evaluations of Public Lighting as Accident Countermeasure," *Transportation Research Record 1485* ,Transportation Research Board, Washington, D.C., pp. 112-123.

Finch, D.M., (1982). "Roadway Visibility using Minimum Energy," *Transportation Research Record 855* ,Transportation Research Board, Washington, D.C., pp.7-12.

Finch, D. M., King, L., and Ellis, K.L. (1967). "A Simplified Method for Obtaining Pavement Reflectance Data," *Highway Research Record 179,* Transportation Research Board, Washington, D.C. pp. 53-60.

Finch, D. M., and Simmons, A. E.,(1950). "Uniformity of Illumination in Highway Lighting," *Illuminating Engineering 45,* p. 561.

Fisher, A.J., (1977). "Road Lighting as an Accident Counter-Measure," *Australian Road Research,* 7(4), Australian Road Research Board, Victoria, Australia.pp 2-16.

Fitzpatrick, J. T., (1960). "Unified Reflective Sign, Pavement and Delineation Treatments for Night Traffic Guidance," *Highway Research Board Bulletin No. 255,* Transportation Research Board, Washington, D.C. pp. 138-145.

Frantzeskakis, J. M., (1983). "Accident Analysis on Two Non-Controlled Access National Highways in Greece," *Institute of Traffic Engineers Journal,* 53(2), pp. 26-32.

Frederiksen, E., and Sorensen, K., (1976). "Reflection Classification of Dry and Wet Road Surfaces," *Lighting Research and Technology,* 8(4). pp. 175-186.

Freedman M., and Davit, P.S., (1982). "Improved Conspicuity to the Sides and Rear of Motorcycles and Mopeds." Final Report, *Report No. DOT HS-806-377,* Department of Transportation, National Highway Traffic Safety Administration, Washington, D.C.

Freedman, M., (1993). "Effects of Reduced Transmittance Film on Automobile Rear Window Visibility," *Human Factors,* 35(3), pp. 535-550.

Freedman, M., (1980). "National Accident Sampling System: Establishment and Operation of the Primary Sampling Unit in Delaware County, PA, 1977-80," *Report No. DOT-HS-805 275,* Department of Transportation, National Highway Traffic Safety Administration, Washington, D.C.

Freedman, M., Decina, L.E., Nick, J.B., and Farber, E.F. (1986). "Reflective Characteristics of Roadway Pavements During Wet Weather," Final Report, *Report No. FHA/RD-86/104*, Federal Highway Administration, Washington, D.C.

Freedman, M., Decina, L.E., and Knoebel, K.Y., (1985). "Traffic Signal Brightness: An Examination of Nighttime Dimming," *Report No. FHWA/RD-85/005,* Federal Highway Administration, Washington, D.C.

Gallagher, Vincent P., (1976). "A Visibility Metric for Safe Lighting of City Streets," *Journal of the Illuminating Engineering Society,* 5(2), Illuminating Engineers Society of North America, New York, New York, pp. 85-91

Gallagher, V., Koth B., and Freedman, M., (1975). "The Specification of Street Lighting Needs," *Report No. FHWA-RD-76-17.* Federal Highway Administration, Washington, D.C.

Gordon, P., (1977). "Appraisal of Visibility on Lighted Dry and Wet Roads," *Lighting Research and Technology 9(4),* pp. 177-188.

Green, B.L., E.A. O'Hair, T. Simpson, T. Krile, W.B. Jones, and W.P. Vann, (1987). "Solar Bowl Subsystems Tests and Analyses," *DOE Technical Report,* US Department of Energy Contract DE-AC04-83AL21557.

Griffin, R., and Woodham, D.B., (1986). "Reduced Freeway Lighting", *Report CDOH-DTP-R-86-19,* Colorado Department of Highways, Boulder, Colorado.

Haber, H. (1955). Safety Hazard of Tinted Automobile Windshields at Night," *Optical Society of America*, 12(6), pp. 1-15.

Hall, R.R., and Fisher, A.J., (1978). "Measures of Visibility and Visual Performance in Road Lighting," *ARRB Research Report No. 74,* Australian Road Research Board, Victoria, Austalia.

Heath, W. and Finch D.M., (1953). "The Effect of tinted Windshields and Vehicle Head lighting on Night Visibility," *Bulletin 68,* Highway Research Board, National Research Council, Washington, D.C.

Helmers, G., and Rumar, K., (1973). "Obstacle Visibility in Rural Night Driving as Related to Road Surface Reflective Qualities," *Transportation Research Record N502,* Transportation Research Board, Washington, D.C. pp. 58-69.

Helms, R. N., (1983). "Methodology for Determining Pavement Reflectivity for Roadway Luminance Calculation," *Transportation Research Record N904,* Transportation Research Board, Washington, D.C. pp. 80-86.

Hilton, M. H., (1978). "Continuous Freeway Illumination and Accidents on a Section of Route I-95," *Report VHTRC 79-R4,* Virginia Highway & Transportation Research Council, Richmond, Virginia.

Hochreither, F.C., (1969). "Analysis of Visibility Observation Methods," *System Development Office Test and Evaluation Laboratory Report*, U.S. Weather Bureau, Sterling, VA.

Holmes, J.G., (1976). "The Road Surface Is Part of the Road Lighting," *Light, Lighting and Environmental Design,* London, England, p. 204.

Hostetter, R.S. (1991). "Trade-off Between Delineation and Lighting on Freeway Interchanges: Investigation on Transient Visual Adaptation," *FHWA-RD-91-041,* U.S. Department of Transportation, Federal Highway Administration, Washington, D.C.

Hostetter, R.S. (1988). "Trade-off Between Delineation and Lighting on Freeway Interchanges: Investigation on Transient Visual Adaptation", *FHWA-RD-88-223,* U.S. Department of Transportation, Federal Highway Administration, Washington, D.C.

Illuminating Engineering Society of North America, (1990), *American National Standard Practice for Roadway Lighting*, ANSI/IES RP-8-1990, Illuminating Engineers Society of North America, New York, New York.

Illuminating Engineering Society of North America, (1983). "Proposed American National Standard Practice for Roadway Lighting," *Journal of the Illuminating Engineering Society,* 12 (2), Illuminating Engineers Society of North America, New York, New York, pp. 146-196.

Janoff, M.S., Koth, B., McCunney, Freedman, M., Duerk, and Berkovitz, M., (1977). "Effectiveness of Highway Arterial Lighting," 1977, *FHWA-RD-77-37,* Federal Highway Administration, Washington, D.C.

Janoff, M.S., (1991). "The Effect of Headlights on Small Target Visibility," *Journal of the Illuminating Engineering Society,* 21(2), Illuminating Engineers Society of North America, New York, New York, pp. 46-53.

Janoff, M.S., (1990). "The Effect of Visibility on Driver Performance: A Dynamic Experiment," *Journal of the Illuminating Engineering Society,* Vol. 9, Illuminating Engineers Society of North America, New York, New York, pp. 57-63.

Janoff, M.S., (1989). "Subjective Ratings of Visibility and Alternative Measures of Roadway Lighting," *Journal of the Illuminating Engineering Society,* Vol. 18, Illuminating Engineers Society of North America, New York, New York, pp. 16-28.

Janoff, M.S., (1993). "Toward Development of a Visibility Model for Roadway Lighting Design," *Journal of the Illuminating Engineering* Society, Illuminating Engineers Society of North America, New York, New York, pp. 122-130.

Janoff, M.S., (1993). "Measured versus Computer-Predicted Luminance in Roadway Lighting Applications," *Journal of the Illuminating Engineering Society,* Illuminating Engineers Society of North America, New York, New York, pp. 75-82.

Janoff, M.S., Freedman, M., and Decina, L.E., (1983). "Partial Lighting of Interchanges," *NCHRP Report 256,* National Cooperative Highway Research Program, National Research Council, Washington, D.C.

Janoff, M.S., Staplin, L.K., and Arens, J.B., (1986). "The Potential for Reduced Lighting on Roadways," *Public Road, 50 (2),* pp. 33-42.

Jung, F.W., and Titishov, A., (1987). "Standard Target Contrast: A Visibility Parameter Beyond Luminance to Evaluate the Quality of Roadway Lighting," *Transportation Research Record 1111,* Transportation Research Board, Washington, D.C. pp. 62-71.

Jung, W., Kazakov, A. and Titshov, A.I., (1984). 'Road Surface Reflectance Measurements in Ontario," *Transportation Research Record 996,* Transportation Research Board, Washington, D.C. pp. 24-37.

Kahl, K.B., and Fambro, D.B, (1994). "Investigation of Object-Related Accidents Affecting Stopping Sight Distances," *Transportation Research Record 1500,* Transportation Research Board, Washington, D.C. pp. 25-30.

Kasturi, R., (1994). "A Model-based Approach for Detection of Runways and Other Objects in Image Sequences Acquired Using an On-board Camera," *NASA Langley Research Center Report,* National Aeronautics and Space Administration, Langley, Virginia.

Keck, M.E., (1996). Memorandum to Douglas D. Gransberg, Texas Tech University, Lubbock, Texas.

Keck, M.E., (1989). "Effect of Luminaire Arrangement on Object Visibility," *Transportation Research Board 1247,* Transportation Research Board, Washington, D.C., pp. 17-22.

Keck, M. E. (1996). *Personal Communication on STV Computer Program and Its Concepts*

Keck, M.E., "Optimization of Lighting Parameters for Maximum Object Visibility and Its Economic Implications," Proceedings, *2nd International Symposium on Visibility and Luminance in Roadway Lighting,* Lighting Research Institute, New York, New York.

Ketron, J. B.(1985). "Reflective Characteristics of Roadway Pavements During Wet Weather," *Transportation Research Circular N297 (Dec 1985),* Transportation Research Board, Washington, D.C. pp. 11-12.

Ketvirtis, A. and Cooper, P.J., (1977). "Detection of Critical Size object as a Criterion for Determining Drivers Visual Needs," Proceedings, 76th Annual Meeting of the Transportation Research Board, Washington, D.C.

King, E.L., (1972). "Luminance Versus Luminance," *Highway Research Board Special Report 134,* Transportation Research Board, Washington, D.C. pp. 10-18.

King, L. E. and Finch, D. M., (1968). "A Laboratory Method for Obtaining Pavement Reflectance Data," *Highway Research Record No. 216,* Transportation Research Board, Washington, D.C. pp. 23-33.

Koth, B. (1978). "Vehicle Fog Lighting: An Analytical Evaluation," *Report No. DOT-HS-803 442,* Department of Transportation, National Highway Traffic Safety Administration, Washington, D.C.

Lamm, R., Kloeckner, J.H., and Choueiri, E.M., (1985). "Freeway Lighting and Traffic Safety-A Long Term Investigation," *Transportation Research Record 1027,* Transportation Research Board, Washington, D.C. *pp. 57-63.*

Lewin, I., (1996). "Advances in Measurement Technology for Vehicle Lighting Systems", *Society of Automotive Engineering, Inc.,* pp. 107-114.

Lewin, I., (1996). "Advances in Measurement Technology for Vehicle Lighting Systems," *SAE Technical Paper Series 960919*, Society of Automotive Engineering.

Lewin, I., Lin, F., and Sisson, C., (1996). "Accuracy Analysis of Video-Based Photometry," *Society of Automotive Engineering, Inc.,* Society of Automotive Engineering pp. 1-10.

Lewin, I., Lin, F., and Sisson, C., (1997). "Accuracy Analysis of Video-Based Photometry," 1997, *SAE Technical Paper series 970231.* Society of Automotive Engineering

Lewis, Alan L., (1976). "The effects of Illumination and Contracts on Visula Processes Affecting Comfort and Performance," *Lighting Design and Applications,* 6(1), Illuminating Engineers Society of North America, New York, New York, p. 16.

Loch, H. C., (1985). "Roadway Lighting Calculations in Perspective," *Journal of the Illuminating Engineering Society, Vol. 12,* Illuminating Engineers Society of North America, New York, New York, pp. 663-669.

Los Angeles Bureau of Street Lighting: (1980). "Intersection Traffic Accident Reduction Through Improved Street Lighting", *OTS Project 127803 Report*, Department of Public Works, City of Los Angeles, California.

Marsden, A. M., (1976). "Road Lighting - Visibility and Accident Reduction," *Public Lighting,* 41 (175), Association of Public Lighting Engineers, pp. 106-111.

Meese, G.E., (1972). "Vehicular Lighting Systems for Two-lane Rural Highways," *Highway Research Board Special Report 134,* Transportation Research Board, Washington, D.C. pp. 41-65.

Merritt, J.O., Newton, R.E., Sanderson, G.A., and Seltzer, M.L., (1979). "Driver Visibility Quality: An Electro-Optical for In-Vehicle Measurement of Module Transfer (MTF)," U.S. Department of Transportation, National Highway Traffic Safety Administration, Washington, D.C.

Moerman, J.J.B., (1977). "Accuracy of Photometry of Retroreflectors and Retroreflective Materials," *Journal of the Illuminating Engineering Society, 9(2),* Illuminating Engineers Society of North America, New York, New York, pp. 85-91.

National Cooperative Highway Research Program. "Practical Guide for Minimizing Tort Liability," *NCHRP Synthesis 106,* Highway Research Board National Research Council, Washington, D.C.

National Cooperative Highway Research Program, (1967). "Effects of Illumination on Operating Characteristics of Freeways," *NCHRP Report No. 60.* Highway Research Board, National Research Council, Washington, D.C.

National Cooperative Highway Research Program, (1978). "Cost and Safety Effectiveness of Highway Design Elements," *NCHRP Report No. 197.* Highway Research Board National Research Council, Washington, D.C.

Nielsen, B.(1979). "Effects of Wear and Composition on Road Surface Reflection Properties," *CIE Proceedings (19th session),* International Commission on Illumination, pp. 425-432.

O'Hair, E.A. and B.L. Green, (1990). "Component Efficiencies from the Operation of the Crosbyton Solar Bowl," Proceedings, *25th Intersociety Energy Conversion Engineering Conference,* Dallas, Texas.

Olson, P.L., and Sivak, M., (1983). "Improved Low-Beam Photometrics," *National Highway Traffic Safety Administration, Report No. DOT HS-9-02304,*U.S. Department of Transportation, National Highway Traffic Safety Administration, Washington, D.C.

Olson, P.L., and Sivak, M., (1983). "Improved Low-Beam Photometrics," 1983, *Report No. DOT HS-806-487,* Department of Transportation, National Highway Traffic Safety Administration, Washington, D.C.

Persaud, B.N. and Mucsi, K., (1994). "Microscopic Accident Potential Models for Two-Lane Rural Roads," *Transportation Research Record 1485,* Transportation Research Board, Washington, D.C. pp. 134-139.

Rackoff, N. J., and Rackwell, T.H., (1975). "Driver Search and Scan Pattern in Night Driving", *Ohio Department of Transportation and The Federal Highway Administration*, Special Report 156. Columbus, Ohio.

Richards, O.H., (1966). "Vision at Levels of Night Road Illumination," *Transportation Research Record 179,* Transportation Research Board, Washington, D.C., pp. 61-66.

Richards, O.W., (1967). "Visual Needs and Possibilities for Night Driving: Part 2," *The Optician,* 154(3999), p. 523.

Richards, S.H., (1981). "Effects of Turning Off selected Roadway Lighting as an Energy Conservation Measure," *Transportation Research Board Record N811,* Transportation Research Board, Washington, D.C. pp. 23-25.

Roper, V.J. (1953). *Bulletin 68*, Highway Research Board, National research Council, Washington, D.C.

Rinalducci, E.J. (1974). "Losses in Nighttime Visibility Caused by Transient Adaptation," *Journal of the Illuminating Engineering Society,* Illuminating Engineers Society of North America, New York, New York, pp.336-345.

Sanderson, J. T., (1985). "An Analysis of Accidents on Freeways With and Without Lighting," *Report No. NTS85/2*, Royal Automobile Club of Victoria, Australia.

Scott, P. P., (1980). "The Relationship Between Road Lighting Quality and Accident Frequency," *TRRL Laboratory Report 929.*Department of Transportation, National Highway Traffic Safety Administration, Washington, D.C.

Scott, P.P., Cobb, J., Hargroved, R. A., and Marsden, A. M., (1979). "Road Lighting and Accidents," *CIE Proceedings,* International Commission on Illumination, Kyoto, Japan.

Shelby, B.L. and Howell, B.G., (1985). "Comparative Analysis of Roadway Lighting Using Both CIE 19/2 and Adrian's Delta L," *Journal of the Illuminating Engineering Society,* Illuminating Engineers Society of North America, New York, New York, pp. 181-211.

Stein, B., Reynolds, J.S., and McGuiness, W.J., (1986). *Mechanical and Electrical Equipment for Buildings, 7th edition,* John Wiley and Son, New York, NY., pp. 857-1114.

Strickland, J., Ward, B. and Allen, M.J., (1968). "The Effect of Low vs. High Beam Headlights and Ametropia on Highway Visilbility at Night," *American Journal of Optometry and Archives of American Academy of Optometry,* 45(2).

Strickland, S.G., and Nowakowski, V.J., (1989). "The Older Driver: A Growing Concern in Roadway Design and Operations," *ITE 1989 Compendium of Technical Papers,* pp. 302-306.

Swanlen, H., and Schnell, T. "Loss of Visibility Distance Caused by Automobile Windshields at Night," *Transportation Research Record 1495,* Transportation Research Board, Washington, D.C. p. 128.

Texas Department of Transportation, (1995). *Highway Illumination, Traffic Operations Manual,* Texas Department of Transportation, Austin, Texas.

U.S. Environmental Protection Agency, (1980). *Interim Guidance for Visibility Monitoring,* Environmental Monitoring System Laboratory, U.S. Environmental Protection Agency, Washington, D.C.

Van Bommel, Wout J.M., (1978). "Design Consideration for Roadway Lighting," *Journal of the Illuminating Engineering Society,* Illuminating Engineers Society of North America, New York, New York, pp. 40-46.

Van Dommelen, C., (1996). "Choosing the Right Lighting for Inspection," *Test and Measurement World,* p. 53.

Waetjen, R., Schiefer, U., Gaigl, A., and Aulhorn, E., (1993). "Der Einfluss von Windschutzscheiben "-Toenung" und "-Neigung" auf den Erkennungsabstand unter Mesopischen Bedingungen," *Zeirschrift fur Verkehrssicherheit,* (in German) 39 (1).

Waldram, J.M. (1938). "The Revealing Power of Street Lighting Installation, "*Transactions,* Illuminating Engineers Society of North America, London, England.

Waldram, J.M. (1966). "The Design of the Visual Field in Street: The Visual Engineer's Contribution," *Transactions,* 31 (1), Illuminating Engineers Society of North America, London, England.

Waldram, J.M., (1976). "Safety on the Road at Night," *Light and Lighting and Environmental Design,* London, England pp. 184-187.

Walton, N.E., (1975). "Fixed Illumination as a Function of Driver Needs," *Ohio Department of Transportation and The Federal Highway Administration*, Special Report 156. Columbus, Ohio.

Wright, W.D., (1976). "Seeing to Drive at Night," *Light and Lighting and Environmental Design,* London, England pp. 188-189.

Zwahlen, H.T., (1993). "Effects of Automobile Windshields or Other Optical Filters on the Visibility and Legibility of Targets within the Driving Context," *Transportation Research Record 94,* Transportation Research Board, Washington, D.C.

Zwahlen, H.T., and Schnell, T. (1994). "Loss of Visibility Distance Caused by Automobile Windshields at Night," *Transportation Research Record 1495,* Transportation Research Board, Washington, D.C. pp. 128-139.

Zwahlen, H.T., and Yu J., (1990). "Color and Shape Recognition of Reflectorized Targets Under Automobile Low-Beam Illumination at Night," *Transportation Research Record 1327,* Transportation Research Board, Washington, D.C. pp. 1-7.